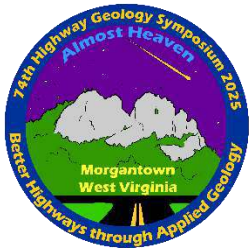
2025

HGS PROCEEDINGS



74TH HIGHWAY GEOLOGY SYMPOSIUM

AUGUST 11-14, 2025
MORGANTOWN, WV



74th Highway Geology Symposium

August 11-14, 2025
Mariott Morgantown Waterfront Place
Morgantown, WV

Grateful Acknowledgments

A huge "Thank You" to the folks who made this Symposium possible:

74th HGS Local Committee:

Wayne Perkins
Dr. Elizabeth Rhenberg
Madison Urse
Emerson Loisel
Chris Ruppen
Kyle Halverson
John Pilipchuk
Ken Ashton

Thanks also to:

Jessica Moore, WVGES Director and State Geologist
John Lasko, Michael Baker International, Inc.
Jeremiah Knavenshue, Michael Baker International, Inc.
Brandon Raines, WVDOT
Phil Dinterman, WVGES Deputy Director
Hannah Sphar, WVGES
Barnes Nugent, WVGES
Randy Toth, WVGES
John Tudek, WVGES
HGS National Steering Committee
Delaney Meeting and Event Management
West Virginia Department of Transportation
The West Virginia Geological and Economic Survey Staff

WVGES
West Virginia Geological and Economic Survey

Geology Underlies it all



74th Highway Geology Symposium

August 11-14, 2025
Mariott Morgantown Waterfront Place
Morgantown, WV

TABLE OF CONTENTS

Acknowledgements....1

Dedication....3

Hotel Map....4

Schedule at a Glance....5

Highway Geology Symposium History Organization and Function....6

HGS National Steering Committee Officers....12

HGS National Steering Committee Members....12

Past, Present, and Future Symposium Contacts....13

Emeritus Steering Committee Members....14

Medallion Award....15

Young Author Award....16

Multi Agency Special Session....17

USGS Special Landslide Session....18

Field Trip Schedule....19

Sponsors....20

Exhibitors....29

Technical Session Schedule....35

Papers....39

The Proceedings of the 74th Highway Geology Symposium are dedicated to

Dr. Terry R. West



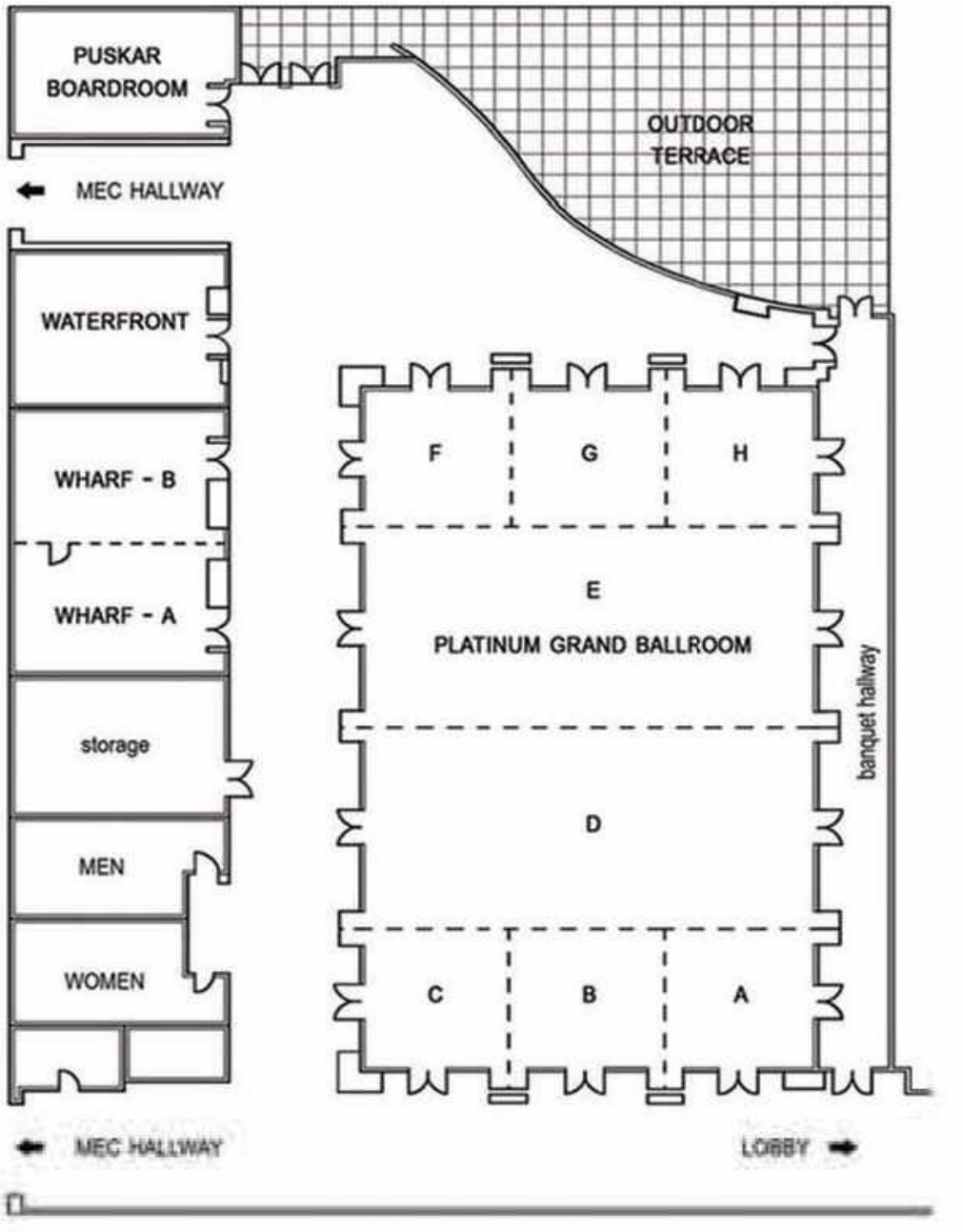
Dr. Terry Ronald West passed away March 4, 2025 at the age of 88. He was born in Saint Louis, MO August 15, 1936. Terry received two undergraduate degrees and a Master's degree from Washington University and another Master's and a PhD from Perdue University. He went on to become a full-time instructor and professor at Perdue, where he taught for 61 years. He was a Perdue multi-sport season ticket holder and enjoyed everything about his beloved Boilermakers.

Dr. West was a long-time member of Association of Environmental and Engineering Geologists and is listed on their web page as "one of the legendary professionals" in the field of engineering geology. Terry authored a widely used textbook, Geology Applied to Engineering, in 2010 and released an updated second edition in 2018.

Terry had a very long history with the Highway Geology Symposium. He was 28 years old when he presented his first paper at the 15th HGS in Rolla, Missouri in 1964. Since then, Terry has authored and presented 28 papers. In 1967, he served as a co-chairman of the local committee for the 18th HGS in Lafayette, IN, and became a member of the HGS National Steering Committee. He remained an active member of the Steering Committee for 59 years, serving on numerous committees. Terry's contributions and longstanding participation with the National Steering Committee and the Symposium will be greatly missed.

74th Highway Geology Symposium
August 11 – 14, 2025
Morgantown, West Virginia

Mariott Morgantown Waterfront Place
Main Floor



74th Highway Geology Symposium

Schedule at a Glance

	Monday, August 11, 2025	Location
9:00 AM - 6:00 PM	Registration Open	Platinum Grand Ballroom Foyer
1:00 PM - 5:00 PM	Multi-Agency Special Session	Platinum Grand Ballroom - Salon ABC
5:00 PM - 6:30 PM	HGS National Steering Committee Meeting	Wharf AB
6:00 PM - 8:00 PM	Icebreaker Reception *Sponsored by GeoStabilization International*	Platinum Grand Ballroom Foyer & Terrace

	Tuesday, August 12, 2025	
7:00 AM - 8:00 AM	Breakfast	Platinum Brand Ballroom Foyer & Salon EFGH
7:00 AM - 5:00 PM	Registration Open	Platinum Grand Ballroom Foyer
7:00 AM - 5:00 PM	Exhibits Open	Platinum Grand Ballroom Foyer
8:00 AM - 9:00 AM	Welcome to West Virginia!	Platinum Grand Ballroom Salon ABCD
9:00 AM - 3:00 PM	Guest Tour & Activity	Offsite - Depart from Hotel Lobby
9:00 AM - 10:00 AM	Technical Session 1: Young Authors	Platinum Grand Ballroom Salon ABCD
10:00 AM - 10:30 AM	Morning Break *Sponsored by Central Mine Equipment Co.*	Platinum Brand Ballroom Foyer & Salon EFGH
10:30 AM - 11:50 AM	Technical Session 2: Young Authors	Platinum Grand Ballroom Salon ABCD
11:50 AM - 1:00	Lunch	Platinum Brand Ballroom Foyer & Salon EFGH
1:00 - 2:40 PM	Technical Session 3	Platinum Grand Ballroom Salon ABCD
2:40 PM - 3:10 PM	Afternoon Break *Sponsored by Hager-Richter Geoscience, Inc.*	Platinum Brand Ballroom Foyer & Salon EFGH
3:10 PM - 5:00 PM	Technical Session 4: Improving Availability of Information on Landslide Loss and Effects	Platinum Grand Ballroom Salon ABCD

	Wednesday, August 13, 2025	
7:00 AM - 8:00 AM	Breakfast	Platinum Brand Ballroom Foyer & Salon EFGH
7:00 AM - 5:00 PM	Registration	Platinum Grand Ballroom Foyer
7:00 AM - 3:00 PM	Exhibits open	Platinum Grand Ballroom Foyer
8:00 AM - 10:00 AM	Technical Session 5	Platinum Grand Ballroom Salon ABCD
10:00 AM - 10:30 AM	Morning Break	Platinum Brand Ballroom Foyer & Salon EFGH
10:30 AM - 11:50 AM	Technical Session 6	Platinum Grand Ballroom Salon ABCD
11:50 AM - 1:10 PM	Lunch	Platinum Brand Ballroom Foyer & Salon EFGH
1:10 PM - 2:30 PM	Technical Session 7	Platinum Grand Ballroom Salon ABCD
2:30 PM - 3:00 PM	Afternoon break	Platinum Brand Ballroom Foyer & Salon EFGH
3:00 PM - 4:00 PM	Technical Session 8	Platinum Grand Ballroom Salon ABCD
4:00 PM - 4:20 PM	Field Trip preview	Platinum Grand Ballroom Salon ABCD
6:00 PM - 7:00 PM	Banquet social	Platinum Grand Ballroom Foyer
7:00 PM - 10:00 PM	HGS Banquet & Awards *Entertainment by Eric Lewis & 80s Enough*	Platinum Brand Ballroom Foyer & Salon EFGH

	Thursday, August 14, 2025	
6:30 AM - 7:00 AM	Grab & Go breakfast *Sponsored by Fragmentation Efficiency Services, Inc. and KESCO, Inc.*	Platinum Brand Ballroom Foyer & Salon EFGH
7:00 AM	Field Trip Departs Breakfast provided by FES, Inc., KESCO, Inc. Transportation sponsored by Maccaferri, Inc. Snacks/soft drinks sponsored by Ameritech Slope Constructors Beer sponsored by Scarptec Snow cones (Kona Ice) sponsored by GSI/Access Limited	Hotel Lobby
12:30 PM	Lunch *Sponsored by Geobrugg*	Blackwater Falls State Park
6:00 PM	Approximate Return to Morgantown	Hotel Lobby

	Friday, August 15, 2025	
8:30 AM - 4:00 PM	Whitewater Rafting Trip - Geology of the Cheat River Narrows *Pre-Registration required*	Offsite - Depart from Hotel Lobby

Highway Geology Symposium
History, Organization, and Function

Inaugural Meeting and Beginnings

Established to foster a better understanding and closer cooperation between geologists and civil engineers in the highway industry, the Highway Geology Symposium (HGS) was organized and held its first meeting on March 14, 1950, in Richmond Virginia. Attending the inaugural meeting were representatives from state highway departments (as referred to at that time) from Georgia, South Carolina, North Carolina, Virginia, Kentucky, West Virginia, Maryland, and Pennsylvania. In addition, a number of federal agencies and universities were represented. A total of nine technical papers were presented. W.T. Parrott, an engineering geologist with the Virginia Department of Highways, chaired the first meeting. It was Mr. Parrott who originated the Highway Geology Symposium. It was at the 1956 meeting that future HGS leader, A.C. Dodson, began his active role in participating in the Symposium. Mr. Dodson was the Chief Geologist for the North Carolina State Highway and Public Works Commission, which sponsored the 7th HGS meeting.

Organization

Unlike most groups and organizations that meet on a regular basis, the Highway Geology Symposium has no central headquarters, no annual dues and no formal membership requirements. The governing body of the Symposium is the National Steering Committee composed of approximately 20 – 25 geologist and geotechnical engineers from state and federal agencies, colleges and universities, as well as private service companies and consulting firms throughout the country. Steering committee members are elected for three-year terms, with their elections and re-elections being determined principally by their interests and participation in and contribution to the Symposium. The officers include a chairman, vice chairman, secretary, and treasurer. all of whom are elected for a two-year term. Officers, except for the treasurer, may only succeed themselves for one additional term. A number of three-member standing committees conduct the affairs of the organization. The lack of rigid requirements, routing and relatively relaxed overall functioning of the organization is what attracts many participants. The symposia are generally run for 3 days, with 2 days for technical papers and a full day field trip. The Symposium is often preceded with a special session or workshop and an opens with an evening Ice-Breaker. Occasionally, an optional workshop or field trip may follow the Symposium

Symposium Locations

Since the initial meeting, 73 annual (2 years missed for COVID) Symposiums have been held in 36 different states. Between 1950 and 1962, the meetings were east of the Mississippi River, with Virginia, West Virginia, Ohio, Maryland, North Carolina, Pennsylvania, Georgia, Florida, and Tennessee serving as host state. In 1962, the symposium moved west for the first time to Phoenix, Arizona where the 13th annual HGS meeting was held. Since then it has alternated, for the most part, back and forth from the east to the west.

1st	1950	Richmond, VA
2nd	1951	Richmond, VA
3rd	1952	Lexington, KY
4th	1953	Charleston, WV
5th	1954	Columbus, OH
6th	1955	Baltimore, MD
7th	1956	Raleigh, NC
8th	1957	State College, PA
9th	1958	Charlottesville, VA
10th	1959	Atlanta, GA
11th	1960	Tallahassee, FL
12th	1961	Knoxville, TN
13th	1962	Phoenix, AX
14th	1963	College Station, TX
15th	1964	Rolla, MO
16th	1965	Lexington, KY
17th	1966	Ames, IA
18th	1967	Lafayette, IN
19th	1968	Morgantown, WV
20th	1969	Urbana, IL
21st	1970	Lawrence, KS
22nd	1971	Norman, OK
23rd	1972	Old Point Comfort, VA
24th	1973	Sheridan, Wy
25th	1974	Raleigh, NC
26th	1975	Coeur d'Alene, ID
27th	1976	Orlando, FL
28th	1977	Rapid City, SD
29th	1978	Annapolis, MD
30th	1979	Portland, OR
31st	1980	Austin, TX
32nd	1981	Gatlinburg, TN
33rd	1982	Vail, Co
34th	1983	Stone Mountain, GA
35th	1984	San Jose, CA
36th	1985	Clarksville, TN
37th	1986	Helena, MT

38th	1987	Pittsburgh, PA
39th	1988	Park City, UT
40th	1989	Birmingham, AL
41st	1990	Albuquerque, NM
42nd	1991	Albany, NY
43rd	1992	Fayetteville, AR
44th	1993	Tampa, FL
45th	1994	Portland, OR
46th	1995	Charleston, WV
47th	1996	Cody, WY
48th	1997	Knoxville, TN
49th	1998	Prescott, AZ
50th	1999	Roanoke, VA
51st	2000	Seattle, WA
52nd	2001	Cumberland, MD
53rd	2002	San Luis Obispo, CA
54th	2003	Burlington, VT
55th	2004	Kansas City, MO
56th	2005	Wilmington, DE
57th	2006	Breckinridge, CO
58th	2007	Pocono Manor, PA
59th	2008	Santa Fe, NM
60th	2009	Buffalo, NY
61st	2010	Oklahoma City, OK
62nd	2011	Lexington, KY
63rd	2012	Redding, CA
64th	2013	North Conway, NH
65th	2014	Laramie, WY
66th	2015	Sturbridge, MA
67th	2016	Colorado Springs, CO
68th	2017	Marietta, GA
69th	2018	Portland, ME
70th	2019	Portland, OR
71st	2022	Asheville, NC
72nd	2023	Tacoma, WA
73rd	2024	Lawrence, KS
74th	2025	Morgantown, WV

Symposium Format

The symposia are scheduled for three days, with two days of technical papers and a full day for the field trip. The Symposium is often preceeded with a special session and/or workshops and opens with evening Ice-Breaker, followed by two days of technical presentations and a full day field trip.

Highway Geology Symposium Field Trip

The field trip is the focus of the meeting. In most cases, the trips cover approximately 150 to 200 miles, with stops visiting geological, geotechnical, and cultural points of interests in the host state or nearby.

Some highlights of past Symposium field trips: In Wyoming (1973), the group viewed landslides in the Big Horn Mountains; Florida's trip (1976) included a tour of Cape Canaveral and the NASA space installation; the Idaho and South Dakota trips dealt principally with mining activities; North Carolina provided stops at a quarry site, a dam construction site, and a nuclear generation site; in Maryland (1978), the group visited the Chesapeake Bay hydraulic model and the Goddard Space Center. The Oregon trip included visits to the Columbia River Gorge and Mount Hood; the Central mine region was visited in Texas.

The Tennessee meeting in 1981 provided stops at several repaired landslide in Appalachia regions of East Tennessee. In Utah (1988) the field trip visited sites in Provo Canyon and stopped at the famous Thistle Landslide.
In New Mexico (1990), the emphasis was on rockfall treatments in the Rio Grande River canyon and included a stop at the Brugg Wire Rope headquarters in Santa Fe. Mount St, Helens was visited by the field trip in 1994 when the meeting was in Portland, Oregon.

1995 the West Virginia meeting took us to the New River Gorge Bridge that has a deck elevation of 876 feet above the water, and at the time, was the longest single arch span in the world. In Cody Wyoming, the 1996 field trip visited the Chief Joseph Scenic Highway and the Beartooth Uplift in northwest Wyoming. In 1997 the meeting in Tennessee visited the newly constructed future I-26 highway in the Blue Ridge of East Tennessee. The Arizona meeting in 1998 visited the Oak Creek Canyon near Sedona and a mining ghost town at Jerome, Arizona. The Virginia meeting in 1999 visited the "Smart Road"



New River Gorge Bridge



Sidling Hill Syncline

Project that was under construction. This was a joint research project of the Virginia Department of Transportation and Virginia Tech University. The Seattle Washington meeting in 2000 visited an ancient lahar in the Mount Rainier area. A highlight of the Maryland symposium in 2001 was visiting the Sideling Hill road cut for I-68, which beautifully exposes a tightly folded syncline, common in the Valley and Ridge physiographic province of the Appalachians. The California field trip in 2002 provided a field demonstration of the effectiveness of rock netting against rock falls along the Pacific Coast Highway. The Kansas City meeting in 2004 visited the Hunt Subtropolis which is said to be the "world's largest underground business complex". It was created through the mining of limestone by way of the room and pillar method. The Rocky Point Quarry provided an opportunity to search for fossils at the North Carolina meeting in 2005. The group also visited the US-17 Wilmington Bypass Bridge which was under construction. Among the stops at the Pennsylvania meeting were the Hickory Run Boulder Field, the No.9 Mine and Wash Shanty Museum, and the Lehigh Tunnel. The New Mexico field trip in 2008 included stops at a soil nailed wall along US-285/84 north of Santa Fe and a road cut through the Bandelier Tuff on highway 502 near Los Alamos where rockfall mesh was used to protect against rockfalls. The New York field trip in 2009 included the Niagara Falls Gorge and the Devil's Hole Trail.

In Oklahoma (2010) the trip saw the complex geology of the Arbuckle Mountains in the southern part of the state along with stops at Tucker's Tower and Turner Falls. In the bluegrass state of Kentucky (2011) the trip included stops at Camp Nelson, the site of the oldest exposed rocks in Kentucky, near the Lexington and Kentucky River Fault Zones. Additional stops at the Darby Dan Farm and the Woodford Reserve Distillery illustrated how the local geology has played such a large part in the success of breeding prized thoroughbred horses and made Kentucky the "Birthplace of Bourbon". In Redding, California, the 2012 field trip included stops at the Whiskeytown Lake, which is one in a series of lakes that provide water and power to northern California. Additional stops included Rocky Point, a roadway construction site containing Naturally Occurring Asbestos (NOA), and Oregon Mountain where the geology and high rainfall amounts have caused Hwy 299 to experience local and global instabilities since first constructed in 1920.

The 2013 field trip in New Hampshire highlighted the topography and geologic remnants left by the Pleistocene glaciation that fully retreated approximately 12,000 years ago. The field trip included stops at various overlooks of glacially carved valleys and ranges; the Old

Man of the Mountain Memorial Plaza, which is a tribute to the famous cantilevered rock mass in the Franconia Notch that collapsed on May 3, 2003; the lacustrine deposits and features of the Glacial Lake Ammonoosuc; views of the Presidential Range; bridges damaged during Tropical Storm Irene in August 2011; and the Willey Slide, located in the Crawford Notch where all members of the Willey family were buried by a landslide in 1826. The 2014 (Wyoming) field trip presented a breathtaking tour of the geology and history of southeast Wyoming, ascending from the high plains surrounding Laramie at 7000 feet to the Medicine Bow Mountains along the Snowy Range Scenic Byway. Visible along the way were a Precambrian shear zone, and glacial deposits and features. From the glacially carved Mirror Lake and the Snowy Range Ski Area, the path wound east to the Laramie Mountains and the Vedauwoo Recreational Area, a popular rock climbing and hiking area. The 2015 field trip in Sturbridge, Massachusetts, focused on the Connecticut Valley, a Mesozoic rift basin that signaled the breakup of Pangea, and the Berkshires, which represents the collision and amalgamation of an island arc system with the North American Laurentian margin.



Garden of the Gods

The field trip in Colorado (2016) was an urban setting along the western edge of Colorado Springs and around Manitou Springs. Stops included the Pikeview Quarry, Garden of the Gods Visitor Center, and several other locations where rockfall and debris flow mitigation, post-flooding highway embankment repair, and a nonconformity in the rock records that spans 1.3 billion years were observed.

The Georgia (2017) field trip provided an opportunity to view the geology of northern Georgia. Stops included the Bellwood Quarry, which, at one time was run by the City of Atlanta and served as a prison labor camp. Upon completion of a tunnel to connect the quarry to two water treatment plants and three pump stations, It will serve as a 2.4 billion-gallon water storage facility for the City of Atlanta. Additional stops included the Buzzi Unicem Cement Plant to get a close up view of the Clairmont Melange, The Cooper Furnace near the Allatoona Dam, and the New Riverside Ochre-Emerson Barite mine.



Penobscot Narrows Bridge

The 2018 field trip of the Portland, Maine Symposium presented a good overview of the geology of coastal Maine. Field trip stops included the Sherman Salt Marsh near Newcastle which was recently restored to its natural state after the dam that carried US Highway 1 washed out during a 2005 storm, the site of the 1996 landslide near Rockland Harbor that consumed several homes, and the rock slope remediation project at the

Penobscot Narrows Bridge near Prospect Maine. A lobster lunch along the shore of Penobscot Bay was one of several highlights of the field trip.

The 2019 field trip in Portland, Oregon travelled the Columbia River Gorge west. Starting at the Crown Point Vista House and Portland Women's Forum State Scenic Viewpoint above the gorge to learn about the river highway. Descending into the gorge, we stopped at scenic Multnomah Falls and Benson Bridge, and saw flexible rockfall fence installed to protect the lodge and historic Columbia River Highway. Other stops included lunch at Cascade Locks, Bonneville Landslide and rockfall areas along the highway

The 2022 field trip in the Ashville, North Carolina area took us through Ordovician (500 my) to Precambrian (1.2 by) migmatized ortho and paragneisses, metamorphosed intrusives, thrust faults and contacts representing three orogenies and complex sequences of basement and terranes. We crossed the Brevard Fault zone several times, which is a structure that has been studied and interpreted for 100 years. Various attempts to define the structure have been made, especially in the pre-plate tectonic era. It has been theorized that these structures were as high, or higher than the Rockies at formation. 200 million years of rifted erosion leave us with an exposed look at deep orogenic roots of multiple thrust events. Precipitation in the areas is between 60-100" per year. There are deep ancient colluvial deposits, complex mineralization and weathering profiles, and non-linear/planar discontinuities. We traveled over I-26 and the Blue Ridge Escarpment where the highway is being widened. Stops included the I-26 Old Howard Gap Slide Area, the US 74 Gerton Slide, a shallow landslide barrier on I-40 W, and the Buckner Gap Cut.

The 2023 Field trip in Tacoma, Washington traveled to Mt Rainer where HGS goers were able to take various hikes around the park. Additional highlights included driving down into the Ohop Valley outwash channel, a drive by of Alder Lake, a drive along Copper Creek Forest Road 59, a view of Nisqually Glacier from Nisqually River and a final stop at Ricksecker Point.

The Lawrence Kansas (2024) symposium field trip took us to the Tallgrass Prairie National Preserve, lunch on the Dakota Formation sandstone bluff at Coronado Heights, and saw the unique differential weathering of the Dakota Formation at Mushroom Rock State Park.



Mushroom Rock State Park

HGS National Steering Committee

Officers

Bill Webster, Chairman CalTrans 5900 Folsom Blvd. Sacremento, CA 95819 916-662-1183 Bill_webster@dot.ca.gov	**Kyle Halverson, Vice-Chairman** Kansas DOT Bureau of Structures and Geotechnical Svc. 700 SW Harrison Street Topeka, KS 66603 785-291-3860 Kyle.halverson@ks.gov
Mark Fish, Secretary WSDOT Geotechnical Office 1655 S. 2nd Ave. Tumwater, WA 98512 360-709-5898 fishm@wsdot.wa.gov	**John Pilipchuk, Treasurer** NCDOT Geotech Engineering Unit (Retired) 1512 US Highway 70 East Hillsborough, NC 27278 919-622-3381 johnpilipchuk@yahoo.com

HGS National Steering Committee Members

Ken Ashton West Virginia Geological Survey 1 Mont Chateau Road Morgantown, WV 26508 304-594-2331 ashton@wvgs.wvnet.edu	**Vanessa Bateman** Geotechnical, Geology, & Materials CoP Leader Eng. & Construction HQ U.S. Army Corp of Engineers 202-761-7423 Vanessa.c.bateman@usace.army.mil	**Simon Boone** Geostabilazation International 10225 Westmoor Drive Westminster, CO 80021 540 420-2678 simon@alcinc.com
James Dahill Wyoming DOT 5300 Bishop Boulevard Cheyenne, WY 82009 307-777-4205 james.dahill@wyo.gov	**Bob Henthorne** PEC 400 S. Kansas Ave. Topeka, KS 66603 785-233-8300 Bob.henthorne@pec1.om	**Jody Kuhne** NCDOT (Retired) 778 Flint Street Asheville, NC 28801 828-779-9482 jodykuhne@gmail.com

HGS National Steering Committee Members (continued)

Sarah McInnes PA DOT Engineering District 6-0 7000 Geerdes Blvd. King of Prussia, PA 19406 610-205-6544 smcinnes@pa.gov	**Krystle Pelham** New Hampshire DOT Bureau of Materials and Research P. O. Box 483 5 Hazen Drive Concord, NH 03302-0483 603-271-1657 Krystle.j.pelham@dot.state.nh.us	**Victoria Porto** PA DOT (Retired) 10 Oine Lake Drive Carlisle, PA 17015 717-805-5941 vamporto@aol.com
Eric Rorem Ameritech Slope Constructors 21 Overland Industrial Blvd. Asheville, NC 28806 505 690-7144 erorem@ameritech.pro	**Christopher Ruppen** Geostabilization International 3808 Sunflower Road New Brighton, PA 15066 727-272-7532 Christopher.ruppen@gsi.us	**Tim Shevlin** Geobrugg North America LLC Salem, OR 97302 503-423-7258 Tim.shevlin.@geobrugg.com
Jay Smerekanicz Scarptec, Inc. P. O. Box 326 Monument Beach, MA 02553 603-493-6274 jay@scarptec.com	**Deana Sneyd** Petrologic Solutions, Inc. 3997 Oak Hill Road Douglasville, GA 30135 678-313-4147 dsneyd@gmail.com	**John Szturo** HNTB Corporation 715 Kirk Drive Kansas City, MO 64105 816-525-2275 jszturo@hntb.com
Cheryl Youngblood NC Dept. of Transportation 1020 Birch Ridge Drive Raleigh, NC 27610 919-707-6873 cyoungblood@ncdot.gov		

Past Present and Future Symposium Contact List

2017	Georgia	Deana Sneyd	678-313-4147	dsneyd@gmail.com
2018	Maine	Krystle Pelham	603-271-1657	krystle.j.pelham@dot.state.nh.us
2019	Oregon	Tim Shevlin	503-423-7258	tim.shevlin@geobrugg.com
2022	North Carolina	John Pilipchuk	919-622-3381	johnpilipchuk@yahoo.com
		Jody Kuhne	828-779-9482	jodykuhne@gmail.com
2023	Washington	Marc Fish	360-709-5898	fishm@wsdot.wa.gov
2024	Kansas	Kyle Halverson	785-600-8165	Kyle.halverson@ks.dot
2025	West Virginia	Ken Ashton	304-594-2331	ashton@wvgs.wvnet.edu
2026	Nevada	Gary Norris	775-331-5582	norris@unr.edu

EMERITUS STEERING COMMITEE MEMBERS

Steering Committee members who have provided outstanding service to the organization but have resigned from the Steering Committee are eligible to become an Emeritus Member. Candidates are nominated and status is granted with a majority vote from the Steering Committee.

R. F. Baker
David Bingham
Virgil E. Burgat
Hugh Chase
Dick Cross
A. C. Dodson
Tom Eliassen
John “Brandy” Gilmore
Robert Goddard
Mike Hager
Pete Ingraham
Richard Lane
Bill Lovell
Willard MaCasland
David Mitchell
W. T. Parrot
Paul H. Price
Bill Sherman
Mitchell Smith
Steve Sweeney
Berke Thompson
Burrell Whitlow

John Baldwin
Vernon Bump
Robert G. Charboneau
Jim Coffin
Jeff Dean
John Duffy
Walter Fredericksen
Russell Glass
Joseph Gutierrez
Rich Humphries
Charles T. Janik
John Lemish
George S. Meadors, Jr.
Henry Mathis
Harry Moore
Nicholas Priznar
David L. Royster
Willard L Sitz
Jim Stroud
Sam Thornton
Mike Vierling
W. A. “Bill” Wisner

Medallion Award

The Medallion Award was instituted in 1969 to recognize individuals who have made significant contributions to the Highway Geology Symposium over many years. The award is a 3.5" medallion mounted on a walnut shield and appropriately inscribed. The Medallion Award is presented during the banquet at the annual symposium.

Medallion Award recipient	Year		Medallion Award recipient	Year
Hugh Chase	1970		Harry Ludowise	2000
Tom Parrott	1970		Bob Henthorne	2004
Paul Price	1970		Michael Hagar	2005
K. B. Woods	1970		Joseph A. Fischer	2007
R. J. Edmonson	1972		Ken Ashton	2008
C. S. Mullin	1974		David Martin	2008
A. C. Dodson	1975		Richard Cross	2009
Burrell Whitlow	1978		Mike Vierling	2009
Bill Sherman	1980		John Szturo	2009
Virgil Burgat	1981		Jeff Dean	2012
Henry Mathis	1982		Chris Ruppen	2012
David Royster	1982		Eric Rorem	2014
Terry West	1983		John Pilipchuk	2015
Dave Bingham	1984		Pete Ingraham	2016
Vernon Bump	1986		Richard Lane	2017
C. W. "Bill" Lovell	1989		Steve Sweeney	2018
Joseph A. Gutierrez	1990		John Duffy	2018
Willard McCasland	1990		Krystle Pelham	2018
W. A. "Bill" Wisner	1991		Vanessa Bateman	2019
David Mitchell	1993		Marc Fish	2023
Harry Moore	1996			
Earl Wright	1997			
Russell Glass	1998			

Young Author Award

The Highway Geology Symposium has always encouraged participation of young professionals knowing that they are the future of the organization. To recognize and promote participation of young professionals, an annual National Young Author Competition was established in 2014. To qualify, participants may be up to 35 years old or younger, must be the principal author, and the sole presenter of the paper at the Symposium. Papers are reviewed and judged based on technical presentation of the paper (including geology), Originality of the Work, Applicability of the Work to Others and Paper Layout. One recipient is selected each year to receive the coveted Young Author Award, consisting of a plaque and cash prize to be presented at the annual Symposium banquet.

Young Author Award winners:

2014 - **Simon Boone**, "Performance of Flexible Debris Flow Barriers in a Narrow Canyon"

2015 - **Cory Rinehart**, "High Quality H20: Utilizing Horizontal Drains for Landslide Stabilization"

2016 - **Todd Hansen**, "Geologic Exploration for Ground Classification: Widening of the I-70 Veterans Memorial Tunnels"

2017 - **James Arthurs**, "Construction of Transportation Infrastructure in Weathered Volcanic Ash Soils"

2018 - **Brian Felber**, "Geotechnical Challenges for Bridge Foundations & Roadway Embankment Design in Peats and Deep Glacial Lake Deposits"

2019 - **Anya Brose**, "The Assessment and Remediation of Wabasha St. Rock Fall"

2022 - **Christopher Mayer** "Using Geophysics to Evaluate the Results of a Grouting Program in Karstic Geology

2023 - **Cody Chaussee**, "Bolt Creek Fire: Post-Wildfire Debris Flow Risk Assessment and Barrier Design on US 2, Near Grotto, WA

2024 - **Katelyn Card**, "Post Wildfire Effects on Geotechnical Assets".

74th Highway Geology Symposium
Multi Agency Special Session
Monday August 10, 2025
1:00 – 5:00 p.m.

Challenges and Solutions for Hiring, Training and Retention of Subsurface Exploration Professionals

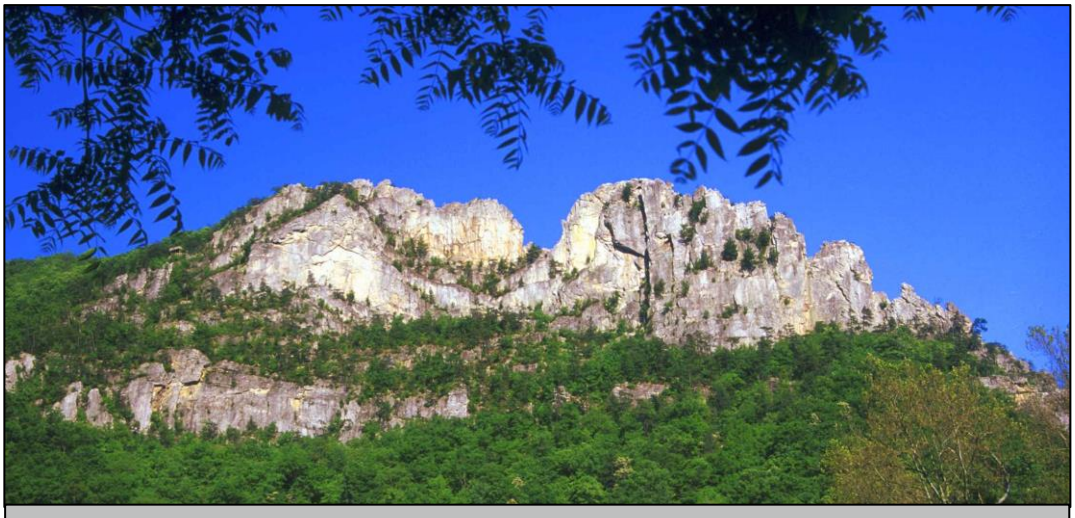
A high-quality subsurface exploration program is the basis for every successful geotechnical construction project and maintaining a reliable and skilled workforce of subsurface exploration professionals is key to gathering the data needed to accomplish this goal. However, consultants and owners in the public and private sectors are facing increasing challenges with hiring and keeping experienced staff for subsurface exploration operations. This panel discussion will address these challenges, with panelists discussing industry trends, pain points, and creative solutions to sustaining this critical workforce. The panel will discuss exploration drilling as well as alternatives like CPT and geophysics and MWD.

Time	Topic	Discussion Lead/presenter
1:00-1:05	Welcome and housekeeping	Krystle Pelham - NHDOT
1:05-1:10	Panel participant introductions	Krystle Pelham - NHDOT
Presentations		
1:10-1:25	*State DOT (discuss structure, drill crews, experience level and requirements for classification by staff geologist and drillers, status of implement new technology, retention and upward mobility, challenges/advantages of maintaining in-house drill crew versus using consultants)*	Kyle Halverson, KDOT
1:25-1:40		Chelsey Brummer, MnDOT
1:40-2:10	*Federal agency (structure, drill crews, experience level and requirements for classification and drillers, implement new technology, retention and upward mobility)*	Jason Wagner or Marty Goff, USACE
2:10-2:30	*Geotechnical drilling contractor (how they train, retain, incentives, provide opportunity for growth)*	Terracon - Tim Cleary
2:30-2:50	*CPT contractor (how they train, retain, incentives, provide opportunity for growth)*	Conetec – Ethan Cargill
2:50-3:10	*Engineering consultant (Procurement of drillers and challenges with quality deliverables)*	HNTB - John Szturo
3:10 - 3:30	***Break***	
3:30-3:45	*Survey Results – Summary of State DOT Practices*	Krystle Pelham - NHDOT
3:40 – 4:50	*Open Discussion/ Research Needs Discussion opportunities*	Matt Riegel
4:50-5:00	*Closing remarks (summary of information)*	Krystle Pelham - NHDOT

74th Highway Geology Symposium
Special Session - U. S. Geological Survey
Tuesday, August 12, 3:10 – 5:00pm

Improving Availability of Information on Landslide Loss and Effects

Landslides are a damaging, disruptive, and sometimes deadly geologic hazard that greatly affect transportation networks in our country. All 225 named roads in the US Interstate highway system are exposed to some level of landslide susceptibility. Sixty-four percent of the total length of these highways are in areas susceptible to landslides. In accordance with the National Strategy for Landslide Loss Reduction, the USGS has created a nationwide compilation of existing, publicly available landslide inventories and is preparing a preliminary data compilation of landslide damage and loss reports in the United States. These preliminary damage and loss data from landslides are heavily biased towards federal data, however much of the costs are borne at the state and local levels. By working together across levels and sectors of government, we can improve our understanding of how much landslides are costing the nation and better prioritize mitigation and preparedness activities. The session will include presentations on the current state of landslide damage accounting and facilitated discussion of how to improve availability and consistency of these data at the national, state, and county levels.

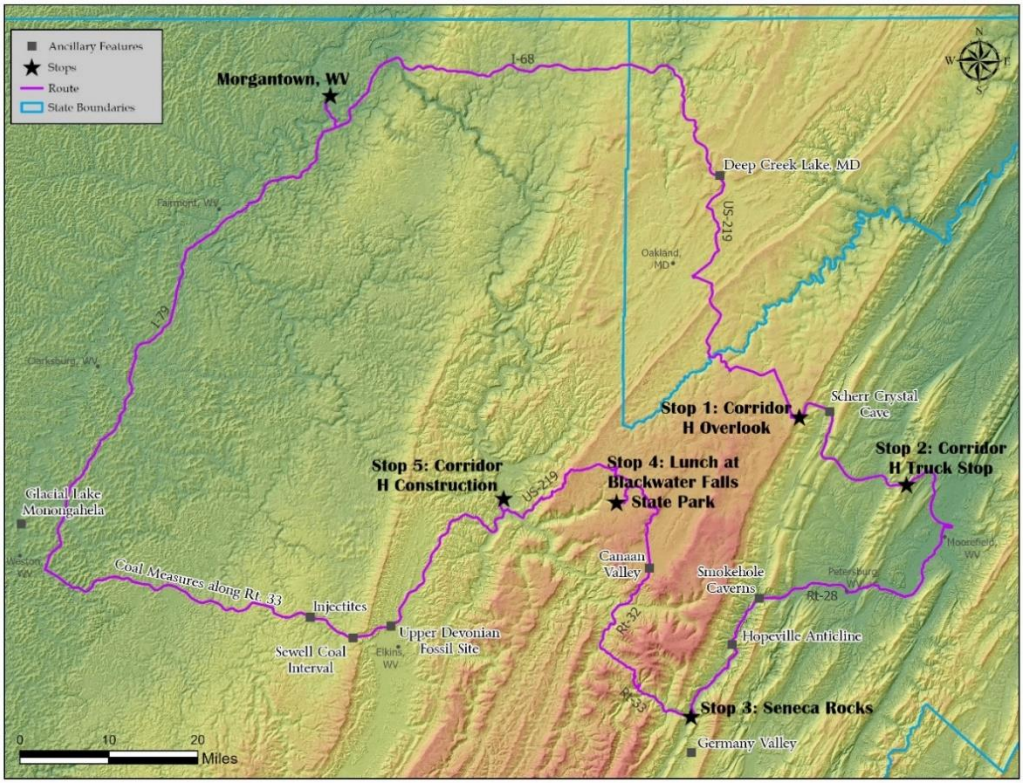


Seneca Rocks – Tuscarora Sandstone

74th Highway Geology Symposium

Field Trip Schedule

Thursday August 14, 2025



Depart	Morgantown Marriott Hotel	7:00 AM	
Stop 1	US 48 Overlook	arrive 8:45 AM	depart 9:15 AM
Stop 2	US 48 Truck stop	arrive 9:35 AM	depart 10:15 AM
Stop 3	Seneca Rocks	arrive 11:15 AM	depart 11:30 AM
Stop 4	Lunch, Blackwater Falls	arrive 12:30 PM	depart 2:00 PM
Stop 5.1	US 48 Cheat Bridge overlook	arrive 2:40 PM	depart 3:10 PM
Stop 5.2	US 48 Cut 29	arrive 3:40 PM	depart 4:40 PM
Arrive	Morgantown Mariott Hotel	6:30 PM	

SPONSORS

The 2025 Highway Geology Symposium extends a huge “Thank You” to the sponsors for their contributions. The Symposium wouldn’t be possible without their generous support!

Platinum Level Sponsors

Geobrugg

Tim Shevlin
E: tim.shevlin@geobrugg.com
P: 503-423-7258
https://www.geobrugg.com/

Field Trip Lunch

True to this guiding principle, we have been developing and manufacturing protection solutions since 1951. High-tensile steel wire nets and matching services monitor and protect against natural hazards such as rockfall, landslides, debris flows, avalanches or coastal erosion. They ensure safety in mining and tunneling as well as on motor sports tracks, in industry and in test facilities. With experience, a spirit of research, continuous internal training and close cooperation with research institutes, we drive innovation and industry standards.

GeoStabilization International

Paige Barnett
E: paige.barnett@gsi.us
P: 855-579-0536
https://www.geostabilization.com

Ice Breaker Reception

GeoStabilization International® and Access Limited provide innovative geohazard mitigation solutions, specializing in landslide repair, rockfall mitigation, slope stabilization, and difficult access projects with cutting-edge technology and emergency response capabilities.

Platinum Level Sponsors

Maccaferri, Inc.

Mike Koutsourais
E: m.koutsourais@maccaferri.com
P: 301-641-8072
https://www.maccaferri.com

Field Trip Transportation

Maccaferri is a worldwide leader in the supply of rockfall protection and geohazard mitigation systems. We offer a wide range of solutions to stabilize rock faces, soil slopes and snow masses, reducing risks to people and infrastructure. Maccaferri's wide variety of engineered systems provide the highest level of performance in the industry. Product offerings include SteelGrid and RockMesh drapery systems, High Energy Absorption (HEA) cable nets, Rockfall Barriers, Embankments and Attenuators, Debris Flow Barriers, and Avalanche Protection. Maccaferri's design software suite includes MacRO software for simple and pinned draperies and Mac S-Design for surface strengthening in soil nailing applications.

Silver Level Sponsors

Ameritech Slope Constructors

Erik Rorem
E: erorem@ameritech.pro
P: 505-690-7144
https://www.ameritech.pro

Field Trip Snacks & Beverage

Ameritech Slope Constructors, Inc. is a geohazard mitigation contractor providing rockfall and debris flow mitigation, anchor drilling and mesh installation, shotcrete application and related rope access services for stabilizing soil and rock slopes. Safely, correctly, and on time. Your geohazard specialists.

Silver Level Sponsors

GFT

Matthew Morris
E: mmorris@gftinc.com
P: 412-503-4938
https://www.gftinc.com

GFT is a recognized leader in geotechnical and geological engineering. We provide consultation for dams, deep foundations, ground improvement, geohazard mitigation, and risk management, offering innovative solutions to safeguard infrastructure and communities. Our team of geoprofessionals specializes in landslide stabilization, rockfall mitigation, debris flow management, and seismic hazard evaluation. Using cutting-edge technology, including LiDAR, remote sensing, and predictive modeling, we assess and address complex geotechnical challenges for transportation, water, energy, and public sector clients. With decades of experience, we develop customized, cost-effective strategies to enhance resilience and protect critical assets from natural hazards, ensuring safety, sustainability, and long-term performance in diverse and challenging environments.

Bronze Level Sponsors

Central Mine Equipment Company

Therrell Hannah
E: hannah@cmeco.com
P: 800-325-8827
https://cmeco.com/

Tuesday Morning Break

CME manufactures auger, core and rotary drilling rigs mounted on trucks, skids, tracks, and rubber-tire all-terrain carriers. We also manufacture hollow stem augers, conventional flight augers, sampling and drilling tools to support our machines.

Bronze Level Sponsors

Fragmentation Efficiency Services, Inc. and KESCO Inc.

Daniel Conn
E: dconn@kesco-fes.com
P: 724-548-2811
https://www.fesconsult.com

Field Trip Breakfast

Designing precise, innovative, and safe explosive engineering solutions that address complex geological environments. we actively partner with leading contractors, engineering firms, state, and federal agencies.

Hager-Richter Geoscience, Inc.

Jeffrey Reid
E: jeff.reid@hager-richter.com
P: 603-893-9944
https://www.hager-richter.com

Tuesday Afternoon Break

HAGER-RICHTER GEOSCIENCE, INC. (HRGS) is an established small business that specializes in surface and borehole geophysics services for engineering and environmental applications (NAICS 541360). The firm has been in business since 1984, has grown to be one of the largest full service geophysical specialty firms in the eastern United States, and has earned a national reputation for quality geophysical services. HRGS has fully staffed and equipped offices in Derry, New Hampshire and Fords, New Jersey, allowing rapid response to projects anywhere in the eastern United States. HRGS specializes in surface and borehole geophysical services for environmental and engineering projects, geotechnical support services, subsurface utility engineering services (designation and mapping), and non-destructive testing services. Routine geophysical services include ground penetrating radar (GPR), electromagnetic induction (EM31 and EM61), magnetics, seismic refraction/reflection, VLF, high resolution borehole geophysical logging (ATV, OTV, HPFM, and conventional logs), and others. The firm owns the equipment it normally uses so that it does not rely on the rental schedules of others.

Bronze Level Sponsors

Jean Lutz North America
Michel Lariau
E: michel@jeanlutzna.com
P: 330-702-1476
https://www.jeanlutzna.com

Manufacture, sales and service of advanced instrumentation applied to deep foundations and Geotechnical Construction.

TabLogs
Declan Vanderhor
E: declan@tablogs.com.au
P: 818-699-3424

TabLogs makes geotechnical investigations simple. As a company founded by a geotechnical engineer, we understand the pain points of the people on the ground. We also understand what is needed to ensure client satisfaction, meaning we're always open to making enhancements to our software. It's our dedication and willingness to listen to our users that has helped us become one of the most trusted tools used by geotechs, drillers, environmental consultants and more - right across the globe.

Voss Signs
Tom Tenerovicz
E: tom@vosssigns.com
P: 315-682-6418
https://vosssigns.com/
Since 1965, Voss Signs, LLC has produced custom and stock signs for various customers that include: Forestry Professionals, Land Owners, State and Federal Government Agencies.

Contributing Sponsor

Scarptec, Inc.

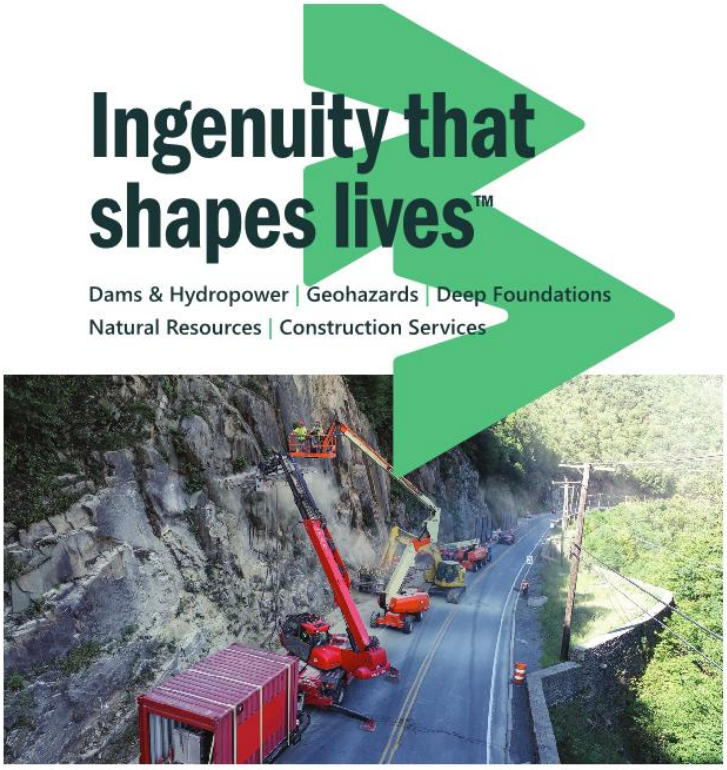
Peter Ingraham
Email: peter@scarptec.com
www.scarptec.com/

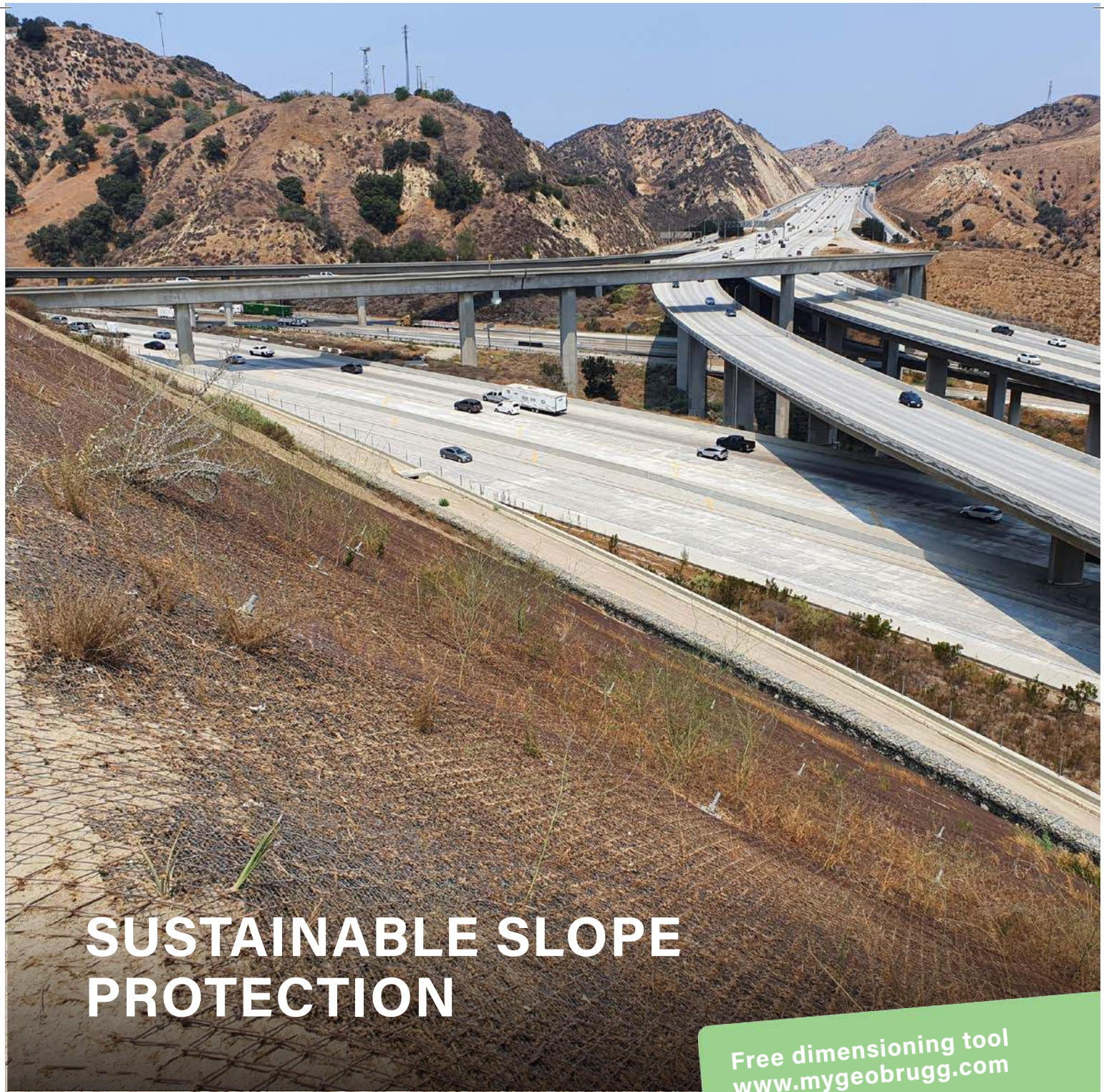
Field Trip Beer

The 74th HGS greatly appreciates the support from this year's sponsors!



Triangle Rock –
Oriskany Sandstone





SUSTAINABLE SLOPE PROTECTION

Free dimensioning tool
www.mygeobrugg.com

TECCO® System made of high-tensile steel mesh

Your local Geobrugg specialist:
www.geobrugg.com/contacts

BRUGG
Geobrugg

Safety is our nature

GSI
GeoStabilization International®

ACCESS LIMITED



Rapid Stabilization Response
Specialty In-House Engineering & Project Management



OUR SERVICES

- ✓ Slope Stabilization
- ✓ Roadway Failure Repair
- ✓ Rockfall Mitigation
- ✓ Retaining Wall Repair
- ✓ Debris Removal
- ✓ River & Stream Channel Restoration
- ✓ Difficult Access Drilling
- ✓ Slope Excavation & Scaling
- ✓ Micropiles



www.geostabilization.com
855.905.2460

www.accesslimited.com
805.590.8510



Enhanced Protection

New Debris flow barriers to mitigate risks and safeguard communities





Maccaferri's debris flow barriers offer reliable protection against destructive debris flows. Designed to contain and slow debris, they help mitigate shallow landslides and protect critical infrastructure. With advanced energy-absorbing systems and certified performance, our barriers ensure long-lasting resilience and effective risk mitigation in high-risk areas.

FIND OUT MORE

maccaferri.com/us/rockfall

The images represented are merely for illustrative purposes and are not to be considered as technical prescriptions or instruct ions of the products herein

MACCAFERRI

Exhibitors

Acker Drill Co., Inc.

Lang Lang
E: jlang@ackerdrill.com
P: 570-575-9163
https://www.ackerdrill.com

Acker Drill Company was founded in 1916 and has been exporting its products worldwide since 1960. Today, we are recognized as a world leader in the manufacture of drill rigs and tooling for the geotechnical, environmental, mineral exploration, mining, and civil engineering industries.

Aero Aggregates

Theresa Loux
E: tloux@aeroaggregates.com
P: 610-447-8900
https://www.aerofga.com/

Aero Aggregates of North America is a manufacturer of Foamed Glass Aggregate - An Ultra-Lightweight fill material made from recycled glass that is durable, sustainable, insulating and free draining, with a low unit weight (<15 pcf) and a high friction angle. Common applications include embankment fill, retaining wall or embankment backfill, and fill over or around utilities or structures.

Collier Geophysics LLC

Jorgen Bergstrom
E: jbergstrom@colliergeophysics.com
P: 943-300-9009
https://colliergeophysics.com

Collier Geophysics is a service-disabled, veteran-owned, small business founded in 2018 with offices in Texas, California, Colorado, Georgia, Massachusetts, North Carolina, Oklahoma, Tennessee, and Wisconsin. We offer a full spectrum of expert surface, borehole, airborne, and marine geophysical solutions for today's needs throughout the U.S. and around the globe. If you have problems or challenges, let us bring you solutions.

Exhibitors

Delve Underground

Allison Halvorson
E: halvorson@delveunderground.com
P: 925-300-5774
https://www.delveunderground.com

Delve Underground is a leader in heavy civil engineering, serving the transportation, water, wastewater, and energy industries. Our team of highly skilled engineering geologists and geotechnical engineers specialize in the characterization and mitigation of a wide variety or geological hazards. Our teams of geoprofessionals are well versed in evaluating complex hazards impacting civil facilities including highways, pipelines, hydropower facilities, dams, and civil structures. Founded in 1954, as Jacobs Associates, Delve Underground is an employee-owned firm with 25 offices and 350 team members throughout the United States, Canada, Australia, and New Zealand.

GEOKON

Siara Dunham
E: marketing@geokon.com
P: 603-448-1562
https://www.geokon.com/

GEOKON, a 100% employee-owned company located in Lebanon, New Hampshire, USA, operates on a worldwide basis through a network of agencies. GEOKON was founded in 1979 by Barrie Sellers and currently has more than 160 employees. GEOKON is a recognized world leader in the manufacture of geotechnical and structural instrumentation due to our quality, responsive customer service and industry-leading designs. Our broad range of geotechnical instrumentation is manufactured at our factory in the USA, by a staff of trained, qualified and experienced machinists and assemblers. In particular, GEOKON, through innovation and experience, has developed a line of vibrating wire sensors unsurpassed anywhere in the world. These highly reliable devices have contributed in no small way to the growing worldwide acceptance of vibrating wire as the most suitable technology for geotechnical applications.

Exhibitors

Geoprobe Systems®

Lori Christensen
E: chril@geoprobe.com
P: 785-404-1160
https://geoprobe.com

Geoprobe Systems® engineers and manufactures drill rigs and tooling focused on making field work simplified by drilling faster, easier, and safer. Our innovative drill rigs employ multiple drilling methods including direct push, augers, air and mud rotary, and rotary sonic. Our rigs can be found on environmental, geotechnical, exploration, geothermal, water well, cathodic protection, and construction job sites worldwide. Developing products focused on making fieldwork simplified includes designing and manufacturing in-situ soil measurement tools for soil lithology and contamination mapping.

Gilson Company Inc

Abbi Smith
E: asmith@gilsonco.com
P: 740-548-7298
https://www.globalgilson.com/

For over 85 years, Gilson has been committed to providing safe, rugged, efficient materials testing equipment that delivers accurate and reliable results. We offer one of the largest selections of equipment for concrete, asphalt, aggregates, and soils in addition to our core products. We regularly update and expand our inventory to meet customer needs and industry demands, and we continue to establish ourselves as a worldwide authority and trusted source for quality equipment.

Hayes Drilling, Inc.

M Luke Schuler
E: lschuler@hayesdrillinginc.com
P: 816-918-7553
https://www.hayesdrillinginc.com

In 1958, Hayes Drilling was founded with a goal to become the premier provider of drilled shaft services in the Midwest. Early on our company established a reputation for quality, dependability and integrity. Today we continue to uphold that reputation with an expanded line of services which includes drilled shafts, design-build excavation support systems, micropiles, soil/rock nailing, permanent rock/soil anchors and secant piles. For over sixty-five

Exhibitors

years, our services have been utilized on significant construction projects in the commercial building, highway/bridge, industrial and power/transmission markets. Geographically, we continue to expand and are currently registered and licensed to perform work in over twenty states. Our corporate headquarters located in Olathe, Kansas is a recently constructed state of the art office and maintenance facility which allows us to service the Midwest region. Our branch office in Georgetown, Kentucky enables us to effectively service the Ohio Valley and Southeast region.The strength of our company continues to be our people. The staff at Hayes Drilling includes highly experienced engineers, project managers and field personnel. This experience combined with a large modern equipment fleet allows us to manage, staff, and equip each of our construction projects ensuring the highest quality of service performed in a safe working environment.States of Operation: KS, MO, OK, AR, CO, NE, IA, IL, KY, TN, IN, OH, WV, MN, TX, WI, AL, MS, NC.

Infinite Engineering, LLC

Tom Pochatko
E: tpochatko@infinite.engineer
P: 724-487-4770
https://www.infinite.engineer

INFINITE ENGINEERING's vision was founded in the pursuit of providing Contractors with specialized, multi-faceted Geotechnical Solutions, providing a wide array of Construction Engineering Services and all types of Surveying. Infinite Engineering provides personal service, and incorporates unique, innovative solutions that are tailored to our Contractors' individual specific needs and resources.

KANE GeoTech, Inc.

Joseph McElhany
E: joey.mcelhany@kanegeotech.com
P: 209-472-1822
https://www.kanegeotech.com

America's Leader in Geohazard Engineering - KANE GeoTech, Inc. specializes in difficult civil and geotechnical engineering problems. Our services include rockfall, debris flow and shallow landslide mitigation, as well as geotechnical instrumentation, and geotechnical analysis and design. We build partnerships with our clients and affiliates, taking time to learn project needs and how we can deliver the best solutions, most effective products and fastest service.

Exhibitors

RE-MONITOR

Tony Simmonds
E: t.simmonds@re-monitor.com
P: 603 443 3626
https://www.re-monitor.com

RE-MONITOR, established in the United States as a subsidiary of NHAZCA S.r.l., brings state-of-the-art monitoring solutions to the North American market. Our core mission is to transform remote sensing practices by integrating advanced technologies, including Satellite and Terrestrial InSAR, and our proprietary Photomonitoring system, to address the growing need for reliable, scalable, and effective monitoring.

Schnabel Engineering, LLC

Brian Banks
E: BBanks@schnabel-eng.com
P: 240-832-6272
https://schnabel-eng.com

In continuous operation since 1956, Schnabel Engineering is a leading national provider of geotechnical, dam, and tunnel engineering services. Specialized services include geotechnical and geostructural engineering as well as dam and tunnel engineering, environmental, geophysical, and geosciences services, construction monitoring, and resident engineering. Schnabel's multi-disciplinary staff of 600+ professionals include geotechnical, geostructural, dam, mining, tunnel, and civil engineers; hydrogeologists; hydrologists; geophysicists and geologists; wetlands specialists; vibration analysts; construction inspectors; and grouting specialists.

SIMCO Drilling Equipment

Ryan Gross
E: rgross@simcodrill.com
P: 800-338-9925
https://www.SIMCODRILL.com

SIMCO manufactures top head hydraulic drilling rigs in the USA for water well drilling, geotechnical and environmental drilling, mineral exploration, geothermal drilling, construction and utility work and a wide range of other diverse applications.

Exhibitors

Solmax

Kooi Kooi
E: mkooi@solmax.com
P: 404-840-8185
https://www.solmax.com
Solmax is the world-leading manufacturer of geomembranes, geotextiles, geonets, geosynthetic clay liners, geogrids and GEOTUBE marine and dewatering.

Trumer Schutzbauten Americas

Ahren Bichler
E: a.bichler@trumer.cc
P: 604-732-0325
https://www.trumer.cc

TRUMER is a world leader in the design and manufacturing of geohazard mitigation structures that protect against rockfall, debris flow, avalanche and unstable slopes.

Williams Form Engineering Corp.

Austin Stephenson
E: AStephenson@williamsform.com
P: 770-949-8300
https:www.williamsform.com/

Williams Form Engineering Corporation has been providing threaded steel bars and accessories for rock, soil and concrete anchors, post-tensioning systems, and concrete forming hardware systems in the construction industry for over 100 years. Our rock and soil anchor product line includes our Spin-Lock mechanical rock anchors, polyester resin anchors, multiple corrosion protection anchors, soil nails, strand anchors, mechanical soil anchors, Geo-Drill Hollow-Bar anchors, and micropiles. For concrete anchoring we offer Spin-Lock anchors, undercut anchors, reusable anchors and cast-in-place anchors. We also have a full line of All-Thread Rebar for tiebacks, micropiles and post-tensioning.

74th Highway Geology Symposium

August 11 – 14, 2025
Morgantown, West Virginia

TECHNICAL SESSION SCHEDULE
Tuesday, August 12

8:00 AM -8:20 AM	Welcome and Opening Remarks	Ken Ashton Jessica Moore, State Geologist	WVGES
8:20 AM - 9:00 AM	Geology of West Virginia	Phil Dinterman, Deputy Director	WVGES
Technical Session 1 - Young Authors			
9:00 AM - 9:20 AM Young Author	The Rockslides of Riggins, ID: A Review of the Road Blocking Events, Rockfall Hazards, and Slope Mitigations Along a 22-Mile Stretch of US-95 between 2020 and 2025	Ethan Guzek & James Struthers	Delve Underground
9:20 AM-9:40 AM Young Author	Geology of the Big Fill Landslide, Teton County, Wyoming	Lief Swanbom	Wyoming Dept. of Transportation, Geology Department
9:40 AM-10:00 AM Young Author	Evaluating the Role of Geology, Hydrology, and Construction Practices in West Virginia Flood-Induced Landslides	Cole Schmidt	GSI
10:00 AM-10:30 AM	**BREAK**		
Technical Session 2			
10:30 AM-10:50 AM Young Author	Monitoring and Mitigation Strategies for Unstable Slopes, a Tennessee Case Study	Sebastion W. Dirringer, Darren Beckstrand, Robert Jowers	Cornforth Consultants, Inc, Landslide Technologies, TDOT
10:50 AM-11:10 AM Young Author	Measuring from a Distance, Teton Pass Remote Sensing Technology	Hunter Hinckley	Wyoming Department of Transportation, Geology Department
11:10 AM-11:30 AM Young Author	Prospective Geohazard Management: The NMDOT District 2 Rockfall Study	Begum Kurtoglu, et al.	WSP USA Inc.
11:30 AM-11:50 AM Young Author	Use of Artificial Intelligence for Identification of Embankment Failures on a Network Level	Aliena Debelak, et al.	WSP
11:50 AM-1:00 PM	**LUNCH**		

74th Highway Geology Symposium
August 11 – 14, 2025
Morgantown, West Virginia

TECHNICAL SESSION SCHEDULE
Tuesday, August 12

Technical Session 3			
1:00-1:20 Young Author	Rockfall Mitigation and Slope Stability Solutions for Interstate 78 in Bethlehem, New Jersey	Christina Comuso, Brian Felber	New Jersey DOT, HNTB Corporation
1:20-1:40	On The Geotechnical Design Considerations and Solutions of the I-80 North Fork Bridges Project	Edward H Barefield & John D. Lasko	Michael Baker International
1:40-2:00	Engineering Judgement, Managing Risk, and the Use of Software	Roch S. V. Player	Braun Intertec Corporation
2:00-2:20	Design Considerations for Consolidation Grouting of the Eisenhower Tunnel	Adam Bedel, et al.	Stantec Consulting, Colorado Department of Transportation
2:20-2:40	River Road in Wilmington, NC - A Study of Small Failures	Nick Moore & Alexandria Jones	North Carolina DOT
2:40-3:10	**BREAK**		
Technical Session 4 – Special Session Improving Availability of Information on Landslide Loss and Effects			
3:10-3:50	Landslide Loss Reporting at the National and State Scale	Aleeza Wilkins, Sarah Hall	U S Geological Survey
3:50-4:10	Discussion 1 – Current landslide loss documentation efforts		
4:10- 4:30	Discussion 2- Future opportunities for landslide loss documentation efforts		
4:30 - 5:00	Group discussion and final wrap-up activity		



74th Highway Geology Symposium
August 11 – 14, 2025
Morgantown, West Virginia

TECHNICAL SESSION SCHEDULE
Wednesday, August 13

Technical Session 5			
8:00-8:20	New Baltimore Landslide Remediation - Lessons Learned	Ala Hajdarwish and Suresh Gutta	A.G.E.S., Inc.
8:20-8:40	Proactive Slope Design: Mechanical Stabilization of Cut Slopes to Reduce Impacts of Landslides and Excavation Footprints	Bryan Radabaugh	Geostabilization International
8:40-9:00	Engineering Geology and Field Fit Solutions for Emergency Landslide Response to SH-64, Kamiah, ID	Shaun Cordes and Jim Struthers	Delve Underground
9:00-9:20	Performance of Micropiles Socketed into Schist Saprolite	Sarah McInnes, et al.	Pennsylvania Department of Transportation
9:20-9:40	The Influence of Particle Shape and Surface Roughness on the Friction Angle of Quartz Sands	Gary Norris	University of Nevada Reno
9:40-10:00	Blasting Design that Ensures Back Slope Stability	Daniel B Conn	Fragmentation Efficiency Services, Inc.
10:00 - 10:30	**BREAK**		
Technical Session 6			
10:30-10:50	Paw Paw Slope Stabilization-Chesapeake & Ohio Canal National Historical Park	Nicholas Strater, et al.	Brierly Associates
10:50-11:10	ATTERRO: A New Design Tool for Rockfall Attenuator Performance	Tim Shevlin and Remo Dudler	Geobrugg
11:10-11:30	Optical and Acoustic Televiewer Logging in Competent and Unstable Rock	Jorgen Bergstrom	Collier Geophysics
11:30-11:50	Integrated Approaches to Landslide Monitoring and Interpretation: Remote Sensing, Field Investigations, and Geomorphic Terrain Analysis in Yellowstone National Park, Montana and Wyoming	Kris Hornsby, et al.	BGC Engineering & Western Federal Lands Highway Division
11:50 - 1:10	**LUNCH**		

74th Highway Geology Symposium
August 11 – 14, 2025
Morgantown, West Virginia

TECHNICAL SESSION SCHEDULE

Wednesday, August 13

Technical Session 7			
1:10-1:30	Engineering Assessment of Field Data from A Unique Drive Point Method	Paritosh Chataut, et al.	Department of Civil and Architectural Engineering, University of Wyoming
1:30-1:50	Enhancing Risk Management in Transportation Geotechnics Through Standardized Data Collection	Declan Vanderhor	Tablogs
1:50-2:10	Subsidence and Sinkhole Geohazard Investigations using Geophysical Methods	Stan Smith	Collier Geophysics
2:10-2:30	Slip Stick: A Low Cost Solution for Shallow Landslide Monitoring in Remote and Difficult-to-Access Terrain	Brett Dougan and Michael Hogue	Pillar Innovations
2:30-3:00	**BREAK**		
Technical Session 8			
3:00-3:20	Geohazard Decision Support: Leveraging AI and Satellite Data for Infrastructure Resilience	Randy Post and Winston Wade	WSP USA Inc.
3:20-3:40	Open Roads, Open Bridge, Open...Frog? Imagining the 3D World of Geological Design with Bentley's latest 3D Subsurface Modeling Tool	D. Crotsley and W.Brandenberger	HDR Engineering
3:40-4:00	Highway Geology and Paleontology and Their Importance to Understanding Earth's History	E. Ray Garton	WVGES Museum
4:00-4:20	Field Trip Preview	Wayne Perkins	WV Geological Survey

The Rockslides of Riggins, ID: A Review of the Road-Blocking Events, Rockfall Hazards, and Slope Mitigations Along a 22-Mile Stretch of US-95 between 2020 and 2025

Ethan Guzek (LEG)
Delve Underground
1011 Western Ave #706
Seattle, WA 98104
425-647-7476
guzek@delveunderground.com

James Struthers (LEG)
Delve Underground
1011 Western Ave #706
Seattle, WA 98104
360-791-2847
struthers@delveunderground.com

Shaun Cordes (LEG)
Delve Underground
2000 SW 1st Ave #410
Portland, OR 97201
971-415-5607
cordes@delveunderground.com

Prepared for the 74th Highway Geology Symposium, August, 2025

Acknowledgments

We would like to thank Idaho Transportation Department for the opportunity to work on the projects discussed in this report. It has been an honor to contribute toward the mitigation and management of rock slope hazards in the subject travel corridor. We also thank William CB Gates for all his guidance and leadership over the years.

Disclaimer

Statements and views presented in this paper are strictly those of the authors, and do not necessarily reflect positions held by their affiliations, the Highway Geology Symposium (HGS), or others acknowledged above. The mention of trade names for commercial products does not imply the approval or endorsement of HGS.

Copyright Notice

Copyright © 2025 Highway Geology Symposium (HGS)

All Rights Reserved. Printed in the United States of America. No part of the publication may be reproduced or copied in any form or by any means – graphic, electronic, or mechanical, including photocopying, taping, or information storage, and retrieval system – without prior written permission of the HGS. This excludes the original author(s).

ABSTRACT

US-95 is the sole north-south route in Idaho, serving as a major economic connector for the state. Located at the center of this route is the highway town of Riggins, ID, a hub for outdoor tourism and home to an impressive concentration of rockfall and rockslide problems.

The canyons bounding US-95 in this region are some of the steepest in the state. Steep roadcuts, complex accreted geology, adverse persistent geologic structure, and narrow roadway geometry set the stage for the rockslides that have blocked the route over the past five years within a particularly hazardous 22-mile stretch of US-95.

Between 2020 and 2025, Delve Underground has been retained by ITD to provide services inclusive of reconnaissance and scoping, design, slope monitoring, exploration, blasting consultation, and slope construction management across five major slopes in this 22-mile stretch.

This paper explores how variations in geology and the activity of rockfall and slope movement have dictated mitigation timelines and different mitigation strategies for the subject slopes located between US-95 Mileposts 188 and 210. This paper also explores how rope-access techniques, remote sensing, and field engineering have allowed our team to be successful in the design, planning, and construction phases of work, despite the challenges related to complex localized geology and difficult access terrain at these sites. Highlighted projects include the MP 188 Emergency Rockslide Response, MP 189 Slope Monitoring, and the recent MP 196 Slope Stabilization Construction. Also discussed are the MP 191 Mousetrap Slope Reconnaissance and MP 210 Landslide Study projects.

INTRODUCTION

For someone local to Riggins, ID, it is not uncommon to pull off of US-95 and kick a few rocks off the road before getting back in their car and resuming travel. For anyone who visits, this may not be entirely surprising on account of the dramatic canyon walls and tight winding highway that contour along the Salmon and Little Salmon Rivers. This has been a challenging route since its inception and today, Idaho Transportation Department (ITD) is in the position of improving ease of travel along a road that has been home to many nicknames. Names such as "The Road of No Return" or "Landslide Alley", with individual slopes acting as characters such as "Bull's Eye" and "Mouse Trap", all aptly named for some sort of event or looming slope hazard. The impressive rockfall problems and unstable slopes along this corridor may contribute to the reasons this route was originally surrounded by controversy and elusive funding, but yet, it now serves as one of the most important economic routes in the state.

US-95 is the sole north-south route in Idaho, connecting major cities and economic hubs along the western margin of the state. This route was not possible until the completion of the arduous section of highway between New Meadows and Grangeville (with Riggins at the center) in the early 1920's. Steep terrain and highly complex geology set the stage for this great achievement and ongoing effort (Figure 1).

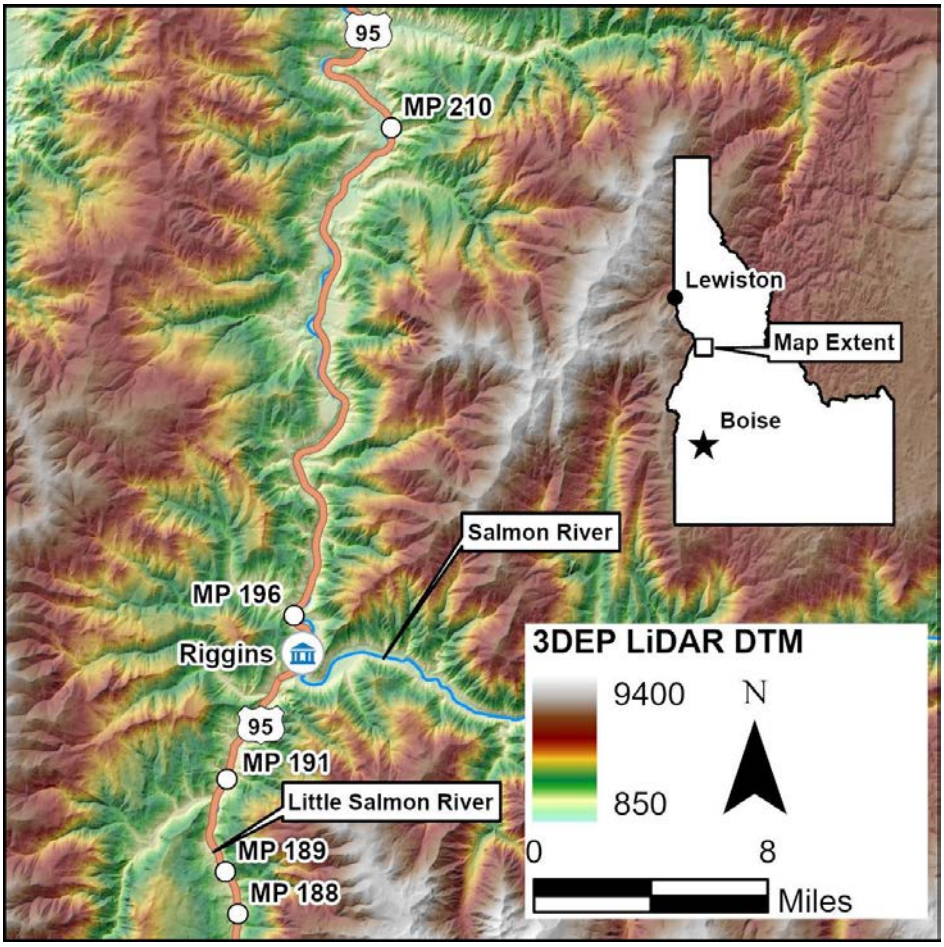


Figure 1 – Corridor Map

Riggins, ID, sits between the two deepest river gorges in North America with the Snake River cutting Columbia River basalts to the west and the Salmon River cutting the granitic Idaho batholiths and accreted terranes to the east (Figure 2). Between these two regions, at the center of our subject corridor, lies accreted island arc terranes that have been subject to multiple episodes of metamorphism, thrust faulting, and rapid regional uplift and fluvial downcutting. In the effort to carve a road through this country, the toe of many slopes had to be cut away, creating typical rock slopes on the order of 200 feet in height. Today, instability related to these large rock cuts includes sporadic to routine rockfall that impacts the roadway, and progressive to sudden rockslides that have proven capable of burying and closing the route.

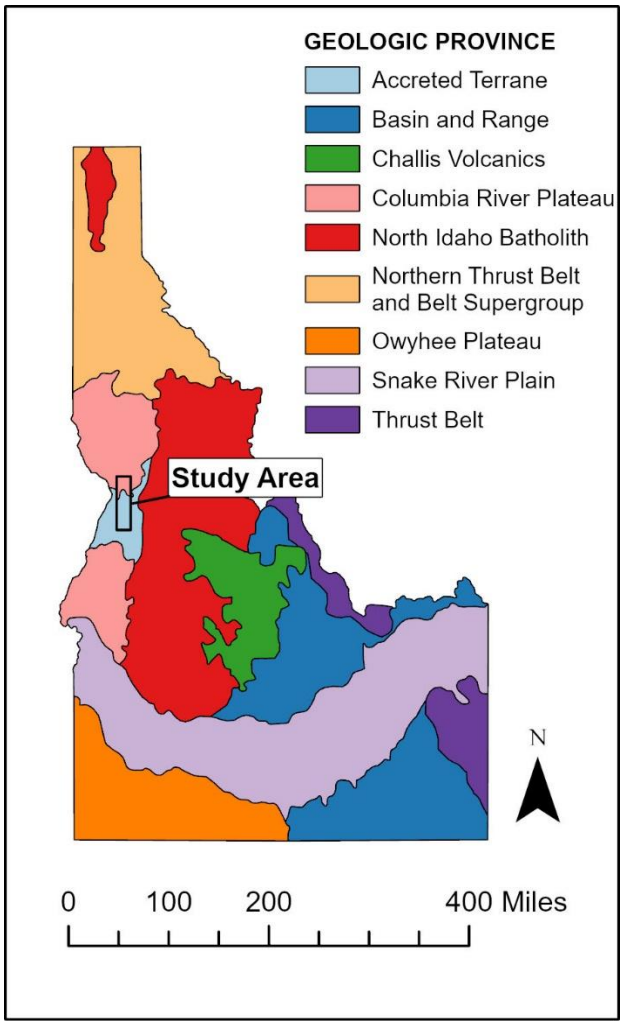


Figure 2 – Geologic Provinces of Idaho (*1*)

Over the past 5 years, Delve Underground engineering geologists have been retained by ITD to assist them in the management, scoping, and mitigation of hazards related to these slopes along an approximate 22-mile section of US-95 centered around Riggins Idaho between Pollock and Slate Creek. While these efforts were initiated by an emergency response to a rock slide near Pollock, efforts since have included reconnaissance and planning, slope monitoring, and construction of designed solutions for the prevention of large rockslides with road blocking

potential. This paper discusses our general approach and lessons learned during recent work on five major rock slopes within this area. Localized variations in geology create unique rock mass settings for each of the five subject slopes, which will be discussed as it relates to the observed instabilities and possible solutions. Additionally, other major constraints and influential factors related to the investigation and response for these slopes are discussed. These include frequency and intensity of any initial rockfall activity, potential for large progressive slope failures, site constraints such as ditch width and road geometry, and long-term roadway planning.

Brief summaries of the US-95 history and local geology are presented below, followed by an overview of the rock slope hazards encountered and solutions implemented (or *being* implemented). Lastly, a brief case study of each slope is presented to highlight unique circumstances encountered during project work.

HISTORY OF US-95

The following summarizes a brief history of US-95 adapted from a 2017 research paper produced by Stevens Historical Research Associates and funded by ITD (*2*).

In 1872, a wagon road was proposed to link the north and south portions of the state along the Little Salmon River. This was approximately 10 years after gold was discovered in the area and pioneering settlement had taken place. Idaho at the time was nearly functioning as two states separated by the 45th parallel, and there was growing motivation to link the two political rivals of Boise and Lewiston by either rail or road, though it was not generally accepted nor prioritized initially.

While Idaho was admitted to the Union in 1890, construction of a wagon road along the Little Salmon River was not authorized until 1893. Between the passing of the State Wagon Roads Act in 1893 and the near-modern roadway finally being completed in the mid 1920's, responsibility of the roadway passed from the Idaho Legislature to the State Highway Commission, and then to the Bureau of Highways in the Department of Public Works. While funding throughout this time was always difficult, funds came from the local, state, and federal levels throughout the process. While a crude wagon road had been established in 1901, it quickly fell into disrepair and some had labeled the effort a failure, but the popularity of the automobile became a key motivator, reinvigorating the effort from 1913 on. Interestingly enough, the route that was once so slow to gain public backing became a high priority during this movement to ready Idaho for the growing popularity of the automobile that was sweeping across the country.

During widening and grading of the roadway in the early 1920s, flooding and rockslides occurred during construction leading to re-work and slowed progress. This did not end with the completion of the road. In the 1940s and 1950s, similar events took out entire segments of the roadway leading to re-building and even re-alignment of the roadway in places. Given the methods, equipment, and technology available at the time, the initial construction of US-95 was an incredible achievement, with similar spirit to that of other American infrastructure projects at the time. With improved technology today, we are better equipped to tackle the complex geologic hazards, now more recognized, that border US-95 and we continue to build on the efforts from those who came before us. Still, this task is not easy, and an old mountaineering saying seems to hold true while performing work in the corridor: "the mountains don't care."

LOCAL GEOLOGY

The project corridor exists within the accreted terrane geologic province of Idaho, a relatively limited zone bordered to the north and south by the Columbia River Plateau, to the west by the Blue Mountains (Oregon), and to the east by North Idaho Batholith (Figure 2). Originally part of an island volcanic arc, the rocks have since been subject to multiple episodes of metamorphism, thrust faulting, and late-stage brittle deformation (*3*). Generally, metamorphic grade increases to the east and south. Further, regional tectonic uplift and rapid downcutting are apparent in the Little Salmon and Salmon River Valleys. During work on these slopes, deposits of stranded alluvium have been encountered during grading activities along the brow of metamorphic outcrops, located hundreds of feet above the present river.

The specific geologic units encountered between Pollock and Slate Creek, located at the respective south and north ends of the study area, are faulted, deformed, and offset by the Rapid River Thrust trending approximately north-south. At the north end of the study area, at the location of MP 210, geologic units are further offset and deformed by the Heavens Gate fault which is located west of the Rapid River Thrust.

The afflicted slopes of MP 210 are comprised of metamorphic rocks associated with the Western Salmon River Belt that include lower greenschist facies of strongly foliated greenstone, phyllite, and marble (*4*). Early mapping identifies the greenstone as part of the Seven Devils Group, and the marble as a part of the Martin Bridge Formation. At this location, the Heavens Gate Fault is positioned mid slope and parallel to US-95 before crossing the highway immediately south of the MP 210 rockslide. Foliation within the slopes at MP 210 dip to the east.

Moving south of MP 210 towards Riggins we move into the overriding Riggins Group which is dominated by the Squaw Creek Schist across the southern four rock slope sites; MP 196, 191, 189, and 188. This unit is composed predominantly of volcanic-sedimentary derived phyllites and schists with varying degrees of foliation apparent in outcrop. Based on site observations, foliation generally dips to the east. Highly persistent and planar joint structure is also present in the four southern rock slope sites discussed in this paper, possibly related to late-stage brittle deformation. These joints have consistently been of significant kinematic influence as it relates to the slope stability of sites across the corridor. In addition to the general metamorphism of the unit, the Squaw Creek Schist is intruded by ultramafic rocks in places such as the MP 188 rock slope. Massive strong blocks of serpentinite dominate the upper 2/3 of the slope at MP 188 and highly persistent, smooth, low-friction joints created conditions for a very large progressive wedge failure. This failure blocked the road in multiple episodes between 2012 and 2020, initiating our story and involvement in the corridor over the past five years.

SLOPE CHARACTERIZATION AND GENERAL MITIGATION STRATEGIES

In managing slope hazards along this corridor, the forefront challenge is to improve slope stability and reduce rockfall risk while keeping the route open. This route has become so critical to the state of Idaho that even 15-minute road closures to support slope work can result in traffic backups measuring multiple miles long, particularly when multiple road projects are happening simultaneously during the dry season. While a typical approach for managing a corridor may involve use of a slope hazard rating system, standard approaches become less useful as the number of high-ranking slopes increase within the corridor. Emphasis on local engineering

geology and an intimate knowledge of how these slopes behave has become critical in assessing the risk, cost, and reward in performing mitigation activities for a particular site. Another key consideration is long-term planning of the corridor inclusive of any potential route modifications. Attempting to reduce rockfall risk for a particular slope can potentially trigger larger global stability issues, increasing project scope, costs, and impacts to the route.

We have found that if not applying a comprehensive slope mitigation scheme, extreme caution must be exercised in scoping project work, especially at locations where realignments are being considered. Relatively small-scale scaling jobs have the potential to turn into expensive ones with little long-term gain. Unfortunately, opportunities for route modifications are limited given the narrow travel corridor between the valley walls and the adjacent rivers. This creates a similar problem in attempting to bypass traffic around slide debris or active hazard zones under emergency response conditions. With respect to long-term planning, construction of material stabilized earth walls along the river are being considered in several locations to allow for higher travel speeds. This would potentially allow for more cost-effective slope hazard reduction at several site locations.

Rockfall throughout the corridor is routine and comes with the territory, given the nearly continuous exposure of outcrops between the roadway and the tops of the adjacent ridgelines. As a society, we have become less tolerant of risk since the original construction of US-95, but there are limitations to quickly reducing rockfall risk to the same level as that achieved along some less hazardous routes. While limited but routine rockfall events related to surficial erosion are pervasive and can be mitigated programmatically, intensive mitigations for well-defined rockslides have been pursued under emergency response and preventative timelines. The management of unstable slopes in this corridor becomes more difficult, when there are numerous sites that produce rockfall on an irregular basis that also correspond to slope features that suggest the potential for global instability. In these cases, slope monitoring can be useful tool for gaining an understanding of slope behavior and informing effective solutions, that can then be incorporated into the transportation department's long-term plan. At the same time, plans must be in place to close the route under emergency conditions, if adverse activity is observed that exceeds risk tolerance thresholds.

To support work related to rockfall incidence response, slope stability assessment, design of mitigation measures, and rockfall construction, it has been critical to maintain a diverse range of investigative tools, design measures, and construction strategies. Discussion, inclusive of insights and lessons learned, is provided below regarding slope work performed in the corridor over the past five years.

In addition to traditional geologic methods related to rock mass characterization, the use of both rope-access techniques and unmanned aerial vehicles (UAVs) has been routine for all types of project work and phases of work. Without one or the other, more assumptions would have to made with respect to mitigation planning on some level. We have found that aerial imagery can even be misleading depending on subtle variations in camera angles and lighting conditions. For any slope reconnaissance specific flight paths are pursued to provide convex (fish-bowl) imagery coverage of the slope for production of 3D point clouds using photogrammetry techniques. The use of aerial imagery and 3D point clouds for conceptual and dimensioning purposes has allowed us to use rope-access methods in a more targeted manner during reconnaissance activities. Rope-access hands-on observation is critical in developing rock

mass parameters for use in design calculations. It is also critical to maintain rope access field personnel to perform field engineering services during construction, as most rock slope mitigations benefit from adjusting and optimizing plans following scaling activities. We have found it very much worth the time we spend annually to train and practice rope maneuvers and rescues, because it has allowed us to perform complicated rope work in emergency response or limited access scenarios. This has included activities such as anchor installation, lead climbing, and extended horizontal aid-climb traverses (Figure 3).



Figure 3 – Horizontal Aid Climbing to Install Telemetered Slope Monitoring Instruments

While scaling to remove loose-detached material is almost always part of slope work, other standard measures such as rock reinforcement (rock dowels) or rockfall mesh (or fence) systems are not always immediately possible. This is often related to rock mass quality or roadway geometry (ditch width), respectively. During any assessment of possible mitigation measures slope-worker safety is considered. Unavoidably, engineering geologists and rockfall contractors have to perform potentially dangerous work to reduce risk along the roadway. While work strategies can be developed to optimize slope-worker safety, sometimes slope conditions are prohibitive and scope must be increased, or alternative strategies must be pursued prior to proceeding with standard rockfall work. Common next steps for these types of situations include blasting, slope monitoring, or route re-alignment if possible. Often, the pursuit of these types of additional measures is in alignment with the overall need of the project or other agency plans for long-term improvement of the corridor

Any blasting performed on these large marginally stable slopes must be highly controlled and performed by experienced blasters. It is key that engineering geologists work with the blaster to target natural weaknesses within the rock; more specifically persistent discontinuities that

bound the slope features and related stability. Access for drilling equipment at the top of a given slope is variable across sites, though substitution of wagon drills in place of larger drill rigs has been successful in some limited-access scenarios. Pursuit of blasting also requires pre-blast surveys be conducted for nearby homes. Additionally, we have discovered that large scheduled blasts require coordination with the local jurisdictions, including law enforcement, to facilitate the management of civilian spectators in effort to secure a safe site.

There are many ways to monitor unstable slopes, but the most important component is to have a good monitoring plan that is followed. Monitoring plans need to have funding for both the establishment of the system and a long-term program as they are not necessarily cheap, though they do not always need to be indefinite either. It is critical to have frequency of readings defined over time, along with thresholds (magnitude and change with time), reporting systems, and specific actions tied to thresholds that include closure of the route. With respect to monitoring, we have implemented simple plastic extensometers using hardware store materials that can be checked using UAVs or rope access. We have installed survey targets on slope for use in conjunction with traditional survey techniques. We have also installed fully telemetered systems inclusive of tilt-meters, extensometers, and automated total stations for the survey of specialized targets. These types of systems have been able to detect movement on such a fine scale that the thermal expansion and cooling of the rock was recorded throughout hot summer days. The ability to receive these readings locally rather than purely by a cell-based or satellite-based system is important for areas of poor connectivity. Nearly live, fine-tuned, readings have allowed us to conduct sensitive work on unstable slopes in a safe manner.

In effort to provide context to the general methods and lessons described above, a brief synopsis is presented for each of the five subject slopes in the following sections. Some of the unique project components are also discussed. Work on some of these sites is ongoing.

MP 188 – 2020 EMERGENCY RESPONSE

In July 2020, on the fourth of July, Delve Underground engineering geologists were contacted and requested to begin mobilizing to MP 188 along US-95 just south of Riggins, ID. Approximately 7,000 cubic yards of material had failed, and debris was blocking both the north and south bound lanes. A team of scalers and engineering geologists inspected the slope using UAV-based methods and rope access techniques and established a crude monitoring system for the slope. Safety scaling was performed to remove fully detached material stranded on the slope and a temporary berm was constructed using slide debris and Connex containers. In addition, a shoofly diversion road was constructed around the toe of the slide debris to let traffic continue to flow. Meanwhile, additional resources were being mobilized to the site to pursue long-term stabilization solutions.

It should be noted that the slope also failed in 2012, blocking the road with a large debris pile. Delve Underground was contracted to provide an emergency response assessment and at the time, progressive failure was not observed following a limited remediation scheme that removed a large, detached mass from the slope by method of blasting.

While a temporary shoofly was constructed around the debris, behind the barrier, slope monitoring remained in effect, and upon further detected movement the route was closed. The movement was detected using crude slope extensometers and was also accompanied by loud

popping noises and loose dry material spraying from underneath the lower-most block at that time. The next day, on July 10th an additional 10,000 cubic yards of material failed, depositing incredibly large blocks onto the roadway as shown in Figure 4.

What remained was a large wedge-shaped mass at the top of the slope. Given the thickness of the block and the documented progression of failure, removal by blasting was the next chosen course of action. Jerry Wallace (Wallace Technical Blasting) was contacted and served as the Blaster-in-Charge to facilitate design of the blasting program. With a fully telemetered monitoring system in place, inclusive of extensometers, tilt-meters, and total station survey points, a highly regimented slope monitoring system was initiated to support drilling for blasting at the top of the slope.



Figure 4 – The July 10th, 2020, Failure at MP 188



Figure 5 – Main Blast to Remove Wedge at MP 188

The cushion line was drilled along the wedge structure at the back of the block, with production holes in the main part of the mass. During this time, traffic was re-routed to the Old Pollock Road located west of the Little Salmon River, which served as the primary alignment before the route was shifted to the east of the river around 1960. The shift of the roadway was coincidentally for the purpose of avoiding landslides on the other side of the valley. The shot successfully removed the remaining rock mass, bringing down an additional 14,000 cubic yards of material (Figure 5). Between the remaining summer months through Thanksgiving of 2020, activities related to post-blast scaling, rock dowel reinforcement, drape mesh, and installation of a rockfall containment fence were performed to provide long term stabilization and rockfall hazard reduction for the site. During this work, a large earth berm was in place to protect traffic from construction related rockfall while passing around the site. This work was completed ahead of schedule and under anticipated budget largely due to effective teaming between ITD, Delve Underground engineering geologists, specialized blasters, and contractors involved in the work.

MP 189 – ONGOING MONITORING FOR POTENTIAL ROCKFALL REDUCTION

In fall 2024, a limited scaling operation, under a contract between ITD and a rockfall contractor, was enacted to reduce rockfall at a location where small-scale rockfall fouled the road several times per month. Approximately one week after the scalers demobilized from the site, a small rockslide occurred which impacted both the north and south -bound lanes. In response to this, ITD contacted Delve Underground to assess the slope for further mitigation recommendations. Upon UAV and rope-based reconnaissance of the site, the slope was discovered to be dilated and shattered nearly from toe to brow, something that was not apparent from the ground or aerial imagery, but characteristic of the Squaw Creek Schist (Figure 6**)**.



Figure 6 – Shattered Squaw Creek Schist at MP 189

During rope-based reconnaissance of the slope it was quickly established that spot or pattern dowel reinforcement would not be a viable option. Despite the foliation of the mass dipping into slope, persistent dilated joints observed throughout the slope suggested that the rockfall at the site could potentially be a symptom of large-scale instability (Figure 7). Though rockfall and large persistent structure were present at the site, it could not be established that a progressive failure was occurring. Because of the shattered texture of the rock mass, installation of simple slope extensometers was not a viable option. To support keeping the route open while further investigative methods were pursued, approximately two weeks of slope observation were employed where direct observers had the ability to close the route by means of a wireless remote system synced with signals positioned to the north and south of the site. During this period, rockfall events were found to be most closely related to poor weather rather than an interval more typical of a progressive rock slope failure.



Figure 7 – Overview of MP 189

To support long-term mitigation at MP 189, routine survey of targets positioned across the slope will be collected to further rule out the potential of a progressive slope failure. If no movement is detected, rockfall management solutions, such as draped mesh, will be considered.

MP 191 – "MOUSE TRAP"

In the spring of 2022 ITD contracted Delve Underground to assess the slope at MP 191. Nicknames at this site include "Mouse Trap", "Tombstone", and "Slab Rock" in reference to the

adverse toppling structure apparent from both the north and south bound lanes of travel. The geology at the site was separated into units based upon the geomechanical and engineering characteristics (Figure 8). At the base of the slope was a schist with foliation oriented sub-horizontally and a lack of persistent joints. Across the middle of the slope existed a more massive rock mass with less developed foliation, though a persistent toppling joint set was present. At the top of the slope was a very platy, jointed rock mass composed of angular blocks on the order of several feet. This upper zone was assessed to be the primary source of rockfall related to sporadic reports of rock in the road near the project site.



Figure 8 – MP 191 Overview

Though an apparent toppling structure was present, photographs of the project site and past reports did not suggest that an ongoing failure was occurring. Based on the fractured rock near the toe of the outer slab, an assessment was made that drilling the outer slab for reinforcement would be too hazardous because of potential for large rockfall on construction crews, and that the marginally stable slope did not warrant immediate action. Though a drape mesh system could have potentially been installed for the upper unit of the slope, it was discovered through further conversation with ITD that the segment of roadway, inclusive of this site, was being considered for realignment to allow for higher travel speeds. Because rockfall hazards at the site were not substantially higher than other areas within the corridor, and the slope did not appear to present an immediate risk to travel, no immediate action was taken. Efforts related to the realignment are currently being pursued, inclusive of public outreach meetings.

MP 196 – "BULL'S EYE"

Delve Underground also was retained in the spring of 2022 to assess a dramatic slope just one mile north of downtown Riggins. Located outboard of a sharp bend in the Salmon River, the slope is dominated by adverse foliation (and possibly bedding), creating a dip-slope condition (Figure 9). The main spine of the rock slope is formed by more massive blocks underlain by highly persistent structure associated with the foliation. Other persistent joints cut this rock mass, inclusive of open release joints that suggest past downslope movement of the mass, likely related to initial construction. Because there is no viable bypass at this location and slope conditions were favorable for rock reinforcement, long term slope stabilization was designed for the site and then constructed in the fall of 2024. The residents of Riggins are no stranger to rocks blocking their roads but at the same time, slope construction results in traffic holds, affecting both the daily operations of the town and regional commerce. This is always a consideration when performing slope work along a major route. During a meeting between ITD, the engineering-contractor team, and the city council, all parties agreed that the effort was worthy, primarily because it would prevent a potential rockslide and a more sustained-unplanned closure of the route.



Figure 9 – MP 196 Overview

During construction, care was taken to avoid unnecessary destabilization of the slope. When marginally stable slopes sit dormant for decades, heavy down-hole hammer drills and the associated vibrations can become the next most likely trigger to cause a rockfall or rockslide. To manage this, the slope was drilled from the top down and grouted as work progressed. In some locations, multiple episodes of scaling and slope reinforcement were phased to further limit the

potential of destabilizing the slope. While the need to sequence reinforcement prolonged the project timeline, it reduced risks related to construction on marginally stable slopes.

Rock slope mitigation at this site was constrained by the virtually non-existent ditch and shoulder along the south bound lane, and Salmon River along the north bound lane. Without a ditch to contain potential rockfall, the general rockfall risk could not be fully mitigated across the site, particularly for the platy rock surrounding the main spine of rock shown in Figure 9. It also created restrictions in executing project work, though sophisticated heavy construction equipment helped maintain project schedule and constructability (Figure 10). While slope stabilization at the site was successful, smaller scale rockfall hazards could only be reduced because solutions were limited to scaling and rock reinforcement on account of available roadway geometry. However, this is another site where more substantial roadway work is being considered to shift the road away from the slope to reduce curvature and increase design speeds. Long-term rockfall management solutions are anticipated to be part of that future roadway work.



Figure 10 – Rock Dowel Installation at MP 196

MP 210 LANDSLIDE

The milepost 210 landslide is located approximately 12.5 miles north of Riggins, Idaho, and is positioned along the eastern margin of the Salmon River Valley (Figure 11). A large failure (approximately 7,000 cy) occurred in 1996 followed by two subsequent failures (7,000 cy and 25,000 cy respectively) in 1997. Unsuccessful efforts to stabilize the slope began in 1998 and were completed in 1999. A post-construction failure in 2000 completely destroyed one of the newly installed rock fall fences, and in 2005 the largest failure to date occurred. The 2005 failures resulted in a 500-foot wide deposit protruding 60 feet out from the slope, with a vertical 70-foot headscarp located at the top of the slide. Total relief of the slide is approximately 400-feet from toe to the crest of the headscarp.



Figure 11 – MP 210 Overview

Delve is currently working with ITD and David Evans and Associates (DEA) on a long-term study to explore feasible mitigation strategies for this slide. In the fall of 2024 baseline UAV and terrestrial LiDAR scanned surveys were performed by DEA. In the spring of 2025, geologic reconnaissance and geotechnical explorations to install slope inclinometers within the slide mass were completed by Delve Underground. Monitoring will likely occur for two years. Although adverse structure has not been ruled out as a driver of instability, this slide does not appear to have originated as the result of persistent joint sets, but rather by the unfortunate geologic conditions that have created a weak, metamorphosed, and highly deformed rock mass.

THE PATH FORWARD

Just as it took years to gain support, funding, and authorization to build US-95, it will take years to address the large, complicated slopes that line the canyon walls above the Salmon and Little Salmon Rivers. A methodical and cautious approach to slope work in this corridor, and the adjacent sections of roadway, is critical for the successful management of numerous unstable slopes. A methodical long-term approach is also critical to the efforts of ITD in securing and allocating funds as part of a comprehensive corridor plan.

By maintaining a comprehensive set of mitigation and monitoring solutions, the route can remain open while slope hazards are reduced over time. Success of projects is not only a product of proper planning, but also of professional execution and teaming between ITD, engineering teams, and heavy civil rockfall contractors. As discussed in this report, work in the corridor is ongoing and we will continue to build on what we have achieved so far, as we face additional challenges in the years to come.

REFERENCES

1. Lifton, Z.M., S. D. Ducar, and C. A. Tate, *Development of a Statewide Landslide Inventory Database for Idaho RP 278.* Report FHWA-ID-20-278. Idaho Transportation Department, 2020.

2. Baldwin A. and J. Stevens. *"Road of No Return" The Story of Travel Through the Little Salmon River Canyon.* Stevens Historical Research Associates, Idaho Transportation Department, 2017.

3. Hamilton, W. *Metamorphism in the Riggins Region Western Idaho.* Geologic Survey Professional Paper 436. United States Department of the Interior, Geological Survey, 1963.

4. Lewis, R.S., et al. *Geologic Map of the Lucile Quadrangle, Idaho County, Idaho.* Idaho Geologic Survey, 2011.

Geology of the Big Fill Landslide, Teton County, Wyoming

Lief Swanbom, P.G.
Wyoming Department of Transportation
Geology Program
5300 Bishop Boulevard
Cheyenne, WY 82009
(307)777-4475
lief.swanbom@wyo.gov

Prepared for the 74th Highway Geology Symposium, August, 2025

Acknowledgments

The author would like to thank the individuals/entities for their contributions in the work described:

James Dahill, P.G. - Wyoming Department of Transportation Geology, Cheyenne, WY
Seth Wittke, P.G. - Wyoming Department of Transportation Geology, Cheyenne, WY
Jeff Booher, P.E. - Wyoming Department of Transportation Geology, Cheyenne, WY
Hunter Hinckley, P.G. - Wyoming Department of Transportation Geology, Cheyenne, WY
Todd Sullivan, P.G. - Wyoming Department of Transportation Geology, Cheyenne, WY
Ben Arndt, P.E. - RJ Engineering, Evergreen, CO
Dr. Bradford Burton, P.G. - Western Colorado University, Gunnison, CO
Dr. James Coogan - Western Colorado University, Gunnison, CO
Alex Branda - Chevron USA, Denver, CO

Disclaimer

Statements and views presented in this paper are strictly those of the authors, and do not necessarily reflect positions held by their affiliations, the Highway Geology Symposium (HGS), or others acknowledged above. The mention of trade names for commercial products does not imply the approval or endorsement of HGS.

Copyright Notice

Copyright © 2025 Highway Geology Symposium (HGS)

All Rights Reserved. Printed in the United States of America. No part of the publication may be reproduced or copied in any form or by any means – graphic, electronic, or mechanical, including photocopying, taping, or information storage, and retrieval system – without prior written permission of the HGS. This excludes the original author(s).

ABSTRACT

The Big Fill Landslide, a “classic” highway embankment failure, occurred on June 8, 2024, at MP 12.8 along Wyoming Highway 22 on the western flank of Teton Pass in Teton County, Wyoming. The failure occurred in a roughly 70-foot-tall embankment section of the highway built in the mid-to-late 1960s and is hypothesized as having occurred due to two primary factors: groundwater and aging infrastructure. Slightly above-average snowpack coupled with rain in Spring 2024 allowed for an above-average release of snow-derived water into, along, and below the surface. Climatic and atmospheric conditions supported this runoff period to raise groundwater levels, eventually enabling the aging, clayey embankment to lose its cohesive strength.

Wyoming Highway 22 roughly follows the boundary between two North American tectonic provinces. Mountains of Laramide age intersect with the Sevier foreland basin Overthrust Belt province. The failed highway embankment traverses an isolated block of mapped, steeply dipping Cretaceous strata created by the northward thrusting Jackson Thrust Fault and the southward thrusting Cache Creek Thrust Fault. The Cretaceous strata are surrounded by various older Mesozoic and Paleozoic formations consisting of sandstone, limestone, and shale. Boreholes drilled for the slide investigation and remediation design confirmed the geologic mapping. Understanding local bedrock geology can indicate and correlate residual material behavior. Further study of climatic conditions preceding the failure has enabled the Wyoming Department of Transportation Geology Program to better monitor and understand winter snowpack, as well as climatic and atmospheric conditions and the affects they can have on mass wasting.

INTRODUCTION

Timeline and Background History

In the few days leading up to the catastrophic embankment failure noted across the United States by national news broadcasts, the fill failure that occurred on June 8, 2024, had been carefully monitored. The following events summary is centered on the Geotechnical Baseline Report by S. Wittke, P.G., (*1*).

Wyoming Department of Transportation (WYDOT) Geology Program staff was notified on June 6 that an arcuate crack had developed in the pavement at MP 12.8 along the average 10.5% grade Wyoming Highway 22 (WY 22) after a motorcyclist had crashed after hitting the offset pavement, though no injuries resulted. Ongoing settlement that developed in 2022 triggered Geology to drill and install an inclinometer at the tangent point of the radial curve of the embankment in September 2022, with an additional inclinometer added in August 2023. This additional inclinometer was added after up to 18 inches of PMP was placed to patch cracks in the road, again. Measurements of that specific inclinometer three weeks prior to the failure on May 15 indicated that the embankment had displayed very minor (< 0.1 inch) movement since the inclinometer's initialization in Fall 2023. The resulting 2023 internal inclinometer installation memorandum by T. Sullivan, P.G., indicated that pavement distress and possible "slumping" had been occurring at the site since 2004 (*2*).

After the discovery of the arcuate crack on June 6, staff from the Jackson Resident Engineers' Office observed lateral cracks in the embankment stemming from the recently formed arcuate crack. At this time too, a spring roughly 45 feet below the roadway surface was observed producing water at flows approximated at less than 1 CFS (*1*).

Geology arrived on site on June 7 to assess. However, a mudslide occurred west of the failure overnight, resulting in the road's closure. Meanwhile, Geology and Jackson staff observed that the arcuate crack had grown up to two inches wide. Tension cracks in the fill were also larger than the day prior. Over an hour's timeframe, the embankment had moved three inches relative to a lathe placed to measure vertical displacement. It was at this time that the under-contract, on-call emergency contractor, Evans Construction of Jackson, Wyoming was directed to begin removing the surfacing section, the inferred driving force. By 6:00 PM on June 7, movement was up to six inches per hour. Work for the day was called at 10:00 PM. That night, a 200-foot horizontal section of the embankment and native ground failed to the north. With Teton Pass closed, the commuter one-way trip from the area of Victor, Idaho where a large majority of the Jackson workforce resides, turned from a 45-minute commute to 2+ hours.



Figure 1 - Picture of failure taken from the toe on June 19, 2024.

While the embankment was being monitored, the degree to which the failure occurred was unprecedented. The embankment, constructed in the mid-to-late 1960s, was upwards of 70 feet tall, and stood at roughly a 1.75H: 1V (~30º) slope for nearly 55 years. The combination of a degrading, aging embankment, complex geology and local climatic conditions, the "perfect storm" of factors, allowed the embankment failure to become catastrophic (Figure 1).

GEOGRAPHIC AND ECOLOGICAL SETTING

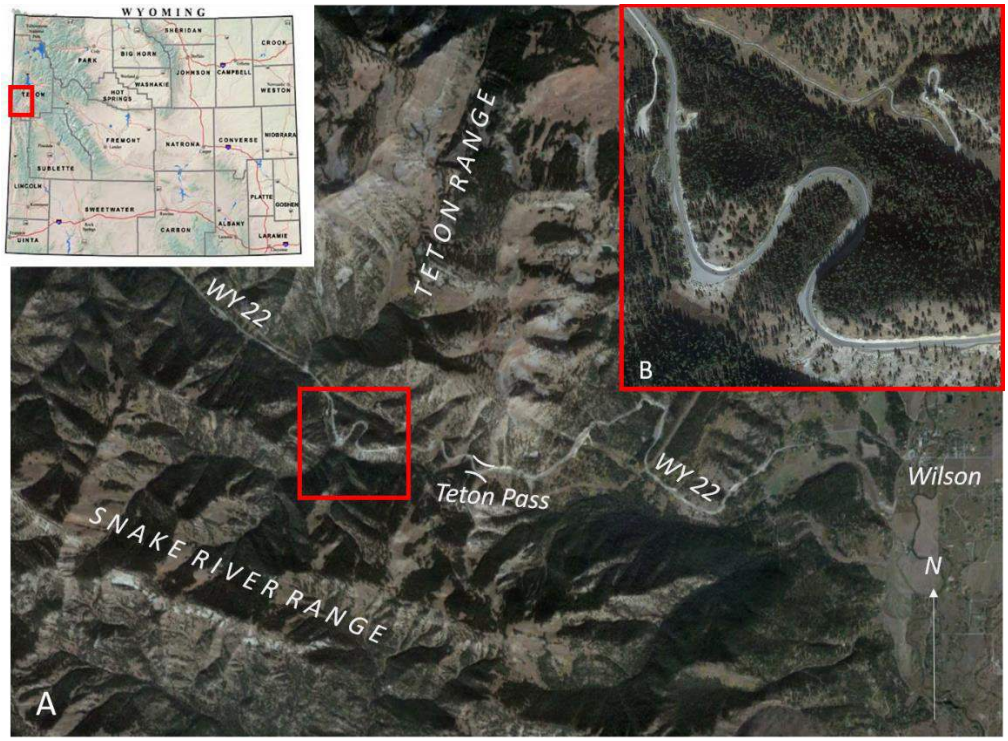


Figure 2 - Location Map of Wyoming and location of the failure in Teton County (Top Left). Map "A" displays the location of the failure (Red Square, Center) along WY 22 west of Wilson, as well as other area geographic features. The Town of Wilson is also shown. Inset "B" (Top Right) displays the location of the radial curve where the failure occurred. State of Wyoming modified from Bureau of Land Management map via wyofile.com. Modified Aerial Imagery courtesy of Google Earth satellite image dated October 3, 2021.

The Big Fill Landslide is located on the western flank of Teton Pass in Teton County, Wyoming. WY 22 ascends from the Town of Wilson on the western edge of Jackson Hole before summiting Teton Pass at 9,655 feet above sea level. WY 22 descends from Teton Pass west into Idaho where the highway becomes Idaho Highway 33 (Figure 2). The landslide is 7.3 miles west of Wilson along WY 22.

Teton Pass separates the Teton Range to the north and the Snake River Range to the south. The east side of Teton Pass drains from Trail Creek to Fish Creek and into the Snake River. Drainage on the west side of the pass is through a different Trail Creek, eventually joining with Warm Creek west of Victor, Idaho. Both sides of Teton Pass lie entirely in the Snake River watershed.

The failure occurred in the Caribou-Targhee National Forest. This area is part of the Greater Yellowstone Ecosystem and is approximately near the boundaries of mapped EPA

Ecoregions 17g, Midelevation Sedimentary Mountains, and 17ap, Sedimentary Subalpine zone (*3*). Ecoregion 17g receives 18 to 24 inches of annual precipitation, while Ecoregion 17ap receives 30 to 50 inches of annual precipitation (*4*).

GEOLOGIC SETTING

Structural Geology Overview

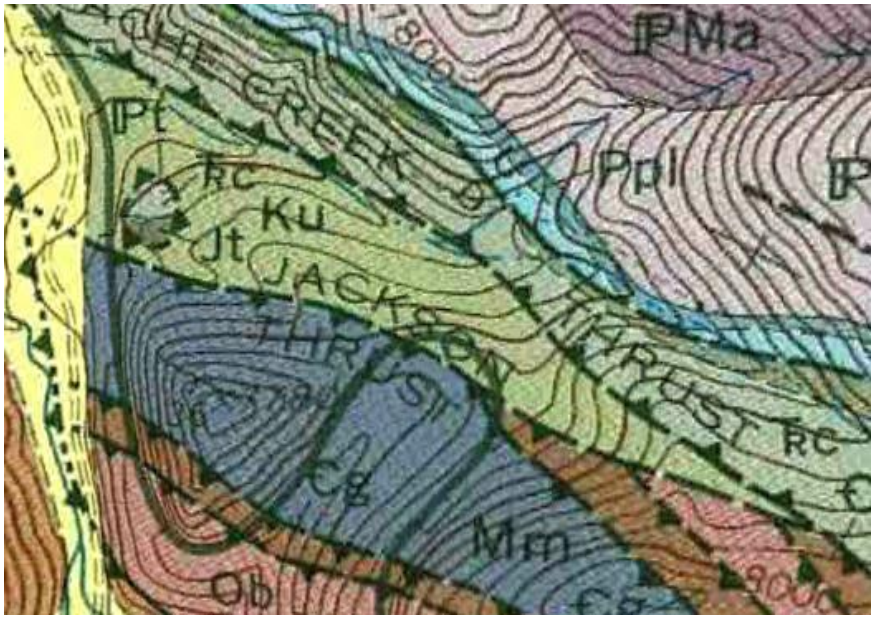


Figure 3 - Geologic map modified from Schroeder's Rendezvous Peak Quadrangle (*5*) displaying the Cretaceous wedge (Ku, Cretaceous undifferentiated) surrounded by the Cache Creek Thrust Fault to the north and the Jackson Fault to the south. Other units of note displayed on the map Cg (Cambrian Gallatin Limestone), Mm (Mississippian Mission Canyon Limestone), Trc (Triassic Chugwater Formation), and Ob (Ordovician Bighorn Dolomite. "Saw teeth" are on the up-thrown blocks. The radial curve of the highway, exemplified by Figure 2, can be observed.

The Big Fill Landslide is located on an isolated Cretaceous strata wedge between two thrust faults of differing age and origin (Figure 3). The first fault of note is the southerly Jackson Fault, an Eocene aged thrust fault associated with the Sevier Orogeny (~140 – ~40 million years ago (MA)) (*6*). The second fault, the northern Cache Creek Thrust Fault, or Cache Creek Fault, is associated with the Laramide Orogeny (~70 - ~45 MA) (*7*). The Sevier Orogeny is referred to as thin-skinned deformation, as strata deformed during the mountain building event was confined to sedimentary rock. The Laramie Orogeny is a thick-skinned deformation mountain building event where both sedimentary and basement rock were involved. The faults and their tectonic overlap are discussed below.

Jackson Thrust Fault

A north-vergent, east-west trending fault, the Jackson Fault notably extends from the west to the east through Jackson Hole. The fault is part of an eastern fault system within the Wyoming salient, consisting of the Crawford, Absaroka, and Hogsback-Darby-Prospect thrusts, active between roughly 70 MA and 50 MA (*6*). This system of faults carried a basal decollement of Cambrian shales as well as thinner Paleozoic and Mesozoic strata (*6*). They are the youngest Sevier-related faults in the salient (*6*). The Prospect Thrust is the easternmost thrust fault and has been dated by Armstrong and Oriel in 1965 (*7)* as early Eocene (~45 MA) while Yonkee and Weil dated movement ending ~ 50 MA (*6).* In the area of the landslide, formations in the hanging wall consist of the Cambrian Gallatin Limestone, the Ordovician Bighorn Dolomite and the Mississippian Mission Canyon Limestone, with the Cretaceous wedge comprising the footwall (*5*).

Cache Creek Thrust Fault

The Cache Creek Fault runs west into Idaho and east across Jackson Hole. The fault is south-vergent, has 5,000 feet of stratigraphic throw (*7*), and represents the southern boundary of local Laramide structures (*7*). The Triassic Chugwater Formation is mapped in the hanging wall adjacent to the Cretaceous wedge in the area of the landslide (*5*).

Tectonic Overlap

During crustal shortening, Sevier thrust faults pushed Paleozoic through Mesozoic strata onto North American cratonic basement rocks as a result of subducting oceanic plates (*6*). Thin-skinned deformation and crustal shortening preceded and overlapped for a short time with the thick-skinned Laramide Orogeny in this area of North America, referred to as the Tectonic Transect by Yonkee and Weil (*6*). Starting about 70 MA, Laramide deformation deformed the older, thin-skinned basal decollement that was actively being faulted. Essentially, the deeper, younger Cache Creek Fault over ran the shallower, older Jackson Fault, cutting through the fault and its basal decollement and bringing with it to the surface a wedge of remnant strata that is interpreted to have been “along for the ride”. It was during this time that bedding within the Cretaceous wedge was stood very steeply with near-vertical dip.

INVESTIGATION AND ANALYSES

Once the catastrophic failure occurred, Geology immediately mobilized its CME 1050 drill rig to the site to begin the investigation and analyses, which began on June 11, 2024, and was conducted almost seven days a week throughout the Summer and into the Fall of 2024. In total, seventeen test holes and test pits were drilled or dug to investigate the area. Test holes 24-01 through 24-14 were drilled with WYDOT Geology’s CME 1050 ATV drill rig, while test pits 24-15, 24-16, and 24-17 were dug with the contractor’s backhoe. Testing and sampling in the test holes consisted of Standard Penetration tests and plastic bag grab samples. Core recovered from the inclinometer installation in 2022 was also utilized as a reference sample.



Figure 4 - WYDOT's CME 1050 drill rig preparing to drill test hole 24-07 looking to the southeast. Snow had fallen overnight. Behind the rig is a mapped, road-cut outcrop of the Mississippian Mission Canyon Limestone and Ordovician Bighorn Dolomite. Evans Construction machinery can also be seen in the photograph. The Jackson Fault is just between the 1050 drill rig and the white box trailer behind it.

Test hole data was shared from the field back to the office daily to update WYDOT's design consultant, RJ Engineering of Evergreen, Colorado, to help expedite modeling of both the temporary detour construction and the long-term embankment reconstruction. The test hole location map (Figure 5) summarizes test hole locations.

Site Geology

While test hole lithology varied to some extent, stratigraphy at the site consisted of three major units: 1) embankment material, 2) native, in-place soils, and 3) weathered to unweathered bedrock mapped by Schroder (*5*) as Cretaceous Undifferentiated. Each unit is discussed in its respective section.

Embankment Material

The failed and in-place embankment consists of loose, brown, very moist to wet, silty sand and gravel with clay. Limestone and dolomite boulders were present in the embankment in the test holes drilled prior to the failure (SL22-01, SL23-01). Boulders are sourced from nearby road-cuts. The unit is essentially boulders within a clay matrix.



Figure 5 - Test hole location map displaying test holes and test pits at the Big Fill Landside site. Test holes were drilled for detour construction and the failure remediation design. For an idea of scale, the Google Earth measured distance between 24-08 and 24-01 is approximately 212 feet. Modified Google Earth imagery dated October 3, 2021.

Native Soil

Underlying the failed and in-place fill material is native soil consisting of stiff, brown to black, slightly moist to moist, silty clay and clay with sand and limestone gravel and cobbles. These soils are derived of local, weathered bedrock. The unit, depending on the location, was influenced during the failure.

Weathered and Unweathered Bedrock

The Cretaceous Undifferentiated bedrock is described in its weathered and unweathered states as follows. Weathered bedrock is medium dense to stiff, yellow-brown to brown to black, dry to slightly moist, hematite stained, lower fine-grained sand, clay, sandstone and shale. Unweathered bedrock is dense to very stiff to very hard, dark gray to maroon to blue-green to white to black, silty to argillaceous shale with carbonaceous shale and coal lenses interbedded with white to black clayey siltstone, and yellow to orange, shaley to silty to very fine grained, poorly calcite cemented “speckled” sandstone. Sedimentary structures within the shale consist of horizontal laminations. It was noted in one test hole (24-07) that the bedrock emitted a sulfuric odor. Shale zones were described as both lean and fat clay, as well as being plastic. The shale also displayed a graphitic luster (24-13). A very pure, uniform white clay was present in test holes 24-01 and 24-02 in bedrock at depths ranging between 32 and 52 feet. A similar clay was present east of the failure along natural outcrops. Shale was dry to wet. Material classifications

ranged from A-4 to A-7-6(101). In test pits 24-15 through 24-17, steep to near-vertical, northerly-dipping bedding was observed. Test pits were dug in the base of the remediation excavation.

Bedrock in one test hole (24-06) was very hard to very dense, white to gray to light brown to yellow, hematite stained, clayey, limy weathered siltstone and weathered shale. Upon review of auger cuttings returned to the surface and samples collected from Standard Penetration tests, the bedrock exhibited a "chewed up" appearance. Table 1 (below) summarizes 2024 test hole and test pit characteristics and can be used in conjunction with Figure 5.

Table 1 – Test Hole and Test Pit Bedrock Summary

Test Hole	Surface Elevation (Post Failure)	Bottom Hole Elevations	Generalized Weathered, Unweathered Bedrock Lithology	Associated Geologic Unit
24-01	7571.7	7530.9	Black shale, siltstone	Cretaceous Undifferentiated
24-02	7585.65	7522.45	Gray shale	
24-03	7576.9	7529.8	Gray shale, shaley sandstone	
24-04	7615.8	7561.6	Gray shale, siltstone	
24-05	7681.1	7610.9	Gray shale	
24-06	7599.5	7545.0	Limy siltstone, shale	Mississippian Mission Canyon
24-07	7691.7	7622.2	Blue-green to gray shale	Cretaceous Undifferentiated
24-08	7606.4	7545.9	Sandstone and shale	
24-09	7661.5	7533.8	Gray silty, clayey shale	
24-10	7660.5	7590.6	Gray to black shale	
24-11	7577.9	7519.4	Brown to black shale	
24-12	7644.9	7566.9	Shale	
24-13	7646.85	7518.85	Gray to black shale	
24-14	7684.9	7636.9	Gray shale	
24-15*	7556.1	7547.6	Gray to black shale	
24-16*	7554.9	7545.6	Carbonaceous to siliceous shale	
24-17*	7554.9	7546.5	Brown to black shale	

***= Test Pits excavated during construction.**

Groundwater

Geology installed three groundwater monitor wells at the site. Groundwater was recorded in the "meat" of the embankment at an elevation of approximately 7611. Groundwater is estimated to have been as high as elevation 7616. The test holes completed for use as monitor wells are 24-10 and 24-14. Initial observations in 24-14 are based on logged cuttings and drill stem observations. Initial groundwater depths and elevations, and next-day (22.5 to 24-hours later) stabilized measurements, are summarized in Table 2 (following page).

Table 2 - Big Fill Landslide Investigation Groundwater Summary						
Test Hole	Date	Depth	Initial Elevation	Test Hole	Stabilized Depth	Stabilized Elevation
24-01	6/11/2024	3.5 feet	7568.2	24-01	Surface (Artesian)	7571.7
24-03	6/11/2024	13 feet	7563.9	24-03	12 feet	7564.9
24-04	6/12/2024	15 feet	7600.8	24-04	30.5 feet	7650.6
24-05	6/13/2024	30.5 feet	7650.6	24-05	12.2 feet	7594.2
24-08	6/18/2024	11.5 feet	7594.9	24-08	82 feet	7579.5
24-09	6/25/2024	82 feet	7579.5	24-09	49.6 feet	7610.9
24-12	6/27/2024	53 feet	7591.9	24-12	53 feet	7591.9
24-14*	8/21/2024	~ 33 feet	~7651.9	24-14	31.95 feet	7654.2

*__24-14 water level taken on 8/22/2024 is from the top of casing in the monitor well, based on Levellogger and Barrolloger Data.__

Instrumentation

Groundwater Monitoring

Beginning in July 2024, Geology installed Solinst Barologgers and Levelloggers to monitor groundwater levels. In August 2024, Geology installed a Solinst Level Sender in 24-14. For more information on long-term groundwater monitoring, see the HGS paper by H. Hinckley, P.G.

2024 Inclinometer Installation

Geology completed two test holes for use in subsurface monitoring. Test hole 24-09 was originally to have the Shape Array installed in it, but the casing was destroyed during construction in July 2024. However, the inclinometer and associated groundwater monitor well (24-10) were salvaged and have been in use as a traditional, probe read inclinometer. Test hole 24-10 was completed to an approximate depth of 128 feet. For more information on slope monitoring systems, see the HGS paper by H. Hinckley, P.G.

Engineering Properties and Slide Modeling

Materials recovered during the investigation were classified by the WYDOT Geology Foundations Laboratory in Cheyenne, Wyoming. Material properties utilized by RJ Engineering (RJ) are derived from WYDOT's drilling, testing, and sampling at the site. Based on the units present, material classifications, and WYDOT's experience with Cretaceous aged shales in Wyoming, the values utilized by RJ in their analyses were authentic and based on fact and experience. RJ developed a failure model based on the mutually agreed-upon engineering properties from materials collected from the drilling investigation. The analysis utilized in generating the failure is referenced in Figure 6. Modeling and analysis software programs used by RJ were Rocscience Slide (2D Limit Equilibrium software) and RS2 (Finite Element software).

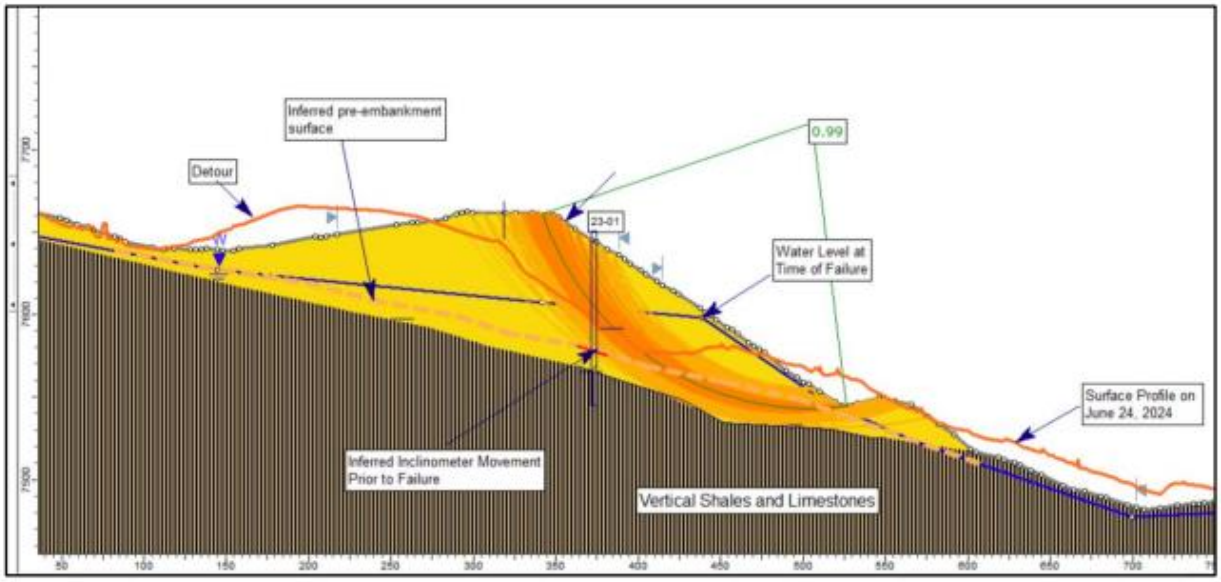


Figure 6 - One of the back analyses generated by RJ Engineering of the Big Fill Landslide. The detour constructed shortly after the failure is detailed. The Yellow unit is the Overburden Clays, Cobbles (Embankment and Native Soils) before the failure, while the gray, vertical line pattern area is the Vertical Shales and Limestone, the Cretaceous Undifferentiated unit of Schroder (*5*). The drilling and analyses indicate that this was not a bedrock failure, but rather an embankment failure.

Units in the analysis are Overburden clays and cobbles (embankment and native soils), while the Vertical Shales and Limestone units are both weathered and unweathered bedrock. The slide analysis consolidates units for simplicity. The low permeability of the shale-dominated wedge allows for the inference that the failure was confined to the embankment and native soils. The May 15 inclinometer reading of 0.1 inches of movement was at an approximate depth of 70 feet, the estimated embankment/native soils contact.

REMEDIATION

Just prior to the failure, the Wyoming State Legislature passed a law that allowed alternative construction methods to be used for WYDOT construction projects. The Big Fill Landslide was the first CM-GC (Construction Manager-General Contractor) project in the State. Potential contractors were solicited, ultimately with Ames Construction at the table in early July 2024.

Geology, RJ Engineering, and Ames Construction collaborated over dozens of meetings during which various remediation methods were discussed. With agreement between all parties, embankment reconstruction material would consist of alternating, four-foot-tall lifts of foamed

glass aggregate and rehabilitated, on-site material reinforced with material separation geotextile and biaxial geogrid, founded on two rows of 140 micropiles, in the base of the remediation excavation. To achieve a target unit weight of approximately 60 PCF, the foamed glass aggregate for the project was sourced from Florida. Due to the time of year, material was stockpiled in Georgia to avoid delays from potential hurricanes. However, the stockpiled material was hit by a hurricane. Florida and the source of the foamed glass aggregate were thereafter hit by another hurricane. Eventually, the material was delivered by rail car and trucked to the failure site, with the storms only causing minor delays in construction time.

Geology continues to track the landslide remotely with its groundwater monitor systems, shape array inclinometer, and snowpack and climate monitoring operations developed from the failure event.

INTERPRETATIONS AND DISCUSSION

The following sections discuss the interpretations of the investigation and analyses conducted at the site. While these interpretations are rooted in scientific evidence, they are not complete and absolute and are subject to refinement.

Bedrock

The site geology aligned well with Schroder's 1972 Cretaceous Undifferentiated unit (*5*), as well as descriptions of both the Cretaceous Upper Bear River and Aspen Formations (*8*), present in Teton County. Both formations have been troublesome with regard to slope stability and mass wasting issues elsewhere in the area. The white, uniform clay layer that was present in test holes 24-01 and 24-02 is believed to be either porcellanite or fault gauge, though that has not yet been determined. Porcellanite is described as being grayish black and pink to white in the Aspen Formations' descriptions from Schroeder's Teton Pass Quadrangle (*8*) and is included in Zeller's formation description (*7*).

However, green shale interbedded with gray sandstone is characteristic of the Bear River Formation. In Zeller's Cross Section B – B' (*7*), located just west of the landslide area, he has both the Bear River, the Aspen, and even the Frontier Formation mapped in Schroder's Cretaceous Undifferentiated unit (*5,7*). This author believes that while a sliver of the Upper Bear River Formation may be present in the southern portion of the wedge, the majority of the investigated bedrock present below the embankment is the Aspen Formation, as per Schroder's formation description in the Teton Pass Quadrangle (*8)*. The presence of dark gray to green shale and speckled sandstone, or "salt and pepper" sandstone (black chert and gray feldspar and quartz grains (*8*)), in the Cretaceous wedge provides the evidence to support this idea. Low permeability of the shale-dominated wedge allows for the inference that the failure was confined to the embankment and native soils, with little to no bedrock movement involved.

The Frontier Formation, described by Zeller, is a fine-grained sandstone and dusky-yellow to yellowish-gray shale, with coal and carbonaceous shale present (*7*). Based on this description alone, the Frontier may be present further north in the Cretaceous wedge as the occurrence of carbonaceous shale in test hole 24-16 provides supporting evidence of this

interpretation. For complete confirmation, more drilling north of the investigation area would need to be conducted.

Detour

Test holes 24-04, 24-06, and 24-07 were drilled to investigate subsurface conditions for the detour route. Test holes 24-04 and 24-07 were drilled into the Upper Bear River and Aspen Formations. The bedrock in test hole 24-06, white to gray to light brown to yellow limy siltstone, is in-line with Schroder's description of the Mississippian Mission Canyon Limestone, in both the Rendezvous Peak and Teton Pass Quadrangles, which outcrops in the road cuts adjacent to the failure to the southeast and west (*5*,*8*). Due to the location of the outcrops and the drilling performed, Geology was confident in the detour being placed inside the original highway curve, onto the perceived, more stable rock, which was confirmed by analysis. Detour analyses and construction were completed in three weeks. Material to construct the detour was mined just west of the failure from the previously mentioned Mission Canyon Limestone outcrop. The detour was constructed on a 12% grade.

Before the detour was opened for travel, around-the-clock monitoring was in place. Monitoring began during construction and was performed by utilizing INSAR (Interferometric Synthetic Aperture Radar) satellite, ground-based side scanning radar, and daily conventional slope monitoring instrument readings. A P.E. stamped detour analysis with a Factor of Safety of 1.2 was also completed. Emergency communication systems were in place in the event road closure was needed. Some systems mentioned above have been in use since their introduction to the site. For more information, see the HGS paper by H. Hinckley, P.G.

Monitored Movement

As mentioned previously, two inclinometers had been installed in the prior two years. Geology had been monitoring the embankment due to offsetting cracks that had been developing in the roadway. The embankment presented itself as vertically settling rather than laterally moving. Geology measured the inclinometers on May 15, 2024, which indicated less than 0.1 inches of movement at an approximate depth of 70 feet, the approximate embankment/native soils contact.

Though the embankment was not moving horizontally, it was moving. Over the years, embankment degradation allowed for the removal of fines to develop void spaces, creating migration pathways for the water to infiltrate the embankment. The settlement experienced by the embankment could have been the consolidation of overlying boulders and upper embankment material into the voids. Fines then collected at the base of the embankment. However, after the initial failure, the embankment remained static, with no additional growth or failures. For more on monitoring the embankment post-failure, see the HGS paper by H. Hinckley, P.G.

Climate Correlations to Failure

After the failure, Geology and RJ Engineering began to investigate the failure causes, with groundwater being the first suspect. Since the winter snowpack had just receded for the year, Geology began to suspect that quick snowmelt coupled with moderate, consistent above-freezing night-time lows was the culprit for the increased groundwater and increased pore fluid pressure in the embankment.

Climate

Studying the United States Geological Survey report, *Temperature, Snowmelt, and the Onset of Spring Landslides in the Central Rockies* by Alan F. Chleborad (*9*), temperature combined with snowmelt was identified as the contributing factors that enable landslides in the Central Rocky Mountains of Wyoming and Colorado. After reading Chleborad's study, WYDOT Geology began to utilize past recorded data from the nearest United States Department of Agriculture's Natural Resources Conservation Service Snow Telemetry (USDA NRCS SNOTEL) Site, Phillips Bench, to understand climatic conditions leading up to the failure (*10*). Phillips Bench is located 3.5 miles east/northeast of the Big Fill site on the eastern slope of the Teton Range at an elevation of 8160. During the Water Year (Oct. 1- Sept. 30), Philips Bench records a maximum median snow water equivalent of 27.7 inches on April 29 and 30 and a median precipitation of 40.8 inches. The data referenced in this section stems from data downloads from the Philips Bench SNOTEL site via the Site Page through the NRCS (Figure 7).

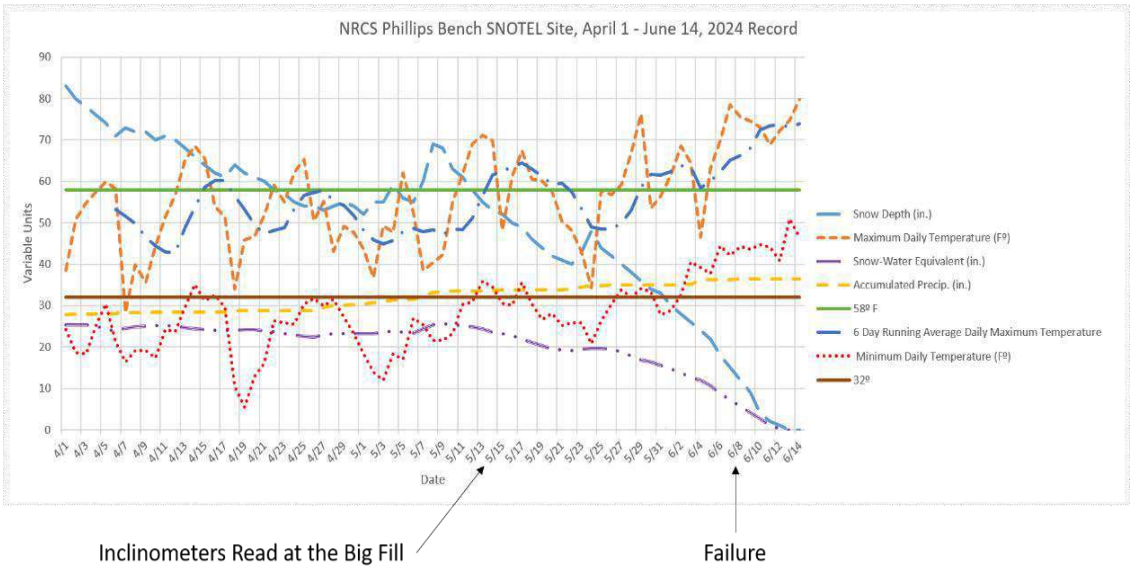


Figure 7 - Graph displaying recorded parameters from Philips Bench SNOTEL Site between April 1 and June 14, 2024. All water-related parameters measured begin at zero on October 1, the beginning of the Water Year. Degrees Fahrenheit was converted from the originally reported Celsius.

From Chleborard, the temperature threshold enabling landslides that must be achieved is a six-day running average maximum temperature of 58° F or greater. By studying the Phillips Bench data, this temperature threshold was first achieved on April 15, 2024, and for three days following. On April 15, 64 inches of snow was present, and the ground is hypothesized to have been thoroughly frozen. It wasn't until May 14, 2024, almost a month before the failure, that the temperature threshold of 58° was achieved again. This warm period lasted until May 21. On May

14 at Phillips Bench, 52.7 inches of snow was measured, and 33.6 inches of accumulated precipitation had been measured in the Water Year. The snow water equivalent was 23.43 inches (Figure 7). By the end of this period on May 21, a recorded snow depth of 41 inches with accumulated precipitation of 33.8 inches was logged. Figure 6 displays snow depths, as well as other measured parameters from Phillips Bench.

The 58º six-day running average daily maximum temperature threshold was again achieved on May 29, 2024, with greater declining snow depth. Average daily maximum temperatures would not fall below 58º again for the rest of the Water Year. On June 3, 2024, a 1.2-inch rainfall event was recorded at Phillips Bench, intensifying melt conditions and the release of water. With this June 3 rainfall event, Philips Bench received 36.3 inches of accumulated precipitation by June 4, 2024, in Water Year 2024 (110% of median for June 4). In the Baseline Geotechnical Report prepared by S. Wittke, P.G., temperature data taken from a WYDOT weather station located at MP 12 of WY 22 (0.8 miles down milepost, elevation 8008) reflects similar temperature conditions to those at Phillips Bench. After May 30, temperatures rose above freezing and did not return to that point (Figure 8; *1*).

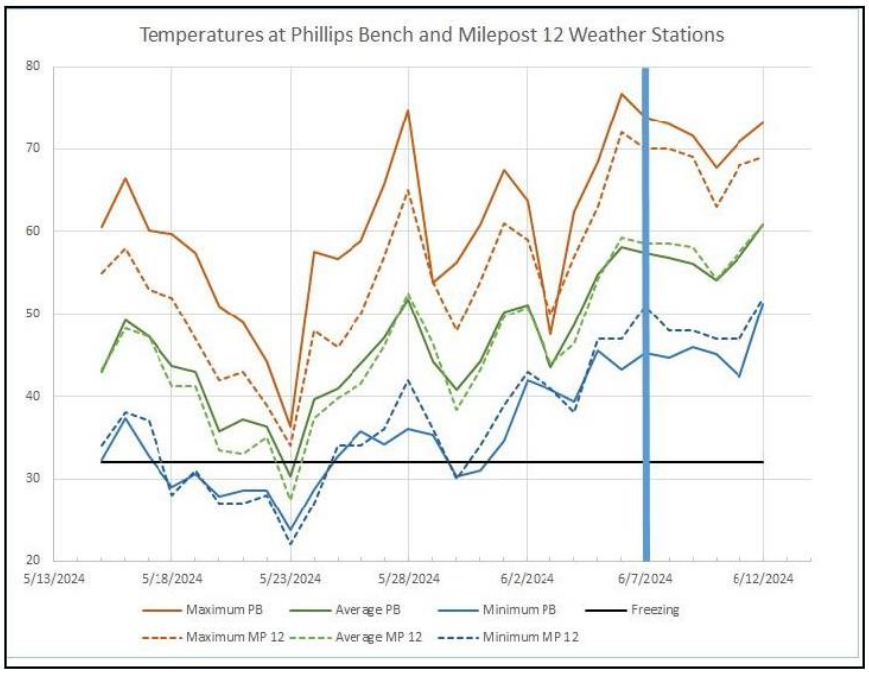


Figure 8 - Wittke's Temperature Graph displaying ambient conditions leading up to the failure. As mentioned, temperatures at all weather stations did not fall below freezing. This graph indicates that conditions were cooler at MP 12 than at Phillips Bench (*1*).

Chleborad also uses a reported relationship between temperature and elevation of -4.5ºF/1000 feet of elevation gain. The Phillips Bench SNOTEL Site is roughly 500 feet higher than the Big Fill (approximate elevation 7665), so daily temperatures can be expected to be approximately 2.25 degrees warmer at the failure site, and roughly the same MP 12 as at Phillips

Bench. However, Wittke's graph displays cooler conditions at MP 12 than at Phillips Bench. Due to uplift of storms crossing the Tetons, snowfall and accumulated precipitation may be expected to be slightly higher on the western flank of the range. Temperatures are being monitored specifically for the Big Fill Landslide by using the WYDOT MP 12 weather station. For more information on climate monitoring at the site, see the HGS paper by H. Hinckley, P.G.

Groundwater Influence and Source

Geology has studied the WYDOT As-Built Construction Plans dated May 8, 1964. The original ground survey displays a slump that was filled in during construction and forgotten about (Figure 9). After overlaying the As-Built Plans with drone footage captured by the WYDOT District 3 Survey team and current satellite photography on the application Google Earth, it was discovered that the location of the failure was the approximate location of the mapped slump. Based on this, the slump was possibly an ephemeral groundwater spring that produced water during Spring runoff. The original groundwater migration corridor became tortuous as the embankment aged and degraded but was still active. To exemplify the pore fluid pressure of the groundwater and the ephemeral spring under the embankment, artesian conditions were met after drilling the initial test hole 24-01, located near the original slump and the failure slump.

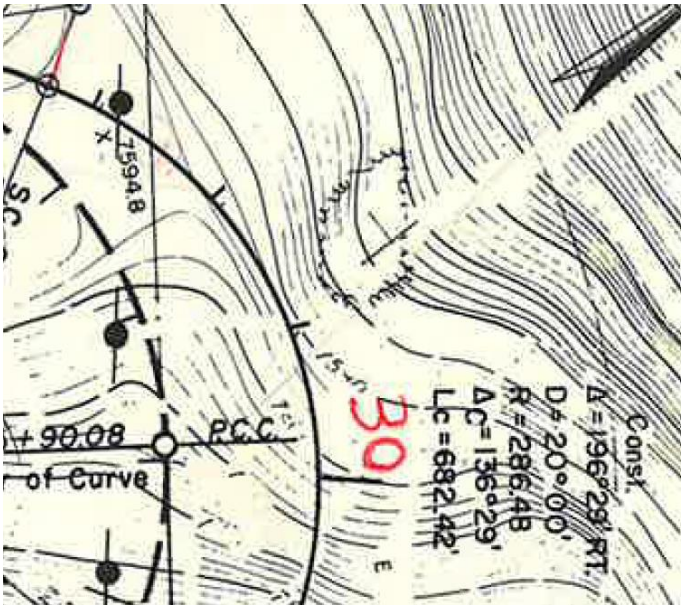


Figure 9 - As-Built Plan Set Sheet 4 (Modified) displaying location of the slump on the original ground line survey. It is interpreted that the slump was actually an ephemeral spring. The tail end of the north arrow can be observed in the top right of the photo.

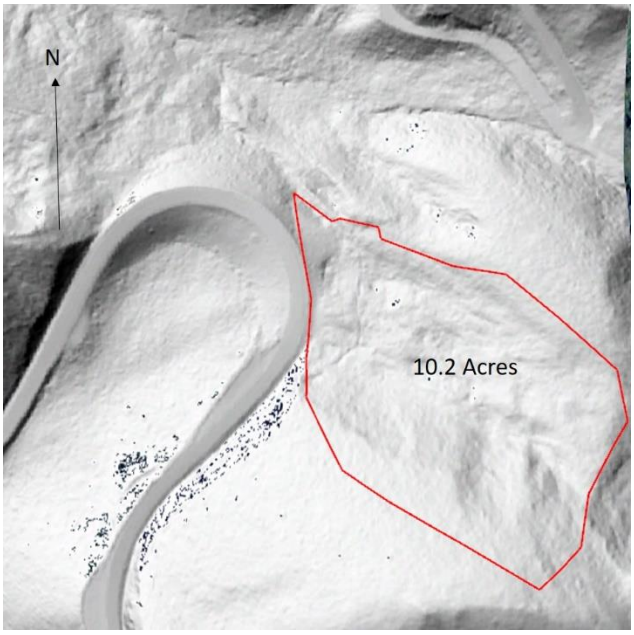


Figure 10 - LiDAR imagery taken of the Big Fill Landslide and surrounding area, pre-failure. Plotted on the map is an estimated drainage area above and adjacent to the embankment that failed during the overnight hours of June 7 into June 8, 2024. LiDAR imagery is from the USGS 3DEP DEM Hillshade layer in the online map viewer.

It is interpreted that all groundwater present at the embankment failure is originally sourced from surficial, overland flow. Based on Google Earth mapping, the drainage area above and adjacent that may drain into and around the embankment is approximately 10.2 acres (Figure 10). A drainage area of this size, with an average annual precipitation of 34 inches (2.83 feet; Ecoregions 17g and 17ap estimated average (*4*)) would produce approximately 28.9 acre-feet of water, or approximately 9,417,092 gallons of water annually.

Pittman (*11*) studied the effects of fault deformed sandstone within the Simpson Group in Oklahoma. Pittman found that both porosity and permeability decrease in these fault zones due to quartz cataclasis and the resulting granulation, leading to a reduction in both grain size and pore size. Cataclasis occurs within areas along and immediately adjacent to faults. The product of granulation is referred to as “clay smear”. Pittman also noted that even sandstone-on-sandstone faults produced clay smear that may disrupt hydrocarbon reservoir permeability. However, weathered sandstones did not produce clay smear while faulting.

With grinding quartz grains creating an impermeable seal along faults studied by Pittman, it is likely that the fine particle clays of the ductile, Wyoming Cretaceous shale have developed an extremely low permeability clay smear along the Jackson Fault. Based on this assumption, it is interpreted that percolated surface water and migrating groundwater within the adjacent Paleozoic dolomite and limestone does not cross the fault into the Cretaceous wedge as it daylights to the south.

Groundwater and Pore Pressure

After the rainfall event, excess runoff surface water migrated and percolated through the embankment and native ground and began to over-saturate the clayey embankment basal layer and adjacent native ground. This over-saturation led to an increase in pore fluid pressure in the embankment which reduced the embankment's cohesive strength. As expected, the clays present did not drain but rather retained water. As described within the Geology Program, the buildup of pore fluid pressure didn't pipe out of the embankment; it completely blew out the embankment. Once the initial failure occurred, the embankment remained stable. This indicates that increased pore fluid pressure had expelled itself, and groundwater-induced pore fluid pressure was no longer an immediate threat to the embankment. Localization of the failure to the fill and some native ground indicates that this failure was not a bedrock failure, but strictly a surficial and embankment failure (Figure 6).

LESSONS LEARNED AND EMPHASIZED

Climatic Conditions

A big lesson learned from the Big Fill Landslide was to utilize already in-place systems used to monitor climate. Since the failure occurred, atmospheric observations and snowpack conditions are being actively monitored, not only in Teton County but statewide. Using existing systems like the USDA NRCS SNOTEL sites around Wyoming, the Geology Program is able to monitor temperatures combined with snowpack and precipitation data in historically mass wasting prone areas of Wyoming. Geology has utilized snowpack data this past Spring to help determine which areas of Wyoming will receive the first inclinometer readings of the year.

Utilizing historical data collected from SNOTEL sites will be able to help indicate late-Winter and Spring conditions leading up to, and at the time of mass wasting events. This data will be used to create criteria to develop a mass wasting advisory system. Essentially, the advisory will help prepare not only WYDOT and other government agencies, but the public too, to anticipate and react accordingly if and when a mass wasting event occurs.

Geology is in the beginning stages of working towards being able to generate a mass wasting advisory. Going forward, the Geology Program will be working with the National Weather Service offices in Cheyenne, WY, Riverton, WY, and Rapid City, SD, to monitor conditions based on the developed mass wasting criteria. Further study to better refine criteria for a mass wasting advisory system will include incorporating existing data and studies from the Wyoming State Geologic Survey.

Water Detectives

The WYDOT Geology Program stresses the importance of being "water detectives" in the field. During initial landslide site visits and the ensuing field investigations, a field reconnaissance of the site to conduct mapping and to begin to look for failure clues and landslide failure mechanisms is performed. In arid environments like Wyoming and the American West, the introduction of abnormal volumes of water into steep or clayey environments usually indicates trouble at some point in the future. Being able to find this source of water is critical in

modeling and analysis, while getting the water to drain ensures a lengthy lifespan of a remediated water problem.

Water causing problems is not confined to landslide events. Whether settlement anticipated at a structure on the Plains or the development of a frost heave above timberline, water is typically the cause of most issues encountered. Understanding where water sources from as well as understanding its influence on material properties and behaviors, will better allow for the Geology Program to help build and maintain safe and efficient infrastructure throughout the State of Wyoming.

REFERENCES

1. Wittke, S., P.G., *Geotechnical Baseline Report for the Big Fill Landslide, M.P. 12.8 Wyoming Highway 22*. Geology Department, Wyoming Department of Transportation, Cheyenne, Wyoming 2024.

2. Sullivan, T., P.G., *Inclinometer Installation, 'The Big Fill', WYO 22, MY 12.8.* Geology Department, Wyoming Department of Transportation, Cheyenne, Wyoming, 2023.

3. United States Environmental Protection Agency. *Level III and IV Ecoregions of Wyoming Map, 1:400,000*. https://www.epa.gov/eco-research/ecoregion-download-files-state-region-8#pane-48. Accessed April 22, 2025.

4. United States Environmental Protection Agency. *Summary Table: Characteristics of the Ecoregions of Wyoming.* Accessed April 22, 2025. https://www.epa.gov/eco-research/ecoregion-download-files-state-region-8#pane-48

5. Schroder, M.L., 1972*, Geologic Map of the Rendezvous Peak Quadrangle, Teton County, Wyoming*. United States Geological Survey, Geologic Quadrangle Map GQ-980, 1:24,000.

6. Yonkee, W.A, and A.B. Weil, Tectonic evolution of the Sevier and Laramide belts within the North American Cordillera orogenic system, *Earth-Science Reviews*, vol. 150, 2015, pp. 531-593.

7. Zeller, C.G., Structural Geology Along Teton Pass, Wyoming, *Rocky Mountain Association of Geologists Geologic Studies of Cordilleran Thrust Belt*, Vol. II, 1982, pp. 831-842.

8. Schroder, M.L., 1969, *Geologic Map of the Teton Pass Quadrangle, Teton County, Wyoming*. United States Geological Survey, Geologic Quadrangle Map GQ-980, 1:24,000.

9. Chleborad, A., *Temperature, Snowmelt, and the Onset of Spring Season Landslides in the Central Rocky Mountains*. Open File Report 97-27, United States Geological Survey, Denver, Colorado, 1997, pp 1-35.

10. Air and Water Database Public Reports. *SNOTEL SITE: Phillips Bench* United States Department of Agriculture, Natural Resources Conservation Service. https://wcc.sc.egov.usda.gov/nwcc/site?sitenum=689. Accessed May 6, 2025.

11. Pittman, E.D, Effect of Fault-Related Granulation of Porosity and Permeability of Quartz Sandstones, Simpson Group (Ordovician), Oklahoma: *American Association of Petroleum Geologists Bulletin,* vol. 65, 1981, pp. 2381-2387.

Evaluating the Role of Geology, Hydrology, and Construction Practices in West Virginia Flood-Induced Landslides

Cole Schmidt, EIT, GIT
GeoStabilization International & Access Limited
102 Smith Street, Columbia, KY 42728
270-250-4054
cole.schmidt@gsi.us

Prepared for the 74th Highway Geology Symposium, August, 2025

Acknowledgments

The author would like to thank the individuals/entities for their contributions in the work described:

Bryan Radabaugh, P.E. – GeoStabilization International
Michael Saylor, P.E – formally GeoStabilization International
Joseph Grecco - GeoStabilization International

Disclaimer

Statements and views presented in this paper are strictly those of the authors, and do not necessarily reflect positions held by their affiliations, the Highway Geology Symposium (HGS), or others acknowledged above. The mention of trade names for commercial products does not imply the approval or endorsement of HGS.

Copyright Notice

Copyright © 2025 Highway Geology Symposium (HGS)

All Rights Reserved. Printed in the United States of America. No part of the publication may be reproduced or copied in any form or by any means – graphic, electronic, or mechanical, including photocopying, taping, or information storage, and retrieval system – without prior written permission of the HGS. This excludes the original author(s).

ABSTRACT

In early April 2024, northern West Virginia experienced two high-intensity flood events that prompted both state and federal emergency declarations. Affected counties—including Brooke, Doddridge, Hancock, Marshall, Ohio, Tyler, and Wetzel—received between 3 to 4 inches of precipitation during each storm, totaling in certain areas up to 18% of the region's average annual rainfall in a single month. These rainfall events, coupled with the region's steep topography, deeply weathered stratigraphy, and aging infrastructure, triggered over 200 documented landslides and caused extensive damage to rural roadways. GeoStabilization International (GSI) led post-disaster field assessments, evaluating slope failures in the context of local geologic conditions, rainfall intensity, historic construction practices, and drainage infrastructure. The majority of landslides were located along low-traffic roadways constructed using "cut-and-side-cast" techniques. Soils were predominantly fine-grained loams derived from weathered mudstones and shales, with failure mechanisms ranging from rotational slumps to translational and block-type failures depending on slope geometry and saturation levels. This study emphasizes the interplay between geology, hydrology, and human activity in the manifestation of landslides. The results underscore the need for updated geotechnical evaluations, modernized drainage design, and risk-informed maintenance practices. A list of twelve strategic recommendations is proposed to support future resilience planning, hazard mitigation, and infrastructure adaptation in geologically sensitive regions like Appalachia. These findings are intended to inform transportation professionals, geologists, and engineers working to protect rural infrastructure in the face of increasing climate variability.

INTRODUCTION

The frequency and intensity of extreme precipitation events have become increasingly apparent across the United States in recent decades. According to national climate assessments, annual precipitation in the contiguous United States has increased at an average rate of 0.2 inches per decade since 1901, with extreme precipitation events—defined as rainfall or snowfall amounts that substantially exceed regional norms—rising at an even faster rate (*1*). While elevated rainfall and localized flooding are often manageable through conventional infrastructure, these hydrologic stressors become significantly more hazardous when coupled with adverse geologic, topographic, and anthropogenic conditions. In such settings, aging and at-risk infrastructure is increasingly vulnerable to geohazards such as landslides.

West Virginia ranks among the most landslide-prone states in the U.S., largely due to its steep terrain, layered sedimentary geology, and widespread development of rural roadways along sensitive slopes as seen in Figure 1 (*2*). The severe flooding that impacted northern West Virginia in early April 2024 serves as a recent and highly consequential example. During this event, the region experienced two major storm systems in rapid succession, resulting in widespread damage to critical infrastructure. The Federal Emergency Management Agency (FEMA) declared a major disaster, initiating federal support for state and local recovery efforts (*3*).

This paper examines the contributing factors that caused the over two hundred landslides documented in the aftermath of the April 2024 flood events. Particular focus is given to slope failures occurring in Brooke, Doddridge, Hancock, Marshall, Ohio, Tyler, and Wetzel counties. The analysis considers the combined influences of extreme precipitation, underlying geologic conditions, and historical construction practices, offering insight into the mechanisms and contributing factors of landslide initiation across West Virginia's vulnerable transportation corridors.

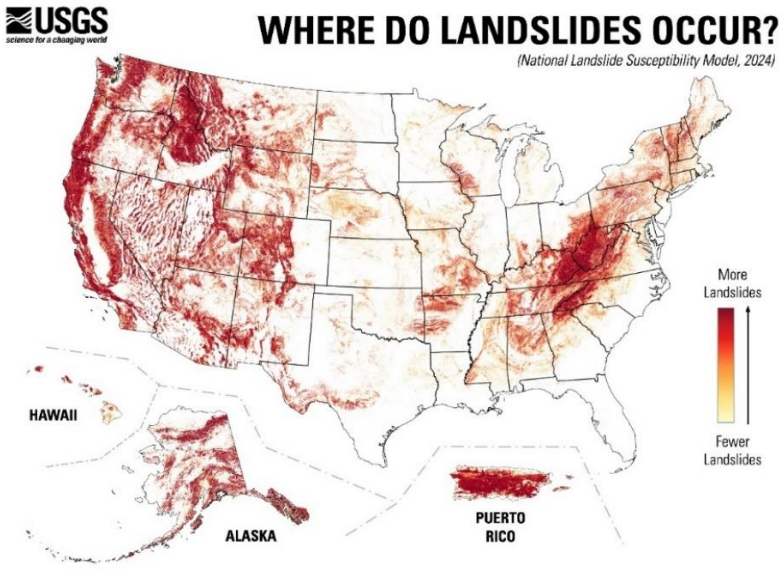


Figure 1 – West Virgina Compared to the United States, USGS "Where Do Landslides Occur" Map

GEOLOGY - FORMATION & GEOMORPHOLOGY OF THE REGION

The primary focus area for this study lies within the Appalachian Plateau and borders the Ridge and Valley physiographic provinces of the central Appalachian Mountains. The region's complex stratigraphy reflects a long geologic history shaped by repeated transgressions and regressions of ancient inland seas. As sea levels fluctuated over time, the alignment of shorelines influenced the deposition of various site-specific lithologies, resulting in a heterogenous stratigraphic record, as illustrated in Figure 2. The bedrock geology of the region consists predominantly of cyclic or interbedded sequences of sandstone, shale, siltstone, limestone, and coal, deposited in both marine and non-marine environments. These strata generally range in age from the Early Pennsylvanian to the transitional Pennsylvanian–Permian periods (approximately 318 to 251 million years ago). Most sedimentary layers exposed at or near the surface are horizontally bedded, having been uplifted but only minimally deformed during the Alleghanian orogeny, in contrast to the more structurally complex Ridge and Valley province to the east (*4*).

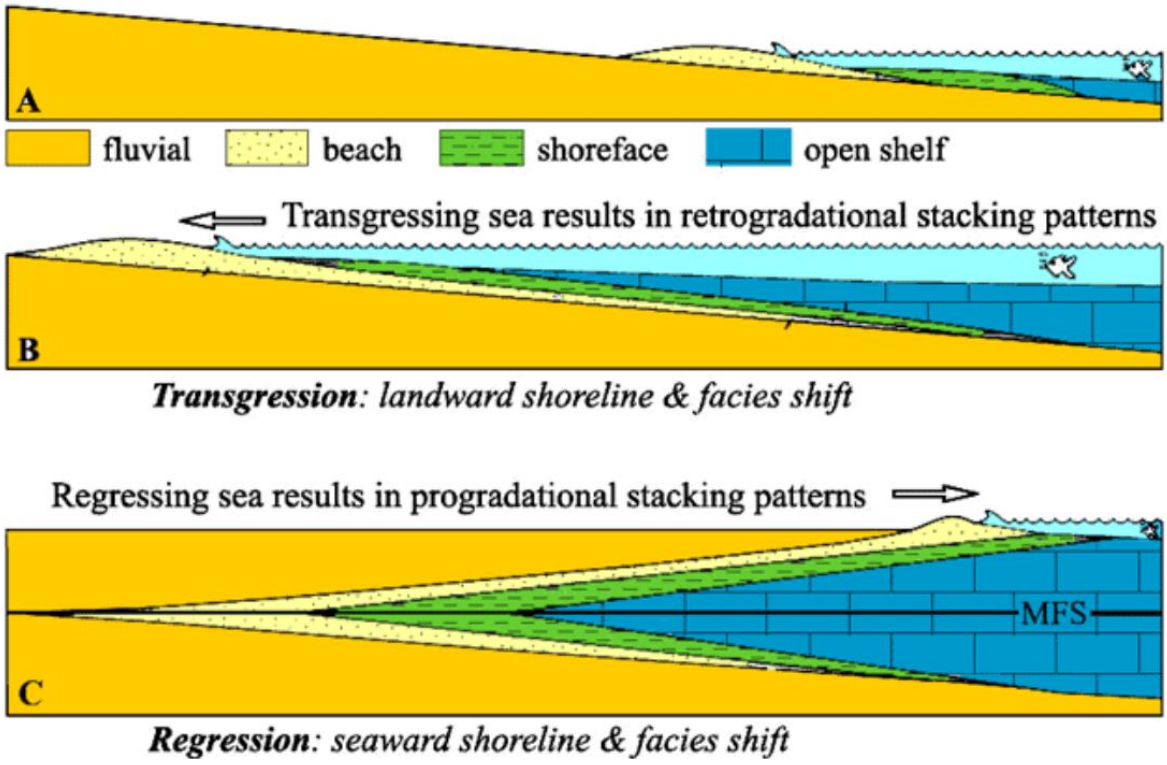


Figure 2 – Typical Transgressive and Regressive Shifts Expected in WV.

Formations that can be found in the research area include the Dunkard Group, Monongahela Group, and Conemaugh Group. Within these groups, the claystones and mudstones are highly susceptible to weathering, which promotes the development of thick residual soil zones, commonly referred to as colluvium (Figure 3). The differential weathering of these fine-grained units relative to more resistant sandstones is frequently observed in roadway cut slopes (*5*). The resulting soil masses typically consist of clayey or silty loams, which were the dominant

materials encountered during GeoStabilization International's (GSI) post-flood landslide inventory survey in April 2024.

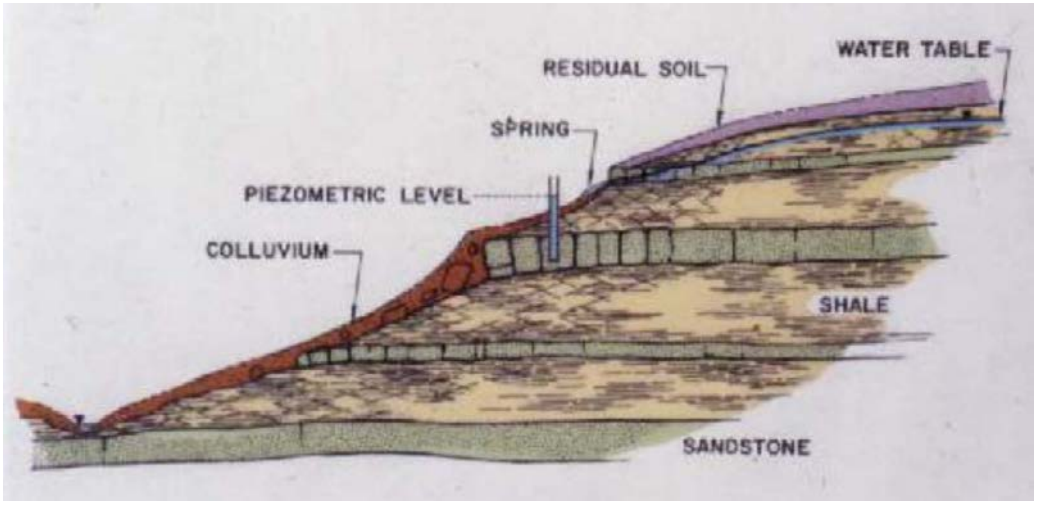


Figure 3 – Typical West Virgina Side Slope Cross Section

With this geologic foundation established, it is important to consider the associated geomorphologic features of the region. The Appalachian Plateau in northern West Virginia is characterized by high local relief, often exceeding 600 feet of elevation difference between ridgetops and valley floors. Elevation varies by county, as does the slope gradient, both of which directly influence local hydrologic response and landslide susceptibility during extreme precipitation events (*6*). When diagnosing the hydrologic contribution to landslides, investigators must consider the topographic setting of the asset. While topography varies across the study area, slope failures are frequently concentrated in local low-lying terrain, such as valleys and drainage ravines. These local depressions act as natural water collection zones during storm events, leading to elevated soil saturation. Although such slopes often support dense vegetation, which typically promotes stability through root reinforcement, the combination of steep gradients and high-intensity rainfall can exceed the absorptive capacity of the soil-vegetation system. This results in increased surface runoff, reduced shear strength, and a heightened risk of slope failure. Table 1 provides a summary of the dominant terrain types and geologic influences for each county in the subject area.

Table 1: Summary of Dominant Geomorphologic Features

County	Dominant Terrain Type	Geologic Influence
Ohio & Marshall	Steep hills, coal-bearing strata	Erosional dissection, mining legacy
Tyler & Wetzel	Rolling to steep hills, narrow valleys	Fluvial erosion, shale instability
Doddridge	Rugged, narrow ridges & hollows	Differential erosion of shales/sandstones
Hancock and Brooke	Dissected plateau, Ohio River terraces	Fluvial Incision with glacial outwash nearby

The region's drainage pattern is predominantly dendritic, consistent with horizontally bedded, uniformly erodible sedimentary units. The prevalence of low-permeability fine-grained soils, coupled with steep slopes and minimal infiltration, contributes to a high stream density (*7*). As a result, the landscape is highly responsive to rainfall, with rapid runoff and short lag times between storm events and peak flow conditions—factors that are critical in the initiation and reactivation of flood-induced landslides.

HYDROLOGY – ACCUMULATING FACTORS

Hydrologic conditions in West Virginia play a critical role in influencing slope stability, particularly in regions with steep terrain, weathered soils, and layered bedrock. As such, water and moisture management should always be a central consideration during site assessments and in the design of slope stabilization measures. Important hydrologic factors include surface water concentration in relation to slope geometry and vegetation, subsurface water conditions (e.g., aquifers and aquitards), the intensity and duration of extreme rainfall events, and the adequacy—or lack thereof—of existing drainage infrastructure.

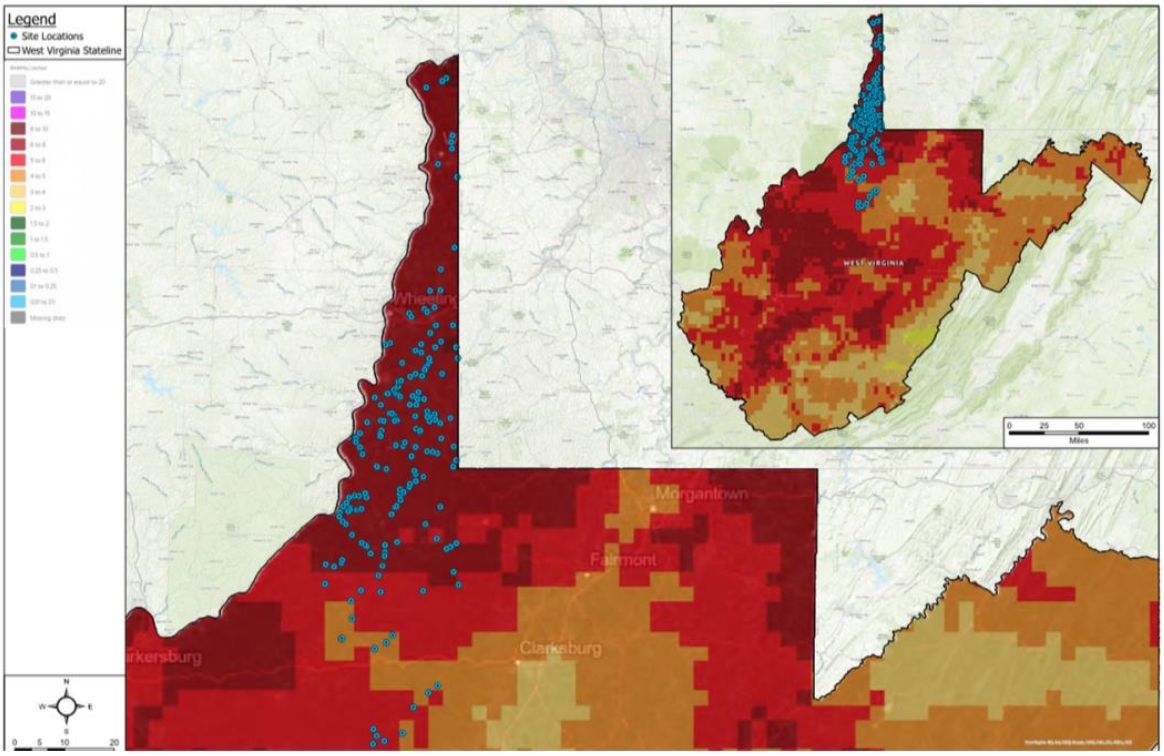


Figure 4 – Regional Map Showing Observed Landslides Sites Caused by Total Estimated Precipitation for April 2024 Flooding Along State Funded Routes

Figure 4 illustrates the location of more than 200 landslides that occurred as a result of the April 2024 flood event. This figure also presents estimated total precipitation for the month of April 2024. On average, the affected region receives approximately 40 to 45 inches of annual rainfall. However, in April 2024, some areas received 10% to 18% of their annual precipitation, indicating a highly anomalous event (*8*). Additionally, Figure 5 highlights the rapid accumulation

of rainfall from successive short-duration storms, each delivering 2 to 4 inches of precipitation over 1 to 2-day periods. In some cases, recorded rainfall in the Wheeling and Moundsville areas exceeded 6 inches between April 1st and 15th, surpassing historical records. Similarly, rain gauge data from the Fairmont and Morgantown areas showed comparable totals, echoing values not seen since 1948. These back-to-back events likely led to full soil saturation and elevated pore water pressures, conditions known to reduce effective stress in soils and trigger slope failures (*9*).

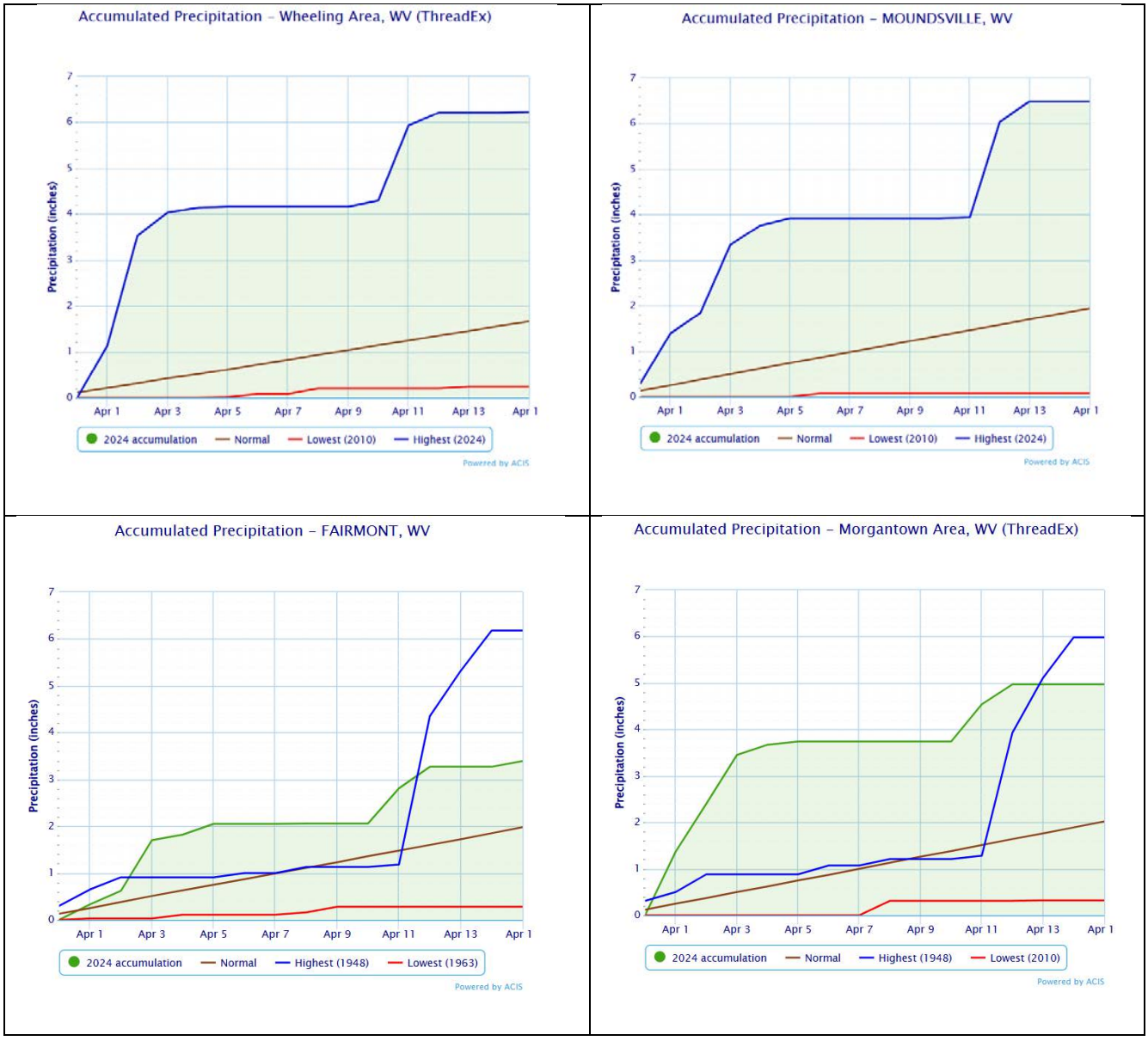


Figure 5 – Rain Gauge Data Showing Accumulation of Rainfall Between April 1st, 2024 and April 15th, 2024 with Lowest, Normal, and Highest Readings

Although antecedent atmospheric moisture levels were generally near or below seasonal norms prior to the April storms—evidenced by roughly 1 inch of precipitation in the final week of March—other hydrologic factors most likely contributed to slope instability. In particular, the

presence of perched water tables observed in areas where permeable sandstone aquifers overlie low-permeability shale units, can create elevated subsurface water pressures along potential failure planes (see Figure 3). These conditions can be common in West Virginia's layered sedimentary terrain, where the outcropping of sandstone and confining shale layers can promote focused water accumulation within slope profiles.

ANTHROPOGENIC INFLUENCES – CONSTRUCTION PRACITCES

Early road builders in West Virginia often had limited resources, technology, and access to earth-moving equipment. As such, roadway alignments were typically selected based on a combination of topographic feasibility, economic efficiency, and practical constraints. Frequently, early roads followed existing footpaths or wagon trails, such as Native American or pioneer routes, which had already demonstrated navigability through the landscape (*10*). These alignments were minimally widened and converted into formal roadbeds, but often lacked modern design considerations, particularly with respect to slope grading and hydrologic management. One of the most pervasive practices to widen roads and contribute to slope instability in the region is the particular use of "cut-and-side-cast" methods in rural, steeply sloped environments. This technique involves excavating material from the uphill side of a slope (the "cut") and depositing it directly downslope (the "side cast") to form a rudimentary road platform. While this method was cost-effective and widely used, especially during early infrastructure development, it often lacked engineered drainage features and stabilization measures, making slopes highly vulnerable to both chronic and episodic failure (*11*). Figure 6 shows an example of a probable "cut-and-side-cast" roadway.



Figure 6 – Probable "Cut-and-Side-Cast" Roadway in Brooke County, WV

When analyzing slope failures associated with historic construction practices, relevant and available data can often be limited. However, with a self-developed and rigorous standard operating procedure GeoStabilization International was able to catalog, assess, and model over 200 landslides caused from the April 2024 event. Several of the failures observed were along "cut-and-side-cast" roadways and the following standard operating procedure to model these slopes is as follows:

1. Field Investigation and Data Collection – Begin with a comprehensive field investigation. Collect site-specific data including photographs, videos, and cross-sectional measurements through and adjacent to the failure. Key features to document include the head scarp, toe bulge, visible water seeps, drainage infrastructure, surface and subsurface utilities, and any rock outcrops.

2. Geotechnical Site Characterization – Compile geologic and geotechnical information derived from field observations, supplemented by publicly available resources such as NRCS soil surveys and regional geologic maps. These secondary sources can guide the classification of soil and rock units, estimate groundwater conditions, and support the assignment of strength parameters when site-specific borings are not available.

3. Development of the Critical Cross Section – Construct two-dimensional slope profiles representing both the pre-failure and post-failure geometries. Pre-failure conditions may be inferred using the "sting line" method, which projects estimated angles of repose upslope and downslope to approximate the original "cut-and-side-cast" boundary (*12*). Post-failure geometry should be based on field survey data or drone imagery. These cross sections will form the foundation for analyses (see Figures 7 and 8).

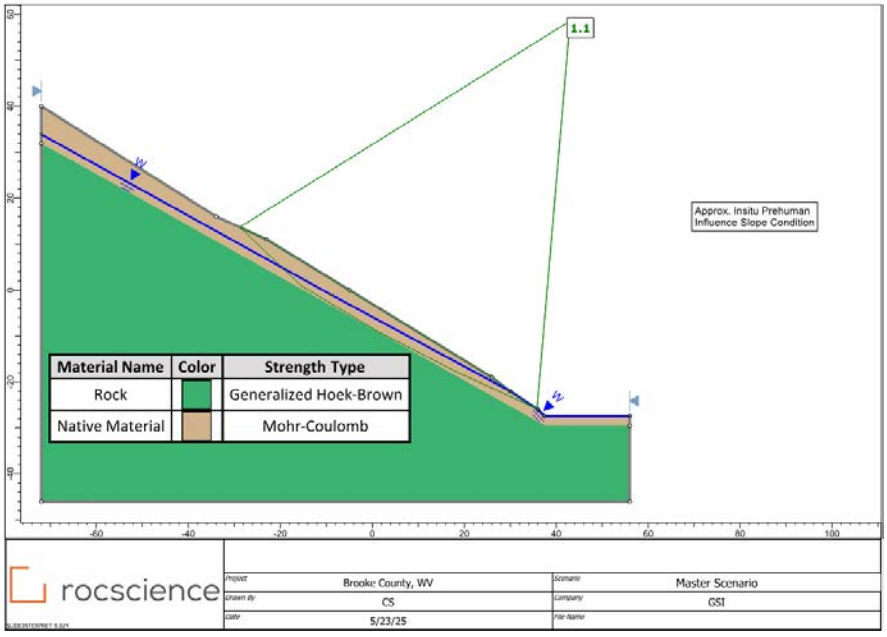


Figure 7 – Pre-Failure or Preconstruction Conditions Based on Assumed Original Slope Angles

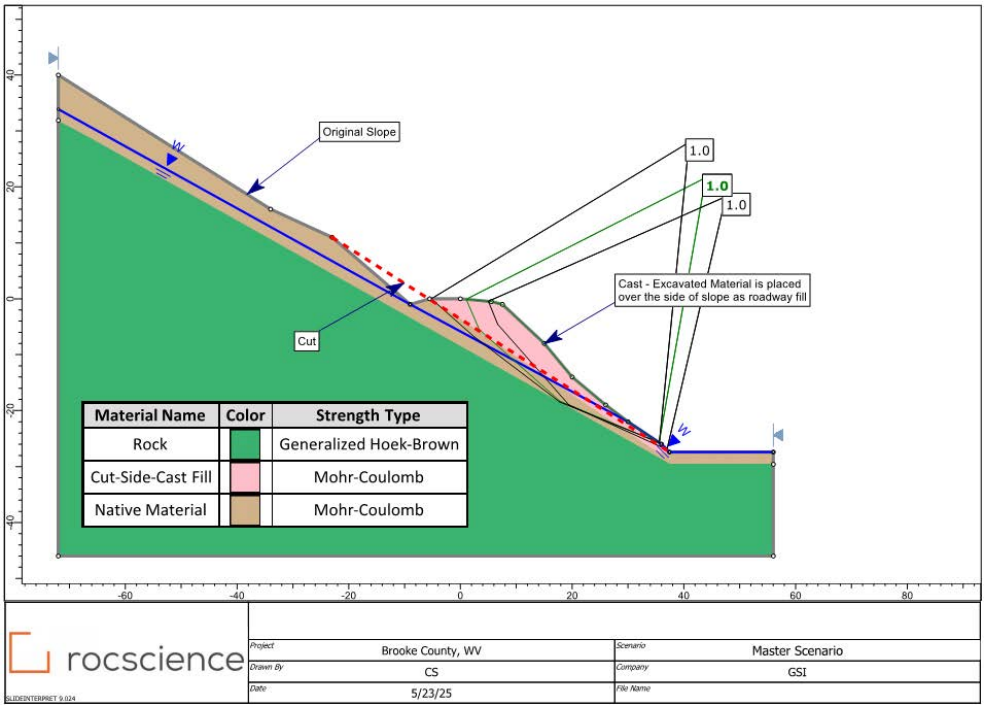


Figure 8 – Post-Failure Conditions Based on Field Survey Data

4. Slope Stability Analyses – Perform slope stability analyses using search methods such as Spencer or Morgenstern-Price to evaluate the factor of safety (FoS) under varying conditions. Undisturbed Appalachian slopes typically exhibit long-term FoS values > 1.1, while post-failure geometries may yield values near or below equilibrium (FoS = 1). At this step, material properties, groundwater assumptions, and boundary conditions should be refined iteratively to achieve representative model outputs.

5. Model Reinforcement or Repair Elements (If Applicable) – Modify the post-failure section to reflect either proposed or implemented mitigation strategies. Repair design should be site-specific and consider practical constraints and project requirements. Common solutions include soil nailing with shotcrete facing, retaining walls, rock buttresses, or slope regrading. Target FoS values may vary by project but typically exceed 1.3–1.5 for long-term stability (Figure 9).

6. Assessment of Extreme Event Scenarios – Many landslides occur after long periods of apparent slope stability. To better understand failure triggers, the model should incorporate extreme event scenarios such as full saturation, rapid drawdown, scour, seismic loading, or temporary surcharge. These conditions can help identify marginal stability zones and better inform the design of resilient infrastructure.

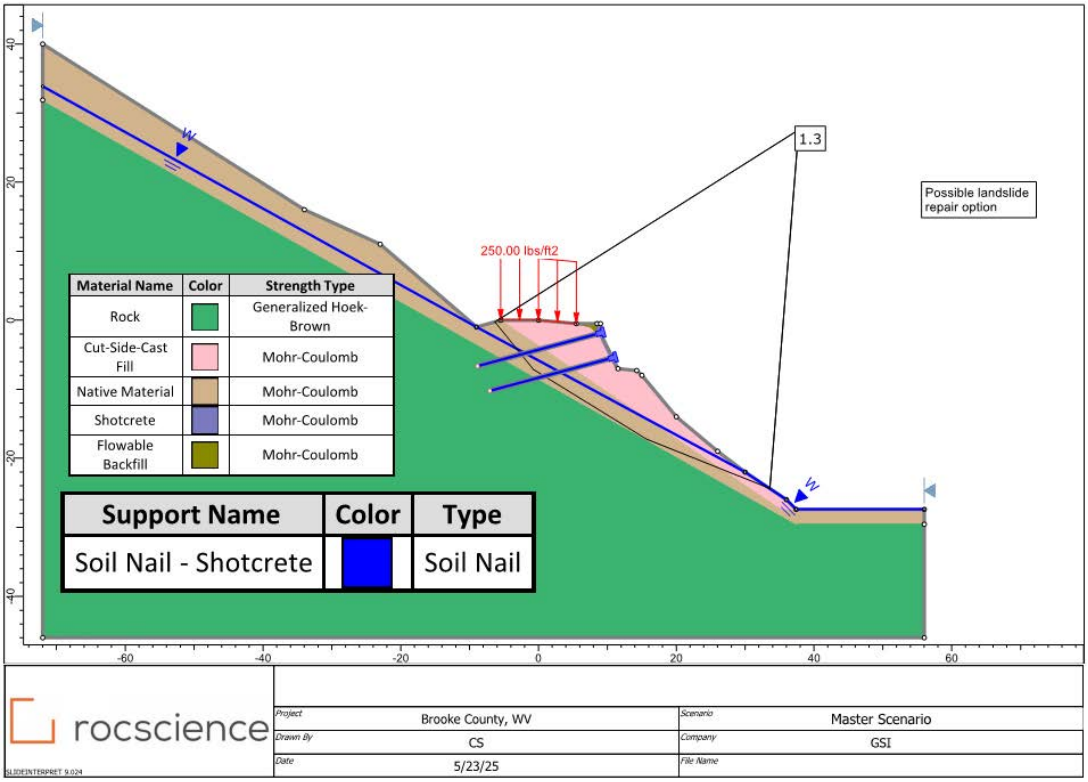


Figure 9 – Potential Repair Conditions Based on Field Survey Data

It is important to recognize that not all cut-and-side-cast slopes are inherently unstable. This construction method remains a common and often practical approach under certain site-specific conditions. Historically, early coal mining and oil and gas operators employed this technique to efficiently and economically develop access routes to resource-bearing locations. However, widespread application of this method—particularly without engineered drainage or slope stabilization—has significantly altered both surface and subsurface conditions throughout much of northern West Virginia.

These alterations have disrupted natural drainage pathways, created voids or zones of weakened material, and modified stress distributions within slope profiles. Under adverse conditions, such as intense precipitation or improper maintenance, these changes can significantly increase the risk of slope failure. As such, the long-term stability of cut-and-side-cast slopes must be evaluated within the broader context of local geology, hydrology, and land-use history.

RECOMMENDATIONS FOR THE FUTURE

As climate variability and extreme weather events continue to challenge historical norms, engineers and geologists must collaboratively evolve the standards of practice to anticipate and adapt to dynamic conditions. Geologically sensitive areas like West Virginia must require proactive action to best protect the health and safety of the general public in this ever-changing

environment. With this attitude in mind, a list of general recommendations to mitigate or alleviate the impacts of landslides in future flood events was generated. Below is a list of strategic and operational recommendations:

1. Develop relationships with local specialists (contractors / consultants) that recognize geohazards pre-failure and can support emergency response procedures.

2. Systematically inventory, assess, and prioritize roadways with known and frequent slope stability issues to create scheduled maintenance programs.

3. Regularly inspect and clear culverts, roadside ditches, and slope drains, especially prior to heavy rainfall events.

4. Develop a flood/landslide maintenance response plan, including pre-identified detour routes and rapid-deployment repair units.

5. Pre-position remediation materials (soil nails, shotcrete, sandbags, drainage pipes) in flood-vulnerable districts.

6. Expand landslide and flood hazard mapping to include predictive modeling based on rainfall thresholds, slopes, and lithologies.

7. Deploy real-time monitoring systems (e.g., rain gauges, piezometers, inclinometers) at known landslide-prone sites.

8. Use LiDAR and UAV imagery to detect early signs of slope movement and drainage failure.

9. Establish interagency coordination protocols between DOT, emergency management, USGS, and environmental agencies.

10. Secure federal or state funding for hazard mitigation projects, leveraging FEMA or FHWA resilience grant programs.

11. Restrict development in known floodways and slide-prone areas through zoning and easement acquisitions.

12. Educate the public in importance of slope reinforcement practices (e.g., soil nails, geogrids, mechanically stabilized earth walls) in high-risk corridors.

CONCLUSIONS

The April 2024 flood events in northern West Virginia offer a compelling case study in the complex interplay of geology, hydrology, and infrastructure design as it pertains to landslide occurrence. This paper has examined over two hundred individual landslides across seven counties—Brooke, Doddridge, Hancock, Marshall, Ohio, Tyler, and Wetzel—emphasizing how

extreme rainfall, weathered stratigraphy, and historically rooted construction practices collectively contribute to widespread slope failures.

The geologic framework of the region, marked by interbedded sequences of sandstone, shale, and mudstone from the Pennsylvanian and Permian periods, creates naturally unstable conditions when subject to deep weathering and saturation. These vulnerabilities are compounded by topographic relief, drainage patterns, and fine-grained soils prone to rapid hydrologic response. From a hydrologic perspective, the accumulation of 2 to 4 inches of rainfall in short-duration storms—amounting to up to 18% of the region's annual average in a single month—was a primary trigger for these landslides. Anthropogenic factors further exacerbate these risks. The widespread use of "cut-and-side-cast" construction, while practical for its time, often lacked engineered drainage and slope stabilization measures. This has left much of West Virginia's rural transportation network vulnerable to modern storm events that exceed historical design assumptions.

Moving forward, there is a clear need for improved integration of geotechnical engineering, hydrologic modeling, and adaptive design in infrastructure maintenance and development. Targeted slope evaluations, modernized drainage design, and data-driven risk mapping can guide future mitigation efforts and ensure the resilience and safety of critical road networks.

REFERENCES

1. Center for Climate and Energy Solutions. *Extreme precipitation and climate change*. (n.d.). https://www.c2es.org/content/extreme-precipitation-and-climate-change/. Accessed May 26, 2025.

2. U.S. Geological Survey. *U.S. Landslide Inventory and Susceptibility Map*. (n.d.). https://www.usgs.gov/tools/us-landslide-inventory-and-susceptibility-map. Accessed May 26, 2025.

3. Federal Emergency Management Agency. *President Joseph R. Biden, Jr. Approves Major Disaster Declaration for West Virginia*. (n.d.). https://www.fema.gov/press-release/20240528/president-joseph-r-biden-jr-approves-major-disaster-declaration-west. Accessed May 26, 2025.

4. West Virginia Geological and Economic Survey (WVGES). *Historical Geology of West Virginia.* Morgantown, January 3, 2020. https://www.wvgs.wvnet.edu. Accessed May 26, 2025.

5. Gray, R., B. Greene, R. Fandray, and R. Turka, *Geology of Pittsburgh* (Educational Series 08, 4th Series). Pennsylvania Geological Survey, (n.d.). https://aeg.memberclicks.net/assets/docs/Geology%20of%20Pittsburgh%20Book.pdf. Accessed May 27, 2025.

6. U.S. Geological Survey. *The National Map Viewer*. (n.d.). https://apps.nationalmap.gov/viewer/. Accessed May 27, 2025.

7. Wiley, J. B. *Drainage areas of West Virginia streams tributary to the Ohio River*. U.S. Geological Survey. (n.d.). https://pubs.usgs.gov/of/1997/0231/report.pdfU.S. Geological Survey. Accessed May 27, 2025.

8. National Oceanic and Atmospheric Administration. *National Water Prediction Service*. (n.d.). https://water.noaa.gov/National Water Prediction Service. Accessed May 26, 2025.

9. National Weather Service. National Oceanic and Atmospheric Administration. *Climate data for Pittsburgh, PA Weather Forecast Office*. (n.d.). https://www.weather.gov/wrh/climate?wfo=pbz. Accessed May 26, 2025.

10. Peyton, B. J. *Highway Development*. e-WV: The West Virginia Encyclopedia. (2024, February 8). https://www.wvencyclopedia.org/entries/349West Virginia Encyclopedia+5. Retrieved May 29, 2025.

11. New Zealand Forest Owners Association. (n.d.). *Cut and side cast construction*. In *NZ Forest Road Engineering Manual: Operators Guide*. Retrieved from https://docs.nzfoa.org.nz/live/nz-forest-road-engineering-manual-operators-guide/earthworks/cut-and-side-cast-construction/. Accessed May 26, 2025.

12. Natural Resources Conservation Service (NRCS). *Web Soil Survey for Northern West Virginia Counties.* U.S. Department of Agriculture. https://websoilsurvey.sc.egov.usda.gov. Accessed May 26, 2025.

Monitoring and Mitigation Strategies for Unstable Slopes, a Tennessee Case Study

Sebastian Dirringer, C.E.G
Cornforth Consultants Inc. - Landslide Technology
9000 SW Gemini Drive
Beaverton, Oregon 97008
Sebastian.Dirringer@ccilt.com

Darren Beckstrand, C.E.G.
Cornforth Consultants Inc. - Landslide Technology
9000 SW Gemini Drive
Beaverton, Oregon 97008
Darren.Beckstrand@ccilt.com

Robert Jowers, P.E.
Tennessee Department of Transportation
Materials & Tests Division-Geotechnical Engineering Section
Building A, 1st Floor
6601 Centennial Blvd., Nashville, TN 37243
Robert.Jowers@tn.gov

Prepared for the 74th Highway Geology Symposium, August, 2025

Acknowledgments

The author would like to thank the individuals for their contributions to this project:

Robert Jowers, P.E. – Tennessee Department of Transportation
Darren Beckstrand, P.G., C.E.G. – Landslide Technology

Disclaimer

Statements and views presented in this paper are strictly those of the authors, and do not necessarily reflect positions held by their affiliations, the Highway Geology Symposium (HGS), or others acknowledged above. The mention of trade names for commercial products does not imply the approval or endorsement of HGS.

Copyright Notice

Copyright © 2025 Highway Geology Symposium (HGS)

All Rights Reserved. Printed in the United States of America. No part of the publication may be reproduced or copied in any form or by any means – graphic, electronic, or mechanical, including photocopying, taping, or information storage, and retrieval system – without prior written permission of the HGS. This excludes the original author(s).

ABSTRACT

The Tennessee Department of Transportation (TDOT) sought to develop an unstable slope monitoring plan for a geotechnically problematic two-lane corridor west of Chattanooga. The subject corridor, SR-2 between Lane Mile (LM) 23 and LM 34 is the designated emergency detour route when the primary Interstate 24 evacuation route is impassable. The corridor is exposed to unstable colluvial slopes of the Pennington Formation and has experienced repeated closures and ongoing distress due to unstable slopes and landslides. The formation is a known problematic unit with low residual strength soils and high groundwater.

The project was subdivided into several phases; background data review, site reconnaissance, conceptual monitoring and early warning system, and conceptual resiliency improvement measures. The Pennington Formation is a thick accumulation of shale and siltstone overlain by thin, unstable colluvial soils. Geotechnical explorations have been carried out at several of the more problematic locations. Groundwater was observed near the top of weathered rock and inclinometers often detected movement at the top of weathered rock.

This paper describes a geologically challenging transportation corridor and evaluates different slope monitoring and mitigation strategies that can be employed anywhere. This paper also presents a framework for developing conceptual monitoring approaches, which include instrumented geotechnical borings and debris flow monitoring stations. Mitigation elements such as geosynthetic-reinforced subgrades and horizontal drains were considered at numerous locations while considering hydrogeologic conditions.

INTRODUCTION

The Tennessee Department of Transportation (TDOT) – Materials & Tests Division Section of Geotechnical Engineering (GES) issued a Work Order to Landslide Technology (LT) for assistance with providing a conceptual unstable slope monitoring plan with prioritization options.

The subject corridor, SR-2 between LM 23 (Hales Bar Road) and LM 34 (Marion/Hamilton County line) is the designated emergency detour route when the primary Interstate 24 evacuation route from Chattanooga is impassable (Figure 1). The corridor is exposed to unstable colluvial slopes of the Pennington Formation and has experienced repeated closures and ongoing distress in several locations due to unstable slopes and landslides. The formation is a known problematic unit with low residual strength soils and often high groundwater.

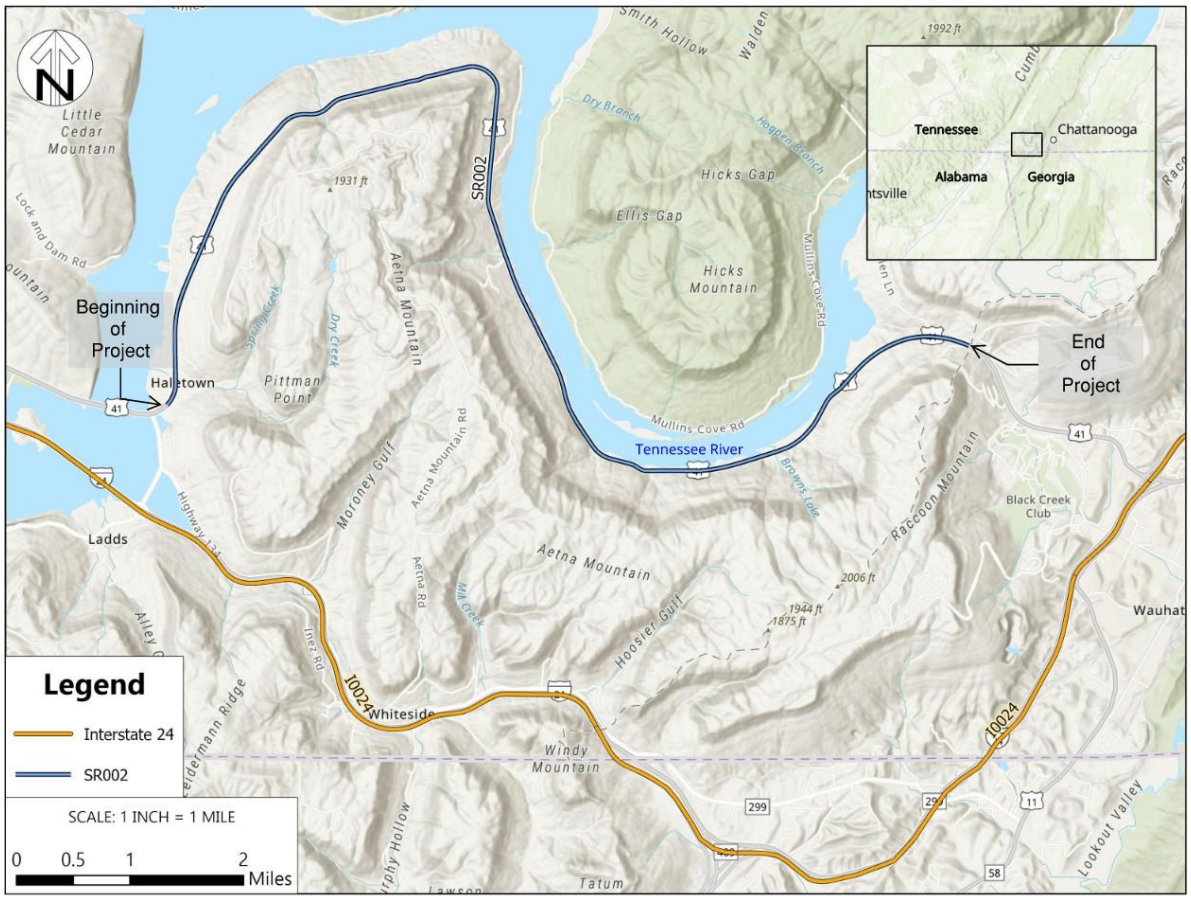


Figure 1 - Vicinity Map of the SR-2 Unstable Slope Project.

This paper describes a geologically challenging transportation corridor and evaluates different slope monitoring and mitigation strategies that can be employed in similar corridors.

Site Engineering Geology

The corridor of interest lies within the Warrior Basin district of the Cumberland Plateau physiographic province. The dissected plateau is known for its incised drainages and slope instability. Aetna Mountain is one of the highest locations within the project vicinity at approximately 1,610 feet above mean sea level, and produces up to 1,000 vertical feet of relief above the SR-2 alignment. Significant vertical relief and unique topographic undulations are present along the entire corridor, which is produced by the underlying soils and geologic formations. Cyclical depositional environments of the Warrior Basin produced varying sedimentary formations, which create present day roadway engineering challenges.

The study area is predominantly situated on the Mississippian Pennington Formation, a thick accumulation of red to green shale and siltstone (Figure 2). Laterally, the formation is known to vary in thickness and lithology due to changes in depositional environments. Intermediate units of limestone, dolomite and sandstone are common within the Pennington Formation. Above the Pennington Formation, Gizzard and Crab Orchard Mountains Groups create more erosion resistant and cliff forming units composed of conglomerate, sandstone and shale (*1*). Formations found along the corridor that compose these groups include the Raccoon Mountain Formation, composed of predominantly silty shale and siltstone, the Warren Point sandstone, Signal Point shale and Sewanee conglomerate (*2*).

As bedrock units described above have weathered, accumulations of colluvial slopes have been produced. Colluvium present along the corridor commonly includes a wide range of grain sizes due to the varying geologic composition of bedrock materials. Thickness of the colluvium appears to range from less than 5 feet to greater than 50 feet. Shale and siltstone of the Pennington Formation produce fine grained sediments such as clay and silt. Sandstone, limestones and conglomerates typically produce coarser sand to boulder sized material. Due to the varying rock sizes, incised drainage systems, and karst conditions, streams often disappear into the subsurface.

Geotechnical investigations performed on behalf of TDOT have been performed for landslide and soil studies at select landslides (*3*). The available documentation describes the encountered native soils as yellowish-brown to reddish-brown clay with some silt, little fine sand, and few rock fragments (shale, limestone, chert). This unit was relatively homogenous through six borings advanced between LM 25.2 and 26.4. Limited explorations reveal soils that are generally less than 20 feet thick and overlie highly weathered shale and siltstone before encountering more competent Pennington Formation shale, siltstone, and limestone. Groundwater was observed near the top of the competent bedrock during drilling. Inclinometers were installed in these completed borings. Later inclinometer results showed landslide displacement, when detected, frequently occurred near the top of the weathered rock.

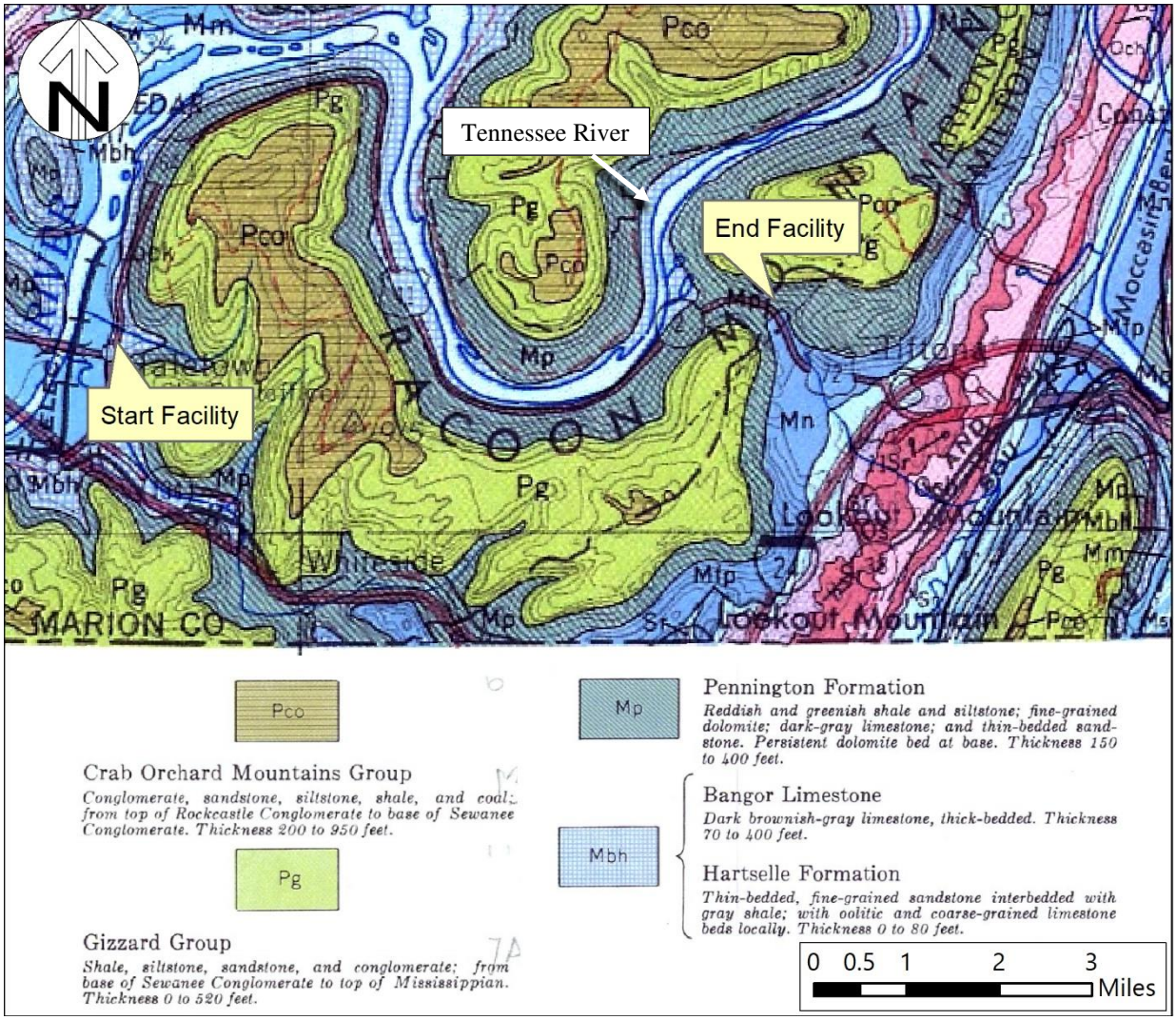


Figure 2 - Area Geologic Map (*1*).

The stability of the subsurface materials along this corridor have been studied by Thomas (*4*). Most of the corridor was mapped on slopes that are susceptible to at least one form of mass wasting. Susceptibility mapping results from the 1981 study include debris flows and debris avalanches, rockfall, and landslides with three different activity qualifiers of 'Active or Recently Active, 'Old Landslide', and 'Combination Landslide'.

TDOT Provided Information

TDOT provided available documentation for geotechnical events along the project corridor between 2011 and 2021. The majority of this information was related to the chronic, significant landslide activity between LM 25.2 and 26.4. Information included event records, photographs, field notes, reports, instrumentation results, PS&E documents, and various communications. This area's landslide activity is well documented and received significant construction activity in the form of walls, soil nails, horizontal drains, and regrading.

FIELD RECONNAISSAINCE

Two site visits were made in 2023 to evaluate the corridor from Guild to the Marion County line on SR-2. During the initial site visit, pavement distress, embankment and retaining wall locations, and landslide conditions were inventoried and were used to develop a framework for further evaluation.

During the second site visit, LT evaluated the locations of pavement distress, assessed locations for slope monitoring programs, and observed the condition of existing unstable slope mitigation and monitoring devices. Conceptual slope investigation and mitigation elements were assessed where unstable slopes were observed. A relative prioritization ranking (A, B, C) was implemented. Priority of subsurface investigation was developed through several factors including relative severity of roadway impact, benefit to designing suitable mitigation, access, historical evidence of mass movement, relative size of impact, and supplementation of existing data.

Deeply incised drainage channels with flow paths across the SR-2 alignment were targeted for debris flow monitoring stations. These monitoring stations were evaluated with several criteria in question, including historical records of debris flows reaching the corridor, relative basin size and slope angle, land use, and potential access requirements and utility conflicts.

Condition of Recently installed Geotechnical Instruments

Monitoring instruments were installed between LM 25.2 and 26.4 where major landslides occurred in 2019 and 2020 with subsequent mitigation constructed in 2020. Geotechnical explorations and instrumentation consisted of of six slope inclinometers (SIs), installed while the mitigation construction was underway. No laboratory or engineering analyses were conducted as part of that study. To our understanding, one of the six SIs continues to be read, while the other five are not viable due to landslide movements that have sheared the casing and it is no longer readable with the SI probe. Remnants of older SIs were also observed in the roadway prism at LM 27.79 and 26.89.

Condition of Recently Installed Slope Stabilization Measures and Horizontal Drains

Previously completed slope stabilization measures have been completed in the study area. Most recently, MSE and shotcrete-faced soil nail walls were completed between LM 25.2 and 26.4 between 2019 to 2020 (Figure 3). Evidence of ground cracking and settlement was observed downslope from SR-2 and associated walls mentioned above, likely from landslide movement.



Figure 3 - Condition of recently installed MSE and shotcrete faced soil nail walls between LM 25.2 and 26.4. The gap between rock fill and the MSE wall is likely landslide and settlement induced. White dotted line indicates location of tension cracks.

Other locations of existing stabilization measures in the form of shotcrete faced soil nail walls, rockfill buttresses, rockfill inlays, and timber crib walls were recorded by lane mile. Locations of asphalt repairs were also recorded which were likely due to embankment and landslide distress.

Horizontal drains were observed in the LM 25.2 to 26.4 area, where 104 drains were identified in orthoimagery collected via UAV photogrammetry. They were installed either at the base of soil nail walls, within the native material below the walls, or above the roadway. Some drains were producing water at the time of our site visits, suggesting that groundwater is being intercepted and drained. Most drains were at the base of the soil nail walls and were typically dry at the time of our visits.

Landslide Conditions

During our field reconnaissance we observed geologic hazards including embankment slope failures, embankment foundation failures, cut slope failures, landslides, debris flow channels, and ground settlement. In general, most roadway pavement distress was observed on the west-bound travel lane and shoulder which is located on the downslope side of SR-2 (Figure 4).



Figure 4 - Example of SR-2 west-bound travel lane roadway embankment and pavement distress near LM 26.9.

Many of the existing retaining walls and slope failure repairs on the downslope side of SR-2 appear to have continued ground movement (Figure 5). Indications of the movement include the distressed pavement and recurring patching, settled and tilted guardrails, and tilted walls. Settled rockfill also are apparent, however, the distress is often difficult to differentiate from final grading during construction that may be irregular in places.

Weathering of local rock formations develop colluvial soils with components ranging from boulders, gravel, to clay with low residual strength. The low strength soil most likely creeps downslope during periods of high ground water condition. The creep movement also appears to develop into basal shearing (landslide), either slumping or as a translating earth flow. Unique topographic conditions may also be from dissolution of limestone, which is common in the area.

Based on Lidar interpretation, our reconnaissance, geologic mapping, and boring logs provided by TDOT, soil thickness varies across the project area from relatively thin, less than 5 feet in

wide areas especially the east facing slopes, to 10-20 feet thick on the north facing slopes. However, based on a brief review of Tennessee water well logs from the vicinity, the surficial soil can attain thicknesses of 40 to 50 feet.



Figure 5 - Example of continued ground movement after repair efforts near LM 29.7.

From our desktop study and field reconnaissance, we learned about historical accounts of debris flows initiating on steep slopes, often in convergent topography and swales. Using available Lidar, incised river drainages through debris flow deposits were inventoried and ground truthed during field reconnaissance efforts. Debris flow deposits ranged in slope location, at times extending to the damned Tennessee River forming Nickajack Lake. Past debris flow events depositing thick accumulations of material across SR-2 have been recorded.

Evidence of landslide movement was discernible by observation of hummocky ground morphology, leaning and fallen trees, ground cracks, sloughing soil, and pressure ridges. Based on the location of gathered landslide evidence, it is likely that:

- Embankments load the colluvium and raise the groundwater, both of which can cause faster creep movement and landslide activity. If embankments foundations do not include drainage systems, increase of groundwater pressures is likely a considerable issue.

- Cut slopes unprotected by shot rock inlays appear to be sloughing or creeping downslope. Occasionally the cut slopes appear to move into the roadway, pinching the ditch, and at least one case, uplifting the roadway within the re-activated slide's toe.
- Slopes without engineered mitigations are susceptible to movement.
- Riprap armored slopes and embankments may also be moving, especially if the rockfill is not keyed into firmer material.

More details can be determined from investigations into the site's materials, for instance how, where, what depths, etc., the inter-bedded shale and limestone weather and contribute to the colluvium.

APPROACHES TO SLOPE STABILITY MONITORING

Remote monitoring systems for purposes of this paper are described as those that use sensors and measurement tools that are not installed on site. As landslides move and debris flows occur the ground surface shifts and elevational differences occur. Some landslide movements, especially those in translational landslides, may not produce a significant elevation difference for the majority of the slide despite significant lateral displacement. In these cases, most change would occur at the landslide's head scarp and toe.

Figure **6** illustrates this relationship where changes at detected at the scarp and a small portion of the landslide toe for a one-year period and greater displacement over a 10-year period. Both illustrate the concept of little elevation change in the landslide's midsection despite either significant or minor landslide displacement. Detection of topographic change is a clear identifier of ongoing landslide movement despite these limitations.

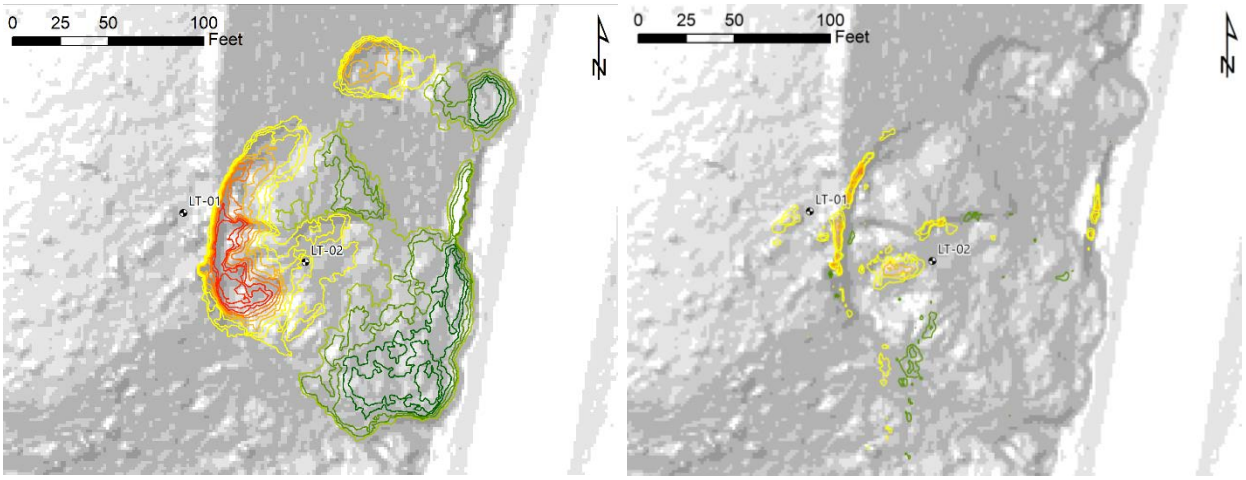


Figure 6: Example change detection for a Missouri landslide using manned aircraft-mounted (2010) and UAV-mounted (2021, 2022) Lidar sensors between 2010 and 2020 (left) and June 2020 and April 2021 (right). (5).

Understanding where topographic changes are occurring due to landslide movement is the primary method for the detection of landslide movement and debris flow occurrence. Selection of remote monitoring techniques should focus on one that can detect topographic changes. Recent literature subdivides remote sensing technologies into those that are passive or active,

depending on if they rely on reflected wave energy (passive) or emit and receive wave energy from the monitored object (*6*). Most of the passive techniques are labor intensive and not commonly used for landslide monitoring and are not suited to detect topographic changes, particularly in areas with heavy vegetation. A passive method often successfully used for change detection of rock slopes and other non-vegetated slopes is use of structure from motion (SfM) photogrammetry. Two active systems are commonly used for change detection, laser surveying using Lidar and synthetic aperture radar (SAR and InSAR). These three candidate remote monitoring methods are well suited for topographic change detection and are discussed below.

Photogrammetry

Structure from motion (SfM) photogrammetry creates 3D models from a series of static photographs obtained from dozens or hundreds of different vantage points. SfM techniques analyze the photographs to estimate three-dimensional structures from the two-dimensional image sequences. LT collected 1,012 images via a UAV-mounted camera of the LM 25.2 to 26.4 segment. This area contains several walls that were constructed in response to a February 2019 storm event and is largely free of dense vegetation. This area is an excellent candidate for photogrammetry-based change detection and is shown in

Figure **7**. Frequency of data collection and analysis could be monthly to annually, based on TDOT's needs. Note that this frequency is insufficient to incorporate into real-time operations decision making, but is most appropriate to monitor ongoing wall distress and landslide movement.

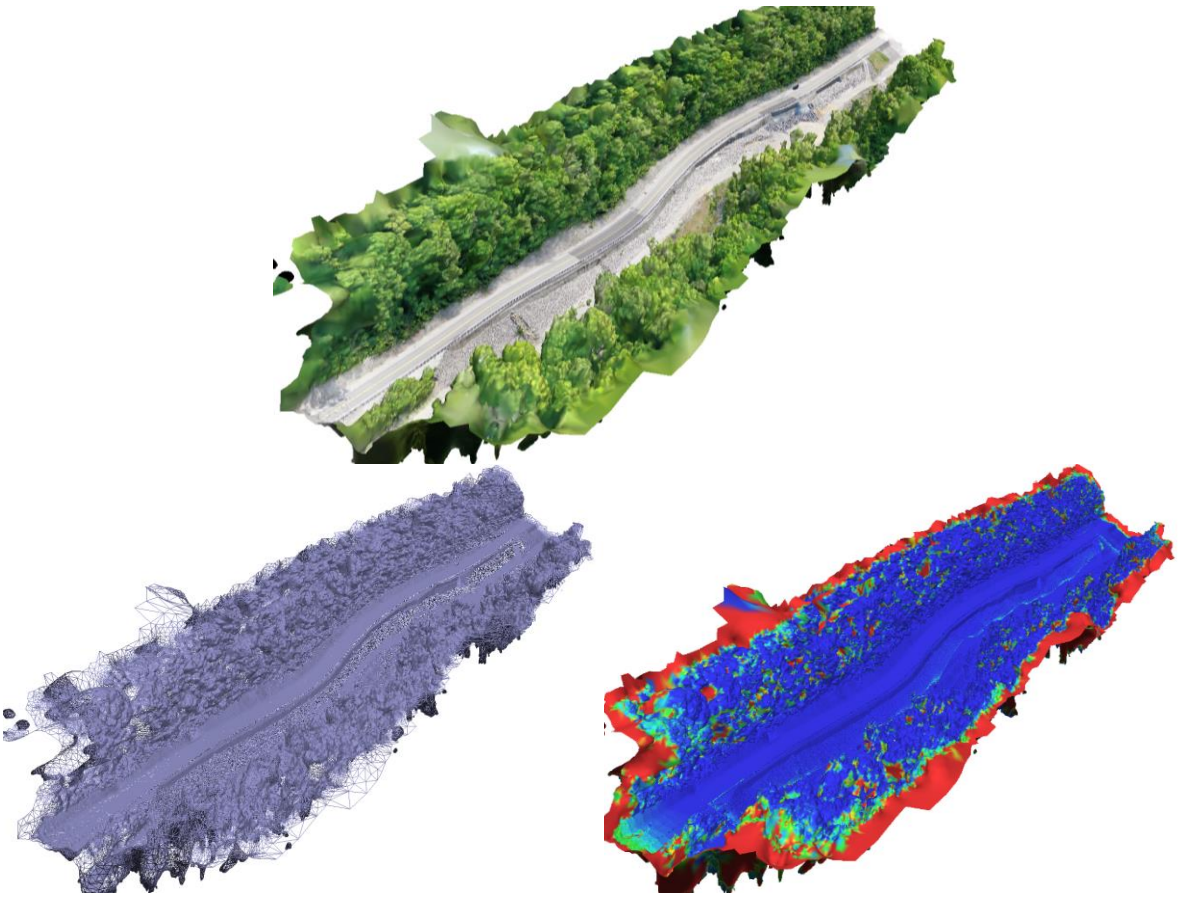


Figure 7: Photogrammetry of the LM 25.2 to 26.4 area. Model shows real color (top), mesh network (lower left), and confidence from high (blue) to low (red) (lower right).

Lidar-based Change Detection

Lidar data can be collected from near the ground via tripod-mounted scanners or vehicle-mounted scanners collecting data while in motion, or via sensors mounted on UAV or passenger aircraft. Ground-based collection is typically not performed for landslide change detection due to their limited field of view, but can be suitable for targeted monitoring of specific features, such as rock inlays for cut slope landslide repairs (*7*). More frequently, landslide change detection is accomplished with repeat Lidar surveys collected by aircraft. Most, but not all, Lidar laser sensors emit several pulses of light and measures the return time of each pulse. The first returns are typically the top of ground cover (trees, shrubs, etc.) while the last return is typically the ground surface in a process of point classification. This provides the ability to see the bare earth surface and has been revelatory to the geotechnical community. Considering the extents of the project area, Lidar-based slope change detection is only feasible via aircraft equipped with sensors capable point classification.

We understand that TDOTs goals included regular, frequent monitoring that could be eventually used as an early warning system that could be expanded to include automated notification measures. This use case necessitates a very high frequency of data acquisition with the accompanying data processing. Typically, when Lidar is used to detect change in a landslide corridor, data is obtained quarterly or semiannually; a timeframe incompatible with making actionable maintenance and operations decisions. A useful, but economically infeasible, data collection frequency would be weekly or biweekly data collection. This may allow equating detected change to specific periods of high intensity storms that would trigger landslide movement. Despite this, our experience in measuring subsurface landslide displacements triggered by storm events suggests that the sub-inch or sub-centimeter movements could not be measured via Lidar. Research carried out for Missouri DOT suggests that reliable detection of landslide displacements under 6-inches with a UAV-based Lidar unit on a ground surface with heavy grass cover was difficult, as shown in Figure 7 (*5*).

A more useful and practical application of Lidar would be via an annual aerial survey. This would help find changes well outside the right-of-way that would otherwise go unnoticed. Examples include detecting debris flows that did not reach the roadway but led to debris accumulation upstream and scarp and toe formation above, across, or below the roadway.

InSAR Satellite Monitoring

The only satellite monitoring technique that utilizes satellite-based remote sensing for change detection is limited to interferometric synthetic aperture radar (InSAR) technologies. Satellite-based InSAR systems rely on phase shifts of radar waves of a series polar-orbiting satellites. Changes within the radar's wavelengths are detected by analyzing repeat data, typically on about a two-week cycle. The technique can potentially measure millimeter-scale changes in ground surface over spans of days to years (*8*,*9*). The technique relies on consistent, identifiable natural or installed reflectors on the ground surface to measure the phase shift. Constantly changing ground conditions, such as those from vegetation or active talus slopes, interferes with

measurement repeatability and prevents accurate readings. Heavy vegetation limits InSAR's ability to gather sufficient data to detect small-scale changes of limited spatial extent typical of most shoulder failures. However, where ground cover is sparse the information collected can provide valuable information.

Much of the SR-2 study corridor is obscured by heavy vegetation except in the LM 25.2 to 26.4 section where much of the ROW was cleared of vegetation during construction activities of the past three years. InSAR may provide quality results regarding landslide extents in the exposed areas. In our opinion, an initial feasibility study is warranted to evaluate its applicability in this area and possibly for other parts of the corridor.

The nature of the SR-2 landslides, the heavy tree cover, the length of the study corridor, and the ultimate use of the data to inform TDOT decision making on both operations and engineering decisions guide the application of several remote monitoring techniques. Table 1 contains a summary of techniques, pro and cons, reading frequency, and recommendations. In general, the following approach would prove useful to TDOT:

1. A pilot study to test the feasibility of InSAR;
2. Quarterly monitoring of the LM 25.2 to 26.4 landslide area with SfM photogrammetry;
3. Annual piloted-aircraft or comparable UAV-mounted Lidar monitoring of the ridgeline down to the Tennessee River.

Table 1: Summary of remote monitoring techniques.

Monitoring Method	Pros	Cons	Practical Reading Frequency	Recommended
Ground-based Lidar	Common equipment, surveyor availability	Low line of sight limits data collection, limited extent, lack of practical real time capability over segment	Monthly or longer	No
Piloted Aircraft Mounted Lidar	Large data collection area, bare earth capable and common	Fewer vendors, lack of practical real time capability	Semi-annually or longer	Yes, at annual or longer interval
UAV-Mounted Lidar	Easily deployable, bare earth capable by specification, higher practical reading frequency	Smaller areal extent than manned aircraft	Monthly or longer	No, if an annual Lidar survey via manned aircraft is selected
SfM Photo-grammetry	Easily deployable, comparatively low cost equipment	Cannot obtain bare earth imagery, has to 'see' through vegetation	Monthly or longer	Yes, at the wall locations only. May be practical at few select additional locations
Satellite-based InSAR	Approximately 14 day reading interval, backward-looking, can incorporate past data	Only measures displacement on line-of-sight axis, can't measure displacement in east – west direction, cannot see through vegetation	14 days	Tentative, recommend a pilot study to determine applicability

Ground Monitoring Systems

Landslide Monitoring

An essential part of modeling a landslide is to determine the depth of the shear zone and the pore water pressure acting on it. This information is obtained by installing and monitoring field instruments consisting of inclinometers and piezometers. Inclinometers monitor the depth and rate of movement at the landslide shear zone and piezometers measure pore water pressure at their installed depth. These two measurement tools are the most valuable methods available for monitoring and understanding landslide movements and their triggers (*10*). Both instrument types can be monitored manually or electronically, with or without radio and cellular data telemetry capabilities. TDOT's goals include the prospect of incorporating landslide data into highway operations, which requires the ability for remote data acquisition and communications.

Inclinometers are currently anticipated for manual readings until landslide displacement is detected. Once movement is detected, an in-place-inclinometer (IPI) can be installed across the shear zone and integrated into the radio network to monitor landslide movement. Alternatively, a continuous in-place inclinometer string, commercially referred to Shape Accel Arrays (SAA) could replace traditional inclinometer casings for a significant added cost. The SAAs permit automated displacement detection prior to observing displacement in inclinometer casing, likely reducing the time from a partially instrumented system from possibly several years (allowing all monitored landslides to displace prior to IPI installation) into only months after drilling is complete.

Debris Flow Detection

Previous studies, site history, and our site reconnaissance indicate that debris flows occur within the steep drainages and have deposited material on the highway (*4*). Debris flows are characterized by the rapid transport and subsequent deposition of a watery slurry of soil, rock, and organic debris. Where the grade becomes gentler or the channel geometry is dammed by an embankment, the slurry is deposited into a debris fan. A monitoring system that senses this deposition near an embankment's culvert inlet is proposed.

The proposed monitoring method would consist of a piezometer and an earth pressure cell, such as Geokon Model 4800 pressure cells, installed within a shallow, sand-filled pit within the creek bed near the culvert's inlet. This would detect the deposition of additional mass and be able to differentiate between loads from high creek flows and loads imparted by additional soil and rock material. This system would also alert TDOT Maintenance personnel about the possibility of clogged or blocked culverts. Ten drainages were identified and the inlets reconnoitered as previously described.

Automated Data Acquisition System

Automated data acquisition systems (ADAS) approaches can range from continuously collected sensor data intermittently downloaded from dataloggers by field personnel to an integrated network of sensors connected via radios and cellular modems and accessible from an office computer or mobile devices. The latter approach provides several benefits, including remote monitoring and automated email alerts to select personnel. The networks are often modular and

can be retrofitted to include additional sensors and peripheral devices, such as lighted signs acting as a warning system in later phases.

A frequently used approach is utilization of a modular, 900mHz radio-equipped datalogger system powered via solar panels with a 35 amp Hr battery and antenna within a polycarbonate enclosure, an example shown in
Figure **8**. Other options could include painted mild steel or stainless-steel enclosures with external antennas. In-ground/in-vault datalogging and radio telemetry are marketed by suppliers and may be more theft resistant; however, below-grade datalogging equipment is vulnerable to and frequently damaged by water intrusion. These 'nodes' communicate with a cellular modem-equipped base station that aggregates and communicates to a data presentation website, our and/or TDOTs servers, and via email or SMS communications.

Initially, notifications would be via scheduled emails and on-demand access via a website. Later, trigger-based notifications would be developed once relationships between water levels and landslide displacements are understood. Note that establishing data-based triggers can take several seasons of observation.



Figure 8: Example of a polycarbonate enclosure with solar panel. Radio communications are facilitated by an antenna within the enclosure.

Proposed Monitoring System with Telemetry Capabilities

System Elements

We recommend a monitoring system centered upon installed inclinometers and piezometers to measure landslide displacement and pore water pressures that triggered the displacement. These would be installed within both observed and interpreted landslides. Each of the locations were given an A, B, or C priority estimated to equate to the corridor's risk exposure due to the monitored landslide. 'A' prioritization are those locations with a higher likelihood of road displacement, 'B' and 'C' prioritizations were judged with medium-high, and medium likelihood, respectively. Due to the USGS mapping and presence of the shale of the Pennington Formation, the entire study area should be considered to have a 'medium-low' likelihood of landslides that could affect the road. Likewise, we recommend a debris flow monitoring and detection system for several candidate debris flow chutes, each with an A or B prioritization.

The installation of IPIs following detection of landslide movement versus installation of SAAs as part of drilling activities depends on TDOT's criteria for immediacy of full system functionality. As noted, SAAs will monitor the full depth of the boring for landslide displacement soon after installation, while IPIs are typically installed after a shear zone has been identified, which could be from weeks to years following drilling and multiple manual inclinometer readings. SAAs also have the benefit of being able to withstand more shear displacement than an IPI installed within an inclinometer casing.

An automated data acquisition system equipped with radios for local, intra-network communication capability and cellular modem(s) for communications with TDOT and/or LT servers and a data presentation website was recommended. A weather station to monitor climatic inputs was also recommended. Table 2 describes monitoring methods and reading intervals recommended for the project.

Table 2: Recommended Monitoring Elements and Reading Intervals

Monitoring Method	Reading Interval
Inclinometers and Piezometers	5-minute reading interval on ADAS, quarterly for manual inclinometer readings
Debris Flow Monitoring	5-minute reading interval
Weather Monitoring Station	5-minute reading interval
Automated Data Acquisition System	Hourly communication with data presentation website
Aircraft-Mounted Lidar	Yes, at annual or longer interval
SfM Photogrammetry	Quarterly to semi-annual
Satellite-based InSAR	A pilot study to determine applicability

SUBGRADE RESILIENCY IMPROVEMENTS

Geosynthetic Subgrade Improvements

Asphalt patches in the corridor were inventoried during our site reconnaissance efforts. Areas of patches, overlays, pavement and shoulder cracking were noted outside of the large landslide area on the north-facing slopes between LM 25.2 to 26.4. Many of these features are likely landslides below the road causing pavement distress. A total of eighteen locations were identified ranging in lengths between 100 to 1010 feet in length. Note that investigation and design activities will likely require adjustments to the approach, including installation of light weight fill, drainage improvements, or retaining walls.

Pavements and subgrades atop slowly displacing landslides can often be made more resilient to the underlying displacement with drainage improvements, geosynthetics, and improved backfill material. Eighteen areas have tentatively been identified for improvement with deep patches or similar resiliency improvement measures. Lengths between 100 and 1,010 feet were approximated. A total of 5,960 lineal feet of possible deep patches were identified. These sites require additional investigations to understand failure mechanisms and to design mitigation measures.

Resiliency Improvements for Deep, Long Horizontal Drains

The major landslide area between LM 25.2 and 26.4 has been experiencing additional distress in the highway, displacement of the haul road and separation of haul road fill and ground armoring from the base of the newly installed soil nail wall in some locations. This landslide area experienced significant displacement in 2019 and mitigation followed with horizontal drains, soil nail walls, and lined ditches. The existing horizontal drains are spaced at about 20 to 100 feet and are up to 100 feet long, based on plan drawings. Two rows of drains were installed, one below the roadway and one above the highway in the road cut. The lower row of drains are generally between 10 and 25 feet below the highway while those above are a similar depth below the ground surface. Some drains were producing water at the time of our site visits, suggesting that groundwater is being intercepted and drained and additional drains would be beneficial. Most drains were at the base of the soil nail walls and were typically dry at the time of our visits. Piezometers have not been installed in the area based on our review of background information.

Horizontal drains are most effective, based on our experience, when installed several hundred feet long in an array pattern with constant adjustment during installation to maximize water withdrawal. The collar location should be as low as possible, often drilled from a topographic low well below the highway to maximize the dewatering effect. Piezometers installed during a design phase and monitored in conjunction with automated or manual inclinometers provide critical information on the groundwater conditions that lead to landslide displacements. Often, lowering background water levels and reducing groundwater pore pressure spikes during and following storms will significantly slow or even stop landslide displacement. A marginal five percent factor of safety improvement, for example from 0.99 during a storm to 1.04, can significantly improve the resilience of roadways threatened by landslides.

To achieve this resilience improvement, GES should discuss temporary or permanent easements or ROW acquisition requirements when significant slope movement is observed. Subsurface easements to allow the drains to pass beyond ROW may be required. This additional permitting effort may require more time than anticipated but will often make the difference between minor and more meaningful stability improvements.

In our opinion, the landslide area defined by LM 25.2 and 26.4 is likely to be a good candidate for an expanded dewatering program consisting of 7 to 10 arrays, each consisting of horizontal drains 250 to 500 feet long. Other installation patterns may also be considered. The annotated cross section below illustrates a 290-foot long drain (red line) collared at a low point about 30 to 35 feet below the roadway. This hypothetical drain begins and ends beyond the ROW, but would have the potential to significantly reduce groundwater pressure (blue lines) acting on the shear zone (
Figure **9**). Pilot programs of one or two drain arrays also help to determine the effectiveness of a dewatering program before bid letting for complete programs and should be considered.

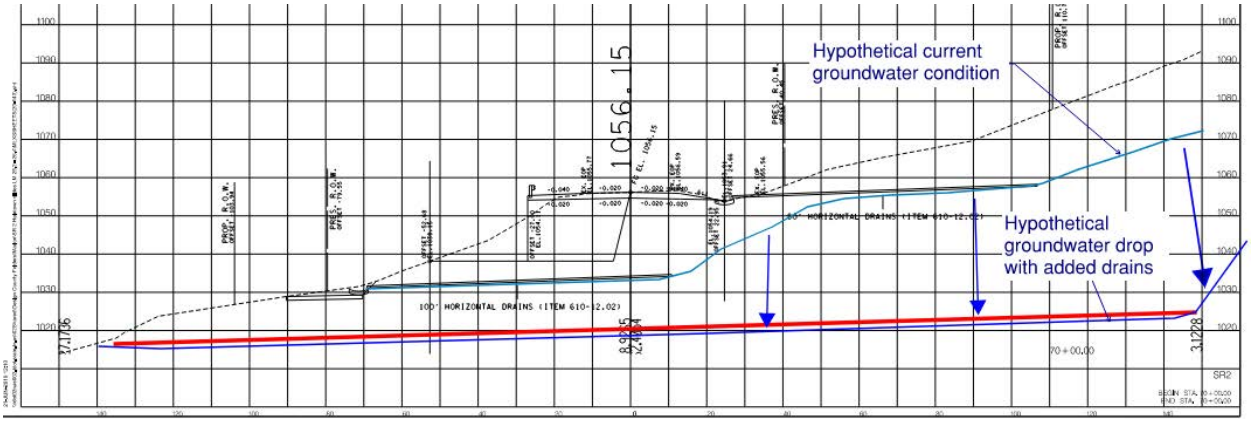


Figure 9: Hypothetical groundwater drawdown with longer drains installed from a lower elevation.

Conclusions

This case study, focusing on SR-2 in Tennessee, offers crucial insights for maintaining critical infrastructure in challenging mountainous regions worldwide. Effective roadway management hinges on understanding geologic conditions and their interaction with geotechnical assets like embankments, slopes, and culverts. By grasping the geomorphic and hydrogeologic characteristics of an area, we can better predict how soil and rock slopes will react to climate-driven changes. Various methods, including geotechnical instrumentation and remote sensing, can then be used to assess shifts in slope behavior. Ultimately, a corridor-wide approach allows for the cost-effective application of slope mitigation strategies across multiple sites sharing similar geological conditions.

REFERENCES

1. Hardeman, W. D., R.A. Miller, and G.D. Swingle, *Geologic map of Tennessee* [Map]. Tennessee Division of Geology, 1996. https://ngmdb.usgs.gov/Prodesc/proddesc_91768.htm

2. Milici, R.C., C.P. Finlayson, R.H. Barnes, and J.M. Colvin, Jr., *Geologic Map and Mineral Resources Summary of the Sequatchie Quadrangle* [Geologic Quadrangle Map 100 SE]. Tennessee Division of Geology, 1986.

3. BFW Engineering and Testing, Inc. *State Route 2 Landslide Investigations State Project Number: 58002-4245-04 PIN Number: 128666.00 GES File Number: 5810918*, 2020.

4. Thomas, R.E. *Landslides and related features, Tennessee-Chattanooga 1 degree x 2 degree sheet [64 quadrangle sheets]* [Map]. U.S. Geological Survey, 1981. https://ngmdb.usgs.gov/Prodesc/proddesc_55234.htm

5. Mines, A.E., D.L. Beckstrand, and M.D. Bunn, Landslide Technology, Missouri Department of Transportation, & Federal Highway Administration. *Landslide Monitoring Methods: Application of Existing Technologies to Long-Term and Real-Time Monitoring of Slope Movements* (01878778; Final Report, p. 87p) [Digital/other], 2023. https://spexternal.modot.mo.gov/sites/cm/CORDT/cmr23-002.pdf

6. Ellis, H.L. and M.J. Vessely,*Visualization of Geotechnical Data for Hazard Mitigation and Disaster Response* (01553725; Issue 467). Transportation Research Board, 2015. http://www.trb.org/Publications/Blurbs/172036.aspx

7. Anderson, S., M. Vessely, and C. Christiansen, *Advances in Unstable Slope Instrumentation and Monitoring* (01747737; Issue 554). Transportation Research Board, 2020. http://www.trb.org/Main/Blurbs/181075.aspx

8. Bürgmann, R., P.A. Rosen, and E.J. Fielding, Synthetic Aperture Radar Interferometry to Measure Earth's Surface Topography and Its Deformation. *Annual Review of Earth and Planetary Sciences*, *28*(1), 2000, pp. 169–209. https://doi.org/10.1146/annurev.earth.28.1.169

9. Fergason, K., B. Panda, D. Williamson, Highway Geology Symposium. (2014). *Utilizing InSAR for Landslide Asset Management in Colorado* (01639998), 2014, pp 149-162. http://www.highwaygeologysymposium.org/wp-content/uploads/65_HGS-OPT.pdf

10. Cornforth, D. (2005). *Landslides in Practice: Investigation, Analysis and Remedial/Preventative Options in Soils* (Vol. 1). John Wiley & Sons, 2005.

Measuring From a Distance
Teton Pass Remote Monitoring Technology

Hunter Hinckley, P.G.
Wyoming Department of Transportation
5300 Bishop Blvd.
Cheyenne, WY 82009
(307) 777-4786
hunter.hinckley@wyo.gov

Prepared for the 74th Highway Geology Symposium, August, 2025

Acknowledgments

The author(s) would like to thank the individuals/entities for their contributions to the work presented in this paper:
James Dahill (PG) – Wyoming Department of Transportation
Jeff Booher (PE) – Wyoming Department of Transportation
Seth Wittke (PG) – Wyoming Department of Transportation
Lief Swanbom (PG) – Wyoming Department of Transportation
Todd Sullivan (PG) – Wyoming Department of Transportation
Michael Killion (PG) – Wyoming Department of Transportation
Ben Arndt (PE) – RJ Engineering and Consulting, Inc.
John S. Metzger – AssetAssurance Monitoring, LLC.

Disclaimer

Statements and views presented in this paper are strictly those of the authors, and do not necessarily reflect positions held by their affiliations, the Highway Geology Symposium (HGS), or others acknowledged above. The mention of trade names for commercial products does not imply the approval or endorsement of HGS.

Copyright Notice

Copyright © 2025 Highway Geology Symposium (HGS)

All Rights Reserved. Printed in the United States of America. No part of the publication may be reproduced or copied in any form or by any means – graphic, electronic, or mechanical, including photocopying, taping, or information storage, and retrieval system – without prior written permission of the HGS. This excludes the original author(s).

ABSTRACT

Weather conditions leading up to June 8, 2024, created a "perfect storm" triggering a catastrophic failure on a hairpin curve located along highway WY-22 of the Teton Pass corridor. The collapse severed a critical scenic and economic route between Victor, Idaho and Jackson Hole, Wyoming, an important lifeline for tourists and commuters. Consequently, WYDOT faced a hyper-compressed timeline with significant reconstruction challenges to open a temporary detour, while simultaneously redesigning and constructing a permanent repair. WYDOT Geology deployed several remote sensing and remotely accessed instruments, safely and efficiently aiding a heavily accelerated reconstruction process.

As reconstruction efforts began, a detour was designed and built in three weeks, and remote monitoring methods became a vital data collection tool, greatly assisting in the observation of site conditions post-failure. Monitoring equipment instrumentation included: InSAR satellite and ground-based side-scanning radar, SAA telemetry inclinometers, and telemetry piezometers. Remote technology provided instant and continuous round-the-clock access to data, enhancing safety while limiting site visits. Due to extensive travel distances, the suite of remote detection tools were maintained throughout the failure and during construction to achieve an accurate assessment of ground conditions. These tools tracked surface heaving and subsidence movement using satellite InSAR and ground-based radar scanning, subsurface shifts using in-ground inclinometers, and water levels using telemetry piezometers. Monitoring communications from remotely accessed equipment and from field personnel over great distances ensured clear understanding and greater situational awareness. This assessment details the steps taken to install, monitor, and analyze a combination of remote sensing and remotely accessed instruments, and lessons learned throughout the process.

INTRODUCTION

A variety of innovative and new project monitoring and modeling tools were implemented to investigate a 200-foot-long landslide affecting highway WY-22 over Teton Pass. The geology and engineering properties of subsurface soil conditions were critical to understand and accurately assess the implementation of a speedy, robust, and safe design. Technologies employed on this project included tools such as InSAR satellite and ground-based side-scanning radar, SAA telemetry inclinometers, and telemetry piezometers. WYDOT's first robust implementation and installation of remote technology provided much-needed information and greatly increased the program's capacity to understand site conditions on a remote and distant project. The tools deployed, in this case, were used to protect workers and the traveling public from further geohazard-related events. During construction, internet connections and real-time data improved communications amongst several entities, including but not limited to WYDOT. This paper will highlight the remote tools used and how the Geology Program implemented these technologies successfully. The objective of this paper is to provide a comprehensive assessment that details the steps taken to install, monitor, and analyze a combination of remotely accessed sensing instruments and lessons learned throughout the process.

SITE DESCRIPTION AND HISTORY

Wyoming Highway 22, otherwise known as the Teton Pass Highway, was originally constructed in the mid-late 1960s. On June 8, 2024, an embankment failure developed on WY-22 at MP 12.8, seven miles west of Wilson, WY in Teton County. The road section at MP 12.8 received the name "The Big Fill" due to the height of the fill placed within a large draw to meet grade. This section of roadway was built on a steeply graded slope averaging 10%. Available As-Built plans show an approximate fill height of 70-75 feet on the North side of the failure, which recedes to fill heights of 40-45 feet moving downgrade and to the South. Material types used for fill were not identified within available original plan sets; however, exposed fill at the headscarp indicates material was likely sourced from exposed outcrops of nearby limestone and dolomite, primarily composed of Mission Canyon Limestone and Bighorn Dolomite Formations. Investigative drilling throughout the site confirmed abundant dolomitic and limestone cobbles and boulders within a clay matrix throughout the fill material *(1)*.

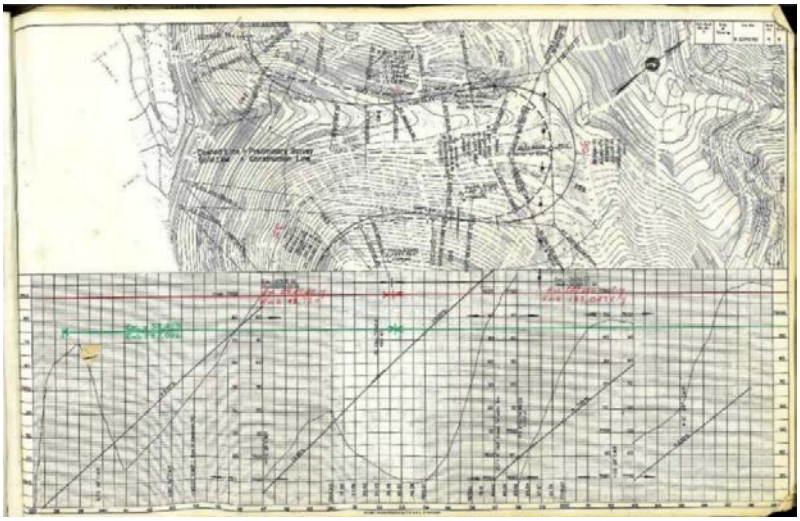


Figure 1 – Schematic for proposed road alignment and grading from original plan set of the hairpin curve of WY-22 at MP 12.8.

GEOLOGIC CONDITIONS

Mapping of the subsurface along the Teton Pass corridor was completed and published by Schroeder M.L. and Zeller *(5,6)*. Each published map has conflicting figures of the bedrock formation positioned below the placed fill, which ranged in thickness from 40 to 70 feet. Concealed by embankment material, numerous mapped faults are located under and near the hairpin turn at MP 12.8. The fill material of "The Big Fill" landslide is situated atop and between two major faults, the Cache Creek Fault and the Jackson Fault. The hairpin curve at MP 12.8 sits upon the footwall, formed between the two hanging walls of the mapped faults, exposing steeply dipping to vertical bedrock identified as the Bear River Formation and Aspen Formation by Schroeder, M.L. and the Frontier Formation by Zeller. Bedrock of the Bear River Formation is composed of olive green to dark gray shale with interbedded olive gray, calcareous sandstone, while exposed Aspen Formation bedrock is described as dark gray to olive green siltstone and shale, with fine to coarse grain arkosic salt and pepper sandstone, containing interspersed, interbedded black and white porcelanite *(5)*. The Frontier Formation is mapped consisting of dusky to yellow fine-grained sandstone and yellowish to gray shale containing interbedded lenses of coal and porcelanite *(6)*. Investigative drilling and dug test pits, confirmed the steeply dipping bedrock of highly interbedded shales, siltstones, and sandstones. For a more detailed and comprehensive analysis on the geologic conditions of this site refer to Lief Swanbom's HGS paper, Geology of the Big Fill Landslide.

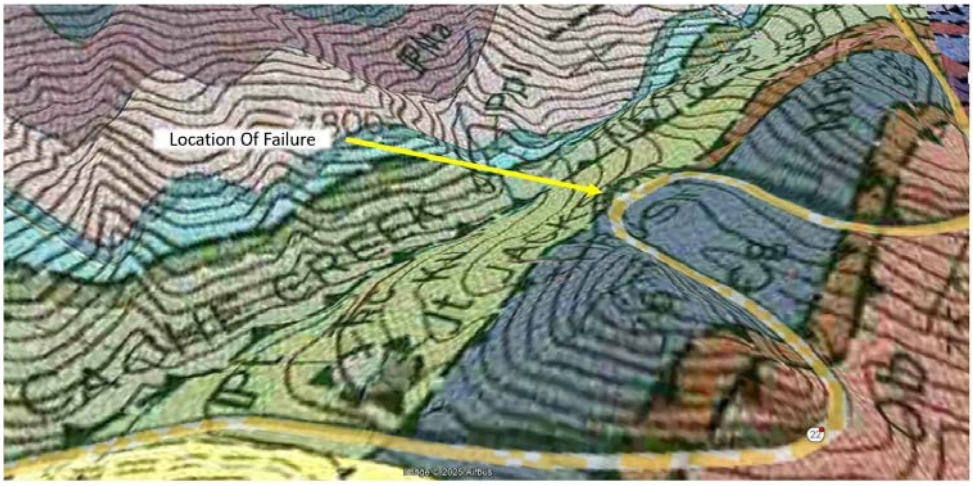


Figure 2 – Subsurface geologic bedrock map at hairpin turn at MP 12.8, mapped by Schroeder, M. L., 1972. Bedrock of the Bear River and Aspen Formations between the Cache Creek and Jackson Fault *(5)*.

TIMELINE OF EVENTS

A brief timeline of events is necessary to demonstrate the flurry of activity post-failure and the necessity for real-time information. An abridged description of the timeline and events detailing the reaction to the catastrophic failure, followed by an organized chronological list of events is in the following paragraphs. Methods, details, and data relating to the installation and monitoring equipment will be elaborated upon later in the report.

Fall 2023

Prior to the catastrophic failure, one inclinometer was installed just beyond the guardrail outside of the hairpin curve in the fall of 2023, providing ground movement information. This inclinometer was installed with a drill rig mobilized via crane, contracted through Salisbury Drilling, Figure 3. Inclinometer completion occurred on August 4, 2023, and initialization followed on August 24, 2023. Subsequent readings of this inclinometer occurred on October 9, 2023 and May 15, 2024, showing a slight 0.07 inches of movement *(2)*. As noted later within this report, warming weather trends from local SNOw TELemetry (SNOTEL) sites were recorded beginning May 23, 2024, sixteen days before the catastrophic failure. The final survey to record data from this inclinometer SL23-01 (TBF-01) occurred during WYDOT Geology's rapid deployment to the site on the afternoon of June 6, 2024, two days before the catastrophic failure. When investigated, the headscarp was actively moving, and the inclinometer probe could not reach past a depth of 70 feet, indicating a shear elevation of 7,592 feet.

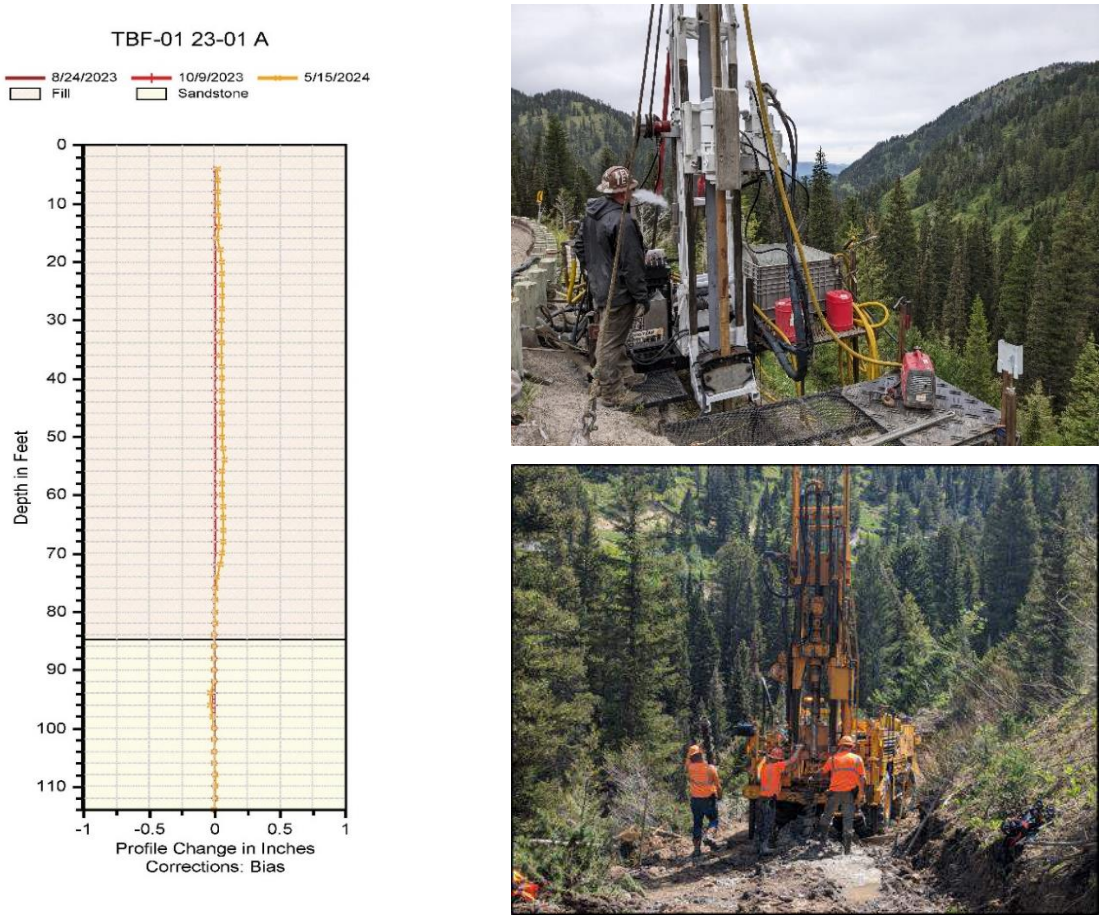


Figure 3 – Left: Inclinometer reading from May 15, 2024, indicating minimal lateral movement (<0.1 inches) at a depth of approximately 74 feet. Right Top: Salisbury portable drill rig installing inclinometer TBF-01. Right Bottom: WYDOT ATV drill rig conducting investigative borehole drilling.

Summer 2024

WYDOT Geology deployed to the site after reports of road distress and a motorcyclist lost control, hitting a crack and suffering minor injuries, on June 6, 2024. The morning of June 7,

2024 a large mudflow at MP 15 closed the Teton Pass Highway. Before the failure at MP 12.8, WYDOT Geology noticed tension cracks with 3-inch vertical offsets, actively widening and growing at a rate of 2-3 inches per hour. As noted, WYDOT Geology gathered measurements from an inclinometer SL23-01 (TBF-01), revealing a slide plane between 70-74 feet below the road surface *(1)*. The highway remained closed due to the mudflow at MP 15 and imminent failure at MP 12.8. That night between June 7 and June 8, a catastrophic failure occurred along the headscarp, affecting both lanes of traffic. Meetings followed between WYDOT and the US Forest Service for preliminary considerations to determine an alternate detour alignment. WYDOT Geology's geotechnical investigation began immediately, drilling five investigative boreholes, simultaneously with detour excavation and construction beginning June 10. Concurrently, WYDOT contracted with RJ Engineering to begin modeling slope failure, performing analysis for a detour route, and beginning analysis for a final roadway fix. On June 11, aerial surveys were conducted throughout the "The Big Fill" failure and the MP 15 mudslide corridor and were compared to previously mapped pre-failure surfaces.



Figure 4 – Left: initial tension cracks forming at the headscarp on June 6, 2024. Right: Widening tension cracks observed at the headscarp on June 7, 2024.

The Geology Program drilled four additional boreholes, three of which were in prospective locations for monitoring instrumentation. Inclinometer cased boreholes SL24-09 (TBF-02) and SL24-12 (TBF-03) were installed near the headscarp while a water-monitoring test hole was drilled and cased. Additionally, RJ Engineering completed its slope stability analysis of the detour roadway. Confirmation from the contracted engineer of the temporary detour's slope stability allowed WYDOT to authorize and open the detour to the public, June 28, 2024. For a more detailed and comprehensive analysis on the drilling, logging, investigation, and subsurface conditions of this site, refer to Lief Swanbom's HGS paper, Geology of the Big Fill Landslide.



Figure 5 – Completed construction of temporary detour, July 2024.

The first week of July, instrumentation monitoring of the failed area began in earnest with the installation of a side-scanning radar, set up and activated to monitor change detection from the hillside opposite the failure. Initialization of inclinometers TBF-02 and TBF-03 allowed for manual downhole probe measurements, while borehole SL24-10 (MW-10) was installed for a piezometer.



Figure 6 – Borehole location map.

Early July, WDOT began the final design through the Construction Manager/General Contractor (CM/GC) process with Ames/Keller and RJ Engineering. In early August 2024, excavation, shoring, and stabilization of failed material within the excavated backslope began. Keller, the subcontractor, installed soil stabilization nails along the entire excavated backslope, while Ames continued to excavate the failed material. WYDOT's existing inclinometers and water monitor casings required removal, as they were positioned within the proposed excavation limits. Consequently, SL24-12 (TBF-03) was destroyed while the inclinometer casing within SL-09 (TBF-02) and the piezometer casing in SL24-10 (MW-10) were severely damaged. Returning to the site, the Geology Program was able to rehabilitate the casing for the piezometer and one

inclinometer, re-establishing new elevations for the damaged casings. Finally, Keller mobilized to begin drilling soil nails 30 to 60 feet into the backslope. Rather than risk damaging the recently shipped remotely accessed SAA inclinometer, it was decided to continue manual downhole probe readings of the inclinometers site-wide until soil nail drilling operations reached an elevation below the bottom of the casing.



Figure 7 – Installation of micropiles at the base of excavation and drilled soil nails shoring the excavation slope, September 2024.

Fall 2024

After the soil nail installation, the remotely accessed SAA inclinometer and telemetered piezometer were initialized on September 24, 2024. Simultaneously, four rows of micropile were drilled vertically at the base of excavation beginning the week of September 20, 2024. After completion of excavation, soil nail shoring and micropile installation, five horizontal drains were installed at the base of excavation on October 8, 2024. Following micropile and drain blanket preparation, work began to rebuild the fill slope. Backfilled material consisted of alternating 4-foot lifts of foamed glass and processed existing material at the site. The lifts were stair stepped, as elevation increased on the foreslope, with material contained by Hilfiker wire baskets.

Side-scanning radar monitoring continued until the fill was constructed to a sufficient height, stabilizing the excavated slope throughout the winter. The contract was completed with the final report occurring on November 3, 2024. Construction ceased on the slope December 13, 2024, moving into the winter season, while WYDOT Geology continued to monitor remote-accessed instruments, sending weekly updates.



Figure 8 – Fill construction utilizing 4-foot alternating lifts of foamed glass and processed backfilled material, December 4, 2024

Spring 2025

Construction would begin again on April 1, 2025, as WYDOT Geology continued to monitor rising groundwater conditions and subsurface movement.

WEATHER

Weather is anticipated to be a large contributing factor prompting the failure. Two weeks prior to the date of the catastrophic failure, temperatures across the south end of the Teton Mountain Range began warming. Weather stations, including a SNOTEL site at Phillips Bench and a weather station located at MP 12, run by the Bridger-Teton Avalanche Center, gathered data confirming this warming weather *(4)*. After May 23, 2024, average temperatures began to rise. After a week of warming, beyond May 30, the daily minimum temperatures no longer dropped below freezing *(1)*. On June 3, 2024, instrumentation at Phillips Bench recorded a rainfall event logging 1.2 inches of rainfall *(3)*. In addition, the absence of daily freezing temperatures led to the continuous melting of snowpack Figure 9. Snow measurements recorded at the Phillips Bench SNOTEL site recorded losses of 53 inches of total snow depth, equating to 18.4 inches of total snow water equivalent precipitation and translating to snowmelt rates of 1.83 inches per day, 0.69 inches per day between May 9, 2024 and June 7, 2024, Figure 9 *(3)*. This rapid snowmelt likely facilitated the catastrophic failure. However, according to historical data gathered from the Phillips Bench SNOTEL site, 2024 spring runoff was not significantly abnormal compared to other years in terms of amount of snowpack or the runoff rate Figure 10 *(3)*. For additional analysis on the broad, regional weather conditions near this site refer to Lief Swanbom's HGS paper, Geology of the Big Fill Landslide.

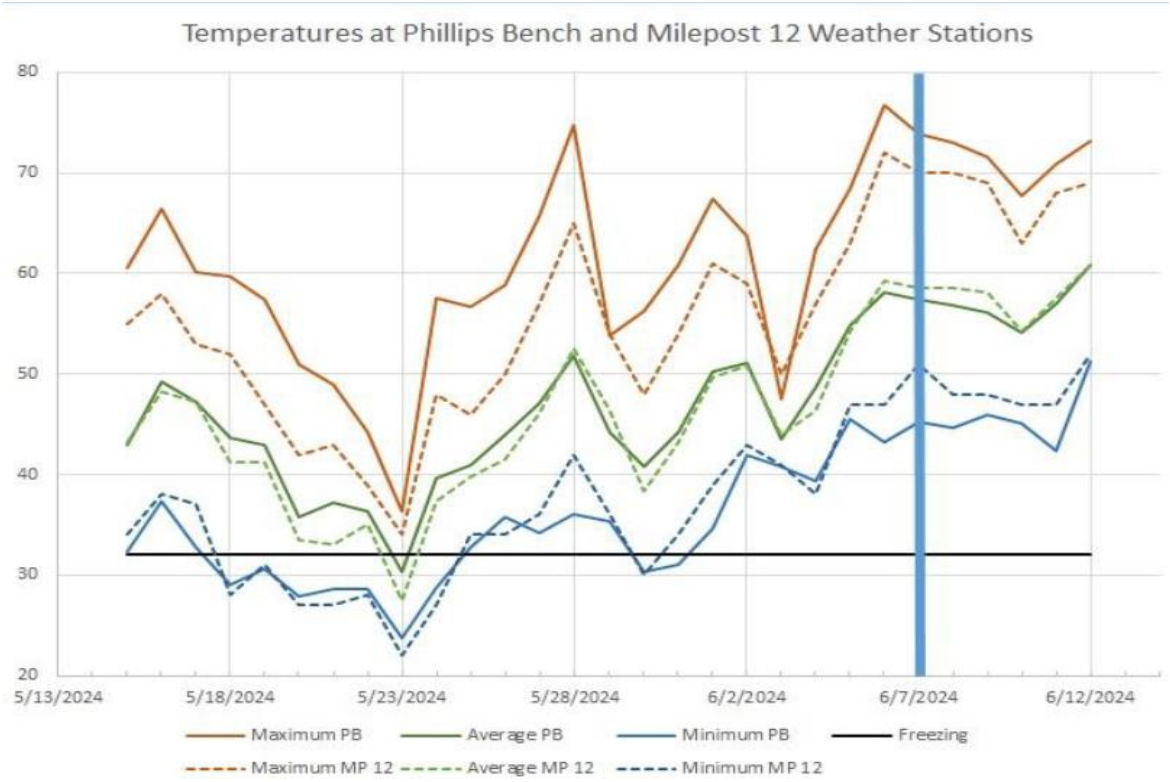


Figure 9 – Graph from Seth Wittke showing maximum, minimum, and average temperatures (F°) at the Phillips Bench (PB) and Milepost 12 (MP 12) weather stations. Black horizontal line denotes 32° F. Blue vertical line denotes June 7th, 2024 *(1)*.

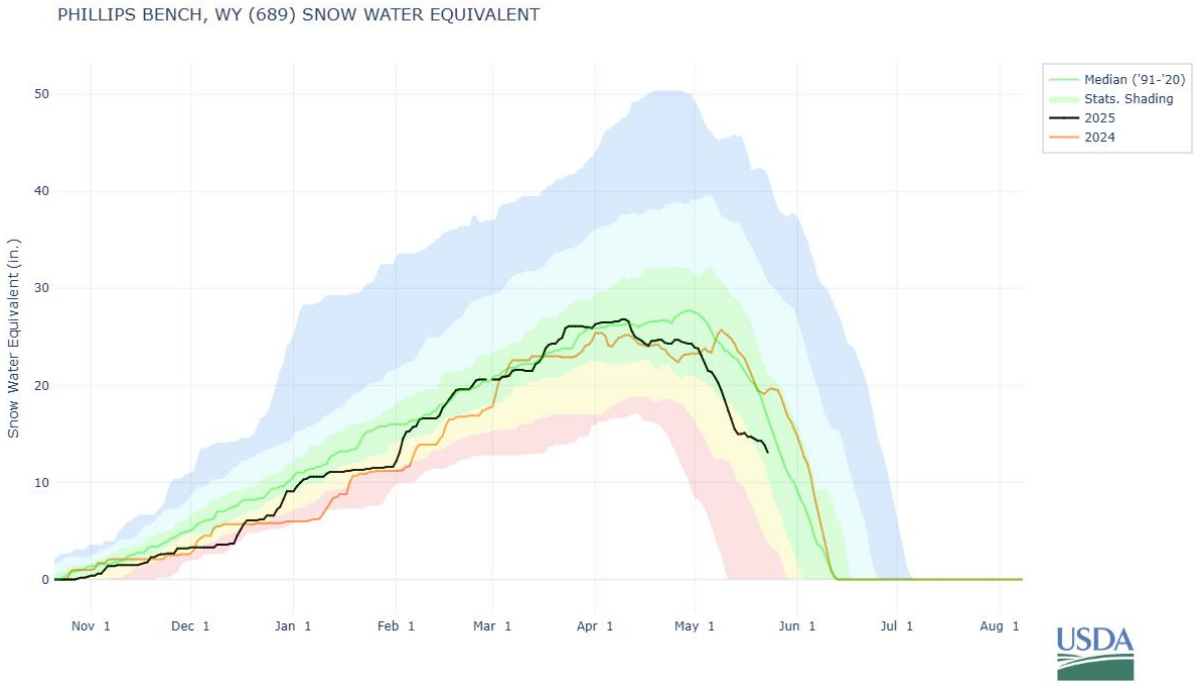


Figure 10 – Phillips Bench SNOTEL site graph showing the last two years of spring runoff compared to mean in measurements of snow water equivalent *(3)*.

REMOTE MONITORING INSTRUMENTATION

Groundwater Monitoring

WYDOT Geology drilled two water monitoring wells to capture information and model groundwater near the headscarp of "The Big Fill" landslide. Boreholes SL24-10 (MW24-10) and SL24-14 (MW24-14) were drilled on June 26 and August 21, 2024 respectively.

On July 3, 2024, WYDOT Geology installed a (non-remote) Solinst M60 barologger and a levelogger piezometer in casing MW24-10. The instrumentation collected water level readings once a day, with data downloads occurring at minimum once a week via the Jackson Hole engineer's office. Daily readings continued until August 2, 2024, when the contractor broke the top of the water monitor casing. WYDOT Geology redeployed to Teton Pass to recover the damaged instrumentation. A heavily damaged barologger was the only water monitoring instrumentation recovered. Assessing workers' safety in the short term and inclement weather in the future, WYDOT Geology saw it imperative to observe groundwater conditions in real-time. On August 2, workers began to occupy the base of the slope with excavation and soil nail installation firmly underway. Limited access, due to snowpack throughout fall, winter, and spring seasons, necessitated telemetry piezometer data.

The remotely accessed piezometer was installed in borehole MW24-10. With the broken casing, a new top of casing elevation was established at 7660.4 feet, reduced 4.98 feet from the prior top of casing elevation 7665.38 feet and leaving 2.25 feet of "stick-up" casing above ground level. With the placement of borehole MW24-10 in the middle of the slope, WYDOT Geology positioned the Solinst M60 levelogger piezometer attached to a Solinst levelsender telemetry system at a depth of 52.9 feet within the monitor well. A heavy influx of sediment was observed within the monitoring well just after it was damaged by equipment. WYDOT Geology made multiple unsuccessful bailing attempts to remove the infilled sediment. Subsequent measurements confirmed the borehole had infilled with 8.32 feet of material, shortening the borehole length from 69.9 to 56.6-feet. The infilled material reduced the bottom hole elevation from 7595.48 feet to 7603.8 feet. Using a water tape, groundwater water measured at an elevation of 7610.79, leaving approximately seven feet of water column within the monitoring well. Installation of the remotely accessed piezometer to a depth of 52.9 feet created a new instrumentation baseline elevation at 7607.5 feet, leaving three feet of measured water column above our instrument.

A subscription plan to the Solinst data cloud allowed readings to be recorded and sent after its installation on October 16, 2024, sending data once a day at 07:00 am. Data collection beginning in June revealed high water levels, which steadily declined until August 27, 2024. At which point water levels maintained an approximate elevation of 7610.6 feet. Minor dips in water elevations occurred throughout the fall and winter. Sensors at MP 12 of the Bridger-Teton Avalanche Center recorded rising minimum daily temperatures above freezing after March 27, 2025, coinciding with an increase of three feet of water in MW24-10, between March 27 and May 26, 2025, Figure 11 *(4)*. Aiding as a control, MW24-14 the (non-remote) piezometer has been recording daily water levels since installation August 22, 2024 and has shown nine feet of water column increase in the same spring season time frame as piezometer MW24-10, Figure 12.

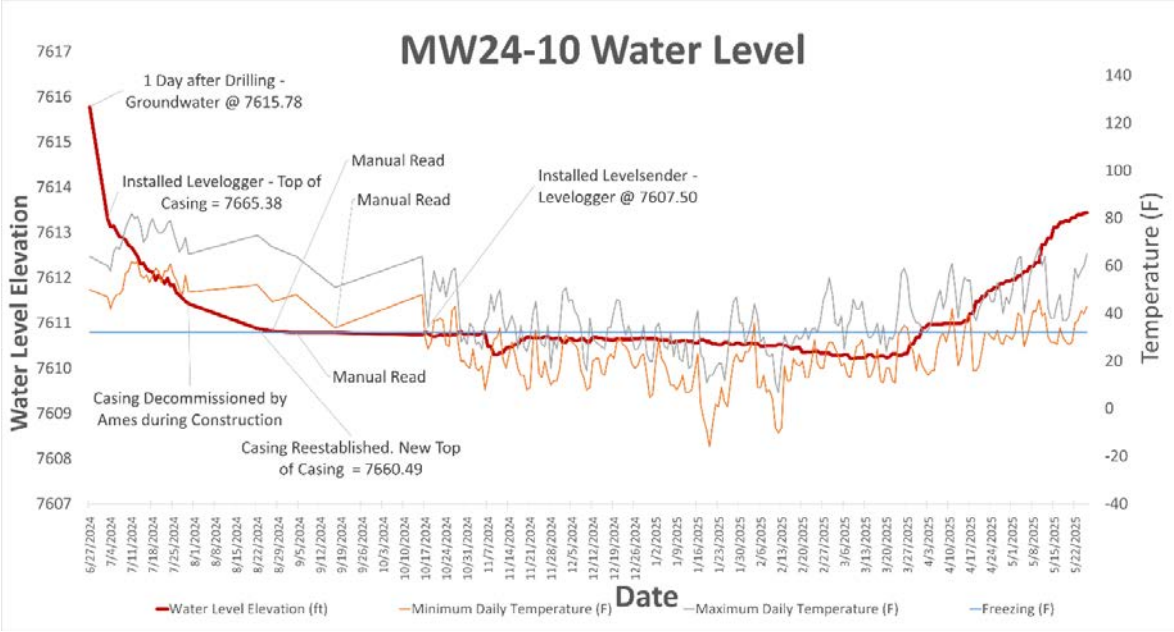


Figure 11 – Graph displays water level data from telemetered piezometer alongside minimum and maximum daily temperatures from the Bridger-Teton Avalanche Center website, spanning June 27, 2024, to May 15, 2025 *(4)*.

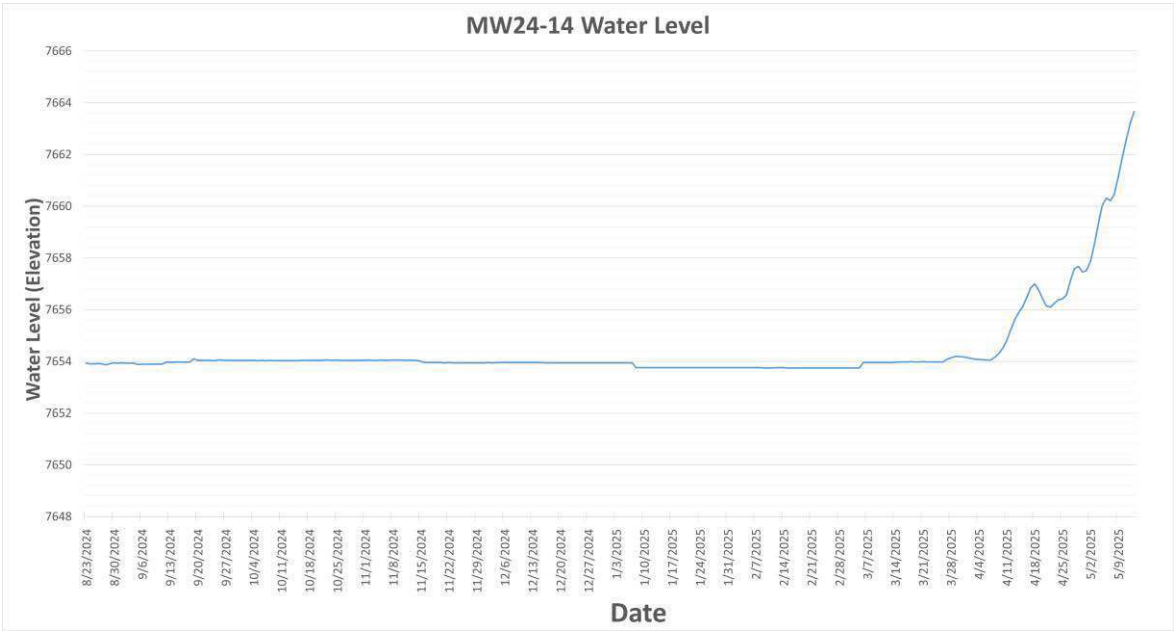


Figure 12 – Graph displays water level data obtained from manually read piezometer measurements, spanning June 27, 2024, to May 15, 2025.

INSAR

Satellite INSAR (Interferometric Synthetic Aperture Radar) technology was employed throughout the Teton Pass corridor. Data of millimeter resolution was retrieved from 625 analysis points within the grid

containing the failure at MP 12.8, detecting surficial displacement *(9)*. Focusing on cross-sections through the hairpin curve at MP 12.8, INSAR data displayed abundant subsidence above the failed section with minor subsidence and some heaving on the switchback downgrade of the failure *(8)*.

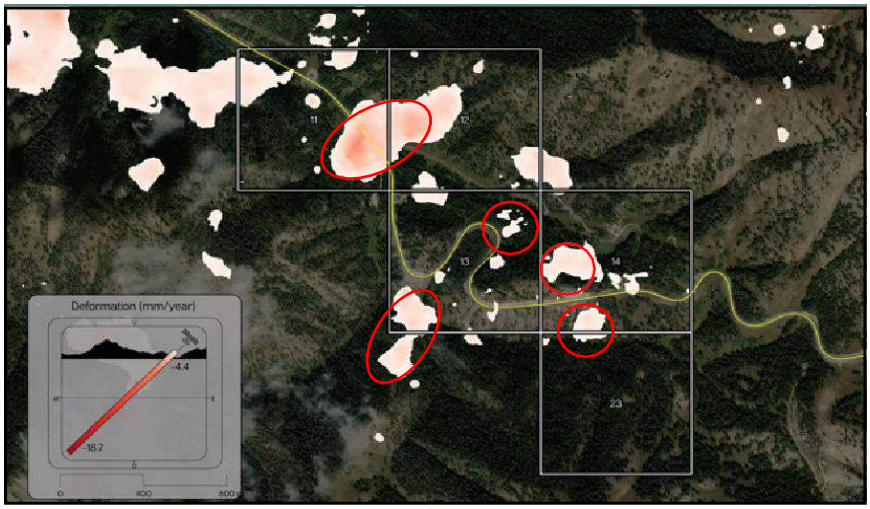


Figure 13 – Subsidence patterns identified peak rates of subsidence at -10.4 mm/year through InSAR analysis along Highway 22. Notable pockets of subsidence were observed in grid cell 13, north of the excavation area, with a larger pocket to the south, confirming previous InSAR reports of east-west trending subsidence *(9)*.

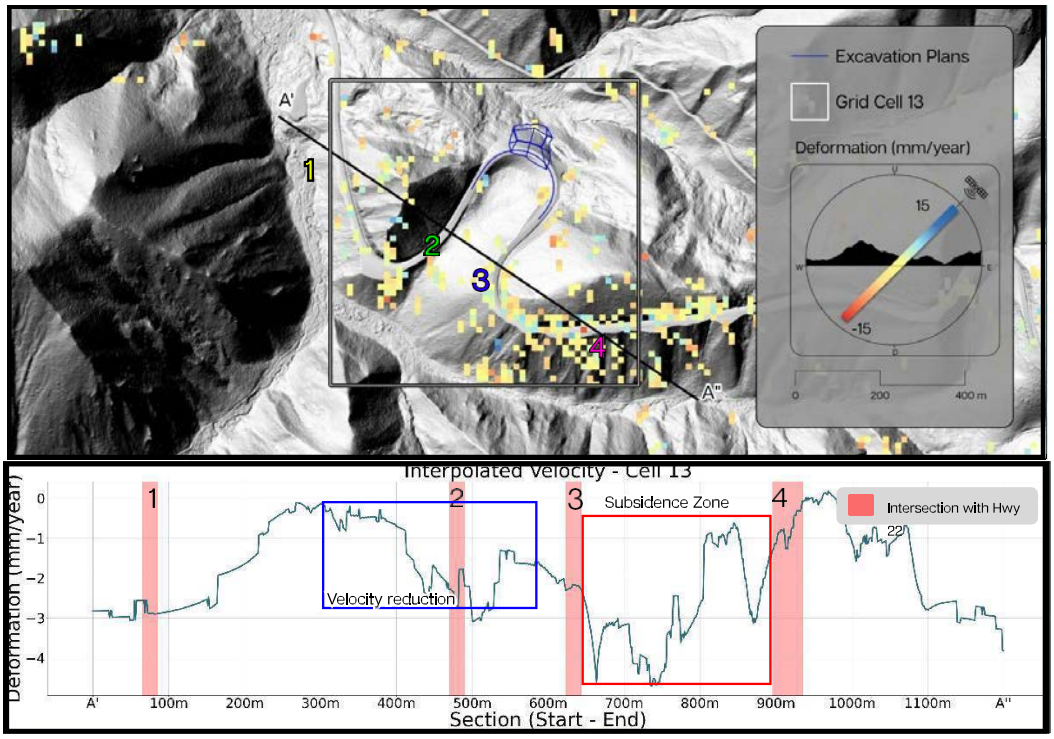


Figure 14 – Plan view and cross-section displaying the velocity surface deformation over grid cell 13. The analysis shows subsidence and westward movement trends, with prominent subsidence on the north-facing slope between intersections 3 and 4, lessening near intersection 2 *(8)*.

GBinSAR

Installed on July 1, 2024, Leica Geosystems (IDS GeoRadar) installed a mobile trailer, containing GBinSAR (Ground Based Interferometric Synthetic Aperture Radar) on the opposite hillside oriented at the failed slope. WYDOT's request consisted of continuous scanning of the failed material to assess displacement and stability, as the temporary detour was constructed and opened. After the temporary detour opened to the public, removal of the failed material began, opening an excavated face of fill material. Heavy machinery operations obscured observations at active work elevations, creating considerable movement signals where the contractor was relocating large amounts of material around the worksite. However, as workers descended, with excavation limits moving lower in elevation, the side scanning radar analyzed the exposed face. To aid in the safety of the workforce and the traveling public, a Trigger Action Response Plan (TARP) was developed to maintain communication between all parties in WYDOT, the construction team, and the slide monitoring team. Priority levels of escalating ground conditions were reported daily in a Level I status. Prospective priority reporting levels during monitoring increased from warning levels, LEVEL I: Project General Stability to Level IV: Impending Slope Failure. At the escalation to Priority Level III, site evacuations and road closures would already be underway, with Level IV initiating emergency evacuations and road closures.

Construction continued into the late fall as the side scanning radar conducted measurement readings every two minutes. Assessing displacement throughout the excavated face, AssetAssurance Monitoring LLC (AAM) continued to send daily monitoring reports to WYDOT personnel. Using hazard maps created within the daily reports, WYDOT Geology tracked displacement areas throughout the excavated and soil nailed face, Figure 16 *(10)*. Observations revealed steady but minor displacement away from the slope throughout the upper soil nail wall. AAM submitted the final daily report tracking displacement on November 3, 2024, while Leica Geosystems removed their instrumented trailer on November 30, 2024.



Figure 15 – Left: Leica Geosystems (IDS GeoRadar) side-scanning radar trailer deployed for remote sensing monitoring. Right: AssetAssurance personnel conducting a site survey above the headscarp of failure.

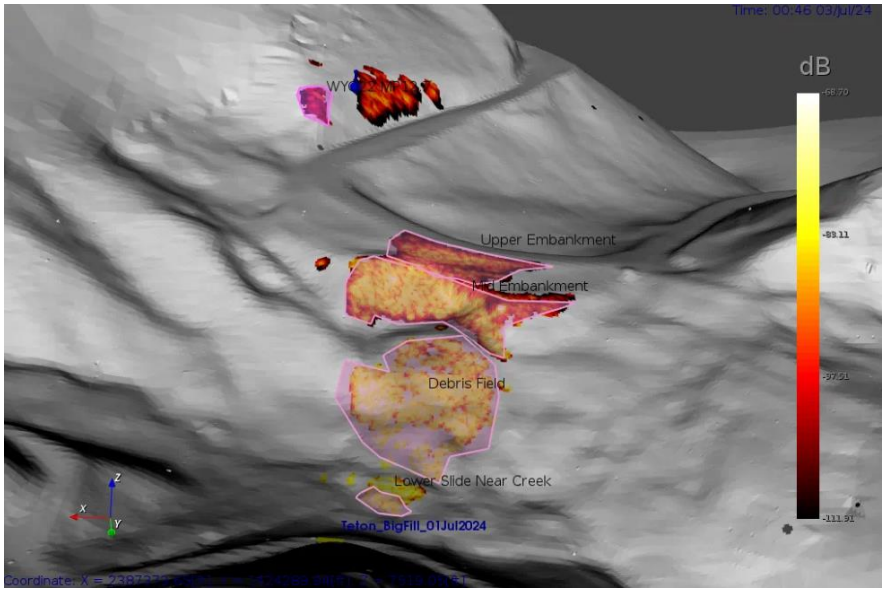


Figure 16 – Heat map illustrates displacement throughout failed material, recorded between July 1 and July 2, 2024 *(10)*.

Shapeaccelarrays Inclinometer (SAAs)

After the failure at MP 12.8, WYDOT entered into an emergency contract to install a temporary detour. The temporary detour consisted of a sharper curve and steeper alignment. The new 600-foot-long temporary curve sat at a grade of 11.2 percent. To monitor and gather data for the potential stability of a temporary detour, inclinometers SL24-09 (TBF-02) and SL 24-12 (TBF-03) were installed near the headscarp of the slide, which were drilled and cased on June 26, 2024 and June 27, 2024 respectively.

Initialization of TBF-02 and TBF-03 occurred on July 2, 2024, via manually operated landslide monitoring instruments, using a DGSI inclinometer probe and reel. Data gathering of inclinometers TBF-02 and TBF-03 occurred frequently, with a steady rate of collection ranging from every day to every other day. WYDOT personnel rotated to the failure site to conduct measurements maintaining a steady rate of monitoring and lasting until both casings were compromised on August 8, 2024.

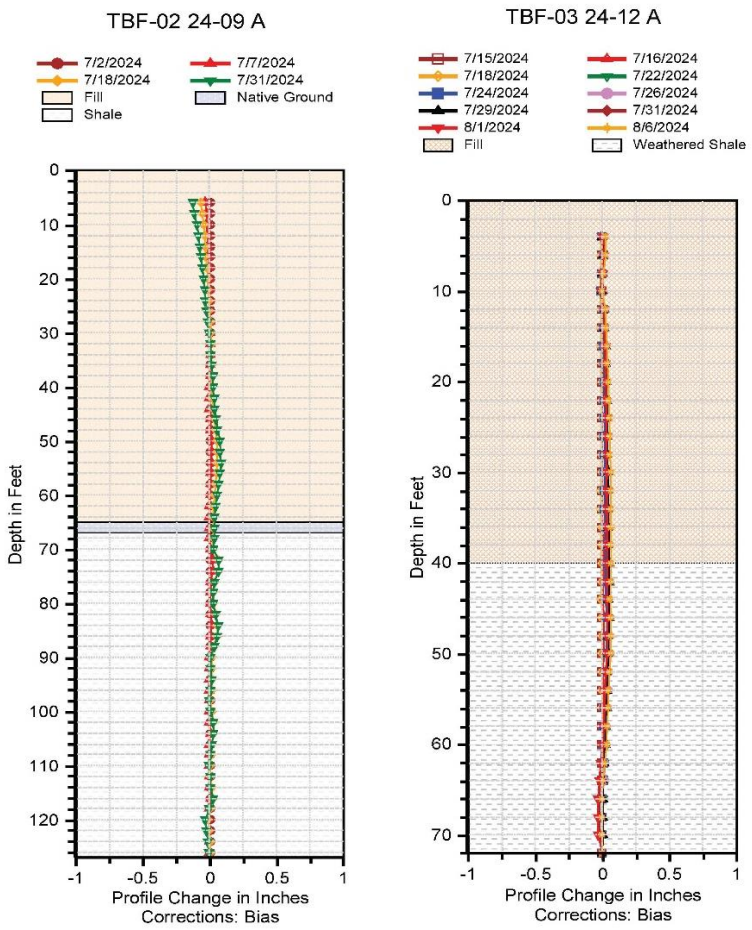


Figure 17 – Manually read inclinometer data from TBF-02 and TBF-03, indicating minimal displacement after slope failure until excavation construction began on August 8, 2024.

On August 8, 2024, the "stick-up" casing in test hole SL24-09 (TBF-02) was severely damaged, while SL24-12 (TBF-03) was damaged beyond repair. Additional drilling occurred on August 20, 2024 to reestablish SL24-12 (TBF-03) in its original location; this location was re-drilled, becoming inclinometer SL24-13 (TBF-05). Additionally, WYDOT Geology was able to remove most of the obstruction, re-establishing communication in borehole labeled SL24-09 and re-establish a new inclinometer SL24-09 (TBF-04). Manual readings continued at both inclinometer locations until September 24, 2024, the date of installation of the SAAs within borehole SL24-13 (TBF-05).

Anticipated installation dates of the SAA inclinometer were scheduled for earlier in the year, however, soil nail installation for temporary shoring during the excavation began August 16, 2024. Four vertical rows of drilled soil nails were positioned extremely close to the inclinometer casing in SL24-13, influencing WYDOT Geology's decision to delay the installation of the SAA inclinometer until drilling reached an elevation below the bottom depth of the existing inclinometer casing.

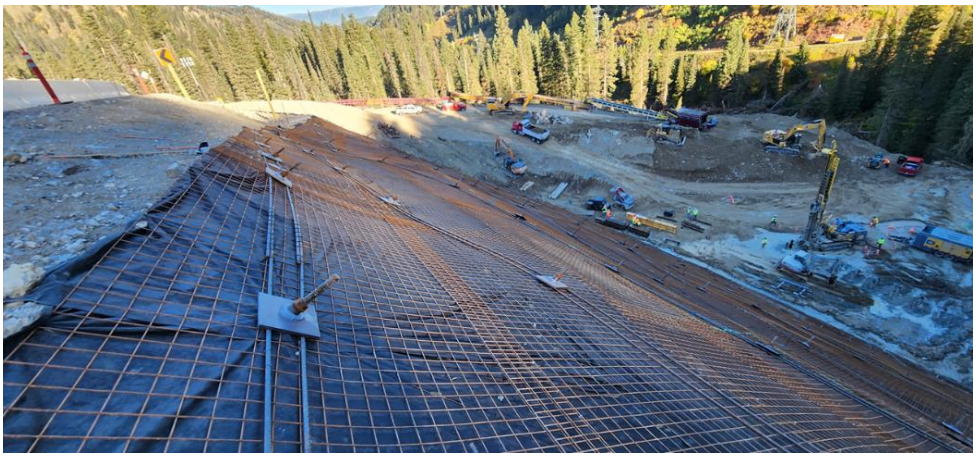


Figure 18 – Installation of soil nails and pinned mesh for slope stabilization following excavation, August 2024.

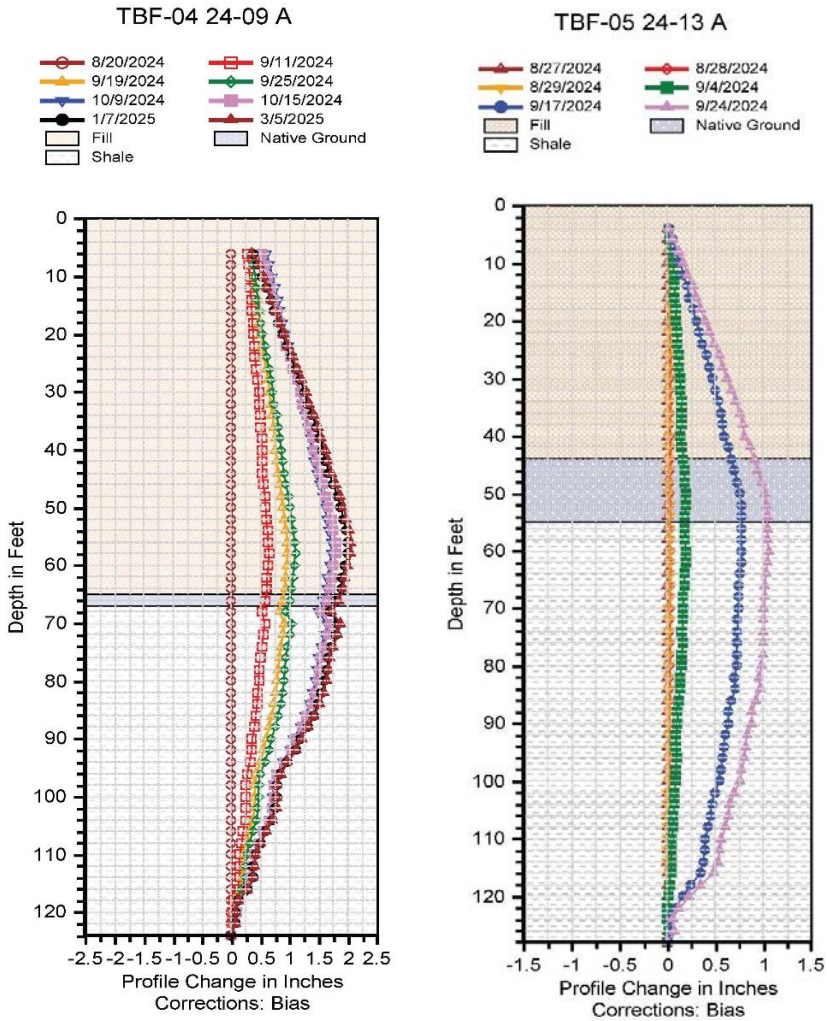


Figure 19 – Manually read inclinometer data from TBF-04 and TBF-05, indicating displacement, post slope excavation after August 8, 2024.

In addition to the SAA inclinometer instrument itself, the data collection package included an Affinity R-star data logger, an Affinity R-star gateway telemetry connector, a marine battery, solar panel, and a modem. The mountainous terrain required the installation of a modem to push a cellular signal strong enough to send real-time data. The data logger, gateway, modem, and solar panel were fitted to a 6-inch by 6-inch, 20-foot-long post Figure 20. The post was set 10 feet into the ground with 10 feet of stick-up. The solar panel had to be strategically placed to capture the appropriate sun angle sweeping around the surrounding peaks, especially in the wintertime with a low sun angle. Additionally, the height had to be enough so that it was not blocked by the excavation slope or susceptible to being completely engulfed by snowpack, snowdrifts, or cast snow from the plows. After September 24, 2024, the SAA inclinometer began to transmit data daily through the internet cloud to WYDOT's office in Cheyenne, WY. Yet, with the deliberate placement of the solar panel, the existing battery could not maintain a charge through the winter months of December and January. To remediate this issue, WYDOT Geology deployed to the location, installing an additional battery to double the stored energy and transmit essential ground movement data.



Figure 20 – Left: Post-installation view of the SAA with all components, September 2024. Right Top: Michael Killion WYDOT installing additional battery, January 2025. Right Bottom: Snowpack and snowdrifts covering the installed SAA below the temporary detour, January 2025.

With the additional real-time data influx into the office, WYDOT Geology reduced the amount of manually operated readings taking place at TBF-04 to a rate of one reading every two weeks. At the beginning of October, contractors concluded full excavation and completed the soil nail

walls for temporary shoring of the slope. Manual readings of TBF-04 recorded approximate rates of lateral movement of 0.13 inches per week, while TBF-05 recorded 0.16 inches per week after the removal of failed material and the excavation face was opened. Five horizontal drains were drilled on October 8, 2024, flushing water, used as drilling fluid, into the excavated slope during the installation, provoking movement within the excavation slope. TBF-04 recorded approximately 0.62 inches of lateral movement between readings on September 24 and October 9, while the SAA inclinometer installed in TBF-05 recorded 0.3 inches of movement on the day of horizontal drain installation. Post installation of the horizontal drains, the rate of movement dropped dramatically, settling into a rate of approximately 0.01 cm per day for both TBF-04 and TBF-05. Subsurface ground monitoring and recording will continue as the runoff season begins and fill re-construction resumes in the spring of 2025.

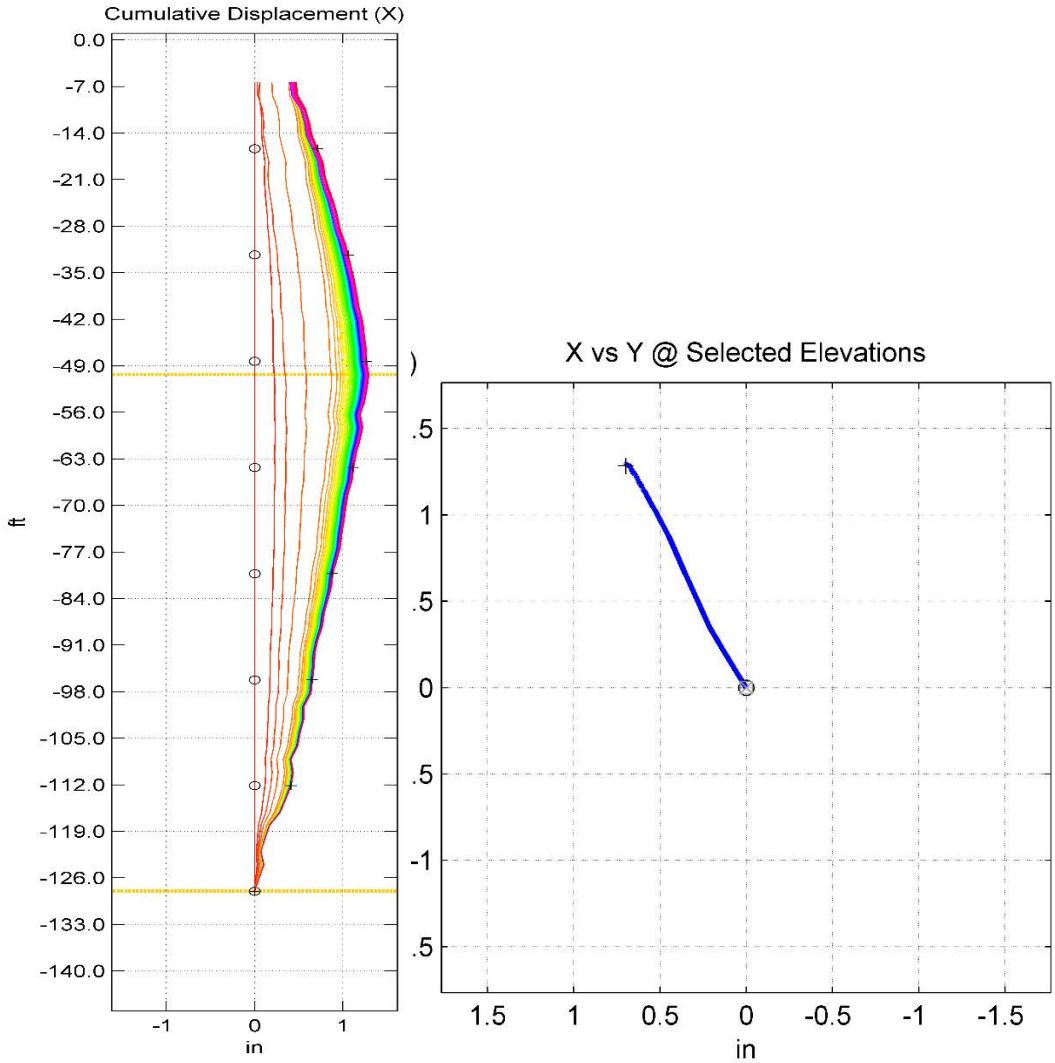


Figure 21 – Left: Graph displays cumulative movement in the X direction, recorded from September 24, 2024 to May 20, 2025. Right: Graph presents top view and directional movement relative to the AO direction, recorded over the same period.

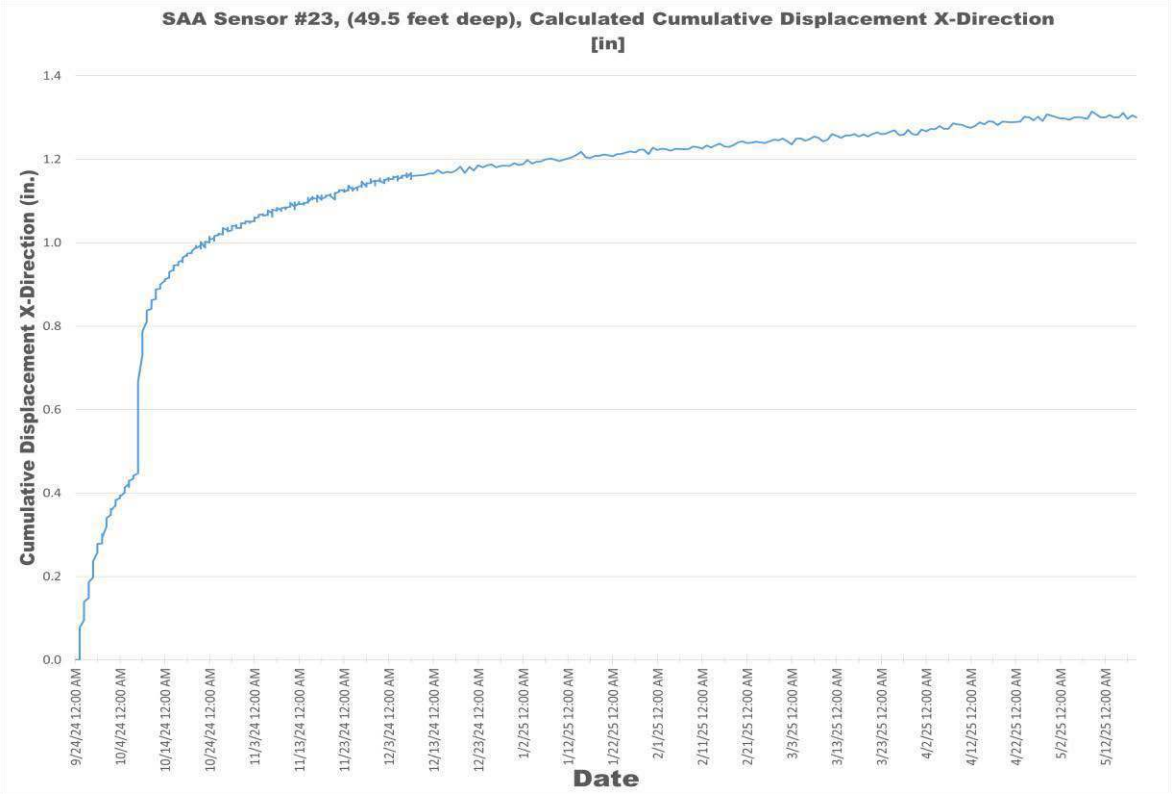


Figure 22 – Graph shows TBF-05 inclinometer data of cumulative movement in the X direction at sensor 23, located at a depth of 49.5 feet, from installation on September 24, 2024 to May 20, 2025. A sharp increase in movement is observed on October 8, 2024, corresponding with the installation of five horizontal drains.

CONCLUSION

The catastrophic failure of "The Big Fill" landslide prompted an urgent and innovative response from WYDOT. Deploying advanced remote sensing and access technology, WYDOT successfully monitored and analyzed the 300-foot section of affected roadway. Ultimately, the data recovered throughout WYDOT's monitoring efforts revealed minimal to no significant surficial or subsurface displacement, while multiple alerting chains and communication redundancies have yet to forewarn of any further instability. These tools enabled timely reconstruction, providing complete confidence in soil conditions while enhancing safety, reducing site visits, and improving communication across multiple entities. The rapid design and construction of a temporary detour, alongside installation of remotely monitored instruments, ensured the protection of workers and the public while facilitating construction of a permanent repair. The broad deployment of cutting-edge instrumentation mitigated geohazard risks while establishing a precedent to manage distant and complex reconstruction projects. This project offered valuable lessons for future emergency geotechnical challenges.

REFERENCES:

1. Wittke, S., *Geotechnical Baseline Report for the Big Fill Landslide*, M.P. 12.8 Wyoming Highway 22, Wyoming Department of Transportation, 23 Aug. 2024.

2. Sullivan, T., *Inclinometer Installation, 'The Big Fill', WYO 22, M.P. 12.8 Wyoming Highway 22*, Wyoming Department of Transportation, 20 Oct. 2023.

3. United States Department of Agriculture, Natural Resources Conservation Service, *Snow Survey and Water Supply Forecasting Program.* National Water and Climate Center, www.nrcs.usda.gov/programs-initiatives/sswsf-snow-survey-and-water-supply-forecasting-program/national-water-and. Accessed 23 May 2025.

4. Bridger-Teton Avalanche Center. *24 Hour Summary of Weather Station Data.* Bridger-Teton Avalanche Center, www.bridgertetonavalanchecenter.org/24-hour-summary-of-weather-station-data/. Accessed 23 May 2025.

5. Schroeder, M. L., *Geologic Map of the Rendezvous Peak Quadrangle*, Teton County, Wyoming, Geological Quadrangle Map GQ-980, U.S. Geological Survey, 1972, scale 1:24,000

6. Zeller, C., *Structural Geology Along Teton Pass, Wyoming*, Geologic Studies of the Cordilleran Thrust Belt, vol. 2, Rocky Mountain Association of Geologists, 1982, pp. 844, Plate #1.

7. Vasko, A.M., *Structural setting of Teton Pass with emphasis on fault breccia associated with the Jackson thrust fault, Wyoming*, Diss. Montana State University-Bozeman, College of Letters & Science, 1982.

8. McEwan, R., and S. Irving., *Historical InSAR Review - Report 3*, KorrAI Technologies Ltd., 15 Nov. 2024.

9. McEwan, R., and S. Irving., *Historical InSAR Review - Report Summary*, KorrAI Technologies Ltd., 19 Jan. 2025.

10. Metzger J., *WYO22 MP 12.8 Big Fill Slide Area Daily Monitoring Report*. AssetAssurance Monitoring LLC., 6 Jul. 2024.

Proactive Geohazard Management: The NMDOT District 2 Rockfall Mitigation Study

Begum Kurtoglu, EIT, GIT
WSP USA Inc.
7245 W Alaska Drive, Suite 200
Lakewood, CO 80226
720-920-4557
begum.kurtoglu@wsp.com

Randy Post, PE
WSP USA Inc.
177 N Church Ave., Suite 1105
Tucson, AZ 85701
520-405-8581
randy.post@wsp.com

Prepared for the 74th Highway Geology Symposium, August, 2025

Acknowledgments

I would like to extend my sincere appreciation to my colleagues at WSP who have contributed their expertise and efforts throughout this study. Also, I wish to acknowledge the individuals at NMDOT who have been involved in various studies and have provided us with the opportunity to be part of this important work.

Disclaimer

Statements and views presented in this paper are strictly those of the authors, and do not necessarily reflect positions held by their affiliations, the Highway Geology Symposium (HGS), or others acknowledged above. The mention of trade names for commercial products does not imply the approval or endorsement of HGS.

Copyright Notice

Copyright © 2025 Highway Geology Symposium (HGS)

All Rights Reserved. Printed in the United States of America. No part of the publication may be reproduced or copied in any form or by any means – graphic, electronic, or mechanical, including photocopying, taping, or information storage, and retrieval system – without prior written permission of the HGS. This excludes the original author(s).

ABSTRACT

The New Mexico Department of Transportation (NMDOT) District 2 Rockfall Mitigation Study is a study aimed at proactively managing geologic hazards along several critical transportation corridors. This study focuses on the innovative approaches and methodologies employed to assess hazards and provide conceptual design of mitigation for rockfall and embankment distress in Otero and Lincoln counties on portions of US 82, NM 380, and NM 532. The study involved a detailed inventory of geohazard sites, drone-based photogrammetry, expert-based qualitative assessment, and the development of a custom geohazard database. Conceptual mitigation options and cost estimates were developed for 56 sites to assist NMDOT with long-term planning and project programming. The study's proactive approach emphasized the importance of early identification of prioritization of high-risk sites, leveraging advanced technologies and interdisciplinary collaboration to enhance safety, mobility, and maintenance efficiency. The findings and recommendations from this study provide a framework for future geohazard management efforts, demonstrating the value of a systematic and data-driven approach to reducing the risks associated with geological hazards. This paper highlights the study's scope, methodologies, and outcomes, offering valuable insights for transportation agencies and geotechnical professionals engaged in similar endeavors.

INTRODUCTION

Highway facilities and those responsible for their maintenance are increasingly impacted by geologic hazards such as rockfall and embankment distress. Traditionally, these hazards have been addressed through reactive measures, responding to incidents after they occur. However, modern asset management practices and technological advancement have enabled a shift toward proactive identification and planning for geohazard risks. Although geohazard management is not yet federally mandated in the same manner as bridge and pavement management, many agencies, including the New Mexico Department of Transportation (NMDOT), are adopting forward-thinking approaches to safeguard critical infrastructure.

The NMDOT District 2 Rockfall Study represents such an effort, focusing on critical transportation corridors within Otero and Lincoln counties along portions of US 82, NM 380, and NM 532. The study emphasized systematic and innovative methodology, including detailed field inventories, drone-based photogrammetry, expert qualitative assessments, and the development of a custom geohazard database. Conceptual mitigation options and cost estimates were developed for 56 sites, providing NMDOT with a critical planning tool to inform future project programming and long-term corridor management. This paper describes the study's scope, methodologies, and outcomes, offering insights into the value of a proactive, data-driven approach for managing geologic hazards along key transportation corridors.

STUDY SCOPE AND BACKGROUND

The purpose of this study was to identify locations along each corridor with the most significant impacts on safety, mobility, and maintenance performance, to support informed decision-making when funding becomes available. While the study does not establish a strict hierarchy for mitigation, it offers a foundation for prioritization efforts when combined with other agency data.

The study was initiated, at least in part, in response to a major rockfall event on US 82 in January of 2023, just west of the tunnel located 8 miles east of Alamogordo, New Mexico. An estimated 100 cubic yards of material fell from a combination cut slope and natural slope. Among the debris was a slab of rock approximately 25 feet across as shown in Figure 1. The event closed US 82 in both directions for two days. This event led to follow-on work to assess the rockfall hazards within approximately one mile above and below the tunnel. This evaluation was conducted by WSP on behalf of NMDOT to address ongoing concerns related to public safety.



Figure 1 - January 2023 rockfall event on US 82, west of the tunnel located 8 miles east of Alamogordo, New Mexico.

The tunnel, located between approximate mileposts (MP) 7.32 and 7.42, including its headwalls and sidewalls which extend from MP 7.21 to MP 7.44, was evaluated for rockfall hazards as part of the 2024 tunnel inspection (Figure 2). While that evaluation was originally conducted under a separate study, the findings are incorporated into this broader Rockfall Mitigation Study, which encompasses the full extent of the surrounding slopes. This study includes evaluations along US 82 from MP 0.0 to MP 35.0, NM 380 from MP 76.0 to MP 107.0, and NM 532 from MP 0.0 to MP 12.0, thereby fully covering the tunnel area and adjacent slopes.



Figure 2 - Overview of west portal (left) and east portal (right) of the tunnel.

GEOLOGICAL SETTING

The three road segments show diverse geological and topography characteristics typical of central New Mexico, where tectonics and volcanism are related to the Rio Grande Rift. The Rift is a feature caused by crustal thinning due to east/west extensional forces as the Colorado Plateau plate moved away from the High Plains plate around 37 million years ago. Thinning of the crust and allowed upward movement of the hot mantel which resulted in the prevalence of volcanos, volcanic deposits and tertiary aged dikes and faulting. The subject road segments are located on the eastern side of the rift where tectonic, volcanic and erosional forces have resulted in the highly variable surface and subsurface conditions.

Lithological variations and differences in the thickness and orientation of bedding account for different levels of rockfall hazard for each formation. Hazard level also varies within each formation due to stratigraphic differences and location of the exposure. The formations related with the greatest safety and mobility impacts are the Gobbler, Yeso and Abo Formations, particularly around the US 82 tunnel at MP 7.2.

1. Geology of US 82

The geological setting along US 82 consists of a complex assemblage of sedimentary rocks that are part of the Magdalena Group, including the Bursum, Holder, Hueco, Beeman, and Gobbler Formations (*1,2*). These formations range from Pennsylvanian to early Permian in age, and include limestone, sandstone, and shale, with varying degrees of lithification and deformation due to tectonic events and diagenesis (USGS, 1990).

From MP 0.0 to MP 6.3, the road cuts expose interbedded limestone and shale from the Hueco and Beeman Formations. Bedding is generally subhorizontal to gently dipping, with local folding and faulting creating structural complexity. Shale layers are more prone to weathering, which can lead to surficial instability and ravelling (*2*).

Between MP 6.3 and MP 8.1, tunnel and portal excavations were performed in alternating beds of buff and gray limestone and shale. East of MP 6.8, bedding dips approximately 10–15° toward N77E, with a strike of N13W—generally subparallel to the road. West of MP 6.5, bedding dips steeply northwest, but remains subparallel to the alignment. The orientation results in bedding dipping into the slope, which generally enhances stability, even when slope angles exceed bedding dip. Bedding thickness is highly variable, ranging from inches to over 8 feet, with differences in rock strength, permeability, and fracture spacing (*3*).

From MP 8.1 to MP 35.0, the route passes through more massive limestone units of the Gobbler and Holder Formations. Bedding here dips moderately toward the southwest, typically into the slope, which supports slope stability. However, localized faulting and variations in rock quality still contribute to potential rockfall hazard zones (*2*,*4*).

2. Geology of NM 380

Between the west project limit at MP 76 to MP 79 the roadway platform is the product of cut and fill construction with modest height cuts up to 50 feet high excavated in the upper Mancos Formation shale and sandstone as well as in the sandstone and shale of the Mesa Verde Group.

These formations are typical of marine to marginal marine environments and form moderate cuts up to 50 feet in height (USGS, 2004; New Mexico Bureau of Geology [NMBG], 2014).

From MP 79 to MP 82, the road crosses into softer Tertiary volcanic units and Paleogene sedimentary rocks, evidenced by low road cuts (<30 ft) and the presence of north-south trending dikes and faults, likely part of Tertiary intrusive activity (*5*). These structural features are expressed as prominent lineations and occasionally visible in road cuts, consistent with the tectonic fabric near Capitan.

Travelling west from MP 82 the bedding is similar to that seen east of the volcanic deposits starting with sandstone and thin shale layers of the Mesa Verde Group forming gentle, rounded hills requiring only small highway cuts and fills. Near Capitan, the soft Mancos Shale forms flat terrain with no highway cuts until slightly more resilient subsurface consisting of sandstone and shale of the Dakota Group. Approaching MP 91, the road crosses Triassic-age Chinle Formation and Permian-age Artesia Group rocks, comprised of sandstone, siltstone, and some evaporite units, forming low-relief landscapes with minor cuts and fills (*6*,*7*).

Between approximate MP 91 and the east end of the study area at MP 107, the road is aligned along the edge of a moderately wide, partially irrigated, valley underlain by alluvium and sandstone, siltstone, gypsum, halite and dolomite of the Yeso Formation. The surrounding rounded hills of the San Andres Formation consist of beds of limestone and dolomite interrupted by occasional shale beds. Cuts along this section are up to 40 feet in height and variable. Soft, erodible siltstone and gypsum cuts occasionally contain large, harder dolomite and limestone boulders creating a hazard to the road. Toward the eastern end of this section, fracture limestone and dolomite cuts are infrequent but present.

3. Geology of NM 532

Between MP 0 at Ruidoso and the western end of this segment near Ski Apache (MP 12), the road is underlain by the Yesso Formation, which consists of interbedded sandstone, siltstone, gypsum, halite, and dolomite (*1*,*2*). These sedimentary units are Permian in age and were deposited in a shallow marine to evaporitic setting. The presence of evaporites, particularly gypsum and halite, suggests potential for subsurface dissolution and related slope instability.

The road alignment follows an east–west valley formed by erosion along a prominent fault zone, with subsidiary faults splaying to the north and south, influencing tributary drainage patterns (*8*). Structurally, the Yesso Formation in this area often displays folding and faulting, contributing to variability in bedding orientation and weathering behavior.

STUDY METHODOLOGIES

To support the identification and prioritization of rockfall hazard sites, several methods were employed to collect and evaluate data throughout the study corridors. These methodologies include a combination of desktop reviews, field visits, drone surveys, and input from maintenance staff. Together, these efforts provided a comprehensive understanding of slope conditions and potential risks. The methods used in this study are summarized below:

1. Desktop Inventory of Sites

WSP began the study by conducting a desktop inventory to identify potential rockfall sites within the study corridors. The primary method involved a “virtual drive-by” using Google Earth and Google Street View to systematically review the alignment and pinpoint areas with visible signs of rockfall hazards. Figure 3 shows an example of a virtual drive-by from one of the NM 532 sites.



Figure 3 - Google Street View image from NM 532 MP 7.58 to 7.62

During this process, WSP assessed several key site characteristics, including slope height, ditch width, the side of the road the slope was on, shoulder conditions, and any visible geological features. This information was used to highlight high-risk locations and develop an initial hazard classification for each site. Sites reviewed included cut slopes in rock, cut slopes in soil with embedded rock blocks, and natural slopes with the potential to produce rockfall. This initial phase laid the groundwork for a focused and efficient field investigation by flagging areas of concern and documenting key features that would be verified and expanded upon during the site visits.

2. Site Visit

WSP conducted field visits to verify and supplement desktop findings. Sites were generally defined as continuous sections of slope with rockfall hazard potential, marked by a start and end point. Most slopes in the study area are cut slopes in rock, soil, or a combination of both.
Occasionally, undisturbed rock outcrops were included when judged to be potential sources of rockfall.

During these visits, a field data collection app was utilized to enhance the efficiency and accuracy of documentation. The app allowed field personnel to mark their exact location using GPS, identify the milepost they were at, take geo-referenced photographs, and write real-time notes. In addition to general observation, the app provided dedicated sections for entering detailed information such as slope geometry, geohazard type, material

characteristics, and conducting risk assessments. This functionality improved the consistency of data collection and enabled better integration of field data into the overall hazard evaluation.

Properties of interest recorded or verified during the site visits included:

- Length of slope hazard
- Estimated maximum slope height or range of heights
- Slope angle and rock characteristics
- Approximate block size or range
- Existing rockfall mitigation
- Ditch configuration, condition, and effectiveness
- Observations or rock debris and pavement or infrastructure damage
- General hazard descriptions
- Estimate of rockfall hazard class

3. Drone Surveys

WSP conducted multiple drone flights to capture photogrammetry images for the creation of 3D meshes and related products. While not survey-grade, these models were useful for making observations from different angles, measuring features (Figure 4), and assessing the potential hazard. The meshes supported evaluations of stability, approximate quantities, and conceptual mitigation options.



Figure 4 - Measurement gathered from the 3D mesh data (NM 380 MP 104.17 to MP 104.29)

4. Maintenance Patrol Input

WSP recognizes the value of institutional knowledge held by maintenance personnel. Several interviews were conducted with different maintenance orgs or patrols to gather insights on the location and severity of known rockfall problem areas within their respective areas. This information was recorded in the study database and factored into the rockfall hazard classifications and mitigation recommendations.

IDENTIFYING ROCKFALL HAZARD CLASS

After completing the desktop inventory, conducting field visits, reviewing available 3D drone- derived models, and incorporating feedback from maintenance patrol meetings, WSP identified and assigned a rockfall hazard class to each site. This multi-step evaluation process helped that each site was assessed from several perspectives helping to develop a comprehensive understanding of the potential hazard and its consequences.

There are many sites within the study area where occasional or non-threatening rockfall occurs whereas other sites present a frequent risk to public health. Time and budget constraints require that an initial screening of sites be part of the study process. In this feasibility-level study, WSP used a subjective classification system that sorts the sites into three classes based on the estimated severity of the risk and consequence in terms of safety, mobility, and maintenance.

Class 1 sites present the most severe hazard, and Class 3 the least. General characteristics of the three hazard classes are described below.

Class 1

Class 1 sites have the most significant impact on safety and, in some cases, maintenance and mobility. These sites should be prioritized for mitigation by NMDOT. They generally have undersized, ineffective ditches, taller slopes, and larger block sizes. There may be boulders that are judged by WSP to be more likely to fall in the near term (0-10 years), although the predicting the exact timing of failures is not possible. Some of these sites are natural slopes where mitigation may be more challenging because stabilization closer to the source may not be an option.

Class 2

Class 2 sites still pose a relatively high safety risk but may not be among the first sites warranting mitigation when considering finite resources. These sites may be grouped with nearby Class 1 sites when packaged into projects. These sites may have ditches that stop a portion of the rocks or other mitigation that is at least partially effective. In terms of risk and

consequence, one component may be relatively high while the other is lower. For example, a slope may have a high likelihood of rockfall, but a lower consequence due to limited traffic exposure or effective catchment.

Class 3

Some slopes fall into the "nuisance" category, where occasional rocks may cause minor property damage or require cleanup by maintenance staff. Class 3 sites are judged to have a low hazard and consequence, or they already have effective mitigation in place. These sites tend to be shorter slopes with ditches and, in some cases, portable concrete barriers. They are relatively clear of debris and other evidence of frequent rockfall activity. Safety and mobility impacts are unlikely at Class 3 sites; therefore, they are not specifically addressed in this study.

DEVELOPMENT OF A CUSTOM GEOHAZARD DATABASE

The geohazard database used to manage the data collected during this study is a combination of ArcGIS desktop, ArcGIS Online (AGOL), and custom components built with python and SQL databases or spreadsheets. AGOL is particularly useful for housing the 3d meshes developed from the photogrammetry models, allowing multiple meshes to be loaded in a browser-based interface and made accessible to a distributed team. Some resolution is lost using this approach, but the benefits of relative ease of managing what are usually very large files and incorporating the ability to load individual drone photos greatly offsets the drawbacks. Field apps were also used collect site photos and data and this data fed into AGOL automatically. Finally, a PowerBI interface was developed to evaluate the results of the study in a dashboard interface and to incorporate various filtering criteria when considering possible sites for advancement to design and construction projects.

DISCUSSION OF ROCKFALL MITIGATION TYPES FOR EACH SITE

Mitigation strategies for rockfall hazards typically consist of a limited set of standard systems that address risk in two primary ways: by stabilizing the source area or providing protection near vulnerable assets. Source area stabilization methods include installing rock bolts, wire mesh, or conducting scaling to remove potentially unstable material (Figure 5). These methods aim to prevent detachment of rocks before they become a hazard. In contrast, proactive systems at the base of slope focus on intercepting or redirecting falling material and may include modifications to ditch geometry, installation of catchment walls, or use of barriers and flexible fences.

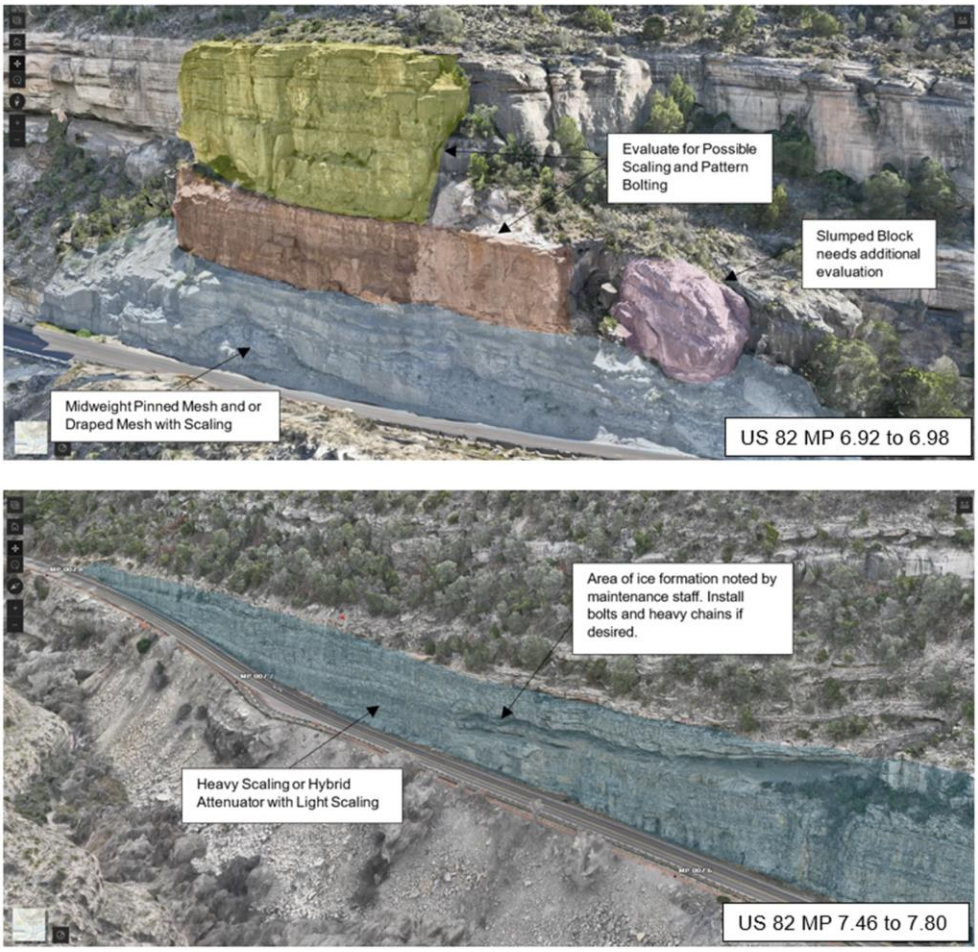


Figure 5 - Examples of recommended mitigation options (3D mesh from US 82 MP 6.92 to 6.98 and US 82 MP 7.46 to 7.80).

When slopes are high, inaccessible, or geologically unstable, treatment at the source may not be feasible. However, in this study area, most slopes are relatively moderate in height and are typically composed of rock and soil cuts. This makes source stabilization not only feasible but often the preferred option for long-term risk reduction. Where appropriate, enhancements to ditch width and backslope geometry should be made carefully to avoid destabilizing the slope above.

Existing mitigation observed within the study area consists of mostly of roadside protection elements, including portable concrete barriers, or permanent walls with a catchment area. These measures provide some degree of impact reduction, but in many cases, additional or more comprehensive systems may be warranted.



Figure 6 - Example of an existing mitigation at US 82 MP 14.19 to 14.28.

Some mitigation measures, such as scaling, are considered temporary and may need to be repeated periodically to remain effective. Others, like catchment ditches or structural barriers, may require ongoing maintenance due to sediment buildup or damage from rock impacts. When selecting the appropriate mitigation strategy for each site, factors such as estimated cost, constructability, long-term maintenance needs, visual impact, and overall effectiveness should be carefully weighed. Consideration of lifecycle costs, not just initial installation, is critical in identifying the most sustainable and efficient approach to hazard reduction.

CALCULATION OF PROBABLE COST FOR CONCEPTUAL OPTIONS

The opinions of probable cost developed for this study are intended for feasibility-level planning and relative comparison among sites. These estimates are based on conceptual mitigation options and preliminary data, with a target accuracy range approximately -50% to +100% of the actual construction costs for the mitigation elements only.

At this stage, the estimates account for the core mitigation system components, including materials, equipment, and labor required and installation. They do not include typical internal and external project costs such as final design, project management, construction management, construction engineering support, material testing, traffic control and devices, environmental compliance, surveying, paving and striping (if needed), or NMDOT in-house costs. Additionally, other pay items not directly related to the rockfall mitigation systems are excluded from these estimates.

To support this study, WSP assembled unit cost data from a database of previous DOT and municipal projects. These cost values were approximately adjusted to reflect current pricing, anticipated installation conditions, and general site considerations within the study corridor. For planning purposes and preliminary total project cost estimation, a multiplier ranging from 1.5 to 2.0 times the estimated mitigation cost may be applied. This factor reflects the typical range of total project expenses based on WSP's experience delivering similar geohazard mitigation projects.

While these estimates are primarily intended for comparing different sites and aiding future prioritization and funding decisions, it is important to carefully consider and account for the additional costs mentioned earlier to ensure more accurate evaluations.

STUDY FINDINGS

A total of 233 potential rockfall hazard sites were evaluated across three highway corridors. The assessment included a combination of desktop review, field visits, 3D slope model interpretation, and patrol staff input.

Based on this multi-step evaluation, sites were classified into three hazard categories reflecting their relative risk and need for action. Of the 233 sites, 56 were identified as Class 1 or Class 2 hazards and selected for conceptual mitigation planning and cost estimating support NMDOT's long-term project development. The remaining sites were classified as Class 3, indicating lower priority or previously mitigated conditions.

Site classifications by corridor are summarized as follows:

- **US 82 (MP 0.0 to MP 6.3 and MP 8.1 to MP 35.0)**

  Class 1 Sites: 1

  Class 2 Sites: 21

- **NM 380 (MP 76.0 to MP 107.0)**

  Class 1 Sites: 3

  Class 2 Sites: 6

- **NM 532 (MP 0.0 to MP 12.0)**

  Class 1 Sites: 2

  Class 2 Sites: 23

These 56 priority sites represent locations where mitigation options were developed, and preliminary cost estimates prepared. They are recommended for further analysis and inclusion in future planning and programming efforts.

CONCLUSIONS

The NMDOT District 2 Rockfall Mitigation Study presents a systematic and data-driven approach to identifying, classifying, and developing conceptual mitigation strategies for rockfall and embankment distress hazards. A total of 233 sites were inventoried along key corridors, including US 82, NM 380, and NM 532. Of these, 56 sites were classified as Class 1 or Class 2, indicating higher priority for mitigation, and were further analyzed for conceptual mitigation options and feasibility-level cost estimates.

The study combined multiple methodologies to create a comprehensive hazard assessment process. Desktop reviews using high-resolution imagery and Google Street View helped establish initial site characteristics and prioritize field visits. Field investigations, drone-based photogrammetry, expert judgment, and patrol meetings provided the necessary inputs to determine rockfall hazard classifications. This tiered approach allowed for efficient evaluation of a large number of sites while maintaining consistency in hazard identification and prioritization.

Mitigation strategies were tailored to each site, considering source stabilization, catchment improvements, and protective barriers, while also evaluating constructability, long-term maintenance, and life cycle costs. Probable costs for each mitigation concept were developed using WSP's internal cost database, with estimated ranges provided to support planning-level decision-making.

The findings from this study will serve as a critical input for long-term planning and programming efforts for NMDOT. Finally, this study also demonstrates how advanced technology and cross-disciplinary collaboration can enhance the effectiveness and efficiency of geohazard assessment and mitigation.

REFERENCES

1. Kues, B. S., and K.A. Giles, *The Geology of New Mexico: A Geologic History*, New Mexico Geological Society, 2004.

2. New Mexico Bureau of Geology and Mineral Resources (NMBGMR), various maps, 2005.

3. USGS (United States Geological Survey), *Geologic Quadrangle Maps and Regional Stratigraphic Bulletins*, 1990.

4. Bachman, G.O., and D.A. Myers, *Geology of the Jicarilla Mountains, Lincoln County, New Mexico*, USGS Professional Paper 600, 1969.

5. McLemore et al., *Volcanic and Structural Geology of the Capitan Region*, 2000.

6. Lucas et al., *Stratigraphy of the Triassic and Permian Rocks in Southeastern New Mexico*, 1997.

7. New Mexico Bureau of Geology and Mineral Resources (NMBGMR), various maps, 2005.

8. USGS (United States Geological Survey), *Geologic Quadrangle Maps and Regional Stratigraphic Bulletins*, 1982.

Use of Artificial Intelligence for Identification of Embankment Failures on a Network Level

Aliena Debelak
8745 W Alaska Drive, Suite 200
Lakewood, CO 80216
720-920-4659
aliena.debelak@wsp.com

Sedrick Bouknight
999 18th St, Suite 1825n
Denver, CO 80202
303-390-5909
sedrick.bouknight@wsp.com

Bailey Fischer
8745 W Alaska Drive, Suite 200
Lakewood, CO 80216
720-920-4586
bailey.fischer@wsp.com

Nicole Oester Mapes
4670 Holly St. Unit A, Denver CO 80216
Denver, CO 80216
720-937-4779
nicole.oester@state.co.us

Roger Pihl
8745 W Alaska Drive, Suite 200
Lakewood, CO 80216
970-379-5341
roger.pihl@wsp.com

Prepared for the 74th Highway Geology Symposium, August, 2025

Acknowledgments

This paper describes the current outcomes of a project developed over the course of 7 months. Many people have contributed their time and talents to aspects of the projects. The authors would like to thank the following individuals (listed in alphabetical order) for their contributions in the work described:

Mudit Argarwal, WSP
Christopher Bente, WSP
Robert Group, CDOT
Bryan Schafroth, WSP
Haoyun Wang, WSP

Disclaimer

Statements and views presented in this paper are strictly those of the authors, and do not necessarily reflect positions held by their affiliations, the Highway Geology Symposium (HGS), or others acknowledged above. The mention of trade names for commercial products does not imply the approval or endorsement of HGS.

Copyright Notice

Copyright © 2025 Highway Geology Symposium (HGS)

All Rights Reserved. Printed in the United States of America. No part of the publication may be reproduced or copied in any form or by any means – graphic, electronic, or mechanical, including photocopying, taping, or information storage, and retrieval system – without prior written permission of the HGS. This excludes the original author(s).

ABSTRACT

Highways in sloping terrain are constructed through cut-fill methods where material removed on the uphill side of the highway is used to construct embankments on the downhill side. Despite improved construction techniques such as benching fill into the existing slope, controlling and testing for moisture content and soil density, and limiting lift heights, embankments experience settlement or sliding, posing risks to transportation systems. Risks vary with the severity of the failure and can include safety impacts, maintenance costs, and in instances of larger failures, user mobility impacts from lane closures. The Colorado Department of Transportation (CDOT) has over 12,000 embankments identified throughout the state, many with indication of failure. Typically, practitioners rely on aerial imagery or detailed corridor-level site assessments to identify these failures. This standard practice is time intensive and only allows for embankment failure identification in localized areas.

The authors of this paper leveraged Artificial Intelligence (AI) and Machine Learning (ML) capabilities to identify the location and severity of embankment failures on a state-wide level. The System integrates a specialized LLM-based expert AI, a reasoning agent, and an autonomous framework that interfaces with tools like ArcGIS and custom ML models. Subject matter expert feedback to fine-tune the models while CDOT data serves as both a training corpus and a key resource. By efficiently identifying embankment failures throughout the state, owners can better quantify risk exposure due to deteriorating embankments and prioritize funds to manage the risk.

Initial results show that the System can successfully identify embankment failures. Model validation exercises along SH 133 demonstrated a strong match with previous feasibility studies, and blind testing on CO-65 confirmed the tool's potential to identify undocumented failures. While further training and system integration are needed, this proof-of-concept illustrates how AI tools can supplement geotechnical risk identification at scale, refine asset inventories, and help prioritize field investigations.

INTRODUCTION

Background

As in many other parts of the United States, much of the primary road network within Colorado was constructed in the 1950's through the 1970's *(1)*. Federal funding of the interstate highway system mandated improvements to the arterial system of US and Colorado State highways *(2)*. Widening, geometric improvements and paving were conducted at a rapid pace as the population and economic importance of intrastate and interstate travel increased. Many of the state's once low volume, unpaved rural roads were upgraded with varying degrees of construction quality control *(2)*.

New alignments and widening projects typically included excavation on the uphill side and placement of the excavated material on the downslope side. Despite improved construction techniques such as benching fill into the existing slope, controlling and testing for moisture content and soil density, and limiting lift heights, embankments experience settlement or sliding, posing risks to transportation systems.

During the intervening years, Colorado's population has more than tripled, and, along with vastly expanded commerce and tourism, increases to the state's dependence on this arterial system are evident *(3)*. User mobility and ever-increasing maintenance costs that result from embankment failures have provided the impetus for creating an inventory to prioritize sites for future funding.

Current State of Practice

Current State of Embankment Failure Inventory

The Colorado Department of Transportation (CDOT) geohazard program has adopted a comprehensive geohazard asset management system to quantify the risk of geohazards on the transportation system in a systematic and repeatable way. Within this system, constructed embankments are considered geotechnical assets which can deteriorate and pose a credible risk to the transportation system. Previously, embankments were only added to the statewide inventory when significant cracking or a larger scale failure had occurred. This incomplete inventory did not fully communicate the level of geotechnical risk from credible geotechnical hazards. Recently, a statewide inventory of embankments was generated from statewide LiDAR datasets, using specific criteria for the initial screening. These criteria included a minimum height of 10 feet, a minimum slope of 3:1 (H:V), and a maximum distance of 80 feet from slope crest to the shoulder *(4,5)*. The inventory generated from these screening criteria significantly increased the number of embankments in the CDOT inventory.

The current number of inventoried embankments and natural proximal slopes is over 12,000 *(5)*. This number is continuously refined but is a large departure from the hundreds of slopes in the previous event-based asset management inventory. While many of these embankments do not show signs of deterioration and pose minimal risk to the transportation network, some do carry risk and need to be managed appropriately. The benefits of understanding where susceptible embankments are located within the transportation network include being able to communicate risk exposure to decision makers, planning future projects for geotechnical assets maintenance or replacement, and assisting with disaster recovery in the instance of large-scale geotechnical asset failures.

Current State of Technology

Artificial Intelligence (AI) often refers to generative models capable of producing complex text-based narratives, high-quality images, and, more recently, advanced reasoning engines capable of solving complex problems across various disciplines. The public release of Generative Pre-Trained Transformer (GPT) models in 2022 marked a significant milestone in AI accessibility, rapidly accelerating innovation in the field *(6,7,8)*. Initially, AI applications were limited to basic chatbots but have since evolved into functional digital assistants and agents capable of interacting with the external environment beyond simple text-based conversations. These agents can now execute tasks, such as operating machinery or interfacing with digital systems, by dynamically leveraging external functions to carry out specific actions.

Project Purpose

Typically, practitioners rely on aerial imagery or detailed corridor-level site assessments to identify failures. This standard practice is time intensive and only allows for embankment failure identification in localized areas. Many of the failures are identified by maintenance personnel after the embankments become problematic for the traveling public due to large pavement cracks, vertical deformation and unsafe guardrails. Pavement overlays and guardrail replacement are common reoccurring temporary fixes when embankments are moving incrementally downslope year after year. These types of temporary maintenance fixes take valuable maintenance personnel time to complete and become costly when considered with a long-term cost benefit analysis. However, as failures progress, mobility risks include single lane closures that require costly and risky 24-hour traffic control. More severe failures may require occasional closure of both lanes of a two-lane road and can mean long detour routes or limited access to homes and businesses. Safety risks such as guardrail in disrepair, and significant cracking also contribute to the total risk exposure caused by embankments.

There are multiple indicators that determine whether a location is experiencing an embankment failure. Characteristic pavement cracking, displaced guardrail, ponding or wet vegetation nearby, location of the cut/fill boundary under the road, and other nuances indicate that slope movement is the underlying factor. No single indicator is definitive. Some are necessary but not sufficient on their own. Previous attempts to inventory failures on a network level have focused on singular factors or a small combination of factors which generally resulted in erroneous identification of large swaths of roadway. The project team recognized the possibility that artificial intelligence and machine learning could be a useful tool because of its ability to assimilate vast amounts of information, reason, and iteratively provide increasingly valuable results.

The purpose of this project was to develop a proof-of-concept level study for an Artificial Intelligence (AI) and Machine Learning (ML) model that could identify and characterize embankment failures and subsidence along Colorado roadways. The model utilizes existing remote sensing data, various reports and studies on embankment failures, and photos to develop and train the model for embankment failure identification. By utilizing previous reports, and identified embankment failures, the intent was to train a model to be able to assist in identifying probable embankment failures on a corridor and potentially state-wide scale. The goal of this project was to understand the feasibility of deploying the model at a larger scale and to determine potential future use cases for the model.

EQUIPMENT & METHODS

Apparatus

At its core, the System consists of a structured database for storing pertinent datasets, a file management system for organizing reports and imagery, and web-based application services tailored for review and testing. Additionally, diagnostic, reporting, and data visualization components enhance the solution's usability, allowing researchers and engineers to analyze patterns, assess site conditions, and interpret findings efficiently. The response output from the system is presented in real-time as the AI is formulating its response. Additionally, the system AI operates in a multi-modal capacity which supports, text, images, and audio inputs.

The System is deployed on Microsoft Azure and leverages cloud-based utilities such as document text indexing to streamline information retrieval. Additionally, it incorporates advanced large language models (LLMs), including those developed by OpenAI, to facilitate automated analysis of geological reports and technical documentation. To further refine its capabilities, a customized LLM has been trained on domain-specific data provided by subject-matter experts, ensuring its applicability to geotechnical challenges. This tailored model is securely hosted in a private, isolated cloud environment, reinforcing data integrity and controlled access.

System Components

The System was developed as a comprehensive application that integrates a range of AI features which continue to evolve and improve with ongoing use. Further enhancing the System, SMEs contribute discipline-specific content, such as Q&A pairs, detailed multi-step instructional procedures with clearly defined outcomes, and annotated technical images. These entries are systematically archived in the System database and later used to fine-tune the large language model. This process ensures that the AI adapts to the specialized needs of the embankment condition assessment application over time. Recognizing some common pitfalls of generative AI, such as producing poor-quality responses or fictionalized "hallucinations", our approach was to incorporate additional modules and components that reinforce accuracy and reliability. A representative illustration of the System components is shown in Figure 1.

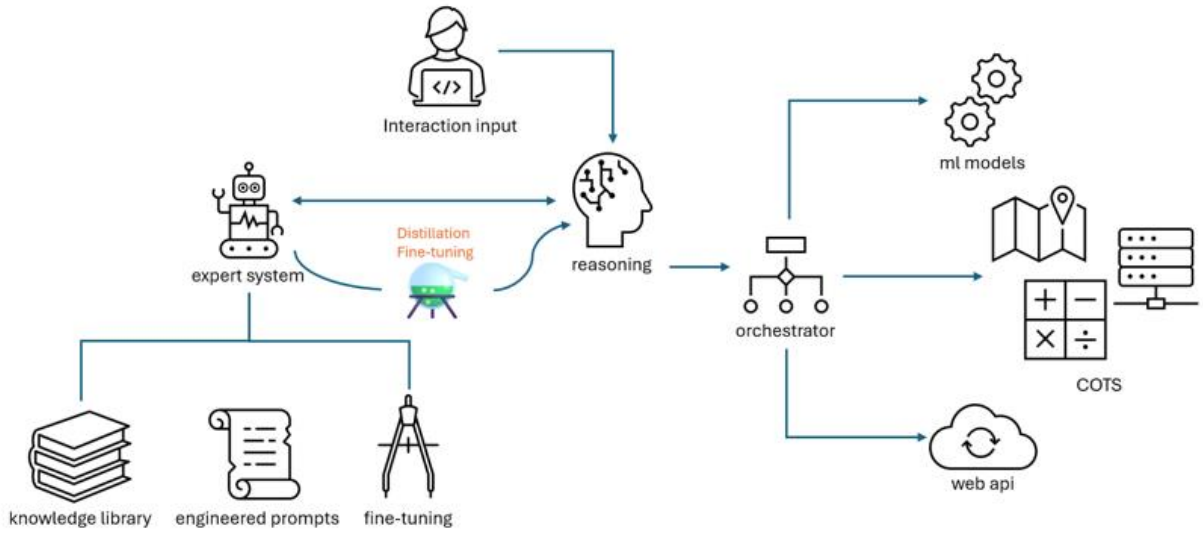


Figure 1 - Representative Illustration of the Various Components of the AI/ML System Developed for the Project.

The System operates much like a "Group Chat GPT," where the different AI agents work together as if they were part of a collaborative conversation. The Expert System agent acts as a trusted source of validated, discipline-specific knowledge, equivalent to a seasoned expert in the discipline or practice domain. The Reasoning Agent focuses on decision-making and can draw on external tools to gather additional data or perform specialized tasks.

In practice, these two agents interact in a dialogue-like manner. When a complex issue arises, the Reasoning Agent consults the Expert System for further context and validation, while also tapping into the integrated toolbox of external tools when needed. This conversation among agents allows the System to improvise and adapt its responses based on real-time inputs, ensuring that outputs are both accurate and contextually relevant. Each component is described in more detail in the subsequent sections.

Expert System

This acts as an advanced digital assistant powered by an LLM. It provides precise, domain-specific information, similar to having a seasoned expert on hand for complex embankment condition assessment queries.

Knowledge Library

The Knowledge Library is a secure document repository that houses exclusive, discipline-specific content not publicly available, such as internal reports and technical studies. Files can be documents, structured data-containing files, spreadsheets, images, reports, and audio and video files. The Knowledge Library allows designated SMEs to contribute relevant files and documents, which provide the base for AI's responses as well as virtually eliminates hallucinations,

The content from the Knowledge Library informs the Expert System, allowing outputs to be grounded in authoritative data and support effective decision-making. When interacting with the

System, users have the option to access all available content, manually select a subset, or filter documents based on category, author, discipline, and date.

The Training Library

The Training Library serves as a dedicated repository for training data used in the System fine-tuning process. SMEs contribute text prompts, Q&A pairs, multi-step instructional procedures, and annotated imagery through a secure web interface. Submissions can be removed, modified, flagged, or marked for exclusion on the next fine-tuning re-training.

Validated training data is systematically archived in the Training Library and integrated into the fine-tuning of the Expert System. By providing a structured and dynamic resource, the Training Library facilitates continuous improvement of the System, ensuring that AI outputs increasingly reflect discipline-specific knowledge. Additionally, users can filter and select training data based on metadata parameters, further refining the quality and alignment of the fine-tuning process.

Prompt Library

The Prompt Library is a dedicated repository for expert-crafted text prompts and templates, designed to guide user interactions with the AI system. Its primary purpose is to facilitate and optimize the composition of prompts to get the best possible responses, or actions, by the AI within the System. SMEs contribute prompts through a secure web interface. Each submission is reviewed such that it meets established standards for accuracy, relevance, and clarity. Users can access the repository to select or adapt prompts that best suit their needs.

Reasoning System

The reasoning system is a separate LLM built on a different foundational model with enhanced reasoning capabilities. It interacts with the Expert System and autonomously calls on external functions when complex decision-making or analysis is needed.

Orchestrator

This intermediary layer organizes external plugins (tools) that the Reasoning System uses to extend its functionality. It provides clear guidelines on how each tool should be utilized by the AI, enabling dynamic problem-solving tailored to geotechnical challenges.

“Genetic Memory” Hivemind

The Genetic Memory is a long-term memory module that accumulates and retains contextually relevant information. By integrating insights from all user interactions across the System, over multiple series of fine-tuning and re-training, it improves the System's knowledge base over time.

Subject Matter Expert Consensus

A comprehensive framework captures interactions between expert users and the AI, quantifies their value through a consensus mechanism, and feeds the outcomes into the AI model’s fine-tuning process. Expert interactions are automatically logged with details such as user identification, discipline, date, and context

A voting system allows SMEs to evaluate each entry through a upvote/downvote interface. The aggregated consensus score determines the importance of each entry. Memory records that achieve a high consensus score are then selected for inclusion in model fine-tuning sessions. This process allows the AI model to be continually refined using only high-value, discipline-relevant insights, enhancing the reliability and practical utility of the System.

External Tools

The System extends its functionality by integrating a range of specialty external tools through a centralized toolbox. This approach enables advanced geospatial and geotechnical analyses by providing standardized access to domain-relevant services. The System can integrate and interact with a variety of other software or data services using industry-standard Application Programming Interfaces (API). At the time of this writing, the System is integrated into two toolboxes, however the System supports virtually limitless extensibility.

ArcGIS

This suite interfaces with the project teams' internal ArcGIS platform containing drone photos and meshes of various highway corridors throughout Colorado. Integrating ArcGIS as a toolbox allows the System to access and interact with content included in the tool, performing queries on ArcGIS and returns the results as formatted data.

CDOT Windshield

This suite connects to the CDOT's custom application, CDOT Windshield. CDOT windshield contains street-level images of highways and interstates throughout Colorado, taken from the perspective of a vehicle. Photos are taken at 0.005 mile intervals and are collected annually as part of the pavement condition data. At the time of this writing, photos are available yearly from 2007 to 2024. This toolbox integration allows the System to execute a query on CDOT Windshield to retrieve condition and highway segment information.

Training Process

While the System can retrieve information from the Expert System and the toolbox, its continuous training allows it to learn new, specialized knowledge. This ongoing learning significantly enhances its ability to interpret data and produce meaningful outcomes. There are three methods that allow the System to learn: training input, Expert System dialogue, and machine learning.

Training Input

The training input module allows a user to provide a question and input the appropriate response to the question. Three different training types are available to be used and are described in **Error! Reference source not found.**.

Table 1: Training Types and Their Uses.		
Training Type	**Description**	**Training Uses**
Simple Mode	Single prompt followed by a single answer	Simple definitions, Tool uses
Advanced Mode	Multi-Turn chat with multiple prompts and multiple responses	Complex definitions
Vision Mode	Single prompt with an image aid and single response	Embankment failure characteristics

Training prompts are entered through dialogue boxes and an example is shown in Figure 2. Once an adequate number of prompts are entered, the user will initiate model retrain, prompting the System to absorb the information entered and apply the data into its future decision making.

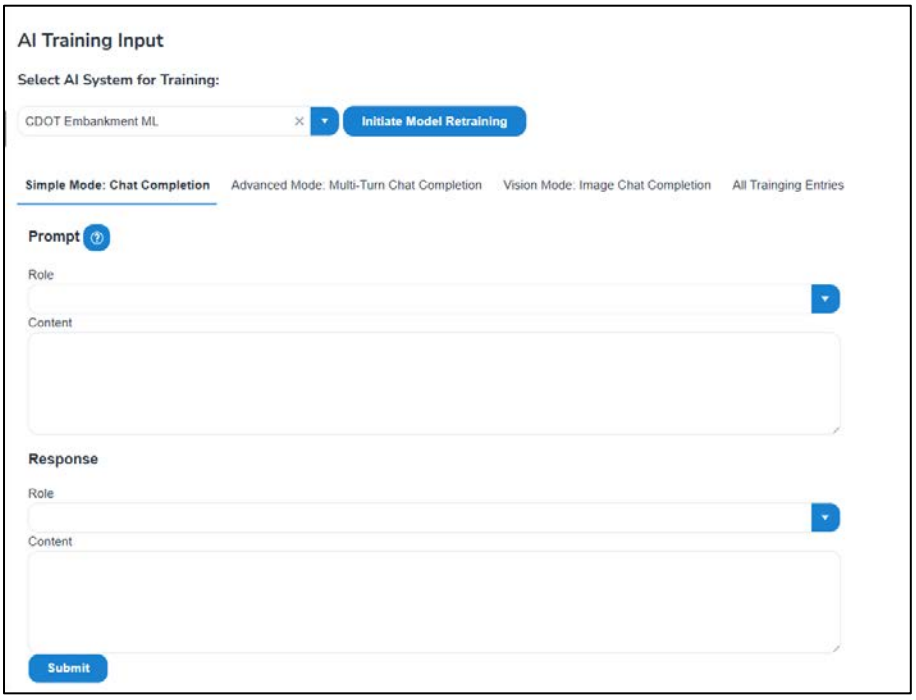


Figure 2 - Training Dialogue Box

The System learns from the dialogue in a way that is analogous to a student learning from homework practice problems. The user can submit prompts as text entries or with images. An example of an image-based training interaction is provided below:

Prompt
Role: User
Content: Both the yellow highlight and red line are not a part of the image and are used for illustrative purposes only. The red line shows the natural slope and the yellow highlight shows a crack in the ground. The red line is drawn parallel to the original ground surface above the cut that existed before the road was constructed. How does the pavement crack indicate an embankment failure and how does the natural slope interact with this crack?



Figure 3 - Photo Used in System Training Modules *(9)*

Response
Role: Assistant
Content: The photo shows pavement cracking which is curved and extends to the edge of the pavement under the guardrail. This crack shape indicates the early stage of embankment failure. The pavement crack is located within three horizontal feet in the plane of the photo to where the natural slope would intersect the pavement. The distance from the yellow lines in the center of the road to the white lines at the edges of the road is approximately 12 feet. The location of the crack on the pavement and where the natural slope intersects the pavement is approximately the boundary between cut and fill. The boundary of cut and fill below the pavement is the location of excavated, native soil and placed fill soil (embankment).

Through this interaction the System knows that concentric circular cracking is indicative of an embankment failure and that when extended through the road cut, the natural slope of the ground will intersect near the pavement crack. Additionally, the System can be trained in multi-turn mode, which involves a back-and-forth interaction between the user and the System, allowing for a more detailed dialogue. This allows the SMEs to train the System through a conversation and focus on the nuances of identifying embankment failures. An example of multi-turn mode is provided below:

Turn 1:
Prompt
Role: User
Content: Can you list the features that would indicate an embankment failure is present?

Response
Role: Assistant
Content: Key features of an embankment failure are (1) concentric circular cracking in the pavement, starting at the edge of pavement and traveling into the lane, located on the downslope side of the road (2) evidence of repaving over previous cracking (3) hydrophilic vegetation present in the area (4) warped and damaged guardrails at the location of the embankment (5) damaged culverts.

Turn 2:
Prompt
Role: User
Content: Are these the only features that indicate an embankment failure? Do these guarantee that there is an embankment failure present?

Response
Role: Assistant
Content: No, these are not the only features that may indicate that an embankment failure is present. Evidence of one these features does not guarantee an embankment failure is present but the more of the features that exist at a site, the higher the probability of the presence of an embankment failure.

In the absence of fine-tuning training, the AI model is limited to the foundational model from which it was derived. Fine-tuning and retraining allow for an iterative and additive performance improvement. As new training data is compiled, the previously fine-tuned model is further fine-tuned and retrained, resulting in a more capable model each generation.

As of the time of this paper, the System has undergone one training session, with 24 training prompts inputted. Based on industry-accepted practices, a training set as small as ten entries can impart specialization improvements. It is recommended that retraining is run with between 100 and 1,000 prompts inputted (a wide range) *(10)*. Until a desired improvement is reached, the lower range is most efficient for rapid validation. Depending on the domain or discipline and the uniqueness of related knowledge, improvement gains may be significant with a small amount of high-quality training data. The process of fine-tuning and training data creation is both art and science. Training inputs have primarily focused on what cracking patterns constitute embankment failures and other visual indicators of a failure, such as hydrophilic vegetation, existing mitigation, warping guardrail, and projecting the original ground slope to determine if the failure is occurring on the cut/fill line. Training has also focused on what does not constitute an embankment failure. Training examples included guard rail damaged from traffic accidents, alligator cracking patterns and circular cracking located on the upslope lane of the highway. Both positive and negative examples aid in the System's ability to properly identify embankment failures.

Expert System

In addition to the training interface, the System can produce dramatically improved results through cues and context provided during prompting. The Expert System not only relies on its robust training interface but also significantly benefits from the practice of "prompt engineering". By carefully crafting the prompt to include necessary background or useful information, the System's AI will better traverse its available reference information more effectively. In practical terms, this has the effect that well-constructed prompts can steer the System to generate responses that are more accurate, relevant, and aligned with the complexities of geotechnical practices.

Machine Learning

The System supports extensive integration capabilities, allowing users to incorporate both commercial and custom software application alongside existing tools like ArcGIS and CDOT Windshield. These models function as additional tools for the Reasoning AI, expanding its ability to analyze data, identify patterns, and support decision-making.

RESULTS

Model Validation on Known Embankment Failures

To initially assess performance, the System was asked to identify embankment failures located along Colorado State Highway 133 (SH133). SH133 has numerous embankment failures extending the length of the corridor and the project team has conducted multiple studies and mitigation designs on embankment failures in this area. Much of the knowledge library was developed from studies the project team conducted on SH133 and many of the training photos are along this highway. As such, the System should be well equipped to identify failures along this corridor. Figure 4 shows an example of the prompt for the validation and an example of the output from the System.

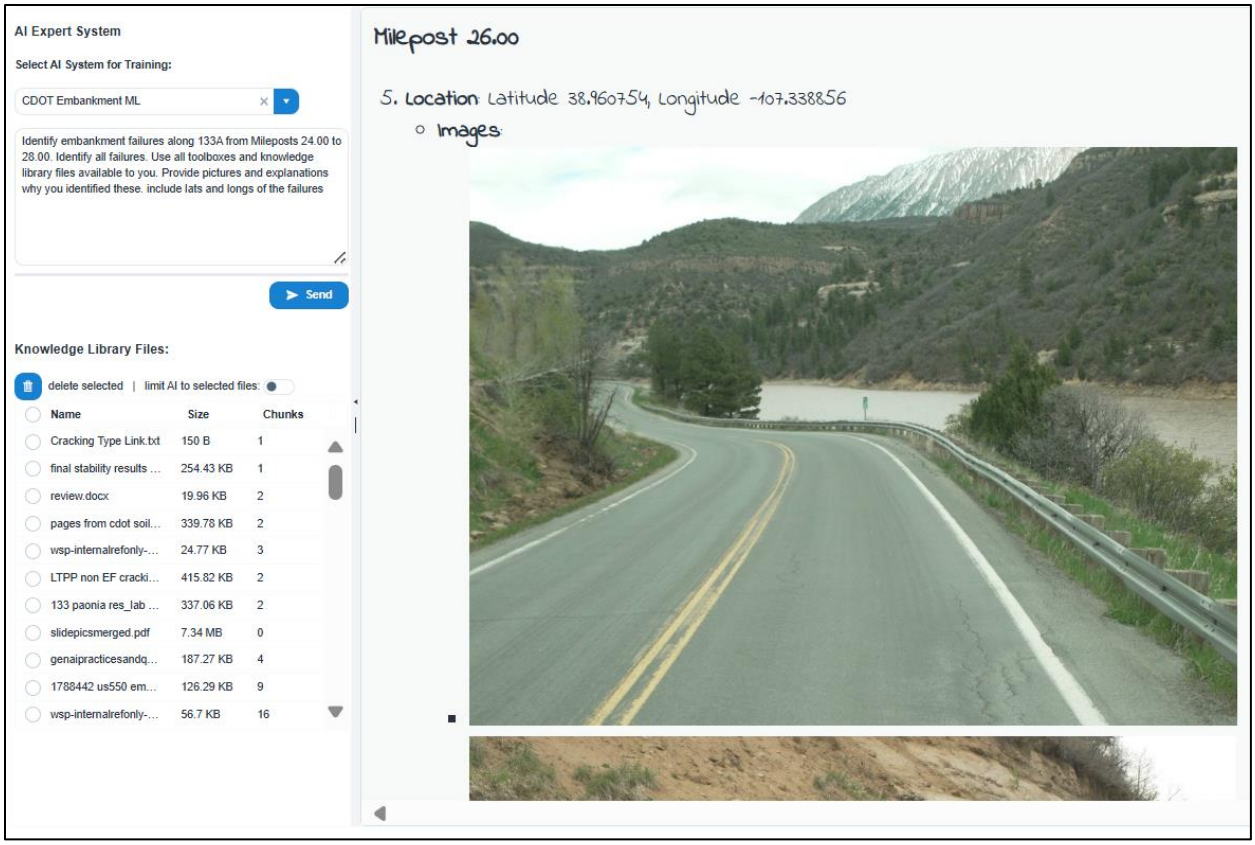


Figure 4 - Example of an Output From the AI System Validation Exercise for Colorado SH 133

Golder 2018 ranked sites based on the consequence of failure and the progression of failure over time *(11)*. **Error! Reference source not found.** shows a comparison between failures identified from Golder's 2018 feasibility report. The System was able to identify 4 of the 5 Consequence A sites and of all the Ranking 1 sites identified in Golder 2018 *(11)*. Initial tests along SH133 show that the System can appropriately identify embankment failures extending over a large length of the road, however it needs further refinement to identify the smaller and less severe failures. Considering that the model has been trained on 25% of the recommended minimum training inputs, the project team considered this initial model validation a success.

Table 2: Priority Sites Identified in Golder 2018 Compared to Sites Identified by the AI System *(11)*.

ID	Approx Begin MP	Approx End MP	Progression[1]	Consequence[2]	Rank	Identified by AI System
9	24.93	24.97	1	A	1	x
16	25.77	25.82	1	A	1	x

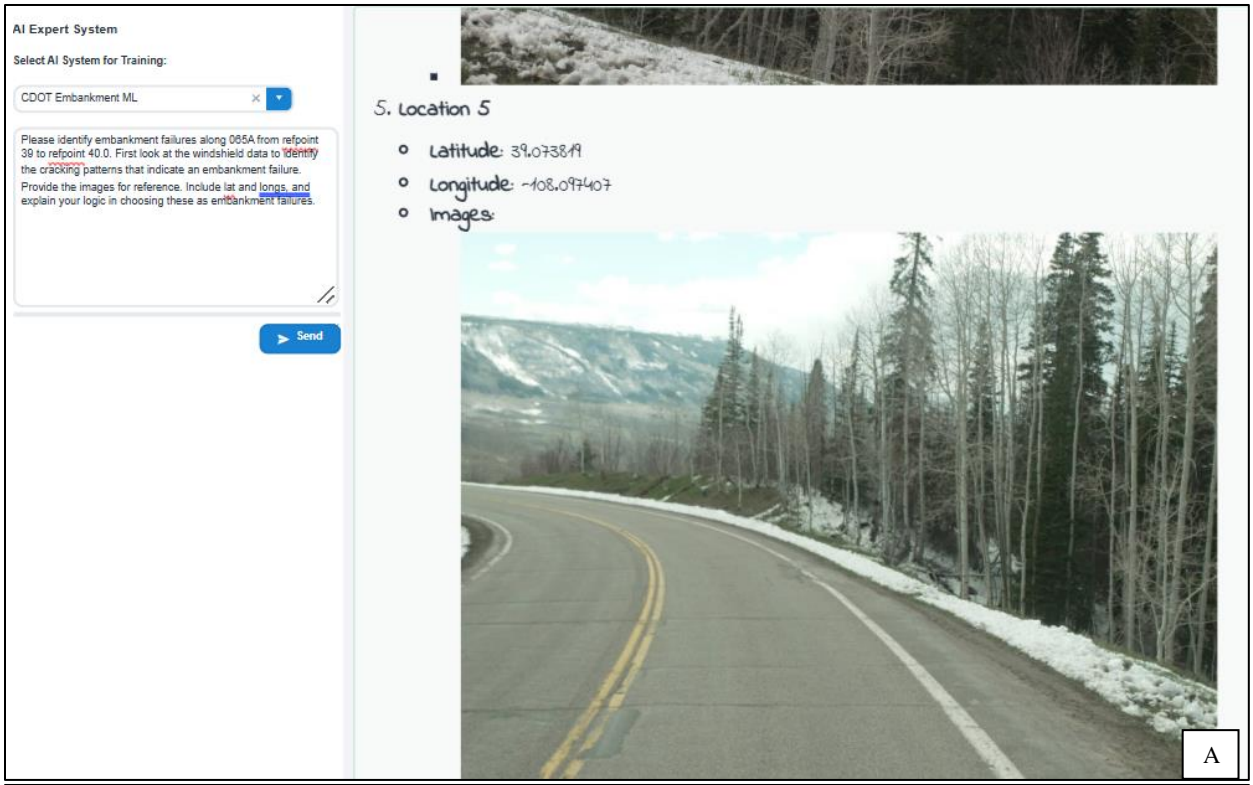
Table 2: Priority Sites Identified in Golder 2018 Compared to Sites Identified by the AI System *(11).*

ID	Approx Begin MP	Approx End MP	Progression[1]	Consequence[2]	Rank	Identified by AI System
25	26.99	27.01	1	A	1	x
8	24.86	24.89	1	B	2	
11	25.16	25.18	1	B	2	
15	25.44	25.47	1	B	2	
23	26.57	26.59	2	A	2	
28	27.29	27.37	2	A	2	x

[1] 1 - Significant movement has already occurred, 2 - Deformation/movement
[2]A - Two lanes, B - One lane

Model Testing on Other Highways

After validating the System with known embankment failures on SH133, the project team tested the model by prompting it to identify failures along Colorado 65 (CO-65) near Grand Mesa, Colorado. This stretch of highway was chosen because the project team is aware of embankment failures along the corridor, but the System does not have any information specific to CO-65 in its knowledge library. Figure 5 shows an example of failures identified by the System.



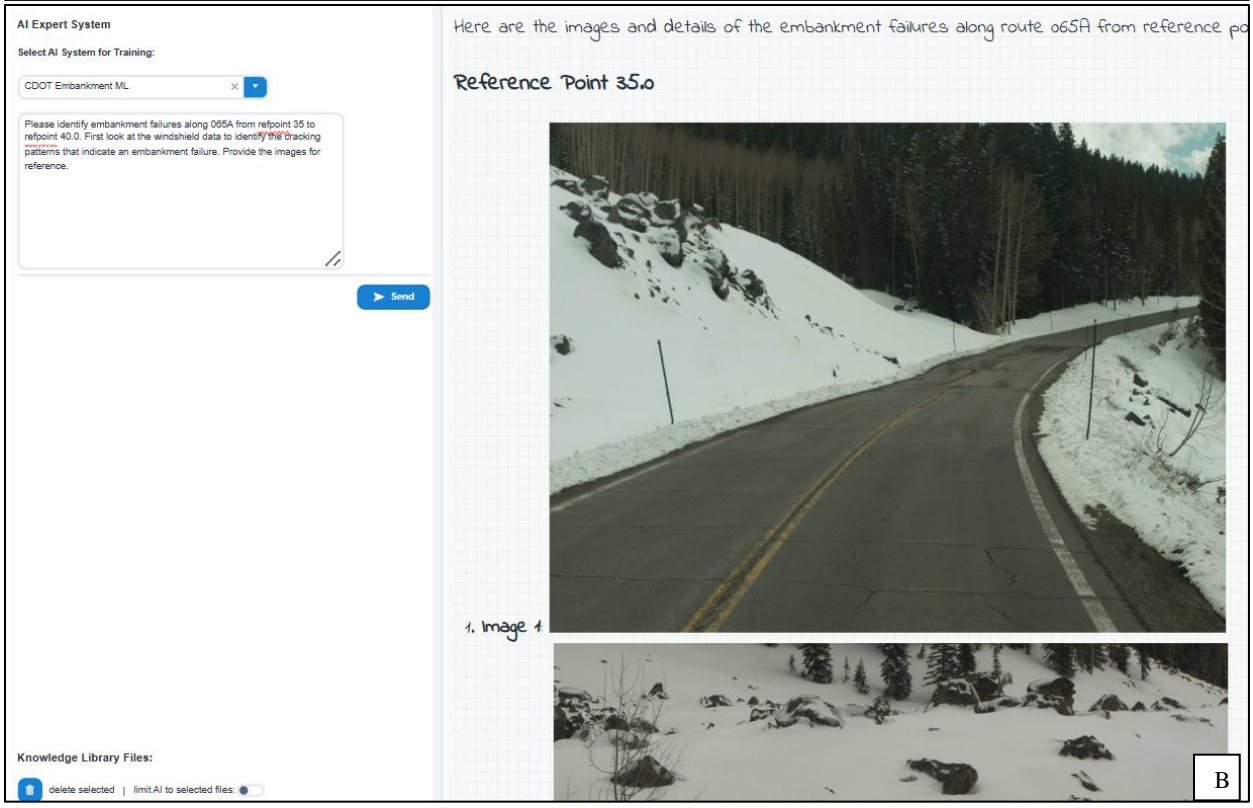


Figure 5 - Examples of a Prompt and Subsequent Result for Embankment Failures Along CO-65.

The System was able to identify known embankment failures for the corridor and indicate several failures that the project team was not previously considering. However, the tests along CO-65 showed an inconsistency in what was identified. Prompting for analysis of longer lengths of highway resulted in non-reported failures.

For example, the prompt "Please identify embankment failures along 065A from MP35 to MP40.0. First look at the windshield data to identify the cracking patterns that indicate an embankment failure. Provide the images for reference." resulted in the System identifying one failure located around MP35 (Figure 5a). However, after re-prompting to search for failures from MP39 to MP40, the System identified a large failure (Figure 5b) at approximately MP39.2.

Conclusions of the initial tests show that the System has successfully identified embankment failures on highways where previous feasibility studies have not been conducted and no inventory tabulation is available to the AI system. This blind test provides confidence in the efficacy of the System for identifying embankment failures and serves as preliminary proof-of-concept. However, considerable effort is required to improve the functionality of the System, as discussed in depth below.

DISCUSSION

The idea for using AI to identify embankment failures came from consideration of the current state of practice for collecting embankment failure information and consideration of whether a more efficient way to refine the inventory could be implemented. Over the past two years, AI has advanced at an unprecedented pace. In March 2023, OpenAI released GPT-4, a milestone that redefined AI's capabilities *(6).* Now, in 2025, autonomous AI agents have emerged with advanced reasoning, problem-solving abilities, and the capacity to interact with the external world beyond their native functions through digitally provisioned tools *(6,7,8).* With these advancements becoming more accessible, affordable, and widely adopted, the opportunity to explore and develop novel applications of AI is greater than ever.

Lessons Learned

Engineering Judgement and AI

Throughout development of the System, the project team gained an understanding of where we can add value to geohazards management through utilizing AI and gained perspective of the required coordination effort between the developers, SMEs, and stakeholders. At the beginning the project, geologists and geotechnical engineers on the project team thought that because identification of embankment failures is conducted primarily through visual assessment, it would be a straightforward task to develop an AI system that can identify these failures. The original goal of the project was to develop a system that could refine CDOT's initial screening inventory and identify embankments that show deterioration and therefore carry risk exposure. While the project team had no intention to replace the need for in-depth investigation or field activities, the hope was to be able to give practitioners probable failure locations to more efficiently conduct field studies.

Despite having the necessary internal resources in terms of computing power and expertise, the project team quickly learned that additional effort was required to achieve the highly specific outputs demanded by embankment condition assessment. A crucial part of this effort involved quantifying a depth of knowledge that was not available in online sources or standard textbooks but rather came from a lifetime of hands-on experience. These AI systems demand meticulous fine-tuning and carefully engineered prompts; in this effort, success was achieved through a blend of art and science, enhanced by extensive experimentation.

Cross-Disciplinary Communication

Even with powerful data handling, advanced computational reasoning, and access to expert human knowledge, the project team spent numerous hours grappling with how best to bridge the gap between domain-specific challenges and the capabilities of AI and machine learning. The geologists and geotechnical engineers who understood embankment failures were not always equipped to leverage AI for the task. Thus, clear, continuous communication was essential. The SMEs provided the necessary tools, training materials, and clear definitions, while the technical team supplied the ML frameworks, component designs, and practical demonstrations.

Realistic Expectations

When the project team began this process, the definition of proof-of-concept was not well defined. The overall concept was to leverage AI to identify embankments on a network level, with the original expectation being that we could simply ask the System to show embankment failures for the state of Colorado. As the project progressed, the SMEs discovered that there was significant work required on training and fine-tuning the System, and additional toolboxes would need to be connected. Despite inputting dozens of technical reports, the AI system needed more context to extract value from the reports. For example, before it could understand information about the cracking patterns listed in the report, the project team needed to give it context on what ‘circular cracking’ meant. Before we had connected the toolboxes, the System had no way to associate ‘SH 133’ with a physical highway. The project team realized that our AI System could not associate different technical information with physical reality, until we trained it on how to do so.

For certain prompts, the System had the ‘intelligence’ to know what it was supposed to do but needed to be connected to specific resources to perform the task. For example, the project team prompted it to draw a cross-section at a certain milepost of highway. Instead of outputting a cross section, the System described how it would draw a cross-section, had it been given the capabilities to do so. Thus, as the work continued, the definition of proof-of-concept morphed from network-level identification with a single button, to developing the System to identify failures along smaller stretches of roadway.

Training Evolution

As the System expands from proof-of-concept into a practical solution for embankment failure identification, the training and training prompts will likewise evolve. To date, training has been focused on the fundamentals of an embankment failure, as this was the most important aspect for the System to complete the desired tasks for the proof-of-concept level goal. There are additional

methods of training and available resources to connect as toolboxes the project team can leverage to improve the functionality of the System.

Future of Work

As the System currently functions, it can identify failures within a specified range of mileposts along a specified highway. As discussed above, further refinement of the AI tools and future training based on other embankment failure signatures will be necessary to ensure reliable results at a larger scale. The next milestone of the project after the System has been fine-tuned and is considered sufficiently reliable for longer stretches of corridor is to have the System properly identify failures along an entire corridor is to expand portion of the state where a complete inventory of embankment failures exists and provide a risk rating of the identified failures.

With considerable additional work and training, the project team believes the System could provide preliminary prioritization of sites and estimate the rate of movement or condition of existing failures. While the tool is helpful as an initial screening for indications of failure, there is no replacement for SMEs. The project team sees this as a tool for practitioners to use in an initial screening of embankments; the intent is not to replace field verification and assessments to understand the embankments' susceptibility to failure and overall stability, but to rather allow the practitioner to efficiently plan and focus field efforts.

Prediction of future failures is not likely achievable, but early detection of failures could result in significantly reduced mobility and maintenance costs as it is much easier to stabilize an embankment before the failing block moves far downhill.

CONCLUSION

The purpose of this project was to explore whether artificial intelligence could assist in identifying embankment failures on a network level using remote sensing data, public GIS tools, and domain-specific training. The project team aimed to understand the feasibility of deploying a trained AI model to assist practitioners in early identification of failure locations, ultimately improving the efficiency of geotechnical asset management.

Initial results from validation and blind testing demonstrated that the System could correctly identify known embankment failures and detect undocumented indicators of failure. These findings affirm the System’s ability to synthesize diverse data sources and emulate aspects of expert judgment, even when working with limited initial training inputs. Limitations of the current system include a dependency on the phrasing of prompts, incomplete toolbox integrations, and the need for additional training to fully capture the complexity of embankment failure mechanisms. The value proposition lies in the ability of this system to supplement traditional field efforts by narrowing the focus of investigations and refining the embankment inventory. By identifying probable failure locations more efficiently, the System can support improved prioritization of sites and early interventions, potentially reducing both mobility and maintenance costs. The System cannot replace SMEs or predict future failures, but it can assist in preliminary screening.

Throughout development, the project team learned that engineering judgment cannot be easily replicated by AI without considerable effort. The knowledge required to identify embankment

failures often resides in the tacit experience of practitioners and must be translated into structured training data. Additionally, aligning the expectations of geotechnical experts with the capabilities of AI required extensive collaboration and clear communication across disciplines. The definition of "proof-of-concept" evolved throughout the project, shaped by iterative testing, system limitations, and technical constraints. In the end, despite the steep learning curve for everyone involved, a system was developed that shows promising results. With ongoing refinements, it is expected that the System will continue to evolve, gradually aligning real-world performance with our original expectations.

REFERENCES

1. Colorado Department of Transportation (CDOT). https://www.codot.gov/about/CDOTHistory. Accessed May 28, 2025.

2. Federal Highway Administration. (FHWA), 2025. https://highways.dot.gov/highway-history. Accessed May 28, 2025.

3. United States Census Bureau (USCB), 2025. https://www.census.gov/. Accessed May 28, 2025.

4. National Academies of Sciences, Engineering, and Medicine (NCHRP), Geotechnical Asset Management for Transportation Agencies, Volume 1: Research Overview, Washington, DC: The National Academies Press, 2019. https://doi.org/10.17226/25363.

5. BGC Engineering, Embankment Risk Assessment Framework, Prepared for the Colorado Department of Transportation, February 2024

6. Sanderson, K., GPT-4 is here: what scientists think, *Nature*, March 16, 2023.

7. Ball, P., Chemistry Nobel Awarded for an AI System that Predicts Protein Structures, October 11, 2024. https://physics.aps.org/articles/v17/149

8. Niemann, D., S. Borenstein, and M. O'Brien, Pioneers in artificial intelligence win the Nobel Prize in physics. Associated Press. October 8, 2023. https://apnews.com/article/nobel-prize-physics-fc0567de3f2ca45f81a7359a017cd542

9. Google Earth, 2025. Accessed May 29, 2025.

10. Microsoft, When to use Azure OpenAI fine-tuning. March 26, 2025. https://learn.microsoft.com/en-us/azure/ai-services/openai/concepts/fine-tuning-considerations

11. Golder Associates Inc. (Golder), SH-133 Paonia Reservoir Embankment Failures – Preliminary Evaluation, Prepared for Colorado Department of Transportation, March 15, 2018.

Rockfall Mitigation and Slope Stability Solutions for Interstate 78 in Bethlehem, New Jersey

Christina M. Comuso
New Jersey Department of Transportation
1035 Parkway Ave.
Ewing, NJ 08618
(856)-357-1141
Christina.Comuso@dot.nj.gov

Brian T. Felber, PE
HNTB Corporation
9 Entin Road, Suite 202
Parsippany, NJ 07054
(973)-800-5502
bfelber@hntb.com

Prepared for the 74th Highway Geology Symposium, August, 2025

Acknowledgments

The authors would like to thank the individuals/entities for their contributions in the work described:

Amanda McElwain – NJDOT, review
John Szturo, PG – HNTB Corporation, review
John Schuring, PhD, PE – HNTB Corporation, review
Matthew Riegel, PE – HNTB Corporation, review
Hager-Richter Geoscience, Inc. providing geophysical surveys

Disclaimer

Statements and views presented in this paper are strictly those of the authors, and do not necessarily reflect positions held by their affiliations, the Highway Geology Symposium (HGS), or others acknowledged above. The mention of trade names for commercial products does not imply the approval or endorsement of HGS.

Copyright Notice

Copyright © 2025 Highway Geology Symposium (HGS)

All Rights Reserved. Printed in the United States of America. No part of the publication may be reproduced or copied in any form or by any means – graphic, electronic, or mechanical, including photocopying, taping, or information storage, and retrieval system – without prior written permission of the HGS. This excludes the original author(s).

ABSTRACT

This paper will discuss the design and construction of rockfall mitigation measures along Interstate 78 in Bethlehem, New Jersey, focusing on the creation of engineered catchment ditches through presplit controlled blasting of two existing rock slopes. These slopes, approximately 1,500 feet long each with inclinations of 0.25H:1V, posed significant construction challenges due to their proximity to high-traffic volumes and environmental restrictions related to snow and endangered wildlife. The project incorporated significant widening of the cross section along with installation of rock dowels, shotcrete, and rock drains to enhance stability and safety. Existing slope heights ranged from 90 to 140 feet with minimal catchment widths, as little as 6 feet, adjacent to the pavement.

The comprehensive site investigation process will be discussed, including subsurface exploration, geophysical surveys, and geologic mapping, which aided with the rock slope stability analysis. Stereographic analysis was utilized to assess kinematic feasibility of failure mechanisms such as planar sliding, wedge, and toppling, while limit equilibrium analysis using RocScience SWedge provided insights into wedge sliding stability.

Key construction challenges included managing blasting operations adjacent to a major interstate with an anticipated 2-Way Average Annual Daily Traffic (AADT) of 87,952 vehicles per day in 2018. The paper discusses strategic approaches to minimize disruptions and ensure public safety during and post construction. An assessment of alternative mitigation strategies is also presented, highlighting the decision-making process and lessons learned.

INTRODUCTION

This paper describes challenges and solutions for rockfall mitigation at the New Jersey Department of Transportation (NJDOT) Interstate 78, Bethlehem Rockfall Mitigation Project. The project was complicated by: limited existing catchment, which was as little as 6 feet, maintenance and protection of traffic considering high AADT, limited work zone area due to the existing slope and lack of a median, limited 15-minute roadway closures allowed per blast, protection of underlying active and abandoned rail tunnels and adjacent structures, protection of a hibernaculum for threatened and endangered bats with seasonal tolerable vibration thresholds, and seasonal restrictions for snow removal.

The primary objective of this project is to improve the safety of the traveling public. The I-78 eastbound (EB) and westbound (WB) slopes were ranked numbers 2 and 4, respectively, in the NJDOT Rockfall Hazard Management System. The project is located along Interstate 78 between Mileposts 10.06 and 10.40 in Bethlehem Township, Hunterdon County, New Jersey. Project limits, existing Right-of-Way limits, and the horizontal location of the underlying active and abandoned Norfolk Southern Pattenburg Tunnels are provided in Figure 1.



Figure 1 – Project limits

Interstate 78 is a rural interstate highway which traverses the state generally in an east-west direction. It serves as a vital transportation corridor that facilitates the movement of freight and the traveling public from New York City to central Pennsylvania, with approximately 22 percent truck traffic. Its rock slopes were excavated between 1958 and 1960, as part of the original construction of I-78, which initially included only two lanes in each direction with a grass median. One additional lane in each direction, separated by a concrete barrier, was added to the median as part of a 1970 widening project without modification of the rock slopes. The 1958 design included rock cut slopes of 0.25H:1V to 1.5H:1V and 12-foot-wide benches at heights of 40 and 80 feet, as shown in Figure 2a, below.

The proposed rock cut slopes for the current mitigation project are shown in Figure 2b, below, and include lower 0.25H:1V or 0.5H:1V rock slopes for the EB and WB roadways, respectively. Up to 30 feet of soil overburden was present above top of rock on the WB slope, therefore, a 10-foot-wide bench and 2H:1V soil slope was excavated above the soil to rock interface.

The method of blasting for the 1958 project is unknown, but very little evidence of pre-splitting or controlled blasting was observed during the field reconnaissance. Evidence of drilling

included a limited number of half-rounds noted in the vicinity of MP 10.2 EB. As a consequence of the original construction practices and subsequent block rockfalls, the cut slopes have evolved to a rough, highly irregular, and non-uniform character. The existing slope is compound, due to the benches from the original construction, with a lower rock cut slope and upper shallower soil or rock slopes. Overall slope heights and lower cut slope heights for the EB rock slope generally range from less than 40 feet to greater than 140 feet and less than 30 feet to greater than 90 feet, respectively. Slope heights for the WB rock cuts generally range from 50 to 80 feet and cut slope heights for the WB rock slope range from 40 to 70 feet. Inclinations for the lower existing cut slopes are generally in the range of 40 to 70 degrees. The upper portions of both slopes are flatter above the crest of the lower slope. Several remnant benches are present on the EB and WB slopes, likely related to the original construction. The benches are relatively flat and approximately 10 to 30 feet wide, 20 feet on average. The rock catchment ditch at the toe of the slope is poorly defined and substandard by current design practice and ranges from 6 to 15 feet and is setback from the guiderail to toe of slope.

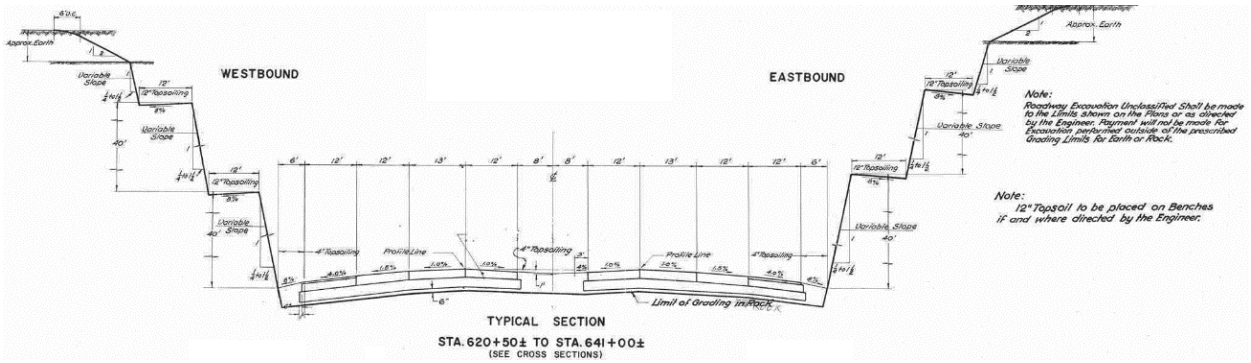


Figure 2a – Original 1958 highway construction section

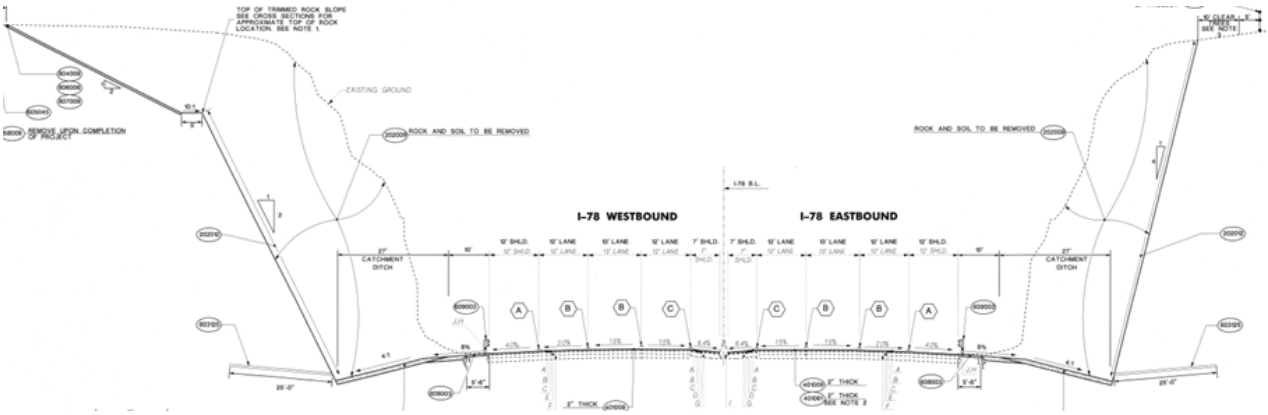


Figure 2b: Typical section for the current rockfall mitigation project

An active Norfolk Southern railroad tunnel and parallel abandoned rail tunnel pass beneath I-78 on a northwest to southeast alignment, approximately 220 feet below highway grade (*1*,*2*,*3*). The Lehigh Valley Railroad Company constructed the Musconetcong Tunnel (also referred to as the Pattenburg Tunnel) to allow coal to be transported along the Easton & Amboy rail line. The original tunnel was in service from 1875 to 1928, at which time, construction of the second tunnel with improved clearance was completed to allow for the passage of larger trains (*4*). The construction of both tunnels predates the construction of the I-78 cut.

ROCKFALL HISTORY

During the site reconnaissance, there was evidence of rockfall (past and present) throughout the project limits, consisting of localized fresh rock faces, impact damage, and debris piles. A complete history of rockfall events is unavailable, however, several events have been documented including the following. Approximately 5 cubic yards of rock fell on April 20, 2015, including roughly a 4-foot diameter rock block, in the WB lane at milepost 10.1. Most of this material was retained behind the guiderail with smaller fragments landing in the right travel lane of WB (Figure 3a).

In March 2021, another rockfall event occurred WB at the easterly end of the project limits, just months before construction activities were set to begin (Figure 3b). Other reported rockfall events came from the traveling public who notified NJDOT of smaller rocks and debris that were in the roadway.



Figure 3a – Remnants of 2015 rockfall event looking north at WB slope, Figure 3b Spring 2022 rockfall event, WB slope Station 639+00 looking West

GEOLOGY

The site is located in the Highlands Physiographic Province, near the border of the Piedmont Physiographic Province (*5*). The Highlands Province generally consists of a series of discontinuous rounded ridges separated by deep, narrow valleys and is primarily underlain by highly metamorphosed and igneous rocks of the Middle Proterozoic Era, roughly 0.9 to 1.2 billion years old. Structurally, the area has been highly disturbed by intrusion and over thrust faulting.

The site lies within the extents of the Pre-Illinoian glaciation, near its terminus, but is located to the south of the more recent Illinoian and Wisconsinan glaciations. The Pre-Illinoian soils were deposited approximately 800,000 years ago. Colluvium, Pre- Illinoian Till, and silty sandy gneiss saprolite and rock rubble are present in the vicinity of the site (*6*). Massive glacial

erratics were observed above the WB Slope. The heterogeneous nature of the surficial geology and glacial origin indicate the depth to bedrock may be variable.

The overburden materials are characterized as glacial, late Wisconsin to Middle Pleistocene colluvial deposits. The literature describes the material as sandy silt, silty sand, clayey silt or gravelly sand deposits, consisting of very poor to poorly sorted matrix of sand, silt and clay, commonly containing 5 to 60 percent angular rock chips, pebbles, cobbles and small boulders; commonly massive and indistinctly layered; locally stratified; deposited on slopes by creep, sheetwash, debris flow, and solifluction processes; and containing local boulder talus. Also mapped nearby, is material characterized as Quaternary and Tertiary Saprolite, Residuum, and Rock Rubble, described as silty, sandy, gneiss saprolite and rock rubble.

The borings along and back of the cut-slope daylight points indicate material is composed of sand with various amounts of gravel and silt. The depth to rock is consistently shallow along the EB slope. However, depth to rock along the WB slope varies considerably. Depth to rock in those borings varies from 1.5 to 34 feet. Large boulders ranging up to 20+ feet in diameter are also noted on the surface north of the I-78 cut. The variable depth to bedrock could be the result of differential weathering (saprolite) of the bedrock, or boulders such as the ones at the surface and the subsurface. The boulders at the surface appear similar to the gneiss bedrock.

Topography

The study area cuts through one of the local northeast trending ridges. The high point of the ridge is approximately 830 feet above mean sea level. The low point of the western edge of the cut is approximately 680 feet above mean sea level, a difference of about 150 feet. The topography slopes down towards the west along I-78 to a low point of approximately 275 feet at the Musconetcong River for an area relief of over 500 feet.

Rock Type and Discontinuities

Bedrock and surficial geology maps are appended as Figures 4a and 4b. The area is underlain by rocks of the Middle Proterozoic Age, Losee Metamorphic Suite, described as Quartz-Oligoclase Gneiss, white when weathered, light greenish gray, medium to coarse grained, moderately layered to indistinctly foliated gneiss and lesser amounts of granfels composed of biotite, hornblende and clinopyroxene (*8*). The rock may also contain granitic plutonic igneous intrusions of middle Proterozoic age consisting of amphibolite or pegmatite, which are described as medium-grained, very dark gray to black, and foliated (*8*). Pockets of magnetite were observed in the pegmatite.

While not mapped in the literature, Hornblende Granite was also noted in lesser areas within the roadway cut. The Hornblende Granite is described as pinkish gray to medium buff, weathering pinkish white or light pinkish gray, medium to coarse grained, gneissoid to indistinctly foliated granite and sparse granite gneiss composed principally of microcline micro perthite, quartz, oligoclase, and hornblende (Figure 5a and 5b). Some phases are quartz syenite or quartz monzonite. The predominant joint set trends northwest and is nearly vertical; a

secondary joint set is nearly perpendicular trending east-northeast with a dip of 70 degrees to the northwest.

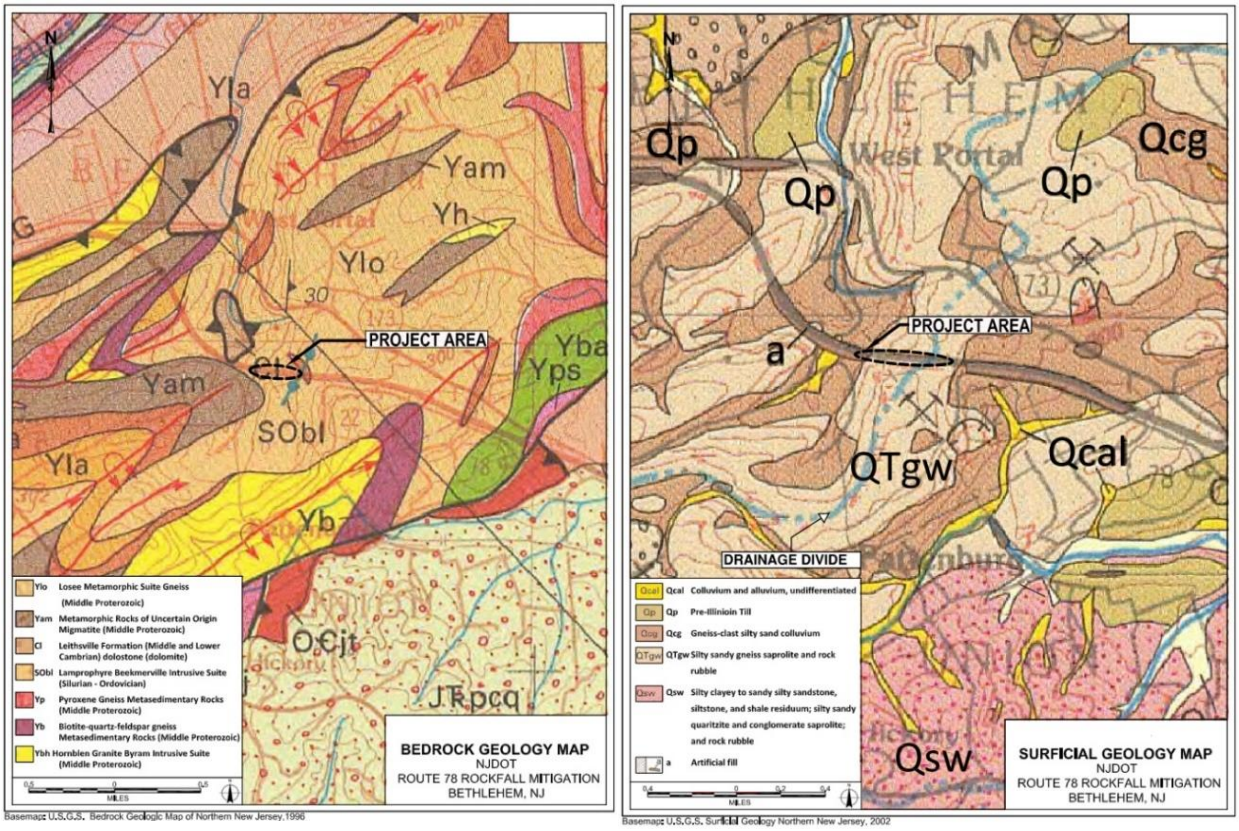


Figure 4a and 4b – Bedrock and Surficial Geology Maps
Left–Bedrock, Ylo-Gneiss, SObl-Beekmerville Intrusive Suite (*6*)
Right–Surficial, (*9*)



Figure 5a – Pegmatite East end of EB and Figure 5b – Granitic Gneiss typical

Water

The rock cut along the EB (south side) slope of I-78 experiences substantial water seepage and is reported to result in a significant accumulation of ice in the winter. The water originates from the ridge area to the south of the cut, an area of approximately 0.5 square miles. The source is most likely rainfall percolating through the thin soil and fractured rock. It travels northwestward along the steeply dipping joint set and intersects the predominant northwest orientated vertical joint set exiting at the roadway cut. The approximate drainage area boundaries are shown in Figure 3b. Typical seepage and ice conditions are shown in Figures 6a and 6b, respectively.



Figure 6a – Typical seepage and Figure 6b – Typical winter ice conditions 2020-2021

SUBSURFACE EXPLORATION

A subsurface exploration program consisting of four borings was performed between December 2016 and January 2017. The borings were advanced using mud rotary drilling techniques with a track mounted Acker XLS drilling rig. The soil was sampled continuously to 12 feet, and every 5 feet, thereafter, extending to a minimum of 10 feet below the toe of slope. A supplemental subsurface exploration phase consisting of four borings was performed in May 2017. Soil sampling was not conducted as part of this exploration; borings were drilled to verify the top of rock along the WB slope. The Standard Penetration Test (SPT) was performed at each boring, in general accordance with ASTM D1586. Soil samples were retrieved using a 24-inch-long split-spoon sampler (2-inch O.D., 1.375-inch I.D.), driven by a 140-lb automatic hammer free falling 30 inches. Groundwater elevations were recorded when encountered. Rock cores were taken at all boring locations and obtained in general accordance with ASTM D2113, “Standard Practice for Diamond Core Drilling for Site Investigation”. An NQ double tube core barrel was used. Nearly continual loss of water during coring was observed. Recovery ranged from 10 to 100% with an average of 90%. Rock Quality Designation (RQD) ranged from 0 to 100% with an average of 70%.

Laboratory Testing

The laboratory testing program included 14 unconfined compressive strength tests on rock core specimen in accordance with ASTM D7012 to obtain the unconfined compressive strength, total unit weight, and elastic modulus, and 18 direct shear tests on saw cut rock core specimen to obtain the basic friction angle in accordance with ASTM D5607. The total unit weight ranged from 162 pcf to 194 pcf with an average of 180 pcf. The unconfined compressive strength of rock core samples ranged from 12,740 to 36,350 psi, with an average of 23,779 psi. The basic friction angle of saw cut rock core samples ranged from 26 degrees to 36 degrees, with an average of 33 degrees. Samples were predominantly comprised of fine grained to medium grained granitic gneiss with varying levels of weathering and jointing.

Geologic Mapping

A site reconnaissance, which focused on the identification of discontinuity orientation and condition, was performed from Wednesday, January 18, 2017 to Thursday, January 19, 2017. At the time of the reconnaissance, the vegetation was dormant, and no snow or ice was present. In general, the slope was viewed from the toe of slope and shoulders of I-78. The upper benches and crests of the EB and WB slopes were accessed on foot and the upper EB slope was also mapped from the bench. The line mapping was performed using a Brunton Compass and the phone application FieldMove Clino. General observations were made about the exposed length of discontinuities, or persistence of discontinuities, and the joint roughness of discontinuities.

Geophysical Surveys

A borehole geophysical logging program consisting of Optical Televiewer (OTV) and Acoustic Televiewer (ATV) logging was performed upon completion of the boreholes. The orientations of bedrock structures (fractures, bedding, foliation, veins, and other planar geologic features) were reported as the dip azimuth (dip direction) and dip angle (dip) of each structure. The OTV and ATV dip azimuth data is referenced to true north using a magnetic declination of 13° west and the bedrock structure dip angle data are reported from horizontal. The discontinuities were compared to the physical rock core and used to filter dip and dip direction data.

Seismic refraction geophysical surveys were performed in February 2017 from the existing ground surface at the proposed EB and WB cut lines to verify the top of rock elevation. Figure 7, below, illustrates the variable overburden thicknesses along the WB slope. There were 3 distinct velocity changes detected at the WB slope and 2 at the EB slope. The velocity changes were used to aid in soil and rock stratification. In general, competent bedrock was found to be present for the full height of the proposed EB cut. However, variable thicknesses of overburden soil were found to be present along the proposed WB slope cut line, which required a bench and shallower upper slope. The borings, observed top of rock in construction, and seismic refraction were in close agreement.

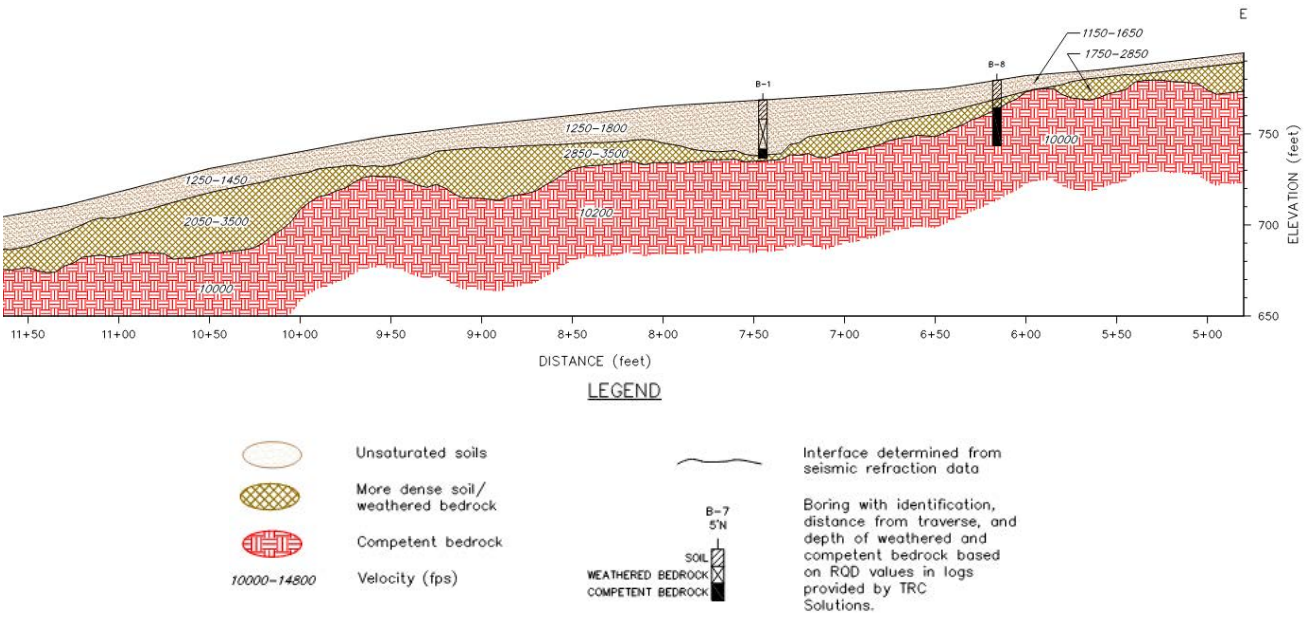


Figure 7- Excerpt from WB subsurface profile from borings and seismic refraction

ALTERNATIVES ASSESSMENT

Concept level mitigation alternatives were developed and compared in an alternatives analysis matrix, which considered the following categories; risk reduction, right-of-way, required maintenance, anticipated service life, construction impact on traffic, construction difficulty, construction duration, costs, environmental and aesthetic impacts. The alternatives considered incorporated combinations of re-grading, rock removal, rock reinforcement, and rockfall control. Ultimately, rock excavation by controlled blasting and pre-splitting final slopes was advanced to achieve stable faces and proper catchment. Additional mitigation efforts include installing rock drains to relieve hydrostatic pressure and reduce the impact of ice jacking and freeze-thaw cycles. Tree removal on and to 10 feet above the crest of slope was performed to prevent root wedging. Structurally controlled failure mechanisms were mitigated with spot rock dowel reinforcement and spot shotcrete. This alternative was preferred for the following reasons:

- High degree of risk reduction
- Virtually maintenance free
- Long service life
- Applicable to variable slope geometry
- Improves sight distance
- Collateral benefit for snow removal/storage
- Nearby rock disposal sites (quarries)
- Minimal aesthetic impact, as proposed rock slope will not be covered with mesh or shotcrete

ROCK SLOPE STABILITY

The shear strength of the individual discontinuities was controlling over the shear strength of the rock mass or the intact rock strength. The shear strength of rock discontinuities was estimated considering the basic friction angle with no contribution from joint roughness or cohesion, as the discontinuities were generally reported to be smooth and planar.

Rock slope stability analysis included stereographic analysis to assess the kinematic viability for planar sliding, wedge, and toppling failure mechanisms using RocScience DIPS software. Generally, low percentages of discontinuities resulted in kinematic viability for the planar sliding and toppling failure mechanisms. Wedge failure was kinematically viable on the WB slope at the existing 0.25H:1V slope inclination. Limit equilibrium analysis to determine factors of safety for the wedge failure mechanism and to assess flattening the cut slope inclination and patterned reinforcement was performed using RocScience SWedge Software. A 0.5H:1V slope provided a factor of safety greater than 1.5 and was preferred over the steeper slope with patterned dowels.

Failure mechanisms are defined as follows:

- Planar Sliding may occur if all of the following conditions are satisfied:
    - The sliding plane strikes nearly parallel (within ±20 degrees) to the slope face
    - The sliding plane "daylights" in the slope face (dip of sliding plane < dip of face)
    - The sliding plane's dip angle is greater than the friction angle
- Wedge Sliding may occur if the dip of the line of intersection of the wedge (intersection of the two planes) is both:
    - Shallower than the inclination of the slope face and
    - Steeper than the friction angle
- Toppling may occur if steeply dipping discontinuities are present and "daylight". Two forms of toppling commonly occur; flexural toppling and block or direct toppling.

The east-west alignment of the interstate produces rock cuts for the WB lanes that are south facing while those on the EB lanes are north facing. As a consequence of this orientation and the fact that the north-facing slopes exhibit active water seepage, severe icing conditions are experienced for the EB rock slopes. It has been reported the buildup of ice can extend several feet beyond the rock face and onto the shoulder of the roadway. Aperture along joints was commonly observed during the field reconnaissance and generally ranged from 0.25 inches to 2 inches. This dilation of joints was inferred to be caused by weathering and ice jacking, possibly made more susceptible by the original rock slope blasting. The north-facing slopes on the EB side are most vulnerable to this condition due to lack of sun exposure in the winter yielding the more pronounced ice build. However, the south-facing slope on the WB side has a greater history of past rockfall events, likely due to sun exposure, which results in more freeze-thaw cycles. Localized instances of root wedging were noted although the lack of vegetation on the lower cut slopes makes this a minor contributor to rockfalls. Similarly, local areas of differential weathering were observed near the crests of some slopes.

Slope failure mechanisms were observed or inferred from the site reconnaissance or determined from stereographic analysis based on limited structural mapping. The most prevalent failure mechanism is wedge failure. The south-facing slopes on the WB side are most susceptible to wedge failure. Although the persistence of the wedge-forming joints on the WB side is

sufficiently large to locally define near full slope height wedges, there is no historical record of large-scale failure events involving volumes more than a few cubic yards. The wedge mechanism appears to be episodic in which a block or group of blocks detach progressively in an upslope direction. Other mechanisms of structurally-controlled failure such as planar sliding and block toppling are locally present, but these tend to define small-scale isolated block falls.

ROCKFALL MITIGATION

The FHWA Rockfall Catchment Area Design Guide (*10*) was utilized to determine the preliminary required catchment widths for 95% rockfall retention based on the proposed slope inclinations and heights. The maximum cut slope height at the site was 80 feet. This resulted in catchment area widths of 25 feet and 22 feet, respectively, for 0.25H:1V and 0.5H:1V cut slopes for a 4H:1V catchment area slope and 37 feet and 26 feet, respectively, for a 6H:1V catchment area slope.

The preliminary catchment area widths were validated with subsequent rockfall simulation modeling using RocScience RocFall and the Colorado Rockfall Simulation Program (CRSP) Version 4.0 software in final design. The rockfall simulation models were based on cross sections cut using LiDAR survey surface data and were used to simulate rocks tumbling down a slope to predict the statistical distribution of speed, bounce height, and kinetic energy to evaluate ditch effectiveness. The programs account for the slope geometry, frictional and rebound characteristics of the slope, rotational energy of the rocks, rock size and shape, starting velocity and location, and ditch geometry. Rockfall block sizes of 4-foot diameter and smaller were simulated with a unit weight of 175 pcf and a spherical shape. Surface roughness, tangential coefficients, and normal coefficients for the various surface coverings (i.e. natural slopes, blasted slopes, graded soil catchment areas, etc.) were selected based on typical values recommended by the software technical manuals.

The rockfall simulation modeling verified a 25-foot width minimum catchment area would stop more than 95% rockfall from reaching the edge of pavement for both the 0.25H:1V and 0.5H:1V cut slopes with a 4H:1V catchment area slope. Ultimately, an additional 12 feet was added to the rockfall catchment areas, 37 feet total, to better utilize existing benches for constructability and provide flexibility for an unplanned future potential widening or climbing lane.

CONSTRUCTION CONSTRAINTS AND LIMITATIONS

Initial scheduling challenges emerged due to the suspected presence of the threatened and endangered Northern Long-Eared bat (NLEB) and Indiana bat. The United States Fish and Wildlife Service (USFWS) identified a reported bat hibernaculum within an abandoned rail tunnel at the west end of the project limits, which was the second largest bat hibernaculum in NJ based on a 1994 study. Required analysis and acoustic surveys were conducted in 2018 and suggested that a NLEB habitat might exist within the limits of the I-78 Rockfall mitigation project. As such, construction activities were obligated to follow USFWS requirements for

threatened and endangered bat species. The acoustic study included documentation of existing noise and vibration levels, along with predictions of the levels generated by necessary construction activities.

Per USFWS activities louder than 75 decibels (dB) would only be permissible between May 15 and August 15. All quieter activities (< 75 dB) may be performed any time of year. The 2018 noise analysis concluded none of the anticipated noise producing construction activities were expected to exceed 75 dBA or the existing background noise in the inactive Pattenburg Tunnel.

Vibration peak particle velocities within the abandoned Norfolk Southern Railroad tunnel had to abide by the following parameters:

- 1.0 inches per second (IPS) or less from May 16- August 15
- 0.25 IPS or less from August 16- November 15 and April 1 – May 15
- 0.02 IPS or less from November 16- March 31

Monitoring of vibration levels of the abandoned railroad tunnel was performed through three (3) bore hole seismographs that were installed across the jobsite. Figure 8 illustrates the proposed depth and location of the bore hole seismographs in relation to the tunnel. An additional two (2) surficial seismographs were installed at nearby dwellings that were within 200 feet of any active blast zones.

To ensure a viable blasting alternative was constructable and met the performance-based requirements while preventing impacts to the Indiana Bat and NLEB, a conceptual blast design was performed. To satisfy the performance-based specification requirements, in-hole (decked charges), hole-to-hole, and row-to-row delays were used to minimize noise and vibration. In addition, blast mats were used to minimize noise and vibration.

To keep from exceeding the *US Bureau of Mines* (*USBM*) maximum safe allowable air overpressure of 136 decibels (dB), the over pressure was not allowed to exceed 22 psi. The New Jersey Administrative Code (NJAC) limits air blast to a 130 decibel peak.

Additional studies performed in 2018 included a tree inventory and evaluation study to help minimize tree removal at the top of the rock cut slope in an effort to maintain any potential bat roosting trees and adhere to the exempt No Net Loss Applicability determination provided by the New Jersey Forest Service. During construction tree clearing was prohibited before April 1st and/or after November 16th as per USFW bat protection requirements.

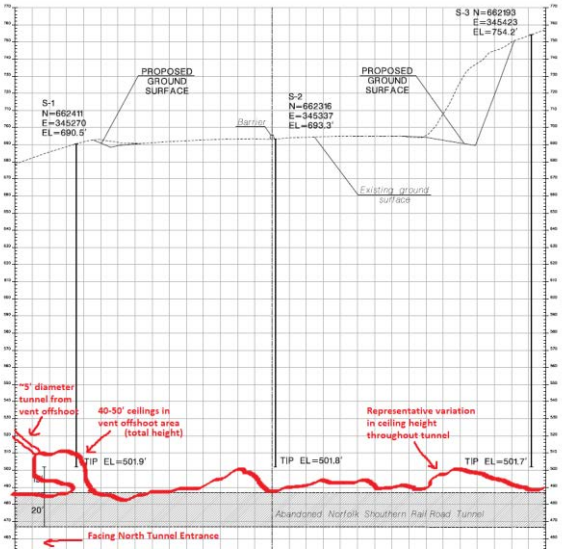


Figure 8- Cross section sketch of bore hole seismograph placement and depth above the abandoned Norfolk Southern Railroad Tunnel. Red line is from USFWS field observations.

The I-78 rockfall mitigation project was originally advertised for construction in September 2020, however due to unforeseen challenges related to snow removal operations during the winter months of construction, the contract required revisions and schedule changes. On August 19, 2021, the required revisions to the contract documents were performed and the project was readvertised. Final contractor bids were due September 9, 2021.

Further timeframe restrictions were imposed during the winter months, specifically from October 1st to April 30th, due to NJDOT snow plowing operations. I-78 is known to be a hazardous area during winter, with significant ice and snow accumulation. To address safety concerns, the work zone had to be configured for winter operations. The original working conditions of the shoulder for the winter formation was 1foot; NJDOT Operations requested a 12-foot shoulder to provide more storage for snow off the roadway. During the construction season the work zone was 22 feet with a shoulder width of 1foot separated by jersey barrier. The winter construction zone was 11 feet with a 12-foot shoulder width also separated by jersey barrier.

In October 2022, a request was submitted by the contractor to delay the winter staging until November. This request was rejected by NJDOT Operations. Instead, the contractor was granted a schedule extension until October 15th, upon which the site needed to be put in winter formation. In the 2023 construction year, additional blasting extensions were granted until early November. The stipulation for this extension was that the site had to be moved into winter formation within 24hrs of any forecasted snow. The contractor was also required to submit two weeks' look ahead for weather and work planned. Lastly, blast volumes needed to be reduced so all muck could be cleared and not staged behind the jersey barriers in case a winter storm was forecasted. Additional rockfall simulation modeling was performed to assess the winter staging conditions, since the EB slope was not completed in the first construction season as anticipated.

Early blasts, including the first test blast, experienced excessive fly rock and poor fragmentation. A primary cause for the blast performance issues was the drill hole deviation, which was identified with borehole deviation surveys, but not significantly rectified in subsequent drillholes. These deviations caused, in some cases, significant back break on the presplit lines of the slopes. This presented challenges for the contractor to access portions of the mid and upper slope to perform scaling and installation of mitigation elements. Moreover, these deviations led to changes in the final slope profile and geometry. Communication between drill holes also caused larger than desired fragmentation in blasted material and excessive fly rock. These rock fragments were too large for construction equipment to move and required jack hammering to break up into manageable sizes. This ultimately caused extensive delays to traffic and longer roadway closures. These road closures were often greater than 30 minutes and on one occurrence as much as 2 hours. This was due to the amount of fly rock, large rock blocks, and volume of blasted material that occupied the roadway (Figures 9a to 9c).

A second drilling and blasting contractor was engaged during the second construction season to work the WB slope while the first drilling and blasting contractor continued on the EB slope. Shortly into the second construction season, the second drilling and blasting contractor was engaged to complete both the EB and WB slopes. It should be noted that the second blasting contractor demonstrated that the original construction schedule could have been achievable based on their production rates.





Figure 9a- Moveable rockfall barrier. Figure 9b- Blasted material occupying roadway



Figure 9c- Excessive fly rock during an early EB blast

From a constructability perspective, access to the upper and mid slopes made it challenging for the contractor to effectively perform pre- and post-blast scaling operations. Through contractors means and methods, mechanical and hand scaling were performed in areas determined by NJDOT and the designer. Several areas required extensive mechanical scaling of larger blocks on the upper slope, as shown in Figure 10. Balancing the need to respect the contractors' means and methods, while ensuring successful scaling and achieving a clean slope, proved challenging and often required multiple attempts and methods.

NJDOT and the design team strongly suggested a specialty scaling contractor be brought onto the project, as required by the specifications, to perform all scaling operations due to the schedule, need to protect the active roadway, and slope accessibility issues. The contractor applied different methods to complete the required work, in lieu of engaging a specialty subcontractor. Drilling activities were also delayed due to the insufficient removal of rock and muck material from the blasted benches.



Figure 10 - Post blast scaling using a contractor constructed scaling tool



Figure 11a- Contractor designed drill rig cage installing a rock dowel on WB slope.
Figure 11b- Drill rig cage mounted to rock face on EB slope.

The original contract plans included the installation of 150 galvanized rock dowels, each measuring 16 ft. Of these, 85 dowels were installed on the WB slope and 52 on the EB slope. The placement of all rock dowels was coordinated by the field engineer, the design team, and NJDOT Geology. To facilitate rock dowel installation, the contractor utilized an innovative proprietary drill cage design that accommodated two crew members, a drill rig, and all necessary mechanical equipment. Refer to Figure 11a and Figure 11b. Although this method improved safety during rock dowel installation, it presented challenges related to access because the cage could not be anchored flush to the rock face. Additionally, the drill rig had limitations on the angles it could drill.

Rock dowel batter angles were predominantly set at 15 degrees below horizontal; however, several locations required a higher angle. In areas where the drill rig cage was unable to achieve a steeper angle, other mitigation measures were used if and where needed.

Shotcrete was applied to areas experiencing weathering and erosion on both the WB and EB slopes. Per the contract documents fiber reinforced shotcrete at a minimum thickness of 6 inches was installed. Significant water seepage, primarily on the EB slope, resulted in the shotcrete showing signs of spalling and cracking within approximately 48 hours of application. To attempt to eliminate water build up behind the shotcrete, vertical strip drains were installed as per the Plans, at a spacing no greater than 5 feet where shotcrete would be applied (Figure 12b). Where water seepage was greater, the spacing of strip drains was reduced to attempt to wick more water away from the slope and shotcrete.

At least one and a half truckloads of unreinforced shotcrete were applied in a thin layer to the lower portion of the EB slope. The contractor was then requested to apply a thicker layer of reinforced shotcrete over the unreinforced section to ensure adequate coverage (Figure 12a). Due to the minimal layer of unreinforced shotcrete applied and the minor level of weathering, erosion, and water seepage in the area, the contractor was not required to remove any unreinforced shotcrete. This incident prompted increased oversight from NJDOT Geology staff and the designer.





Figure 12a - Initial application of unreinforced shotcrete on the EB slope.
Figure 12b - Vertical strip drains installed on the WB slope.

The contract plans also included approximately 300 rock drains to be installed at a height of 10 feet above the toe of the slope and spaced 15 feet apart. Due to elevation variations from the blasted toe of slope, rock drains could not be installed at the correct height. The contractor had to excavate below the toe of slope to enable the drill rig to access and install the rock drains to the specified height. Since many of the rock drains were installed prior to final scaling efforts, several of the PVC tips were broken off, many of which were not replaced as of May 2025. This did not compromise the integrity or effectiveness of the drains.

Hydroseeding was applied to portions of the slope where overburden was present to help with erosion control. This involved spraying a slurry of mulch, seed, and water onto the slope to promote vegetation and reduce the risk of erosion over time. Extended levels of drought and insufficient watering resulted in patchy grass growth in some areas. The contractor applied a second application of hydroseeding to areas with minimal growth.

To finalize the construction phase of this project, several items outside the rockfall mitigation work needed to be performed. This included replacement of the drainage along and under the roadway, perimeter fencing to secure the site on the upper and lower slopes for both EB and WB, installation of guide rail, and lastly repaving of the roadway.

CONCLUDING THOUGHTS AND LESSONS LEARNED

After three years of shortened construction seasons and a plethora of complications, beyond what is mentioned in this paper, the I-78 project came to a successful completion in June 2025. Working with other state and federal organizations on threatened and endangered species has provided insight on how to proceed with site evaluation and scheduling for other projects. Areas impacted with heavy traffic and intense winter weather also shed light on how to prepare a work zone for snow removal while continuing construction activities. One of the biggest take-aways is that when performing a rockfall blasting project, it is critical that all parties involved are well acquainted with all relevant contract documents, including the plan sets and special provisions. Additionally, it is imperative that the resident engineer and site inspectors are trained and informed of all potential issues that may occur in this type of work. It is equally important to ensure the project team has an open line of communication and raises any concerns to the subject matter experts and design team.

Overall, the high Average Annual Daily Traffic (AADT) counts along I-78 MP 10.04 - 10.40, combined with limited shoulder space and catchment areas, made this site an ideal candidate for a comprehensive rockfall mitigation design. The implementation of blasting techniques not only increased catchment width and achieved 95% rock retention but also enhanced the overall global stability of the rock corridor. Furthermore, the use of blasting, along with colored shotcrete, helped to showcase and preserve the unique geological features along the roadway. In-depth studies on threatened and endangered species, vegetation, and both subsurface and surficial geology provided the essential framework for the project's design. The innovative techniques employed by the design team and contractors successfully addressed unexpected delays and deviations during construction. Ultimately, the lessons learned from the design and

construction of this project offer valuable insights into minimizing potential challenges in future rockfall mitigation projects.

REFERENCES

1. State of New Jersey Highway Department, *Plans of Route 78 Section 2E – From Central Railroad of New Jersey to Mulhockaway Creek* (Original Construction), September 1958.

2. State of New Jersey Highway Department, *As-Built Plans of Route 78 Section 2E – From Central Railroad of New Jersey to Mulhockaway Creek* (Original Construction), August 1960.

3. State of New Jersey Highway Department, *As-Built Plans of Route 78 Section 2G From Still Valley to Clinton Farms* (Widening), March 1970.

4. Township of Union, Hunterdon County, New Jersey, *A Brief History of Union Township*. http://www.uniontwp-hcnj.gov/history.html

5. NJGS, *Physiographic Provinces of New Jersey*, 2006. http://www.nj.gov/dep/njgs/enviroed/infocirc/provinces.pdf

6. NJGS, *Bedrock Geologic Map of Northern New Jersey*, 1984.

7. USGS, *Mineral Resources On-Line Spatial Data. Quartz-Oligoclase Gneiss*, http://mrdata.usgs.gov/geology/state/sgmc-unit.php?unit=NJYlo%253B11

8. USGS, *Mineral Resources On-Line Spatial Data. Amphibolite*, http://mrdata.usgs.gov/geology/state/sgmc-unit.php?unit=NJYa%3B3

9. NJGS, *Surficial Geology of Northern New Jersey*, 2002.

10. FHWA, *Rockfall Catchment Area Design Guide, Final Report, SPR-3(032)*, Oregon Department of Transportation, FHWA-OR-RD-02-04, January, 2002.

a. FHWA, *Rockfall Hazard Rating System Participant's Manual*. FHWA SA-93-057, November 1993.

b. FHWA, *Rock Slopes: Design, Excavation, Stabilization*, FHWA-TS-89-045, September, 1989.

c. Harper, David P, *Roadside Geology of New Jersey*, March 2013.

d. NJAC, New Jersey Administrative Code. https://www.nj.gov/labor/lsse/laws/Explosives_Law.html

e. Transportation Research Board, *Rockfall Characterization and Control*, 2012.

f. USBM, Structure Response and Damage Produced by Ground Vibration from Surface Mine Blasting, 1989.

g. USFWS, Northern Long-Eared Bat Interim Conference and Planning Guidance for USFWS Regions 2, 3, 4, 5, and 6, January 6, 2014.

h. USFWS, Range-Wide Indiana Bat Survey Guidelines, April 2018.

i. USGS, *Bloomsbury, NJ Quadrangle*, 2014.

j. USGS, *Mineral Resources On-Line Spatial Data. SObl Undifferentiated*. http://mrdata.usgs.gov/geology/state/sgmc-unit.php?unit=NJSObl%253B7

*References a-j are not cited in the body of text

On the Geotechnical Design Considerations and Solutions of the I-80 North Fork Bridges Project

Edward H. Barefield, P.G., P.E.
Michael Baker International
100 Airside Drive
Moon Township, PA 15108
(330)-831-1662
ebarefield@mbakerintl.com

John D. Lasko, P.G.
Michael Baker International
100 Airside Drive
Moon Township, PA 15108
(724)-312-2794
john.lasko@mbakerintl.com

Prepared for the 74th Highway Geology Symposium, August, 2025

Acknowledgments

The authors would like to thank the following for their support of this paper and/or in the prosecution of the work described herein:
Joel Borrelli, P.E. -Michael Baker International Pittsburgh Bridge Practice -Michael Baker International Pittsburgh Transportation Practice -Michael Baker International

Disclaimer

Statements and views presented in this paper are strictly those of the authors, and do not necessarily reflect positions held by their affiliations, the Highway Geology Symposium (HGS), or others acknowledged above. The mention of trade names for commercial products does not imply the approval or endorsement of HGS.

Copyright Notice

Copyright © 2025 Highway Geology Symposium (HGS)

All Rights Reserved. Printed in the United States of America. No part of the publication may be reproduced or copied in any form or by any means – graphic, electronic, or mechanical, including photocopying, taping, or information storage, and retrieval system – without prior written permission of the HGS. This excludes the original author(s).

ABSTRACT

The I-80 North Fork Bridges project involves the reconstruction of approximately 2 ¼ miles of SR 0080 in northwestern Pennsylvania. Realignment of the eastbound corridor and corresponding relocation of the eastbound SR 0080 bridge over the gorge of North Fork Redbank Creek results in significant cut and fill earthwork necessary to establish the realigned portion of SR 0080 eastbound and for construction of the eastbound and westbound bridges. Coupled with the significant earthwork component of the project, site investigations revealed geohazards and site constraints related to the presence of multiple horizons of acid producing rock stratigraphy and coal measures within the roadway template and challenging foundation conditions at the locations of the proposed bridge pier foundations adjacent to North Fork Redbank Creek, e.g. weak sedimentary stratigraphy, non-uniform sloping top of rock surface, boulder conditions along the valley sidewalls, and proximity of an existing in-service municipal water supply dam.

This discussion explores the various transportation geotechnical design challenges offered by the geologic framework, steep terrain, and site constraints within the project limits as well as considerations and solutions for resolution of the challenges. Specific attention will be allocated to design considerations for integrating acid producing encapsulation zones within the proposed embankments along with select borrow material zones needed to satisfy long-term slope stability requirements, cut slope face treatment measures employed for mitigating exposed acid producing rock material, and considerations for design of drilled shaft foundations within the gorge of North Fork Redbank Creek.

INTRODUCTION

The title of Norman Maclean's novel "A River Runs Through It and Other Stories" (*1*) provides a useful framework for discussion on the geologic and geotechnical aspects of the I-80 North Fork Bridges project. This title highlights not only the physical bisecting of the project by the erosional gorge of North Fork Redbank Creek, but also the variety of geohazard considerations found within the project limits, each yielding the necessity to apply sound engineering geologic characterization procedures and geotechnical engineering solutions to rectify the geohazards for design and construction purposes.

Based on the experiences of the authors throughout the execution of the design phase of the I-80 North Fork Bridges project, and experiences during the early stages of the construction phase, the aim of the authors is to provide a useful project case example concerning the geotechnical-related challenges that were encountered and how solutions were devised and implemented to address those challenges. The intent is that these experiences will serve as a useful reference for geotechnical engineering practitioners regionally and nationally working or planning to work in and under similar conditions and circumstances.

PROJECT OVERVIEW

The I-80 North Fork Bridges project involves the reconstruction of approximately 2 ¼ miles of SR 0080 in Brookville Borough and Pine Creek Township, Jefferson County, Pennsylvania. As indicated in Figure 1, the project limits extend approximately from the SR 0036 Interchange through to the SR 0028 Interchange on the east side of the project. The distinctive geographic feature in the area is the gorge of North Fork Redbank Creek, which flows from north to south, effectively bisecting the project into two halves. Original construction of SR 0080 in the 1960s involved bifurcating the highway corridor and pushing the eastbound travel lanes to the south, resulting in construction of the eastbound bridge approximately 1,100 feet to the south of the corresponding westbound bridge over North Fork Redbank Creek.

The project involves the replacement of the eastbound and westbound bridges over North Fork Redbank Creek, roadway and pavement reconstruction, and replacement of smaller intersecting bridges within the project limits. Realignment of SR 0080 eastbound to permit construction of the new eastbound bridge adjacent to the new westbound bridge involves significant new embankment and cut slope construction on the approaches to the new eastbound bridge. The mainline SR 0080 eastbound and westbound bridges will consist of new 4-span continuous weathering steel plate girder bridges constructed adjacent to one another. In addition to North Fork Redbank Creek, the bridges will span over Water Plant Road, the Walter Dick Memorial Park, the municipal water treatment facility serving the Borough of Brookville, and a regulated municipal water supply dam and reservoir.

The I-80 North Fork Bridges project is a part of the Major Bridge Public Private Partnership (MBP3) for the replacement or rehabilitation of nine major interstate bridges across the Commonwealth of Pennsylvania in concert with the Pennsylvania Department of Transportation (PennDOT). The Design/Build project delivery mechanism was implemented to facilitate the design, permitting, and construction of the project.

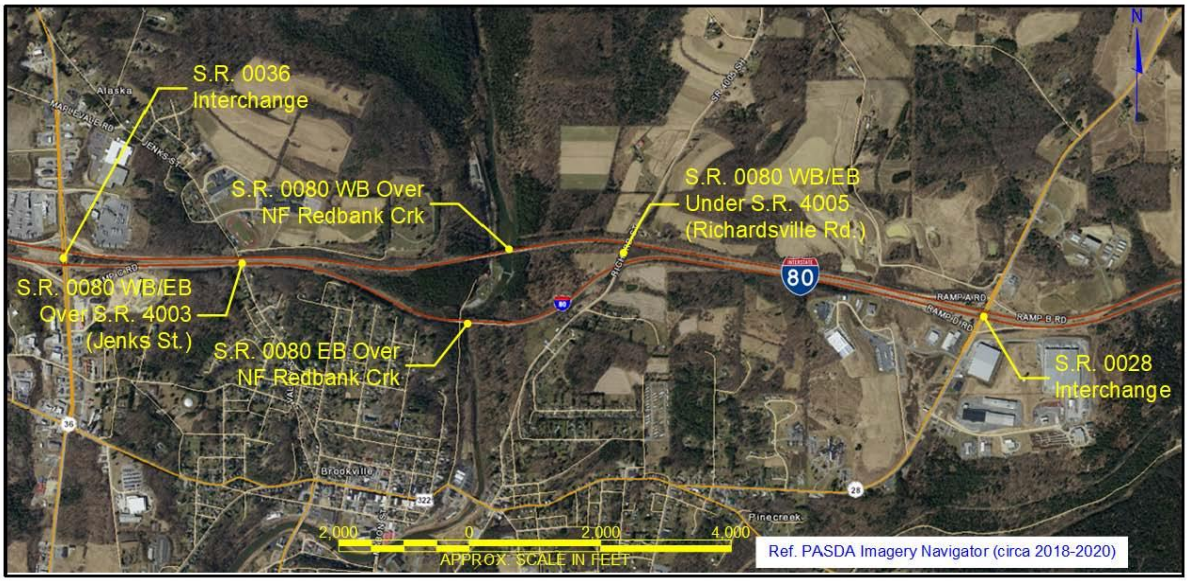


Figure 1 - Overview of I-80 North Fork Bridges Project (*2*)

REGIONAL GEOLOGIC FRAMEWORK

Physiographic Setting

The site is located in the Pittsburgh Low Plateau Section of the Appalachian Plateau physiographic province (*3*). The Pittsburgh Low Plateau Section is an extensive mature plateau of moderate relief. Local relief within the project location from North Fork Redbank Creek to the top of the valley is approximately 200 feet. The North Fork Creek is a tributary to Redbank Creek and is formed by the confluence of Muddy Run and Williams Run to the north of the project site, joining Sandy Lick Creek at Brookville, PA to form the Redbank Creek (*4*).

Sedimentary Rock Stratigraphy and Bituminous Coal Measures

Allegheny Group

Bedrock units along the upper portion of the project site belong to the lower part of the Allegheny Group (*5*). The Allegheny Group consists of cyclic sequences of sandstone, shale, siltstone, claystone, limestone, coal, and underclay. The Allegheny Group is characterized by the presence of economically significant coal beds, primarily concerning the Clarion and Brookville coal seams for this project. The Brookville coal, where present, defines the base of the Allegheny Group. The expected units within the project limits are from the Clarion sandstone (Clarion Formation) and encountering the Clarion and Brookville coal seams at the approximate elevation of SR 0080 on the approaches to the main bridge crossings. Refer to Figure 2 for a stratigraphic section depicting these key stratigraphic markers.

Pottsville Group and Mississippian System

The Pottsville Group (Pennsylvanian) is present along the valley sidewalls of the North Fork Redbank Creek gorge, consisting of fine-grained to coarsely conglomeratic sandstone with

minor shale, siltstone, claystone, limestone, and thin discontinuous coals (*5*). Coal bed markers expected within this group are the Mercer and Quakertown with the expected units within the project limits ranging from the Upper Connoquenessing sandstone to the Homewood sandstone.

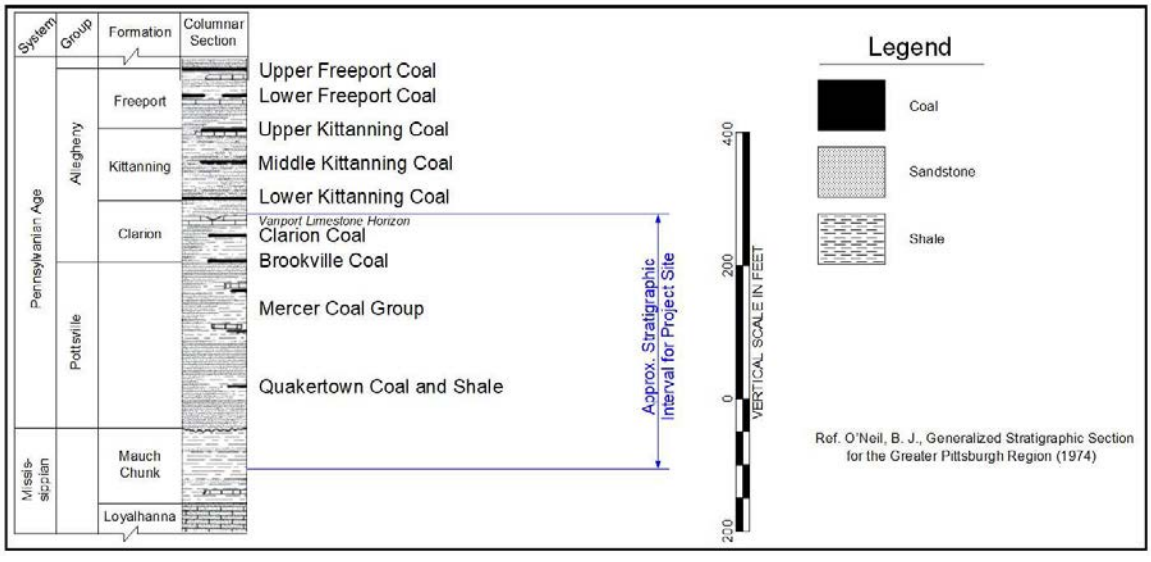


Figure 2 - Project Stratigraphic Section and Pennsylvanian Coal Measures (*6*)

Mississippian geologic units are present below the valley bottom of North Fork Redbank Creek within the project limits, consisting primarily of the upper part of the Mauch Chunk Formation (*5*). The Mauch Chunk Formation consists of red shale and subordinate sandstone and limestone units. The proposed bridge pier locations for both proposed eastbound and westbound bridges are expected to encounter bedrock units of the Mauch Chunk Formation, and potentially lower stratigraphic units.

Structural Geologic Setting

The bedrock of the Brookville 7.5-minute quadrangle, in which the project site resides, consists of a series of broad and irregular folds with the fold axes trending approximately north 50 degrees east (*5*). The structure is not reflected in the topographic ridges and valleys but is likely responsible for the character of the uplands and valleys depending on the location of the more resistant rock strata. Local drainage appears to have no relation to the geologic structure as the principal streams and rivers maintain their courses regardless of the geologic structure. The site is located within the western limb of the southwest plunging Fairmont Syncline. Locally, the bedrock dip is southeast at less than 1 degree within the project.

Potential Acid Producing Rock

As documented in PennDOT Publication 293 (*7*), sulfur bearing deposits with the potential to produce Acid Rock Drainage (ARD) occur in Pennsylvania in the form of either veined rock deposits, sedimentary rock deposits (i.e. black shales and coals), mine spoils resulting from economic extraction, and supergene acid sulfate soils. Occurrence of these sulfur

bearing deposits is given in the publication concerning Geologic Units Containing Potentially Significant Acid-Producing Sulfide Minerals (*8*). The I-80 North Fork Bridges project resides in the western region of Pennsylvania where these types of sedimentary rock deposits occur.

Alluvial and Glacial Geology of North Fork Redbank Creek

Pleistocene Periglacial Climate Effects and Glacial Lake Monongahela

Glacial Lake Monongahela (Figure 3) formed when outwash and or glacier ice dammed the Monongahela River and ancestral Ohio River that previously flowed northward (*9*). Glacial Lake Monongahela was estimated to reach an elevation of 1,100 feet. The water inundated existing landforms, but did not erode the topography and covered the land with lacustrine sediments. Existing terraces and abandoned meander channels, low hills, slopes, and valley bottoms were covered by the lacustrine deposits, typically consisting of highly weathered clay, silt, and sand and gravel.

The project site is located outside the limits of Glacial Lake Monongahela but was subject to periglaciation geomorphic processes resulting from seasonal freezing and thawing, creating frost-shattered rock outcrops, boulder fields and lobes, and debris mantled slopes. Redbank Creek and the North Fork Creek tributary are both mature, well-developed streams that were not subject to significant glacial meltwaters, each forming part of the ancestral Lower Allegheny



Figure 3 - Glacial Lake Monongahela with respect to I-80 North Fork Bridges (*10*)

River drainage system. This area is characterized by rounded hills, narrow valleys, entrenched streams with sloping valley walls, steep and variable top of rock slopes, large meanders, and

narrow floodplains. The deeply incised stream exposed river valley walls throughout the stream's development, inducing deep weathering and bedrock decomposition.

GEOTECHNICAL CHALLENGES ASSOCIATED WITH THE GEOLOGIC HAZARDS

Based on the geohazards revealed by the geologic framework outlined in the preceding section, the following discussion provides select cases from the I-80 North Fork Bridges project to provide additional insight into how the geologic hazards were addressed and the geotechnical design and construction solutions applied.

Investigation and Occurrence of Acid Producing Rock and Bituminous Coal Seams

Environmental Impact Potential of Acid Producing Rock

Based on the geologic framework in which the I-80 North Fork Bridges project resides, the potential for Acid Producing Rock (APR) to be encountered during construction represented a significant investigative and design effort on the project. The principal goal of this effort was to proactively mitigate the potential for ARD to occur where APR materials are being disturbed by cut earthwork necessary for the project, as this disturbance has the potential to expose naturally occurring iron sulfide minerals, principally pyrite, contained within the sedimentary rock stratigraphy underlying the project site. This potential is borne from an understanding of the chemical reaction that may occur where pyrite minerals are exposed to atmospheric oxygen and water, resulting in generation of acidic, high metallicity leachate with toxic capacity towards vegetation and aquatic life and towards surficial and ground waters.

Subsurface Characterization Targeting Acid Producing Rock

The APR investigation on the I-80 North Fork Bridges project, conducted in general accordance with PennDOT Publication 222 guidelines (*11*), consisted of a total of 47 roadway test borings and 16 test pits conducted throughout the project limits to collect bedrock samples to be used for laboratory testing to identify index properties indicative of acid producing potential. The test boring and test pit program targeted locations on the project where cut earthwork was proposed, with boring locations sited to spatially define APR zones laterally and vertically. Test pits were also utilized where bedrock was exposed in existing roadway cuts. 421 APR tests were performed on the collected bedrock samples, with testing consisting of fizz, paste pH, Total % Sulfur, and Neutralization Potential (NP) tests.

Laboratory testing of bedrock samples collected from the roadway test borings and test pits identified bedrock that was designated as APR. For the purposes of delineating the limits of APR within the project, APR was defined as bedrock with a Total Sulfur (%S) content greater than 0.5. Plotted roadway test borings/test pits and APR laboratory testing results were placed on the roadway cross sections and the available data projected laterally left and/or right, as well as ahead and back station, to interpret the horizontal extent and elevation interval of APR planned to be encountered during the proposed excavations. The APR with %S greater than 0.5 was considered as material that may generate significant acidity, where treatment and proper handling/disposal of the excavated material would be required in addition to application of acid-neutralizing treatments to exposed rock cut faces. Figures 4 and 5 below provide an overview of

the individual cut earthwork locations (cut sections) where APR was delineated within the project limits. As seen in these figures, APR was primarily concentrated in the project areas to the east of North Fork Redbank Creek, which bisects the project.

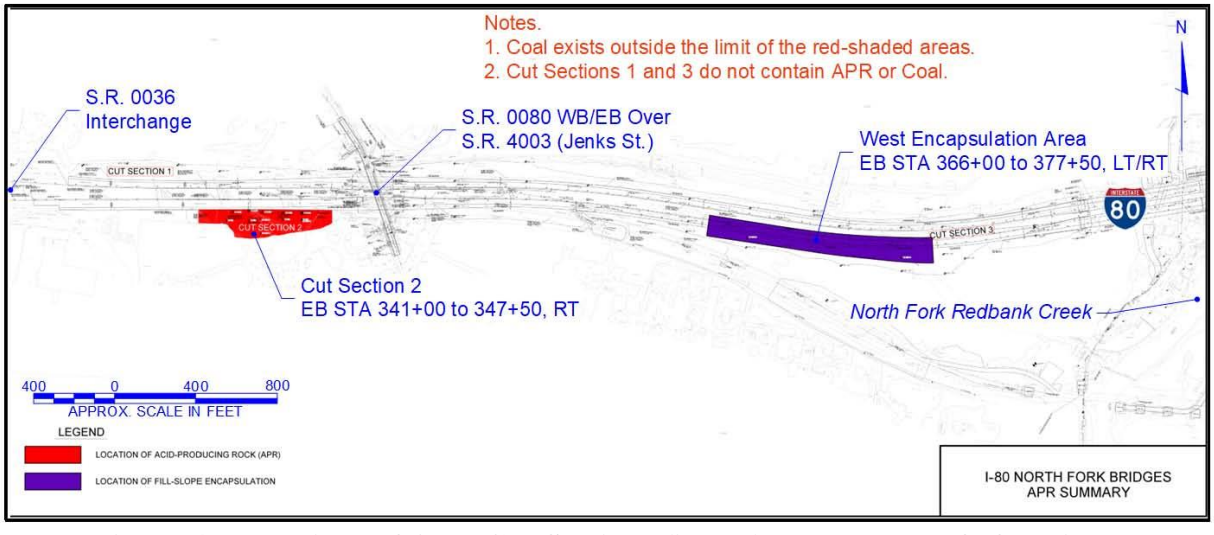


Figure 4 - Locations of APR Cut Sections (in red) -Western Half of Project

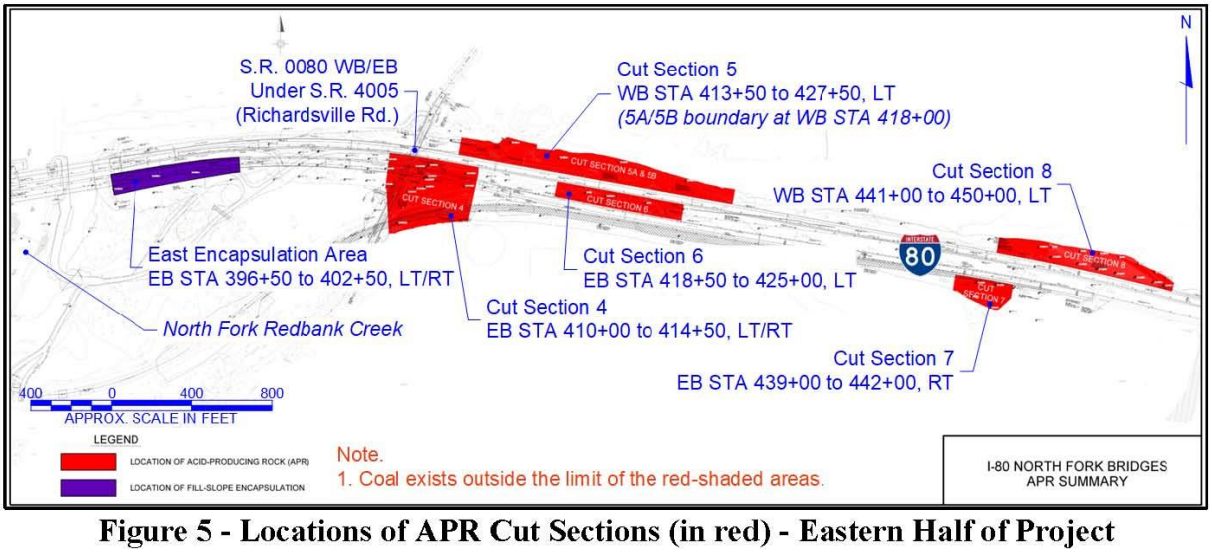


Figure 5 - Locations of APR Cut Sections (in red) - Eastern Half of Project

In the case of the I-80 North Fork Bridges project, sedimentary rock lithologies varying amongst siltstone, sandstone, and shale as well as materials described as carbonaceous shale and carbonaceous siltstone exhibited %S greater than 0.5. In many instances, bedrock material sampled from the test borings/test pits exhibiting laboratory-tested %S greater than 0.5 did not show outward visual signs of carbonaceous material (i.e. dark gray to black color) or visible pyrite crystals. This highlights the point that visual inspection of rock core or exposed bedrock material in the field can be a poor diagnostic means of identifying APR, underscoring the importance of laboratory testing of samples collected from the field to positively identify the material. However, in most cases bedrock material that exhibited obvious signs of containing an appreciable amount of carbonaceous material did exhibit %S greater than 0.5.

Bituminous Coal Seams and Association with Acid Producing Rock

As stated in a preceding section, the Clarion and Brookville coal seams occur at the approximate elevation of SR 0080 on the approaches to the main bridge crossings over North Fork Redbank Creek. These coal seams generally tend to occur along the existing cut slopes to the left and right of the existing SR 0080 corridor. As part of the APR subsurface characterization work, identification of the location, thickness, and lateral extent of these coal seams was undertaken in locations of the project where cut earthwork was anticipated to intercept the coal seams. Coal seams on the project greater than 6 inches in thickness were considered as APR material (regardless of %S content) and as having sufficient thickness that they could be excavated in a manner to be segregated from the bedrock material above and below the coal seam. Similar to identified APR materials, coal seams intercepted by the project test borings were plotted on the roadway cross sections and interpolation with adjoining test borings encountering coal was made to interpret the lateral extent and elevation interval of the coal seams to be encountered in the roadway excavations for the project.

Bituminous coal seams on the I-80 North Fork Bridges project were found to vary in thickness from 'stringers' less than 6 inches thick up to 2.8 feet in thickness, frequently laterally discontinuous and variable in thickness, and primarily occurring at the anticipated elevation horizons of the Brookville and Clarion coal seams. Coal seams were not identified at the elevation horizons of the Quakertown and Mercer coals of the Pottsville Group, although these coals may have been too laterally impersistent to be identified by the test boring program conducted for the project. A trend revealed in comparison with the APR laboratory testing data was the prevalence of non-coal APR sedimentary rock materials (e.g. sandstone, siltstone, and shale) above and below encountered coal seams, i.e. where coal seams occurred, APR frequently occurred in the stratigraphic interval above and below the coal seam. This point is made as the location of coal seams frequently correlated with the occurrence of other rock materials with elevated %S.

Commentary On Soil as an Acid Producing Material

Given the lack of identified surficial or deep mining of bituminous coal seams within the project limits, mine spoils with the potential to contain coal fragments and/or non-coal APR materials were not considered a concern for the APR subsurface characterization work. Additionally, the non-glaciated geomorphic framework of the region suggests that comparatively deep weathering of the sedimentary bedrock in the geologic past has resulted in a residual soil mantle where sulfide minerals, regardless of rock lithology, have likely already undergone the oxidation chemical reaction that results in ARD, with natural attenuation of acidic effluent from this process long having since taken place. Hence, naturally occurring residual soils weathered from the underlying sedimentary stratigraphy were not considered as a potential APR material where cut earthwork for the highway construction required excavation of these materials.

Geotechnical Design to Mitigate Acid Producing Rock and Bituminous Coal Seams

Geotechnical design activities to mitigate APR and coal occurring within the project focused on three distinct considerations: 1.) segregation, treatment, and encapsulation of APR generated from project earthwork excavations, 2.) segregation and disposal of coal seams, and

3.) application of treatments to cut slope faces where APR and coal horizons are to be intercepted by the project excavations. Development of geotechnical design and construction specifications were coordinated with the Pennsylvania Department of Environmental Protection (PADEP), including development of an APR Handling Work Plan that was included as part of the National Pollutant Discharge Elimination System (NPDES) permit for the project.

Segregation, Treatment, and Encapsulation of Acid Producing Rock

Rock material with %S greater than 0.5, including carbonaceous shale regardless of %S, was designated as APR having the potential to generate significant acidity without treatment on the project. As a result, this material was designated as unsuitable for use as common borrow on the project if not treated. Quantity estimation of the in-place bank volume of APR requiring excavation on the project was approximately 72,000 c.y. The challenge of this large volume of material unsuitable for use as compacted embankment was compounded by the limited availability of right-of-way in which material might be permanently stockpiled within the project limits. Hauling the APR material to an offsite waste area was deemed cost prohibitive. Given the availability of space in which to encapsulate the APR material directly within the eastbound approach embankments, treatment of excavated APR materials followed by hauling to designated encapsulation areas was selected as the most economical means to address APR material on the project.

Two APR encapsulation areas were designed as indicated in Figures 4 and 5. The encapsulation areas were designed to provide sufficient volumetric capacity to hold the entirety of APR excavated after consideration of volumetric earthwork swell of the APR (10% increase estimated) and volumetric addition of Supplemental Alkaline Material (SAM) (8% increase estimated). Design of the encapsulation areas aimed to achieve a 20% buffer between the total available encapsulation volume and the quantity of APR and SAM treatment material to ensure sufficient encapsulation volume would be available in the event that unforeseen APR was encountered. This measure was implemented to reduce the risk that unforeseen APR would require offsite disposal and corresponding construction cost and schedule ramifications.

A key challenge in design of the 2H:1V slope encapsulation embankments involved balancing long term slope stability considerations with the need to maximize the volume of embankment available for encapsulation of SAM-treated APR. Additional considerations involved meeting minimum PennDOT Publication 293 (*7*) burial depth requirements for the SAM-treated APR (to limit long-term exposure to atmospheric oxygen and water) and minimum vertical offset requirements above the 100-year flood plain of nearby relocated stream tributaries.

Slope stability analyses were first performed to design the geometry and dimensions of Selected Borrow Excavation Rock needed to achieve a long-term slope stability Factor of Safety of 1.5 using compacted embankment design parameters informed by shear strength testing (Direct Shear) of remolded soil samples collected from the site (example analysis plot for the East Encapsulation area provided as Figure 6). This in essence established the outer-right boundary of embankment available for encapsulation of SAM-treated APR. Key to this exercise was recognition that the SAM-treated APR in the encapsulation area could not be utilized as exhibiting elevated rock aggregate shear strength due to the preponderance of shale and siltstone rock types in the APR. This consideration was justified by the expectation that

these shale and siltstone materials would break down during excavation, compaction, and placement, ultimately performing similar to a compacted soil embankment material.

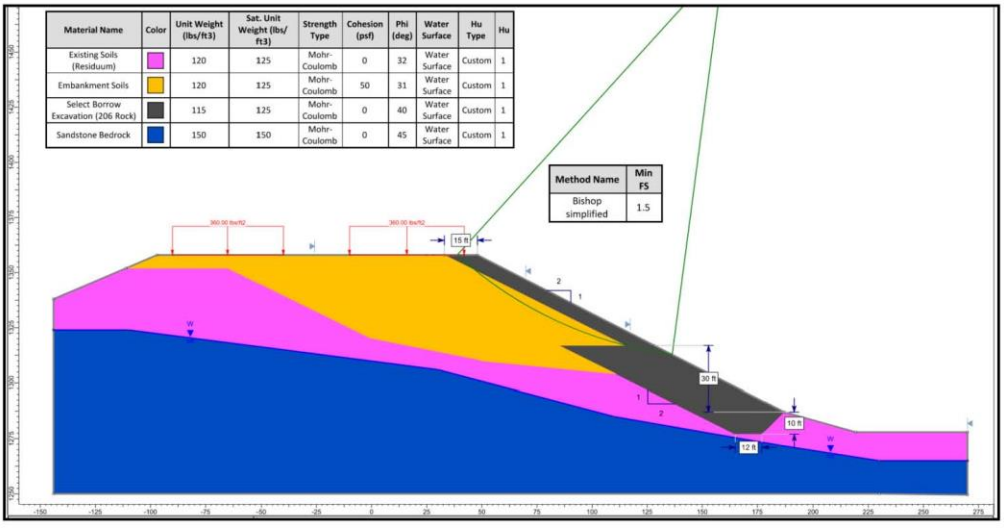


Figure 6 - Slope Stability Analysis -East Encapsulation STA 397+50 (Slide© -Rocscience)

Hydrologic and Hydraulic (H&H) analysis were utilized to develop a 100-year water surface elevation for the relocated tributaries below the encapsulation embankments, with a 5 feet minimum vertical offset applied between the 100-year water surface and base of the encapsulated material, consistent with Publication 293 requirements (*7*). A minimum 10 feet vertical offset was applied between the roadway surface and top of the encapsulated APR material to set the upper boundary of the encapsulation zone. In the case of the east encapsulation area, additional space constraints imposed by the need to avoid the area of the predrilled pile supported Abutment 2 of the mainline eastbound bridge were taken into account.

Balancing all of these considerations resulted in an estimated capacity of approximately 107,000 c.y. of combined volume between the east and west encapsulation areas on the project, which was sufficient to encapsulate all SAM-treated APR material entirely within the project limits with a capacity buffer of 20%. Refer to Figures 7 and 8 for a plan and cross section view highlighting the location and geometric configuration of the East Encapsulation Area.

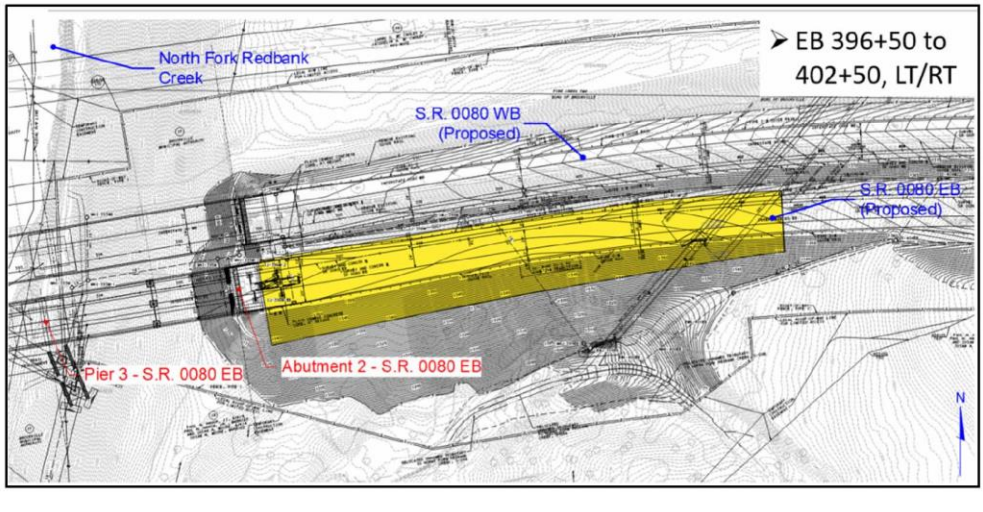


Figure 7 - Plan View of East Encapsulation Area (in yellow), EB STA 396+50 to 402+50

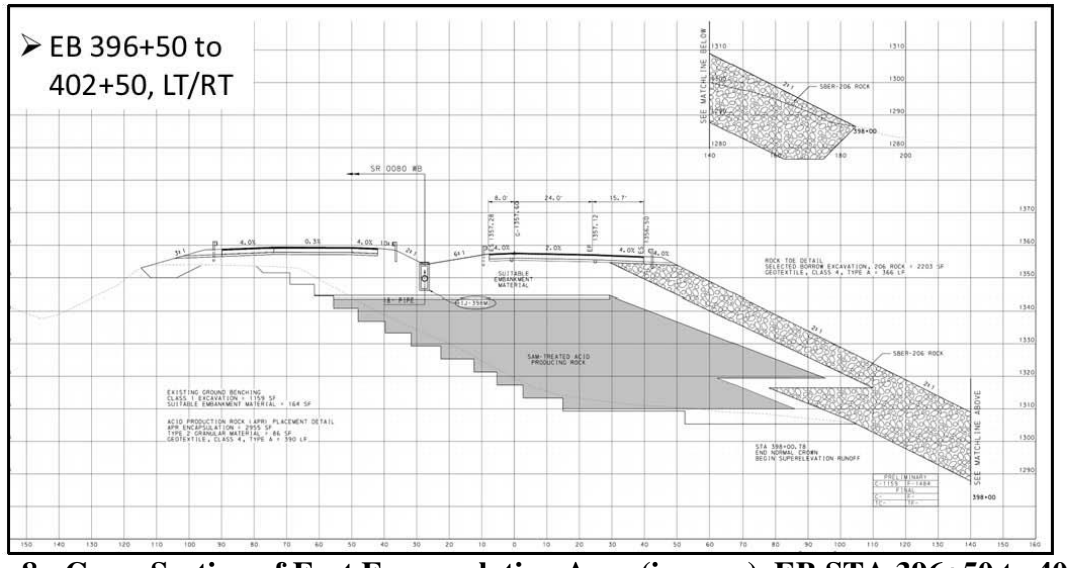


Figure 8 - Cross Section of East Encapsulation Area (in gray), EB STA 396+50 to 402+50

Acid-Base Accounting (ABA) was performed utilizing the APR testing results for each APR cut section to estimate the proportion of SAM material needed to achieve a target Net Neutralization Potential (NNP) of 12 ppt. A Factor of Safety of 2.0 was applied to account for non-uniform mixing of the material in the encapsulation areas, resulting in an NNP of 24 ppt being used to calculate the dosing rates. Graymont Baghouse Lime® was estimated to be used as the SAM material with a moisture content of 11.2% and Calcium Carbonate Equivalent (CCE) of 114.4%. SAM Addition Rates were calculated to achieve an NNP of 24 ppt considering the neutralizing capacity of the SAM material (CCE) and reduction due to moisture content (Figure 9). Dosing rates were resolved to tons of SAM material per loaded 40-ton articulated truck or triaxale truck. An approximately uniform dosing rate was calculated for the cut sections on the project, although cut section 4 exhibited APR testing results with an elevated APR potential, requiring approximately double the SAM dosing per ton of APR compared with the other cut sections. No endorsement of Graymont products is implied by the use of Figure 9.

APR Section	Location/Station Limits	SAM Addition Rate (tons / 1000 tons of APR	*40 Ton Artic - Approximate Tons of Lime per truck load of APR	**Triaxle - Approximate Tons of Lime per truck load of APR
8	WB, 441+00 to 450+00, LT	47.25	1.61	0.80
7	EB, 439+00 to 442+00, RT	52.17	1.77	0.89
6	EB, 418+50 to 425+00, LT	59.06	2.01	1.00
5a	WB, 413+50 to 418+00, LT	64.97	2.21	1.10
5b	WB, 418+00 to 427+50, LT	64.97	2.21	1.10
4	EB, 410+00 to 414+50, LT/RT	136.83	4.65	2.33
2	EB, 341+00 to 347+50, RT	53.16	1.81	0.90

SAM = Lime; * 20 cy/ld x 3,400 lbs/cy = 68,000 lbs/ld = 34 tons/ld; ** 10 cy/ld x 3,400 lbs/cy = 34,000 lbs/ld = 17 tons/ld

$$\%CCE_{ma} = \frac{100 - \%moisture}{100} \times \%CCE$$

$\%CCE$: *Calcium Carbonate Equivalent*
$\%CCE_{ma}$: *Calcium Carbonate Equivalent, moisture adjusted*

$$SAM\ Addition\ Rate\ \left(\frac{tons\ SAM}{1{,}000\ tons\ APR}\right) = \frac{Required\ SAM\ Addition\ Rate}{\%CCE_{ma}}$$

Updated Based on Graymont Baghouse Lime CCE & percent Moisture Content

Figure 9 - Varying Cut Slope Dosing Rates for SAM Treatment

Segregation and Disposal of Coal Seams

Coal seams related to the Brookville and Clarion coal horizons were identified within several existing cut sections needed to widen the I-80 corridor. Coal seams on the project greater than 6 inches in thickness were considered as having sufficient thickness to be segregated from the bedrock material above and below. Due to their unsuitability as compacted embankment material, identified coal seams were plotted on the roadway cross sections and interpolation between adjacent test borings performed to spatially characterize the coal seam extents. This was performed to aid in quantity estimation of volumetric coal that would require segregation and offsite disposal. Coal seams 6 inches or less in thickness were permitted to be incorporated into other excavations and placed provided the material was blended with suitable cohesive soil.

Cut Slope Face Treatments for Acid Producing Rock and Bituminous Coal

Subsurface investigations at the site further identified that exposure of APR and coal seams would occur during cut slope excavations to establish the final I-80 roadway template. Acidic runoff from APR and coal seams left untreated on cut slope faces was considered to be a concern that needed to be addressed during design and construction. Cut slope face treatments were designed to address this concern by overexcavating APR and coal beyond the finished cut slope face and backfilling the overexcavation with either Best Available Rock acquired from onsite (non-APR) excavations, suitable soil embankment material, or special capping soil consisting of cohesive material with a Plasticity Index > 3 (fraction passing the #40 sieve). A minimum bottom bench width of 8 feet was utilized to provide a stable base for the backfill materials while providing sufficient cover over the exposed APR/coal to limit oxygen interaction leading to the ARD chemical reaction. Slope stability analyses were performed where cut slope face treatments exceeded approximately 20 feet in vertical height to validate long term stability of the backfill, with vertical heights of backfill with soil material being limited to 20 feet. As an additional measure to prevent acid production, application of lime slurry to the overexcavated APR/coal surface was specified to provide a preventative neutralizing agent at the exposed rock surface. Refer to Figure 10 for a typical APR cut slope face treatment detail.

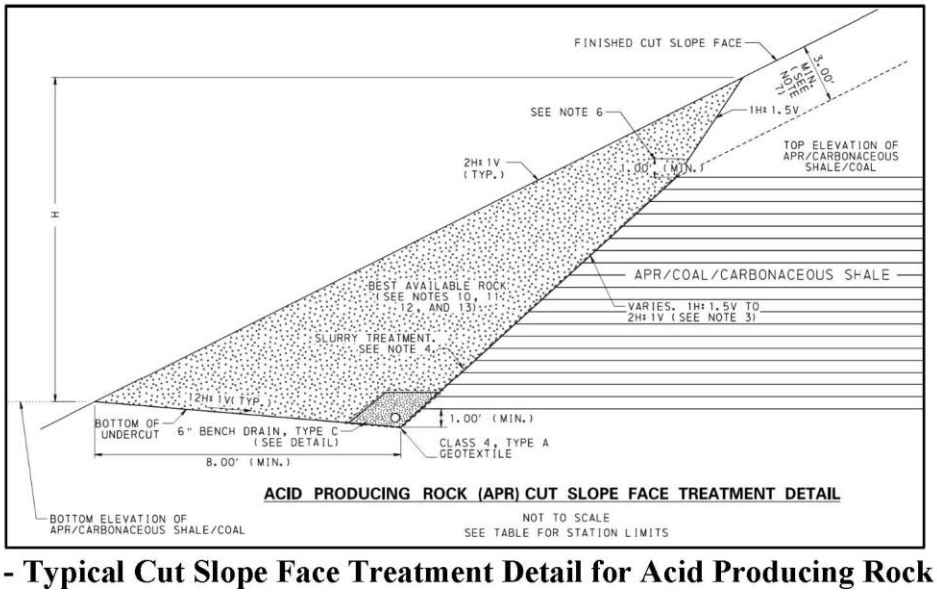


Figure 10 - Typical Cut Slope Face Treatment Detail for Acid Producing Rock and Coal

Figure 11 provides a visual depiction of how the cut slope face treatment details were depicted on the roadway cross sections. In instances such as that depicted on Figure 11, the application of cut slope face treatments to multiple horizons of APR and coal required overexcavation of non-APR rock materials. Where practical, excavated non-APR rock materials separating APR horizons were permitted to be segregated from the APR and utilized for embankment construction without treatment and encapsulation. Note that the approach to overexcavate APR/coal materials beyond the finished cut slope face contributed significant quantities of additional APR and coal that needed to be treated and encapsulated or hauled offsite. As a result, design of cut slope face treatments such as this should be planned to consider the additional costs associated with generating additional quantities of APR and coal.

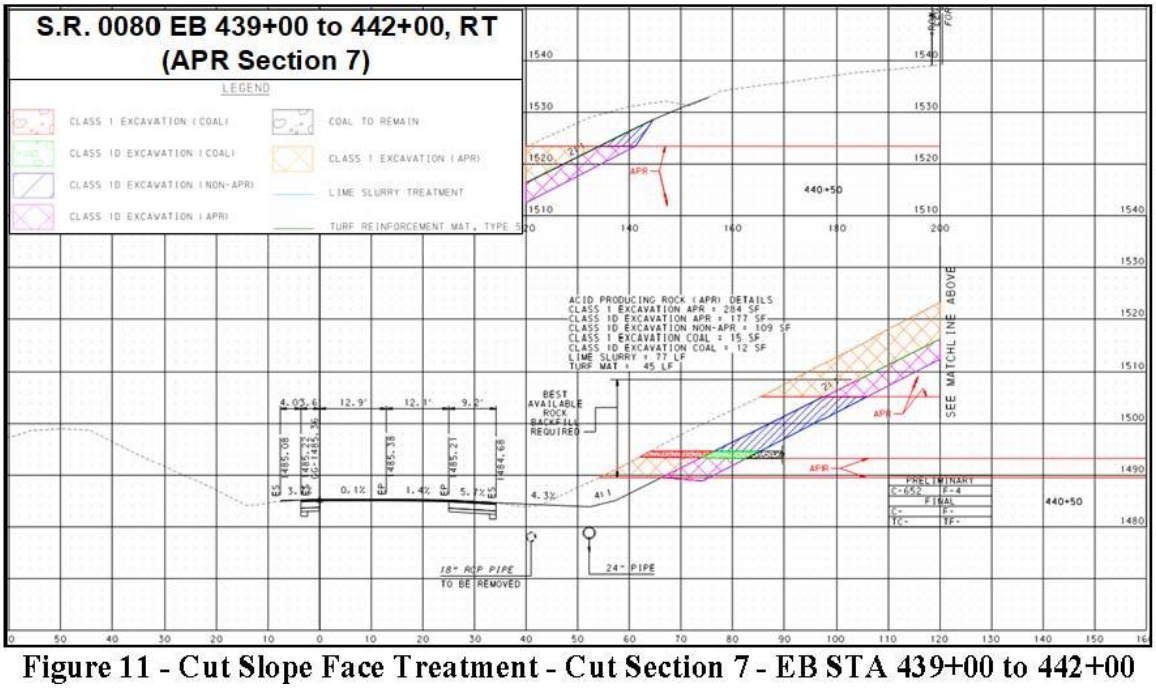


Figure 11 - Cut Slope Face Treatment - Cut Section 7 - EB STA 439+00 to 442+00

Embankment Settlement Analysis and Monitoring

Geotechnical exploration and design considerations were made for the significant fill placements required to establish the realignment of the SR 0080 eastbound corridor. Fill placements involved widening of the existing SR 0080 westbound approach embankments to the existing bridge crossing over North Fork Redbank Creek, with fill slope vertical heights ranging up to approximately 60 feet. Site geotechnical explorations generally revealed granular residual soils of sandstone, siltstone, and shale through the footprint limits of the proposed embankments, with relative densities frequently in the medium dense to very dense range, i.e. soft, fine grained soils with elevated moisture contents were generally not encountered that would present concerns for long-term consolidation settlement. This finding of a residual soil mantle across the project site was found to be consistent with the non-glaciated geomorphic framework of the region and comparatively deep weathering of the sedimentary bedrock. Correspondingly, calculated settlements of the residual soils induced by stress change from the embankment fill placements were primarily anticipated to occur over the time period that the embankments were constructed, with settlements concluding once the fills achieved their final proposed elevations.

Despite the general lack of site soils with the likelihood of exhibiting time-dependent consolidation settlement behavior at the major embankment locations, concerns were raised during the design phase regarding settlement of the compacted embankment fills once in place due to reorientation of the soil and rock particles within the embankment mass itself due to embankment self-weight. This correspondingly led to settlement monitoring being recommended during construction following fill completion to confirm that no post-placement embankment settlement was occurring. The concern raised focused on a postulated process that breakdown of point-to-point contacts between rock fragments in the compacted embankment fill due to overburden stresses would lead to additional settlement occurring within the embankment after completion. This concern was compounded by the sensitivity of proposed permanent pavements supported by the embankment fills and proposed driven battered pile foundations for the eastbound bridge to be installed through the embankment.

A case is noted below where a surface settlement monument was installed at the location of Abutment 2 of the eastbound bridge (Figure 7) following completion of the supporting compacted embankment fill, where vertical and battered HP12x74 piles were proposed to be driven through holes predrilled through the fill. Survey monitoring of the surface settlement monument was performed during a quarantine period imposed on the embankment fill before pile installations could begin. As seen in Figure 12, monitoring of the surface monument revealed negligible settlement over an approximate 2-month monitoring period, suggesting that the speculated settlement of the embankment under its own self weight was not occurring (or not detectable based on the survey instrument sensitivity), and that any elastic settlement of the residual soils beneath the embankment occurred and concluded over the time period that the compacted embankment was constructed. Additional settlement monitoring of embankment fill placements along other reaches of the realigned SR 0080 eastbound roadway are planned.

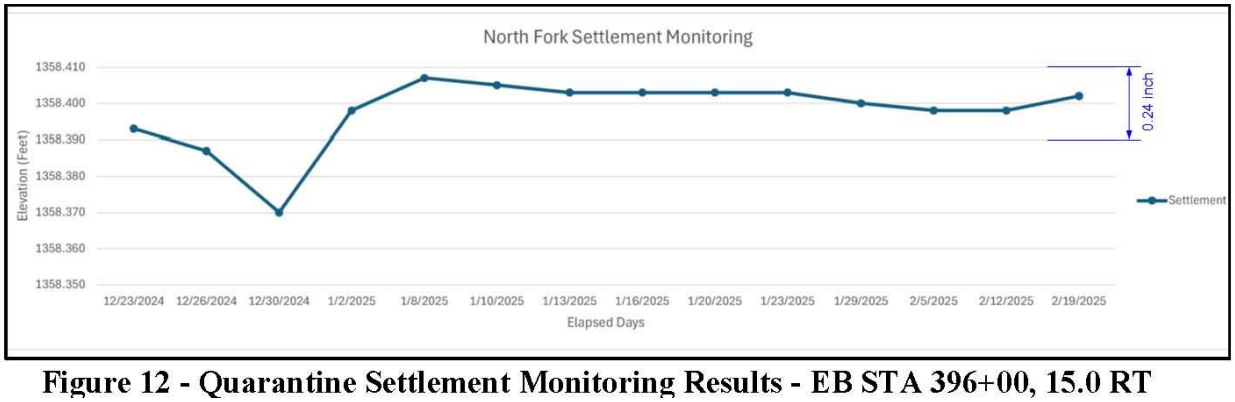


Figure 12 - Quarantine Settlement Monitoring Results - EB STA 396+00, 15.0 RT

Unique Subsurface Conditions at Pier 2 and Pier 3 -SR 0080 Eastbound Bridge

Summary of Proposed Construction

The Pier 2 and Pier 3 substructures for the SR0080 eastbound bridge are proposed to be constructed along the west and east banks of North Fork Redbank Creek. The creek at the pier locations is impounded by an embankment dam with a concrete spillway, serving as a municipal water supply for the Borough of Brookville. The pier substructures were designed as 36 feet square cast in place reinforced concrete footings, each supported by six 72-inch diameter caisson

foundations installed with permanent steel casing and socketed with 66-inch diameter rock sockets into bedrock of the Mauch Chunk Formation. Steel cofferdams are proposed to be installed to permit excavations and dewatering needed to construct the pile caps. Non-Uniform Sloping Bedrock Conditions and Deep Residual Soils

At Pier 2, approximately level top of rock surface conditions were identified by test borings/test holes conducted to support design of the caisson foundations. As seen in Figure 13, distinctly different top of rock surface conditions were encountered at Pier 3, which is located along the east edge of the impounded creek. Due to site access constraints, the location of the test borings relative to the proposed Pier 3 did not fully disclose the steeply dipping nature and configuration of the top of rock surface across the pier footprint, which was only fully revealed by test holes performed during construction. Additionally, this top of rock surface was found to be non-planar when projected through the bottom of pile cap elevation (1,214.0 feet), exhibiting a profile dissimilar to the sloping surface of the valley sidewall. This suggests a significant influence of erosion and non-uniform bedrock weathering on the geomorphology and subsurface conditions during downcutting of the North Fork Redbank Creek gorge in the geologic past. This suggested influence is reinforced by the deeply weathered residual soils disclosed by the test borings and test holes at Pier 3. Refer to Figure 7 for a depiction of the Pier 3 location.

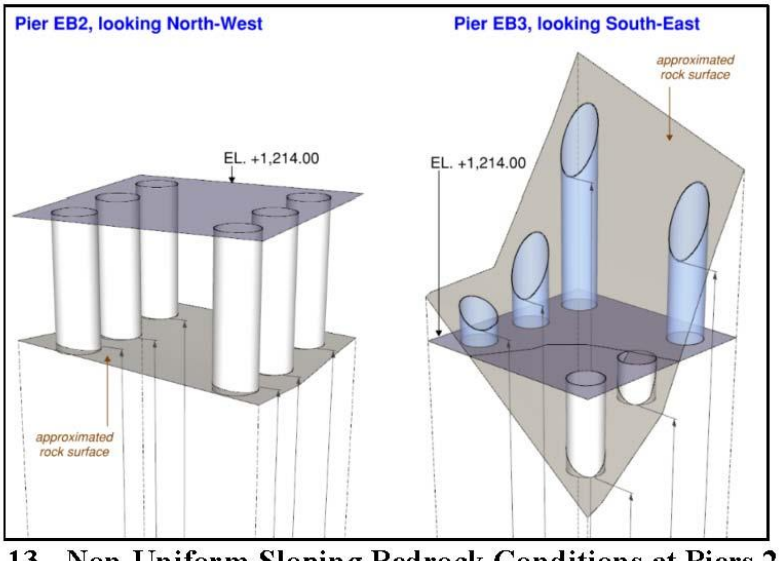


Figure 13 - Non-Uniform Sloping Bedrock Conditions at Piers 2 and 3 SR 0080 Eastbound Bridge Over North Fork Redbank Creek

Drilled Shaft Design and Construction Considerations at Pier 3 Special consideration was made for design of the Pier 3 caisson foundations to account for the steeply dipping, non-uniform top of rock surface conditions and the presence of deep residual soils while meeting the requirements of PennDOT Design Manual Part 4 (*12*). Original design of the caisson foundations considered that a full 72-inch diameter caisson through soil would be necessary to reach bedrock for the majority of the drilled shafts. However, projection of the top of rock surface through the bottom of pile cap elevation during construction revealed four out of the six proposed caissons with sandstone bedrock present at the bottom of pile cap elevation. To account for this condition, the caisson design was adjusted at these locations to eliminate the 72-inch diameter caissons section

and corresponding permanent steel casing and advance the 66-inch diameter rock socket directly from the bottom of pile cap elevation. For the two remaining caissons, the length of the 72-inch diameter caisson section was adjusted to provide a minimum 2 feet of vertical embedment below the top of rock surface. Considering the steeply dipping nature of the top of rock surface at Pier 3, which resulted in several vertical feet of difference in top of rock surface around the perimeter of the caissons, special attention was made to utilize the lowest top of rock elevation around the caissons perimeter to ensure a full 2 feet of permanent casing embedment into sandstone bedrock.

Analysis of the lateral response of the caisson group made similar consideration of the most severe low top of rock condition (i.e. deepest residual soil zone) to ensure that the effect of the sloping bedrock surface across the caisson group was accounted for in the design. As a result, following evaluation of the caisson test hole information, a revised subsurface model was developed to analyze the most severe low top of rock condition to validate the adequacy of the as-designed structural reinforcement and confirm that deflections at the top of caisson fell within tolerable limits using the maximum load combinations imposed by the pile cap. Conservative application of p-multipliers were applied to the supplemental lateral analysis to account for the group behavior of the caissons based on the caisson spacings within the group. Based on the results of the analysis, maximum moments and shears with overstress allowance factors applied were found to be tolerable for the structural reinforcement of the caissons and with lateral deflections of 0.10 inches or less, which were also considered to be within tolerable limits.

Interbedded Sedimentary Rock Stratigraphy Considerations on Rock Socket Design at Pier 3

Original design of the Pier 3 caisson rock sockets embedment into the Mauch Chunk Formation was developed in consideration of anticipated sandstone and siltstone rock units with a minimum unconfined compressive strength of 4 ksi. Test holes performed at each of the six caissons revealed conditions of weak, weathered rock units within the elevation interval of the rock sockets in which geotechnical axial side resistance was to be developed for support of factored axial loads. These adverse rock units were found to consist of soft to hard, slightly weathered to weathered shale and soft to hard, slightly weathered to weathered siltstone, and were found to be in an interbedded state, i.e. these units were interbedded with more competent rock strata similar to the conditions originally anticipated. These conditions were considered unacceptable for development of the required factored geotechnical axial side resistance in comparison with the originally anticipated conditions utilized for design.

Based on the presence of these adverse rock units within the originally designed elevation interval of effective unit side resistance, coupled with the presence of generally hard to very hard, largely unweathered sandstone bedrock below the originally planned rock sockets, the rock socket lengths for all six caissons were increased approximately 8 to 11 feet to provide sufficient development of axial side resistance within the more competent rock mass present at a greater depth. Calculations performed to develop the new rock socket lengths took into account the self-weight of the concrete and length of permanent steel casing that was adjusted based on the test hole results as described above, and a geotechnical resistance factor was applied considering that no load testing was planned once the caissons were installed. Although construction quality control procedures required inspection of the bottom of each rock socket prior to placement of reinforcing steel and concrete, contribution of end bearing was discounted entirely in sizing the

lengths of the rock sockets to conform with PennDOT guidelines concerning vertical displacement required to develop end bearing resistance in comparison with side resistance.

CONCLUSIONS, RECOMMENDATIONS, AND COMMENTARY ON LESSONS LEARNED

A presentation follows below concerning selected conclusions, recommendations, and lessons learned based on the author's experiences during design through the initial phases of construction on the I-80 North Fork Bridges project. The intent here is to provide a succinct, useful summary of important takeaways for the practical consideration of and use by the reader.

1. Careful examination and consideration of the regional geologic framework in which a highway project site resides will reveal key insights concerning likely geohazards and challenging subsurface considerations that will require geotechnical engineering design and construction solutions to solve. In the case of the I-80 North Fork Bridges, the sedimentary rock and coal stratigraphy resulted in significant geotechnical engineering and project earthwork planning to address Acid Producing Rock (APR) and disposal of coals intercepted by project site excavations. Additionally, the non-glaciated setting at the project site was found to result in comparatively deep weathering across the project site, especially along the valley walls of North Fork Redbank Creek, which required special engineering considerations for foundation design of the structures on the project.

2. Careful planning and execution of geotechnical subsurface explorations for highway projects is essential, especially in areas where geologic literature and geomorphology at specific structure locations suggest challenging conditions for construction of foundations. Every attempt must be made to complete design test borings within the limits of the proposed substructures, even where existing site terrain makes access for investigation equipment difficult. Money saved in conducting less than ideal geotechnical subsurface explorations will typically be offset by additional construction costs incurred during redesign work done to account for the true subsurface conditions once revealed during construction.

3. Close interaction between highway, structural, and traffic engineers and engineering geologists and geotechnical engineers from early in the project planning phases through design and into the construction phase will allow for geohazards to be considered throughout the design planning and decision-making process. It is suggested here that this planned close interaction is essential to optimize highway project designs to be both economical and constructible while serving the best interests of the public and in consideration of the surrounding environment and community. The importance of this consideration is especially pronounced when designing highway projects where APR and coal need to be considered.

4. Provided proper quality procedures concerning material types, lift thicknesses, and moisture-density controls are implemented during construction, potential settlement of underlying materials on which the fills are placed should generally be the focus during highway project geotechnical engineering. Mechanical compaction of soil and rock materials should serve to

densify and reorient particles such that overburden stresses imposed by overlying fill lifts should not cause further long-term densification and corresponding settlement of the materials. Evaluation of settlement monitoring results acquired relatively early in the construction phase on the I-80 North Fork Bridges project appears to support this notion.

REFERENCES

1. Maclean, N., A River Runs Through It and Other Stories, The University of Chicago Press, Chicago, IL, 1976.

2. Pennsylvania Spatial Design Access (PASDA). Pennsylvania Imagery Navigator. Pennsylvania Public Access Open Geospatial Data Portal. maps.psiee.psu.edu/ImageryNavigator. Accessed 2024.

3. Sevon, D. W., Map 13 -Physiographic Provinces of Pennsylvania, Commonwealth of Pennsylvania, Department of Conservation and Natural Resources, Bureau of Geological Survey, 3rd Printing, Harrisburg, PA, 2023.

4. Scott, K., History of Jefferson County, Chapter II Natural Characteristics, D. Mason & Co, Syracuse, NY, 1888.

5. Graeber, C.K. and R.M. Foose, Geology and Mineral Resources of the Brookville Quadrangle, Pennsylvania, Atlas 54, Pennsylvania Geological Survey, Harrisburg, PA, 1954.

6. O'Neill, B. J., Jr., Greater Pittsburgh Region Construction Aggregates, Plate 3, Mineral Resource Report 67, Pennsylvania Geological Survey, 4th series, Harrisburg, PA, 1974.

7. Publication 293, Geotechnical Engineering Manual, Pennsylvania Department of Transportation, December 2022 Edition, 12/14/2022.

8. Open File Report OFMI-05-01.1, Geologic Units Containing Potentially Significant Acid-Producing Sulfide Minerals, Pennsylvania Geological Survey, Fourth Series, Harrisburg, PA, 2005.

9. The Geology of Pennsylvania, Commonwealth of Pennsylvania, Department of Conservation and Natural Resources, Bureau of Topographic and Geologic Survey and Pittsburgh Geological Survey, Harrisburg, PA, 1999.

10. Harper, J. A., Lake Monongahela: Anatomy of an Immense Ice Age Pond. In Pennsylvania Geology, Pennsylvania Department of Conservation and Natural Resources, Bureau of Topographic and Geologic Survey, Vol. 32, No. 1, Harrisburg, PA, 2002, pp. 2-12.

11. Publication 222, Geotechnical Investigation Manual, Pennsylvania Department of Transportation, November 2022 Edition, 11/15/2022.

12. Publication 15M, Design Manual Part 4 (DM-4), Structures, Pennsylvania Department of Transportation, December 2019 Edition, 12/30/2019.

Engineering Judgment, Managing Risk, and the Use of Software

Roch S. V. Player, PE, BC.GE, PMP
Braun Intertec Corporation
1901 16th Ave SW, Suite2
Cedar Rapids, IA 52404
(319)-423-0509
RPlayer@braunintertec.com

Prepared for the 74th Highway Geology Symposium, August, 2025

Acknowledgments

The author would like to thank the following individuals and entities for their contributions to the work described in this paper:

Charles D. Hubbard, PE, PG – Braun Intertec Corporation
John Puls, PE – HNTB
Walter Turnbull, PE – GeoStabilization International

Disclaimer

Statements and views presented in this paper are strictly those of the authors, and do not necessarily reflect positions held by their affiliations, the Highway Geology Symposium (HGS), or others acknowledged above. The mention of trade names for commercial products does not imply the approval or endorsement of HGS.

Copyright Notice

Copyright © 2025 Highway Geology Symposium (HGS)

All Rights Reserved. Printed in the United States of America. No part of the publication may be reproduced or copied in any form or by any means – graphic, electronic, or mechanical, including photocopying, taping, or information storage, and retrieval system – without prior written permission of the HGS. This excludes the original author(s).

ABSTRACT

The power and scope of geotechnical engineering software have accelerated. The geoprofessional's ability to perform complex calculations rapidly, and the commercialization and accessibility of artificial intelligence (AI), have created unprecedented opportunities to evaluate engineering problems and develop solutions. However, the ease of use of these tools increases the risk of decoupling the analytical modeling from the inherent variability and complexity of the natural world. Therefore, rather than replacing the engineer, human engineering judgment is more vital than ever to manage risk and create solutions!

This paper will discuss putting analytical modeling into the context of the natural world by discussing the goals of modeling and prerequisites for effective modeling. The Conceptual Site Model will be presented as a tool for improved analytical modeling. Case studies will be presented showing the risks of insufficient site understanding and knowledge of soil and rock behavior, and the resulting numerically correct analytical results providing incorrect engineering answers or solutions for transportation and other projects, as well as successful use of analytical tools to understand and predict site behavior to create effective repair solutions. The purpose of this paper is to prompt better understanding of effective modeling and methods for truing-up analytical results with observed site behavior, leading to better outcomes and improved risk management.

INTRODUCTION

The rate of change relative to the power and scope of geotechnical engineering software has accelerated. The geoprofessional's ability to perform complex calculations rapidly, and the commercialization and accessibility of artificial intelligence (AI), have created unprecedented opportunities to evaluate engineering problems and develop solutions. Analytical tools are increasingly easy to use and can produce outputs with minimal user inputs. However, the ease of use of these tools increases the risk of decoupling the analytical modeling from the inherent variability and complexity of the natural world. With these advancements, rather than replacing the engineer, the need for engineering expertise and judgment has become more vital.

Artificial Intelligence

Artificial Intelligence (AI) is the common, broad term for computer systems and software created to simulate human intelligence to perform tasks that normally would require human intelligence. Included within AI is machine learning, where algorithms allow computers to review, learn from, and make decisions based on data patterns. Generative AI (GAI) refers to AI systems, trained using machine learning, that have the capability to perform higher level tasks in response to prompts from users. For example, GAI systems such as Google's Gemini™ can be queried about a subject, and it will respond with GAI generated text to answer the question.

GAI and other machine learning based-AI systems are trained by providing the models with input data that is used by the model to fine-tune the model parameters, also known as hyperparameter optimization, to best match the training data. These trained models are tested to evaluate the effectiveness of the model in producing results by using new data not seen during the training process. The quality, breadth, and bias of the data sets direct the creation of, and therefore, the results produced by, the model. Thus, these models are empirical and are limited by the data sets used to train and verify the models and the old maxim "garbage in equals garbage out" applies.

Analytical Tools

Analytical tools are tools used to process, evaluate, analyze, and visualize data to allow users to make informed decisions. Analytical tools can range from simple pen and paper processes to complex software platforms that include aspects of AI. In geotechnical engineering, analytical tools allow geoprofessionals to evaluate the response and/or behavior of a system when subjected to stress changes. As computing power has continued to improve, complex analytical software tools have been created for use by geotechnical engineers. For slope stability evaluation, there are two general types of analytical tools that have been developed – limit equilibrium (LEM) and numerical analysis, particularly finite element (FEM)

LEM analysis considers the equilibrium of a soil mass under the influence of gravity and external loads. The method compares the driving forces, moments, or stresses that are potentially causing mass instability with the forces, moments, or stresses resisting instability. The driving and resisting forces are evaluated along a known or assumed potential failure surface represented by a free-body diagram of the overall soil mass bounded at the bottom by the failure

surface being evaluated. The most common method to evaluate these surfaces is the method of slices where the soil mass above the assumed slip surface is divided into multiple vertical slices to simplify the calculations. Multiple methods of slices have been developed and vary depending on simplifications and assumptions of interslice forces and satisfaction of moment, force, or moment and force equilibrium. The factor of safety (FS) against slope instability is simply the ratio of the available resistance to the demand required for equilibrium. A FS>1.0 indicates resistance is greater than demand. LEM analysis further simplifies the calculations by assuming that the FS is the same along the entire slip surface. Deformation is not explicitly considered in LEM analysis (*1*).

FEMs are numerical analytical methods that are used to solve complex problems by subdividing larger systems into simpler, smaller parts. These smaller parts are the finite elements. Each finite element has its own equations describing its physical properties. They are connected together by nodes and assembled into an overall system to represent the model of the overall system. Calculations are performed on the system to evaluate how the overall system will behave. FEM can provide magnitude and direction of displacement. For slope stability analysis, FEM methods do not require the LEM assumptions regarding the shape or location of failure surfaces, the FS along the entire slip surface, or interslice forces. They do require selection of the appropriate general soil behavior models that have been developed (*2*).

MODELING

In the context of this paper, the author defines a model as an understanding of the interrelated variables that can be used to explain site conditions. An effective model captures the behavior of systems to allow users to “observe” what is going on. It displays what the modeler understands the conditions to be. Adjustments to variables within a modeling can be used to evaluate system response to changes.

Models by their nature are simplifications of extremely complex systems and scenarios. To be meaningful, a model must produce results that correlate to the observed conditions that are being modeled. For example, if an analytical model indicates a slope should be actively failing and the observed conditions do not show failure, either the analytical model is incorrect, or the observations are wrong. Since observed conditions can be directly measured, likely the analytical model is wrong and needs to be updated, refined, or discarded.

Accuracy, Precision, Reliability, And Validity

As models are created and analysis performed, the quality of the results can be evaluated by their accuracy, precision, reliability, and validity. Accuracy is how close a result is to a measured value, standard, or known results. Precision is how close the results are to each other. Reliability is how repeatable the results are from similar input. Validity is how well the results meet the intended purpose. Figure 1 illustrates this principle.

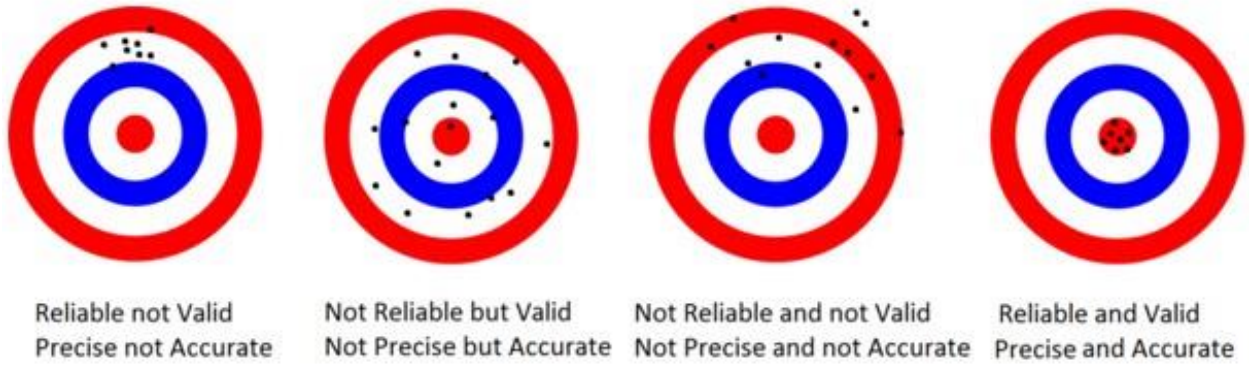


Figure 1 - Modeling and Analysis Categorization

A quality result from a model or analytical tool provides accurate, precise, reliable, and valid results. Comparing results to known and measured information provides a method to assess quality.

Challenges

Analytical modeling for geotechnical and geological engineering is particularly challenging. Earth materials are inherently variable and can vary over time and relatively short distances, both vertically and horizontally. Material responses are based on multiple variables such as:

- Depositional environment
- Previous stress history
- Strain rate of loading
- Duration of loading
- Minerology
- Shape
- Size
- Void ratio/porosity
- Water content
- Discontinuities

The amount and quality of geotechnical and geological data varies widely. General industry practice does not collect continuous data nor are all samples tested (or able to be tested) for all the possible variables. Investigation locations are also widely spaced, therefore only a small percentage of the subsurface is characterized sufficiently to provide high quality, objective data.

Many of the methods used to estimate soil properties are empirically-based with highly variable reliability, such as estimating clay undrained shear strength by counting standard penetrometer test (SPT) blow counts or using SPT values to estimate the internal angle of friction of a sand. These roughly estimated soil properties are then used in sophisticated models which provide high accuracy calculation results.

In other cases, like developing p-y curves for evaluating lateral response of deep foundations, field tests were run and models created using test results for specific elements (such as small diameter driven piles). These models are then applied to evaluate a wide range of deep foundation types, such large diameter drilled shafts, which are outside the data set used to create the models.

Need For Engineering Judgment

Because of the inherent uncertainty in geomaterials and the challenges with quality and reliability of the associated collected data, coupled with the wider development of AI use and accessibility and ease of use of analytical tools, the need for human judgment has never been greater. Experienced geoprofessionals are indispensable to critically evaluate both the input to, and output from, AI answers and analytical tools. They must be capable of distinguishing between mathematically correct answers and realistically possible results.

Analytical models require explicit input parameters, but these geotechnical input parameters have significant variability and uncertainty. One way to demonstrate is by using the Coefficient of Variation (COV) of geotechnical properties. COV is an expression of the relative amount of spread within a data set and is calculated by dividing the standard deviation by the mean of a data set. A low COV means low variability and high COV a high variability. Jones, Kramer, and Arduino (*3*) discussed the uncertainty in geotechnical properties and reported the COV for multiple soil parameters. A listing of a few of these parameters with their associated COV for lab measured properties from their report are in Table 1.

Table 1 - Variability of Geotechnical Properties

	γ COV (%)		ϕ (deg) COV (%)		PI COV (%)		Unconfined Compression Test, Su COV (%)	
Material	**Range**	**Mean**	**Range**	**Mean**	**Range**	**Mean**	**Range**	**Mean**
Clay	2 -13	7	10 – 56	21	9 -57	29	6 – 56	33
Sand	0 - 10	NR	5 – 11	9	NA	NA	NA	NA

NR = Not Reported
NA = Not Applicable

As Table 1 illustrates, even in controlled laboratory tests, the variability of soil properties is great. The founders of geotechnical engineering understood this uncertainty. Ralph Peck in his 1969 Rankin Lecture, quoted Karl Terzaghi as follows (*4*, emphasis added): "In the engineering for such works as large foundations, tunnels, cuts, or earth dams, a vast amount of effort and labor goes into securing **only roughly approximate values for the physical constants that appear in the equations**. Many variables… remain unknown. Therefore, the results of the computations are **not more than working hypotheses**, subject to confirmation or modification during construction…"

As such, the geoprofessional needs to test the results of the AI outputs and analytical tools against the observed, measured world. One method to test these results is the Conceptual Site Model prepared by an experienced geoprofessional.

CONCEPTUAL SITE MODEL

The Conceptual Site Model is a working model that is a synthesis of the known information about a site. It is the model from which site activities are planned and against which analytical results are compared. It consists of multiple data sources, such as:

- Geologic data
- Geomorphological history
- Geotechnical results, such as borings and lab testing
- Geographic information
- Aerial photographs
- Topography
- Hydrology
- Site uses (historic, current, and planned)

These data sources are integrated and interpreted to create an understanding of the actual site conditions based on observed and accepted facts. The Conceputal Site Model is constantly refined as more factual information is collected.

To create the Conceptual Site Model, data is collected through both desktop and field studies. The geoprofessional then takes the collected data and integrates it. The integrated data is then analyzed using science (physical laws, mechanics, statics, dynamics, etc.) and art (creativity, interpretation, intuition, experience, etc.), by asking questions such as:

- What is the significance of the data collected?
- What are the data interdependencies?
- Do I have a sense of the morphology of the site?
- Do I understand the constraints?
- Can I explain the site and the above to another person?

The geoprofessional should identify areas of continued uncertainty and associated risks requiring additional data collection.

Many tools can be used to assist this effort, such as Geographic Information Systems (GIS), computer files, electronic notebooks, pen and paper, and/or simply the mind of the geoprofessional. The Conceptual Site Model is not a specific tool, rather it is a process to create a documented, educated understanding of what the site is, why it is that way, and how it will respond to change. This requires the engineer to take time to research the site, digest the data, and develop the conceptual understanding (site model) that presents an educated hypothesis of the materials and the mechanisms of failure PRIOR to creating an analytical model. The Conceptual Site Model then becomes the basis for analysis and design and the standard against which the analytical models are judged.

CASE HISTORIES

To illustrate the need for engineering judgement and the power of the Conceptual Site Model, two case histories are presented. Case History 1 illustrates how precise analytical results can result in failure when actual site conditions are not understood correctly. The use of the Conceptual Site Model in determining the repair solutions is also presented. Case History 2 illustrates how precise analytical results result in correct, but inaccurate, answers when the incorrect analytical methods are used.

Case History 1

Fort Dodge, Iowa, is located in the Des Moines Lobe physiographic province of Iowa (Figure 2). Glacial processes dominated the recent geologic history of the area. The Des Moines Lobe was formed during the advance, stagnation, and retreat of the continental glaciers during last Ice Age and is the youngest geologic surface in Iowa. As such, the drainage networks are continuing to be established. River and major stream tributaries are relatively short, deeply incised, and have steep sidewalls that are actively failing due to headward erosion. Human infrastructure has been superimposed on the dynamic landscape, leading to failures when the geologic processes are not recognized, as illustrated in Case History 1.

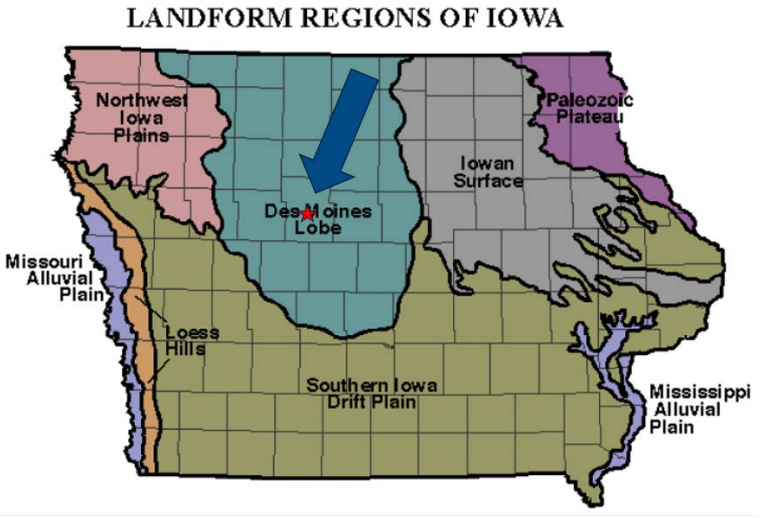


Figure 2 - Landform Regions of Iowa (after *5*)

To expand its parking area, the Fort Dodge Hospital built a series of reinforced soil slope (RSS) structures to maximize the parking area available. These RSS structures incorporated primary and secondary geogrid reinforcement to construct 1:1 horizontal (H): vertical (V) finished slopes extending from the parking lot down to the original grade (Figure 3). After a period of heavy rainfall, the parking area above the RSS experienced cracking and settlement (Figure 4). Inspection determined that the RSS had been undermined and failed (Figure 5).

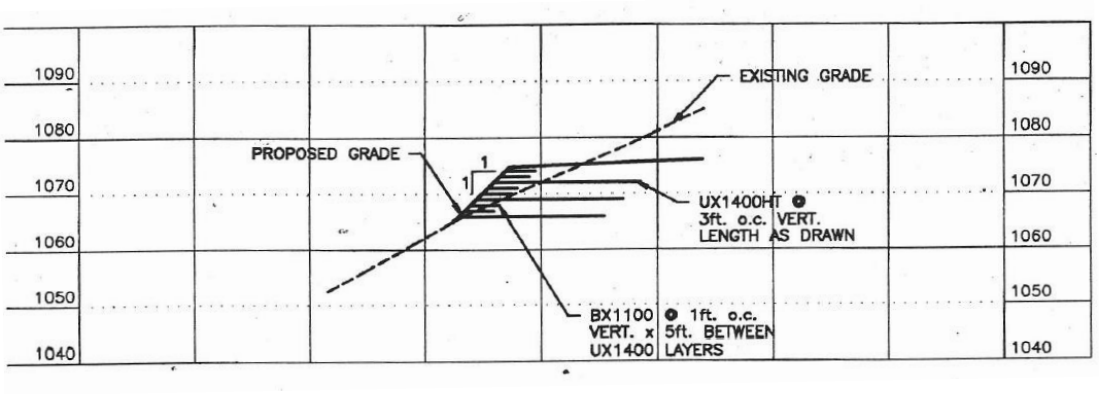


Figure 3: RSS Design from original plans



Figure 4: Pavement cracking and settlement above RSS



Figure 5 - Failed slope, circa 2008. Left photo indicates top of slope and bottom of RSS. Right photo shows eroded toe at creek.

A site investigation was performed to investigate subsurface conditions. Several repair options were considered and the area above the failure was blocked off from parking. A design/build stabilization solution utilizing an in-place soil nail wall was eventually selected. The author was involved in both the design and construction of the repair.

To design the repair, a desktop study was first performed. Existing information was gathered and integrated to develop the initial understanding of the site and the site history. Information collected included:

- Design plans and construction records and photographs of the original RSS slope
- Photographs of the failure taken soon after the damage was found
- Current and historical aerial images
- Topographic maps
- Soil surveys
- Conceptual repair solution alternative and budget pricing
- Previous soil borings and lab testing
- Previous geotechnical reports
- Previous site surveys
- General geologic maps and GIS databases

The desktop study was used to develop the initial Conceptual Site Model to understand the site and the causes of the failure. The Conceptual Site Model indicated:

- The parking area was located upland above the Des Moines River
- The site was in the Des Moines Lobe and was still coming to equilibrium
- The soil borings showed competent foundation and retained material consisting of very stiff to hard sandy lean clay till, consistent with the soil survey and geologic mapping
- The RSS widened the parking area onto a steep slope above an intermittent stream that fed into the Des Moines River
- Per the design documents, the RSS internal design met the required factor of safety
- The design documents showed a slope in front of the RSS
- Failure of the RSS was not general along the entire length of the slope
- The portion of the RSS that failed was above the outside of a stream meander (Figure 7)



Figure 6 - Parking lot setting. Note edge of parking lot in yellow. Location of failure marked by red arrow.

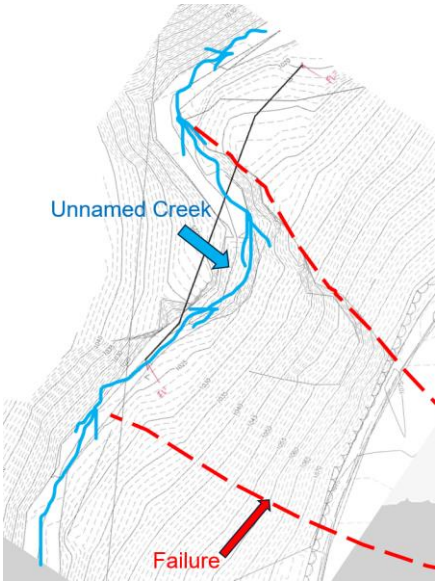


Figure 7 - Failure location in proximity to unnamed creek.

Several observations were made from the initial Conceptual Site Model:

- Stability of the RSS seemed dependent upon its location along the creek
- Erosion of the cut bank could have caused a slope failure that undermined the toe of the RSS
- Continued erosion and toe loss could have resulted in a progressive failure of the RSS

To confirm the initial Conceptual Site Model, a detailed geotechnical site reconnaissance was performed by the author to gather additional, project-specific information, including collecting critical cross-section information from downslope of the RSS. The Conceptual Site Model was updated with this new information. The site reconnaissance confirmed the observations of the desktop study and found:

- Along and on both sides of the entire stream length, the slopes were actively failing above the cut banks
- The portions of the RSS above the inside of meander bends showed no signs of distress
- The slope below the failed portion of the RSS continued to fail and undermine the RSS
- The RSS face had retreated and was standing near vertically, supported by the layers of geogrid (Figure 8)
- The parking lot continued to settle as soil was lost



Figure 8 - Failed RSS face

To test the mechanism of failure hypothesis, the Conceptual Site Model was used to develop an analytical model to perform a slope stability back analysis for:

- Post-failure (existing) conditions.
- Pre-failure showing a continuous slope below the RSS
- Pre-failure showing saturation and soil loss at the toe of the slope
- At-failure modeling the loss of soil due to erosion of the toe

Limit equilibrium methods were used to analyze slope stability. The post-failure analysis was used to calibrate the soil properties estimated from the soil borings, lab tests, and local experience. These properties were then used in the pre-failure model that showed a continuous slope below the RSS. The results confirmed the conclusions of the initial RSS design, showing a FS>1.3 against global stability (Figure 9). Therefore, the calculated results in the initial design were correct mathematically. However, the model was wrong because the initial design missed the actual topographic and geologic conditions, as well as processes that were acting on the site, such as the erosion caused by the creek.

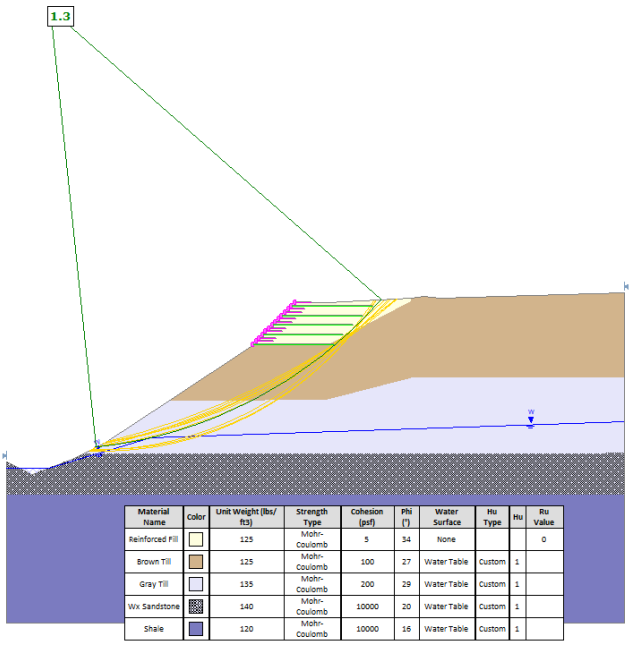


Figure 9 - Pre-failure condition, no erosion

The pre-failure with saturation and soil loss case modeled the topographic and geologic conditions that existed at the time the RSS was constructed. The analytical model was run and showed failure surfaces with FS<1.0 in the slope below the toe of the RSS, as anticipated in the Conceptual Site Model (Figure 10). Next, the analytical model was adjusted, removing the soil that showed failure in the previous model, assuming it failed and was eroded away by the stream. This new, at-failure analytical was run and showed failure surfaces with FS<1.0 extending up into the RSS, indicating a failure mechanism consistent with the conditions observed at the site and summarized in the Conceptual Site Model. Existing, post-failure, conditions are shown in Figure 11.

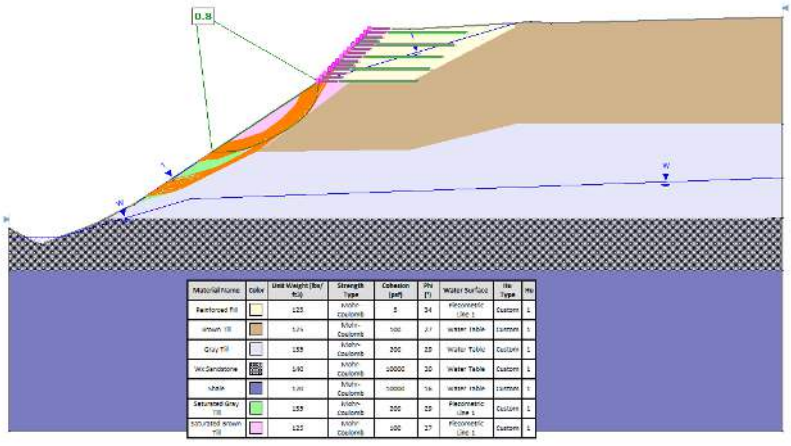


Figure 10 - Failure surfaces below the RSS toe, FS~0.8.

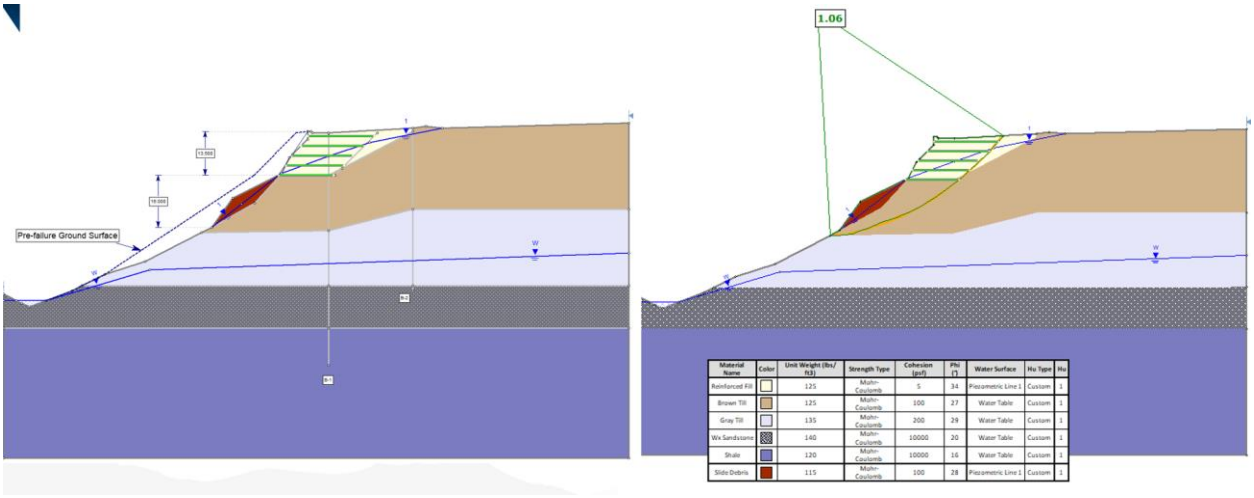


Figure 11 - Post-failure conditions. Left graphic illustrates material lost due to failure. Right graphic illustrates FS prior to repair.

The calibrated analytical model was then used to develop the repair. The repair accounted for the creek erosion and additional loss of soil at the toe by preemptively removing soil thereby increasing the height of the retained slope and flattening the slope in front of the toe. Stability checks were performed for normal, service conditions, and as well as extreme conditions with soil loss due to erosion. The repair was designed to provide FS>1.3 (Figure 12). The repair consisted of hollow bar soil nails at 4.5 feet vertical and 5 feet horizonal spacing, up to 30 feet long. An 8-inch thick reinforced shotcrete face was used to tie the system together. The repair system was installed and has been performing as designed.

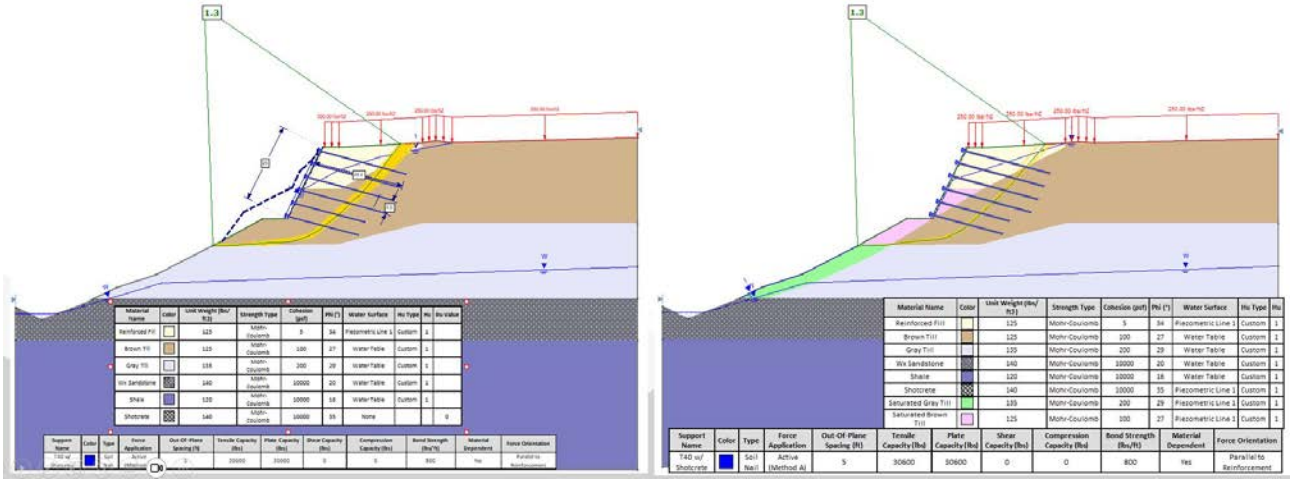


Figure 12 - Repaired slope. Left graphic indicates normal conditions. Right graphic shows saturated foreslope conditions.

Case History 1 illustrates that analytical modeling may create results that are precise, but not accurate. The models were precise, in that independent checks, using the same assumptions, resulted in the same answers. However, the results were inaccurate and failure occurred because

the analytical model did not represent the actual geologic conditions at the site or consider the geologic processes that impacted, and would continue to impact, the site.

Case History 2

A roadway in Oklahoma had experienced global stability failure resulting in loss of use of the shoulder and driving lane (Figure 13). The agency hired a geotechnical engineering consultant to perform a site investigation and design a repair to the slope. The consultant designed an earthwork fix using a combination of regrading and RSS. The design and construction followed the agency specifications for materials and compaction. Unfortunately, soon after the road was repaved, the slope failed again in the same location and the failure surfaces extended up through and behind the RSS reinforcement.



Figure 13 - Left photo shows original roadway failure. Right photo shows the failure of the original RSS repair.

The highway department then chose to pursue a design/build solution to repair the failed roadway embankment. The author served as the senior reviewer of the repair solution design. The design engineer performed a desktop study, created the initial Conceptual Site Model, and then performed a detailed geotechnical site reconnaissance to confirm the desktop study and gather additional information to update the site understanding.

The Conceptual Site Model included the results of the original geotechnical consultant's site investigation and repair design. The consultant had collected good geotechnical data showing a subsurface that consisted of fill and native soil overlying shale. This data was used by the design engineer to create an analytical model of the site to evaluate existing and at-failure conditions, including modeling the RSS. As he ran the back analysis to calibrate analytical model to the observed site conditions, he was able to create failure surfaces that resembled those observed in the field. He then took this calibrated model and began to evaluate repair solutions.

Prior to finalizing the design solution, the author was engaged by the design engineer to review the progress and discuss concerns about the apparent robustness of the repair solution. During the review, we discussed the Conceptual Site Model observations and the back analysis.

The design engineer pointed out that his initial analytical inputs were based on best estimates of soil properties, including in-specification, compacted embankment materials. However, when using those best estimates, the analytical model did not show failure as observed in the field, but rather similar acceptable factors of safety to those shown in the geotechnical consultant's original design (Figure 14). He therefore adjusted the soil properties by reducing the effective friction angles until the analytical model behaved as observed in the field. The model required the in-specification, low-plasticity compacted embankment materials to have an effective friction angle of 20 degrees (Figure 15).

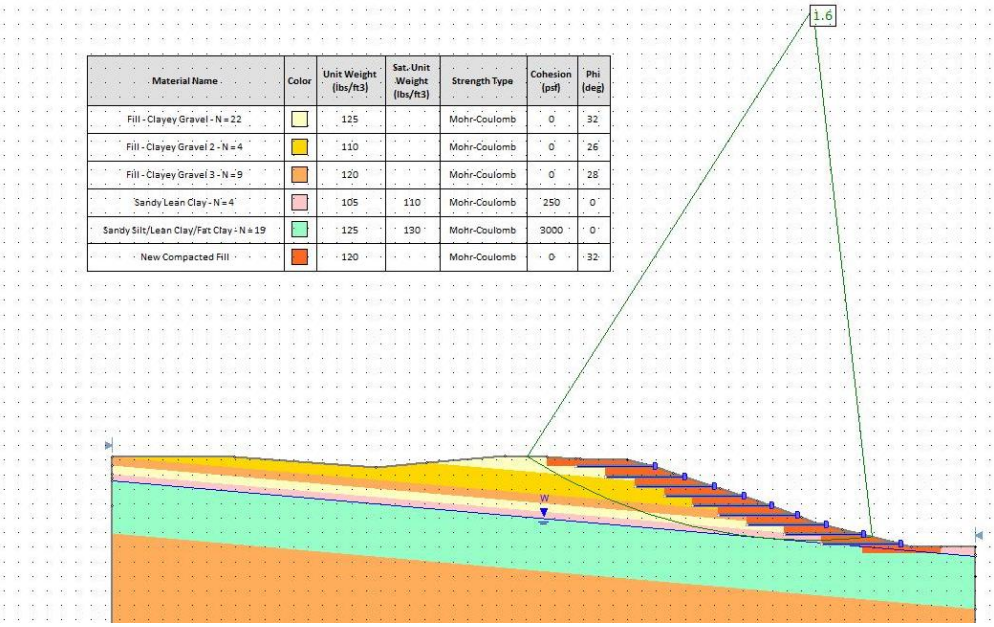


Figure 14 - Initial model, best estimate soil properties, FS~1.6

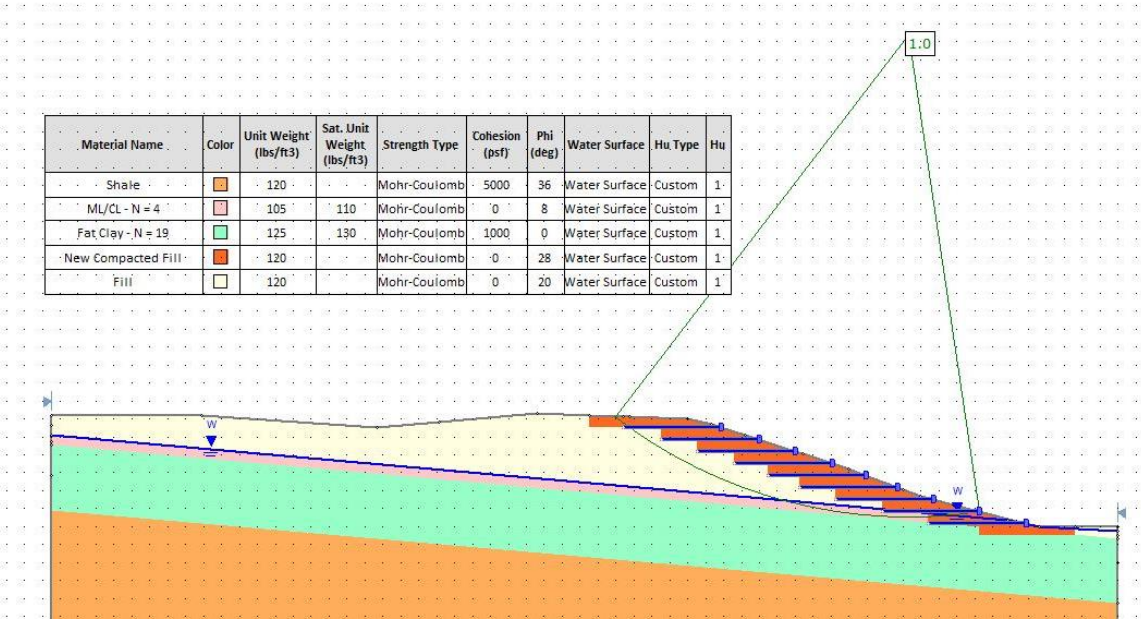


Figure 15 - Revised model, reduced soil properties, FS~1.0

The low effective shear strength parameters in the "calibrated" analytical model were not reasonable when comparing the soil shear strength to those estimated from the Conceptual Site Model. The "calibrated" shear strengths represented soils that were out of specification and would not be allowed by the contract documents. The roadway agency had confirmed during the development of the Conceptual Site Model that only in-spec material was placed and that the contract documents were followed. The subsurface soil layers, RSS geogrid layering, and groundwater conditions used in the analytical model were reviewed and matched those in the Conceptual Site Model. So, although the failure surfaces appeared to match the observed site conditions, the analytical model was wrong because the shear strength parameters required to match field observations were unreasonable. Any repair based on that analytical model had to be very robust because the soil properties were so weak.

Next, we reviewed the methods of slope stability analysis used. The design engineer used appropriate methods which satisfied both moment and force equilibrium (Spencer and GLE/ Morgenstern-Price), however he only checked using circular surfaces (the original geotechnical consultant also had only used circular surfaces to check global stability of their repair). The design engineer re-ran the analysis using non-circular surfaces and the original, best estimate soil properties. The resulting FS was less than 1.0, indicating failure (Figure 16).

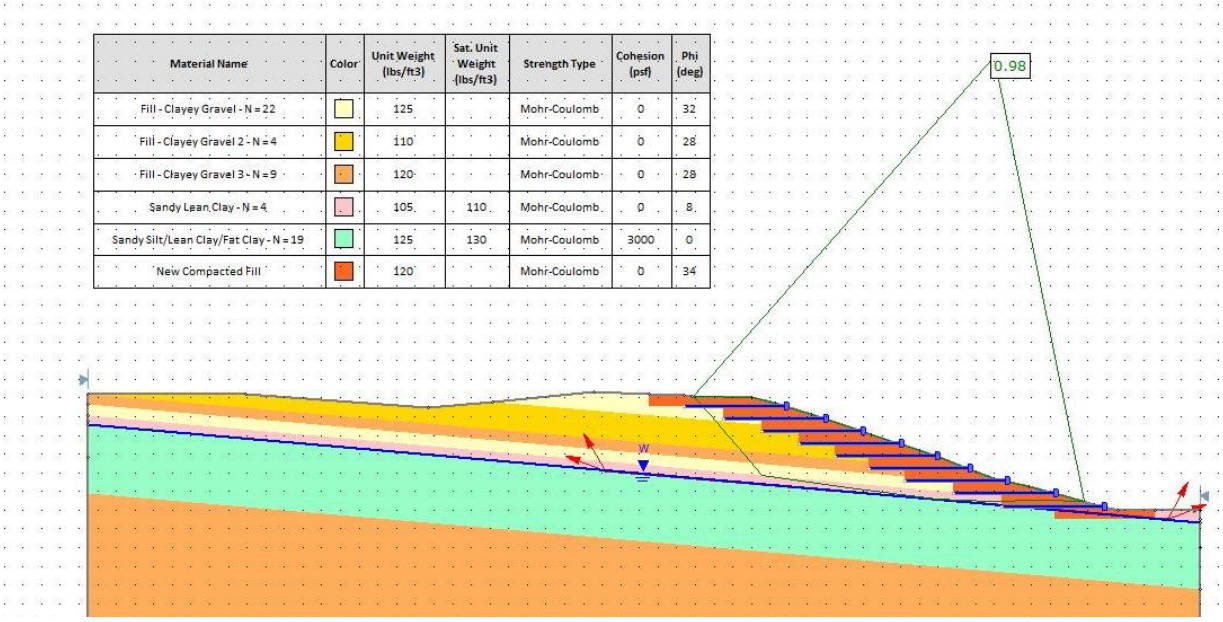


Figure 16 - Best estimate soil properties, non-circular failure surfaces, FS<1.0

The identified failure mechanism was along the sloping, weathered top of the underlying shale. This weathered layer was identified in the geotechnical investigation and included in the Conceptual Site Model. Both the original geotechnical engineer's and the design engineer's analytical models included this layer. However, the circular surfaces generated by the two different modeling programs missed the influence of this layer on global stability. Precise, but inaccurate modeling results were produced.

The recalibrated analytical model was then used to develop the repair. The repair consisted of unloading the slope by removing the RSS and supporting the roadway platform with a soil nail wall. The RSS and other embankment materials were used at the toe of the slope to provide a stabilizing buttress (Figure 17). The repair system was installed and has been performing as designed.

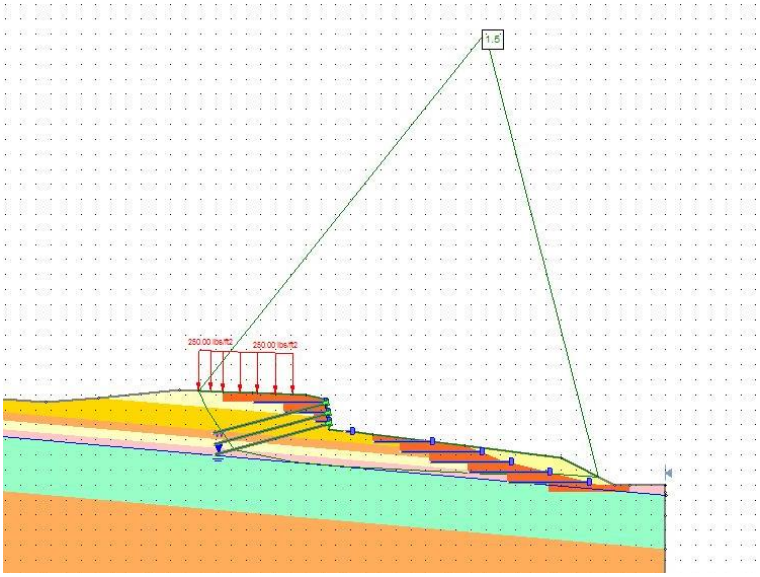


Figure 17 - Repaired slope, FS~1.5

Case History 2 again illustrates that analytical modeling may create results that are precise, but not accurate. Although the analytical model represented the actual geologic conditions at the site, using the wrong surface shape missed the significance of the geologic conditions. A key take-away is that the programs still produced results and those results mislead the designers and resulted in failure.

CONCLUSION

As discussed in this paper, the geoprofessional's ability to perform complex calculations rapidly has created unprecedented opportunities to evaluate engineering problems and develop solutions. However, the ease of use of these tools increases the risk of decoupling the analytical modeling from the inherent variability and complexity of the natural world. Because the Conceptual Site Model is not a software tool but rather is developed by the geoprofessional through experience and judgement, the Conceptual Site Model can be used to calibrate and verify the analytical modeling to observed, known site conditions. Human engineering judgment is more vital than ever to manage risk and create solutions!

REFERENCES:

1. U.S. Army Corps of Engineers, *Engineering and Design, Slope Stability.* Engineer Manual EM 1110-2-1902, Department of the Army, October 31, 2003.

2. Rocscience, Application of the Finite Element Method to Slope Stability, 2004.

3. Jones, A.L., S. L. Kramer, and P. Arduino, Estimation of Uncertainty in Geotechnical Properties for Performance-Based Earthquake Engineering. *PEER Report 2002/16,* Pacific Earthquake Engineering Research Center, College of Engineering, University of California, Berkeley, December 2002.

4. Peck, R.B., Advantages and Limitations of the Observational Method in Applied Soil Mechanics, Ninth Rankine Lecture, *Geotechnique 19*, No. 2, 1969, pp. 171-187.

5. Prior, J.C., *Landforms of Iowa,* University of Iowa Press, Iowa City, Iowa, 1991.

Design Considerations for Consolidation Grouting of the Eisenhower Tunnel

Adam Bedell, PG
Stantec Consulting
167 Selu Creek Road
Cleveland, Georgia 30528
Adam.bedell@stantec.com

Nick Cioffredi, PE
Stantec Consulting
410 17th Street, Suite 1400
Denver, Colorado 80202
Nick.cioffredi@stantec.com

Jeff Hampton, PE
Colorado Department of Transportation
425B Corporate Circle
Golden, Colorado 80401
Jeffery.hampton@state.co.us

Prepared for the 74th Highway Geology Symposium, August, 2025

Acknowledgments

Steve Fradkin-Stantec
Barry Doyle-Stantec
Tao Jiang-Stantec
Michael Boatman-Stantec
Mike Salamon-Retired CDOT/Stantec
Bernie Guevara-Stantec

Disclaimer

Statements and views presented in this paper are strictly those of the authors, and do not necessarily reflect positions held by their affiliations, the Highway Geology Symposium (HGS), or others acknowledged above. The mention of trade names for commercial products does not imply the approval or endorsement of HGS.

Copyright Notice

Copyright © 2025 Highway Geology Symposium (HGS)

All Rights Reserved. Printed in the United States of America. No part of the publication may be reproduced or copied in any form or by any means – graphic, electronic, or mechanical, including photocopying, taping, or information storage, and retrieval system – without prior written permission of the HGS. This excludes the original author(s).

ABSTRACT

The Eisenhower Tunnel was completed over 50 years ago and continues to be a testament to tunnel design and construction professionals demonstrating how the underground industry rises to overcome challenges during construction. During design of the Eisenhower Tunnel, potential high rates of groundwater infiltration into the excavation during construction was expected based off construction records of two tunnels completed earlier—The Moffat Tunnel and the Roberts Tunnel which produced 1,800 gpm and 200 gpm, respectively.

Since traffic started flowing through the completed bore in 1973, groundwater continues to flow into the Eisenhower Tunnel. Water that makes it to the roadway is collected and transmitted to a water treatment facility located in the basement of the east ventilation building. Groundwater that intercepts the horizontal collectors, seep drains, and vertical wall drains bypasses the water treatment facility. Once captured water is discharged from the water treatment facility, it combines with groundwater from the mountain and together they flow into Clear Creek and down the mountains; their use governed by Colorado Water Rights legislation.

Over the past 52 years, continued groundwater infiltration into the Eisenhower Tunnel not controlled by the installed plumbing system has caused numerous challenges from an operational and maintenance perspective. In efforts to protect and ensure continued use of Colorado Department of Transportation's "Crown Jewel" and most valuable asset, a consolidation grouting program was designed as part of a pilot program to mitigate groundwater infiltration into the Eisenhower supply air plenum. The purpose of this paper is to present design considerations for the consolidation grouting program currently in construction.

PROJECT BACKGROUND AND CONSTRUCTION HISTORY

The Eisenhower Memorial Tunnel is located along Interstate 70 (I-70) about 60 miles west of Denver, Colorado. The tunnel is approximately 2 miles long at an elevation of approximately 11,000 ft above sea level. For the early years of its operation, it was the highest vehicular tunnel in the world.

The original tunnel design was performed by Tibbets, Abbets, McCarthy and Stratton of New York. Because of the location at elevation 11,000 feet, ventilation was a huge consideration. At the time in the late 1960's, the effects of elevation on the behavior of carbon monoxide exhaust from mechanized underground excavation equipment was not what it is today.

Following detailed design, as part of the project delivery method (design-bid-build), contractor pre-qualification was required. The pre-qualification requirements were let prior to bid. The major requirements included:

- At least 5 years of experience in major construction work similar to Straight Creek Tunnel
- Satisfactory completion of $10 million project
- Completed 10,000 ft of tunnel excavation
- Establish a net quick asset condition of at least $1,500,000. All bids must be accompanied by a certified or cashiers check for $1,000,000.

Colorado Department of Highways (prior to renaming as the Colorado Department of Transportation) received six bids in October 1967 from joint ventures comprising 18 of the country's major contractors. The Eisenhower Tunnel contract was awarded at $50 million, and construction started in 1968. The winning bid was submitted by Straight Creek Constructors, a joint venture of Al Johnson Construction Company (Minneapolis, MN), Sponsor--Gibbons and Reed (Salt Lake City, UT), Western Paving (Denver, CO), and Kemper Construction (Los Angeles, CA). The bidding phase lasted 6 weeks and Straight Creek Constructors spent $50,000 on consultants and pre-bid work (over $420,000 in 2022 dollars). Straight Creek Constructors understood that the complexity of geology was a key component and hired key consultants such as a Construction Geologist and a Rock Mechanic Consultant. The maximum cover above the tunnel was approximately 1,450 ft and the tunnel was going to be approximately 48 feet wide and 50 feet tall.

In 1967, this represented the largest contract awarded for the Interstate Freeway System as Federal funding accounted for 92% of the project cost.

Geology

Both the Eisenhower and Johnson Memorial Tunnels pass through 75% granite of the Silver Plume Granite and 25% schists and gneisses of the Idaho Springs Formation. The schists and gneisses occur as migmatitic inclusions within the granite. At the Loveland Fault, the rock has been crushed and altered to almost a soil-like condition. The terrain was mapped in 1962 by the U.S. Geological Survey.

During detailed design, the tunnel was divided into five zones based on characteristics developed during design. The following zones are broken down as follows, from west to east:

- Station 38+06 to 81+57 (West Portal to Loveland Fault—Zone 1)
- Station 81+57 to 100+30 (Zone 2-Loveland Fault)
- Station 100+30 to 109+07 (Zone 3)
- Station 109+07 to 118+05 (Zone 4)
- Station 118+05 to 122+30 (Ends at Eastern Portal--Zone 5)

Rock Tunnel Initial Support

The western heading began in 1968 using a top heading and bench excavation sequence and advanced approximately 4,300 feet without issue. The top heading had steel ribs in the arch, set on I50 wall plates. Concrete was placed between steel ribs 4 feet above the wall plate. Rockbolts (10-foot) were installed between the ribs and through the concrete. It was estimated that 30 feet of bench could be safely removed prior to placing posts under the wall plates. Using this sequence, the bench was removed without issue for 1,600 feet from the portal. Because of good ground conditions, the bench length was increased from 30 to 60 feet. This resulted in a collapse of approximately 60 feet of arch. The collapse was judged to be due to joints with talc, clay, and calcite dipping into the tunnel causing lateral loads on the ribs and wall plates. Original rock reinforcement was supplemented with 20-foot grouted rock bolts and in some cases the ribs were pinned with 10-, 15-, and 20-foot-long rockbolts. This continued until the heading reached the Loveland Fault. Figure 1 shows the different zones for the initial support types.

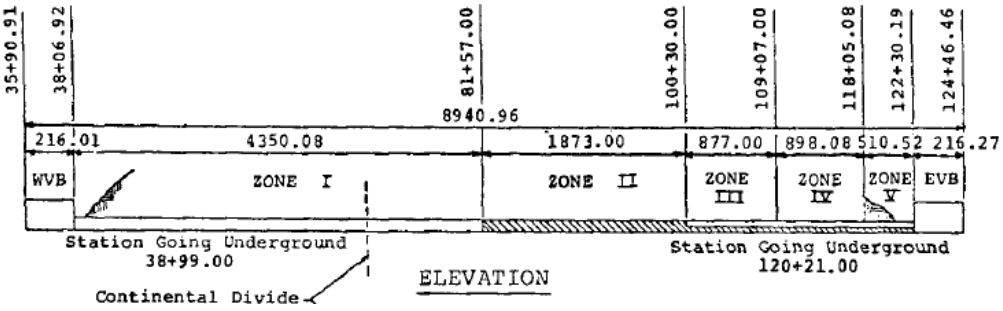


Figure 1 - Plan view of the different initial support zones. Profile is from west to east. From RETC 1972, Construction of the Straight Creek Tunnel.

The eastern heading started in late 1968 and proceeded through the landslide area. Spiling was required once blocky ground was encountered past the landslide area. As the western edge of Zone 3 was advanced, it was noted that large loads were unsymmetrically loading the ribs and deforming and twisting the ribs in Zones 5, 4, and 3. Wall plates were deforming in Zone 3 and allowing the arch ribs to settle.

In September 1969, a shield was to be used to advance the heading from the west into the Loveland Fault. The shield concept was also to be used in the eastern heading. As excavation progressed without issue on the western heading (up to 1,600 feet in from the portal), the contractor abandoned the shield concept for the eastern heading as they felt that experience gained from the western heading would allow for a top heading and bench excavation. As it turned out, great difficulties were encountered with the use of the shield approaching the Loveland Fault, and it was abandoned.

On December 6th, 1969, the east heading stopped due to unexpected convergence and deformation of the steel support sets. All underground construction stopped for just over a year, resuming on January 7th, 1971. The difficulties from both the east and west headings caused a re-evaluation of tunnel initial support and procedures to complete tunnel excavation. Figure 2 shows a partial schedule of excavation sequences up to the re-evaluation of tunnel initial support and excavation sequences.

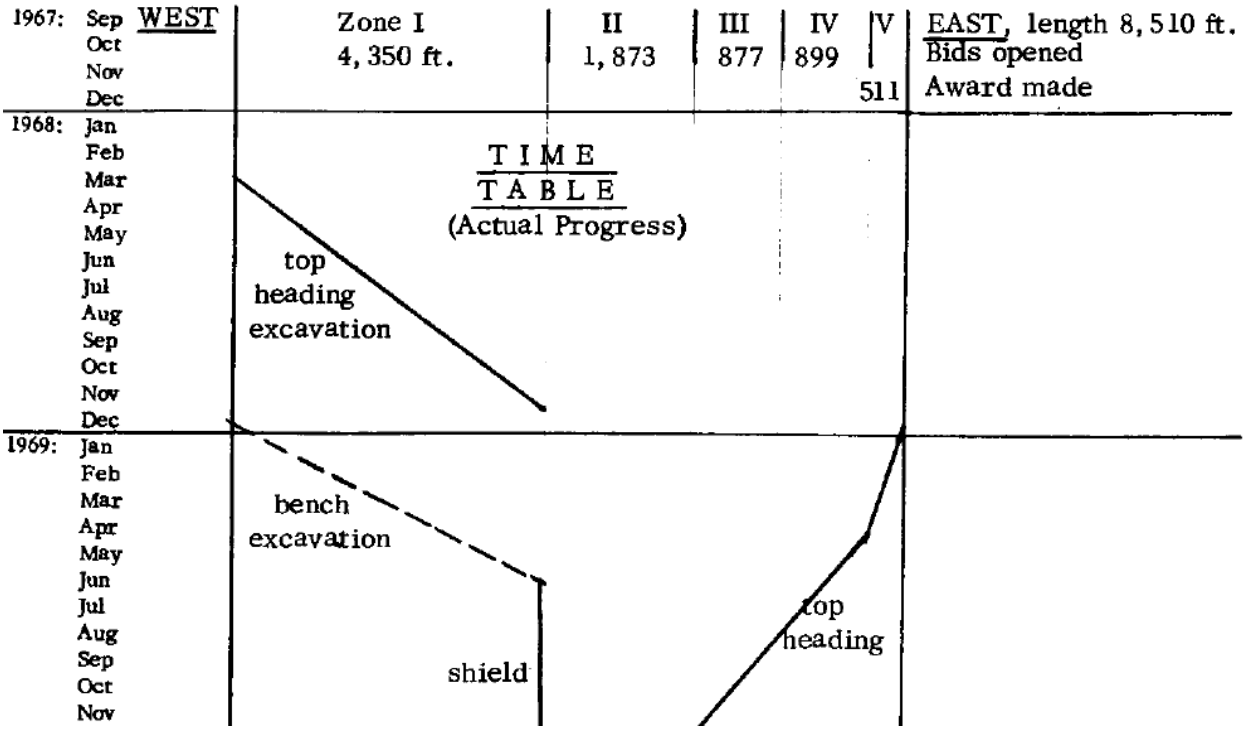


Figure 2 - Schedule shows construction stopping during tunnel initial support re-design. From RETC 1974, Lining and Finishing of the Eisenhower Memorial Tunnel.

The immediate need was to stabilize the heading as most severe conditions existed in Zone 3 from the eastern heading. The bearing failure and collapse of the wall plates and distress in the arch ribs was observed initially. The first remedial action was to install 5-foot wide by 6-foot high concrete buttresses. In addition to buttresses, jacket sets and invert struts were installed but did not arrest ground movement.

During design re-evaluation, it was determined that the amount of overbreak and cribbing between the steel sets and the rockmass created a “soft spot” and rock in close contact with the

steel sets created a “hard spot”. The substantial cribbing used acted as a cushion and allowed for deflection of the steel sets. This condition was corrected through encasement of the ribs with either concrete or shotcrete and filling all remaining voids in the cribbing and blocking with grout. No 8 bars, 20 feet long were installed on a 5- by 5-foot pattern over the entire arch. The invert was also lowered throughout Zone 3.

Removal of the eastern heading bench had two issues—first undermining of the arch support that had already experienced movement and distress. The original planned support did not account for horizontal ground movements (the design intended to use straight side posts). This was complicated as curved side-posts and struts could not easily be adapted. Rock dowels 20 feet long were installed through the wall plates and concrete was placed between the invert struts. Concrete footings from previous drifts added safety by reducing the time supporting the arch and bench face. It was determined that concrete footage drifts would be driven for Zone 4 in addition to the concrete buttress. Additional rock support stabilizing the ground was used.

Excavation in Zone 2 would encounter conditions worse than Zone 3 due to squeezing ground in the Loveland Fault. A full shield driven on concrete footings from the footing drifts (also called foundation drifts – 8- by 8-foot excavations) with arches and invert struts on 3-foot centers would support the excavation. The best ground conditions would utilize 12WF106 arch ribs and the worst conditions would receive 14WF287 invert struts. When excavated, the footing drifts confirmed the ground conditions indicated by the pilot tunnel.

Given ground conditions in Zone 3, and observed extensometer readings, ground loads in Zone 2 could be considerably higher than both primary tunnel liner or the shield had been designed for. The original project team also looked at the Carley V. Porter Tunnel in California for potential risks. Due to the low probability of successfully driving a shield through Zone 2, a multiple drift attack was chosen for tunnel excavation through Zone 2. Dr. R.L. Taylor and Dr. T.L. Brekke in Berkely, California utilized quadrilateral “linear strain elements” to determine high strain gradients.

For most of Zone 2, five drifts were used and were composed of a crown drift, two wall plate drifts, and two footing drifts. In portions where bearing capacity of concrete wall plate was estimated to be too low, an additional sidewall drift was driven on top of the existing footing drift and backfilled with concrete. Within the Loveland Fault, 13 stacked drifts were used continuing across the crown. Each drift was backfilled with concrete before the next drift was excavated. In essence, a concrete arch was constructed before the core of the tunnel was excavated. The crown drift experienced the greatest distortion in initial support members than any of the other drifts excavated in the Loveland Fault.

The zones were heavily instrumented using multiple position borehole extensometers, miniature weldable strain gauges, rock pressure cells, load cells, rockbolt deformeters, and tape extensometers. Locations of instrumentation were based on the geology and construction history for the various zones within the tunnel. As one would expect, the poorest ground conditions were the most heavily instrumented. Figure 3 shows a model that depicts the tunnel and generalized support styles through the excavation.

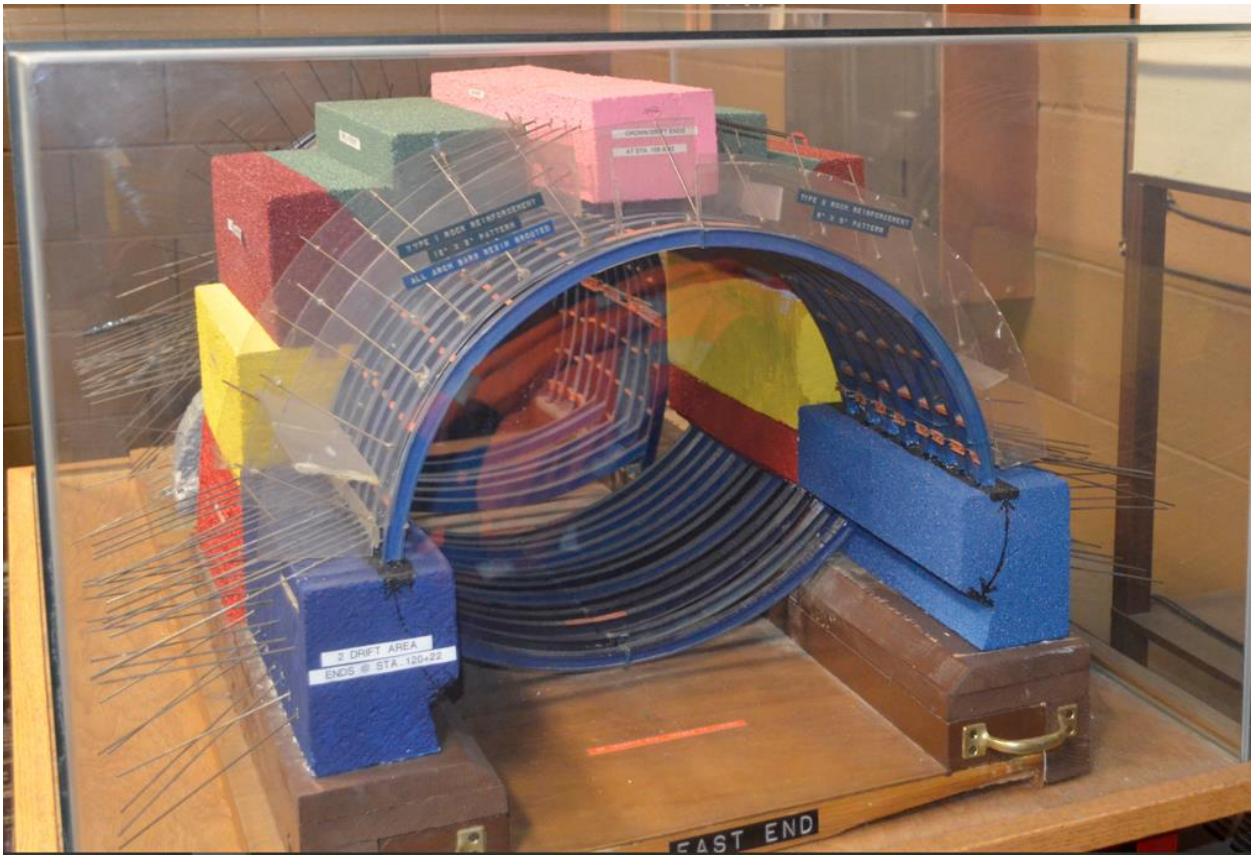


Figure 3 - Model shows the stacked drifts and overall tunnel initial support elements.

A key component to the schedule savings involved the overlapping of activities. This included the overlap of finishing work and tunnel excavation from February 1971 through 1972 and the overlap of finishing work and concrete lining for arch and invert from August 1972 through November 1972.

Completion was delayed by 2 years and construction costs escalated from $52M to $108M ($327M and $678M in 2022, respectively). The original completion date was 1971 (3 years) and it took 5 years. The Eisenhower Tunnel represents one of the most challenging tunnel projects constructed in the United States. Its scope and breadth are remarkable by today's standards, but are made even more so considering the time period in which it was constructed—the late 1960's and early 1970's. Solutions to challenges met and overcome during the construction have filtered into all aspects of the underground industry, including the creation and use of Dispute Review Boards and Escrow documents (implemented for construction of the Johnson Memorial Tunnel).

TUNNEL INSPECTIONS

Tunnel inspections at Eisenhower Memorial Tunnel have been performed since the facility came online. The inspections were non-standardized for many years, as with most tunnel assets across the country. The National Tunnel Inspection Standards (NTIS) were established in 2015 by the Federal Highway Administration (FHWA) to establish and create a national standard for tunnel

inspection for federal and state transportation roadways. This allows each tunnel used for transportation purposes to be held to a national standard and documented on at least a semi-annual basis.

Tunnel construction is always an expensive remedy to traditional transportation problems. Geotechnical risk and uncertainty, permitting, and cost all contribute to overall project cost. Often, problems that arise during the operational lifespan of the tunnel are dealt with as schedule and transportation division budgets allow. Proper asset management and maintenance is the preferred method to address problems that arise over the life span of any transportation asset, especially one that is as difficult to replace or rehab as a tunnel.

Stantec has been performing tunnel inspections on all of CDOT's underground assets since NTIS was established. In addition to the standard FHWA inspection standards, tunnel condition assessments involving facilities operations and maintenance programs are reviewed. Groundwater infiltration mitigation measures are reviewed in addition to other structural deficiencies.

PAST GROUNDWATER REMEDIAL TECHNIQUES

The original detailed design of the Eisenhower Tunnel included measures to deal with groundwater. While waterproof membranes were not specified, the design did include radial holes penetrating the rock mass. These holes intercepted groundwater and conveyed flow to vertical seep drains installed on top of initial support elements and behind tunnel permanent support elements. These vertical seep drains connected to a plumbing system that transmits groundwater underneath the roadway. This system combines with water discharged from the wastewater treatment system located in the basement of the east ventilation building.

During the operational history of the Eisenhower Tunnel, groundwater has infiltrated the permanent liner including into the upper plenum above the roadway. A suspended plenum floor separates the plenum area from the travel lanes, and the plenum area is divided into two areas-the supply side and the exhaust side. See Figure 4.



Figure 4 - Historical photo from the Denver Post. Installation of the plenum dividing wall and floor slabs during construction progressing from west to east. View is looking west. The left plenum is the exhaust air and the right side of the plenum is fresh supply air. From Denver Post archives.

Historically, groundwater infiltration has been the heaviest in the supply side plenum. This portion of the plenum is on the north side of the tunnel where the ground elevation increases to the north and decreases to the south of the tunnel. Groundwater does enter the supply side plenum (during non-freezing periods) and will collect on the plenum floor until accumulation is such that the groundwater enters the seep drain and the collection system.

During the winter season (roughly October through April), groundwater infiltration enters the tunnel plenum and forms “ice monsters”. Figure 5 shows typical accumulation after a 2-month period. Ice accumulation adds both increased weight to the suspended plenum floor as well as adds additional workload to facility employees that must break up the ice, load, transport, and then dispose of the ice outside of the facility. All during the height of Colorado’s winter and spring tourist snow season.



Figure 5 - Groundwater infiltration during the winter months adds additional weight to the plenum floor suspended above active traffic. This accumulated after 2 months of freezing temperatures.

This presents annual conditions that require maintenance. The facility personnel applied various remediation techniques through the operational history of the Eisenhower Tunnel. This included the application of geo-drains.

Geo-drains were drilled through the concrete liner where the tunnel permanent support ended and the tunnel initial support started. Geo-drains are holes that allow groundwater to freely drain from behind the permanent, reinforced concrete liner and is channeled into PVC piping that collects and diverts the flow into drains located at the edge of the plenum floor and the tunnel wall. These were installed by facility staff in efforts to control groundwater infiltration that was concentrated in areas of the tunnel plenum. They were installed primarily in the supply side plenum, though some were installed in the exhaust plenum. A typical arrangement is shown in Figure 6.

The exact date of geo-drain installation is not known, though the majority was gradually installed during the 1980's to early 2000's. Geo-drains provided short term relief from drips and seeps accumulating on the plenum floor. Maintenance of the system proved problematic and over time and multiple freeze thaw cycles, the system became only partially functional while accelerating deterioration of other tunnel elements.



Figure 6 - Geo-drains are the piping that penetrate into the tunnel permanent lining and terminate at the initial support / rock interface. They capture and divert ground infiltration entering the tunnel.

Chemical grout has been applied numerous times along various cracks in the tunnel permanent concrete liner. Chemical grout injection involves drilling holes and installing small grout ports along the crack, alternating sides of the crack. A chemical grout is selected based on conditions (groundwater flow, thickness of concrete, set times, etc.) and is sequentially injected through the grout ports into the concrete liner in effort to seal the crack and provide potential protection along the back side of the permanent concrete liner.

Figure 7 shows the pattern of grout ports along numerous cracks in the supply plenum. Chemical grouting of the supply side plenum has been occurring sporadically for over 20 years. Effectiveness of each chemical grouting campaign is determined by the duration of time before the next campaign of chemical grouting. Chemical grouting in deep tunnel applications is often not as effective when compared to municipal sewer applications. The overburden pressure is greater and often the chemical grout does not penetrate all areas to be effective from a long-term perspective.

Chemical grouting is more expensive than cementitious grouting. Advantages to chemical grouting include overall mobility of the grouting operations as well as simplicity of the

operation. Large, complex equipment is not needed to inject chemical grout, and the single or double component grouts are transported in 5-gallon buckets. Chemical grout mixers are typically pneumatically driven.



Figure 7 - Numerous chemical grout ports are observed along cracks in the permanent tunnel liner. Note the icicles also forming along the cracks. Photo is looking west.

CURRENT GROUNDWATER INFILTRATION ISSUES

Groundwater infiltration into the supply side plenum of the Eisenhower tunnel has been creating challenges for facility staff for decades. Challenges during the summer months include increased calcification of the seep drains. Calcite deposits along concrete cracks and flow paths increase with time. These deposits have grown large around the seep drain inlets on the plenum floor.

Challenges during the winter are obvious with ice accumulation. Ice accumulation presents two fronts that must be dealt with. The first challenge is accumulation. Ice accumulation presents a hazard should facility personnel require access to the plenum for emergency operations, large ice patches are hazardous for walking. The second challenge is weight. Ice that accumulates on the plenum floor increases the weight of the plenum floor slab. The plenum floor slab is suspended from the sidewall and the vertical dividing wall separating the supply and exhaust sides of the plenum. The dividing wall is suspended from the permanent concrete liner by hanging rods. Additional loading of the plenum floor becomes an important consideration given the arrangement of components in the tunnel plenum.

Associated as a by-product of the challenges of ice accumulation is another operational challenge. The ice must be chipped and removed by facility personnel. This is accomplished with wheelbarrows, spades, and shovels or even melting. The process is labor intensive as well as time consuming as the ice locations may be a few thousand feet inside the tunnel. This also involves taking away personnel from other daily activities that must be performed for facility operation. Figure 8 shows another area of ice accumulation.



Figure 8 - Ice accumulation can create a point load and slippery surface on the plenum floor slab. This requires demolition and removal by hand to outside the ventilation buildings.

Numerous solutions to these challenges have been attempted through the years. Heat tape has been applied to geo-drains as well as heat blankets on ice sheets that have formed on the plenum floor. Every remedy only provided short term relief to the facility personnel. Groundwater eventually returns, geo-drain piping breaks due to numerous freeze-thaw cycles, and blankets electrically short or are misplaced.

SOLUTION

Colorado Department of Transportation needed a long-term solution for groundwater infiltration into the Eisenhower Tunnel. All the previous attempts to arrest or manage the infiltration that entered the supply plenum were reactionary and none addressed *why* groundwater wants to flow

into the tunnel. Understanding why and how groundwater infiltrates into the tunnel is the first step in mitigating the ongoing issue.

The Eisenhower Tunnel, at the deepest point, is approximately 1,470 feet below ground surface, well below the natural groundwater table. After construction of the tunnel, an area of negative pressure is created by the excavation and a pressure gradient into the excavation is created. Fractures within the rockmass act as conduits transmitting water from the rockmass into the excavation. The rockmass permeability surrounding the tunnel must be lowered to lessen the pressure gradient acting on the groundwater.

There were two operational requests that the solution needed to satisfy, if possible. The first request was that the solution would require very little if any impact or participation from CDOT staff working at the facility. Staffing levels and providing daily routine maintenance keeping the tunnel operational is a large labor effort for CDOT. The second request was the electrical or energy component would be kept to a minimum. Flipped breakers, extension cords, or other components that would require assistance or continual maintenance from the facility electrician and team were to be avoided if possible.

Two solutions were identified to provide long term groundwater infiltration mitigation to CDOT. Consolidation grouting of the rockmass with a cementitious grout would lower the overall permeability of the rockmass, provided the water bearing fractures could be intercepted and filled with grout. This would greatly reduce or minimize the amount of ice developed in the plenum for the longer-term operational future of the tunnel. In addition, this solution would decrease the impact to the facility workers as well as not include an electrical component at all.

If cementitious grouting was not possible, an engineered drainage system to provide capture and diversion of groundwater infiltration into the existing plumbing system would need to be designed and installed. The design would need to account for extreme cold conditions during the winter season as well as operational simplicity to lessen the impacts on facility workers.

It was determined that consolidation grouting of the rockmass to lower overall permeability would provide longer term benefit to CDOT. While potentially more expensive than a designed, engineered capture and diversion system, it was judged that a proactive approach addressing the fundamental reason why groundwater enters into the tunnel provided more value and benefit than a reactionary system. In addition, the capture and diversion option would still be available if consolidation grouting were not feasible.

Fundamental Question

If grout could not be delivered back into the rockmass, then consolidation grouting would not be an option and force a capture and divert solution. Knowledge of tunnel construction methodologies and techniques of construction are needed to determine the viability of penetrating both the tunnel permanent support elements as well as the tunnel initial support member in order to deliver the grout into the rockmass. All historical documentation including pilot tunnel and geotechnical reports, original design and as-built drawings and construction documentation including photographs were reviewed.

There was no way of determining if any of the grout holes would miss the steel sets installed during tunnel construction. As the permanent tunnel liner is designed to withstand the full load of the structure and act independently from the initial tunnel support elements, the probability of penetrating initial tunnel support members during drilling the grout holes was reasonable. Structural analysis determined that penetration of initial support member such as steel sets or spiling was acceptable. Structural reinforcing steel in the permanent reinforced concrete liner, however, would need to be avoided. The basic answer of whether consolidation grouting was possible was answered, though more answers were needed.

Given the complicated construction history of the tunnel, it was determined that advancement of the grout hole would pass through 2 main zones, the concrete and rock zones. The concrete zone contained structural reinforcement, the tunnel permanent concrete liner and the tunnel initial support, including steel sets, rock bolts, and timber lagging. The rock zone extended back into the rockmass, starting past the end of the tunnel initial support.

DETAILED DESIGN OF CONSOLIDATION GROUTING PROGRAM

Tunnel inspection data for the previous 8 years was reviewed. Attention was given to areas that consistently had documented levels of elevated groundwater infiltration. Tunnel inspection data referenced segment and panel numbers for locations in the tunnel. During concrete placement in construction, concrete forms leave an imprint on the concrete surface. Concrete forms are made up of 3-4 sections and each concrete placement will use anywhere from 1-4 of the form sections, depending on construction schedule, concrete availability, and form strength. In Eisenhower, each form section length is approximately 50 ft long, and each section is referred to as a segment and segments are numbered sequentially in the tunnel from west to east. The segments are delineated by cold joints or formed construction joints every 50’ 3”. The panels are in sets of 8 or 10 and are the imprint from the form skins/sheets.

In tunnel construction, all positioning is referenced to stationing that starts from a point. Areas of groundwater infiltration identified from tunnel inspection records were then correlated to tunnel stationing during construction. As Eisenhower had multiple initial support styles, including 13 stacked drifts used for excavation support crossing the Loveland Fault, correlation between groundwater infiltration and tunnel initial support style was needed to determine what the grout holes needed to penetrate to access the rockmass. Figure 9 shows typical initial support used during construction.

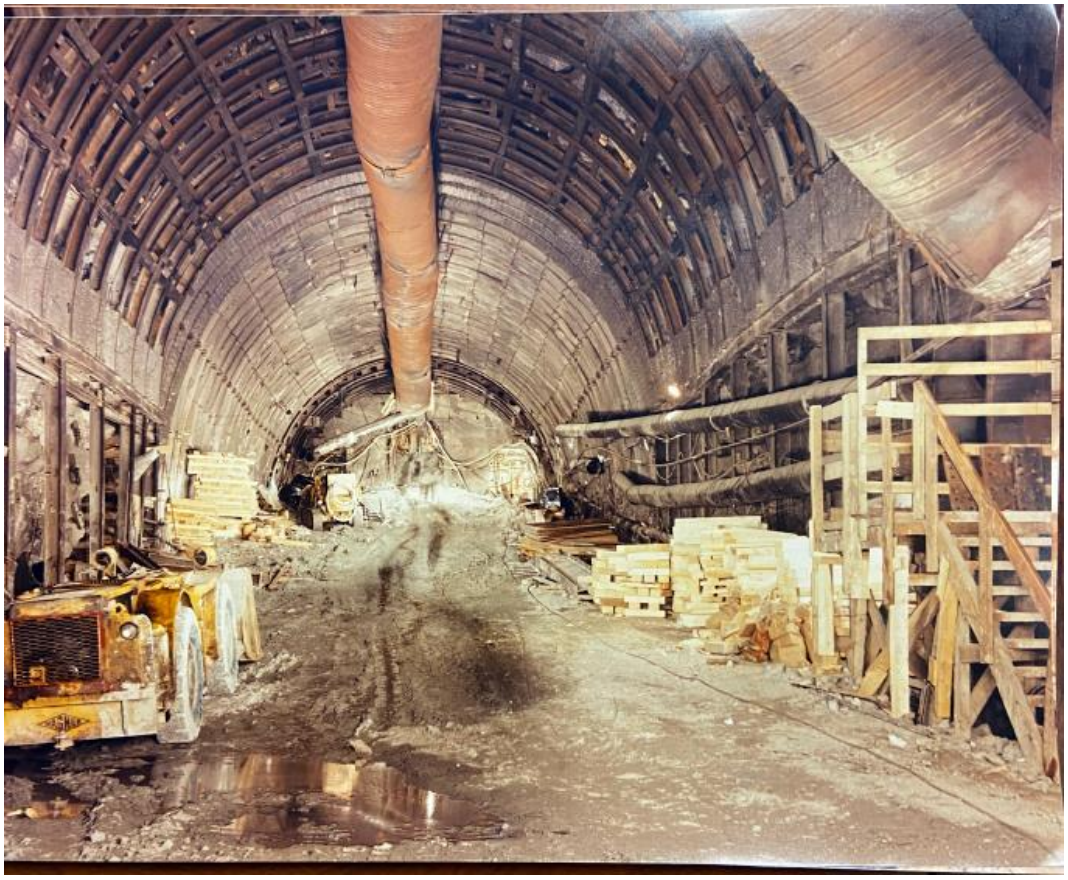


Figure 9 - Steel sets from the east portal looking west. Tunnel support becomes more robust as the arch concrete transitions to full arch concrete in between the steel sets halfway down the excavation. Figure also shows multiple support styles that the consolidation grout holes would need to penetrate to deliver grout into the rockmass.

Three zones for consolidation grouting were identified. It was decided that the initial project would serve as a pilot program. The pilot program would assess grouting effectiveness as well as cost following project completion. Zones identified were then compared to construction as-builts created during tunnel construction. Fracture orientations were compared to the tunnel alignment to determine if grout holes needed to be oriented or if they could simply be perpendicular to the excavation. See Figure 10.

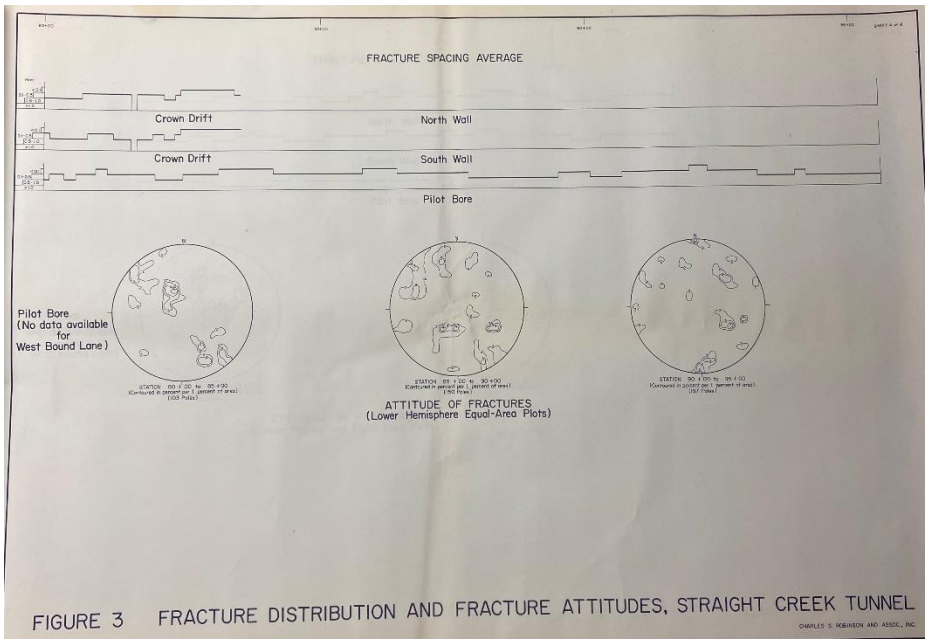


Figure 10 - Stereonets from as-builts from the Straight Creek Tunnel. Used to determine consolidation grout hole orientation.

It was decided that advance stage grouting would be used to advance the consolidation grout hole. Advance stage grouting involves drilling to a depth, then grouting the stage, then re-entering the grouted hole and drilling to a new depth. This is commonly used in cases that involve difficult ground or when additional control of the injected grout is needed. Additional control of the injected grout in this case also lowers the potential for grout to bypass the packers returning to the tunnel. There would be a high potential for this to occur if downstage grouting had been specified.

The first grout stage involved advancing the grout hole through the permanent tunnel liner as well as through the tunnel initial support members and was called the concrete stage. The concrete stage could be anywhere from 3-7 ft long. The variability in concrete stage thickness is dependent on the amount of overbreak that is present at the location of the grout hole. The concrete stage ended at the beginning of the excavated rock surface. The second and third stages were both 10 ft long and in rock for a total of 20 ft into the rockmass.

It was decided the ultra-fine cementitious cement would be best to provide grout penetration into the rockmass. During construction in the early 1970's, contact grouting was performed after the permanent concrete liner was placed. Contact grouting, as detailed on the as-builts and in line with industry standards at the time of construction, included sanded grouts injected at lower pressures at grout ports placed approximately every 50 ft. This practice often led to numerous voids between the permanent and initial tunnel support and large grout takes could be anticipated during the concrete stage in the program. It was decided it would be easier for the Contractor to expect microfine cement then switch to Type IL or Type 1/ Type II rather than vice versa. This change in cement type can be easily discussed on the project site during grouting operations and then addressed through standard contract protocols (Request for Information).

In addition to specifying microfine cement, Xypex was specified for use in all grout mixes as well as for patching grout holes following completion. Xypex is a crystalline, waterproofing admixture commonly used in the concrete industry where water leakage may occur through shrinkage cracks in the concrete. Xypex, in conjunction with compounds in the concrete and water nucleate insoluble, acicular crystals that propagate across microcracks within the concrete. Based on previous tunnel industry applications, a highly Xypex dosed cementitious grout provides an avenue for Xypex to migrate from the grout into concrete thus providing an additional layer of water proofing to the permanent tunnel liner.

Grouting Quantities

Estimated quantities were provided for bidding purposes. Quantities were broken down into the following items:

- Concrete Drilling—Advancing the grout hole through the concrete and initial support members until rock has been encountered.
- Obstruction Drilling—Obstruction drilling separated the concrete drilling from drilling through the tunnel initial support elements including steel and timber.
- Rock Drilling—Advancing the grout hole from the edge of excavation to the prescribed depth of rock.
- Cement—Cement in tons used for mixing grout (including Xypex and superplasticizers).
- Stages—The number of grouting stages.

Estimated quantities were provided on the drawings as well as the bid sheet as part of the project contract drawings.

CONSTRUCTION CONSIDERATIONS

A large part of the detailed design had to account for how the selected contractor would accomplish the work. It was not sufficient to simply make the judgement that all the challenges would fall under Means and Methods of the contractor. The following are examples of such construction considerations.

Active Traffic During Construction

Traffic along I-70 through the Eisenhower Tunnel could not be stopped for long periods given the critical nature of CDOT's asset. The contract specified for the Contractor to utilize spotters during grouting periods to ensure grout communication to the roadway was stopped and addressed to minimize impacts to passing vehicles. The Contractor would also double anchor the grout injection packers for secondary anchorage. In addition, the grouting contractor is required to maintain catch basins to collect any additional fluid (grout or drilling water) to prevent accidental spillage into drains or vents that lead to the roadway.

Plenum Floor Slab Loading

As mentioned, the plenum floor slab is keyed into the tunnel permanent liner on the side wall and then is suspended in the middle by the plenum dividing wall. The plenum dividing wall is held in place by hanging rods embedded into the tunnel permanent liner in the crown. Loads on the

plenum floor had to be restricted to prevent overloading of the hanging rods and plenum floor panels. A suspended floor would need to be constructed for the drilling portion of this work. This would allow the drilling operations to move up and down the tunnel between tunnel segments and different stages of drilling.

Grout Mixing

Distances from the grout mixer to the point of injection were measured. Given that neat cement grout is routinely pumped underground during tunnel construction upwards of 10,000 ft, the fan decks in the ventilation buildings were judged to be more than adequate to stage the grout mixers. An agitator, grout pump, and grout mixer could be placed out of the normal operational space of the facility maintenance crews. The grout hoses (or steel pipes for hard lines) could then be run to the point of grout injection. The only equipment needed at the point of injection would be a flow meter, pressure gauge, and header to control whether the grout is injected or directed back to the agitator in the grout return lines.

Cement

Cement could also be staged on the ventilation fan deck in both the east and west buildings. The two loop roads (on either side of the tunnel) could provide loading and unloading access for cement deliveries or other equipment and materials.

Water

Access to water to support drilling and grouting operations was a major concern during detailed design. Colorado already possesses strict water rights laws and the Eisenhower Tunnel is at 11,000 ft elevation, thus available options to the selected contractor to obtain water for drilling and grouting operations had to be evaluated. Four different perspectives were looked at.

Idaho Springs Tunnel Enlargement Project

The construction history and conditions for this project were reviewed. The contractor was responsible for trucking water to the project site. The Contractor was required to purchase and deliver water trucks for daily drilling and grouting activities.

Water from Eisenhower Operational Facilities

CDOT maintains a storage tank of water for use at the facility. Straight Creek flows from the mountain and fills the tank if the tank water level is low. If the water level is fine, then water is diverted back to Straight Creek. The water stored at Eisenhower supports basic utilities at the tunnel, fire hydrants at the facility, as well as the fixed fire suppression system at the facility.

Water volumes needed for support of drilling and grouting activities were compared to the volume stored onsite. Drilling and grouting activities would significantly exceed the available water CDOT has onsite. It was determined the risk of an emergency occurring in the tunnel while drilling and grouting were occurring was far greater than any party was willing to accept. For this reason, CDOT's onsite water storage was not available for Contractor's use.

Purchase Water from Local Municipality

Rather than acquiring the services from various water delivery vendors in the Denver Metro area, the Contractor had the option of purchasing water from either Dillon or Georgetown, the two closest municipalities west or east of the tunnel, respectively. This would lower transportation costs and allow for flexibility to accommodate traffic or construction issues along I-70.

Capture and Re-use

The Contractor would be responsible for management of all drilling and grouting waste. Water from the drilling process could be pumped from retention basins into settling basins to allow rock and concrete fines to settle out. This would also include any groundwater that was intercepted during the drilling operation. The captured and filtered water could then be re-used for drilling purposes. This would reduce the amount of water purchased to support the drilling operation. This process would not be preferred for grouting as there could still be silts and clays within the water that could limit the grout's penetrability into the rockmass.

Means and Methods

The following two items were considered to fall under means and methods of the selected contractor. The Engineer would not know what system would be used by the Contractor to protect the plenum floor slab, nor would we know how the Contractor would determine where to place their grouting equipment or mixing operations. What was known were lessons from general tunnel construction. The Contractor would need to know what their responsibilities were and what the practical expectation was.

Plenum Seep, Vertical, and Horizontal Drain Protection

Protection of the internal drainage system for the tunnel was very important. Drilling and grouting are not clean operations and routinely make a mess. This applies to both cementitious and chemical grouts. The contractor needed to apply best practices to protect grout or drilling cuttings into the internal drainage system for the tunnel.

It was envisioned that the Contractor would establish a catch basin for both drilling and grouting operations. Catch basins are routinely used in underground construction and all involve a small, electrical pump to discharge the fluids and particulate to a storage container. Small booms or sandbags provide a semi-rigid edge that contains the fluid. This would not be a large structure, but large enough to capture water from drilling or grout escaping from cracks in the concrete liner.

Drilling and Grouting Spoils

Drilling and grouting spoils would need to be disposed of at the end of each shift. It was envisioned that either 250-gallon totes or 55-gallon drums would be used for drilling and grouting spoils. Either of these containers could be moved in and out of the tunnel. The manner in which they would be transported would be dependent on scaffolding or protection of loading of the plenum floor would be employed.

CONCLUSION

Groundwater has been flowing into the Eisenhower Tunnel since the tunnel went online in March of 1973. Numerous methods to arrest groundwater infiltration have been tried during its history with little success. A pilot consolidation grouting program has been designed and is currently under construction. To effectively address groundwater infiltration into existing transportation tunnels, a knowledge of tunnel construction and geology is needed to facilitate a proactive solution. Given the complicated design and construction history of the Eisenhower Tunnel, a detailed investigation into all historical construction documents was performed.

Consolidation grouting of the rock mass surrounding an existing transportation tunnel may not always be feasible, practical, or cost effective. Considerations of how the grouting contractor will perform the work must be accountable in the detailed design and communicated to the contractor such that the level of effort, level of expectations, and challenges of the project are clear and concise.

This pilot program should reduce the operational and maintenance challenges associated with operation during seasonal cycles at the facility. Electrical components are not included in the solution as well as minimal impacts to the facility workers. Facility maintenance workers can focus on tunnel operations and traffic management rather than determining who has to scrape ice in the supply plenum when it's 20 below zero.

REFERENCES

a. Bedell, A. and N. Cioffredi,, Eisenhower Memorial Tunnel—50 Years Later, Rapid Excavation and Tunneling, 2023.

b. Bedell, A., B. Crenshaw, and P. Derby, Grouting Cast-In-Place Concrete Tunnel Liners--What Have We Learned?, Rapid Excavation and Tunneling, 2021.

c. Hopper, R., T. Lang, and W. Mathews, Construction of the Straight Creek Tunnel, Colorado, Rapid Excavation and Tunneling, 1972.

d. Hurr, R., and D. Richards, Ground-Water Engineering of the Straight Creek Tunnel (Pilot Bore), Colorado, Bulletin of the Association of Engineering Geologists, Vol. 3, Nos 1 and 2, 1966.

e. Jordan, K., Notion of a Tunnel under Divide Predates Reality by 100-Plus Years, The Daily Sentinel, December 2011.

f. Kellog, J., The Straight Creek Tunnel-An Engineering and Constructor's Challenge, American Society of Civil Engineers, National Structural Engineering Meeting, 1969.

g. Lee, F., et.al, Geological, Geophysical, and Engineering Investigations of the Loveland Basin Landslide, Clear Creek County, Colorado, 1963-1965, Geological Survey Professional Paper 673-A, B, C, D, E F, G, United States Government Printing Office, Washington, 1972.

h. Lee, F., et.al, Engineering Geologic, Geophysical, Hydrologic and Rock Mechanics Investigations of the Straight Creek Tunnel Site and Pilot Bore, Colorado, Geologic Survey Professional Paper 815, United States Government Printing Office, Washington, 1974.

i. Lee, F. and W. Mystkowski, Chapter 13-Loveland Slide Basin, Colorado, USA, Developments in Geotechnical Engineering, Volume 14, Part B, 1979, pp. 473-514.

j. McOllough, P., Contractual Requirements and Design Philosophies Employed to Minimize Adversary Relationships : Eisenhower Memorial Tunnel, Second Bore, Transportation Research Record, Issue 792, 1981.

k. Merten, F., Straight Creek Tunnel Construction, Route I-70, Colorado, Highway Geology Symposium, 1975.

l. Robinson, C. and F. Lee, Geologic Research at the Straight Creek Tunnel Site, Colorado, U.S. Geologic Survey.

m. Robinson, C. and F. Lee, The Validity of Geologic Projection; a Successful Example : The Straight Creek Tunnel Pilot Bore, Colorado, U.S. Geologic Survey, 1966.

n. Ruemmele, W, Lining and Finishing Eisenhower Memorial Tunnel, Rapid Excavation and Tunneling, 1974.

o. Trapani, R., J. Kaneshiro, D. Jurich, M. Salamon, M., and S. Quick., Structural Inspections of Colorado's Eisenhower Johnson Memorial Tunnel, Hanging Lake Tunnel, and Reverse Curve Tunnel, North American Tunneling, 2010.

p. Water Inflows and Drainage at the Eisenhower Memorial Tunnel, Technical Memorandum 237.120-6, 1974.

*References a-p are not cited in the body of text

River Road in Wilmington, NC – A Study of Small Failures

Nick Moore, LG
North Carolina Department of Transportation
3301 Jones Sausage Road, Suite 100
Garner, NC 27529
984-920-8914
nomoore1@ncdot.gov

Alexandria Jones, LG
North Carolina Department of Transportation
1020 Birch Ridge Drive
Raleigh, NC 27610
919-707-6875
anjones4@ncdot.gov

Prepared for the 74th Highway Geology Symposium, August, 2025

Acknowledgements

The authors would like to thank the individuals for their contributions in the work described:

Tom Santee, PE – North Carolina Department of Transportation
Umesh Neupane, PE – North Carolina Department of Transportation
Neil Roberson, LG – North Carolina Department of Transportation
Nick Zimarino, LG – North Carolina Department of Transportation
Thomas Miller, LG – North Carolina Department of Transportation
Dave Pinter, Retired – North Carolina Department of Transportation
Ricky Smith, Retired – North Carolina Department of Transportation

Disclaimer

Statements and views presented in this paper are strictly those of the authors, and do not necessarily reflect positions held by their affiliations, the Highway Geology Symposium (HGS), or others acknowledged above. The mention of trade names for commercial products does not imply the approval or endorsement of HGS.

Copyright Notice

Copyright © 2025 Highway Geology Symposium (HGS)

All Rights Reserved. Printed in the United States of America. No part of the publication may be reproduced or copied in any form or by any means – graphic, electronic, or mechanical, including photocopying, taping, or information storage, and retrieval system – without prior written permission of the HGS. This excludes the original author(s).

ABSTRACT

New Hanover County Bridge No. 19 is a 3-span bridge on River Road over Lords Creek in Wilmington, NC built in 2018. The project carries a high-volume, two-lane roadway over a 600 foot-wide tidal creek with inundation from diurnal tides. The original subsurface investigation was completed in 2014 and noted saturated, loose sand with moderate organic content to about 18 feet below the ground surface. No recommendations were made addressing embankment settlement due to the suitable quality of sand that was reported. However, embankment settlement and longitudinal pavement cracking began north of the bridge soon after completion of the project, requiring regular maintenance. NCDOT maintenance department contacted the Geotechnical Engineering Unit to investigate the failures and recommend a long-term solution.

Our investigation consisted of 5 mud-rotary borings approximately 80 feet in depth through the failing embankments with SPT samples at 2.5 feet intervals. We sampled for grain size analysis, Atterberg limits, moisture, and organic content, and collected 5 Shelby Tubes for confined-undrained triaxial shear and consolidation testing. We discovered a 15 to 18 foot-thick layer of saturated, very soft, highly plastic, highly organic, alluvial clay. This clay layer was identified as the source of the failure by consolidation due to the addition of the new embankment loads.

The oversight of this alluvial clay layer from the original investigation was costly to NCDOT and highlights the importance of a sound field investigation by locating and identifying potential pitfalls for construction or long-term maintenance. Failure to recognize potential geotechnical liabilities can result in construction delays, cost overruns, negative public relations and unsafe infrastructure.

INTRODUCTION

A sound geotechnical investigation is literally the foundation to the success of a construction project. Pre-field planning is also critical to a successful project. A detailed geologic review should be conducted to help facilitate the boring plan development and anticipate potential geotechnical liabilities before field work begins. The field professional's job is to identify and record problems that could affect the design, the construction phase, or post-construction phase of a project. It is imperative that the field professional correctly identifies these geotechnical liabilities in the field to prevent construction delays, cost overruns, negative public relations and unsafe infrastructure. North Carolina Coastal Plain geology is complex with many unconsolidated surficial soils and high water tables with numerous tidal inlets for sea water, river water, and brackish water to migrate. A bridge replacement on River Road in Wilmington, North Carolina has illustrated when these complex Coastal Plain soils cause infrastructure and engineering problems. Loading roadway embankement soils on a highly compressible alluvial clay layer led to unsafe infrastructure, negative public relations, and hundreds of thousands of dollars were spent on remediation efforts plus future detailed monitoring of the site. This case study is to show the importance of preliminary field work planning and choosing the proper drilling strategy to conduct a sound geotechnical field investigation.

BACKGROUND

North Carolina Geology

North Carolina has a 1.8 Ga. (Ga. stands for "giga annum" and represents one billion years) complex geologic history characterized by the Greenville orogeny (1.8 Ga.-980 Ma. Ma. stands for "mega annum" and represents one million years), Taconic orogeny (470 Ma.-440 Ma.), Acadian orogeny (375 Ma.-325 Ma.), and Alleghenian orogeny (325 Ma.-260 Ma.), rifting of Pangea (235 Ma.-200 Ma.), and mountain erosion, sediment deposition, and creation of the Atlantic coastal plain (66 Ma.-present day; Figure 1; *1*). North Carolina has numerous folds, thrust faults, reverse faults, normal faults, unconformities, accreted volcanic arcs, plutons, rift basins, and fluvial to marine sedimentary formations.

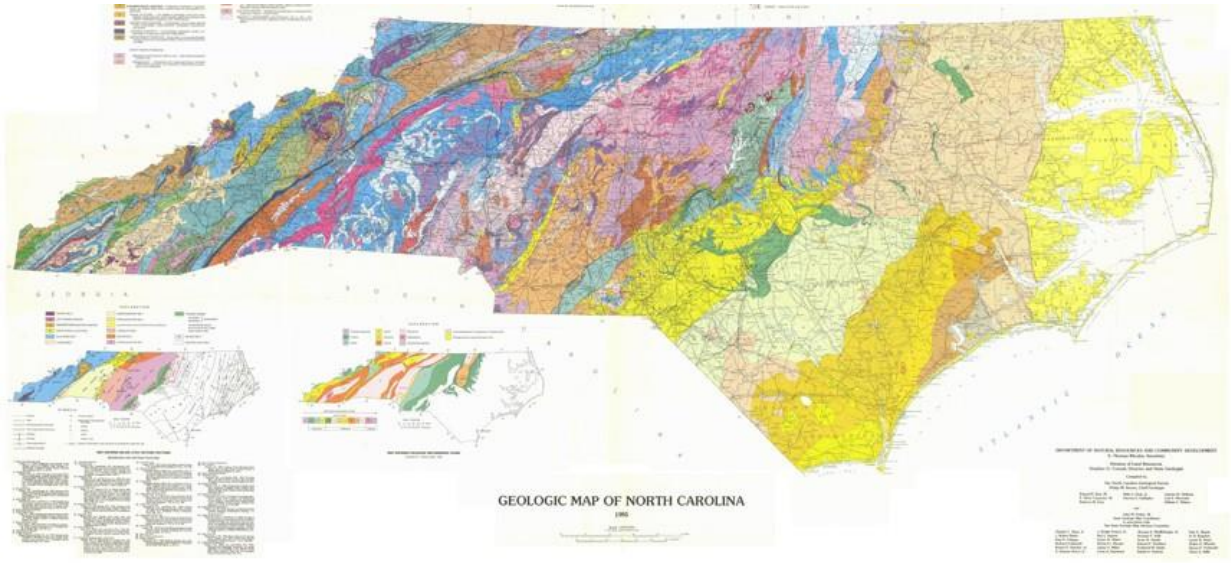


Figure 1 - Generalized Geologic Map of North Carolina.

North Carolina is divided into three physiographical provinces (Figure 2). The Blue Ridge province is the mountainous region in the western NC and contains Proterozoic-aged sedimentary, volcanic, igneous, and metamorphic rocks. The Blue Ridge province contains the Blue Ridge Mountains which are part of the eastern Appalacian Mountains chain. The Piedmont province is the region in central NC and contains mainly igneous and metamorphic rocks. Evidence of volcanic activity during the Allegenian orogeny is observed in the Carolina Slate Belt. The Triassic rift basins from the breakup of Pangea are also found in the Piedmont. The Coastal Plain province is North Carolina's largest geologic region and covers about 45% of the state. Sediments and sedimentary rocks comprise the Coastal Plain region. The following section will cover the Coastal Plain province in more detail.

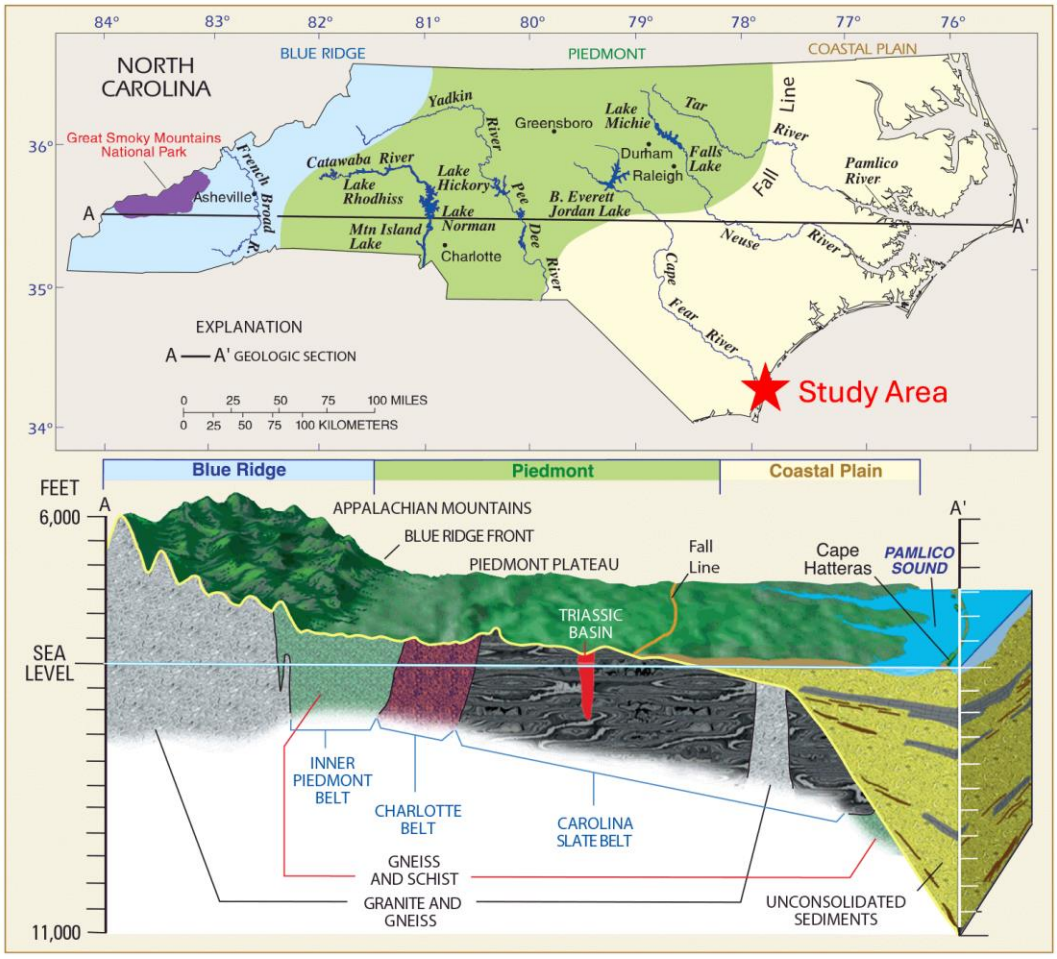


Figure 2 – Physiographic Province Map of North Carolina with a Generalized Geologic Cross Section of the state from A-A'. Study Area is Denoted by Red Star.

North Carolina Coastal Plain Geology

The Coastal Plain itself is part of the larger Atlantic Coastal Plain, stretching from New Jersey to Texas. The North Carolina Coastal Plain province is uniquely complex with multiple transgression and regression sequences, rich fossil assemblages, multiple unconformities, and heavily influenced by a Paleozoic tectonic structure. The North Carolina Coastal Plain province is relatively thin at the western boundary with the Piedmont province and thickens eastward towards the present-day coastline and beyond to at least the continental shelf break (*1*). The Coastal Plain province is characterized by unconsolidated sediments such as gravel, sand, silt and clay and sedimentary rocks such as sandstone, shale, limestone, and marl.

The coastal plain sediments were deposited on broad structural upwarps (arches) and basins (downwarps). These structures occur along the entire eastern seaboard of United States (Figure 3; *2*). The Cape Fear arch is a major upwarp near the North Carolina-South Carolina border and the Albermarle embayment is major downwarp in northeastern North Carolina (Figure 3). The Cape Fear arch is composed of Paleozoic metamorphic rocks of the Charleston,

Roanoke Rapids, and Spring Hope terranes, and igneous and metamorphic rocks of the Hatteras belt near the coast (*3*). The Charleston, Roanoke Rapids, and Spring Hope terranes consist primarily of slaty to schistose metamorphosed mafic, intermediate, and felsic tuffs and flows, volcaniclastic mudstones, siltstones, sandstones, and minor quartzite. The Hatteras belt consists of large granitic batholiths that are bounded to the west by amphibolite facies rocks. In general, Coastal Plain sediments are thinner on the arches and provide a less complete depositional record, whereas Coastal Plain sediments deposited in the embayments are considerably thicker and provide a more complete depositional record.

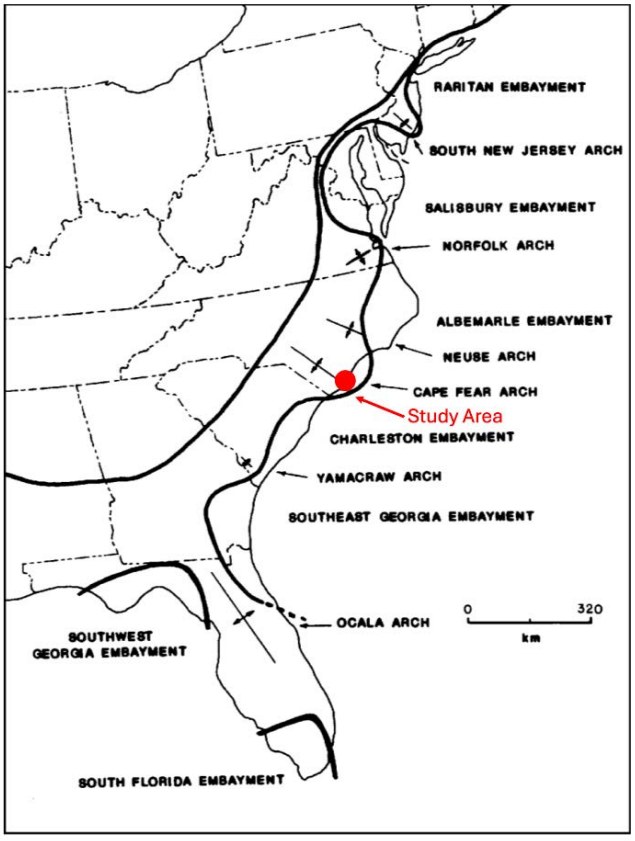


Figure 3 – The Cape Fear arch and other structural features of the Atlantic Coast (Adapted from *2*).

The North Carolina Coastal Plain stratigraphy is largely shaped by a combination of shallow marine, marginal marine, and terrestrial processes from Late Cretaceous to present-day (~90 Ma.—present-day; *4*). The Coastal Plain Cretaceous stratigraphy is composed of, from oldest to youngest, the Cape Fear Formation, the Middendorf Formation, the Black Creek Formation, and the Peedee Formation. The Cape Fear Formation, Middendorf Formation, and Black Creek Formation were deposited in fluvial, deltaic, and estuarine environments during the Late Cretaceous period. The Peedee Formation was deposited in a shallow marine shelf environment and is abundant in marine fossils and glauconitic sand.

The basal unit of the Paleogene period is the Beaufort Formation which formed during rapidly changing conditions on a shallow continental shelf. The mineral cristobalite is present within the layers of the Beaufort Formation. Cristobalite is a high temperature polymorph of quartz found in volcanic environments. The material was likely transported by wind suggesting volcanic activity was occurring near the area. Erosion of the land surface caused the crust to rise slowly and the entire Coastal Plain was above sea level by the end of the Paleocene time (*5, 6)*. The oceans rose during the Eocene during warm and semi-tropical conditions. These conditions allowed the abundant growth of calcareous green algae and marine life flourished. The limy mud was consolidated in limestone over millions of years. Ground water leached most of the original shell material, leaving behind only molds and rare shells. The Castle Hayne Formation is easily recognized by its grey color and the presence of abundant mollusk fossil molds. The ocean retreated and erosion carved the entire coastal plain surface. The sea advanced again during the Oligocene epoch (~31 Ma.) and layers of sand and sandy limestone were deposited in deepening waters. These deposits make up the River Bend Formation. The uppermost deposits of the River Bend Formation are characterized by surf-zone deposits, indicating the ocean retreated again.

The sea began advancing again during the late Oligocene to early Miocene and deposited sand and sandy clay containing numerous marine fossils including barnacles. This formed the Belgrade Formation. After this deposition sequence, the ocean retreated completely from the Coastal Plain and erosion was the dominant process across all of North Carolina. Another sea transgression occurred in the early Miocene (19.0—11.6 Ma) and created unique environmental conditions. A shallow sea in a closed basin with oxygen-depleted water caused phosphate deposits to form in shallow troughs and lime-rich layers developed on slightly higher ridges. Scattered layers of clay from the coast and thin layers of volcanic ash were also present. These sediments form the Pungo River Formation and are completely buried beneath younger Coastal Plain sediments. The Pungo River Formation is also rich in diverse marine fossils including *Carcharocles megalodon* teeth and whale bones. The Pungo River Formation is also mined for phosphate in one of the largest phosphate mines in the world, located in Aurora, NC. Roughly 13 Ma, the sea regressed again and streams eroded the underlying Coastal Plain deposits. The ocean advanced inland about 9 Ma and deposited tan sands of the Eastover Formation in a shallow open environment in the northeastern area of North Carolina.

About 400,000 years later, the sea withdrew and erosion continued in the Coastal Plain for the remainder of the Miocene epoch into the early Pliocene (~5 Ma). Erosion stopped around 5 Ma as the sea advanced and covered the entire eastern portion of the Coastal Plain. Sandy beds were deposited in a shallow, open continental shelf environment. Then, a barrier island system formed and created a large and protected, shallow basin. Fresh water from the mainland interacted with salt water from the ocean and became brackish. Abundant and varied animals thrived in this environment. Interbedded layers of sand, bluish clay, and shell-marl sediments formed the Yorktown Formation. Sediments with similar lithology and age have been mapped south of the Neuse River in North Carolina and into South Carolina; however, these sediments contain species of invertebrate fossils that are distinctly different from the Yorktown Formation. As a result, the Duplin Formation is used to represent this area that contains the different invertebrate fossil species (*7*). The sea retreated again about 3 Ma and major erosion occurred in the Yorktown Formation for about 500,000 years. Around 2.5 Ma the sea advanced inland and

deposited laminate estuarine or lagoonal clays containing interbedded shelly sands of the Chowan Formation in northeastern North Carolina (*2*). The sediment beds associated with the Chowan Formation become more calcareous in southeastern North Carolina, reflecting a slightly deeper sea continental shelf and deltaic environment. These coarse-grained lime-cemented sand and silts are known as the Bear Bluff Formation and correlative with Chowan Formation in northeastern North Carolina.

After a brief 100,000 year erosional period, marine transgression occurred around 1.9 Ma and deposited bluish gray, lime-rich clays and molluscan fossil-rich sands in an open-marine, shallow-shelf environment in northeastern North Carolina. These sediments are known as the James River Formation. During this same time period highly fossiliferous quartz sands and shelly marls were being deposited in a very near shore environment located in southeastern North Carolina. The rich fossil assemblage makes the Waccamaw Formation a critical unit for correlating marine Pleistocene deposits along the Atlantic Coastal Plain. Glacial and interglacial periods dominated the Pleistocene epoch. Glacial periods caused marine regression sequences and interglacial periods caused marine transgression sequences in the Coastal plain. An interglacial period occurred during the late Pleistocene and caused sea level to rise in east-central North Carolina and deposit pebbly sands, silt, and clay of the Flanner Beach Formation in a barrier-lagoon environment. Deposits of peat with cypress tree stumps are also located in this formation. The coarsely grained fossiliferous sand and arenaceous fossiliferous limestone of the Neuse Formation was being deposited in an estuarian to shallow marine environment in southeastern North Carolina also during the late Pleistocene (*8*). The Neuse Formation is the youngest named formation in the North Carolina Coastal Plain. Undivided coastal plain soils are deposits found within Coastal Plain province that have not been formally classified into a specific geologic formation. These unconsolidated soils are highly variable and include sand, silt, clay, gravel, or marl.

Project B-5236: River Road over Lords Creek, Wilmington, NC

New Hanover County Bridge No. 19 is a 3-span bridge on River Road over Lords Creek in Wilmington, NC and was originally built in 1974 (Figure 4). NCDOT Bridge Management Unit considered the bridge structurally deficient and functionally obsolete. The original bridge foundation was timber piles and the superstructure was constructed of concrete. The traffic study perfomed in 2014 indicated Bridge No. 19 carries 5,220 vehicles per day and 8,700 vehicles per day is predicted for the year 2035. The original bridge length was 91 feet and the replacement bridge would be lengthened to 110 feet. The replacement bridge would include two 11-foot lanes and 4’3” offsets to accommodate bicycles. The approach roadway would extend 284 feet from the north end of the replacement bridge and 355 feet from the south end of the replacement bridge. The approaches would be widened to include a 22-foot pavement width to provide two 11-foot lanes. Six-foot grass shoulders and four-foot paved shoulders would be provided on both sides.

The original geotechnical investigation for the roadway was performed by a consulting firm in September and December of 2014. Twenty-two hand auger borings and 2 vane shear tests were performed (Figure 5). Roadway embankment soils were present throughout the entire project and consisted of gray, moist to saturated, loose, fine sand (A-3). Alluvial soils were also

present throughout the entire project and consisted of orange, brown, and gray, moist to saturated, loose, silty and fine sand (A-2-4, A-3) with 3-6% organic content. Vane Shear Test data indicated shear strengths ranging from 43-1963 psf. Ground water elevations were collected in September 2014 during normal precipitation time and ranged from 0-3 feet below ground surface.



Figure 4 – Satellite Image of the Bridge No. 19 on River Road. Notice the wide historical floodplain on the north side of the bridge.

The original geotechnical investigation for the bridge was perfomed during January 2015 by a different consulting firm. Six mud-rotary SPT borings with one core boring were performed (Figure 5). Roadway embankment silty, fine, and coarse sands (A-2-4, A-3, A-1-b) were reported similar to the roadway investigation report. Alluvial soils consisted of brown, gray, and black, saturated, very soft to soft, sandy silt (A-4) with an organic content of 14-21%. Wood fragments were also noted in the organic content. Undivided coastal plain soils were also reported and consisted of tan, black, and gray, saturated, very loose to medium dense silty, fine, and coarse sands (A-2-4, A-3, A-1-b). The Castle Hayne Formation soils were reported around 55-60 feet below the ground surface and consisted of gray, wet, medium dense to dense, fine sand (A-3) and gray, wet, stiff, sandy silt (A-4). Three- to four- foot-thick layers of dark gray and tan, indurated to friable, sandy limestone were also recorded in the Castle Hayne Formation.

Bridge construction began in November of 2017. This section of River Road was closed to the public during construction which required a 12-mile detour. The bridge was completed and the road reopened in June of 2018. Transverse and longitudinal pavement cracks began to

form due to differential embankment settlement of up to one inch by mid-July of 2018 (Figure 6A, settlement graphs/plan view). The north side of River Road was repaved in July of 2019, November of 2019, and January of 2021. Longitudinal pavement cracks formed shortly after each repave (Figure 6B, 6C, 6D). Finally, the NCDOT maintenance department contacted the Geotechnical Engineering Unit to investigate the failures and recommend a long-term solution.

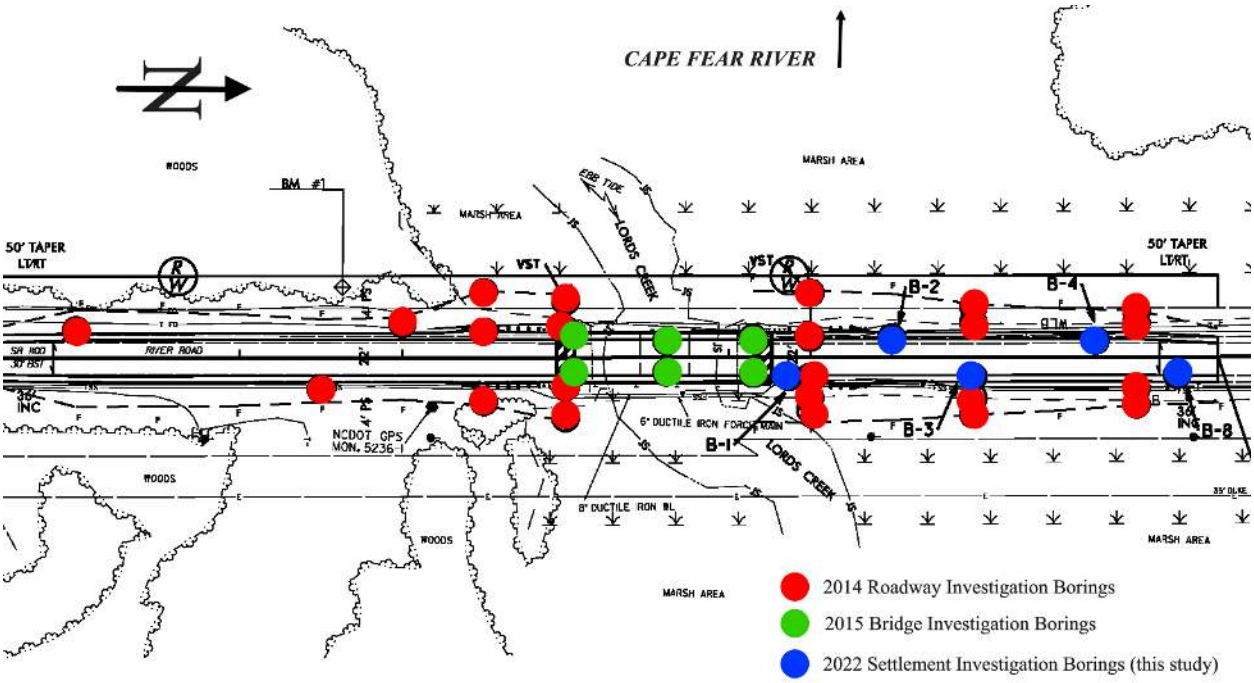


Figure 5 – Plan View of Bridge No. 19 on River Road and the Location of the Original Roadway and Bridge Investigation Borings as well as the Settlement Investigation Borings from this Study. VST = Vane Shear Test.



Figure 6 – A) Transverse Pavement Cracks on North Side of Bridge in July 2018, Less Than One Month After New Bridge Opened. B) Longitudinal Pavement Cracks in 2020 After Repave. C) Longitudinal Pavement Cracks in 2022 After Repave. Also, Notice the Slumping Guardrail. D) Longitudinal Pavement Cracks and Slumping Guardrail in 2024 After Repave.

METHODOLOGY

The initial phase of our investigation involved a review of the 2014 roadway and 2015 bridge inventories to help develop our field plan. Our reviews revealed the bridge inventory had noted an 8 to 22-foot layer of moderately to highly organic, alluvial silt and this silt layer was absent in the roadway investigation . We also utilized Google Earth to review satellite imagery of the field area and noticed a wide historical floodplain on the north side of the bridge that could be main reason for the embankment settlement (Figure 4). Historical floodplains can contain organic, soft, compressible soils that were deposited in the geologic past by water. It is important to note these floodplains because they can be geotechnical liability.

Our investigation consisted of five mud rotary SPT borings on the north side of the bridge (Figure 5). We recorded SPT drives at 2.5-foot intervals through the roadway embankment and alluvial soils to accurately determine the top and bottom contactS of the alluvial soil in the 2 borings closest to the bridge (Boring B-1 and B-2; Figure 7). We also drilled boring B-1 to a total depth of 105.6 feet and boring B-2 to a total depth of 102.6 feet. After we drilled boring B-1, we offset 5 feet and drilled boring B-1A so we could push 9 consecutive shelby tubes in the

alluvial layer to have a complete and undisturbed soil record of this layer. We wanted to determine the thickness of the alluvial layer as we traveled North and farther away from the bridge so our boring termination criterion was to terminate the boring once we drilled through the bottom of the alluvial layer. We drilled borings B-3, B-4, and B-8 to depths of 30.1 feet, 30.1 feet, and 22.5 feet, respectively (Figure 7). Twenty five soil samples were submitted to the NCDOT Materials and Test Laboratory for grain size analysis, Atterberg limits, moisture percentage, and organic content. Five Shelby Tube samples were also submitted to the NCDOT Materials and Test Laboratory for confined-undrained triaxial shear and consolidation testing. An updated report was created combining the original 2014 roadway borings, 2015 bridge borings, and our 2022 roadway borings to show a plan view of the boring locations (Figure 5), a profile view along the L alignment with the subsurface stratigraphy, and cross sections from the beginning of the bridge and approach going northward with the subsurface inventory. Settlement analyses were conducted on the samples from the alluvial layer. Settlement remediation options were also analyzed and produced.

RESULTS

The roadway embankment soils present throughout the entire project consisted of gray and brown, moist to saturated, very loose to loose, silty, fine, and corse sand (A-2-4, A-3, A-1-B) with trace gravel. The roadway embankment layer was about 23 feet-thick by the bridge and thinned out to about 10 feet-thick northward from the bridge (Figure 7).

Alluvial soils were also present throughout the entire project and consisted of dark gray to black, saturated, very soft to soft, highly plastic, highly organic, silty clay (A-7-6) with moderate wood fragments (Figure 8A-D) interbedded with gray and black, saturated, very loose, highly organic, silty sand (A-2-4). The liquid limit (LL) for the alluvial layer ranged from 81 to 128 and the plastic index (PI) from the clay layer ranged from 40 to 57 (Figure 7). The moisture percentage (w) of the alluvial layer ranged from 80% to 313% and the organic percentage (ORG) ranged from 11% to 62% (Figure 7). The alluvial layer was about 18 feet-thick by the bridge and thinned out to about 8 feet-thick northward from the bridge (Figure 7).

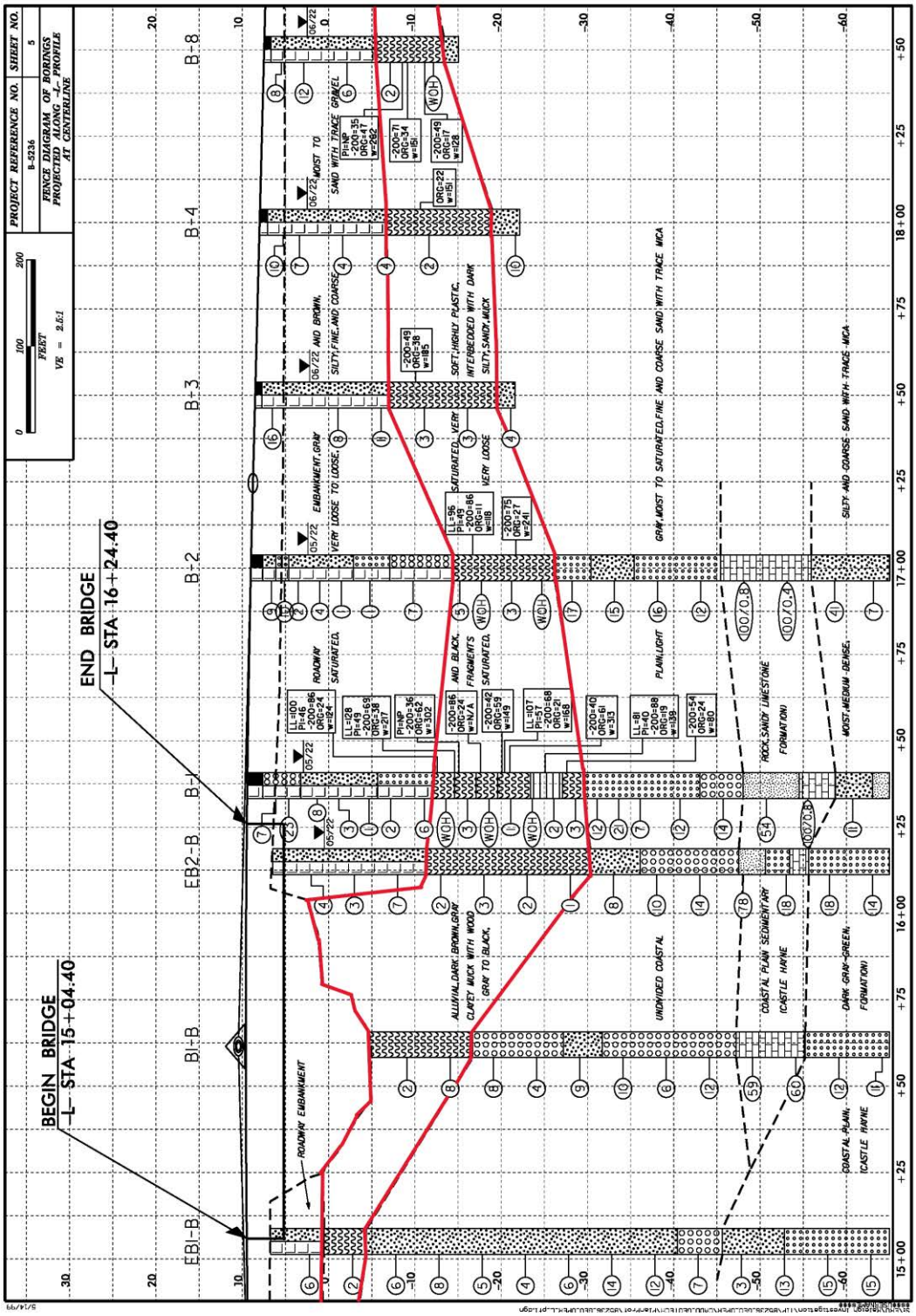


Figure 7 – Profile Showing the Subsurface Geology Along Centerline of Bridge No. 19 on River Road. The Red Outlined Layer is the Highly Compressible Alluvial Layer Responsible for the Embankment Settlement. Borings B-1, B-2, B-3, B-4, and B-5 are from This Investigation. Borings EB1-B, B1-B, and EB2-B are from the 2015 Bridge Inventory. PI = Plastic Index, LL = Liquid Limit, -200 = % Sample Pass #200 Sieve, ORG = % Organic Material, w = Moisture %, NP = Non-Plastic



Figure 8 – Alluvial sediments encountered at River Road. A) Example of highly organic, silty clay with root fragments. B) Large wood fragments that were returned to the surface from recirculated water. C-D) Large wood fragments removed from a Shelby Tube.

Undivided Coastal Plain (UCP) soils were also present throughout the entire project and characterized by light gray, moist to saturated, medium dense, fine and coarse sand (A-3, A-1-b) with trace mica. The UCP layer was about 40 feet thick just south of the bridge and thins to about 12 feet thick just north of the bridge where the highest amount of settlement was occuring (Figure 7).

Coastal Plain soils were also present thoughout the entire project in borings that were drilled to a depth of greater than 50 feet below ground surface. The Castle Hayne Formation represents the Coastal Plain geology in this area. The Castle Hayne Formation at this site is characterized by 7-10-foot-thick layers of sandy limestone interbedded with dark gray and green, moist, medium dense, silty and coarse sand (A-2-4, A-1-b). The sandy limestone layers are discontinuous and commonly pinch out in the Castle Hayne Formation (Figure 7).

The settlement analysis shows 10 inches of primary consolidation settlement would occurr in the first 4.3 years after the new roadway embankment fill was completed and 7” of secondary consolidation settlement would occur between 4.3 and 100 years (Figure 9A-B, Table 1).

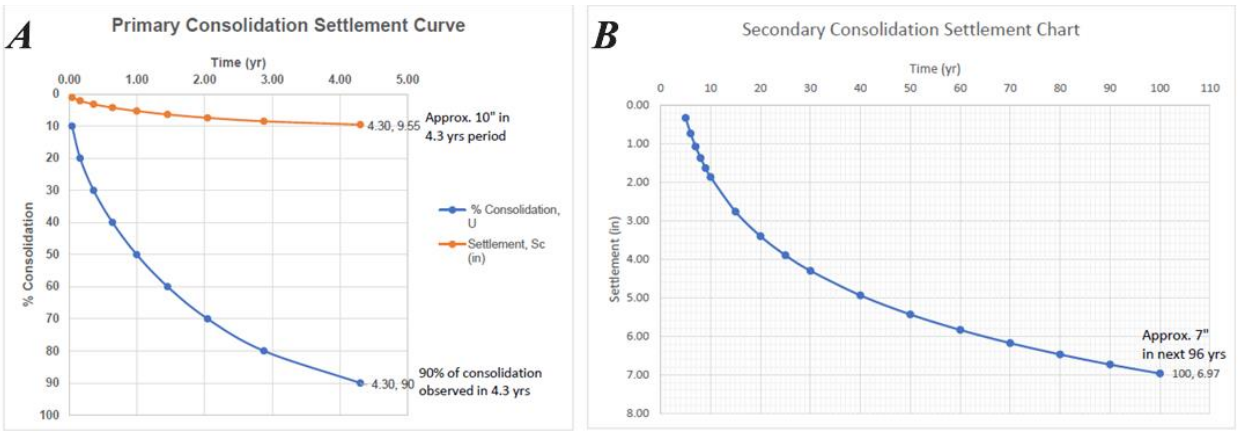


Figure 9 – A) Primary Consolidation Settlement Curve. B) Secondary Consolidation Settlement Curve.

Table 1: Settlement Estimated/Observed Summary		
Year	Approximate Settlement (in.)	Remarks
0-4.3	10.0	Primary Consolidation Settlement (Estimated/Observed)
4.3-100	7.0	Secondary Consolidation Settlement (Estimated)

DISCUSSION

The project has incurred a total cost of $230,000 to date, including initial investigation and subsequent failure investigation and repairs. Of this, post-construction differential settlement has led to ongoing maintenance expenses of $95,000. These unanticipated costs are directly attributable to subgrade instability, which could likely have been identified and mitigated through a more comprehensive geotechnical investigation during the design phase. Critical subsurface data—such as N-values—would likely have indicated the presence of soft or compressible soils if in-lane Standard Penetration Testing (SPT) had been perfomred. This information could have prompted proactive measures, such as implementing surcharging during initial construction. The cost of performing both the SPT and surcharging would have been approximately $60,000—substantially lower than the current cumulative maintenance cost and significantly less than the more invasive and expensive retrofit options later considered.

Several remedial strategies were evaluated to address the ongoing settlement (Table 2). Solution 1, which involves repeated resurfacing of the roadway until settlement naturally ceases over a projected 40-year span, was selected due to its lower immediate cost of $70,000. However, this method does not address the root cause of settlement and has already led to costly maintenance. More comprehensive alternatives were considered and dismissed due to their higher upfront capital costs: surcharging ($325,000, requiring full bridge closure for four months), undercutting and replacement with lightweight fill ($750,000 with single-lane closure for four months), and installation of rigid inclusions beneath a load transfer platform ($1,000,000 with single-lane closure for six months). Although more expensive initially, these options would

have offered long-term geotechnical stability and predictable performance. The absence of early-stage site investigation—particularly through SPT-based profiling—resulted in a reactive maintenance strategy rather than a proactive design approach. This case underscores how omitting relatively low-cost investigative efforts can lead to substantially greater lifecycle costs and elevated engineering risk.

Table 2 – Settlement Remediation Options

Option	Estimated Cost ($)	Road Closure
Resurfacing/Leveling	70,000	Single Lane for 2 days per repair
Surcharging	325,000	Full closure of bridge for 4 months
Undercutting the existing embankment and replacing with light weight fill	750,000	Single lane traffic for 4 months
Adding rigid inclusions (concrete column or timber piles) below a load transfer platform	1,000,000	Single lane traffic for 6 months

Comprehensive and accurate geotechnical investigations are critical to the financial and technical success of transportation projects throughout their lifecycle. Borehole drilling, paired with in-situ tests such as SPT per ASTM D1586, provides essential data on soil stratigraphy, bearing capacity, groundwater levels, and settlement potential. Among the most valuable outputs of the SPT are N-values, which indicate the number of hammer blows required to advance a standard sampler and are directly correlated with soil density and strength—particularly for cohesionless soils such as sands and gravels. Accurate N-values inform design decisions for foundations, pavement systems, and slope stability. Without this information, engineers must rely on assumptions, significantly increasing the likelihood of encountering unanticipated subsurface conditions during construction.

When site investigations are rushed or insufficient, the risk of encountering problematic soil conditions—such as loose sands with low N-values or highly compressible clays—greatly increases. These materials can cause excessive settlement or bearing failures, leading to costly redesigns or retrofits, such as the installation of deep foundations, ground improvement techniques, or enhanced drainage systems. Insufficient or improperly interpreted N-value data can result in inaccurate estimations of bearing capacity or unrecognized liquefaction potential in seismic zones. These oversights can compromise structural integrity and dramatically increase long-term maintenance costs. Conversely, a comprensive field study review coupled with a high-quality site investigation program that includes corrected and representative N-values allows engineers to optimize designs with appropriate safety factors and mitigation strategies, ultimately reducing cost overruns, construction claims, and schedule delays.

Investing in a robust geotechnical investigation—comprising adequately spaced boreholes and standardized SPT testing—yields accurate subsurface models and supports risk-informed design. Corrected N-values enhance empirical correlations for key design parameters such as relative density, internal friction angle, and anticipated settlement, all of which are essential for the reliable design of transportation infrastructure. A comprehensive preliminary field review including site reconnaissance, geologic review, and previous nearby geotechnical reports reviews can help determine the correct testing and sampling techniques for the project. Choosing the correct testing and sampling techniques can lead to early identification of weak or

problematic soil layers and enable the integration of targeted ground improvement methods (e.g., surcharging, over-excavation, soil replacement) into the original project scope, avoiding expensive and disruptive change orders during construction. Furthermore, high-quality geotechnical data improves bid accuracy, reduces contractor risk premiums, and supports the development of realistic schedules. Ultimately, thorough geologic and geotechnical investigations lead to more resilient, cost-effective infrastructure that performs predictably throughout its intended service life.

Within six months of the bridge opening in 2018, two local newspaper articles reported visible sinking of the roadway leading up to the structure (*9,10*). Transportation infrastructure projects are often subject to intense public scrutiny. Preventing negative public relations is vital, as early reputational damage can be difficult to recover from and may jeopardize long-term project support. These projects typically involve significant public funding, political involvement, and direct community impact, all of which heighten sensitivity to perceived failures. If issues such as cost overruns, environmental concerns, safety risks, or inequity are not proactively addressed, they can rapidly escalate into widespread public distrust. Strategic communication, transparent reporting, and active community engagement are critical tools to prevent such outcomes. Doing so protects a project's reputation and preserves public, political, and financial support across multi-year timelines.

Proactive public relations also enables agencies to shape the narrative around the project—highlighting public benefits and long-term value instead of allowing negative incidents to dominate public discourse. Consistent and early communication builds public goodwill, making stakeholders more resilient to challenges or delays. Agencies foster collaborative relationships with the public by anticipating and addressing community concerns before they escalate. In the context of transportation infrastructure, it is a fundamental aspect of project continuity, public accountability, and long-term success with public relations.

REFERENCES

1. Horton, J.W. and V.A. Zullo, Carolina Geological Society Fiftieth Anniversary Volume, The Geology of the Carolinas, University of Tennessee Press, Knoxville, 1991, pp. 1-10.

2. Ward, L.W., R.H. Bailey, and J.G. Carter, Carolina Geological Society Fiftieth Anniversary Volume, The Geology of the Carolinas, University of Tennessee Press, Knoxville, 1991, pp. 274-289.

3. Lawrence, D.P. and C.W. Hoffman, Geology of basement rocks beneath North Carolina Coastal Plain. *North Carolina Geological Survey*, Bulletin 95, 1993, 60 p.

4. Sohl, N.F. and J.P Owens, Carolina Geological Society Fiftieth Anniversary Volume, The Geology of the Carolinas, University of Tennessee Press, Knoxville, 1991, pp. 191-220.

5. Harris, W.B., G.R. Baum, and M.L. Bottino, The Paleocene Beaufort Formation, North Carolina: Microfauna and Radiometric Age (abs.). *Northeastern and Southeastern Sections, Geological Society of America*, v. 8, n. 2, 1976, p. 191

6. Brown, P.M. and J.A. Miller, Cretaceous-Paleocene Boundary, Lenoir County, North Carolina *in* Textoris, D.A., ed., *SEPM Field Guidebook*. Society of Economic Paleontologists an Mineralogists, Third Annual Midyear Meeting, 1986, pp. 119-128.

7. Colquhoun, D.J., Cyclic Surficial Stratigraphic Units of the Middle and Lower Coastal Plain Central South Carolina *in* Oaks, R.O. and Dubar, J.R., eds., *Post-Miocene Stratigraphy Central and Southern Atlantic Coastal Plain*. Utah State University Press, Logan, 1974, pp. 179-190.

8. Dockal, J.A., The Coquinas of the Neuse Formation, New Hanover County, North Carolina. *Environmental Coastal Geology: Cape Lookout to Cape Fear, NC*. Carolina Geological Society, Guidebook for Annual Meeting, 1996, pp. 9-18.

9. Ratcliff, K., *Dips and Cracks Impacting New Bridge in New Hanover County.* WECT News, Wilmington, NC, November 7, 2018.

10. WWAY News, *Safety Concerns Raised After New Bridge Begins Sinking*, WWAY News, Wilmington, NC, July 31, 2018.

New Baltimore Landslide Remediation – Lessons Learned

Suresh Gutta, Ph.D., P.E.
Senior Geotechnical Manager
American Geotechnical & Environmental Services, Inc.
4 Grandview Circle, Suite 100
Canonsburg, PA 15317
724-916-0300 Ext. 744
SGutta@agesinc.com

Ala M. Hajdarwish, Ph.D., P.G.
Senior Engineering Geologist
American Geotechnical & Environmental Services, Inc.
4 Grandview Circle, Suite 100
Canonsburg, PA 15317
724-916-0300 Ext. 751
AHajdarwish@agesinc.com

Prepared for the 74th Highway Geology Symposium, August, 2025

Disclaimer

Statements and views presented in this paper are strictly those of the authors, and do not necessarily reflect positions held by their affiliations, the Highway Geology Symposium (HGS), or others acknowledged above. The mention of trade names for commercial products does not imply the approval or endorsement of HGS.

Copyright Notice

Copyright © 2025 Highway Geology Symposium (HGS)

All Rights Reserved. Printed in the United States of America. No part of the publication may be reproduced or copied in any form or by any means – graphic, electronic, or mechanical, including photocopying, taping, or information storage, and retrieval system – without prior written permission of the HGS. This excludes the original author(s).

ABSTRACT

In 1940, the Pennsylvania Turnpike was constructed mostly along the path of the original alignment of the old South Penn Railroad and as a result, passed through the Borough of New Baltimore, PA, and the Allegheny Mountains. The original construction reactivated an ancient landslide, referred to as the "New Baltimore Slide" that had occurred in the geologic past due to undercutting of the mountain slope by the Raystown Branch of the Juniata River, which lies in the valley beneath the Turnpike. This slide zone eventually extended to 800 feet wide, 1,500 feet upslope of the roadway, with an average overburden thickness of 60 feet sliding along a weathered clayey siltstone bedrock surface defined as the failure plane for over 70 years.

Historical records indicate that the slide moved 13 feet in 1940. Such large movements had resulted in major scarps as much as 80 feet wide on the mountainside. Over the past 20 years, active movements have been closer to 10 inches/year, with peak movements of 2 inches/month in the spring season. The proposed widening and reconstruction of the Turnpike required removal of the toe of this active landslide. The design involved characterizing the failure mechanism, instrumentation, treatment, development of a sequence of construction, and development of safety systems for the protection of traffic during construction. Construction of the slide remediation was successfully completed in September 2016.

HISTORICAL BACKGROUND

The landslide is located along the eastbound lanes of the Pennsylvania Turnpike (I-76), near the town of New Baltimore in Somerset County, PA. Refer to Figure 1 for the project location. In 1940, the Turnpike was constructed mostly along the path of the original alignment of the old South Penn Railroad, thus passing through the Borough of New Baltimore and the Allegheny Mountains. The original highway construction reactivated what is believed to be an ancient landslide, referred to as the "New Baltimore Slide."

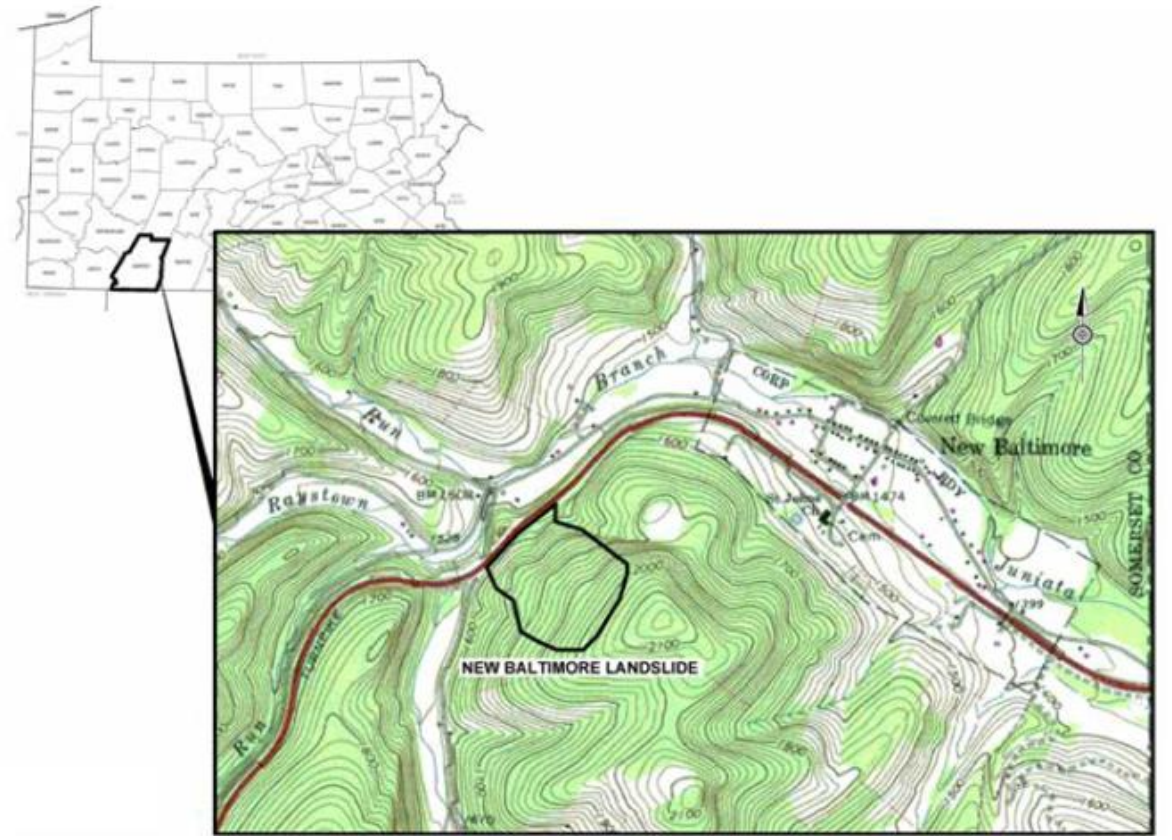


Figure 1 – Project Location Map

The New Baltimore Landslide is a major rockslide that has created maintenance issues for the Turnpike since original roadway construction in 1940. During construction, the roadway alignment and grade were revised to minimize disturbance to the unstable slope area. Historical records from the original Turnpike construction indicate movements of up to 13 ft/year at that time. These large movements resulted in major scarps up to 80 ft wide on the hillside above the roadway. This slide zone eventually extended to 800 ft wide x 1,500 ft upslope x 60-ft-deep sliding along a weathered mudrock defined as a failure plane (Figure 2). As the landslide mass moved, the heaving of the eastbound shoulder required milling of the pavement up to 8 in./year and clearing of toppled debris from the shoulder. The majority of the movement and subsequent pavement milling has reportedly occurred annually during the spring. In addition to the shoulder heave, there has been some distortion of the pavement along the outside eastbound travel lane. The failure has been occurring for the past 60 years, with a peak movement rate of 1-2 in./month.

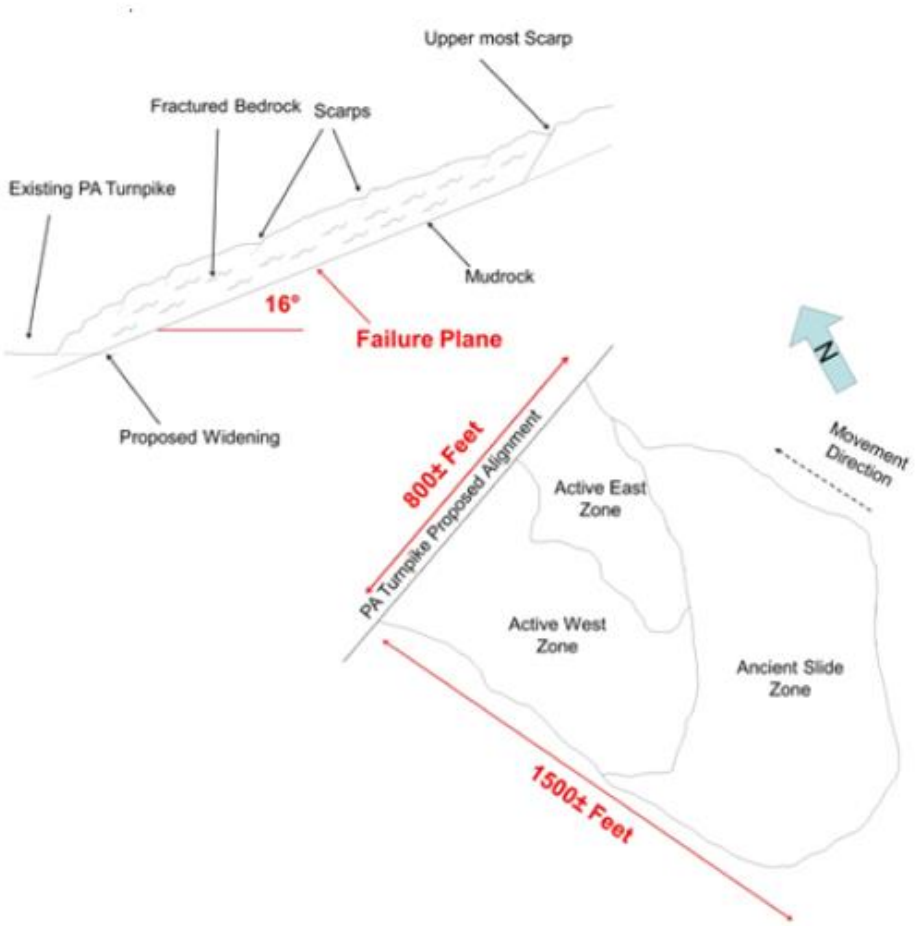


Figure 2 – Schematic Plan and Elevation of the Slide

GEOLOGIC MODEL AND CONTROLLING FACTORS

The total geologic model was established based on more than 15 years of subsurface investigation and instrumentation data. The model is controlled by five factors that shaped the understanding and eventually the solution for the landslide.

1. *Bedrock Orientation* —The New Baltimore landslide is a classic example of a low angle dipping lithology bedrock failure. The bedding strike is nearly parallel to the roadway, with a dip angle of 15-16 degrees (3.5H:1V) toward the roadway with kinematic conditions that are favorable for sliding. The bedding planes daylight the ground surface and roadway cut slope.
2. *Interbedded Layering* —The bedrock within the landslide mass belongs to the Devonian-aged Catskill Formation. This formation consists of alternating layers of interbedded sandstone and siltstone, with some weak layers of mudstone. The mudstone layers are

prone to relatively quick weathering when exposed to fluctuating groundwater conditions and can weather in place to almost soil-like material, with friction angle values less than 16 degrees and almost zero cohesion.

3. *Geomorphology* —The geomorphology of the region is characterized by continuous hills and wide recharge areas, with the exception of a few areas where the topography formed isolated hills with limited recharge zones created by past surface weathering. The New Baltimore landslide is the perfect example of that exception.

4. *Local Hydrogeology* —The geomorphology of the site and its limited recharge area limits water supply into the failure layer to only the amount of rain that falls on the landslide recharge zone uphill. Therefore, if it rains or when snow melts, the groundwater rises along the slide that acts as an aquitard. If a period of little rain occurs, the layers become relatively dry. This creates a cycle of wet and dry periods, which contributes to the accelerated weathering of the mudstone.

5. *Roadway Construction* —As the roadway construction undercuts the slope, it also connects *the above four factors* together. It does this by creating a cut slope surface for the bedding to daylight, by making an outlet for the groundwater to flow through the weak layers of mudstone, and by reducing the overall factor of safety of the rock mass above the failure plane.

A detailed site reconnaissance was completed to establish the landslide limits by mapping the scarps and tension cracks as well as the disturbed topography limits and water seeps. Bedding orientation and types of exposed bedrock were mapped and measured within and outside the limits of the landslide. The strike orientation of the bedding was generally consistent within these areas at N40ºE and a dip direction at 16° towards the northwest. The rate of slide movements was typically high during the spring, especially during periods of high precipitation. The subsurface investigation was focused mainly within the limits observed by the site reconnaissance.

SITE INVESTIGATION AND INSTRUMENTATION

An extensive site exploration program was developed to characterize the slide mechanism, to determine rates of movements, and to delineate the boundaries of the landslide. The exploration program involved: a) test borings and lab testing, b) instrumentation, c) surface and subsurface survey monitoring,and d) test blasting.

The drilling program included over 50 test borings in the slide area. A few borings were drilled outside the landslide limits to compare with the landslide conditions. Samples recovered from the failure zone showed that the mudstone layer became a soft, soil-like clay as a result of weathering, fluctuating groundwater flow, and intense shearing and movement along the failure plane. Direct shear tests conducted on samples taken from the failure zone showed residual friction angle of 16 degrees, which generally corresponded with value back-calculated for soils with marginal stability.

Various types of instrumentation were utilized for the monitoring of the slide movements, groundwater levels, and changes in porewater pressures. From 1998 to 2012, time domain reflectometers (TDRs), vibrating wire piezometers, and vertical inclinometers were utilized to monitor the landslide. As instrumentation technology evolved, original inclinometers were replaced with in-place inclinometers in 2012 to allow remote collection of slide movement data on a real-time basis. This instrumentation allowed correlation of the rainfall data with changes in rate of movements in real-time.

Surface movements of the slide were also monitored by surveying more than 50 surface monuments for the duration of the design phase. Refer to Figure 3 for the survey data of surface monuments in the active slide area from 2000 to 2014. Figure 4 provides an example of data collected from one of the in-place inclinometers. Based on the data collected over the years, the New Baltimore landslide was characterized to consist of two portions: the lower portion, with a faster moving rate and referred to as the active landslide, and the upper portion, with a relatively slower sliding rate and referred to as the ancient landslide.

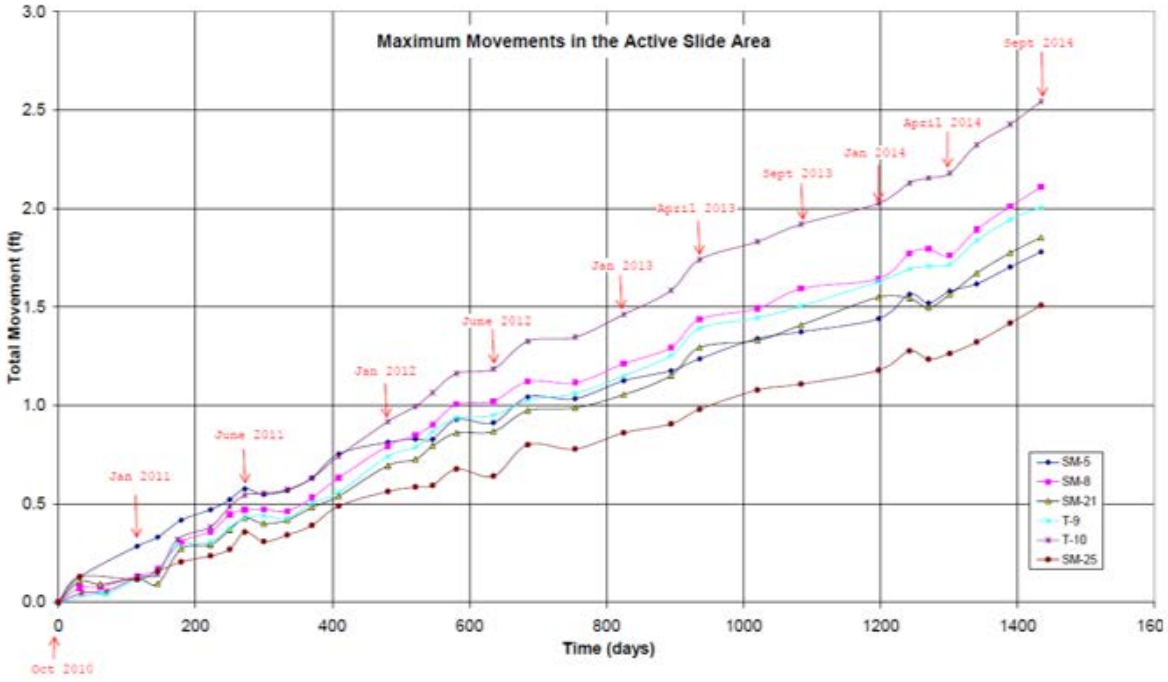


Figure 3 – Survey Data

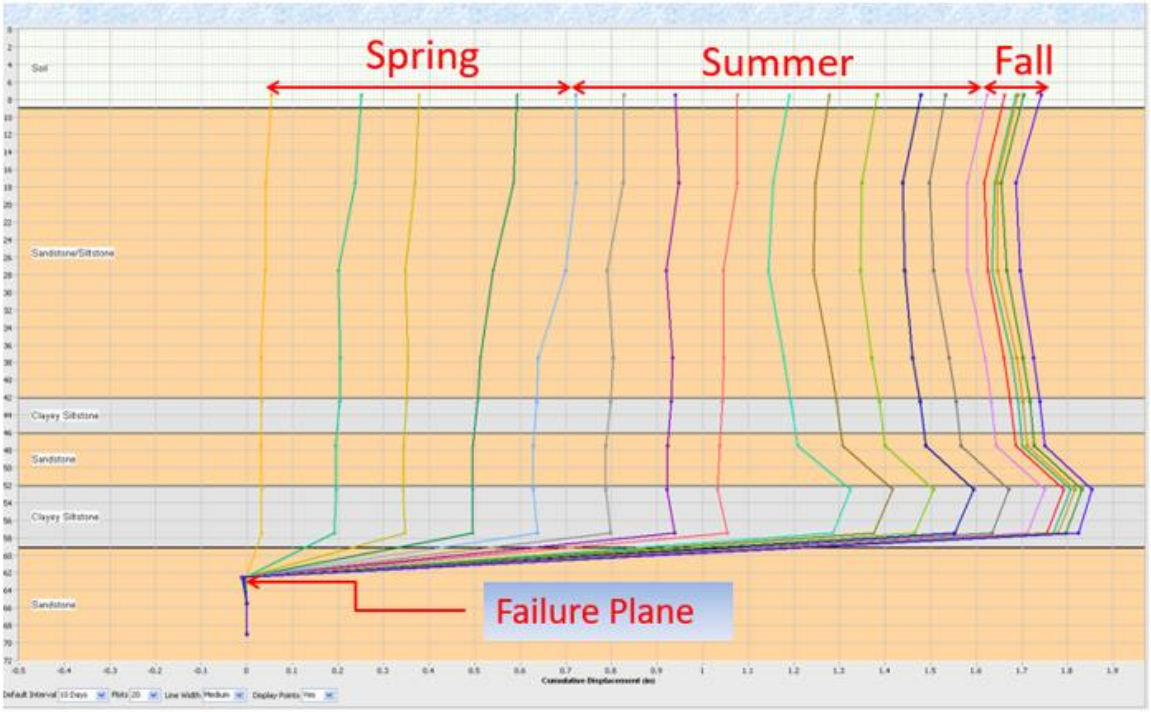


Figure 4 – Inclinometer Data

SLIDE REMEDIATION

Remediation design was controlled by the presence of heavy vehicular traffic immediately next to the toe of the active landslide. Based on the feasibility, risk, and cost analyses, three alternates were considered for the remediation:

1. Remove the active portion of the landslide and construct a rock buttress against the ancient portion of the upper slope or use rock nails to protect the upper slope.
2. Complete removal of the overburden slide material.
3. Removal and reconstruction of the slope with an engineered sequence of construction.

Alternates 1 and 2 were not considered due to high costs associated with hauling the excavated material offsite to waste areas. Alternate 3 was selected as the most feasible and cost-effective solution as it allowed reuse of the excavated material to reconstruct the new slope.

SEQUENCE OF CONSTRUCTION

Although the chosen remediation concept was simple, execution of the design required careful considerations to minimize traffic interruptions, ensure traffic safety, avoid activation of slides, and minimize the potential for catastrophic failures. To achieve these objectives, a detailed sequence of construction plan was developed as part of the contract documents.

A sequential top-to-bottom construction method, with limited width excavation zones, was used to avoid rapid movements of the slide. The hillside slope continues well beyond the upper boundary of the landslide. Although there were no movements in the upper slope, there was a concern that the removal of the landslide overburden during construction could essentially remove the toe for that upslope area and could possibly create a new landslide beyond the upper limits of the ancient portion of the slide. To address this issue, a limited 300-ft-wide excavation was proposed along the direction of slide movements within the ancient portion of the slide. This excavation would extend to 1ft below the bottom of the failure plane. Material from the Stage 1 excavation would be disposed offsite. The factor of safety of the upslope based on 2D slope stability analyses for the Stage 1 temporary condition was 1.0. However, 3-D effects due to the presence of overburden on both sides of the Stage 1 excavation, improved the factor of safety to 1.3. In Stage 2, another row of 150-ft–wide, limited-width excavations would be made adjacent to the Stage 1 trench. The material excavated from Stage 2 would be flipped and used to reconstruct the slope in the already excavated area of Stage 1.

Upon completion of Stage 2, another row of 150-ft-wide excavations would be made next to the previous trench. At any stage, excavation widths of no more than 300-ft would be open during the earthwork. This process would continue until the ancient portion of the slide was removed and reconstructed. After the ancient part of the slide had been reconstructed, excavation in the bottom portion (active slide) would continue in limited-width trenches, except that the trenches would run parallel to the strike of the bedrock. The final, reconstructed slope would generally match the pre-existing slope at 3H:1V.

Groundwater was one of the major contributors to the landslide movements. Therefore, design details were developed to address various sources of water-surface runoff at the upslope of the slide area, groundwater from the cut zones during excavation, and drainage for the final reconstructed slope.

During the design phase, test blasting was performed to verify the feasibility of drilling and blasting within the overburden, and to develop parameters for the production-blasting design. The test blast data was also utilized to perform finite element analyses to verify the temporary stability of the active slide zone due to blasting of the nearby upslope.

Using the historical movement data from the survey and instrumentation, various trigger and action levels were developed for slide movements in various zones of the landslide. An automated motorized laser total station system was installed nine months prior to beginning of the construction to monitor the slope movements and to develop baseline data. The slide movements were monitored for the entire duration of construction in real-time using the total station system and the in-place inclinometers.

The earthwork associated with the landslide involved approximately 2.5 million cubic yards of material. As the excavated landslide overburden material was recycled for reconstruction of the slope, hauling costs were significantly reduced, resulting in cost savings for the Turnpike Commission. The construction was successfully completed in 2017. None of the action levels were triggered during the construction. Figures 5 and 6 depict before and after views of the landslide slope.



Figure 5 – Landslide prior to Remediation



Figure 6 – Slope after Remediation

CONCLUSION

The importance of characterization of the factors contributing to the failure mechanism, sufficient subsurface exploration, monitoring, and design and installation of appropriate instrumentation cannot be overstated in designing the most economical, practical, and environmentally friendly remediation for complex and large scale landslides. With the Pennsylvania Turnpike Commission as the client, the designers did not have to compromise on the extent of the subsurface investigation, slide monitoring, instrumentation, and test blasting. Equipped with great quality data, the sliding zone and the boundaries of the landslide were well defined, and the surface elevation model of the bottom of the failure plane was developed. Preparation of detailed construction sequence plans, details, and specifications limited uncertainties during construction.

Removal of overburden and reconstruction of a new slope with the same material for smaller-scale landslides is not uncommon. However, what makes the New Baltimore Landslide project unique was the sequential removal of the overburden and reconstruction of the slope as excavation progressed from the top-to-bottom of the slope in a systematic manner, control of groundwater and surface runoff throughout the construction, real-time monitoring of slope movements and change in porewater pressures during construction, and ensuring the protection of active traffic at the toe of the landslide during construction. The landslide was successfully remediated in 2016.

PROACTIVE SLOPE DESIGN: MECHANICAL STABILIZATION OF CUT SLOPES TO REDUCE IMPACTS OF LANDSLIDES AND EXCAVATION FOOTPRINTS

Bryan Radabaugh
Geostabilization International
2 White Oak Drive
Ripley, WV 25271
Bryan.radabaugh@gsi.us

ABSTRACT

Due to West Virginia's physiographic, geomorphologic, and geologic setting, infrastructure development and expansion projects often face technical challenges which can impact the viability and cost of the project. As roadway and infrastructure expansions are initiated in Appalachia, and specifically in West Virginia, cut slopes frequently encroach into landslide-prone slopes. Slopes consisting of thick colluvium, thick residuum, and highly weathered soils are consistently encountered. Encroachment into landslide prone slopes can result in several negative consequences including:

- safety impacts to the contractor and the public as these landslide areas are exposed.
- expanded right of way as cut slopes are flattened and extended upwards.
- potential impacts to adjacent property.
- larger and/or additional waste areas for excess materials generated.
- potential impacts to adjacent infrastructure.
- additional right of way acquisition.
- environmental and permitting impacts due to expanded cuts and fills.
- extended construction schedules and project budgets.

To mitigate these potential negative impacts, non-traditional construction practices can be utilized. Recent highway expansion along US 52 in Mingo County, WV, and new school construction in Lincoln County, WV, both resulted in extensive mass excavation within landslide prone slopes. To reduce the extent of the cut slopes and reduce the risk of slope failures during and after construction, final designs for both projects include pinned and draped high-tension mesh systems, complementing conventional earthwork.

Our paper and presentation will provide two case histories, focusing on the geologic setting, right-of-way considerations, mass excavation placement, and slope stability concerns addressed by the project teams through proactive design and construction phases.

Engineering Geology and Field Fit Solutions for Emergency Landslide Response to SH-64, Kamiah, Idaho

Shaun Cordes, CEG
Delve Underground
2000 SW 1st Avenue
Portland, Oregon 97201, Suite 410
971.415.5607
cordes@delveunderground.com

Jim Struthers, CEG
Delve Underground
1011 Western Avenue, Suite 706
Seattle, Washington 98104
206.260.2591
struthers@delveunderground.com

Prepared for the 74th Highway Geology Symposium, August, 2025

Acknowledgments

We would like to thank Jared Hopkins, Jesse Webb, and the engineering and maintenance team at ITD District 2. Their insight into the timing of the events and ground conditions were invaluable. In addition, we would like to thank Cecilia Burke and Mark Pinske, of Delve Underground. Their dedication and support to the project made this rapid delivery possible.

Disclaimer

Statements and views presented in this paper are strictly those of the authors, and do not necessarily reflect positions held by their affiliations, the Highway Geology Symposium (HGS), or others acknowledged above. The mention of trade names for commercial products does not imply the approval or endorsement of HGS.

Copyright Notice

Copyright © 2025 Highway Geology Symposium (HGS)

All Rights Reserved. Printed in the United States of America. No part of the publication may be reproduced or copied in any form or by any means – graphic, electronic, or mechanical, including photocopying, taping, or information storage, and retrieval system – without prior written permission of the HGS. This excludes the original author(s).

ABSTRACT

During the week of April 14, 2024, a concentrated, slow-moving, high-intensity storm event dropped an estimated 2- to 2.5 inches of rain over the duration of 2 hours near the town of Kamiah, Idaho. The event severely impacted SH-64 between milepost 25.1 and 26.6, resulting in scour and erosion of the road prism, undermining existing retaining walls, plugging and damage to existing culverts, landslides, and generation of debris flows within ravines.

At the request of the Idaho Transportation Department (ITD), Delve Underground mobilized two engineering geologists to perform a site reconnaissance of the damaged roadway. ITD's ultimate goal was to develop plans for emergency mitigation, advertise and award the work in summer 2024, and finish construction of the repairs during the 2024 construction season. We identified and prioritized 12 key areas of damage along the alignment with ITD staff. We then collected information, including the failure mode, geotechnical materials present, and failure geometry, to be used in final emergency mitigation design. Site characterization was followed by rapid design and contract development with advertisement soliciting bids within 3 months of the storm event.

During construction of the 12 damaged areas, ITD personnel and Delve Underground worked in close collaboration with the contractor to coordinate the phasing of work and provide adjustments and field fitting to the final design based on expected variations of subsurface conditions. This case study provides an example of rapid development, contracting, and construction of landslide mitigation work within a constrained corridor.

INTRODUCTION

During the week of April 14, 2024, a concentrated, slow-moving, high-intensity storm dropped an estimated 2- to 2.5 inches of rain within a 2-hour period near the town of Kamiah, Idaho (Figure 1). The event severely impacted SH-64, resulting in numerous landslides, debris flows, and scour and erosion that led to significant damage to the roadway. Damage included scour and erosion of the road prism, undermining existing retaining walls, plugging and damage to existing culverts, and generation of debris flows within ravines.

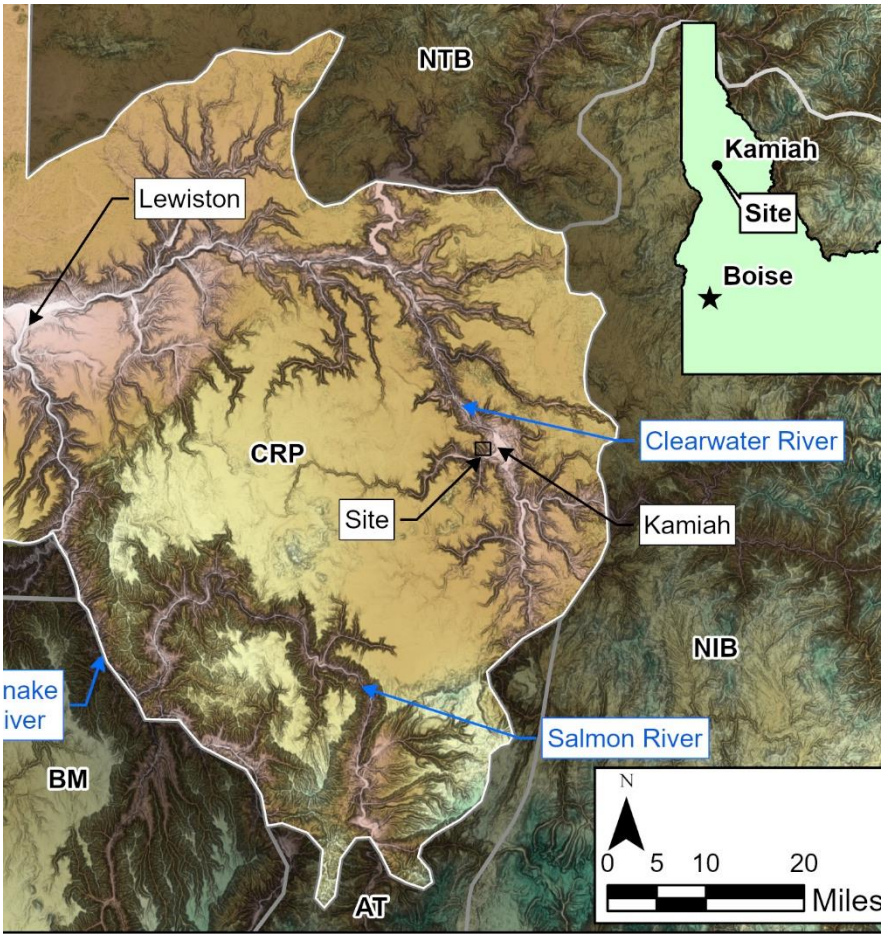


Figure 1 – Site location and geologic provinces; Columbia River Plateau (CRP), Northern Thrust Belt (NTB), Northern Idaho Batholith (NIB), Accreted Terrane (AT), and Blue Mountains (BM). Note the dissected and dendritic drainage pattern of the CRP waterways. SR-12 follows the Clearwater River from Kamiah, Idaho, to Lewiston, Idaho.

The Idaho Transportation Department (ITD) notified Delve Underground of the storm event and damages on Tuesday, April 16, 2024. Delve Underground mobilized to the site on April 22, 2024, to perform a site reconnaissance of the failures. The initial goal of this site visit

was to assess the subject failures, develop conceptual designs for potential repair, and assist ITD in prioritizing the failures for repair. In addition, during this site visit, Delve Underground collected information on the failure mode, geotechnical materials present, and failure geometry for use in the final emergency mitigation design.

Early discussions with ITD District 2 management indicated that it was their preference that mitigation designs for this emergency repair be prepared under a rapid delivery timeline. The ultimate goal of ITD was to develop plans for emergency mitigation, advertise and award the work in summer 2024, and finish construction of the repairs during the 2024 construction season. Because of an expedited schedule and the difficult site access constraints, detailed subsurface investigation (e.g., borings) was not conducted as part of our geotechnical scope. Field investigation was limited to surface observation, excavation of shallow hand-dug test pits, and hand-probing of soils in the failure areas.

Because of this rapid delivery approach, it was acknowledged that the base elevation and foundation conditions of each repair would need to be confirmed and potentially adjusted during construction. Field fitting and adjustments would require geotechnical support throughout construction.

GEOLOGIC CONDITIONS

The SH-64 alignment is located along the eastern margin of the Columbia River Plateau geologic province and is positioned immediately west of the Clearwater River (Figure 1). The Columbia River Plateau geologic province is synonymous with the Columbia Basin of Washington, and the Deschutes-Columbia Plateau of Oregon. Within the region of the site, the plateau is bordered to the west by the Blue Mountains of Oregon, to the north by the Northern Thrust Belt, and to the south by accreted terrane. The plateau is composed of approximately 208,000 km^2 of regional scale flood basalts that extend from Western Idaho to the Pacific Ocean in Oregon (*1*; Figure 2). These basalts are collectively known as the Columbia River Basalt Group (CRBG) and are stratigraphically subdivided into smaller recognizable flows and members.

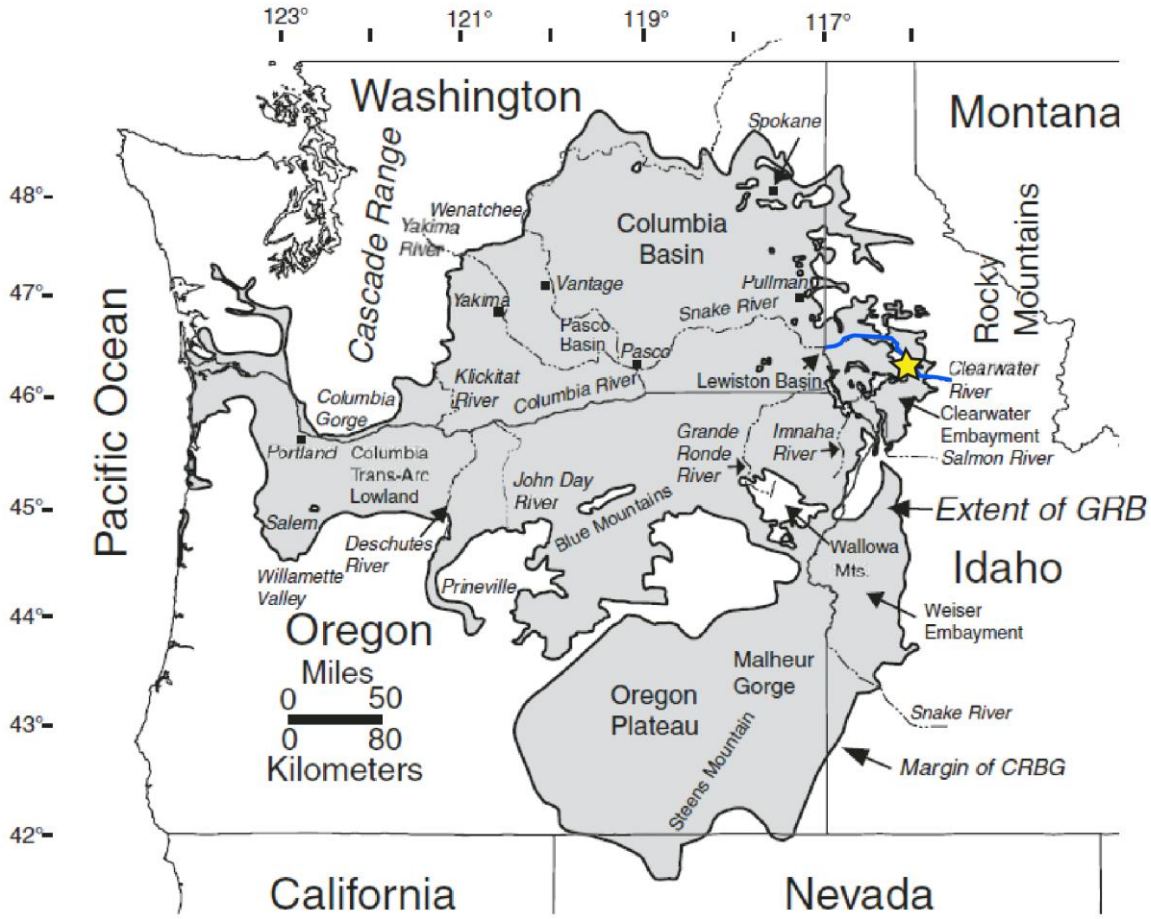


Figure 2 – Modified from Barry et al. (*1*), extent of CRBG indicated in dark gray, approximate location of site indicated with yellow star, and the Clearwater River outlined in blue.

The Columbia River Plateau is deeply incised by prominent rivers, including the Clearwater River, Snake River, and Salmon River, that drain westward to the Columbia River and ultimately to the Pacific Ocean. The drainage network exhibits immense topographic relief relative to the surrounding flat surface of the plateau in the form of deep canyons that cut through the underlying CRBG rocks (Figure 1). Cliff bands of CRBG rocks are exposed throughout these canyons.

The alignment and the adjacent slopes are composed of Miocene-age Grande Ronde basalt, as mapped by Kauffman et al. (*2*). Within the alignment, the Grande Ronde basalt is subdivided into units defined by magnetic polarity. However, Kauffman et al. (*2*) note that the recognition of magnetic polarity is questionable, and for the purpose of this study, we recognize a single unit of Grande Ronde basalt consisting of multiple flows. Geologic and geotechnical observations are presented within the unit description below.

FIELD RECONNAISSANCE AND CONCEPTUAL DESIGN

During our pre-field desktop study, three important observations were made that would dramatically impact design: (1) the adjacent hillslopes were steep (Figure 3), (2) the underlying bedrock consisted of basalt flows of the CRBG with cliff bands found throughout the slopes (Figure 4), and (3) the site slopes did not appear to have widespread evidence of large-scale slope failures at the time of LiDAR acquisition (*3*). Based on this knowledge, our assumptions heading into the field were that bedrock was shallow, slope geometry would play a key role in repairs, and construction equipment access would be limited.

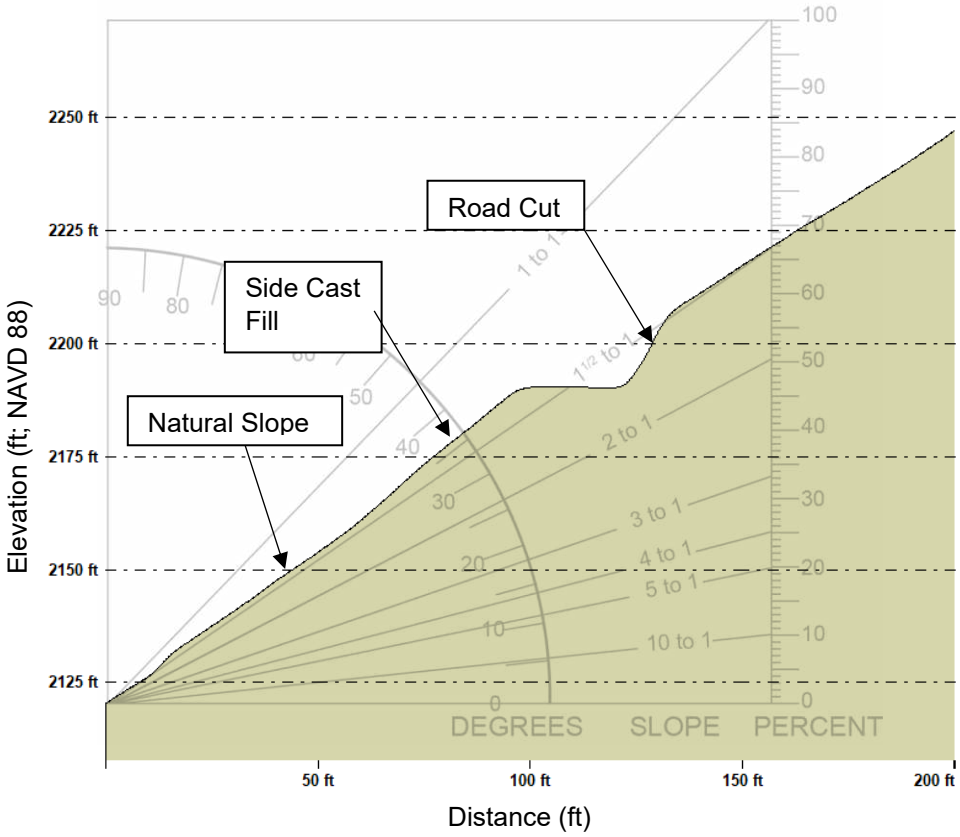


Figure 3 – Typical slope profile of SH-64 with slope inclination overlay. Elevation data derived from USGS LiDAR. Note that natural slope occurrence is typically around 35°.

ITD personnel were present at the beginning of our reconnaissance and were invaluable in introducing basic information regarding the timing of the failures, site conditions during the failure, and, most critically, in defining the locations and limits of failure that would be the subject of emergency repairs to the route. Damaged sections of SH-64 were identified with ITD personnel and designated Slide 1 through Slide 12 (Figure 4).

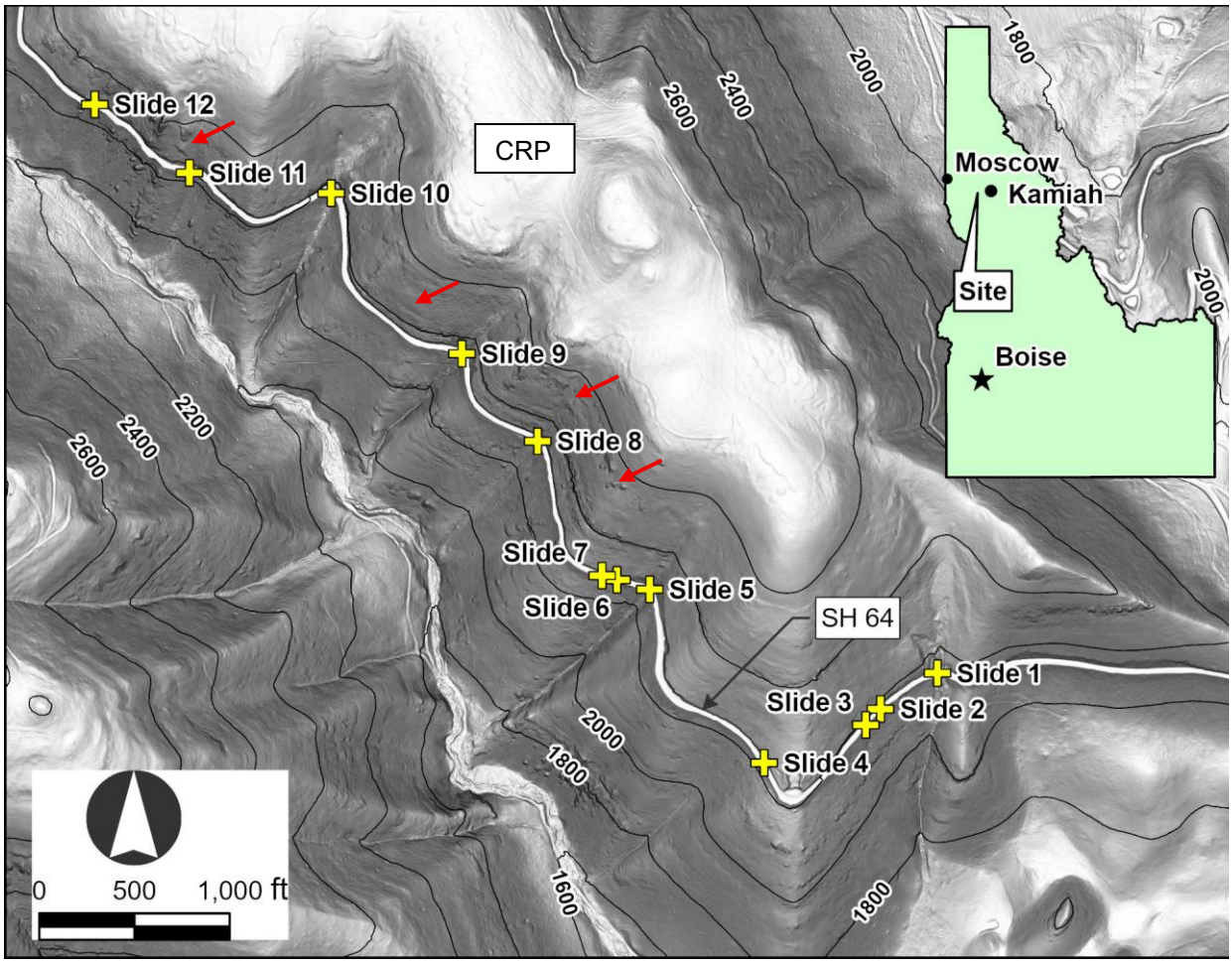


Figure 4 – LiDAR hillshade of the SH-64 corridor outside of Kamiah, Idaho. Red arrows indicate cliff bands. Note the uniform appearance of the slopes and the relatively flat surface of the CRP at the top of the slope.

Along the inboard drainage ditches, small slumps of upslope material frequently blocked surface water and redirected flows across the road, resulting in scouring and erosion of the downslope road embankment or undermining of existing gabion basket walls (Figure 5a, 5b). Damage to walls typically resulted from erosion of the underlying soils at the wall base, which were typically not found in bedrock, leaving baskets suspended and sagging (Figure 5a). Within the drainage ravines, culverts were overwhelmed and blocked by debris flows, which buried the roadway and deposited rocky debris upward of 5 feet thick. The downslope embankments suffered considerable erosion, resulting in upwards of 10 feet in roadway loss in some locations (Figure 5c, 5d). At Slide 1, roadway failure was found to have resulted from a partial reactivation of an existing landslide that was recognizable in the 2019 LiDAR, but clearly exhibited evidence of recent movement in the form of extensive tension cracks and a headscarp with slickenlines.



Figure 5 – (a) Sagging gabion baskets from scour and erosion of subgrade materials at the location of Slide 12. (b) Erosion of the road prism revealing the roadway fill at Slide 2. (c) UAV photo of Slide 9 showing the deep incision of colluvium within the ravine. Note car for scale left of the failure. (d) Slide 8 debris flow and scouring of the road prism. Note undercut and overhanging fill left of the geologists.

After the initial site walk, we began systematically inventorying each of the 12 locations and documented (1) stratigraphy and geotechnical properties of the materials encountered, (2) depth to bedrock, (3) bedrock conditions, (4) geometry of the afflicted sections of road, (5) unmanned aerial vehicle (UAV) photos, and (6) the likely repair solution (e.g., wall or buttress).

Site Stratigraphy

During our reconnaissance, we established the site stratigraphy as consisting of fill, colluvium, weathered basalt, and basalt. Weathered basalt was differentiated from basalt based on its geotechnical properties.

Fill

Fill related to original roadway construction was confined to the road prism and embankments and consisted primarily of gravel with various amounts of fines. The embankments appeared to be predominantly side-cast fill from cutting the inboard side of the road. In some locations, riprap had been previously placed where older embankment failures had occurred. In many locations, the fill could hold a vertical face, and in some locations, the fill was overhung (e.g., Slide 8, Figure 5d).

Colluvium

The colluvium was low plasticity silt (ML) and clay (CL) with various amounts of sand, gravel, cobbles, and occasional boulders, and was sourced locally from the underlying rock mass. Colluvium mantling the slopes was typically less than 2 feet thick, as observed in numerous shallow landslides that revealed the underlying weathered rock or fresh rock. Colluvium had a much thicker accumulation within the ravine, as apparent from the depth of incision on the order of 3 to 5 feet, which often did not reveal the underlying rock mass. The thickness of colluvium downslope of the roadway within the ravines often masked the underlying bedrock, making direct observations limited to the flanks of the ravines. In addition, roadway-clearing activity by ITD maintenance crews generated local side-cast fill that added cover above bedrock within the ravines.

Weathered Basalt

Weathered basalt was exposed within newly formed eroded channels and was easily distinguishable from the overlying colluvium by its distinct reddish color. It was extremely weak in strength (R0) and could be textured under manual pressure to clay (CL) with sand, to silt (ML) with sand. Corestones from differential weathering surrounded by preserved rock fabric were also present. The thickness of the weathered bedrock was typically less than 1 foot, but the difference of appearance from the colluvium would ultimately be a key indicator for the near presence of fresher bedrock during construction.

Basalt

The basalt within the project limits was moderately weathered to fresh, medium strong (R3), and was blocky in appearance with irregular joints and fractures spaced on the order of 2 to 8 inches. Exposed bedrock within the existing roadcuts did not appear to have been excavated by drill-and-blast techniques, and ITD personnel were observed excavating into the existing cuts with conventional earth working equipment while clearing debris from the roadway. Areas downslope of the roadway that were scoured down to the bedrock contact exhibited similar blockiness and joint fracture spacing, as observed within the roadcuts.

Conceptual Design

Conceptual mitigation design was performed in the field and ultimately focused on the use of welded wire mechanically stabilized earth (MSE) walls and rock fill buttresses, as discussed in greater detail below. Additional repair options such as soldier piles, gabion baskets, and gravity block walls were discussed with ITD personnel during the reconnaissance. However, it was recognized that soldier piles would be problematic due to the limited space available for construction equipment, costs, and scheduling complications with the need for a specialty contractor on site. Gabion baskets were ruled out because they would be cumbersome to construct in the field, which in turn could dramatically slow down construction and increase costs. Gravity block walls were considered a less favorable option due to their relative inflexibility with respect to both settlement and subgrade preparation. Because of the potential for variable foundation depth and condition, it was recognized that the selected mitigation options would need to be easily adjusted based on field conditions encountered during construction.

MSE walls and rock fill buttresses were ultimately selected because they could be constructed by a single contractor, without the need for specialty equipment. In addition, MSE walls are easy to assemble on site and are modular, meaning that if adjustments were required in the field (as we suspected), the contractor would simply need to “step up” or “step down” the excavation to accommodate the walls. MSE walls also have a high tolerance for variable foundation conditions and do not require the same degree of foundation preparation as a rigid gravity block wall, as their tolerance for differential settlement is greater.

The damaged portions of the roadway located outside the ravines would be relatively simple to repair and would consist of MSE walls keyed into the shallow bedrock revealed in the downslope rills. Ravine crossings where the depth of bedrock was less constrained would be mitigated by the construction of buttresses keyed into bedrock observed further downslope. Alternatively, ravine crossings could be designed using MSE walls to limit the downslope extent of excavation, with the understanding that differential bedrock depths could be resolved with field fitting at the time of construction. However, we suspected this approach in some of the ravines could push the limit of MSE wall construction given the steep slope conditions.

Survey

Site-specific survey was performed by J-U-B Engineers after our reconnaissance and utilized UAV LiDAR and photogrammetry. The flights were tied into control points positioned throughout the alignment. During our field reconnaissance, flagging and other markers were placed along the slopes at our preferred foundation locations, knowing that UAV imagery would capture the locations and allow for easy elevation correlations between the imagery and the derived surface model. This information could then be used to build slope stability models and establish repair geometries as soon as survey deliverables were provided. The digital surface model (DSM) derived from the point cloud captured incredible detail of the resulting damage and the location of rock outcrops became more apparent (Figure 6). This level of detail was valuable in confirming field observations and validating the assumptions underlying our initial mitigation concepts.

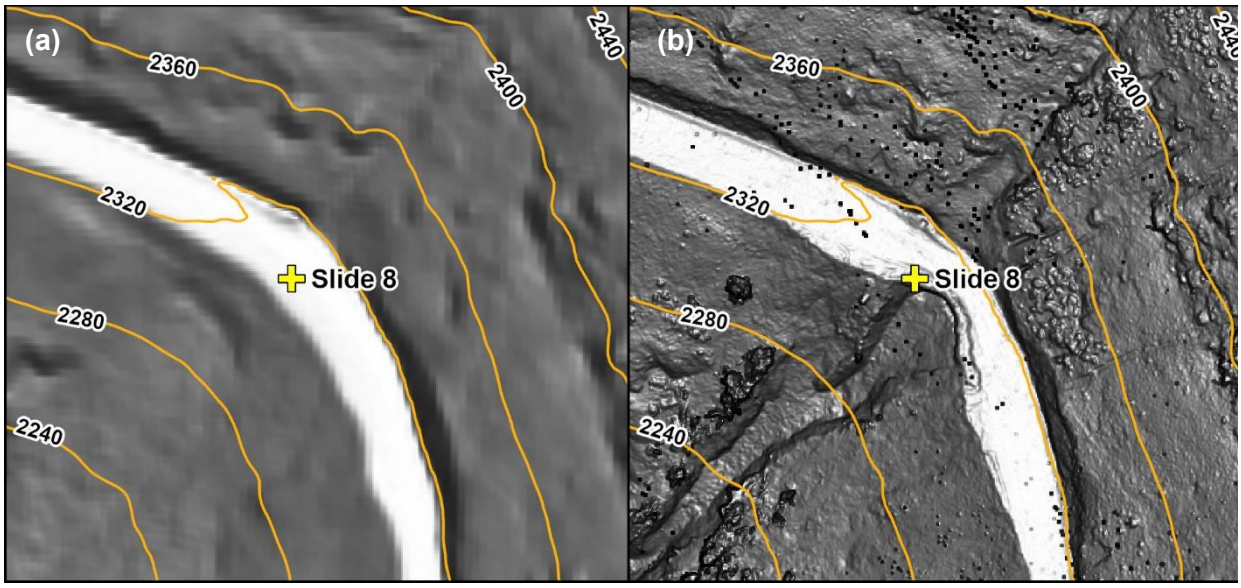


Figure 6 – (a) Pre-failure hillshade derived from USGS LiDAR of Slide 8. (b) Post-failure hillshade derived from UAV DSM. Elevations in NAVD 88.

ENGINEERING AND DESIGN

Field observations and site access limitations ultimately drove the design of MSE walls and rock fill buttresses. The well-documented presence of shallow bedrock allowed us to eliminate or significantly reduce global stability as an issue for wall and buttress design. As previously mentioned, the depth of bedrock within the ravines was generally greater than the areas outside of the ravines. Consequently, our confidence in our field estimates of the depth to bedrock in some of the ravines was less than in other ravines. As such, we modeled an overthickened colluvium beneath the walls in areas of uncertainty (Figure 7). This forced failures above the more resistant bedrock to ensure the factor of safety was still achieved if a field adjustment was needed. In addition, we increased the height of the walls to coincide with the potential for deeper bedrock conditions.

As an additional safeguard to protect the foundations of the MSE walls, we recommend a 2-foot buffer be placed in front of the toe of the walls and armored with riprap. If a portion of the wall was not founded entirely in bedrock due to variable site conditions during construction, this would help mitigate scour and erosion at the toe of the wall that damaged many of the existing walls during this subject storm event.

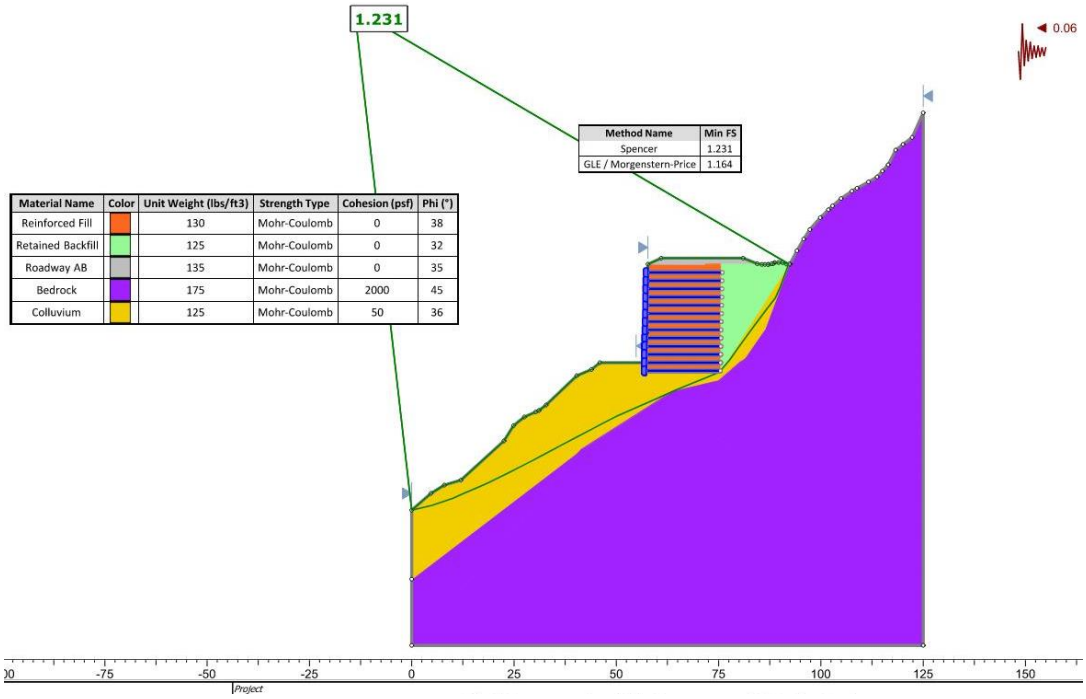


Figure 7 – Example of slope stability modeling with overthickened colluvium to force failures above the bedrock contact.

CONSTRUCTION

Like all construction projects, this project had its own challenges. We knew construction would ultimately be limited by the slope conditions and access, and sequencing would be key, particularly within the ravines (Figure 6, 8). For instance, excavating a damaged portion of the road prism would render access to the opposite side impossible to temporarily access by vehicle. Therefore, materials and equipment needed to be staged accordingly to avoid delays. For the first month of construction, this proved to be a challenge, and the schedule was frequently disrupted for a variety of contractor-related reasons.

In order to facilitate field adjustment of MSE wall geometry, the project specification included provisions for field confirmation of subgrade conditions and iteration of the wall design. Despite initial coordination difficulties that resulted in greater than necessary excavation of bedrock, this incorporation of field engineering of the walls was largely successful in limiting wall heights based on encountered conditions and in appropriate adjustment of wall geometry to match the existing slope at the margins of the wall repairs. Keys to streamlining this process were coordinating with the contractor regarding the need for consistent survey support during excavation and timely submission of requests for information (RFI) to the wall manufacturer regarding adjustments to wall geometry.



Figure 8 – Tight working conditions made for slow progress with heavy equipment, particularly the haul trucks.

Despite these challenges and delays, progress was made, and issues with sequencing and field fitting were resolved. A final major hurdle was the completion of the Slide 9 buttress which required flawless sequencing to maintain access to slides 11 and 12 that were undergoing repairs simultaneously. The contractor initially pioneered an access road to the middle of the failure to begin excavating benches to the toe of the buttress. Once complete, the contractor excavated the remaining benches up to the road surface (Figure 9). Maintaining access to the slides further up the road during construction of this buttress allowed the contractor to maintain the tight schedule.



Figure 9 – Excavating the Slide 8 rock fill buttress.

CONCLUSIONS

Rapid emergency response and mitigation scenarios are a challenge due to the compressed time frame for both construction and design. The SH-64 failures described in this paper were successfully mitigated within a single construction season despite tight design time frames, limited ability to perform subsurface investigation, and difficult site access constraints. The successful completion of the work was driven by field conditions that could be reasonably well-constrained and the incorporation of mechanisms in the plans and specifications to adjust design, as necessary to match field conditions. Rapid development of project plans and specifications was made possible by close coordination between the geotechnical staff and ITD designers and management.

Of the 12 failure sites on this portion of SH-64, eight were mitigated with new MSE walls, two with rock buttresses, one damaged gabion basket wall was repaired in place, and one ravine failure was mitigated by partial realignment of the route. Following the initial failure, preparation of plans and specifications was accomplished within 2 months and construction was completed prior to mid-November. Timely delivery of construction was dependent upon on

having a licensed engineer staffed in the field with the ability to translate field observations into adjustments to the design. This support, combined with close coordination of redesign with the contractor, allowed for sensible and practical adjustment of the work throughout construction.

REFERENCES

1. Barry, T.L., S.P. Kelley, S.P. Reidel, V.E. Camp, S. Self, N.A. Jarboe, R. A. Duncan, and P.R. Renne, Eruption chronology of the Columbia River Basalt Group, Geological Society of America, Special Paper 497, 2013.

2. Kauffman, J.D., R. S. Lewis, and P.E. Myers, Geologic Map of the Kamiah Quadrangle, Lewis and Idaho Counties, Idaho, Idaho Geological Survey, Geologic Map GM-42, 1:24,000 scale, 2006.

3. United States Geological Survey (USGS), One meter x57y513 ID Nez Perce QL2 TL 2016, 3D Elevation Program (3DEP), acquisition: 10/29/2016–11/13/2016, publication date September 16, 2019.

Performance of Micropiles Socketed into Schist Saprolite

Sarah McInnes, P.E.
Senior Assistant Construction Engineer
Pennsylvania Department of Transportation
Engineering District 6-0
7000 Geerdes Boulevard
King of Prussia, PA 19406
610-205-6544
smcinnes@pa.gov

Shimeles Badane, P.E.
District Geotechnical Engineer
Pennsylvania Department of Transportation
Engineering District 6-0
7000 Geerdes Boulevard
King of Prussia, PA 19406
610-205-6544
sbadane@pa.gov

Robert Crawford, P.E.
Chief Engineer – Structures
James J. Anderson Construction Company, Inc.
6958 Torresdale Ave, Suite 200
Philadelphia, PA 19135
215-768-6724
bobc@jjaconstruction.com

Matthew Lunemann, P.E.
Engineering Director – Geotechnical
STV, Inc.
1818 Market Street, Suite 2300
Philadelphia, PA 19103
609-530-9610
matthew.lunemann@stvinc.com

Lei Gu, P.E.
Technical Manager – Geotechnical Engineering
Michael Baker International, Inc.
300 American Metro Boulevard
Hamilton, NJ 08619
609-438-6549
lei.gu@mbakerintl.com

Prepared for the 74th Highway Geology Symposium, August, 2025

Disclaimer

Statements and views presented in this paper are strictly those of the authors, and do not necessarily reflect positions held by their affiliations, the Highway Geology Symposium (HGS), or others acknowledged above. The mention of trade names for commercial products does not imply the approval or endorsement of HGS.

Copyright Notice

Copyright © 2025 Highway Geology Symposium (HGS)

All Rights Reserved. Printed in the United States of America. No part of the publication may be reproduced or copied in any form or by any means – graphic, electronic, or mechanical, including photocopying, taping, or information storage, and retrieval system – without prior written permission of the HGS. This excludes the original author(s).

ABSTRACT

Although micropiles are increasingly utilized as a reliable solution in challenging ground conditions for bridge foundations, rock socket design in weathered saprolite/intermediate geomaterial (IGM) layers remains a great design and construction challenge. The saprolite layers of the Wissahickon Schist Formation/Wissahickon Group vary significantly with depth and have varying degrees of weathering and geotechnical properties, which can result in structural instability if not properly accounted for during design and construction. This paper explores a case study of micropiles socketed into very dense saprolite in the City of Philadelphia focusing on key considerations for successful implementation. Highlighted is the importance of thorough site investigation to characterize the saprolite's heterogeneity, including its strength and degree of weathering. The paper further discusses the design aspects of micropiles in saprolite, encompassing load transfer mechanisms, grout techniques, and the influence of groundwater conditions. Both sacrificial verification and production proof load tests were conducted on the micropiles to confirm performance. Mobilized bond stresses (44 to 55 psi) between the micropile and saprolite during load testing are compared with the design value (40 psi) as well as published values for similar geomaterials. Finally, the paper summarizes the benefits of micropiles in saprolite, which makes them a valuable solution for infrastructure development in weathered rock and provides recommendations for future projects with similar design challenges.

INTRODUCTION

Micropiles have been an effective foundation alternative due to their ability to withstand large axial and lateral loads. Both contractors and engineers need to have a thorough understanding of soil-structure interaction for rock-socketed micropiles in weathered saprolite layers during design as well as construction. This paper presents a case study of micropiles socketed into very dense saprolite in Philadelphia, Pennsylvania. The Interstate 95 (I-95), Section BSR project (construction Section BS2) involves the reconstruction and widening of I-95 between Margaret and Carver Streets. The proposed Wall 3 SB structure is designed as a cast-in-place retaining wall founded on micropile foundations to mitigate potential adverse effects on nearby structures and residents from vibrations associated with driven pile installation. As a part of the construction plan, sacrificial load testing prior to installation and proof testing on selected production piles was conducted to verify the design resistance. Bond stresses between the rock socket and mica schist saprolite, with various degrees of weathering and strengths, were measured in the load tests. Design and construction practices generally applicable to sites with similar challenges are presented, and best practices are recommended.

BACKGROUND

Subsurface Conditions

The project site is underlain by man-made fill atop the Trenton Gravel Formation followed by the Wissahickon Formation, consisting of highly micaceous, coarsely crystalline rock, as shown in Figure 1. The Trenton Gravel consists of gravelly sand with cross-bedded sand and clayey silt layers and is composed of highly weathered outwash and alluvium.

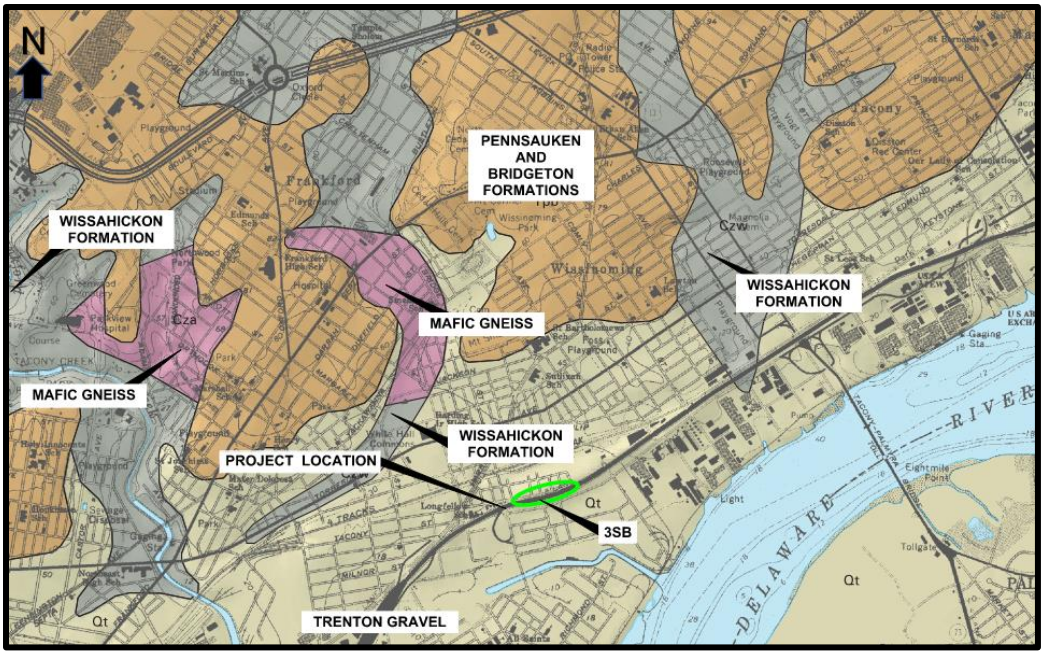


Figure 1 - Geologic Map of the Project Site

Typically, the Wissahickon Formation is composed of schist and mica schist. The schists are quartz and feldspar rich. The Wissahickon Schist encountered at the project site is more excessively micaceous and more crystalline than other variations. Above the competent bedrock, is a very dense, silty sand, saprolitic stratum of varying thickness. The residuum/saprolite composition varies based on the degree of material weathering but predominantly consists of sand and silt with varying amounts of gravel and lesser amounts of clay. The residuum/saprolite consistency is generally dense to very dense. The residuum/saprolite layer consists mostly of weathered rock and retains the fabric and structure of the parent bedrock, resulting in significant blow count refusals during SPT sampling and rock-like behavior but can be subject to soil-like behavior such as heaving and sidewall sloughing if left exposed in an unsupported excavation for an extended duration. Where identified, the saprolite thickness varied from approximately 14 feet to greater than 50 feet based on degree of weathering and depth to underlying rock; however, the top of the residuum/saprolite layer was fairly consistently encountered at or near elevation -10.0 feet at the project site. Groundwater was generally encountered between approximately elevation +3.0 and +8.0 across the length of the retaining wall.

Wissahickon Mica Schist Saprolite Characteristics

Saprolite is a chemically weathered rock. The rock surface of the Wissahickon Formation is overlain by a layer of saprolite, usually locally referred to as “decomposed mica schist”. The saprolite was formed in place by severe chemical weathering on the exposed Wissahickon Formation surface both prior to and after the deposition of the overlying Cretaceous rocks (*1*). The saprolite layer is completely weathered but retains the fabric and structure of the parent bedrock. The Wissahickon Formation is characterized by extremely variable physical characteristics dependent upon the orientation of the steeply dipping rock beds that are crosscut by closely spaced, steeply dipping, and open joints. This geometrical complexity is further complicated by the degree and nature of the weathering of the upper surface of the Wissahickon Formation.

Excavation of the Wissahickon Formation and the Pennsauken and Bridgeton Formations are moderately easy, and foundation stability is generally good (*2*). Unweathered sound Wissahickon may have an unconfined compressive strength of 200 tons per square foot (tsf) whereas highly weathered soft Wissahickon has a strength of 10 tsf or less (*1*).

Installing deep foundations in a saprolite stratum poses a very challenging problem. Ferguson and Glynn (1988) described that a foundation failure of a 22-story federal courthouse in Philadelphia occurred due to an inadequate assessment of the Wissahickon Schist. Caissons improperly installed on the top weathered surface of the mica schist and the overlying saprolite caused significant settlements of some columns of the building. The extensive repairs resulted in a cost of approximately 6 million dollars in 1982.

PILE DESIGN

Based on the encountered subsurface conditions and proximity to nearby existing residential structures, micropiles were designed to be drilled into the residuum/saprolite stratum with the bond zone beginning at the top of the residuum/saprolite layer which fairly consistently corresponded to elevation -10 feet.

The relative stiffness of the geotechnical materials that micropiles bond into to develop axial resistance is of significant importance to the designer. As piles begin to transition axial load in the bond zone through grout-to-ground adhesion, the basic principles of material stiffness and load transfer need to be carefully considered. The Wissahickon Schist in the Philadelphia area has variable quality, weathering, and strength. As such, the design originally considered the residuum/saprolite layer as exhibiting soil-like behavior for conservatism. As the design progressed and the team was able to confirm differences and consistencies in material stiffness and properties within the wall limits, a higher bond strength and rock-like behavior was determined to be more representative of the in-situ conditions. Based on the expected rock-like behavior, the design utilized a bond resistance that considered both the composite stiffness and mechanical bonding characteristics of the saprolite zone. Based on the lower range of typical bond strengths for soft rock material descriptions from the FHWA Micropile Design Manual as well as PennDOT Design Manual 4 (*3*) and AAHSTO LRFD specifications, a design bond strength of 40 psi was applied for the residuum/saprolite layer, considering the rock-like material with variable degrees of weathering throughout the layer.

Using this nominal grout-to-ground bond strength, the micropile factored axial resistance was computed in accordance with AASHTO LRFD methodology for a 9-5/8" diameter, with a wall thickness of 0.472". Based on laboratory testing results, the design team accounted for corrosive ground conditions by applying sacrificial section loss of 0.075 inches around the perimeter of the micropile steel casing. Type A micropiles were used, with 5 ksi grout applied under normal gravity pressure. The pile layout was determined using ABLRFD software using the single pile axial resistance and rock-like characteristics with the first several rows battered to take the full lateral load in accordance with PennDOT requirements. For added assurance, the design team also performed group pile analyses considering potential soil-like behavior of the saprolite as a dense sand to account for potential pile shadowing effects. Both cases resulted in single pile loads and lateral deflections well within the micropile capacities.

Based on wall heights and associated loading, the wall was divided into three representative segments for geotechnical design purposes. A summary of the micropile design by segment, including micropile tip elevations and computed axial pile resistances, is presented in Table 1 considering a grout-to-ground bond resistance of 40 psi. Casing was terminated at the top of saprolite for improved constructability, resulting in a top of bond zone at elevation -10.0 feet.

Table 1 - Micropile Design Summary by Retaining Wall Segment

Segment	Wall Height (ft)	Micropile Bond Length (ft)	Minimum Micropile Tip Elevation (ft)	Factored Geotechnical Axial Resistance (kips)	Maximum Factored Single Pile Axial Load (kips)	Maximum Service Load (kips)
1	< 19	20	-30	183	111	72
2	19 to 26	25	-35	228	149	102
3	26 to 33.25	30	-40	274	225	155

To confirm the rock-like behavior and corresponding bond strength, the design required five sacrificial test piles to be installed prior to production and spaced along the different zones of the wall. The design loads for the tests were based on the maximum service load from Table 1 per PennDOT specifications. While testing was originally intended to be performed until failure, the maximum testing load was limited to 80 percent of the structural capacity of the central rebar reinforcement to avoid a sudden and dangerous failure during testing. To maximize the test loads, a #28 central reinforcement bar was used for the sacrificial test micropiles, while a #24 central reinforcement bar was used for the production piles and proof test micropiles. Additionally, to mitigate the risk of heave and sidewall collapse within the saprolite, micropile drilling and grouting below the cased length were performed in a continuous manner.

TEST PILE CONSTRUCTION AND LOAD TESTING

Construction Overview

The design discussed above resulted in 730 micropiles being required to support the vertical and lateral loads for a 1,200-foot-long retaining wall with a maximum height of 33.25 feet high supporting the roadway embankment. The project schedule required that excavation to bottom of pile cap, micropile installation, and micropile testing be completed in 5 months so completion of the wall, backfill, roadway paving, barrier, and sound wall installation would be complete within one construction season. The project micropile subcontractor, 3C Drilling of Quakertown, Pennsylvania proposed the following installation methodology and testing program to meet this requirement.

Micropile Installation Methodology

A Commachio MC-15p drilling rig would be used for the plumb verification test piles and a Rev Drill 40HD/60HD drilling rig would be used for the plumb proof test piles and all production piles. More than half of the micropiles were to be installed on a 3H:12V batter. Using these drilling rigs, all verification test, proof test and production micropiles would be installed in two steps. The first step was to install the 9-5/8 inch diameter with 0.472 inch wall permanent casing. The casing was advanced with the respective drill rig to the elevation that attained a 1 foot minimum penetration into the saprolite layer. For this project, that was approximately elevation -11.0. At all times during casing advancement, a minimum of one foot of casing remained above ground elevation. Alignment criteria for battered micropiles was specified and maintained at +/- 2% of the total length. The second step was to drill the socket into the saprolite layer to the design elevation, then clean the hole, install the reinforcement and grout. For this step, the hammer with drill bit is reinserted to the bottom of the already installed casing and advanced into the saprolite layer to the socket depth elevation directed by the designer. While advancing, the cuttings are removed via an air flushing medium and collected. When the planed socket depth was attained, the hole was again flushed with air until a clean return was observed. For this project the air lift was sufficient to accommodate the presence of groundwater during flushing. The hammer was then extracted from the hole and the hole and socket are reviewed for acceptance. Upon approval, a central reinforcing bar with attached tremie tube are lowered into the hole. As noted, proof and production micropiles received a #24 central reinforcement bar and sacrificial verification micropiles received a #28 central

reinforcement bar. All central reinforcement bars were fitted with centralizers placed at a maximum 10’ spacing with the first and last centralizers being a maximum of 3 feet from the end of the bar. 5000 psi. sand-cement grout was then placed via the tremie tube in a bottom-up manner until clean grout returned to the surface.

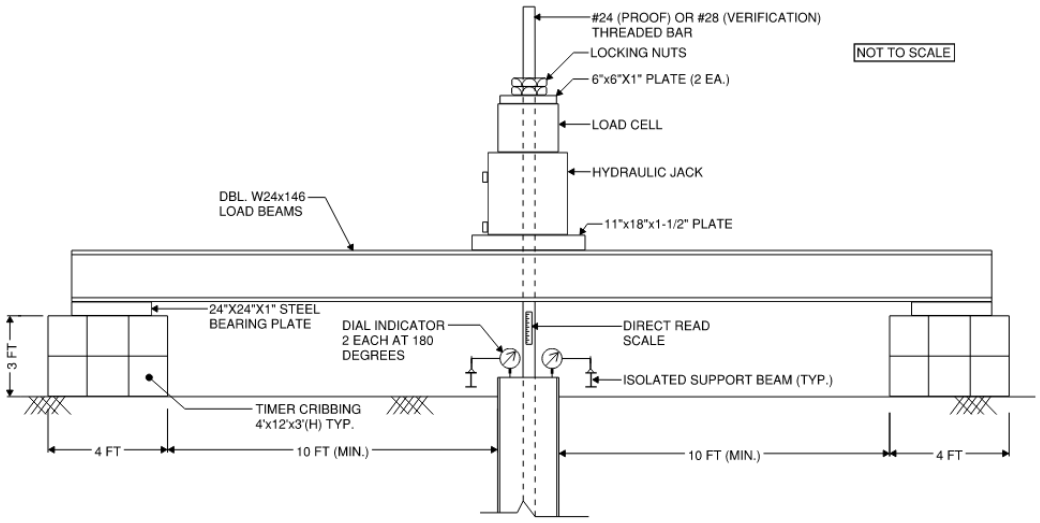


Figure 2 - Verification Test Load Frame Schematic

Field Verification Testing For Design Bond Strength

The design bond strength was confirmed via tension tests (Figure 2) on sacrificial micropiles prior to the start of production micropile installation. A total of five (5) sacrificial, non-production test micropiles were installed at a sufficient offset to not disturb the ground at the production micropile locations. Tests were performed in tension with a design load (DL) range of 72 kips to 155 kips resulting in a verification test load range of 360 kips to 428 kips within the respective retaining wall segment. Sacrificial load tests are restricted to an upper bound load of 80 percent of the structural capacity of the central rebar reinforcement. To accommodate this upper bound during verification testing, a #28 rebar size was used for the verification test micropiles. Testing was performed using a structural beam load frame on dunnage fitted with a calibrated hydraulic jack for tensile load application to the #28 bar central reinforcing bar. Top of pile movement was monitored using two (2) dial gauge indicators with a travel of 3 inches and a precision of 0.001 inches. Gauges were spaced at 180 degrees to each other on the pile top. In addition, back up movement monitoring was done using a piano wire, scale and mirror attached to the pile bar.



Figure 3 - Micropile Installation and Load Test Setup

LOAD TEST RESULTS AND DISCUSSIONS

It is essential to understand the load-displacement behavior of micropiles socketed in the saprolite layers and correctly interpret the load test results. The sacrificial micropile load testing results indicated the pile design and performance was acceptable. The sacrificial test piles comprised cased lengths ranging from 30 to 35.3 feet and bond lengths of 20.5 to 30 feet, resulting in total lengths of 51 to 64.5 feet. As seen in Figure 4, the axial load-displacement responses follow a similar pattern for all test piles. The test pile behavior was essentially elastic (mostly recoverable) even after the design load was exceeded. These axial load-displacement curves can generally be simplified into two stages (i.e., an initial linear stage and a curvilinear transition stage). One of the objectives of these sacrificial load tests is to pull the piles into the final stage (failure stage), where a small increase in load provides a large increase in settlement as described by Jeon and Kulhawy (*4*); however, none of the test piles appears to be tested beyond the transition stage.

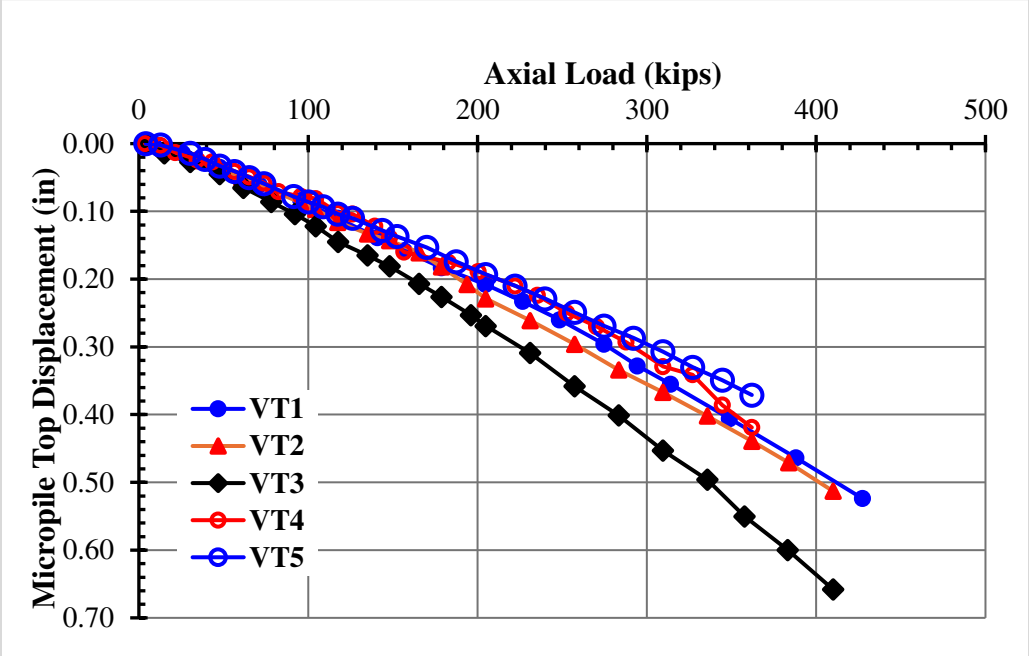


Figure 4 - Measured Load-Displacement Curves

Micropile Acceptance Criteria and Failure Load

Similar to the Deep Foundations Institute (*5*) micropile load test acceptance criteria, PennDOT publication 408 Section 1007.3 (j) specifies the following general acceptance criteria for load tests conducted on high capacity drilled and grouted micropiles:

- The pile must sustain the design load (DL) with no more than 0.75 inches of total vertical movement at the top of the pile as measured relative to the top of the pile prior to the start of testing.

- Test piles must have a creep rate at the end of the 1.3 DL increment that is not greater than 1/32" (0.031") between 1 and 10 minutes, or 1/16" (0.063") between 6 and 60 minutes and has a linear or decreasing creep rate.

- Failure does not occur by 2.0 DL. Failure is defined as a slope of the load versus deflection curve (at end of increment) less than 40 kips/inch.

All test piles were considered acceptable for limited vertical displacements under service limit state, creep as well as failure criteria. For piles installed in the saprolite material, creep is not a significant design concern and will not be discussed further in this paper.

As mentioned previously, the micropile acceptance criteria define the failure load as the point on the load-displacement curve at which the slope of the curve begins to fall below 40 kips/inch. The maximum testing loads of up to 5.0 DL were applied to the sacrificial test piles. The axial load test data indicate that at the maximum test load the smallest value of load-deflection slope encountered was 450 kips/inch (Pile VT4), with a corresponding maximum deflection of 0.607 inch which is much less than the failure criterion of 40 kips/inch. Therefore, none of the micropiles tested reached the failure load as defined by PennDOT (*6*).

In order to further investigate the failure loads for micropiles socketed in saprolite, slopes with load over deflection at maximum testing loads are plotted against the corresponding deflections. Figure 5 indicates that a relationship exists between the two parameters for these micropiles in saprolite. Considering the limited data presented, it is reasonable to assume that the failure criterion of a slope value of 40 kips/inch corresponds to a deflection around 1.0 inch for these micropiles, given not exceeding the structural capacity of the piles.

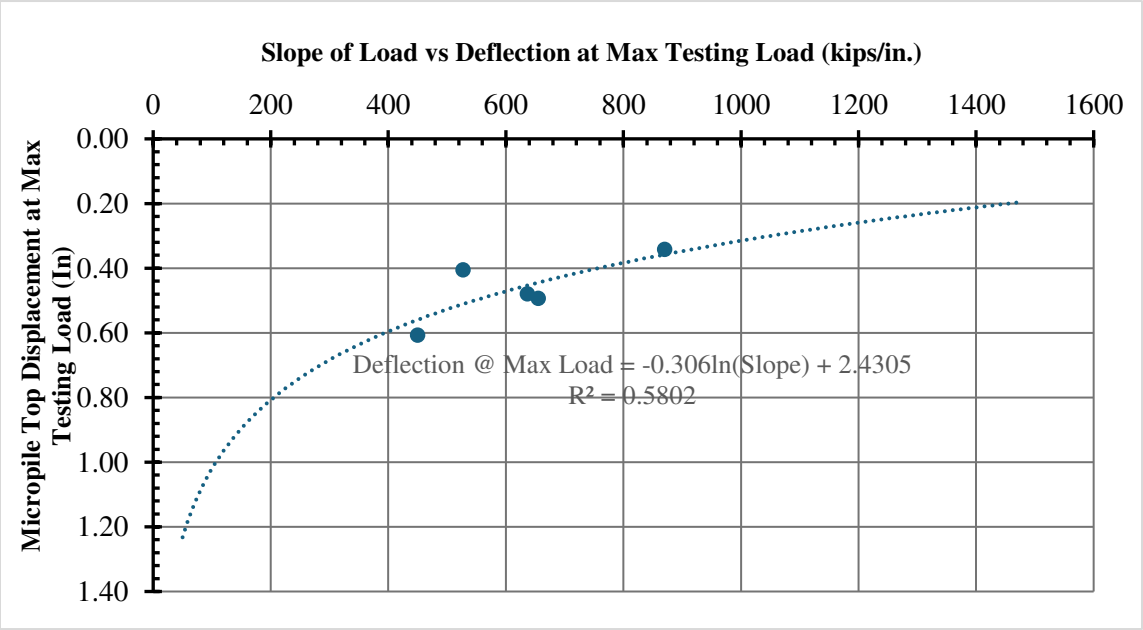


Figure 5 - Load Over Deflection at Maximum Testing Loads Versus Deflection

Side Resistance and Bond Stress

Micropiles could be considered as frictional pile foundations due to the large ratios of length to shaft diameter. The vertical tensile and compressive load-carrying capacities were mainly determined from shaft friction and pile length. The maximum measured average grout-to-saprolite bond stress was calculated using the maximum applied load divided by the side area of the socket. The results in Table 2 indicate that the measured bond stresses ranges from 44 to 55 psi, up to 40% higher than the design values. Note that back-calculated bond zone diameters using actual grout take are relatively similar to the theoretical ones. This is because the grouting technique does not force the grout against the wall of the hole. Considering all the piles were not tested to failure, it is reasonable to assume that even higher grout-saprolite bond stress could be developed with increasing loads.

Table 2 - Comparison Between Design Bond Stress and Measured Bond Stress

Pile Designation	Pile Bond Zone Length (ft)	Design Bond Stress (psi)	Unfactored Axial Design Resistance (kips)	Max. Testing Loads (kips)	Max. Measured Ave. Bond Stress (psi)	Ratio of Measured/Design Bond Stress
VTP-1	30.0	40	385	428 (2.75 DL)	44	1.1
VTP-2	25.0		320	410 (4.0 DL)	51	1.3
VTP-3	24.1		309	410 (4.0 DL)	53	1.3
VTP-4	20.5		263	360 (5.0 DL)	55	1.4
VTP-5	21.0		269	360 (5.0 DL)	53	1.3

CONCLUSIONS

Design and construction of micropiles socketed in saprolite are presented in this paper. Together with the sacrificial verification load test results, the following conclusions are suggested from this study:

1. Mica schist saprolite mechanical properties are complicated and can vary significantly. Extensive geotechnical investigations and a comprehensive load testing program will be needed for micropile design.

2. Air flushing medium worked well inside the saprolite socket. For this project, the air lift was sufficient to accommodate the presence of groundwater during flushing.

3. With this project design loads, deflections in the saprolite socket are relatively small. Load test results indicate these micropiles socketed into saprolite could carry a load much higher than the design load.

4. Higher mobilized bond stresses between the micropile and saprolite are obtained from load tests compared to the published values for similar geomaterials.

REFERENCES

1. Ferguson, W.B., E.F. and Glynn, A foundation failure in Philadelphia, Second International Conference on Case Studies in Geotechnical Engineering; Proceedings, v. 2, 1988, p. 1293-1296.

2. Geyer, A.R., and J.P. Wilshusen, Engineering Characteristics of the Rocks of Pennsylvania, Pennsylvania Geological Survey, 4th Series, 1982.

3. Pennsylvania Department of Transportation, *Design Manual, Part 4,* Publication 15M, Harrisburg, Pennsylvania, 2019.

4. Jeon, S.S., and F.H. Kulhawy, Evaluation of Axial Compression Behavior of Micropiles, Foundations and Ground Improvement, GSP No. 113, T.L. Brandon, Ed., ASCE, Reston, Virginia, 2001, pp. 460-471.

5. DFI, Guide to Drafting a Specification for High Capacity Drilled and Grouted Micropiles for Structural Support, Deep Foundations Institute, 2001.

6. Pennsylvania Department of Transportation, *Specifications,* Publication 408, Harrisburg, Pennsylvania, 2023.

The Influence of Particle Shape and Surface Roughness on the Friction Angle of Quartz Sands

Gary Norris
Emeritus Professor
University of Nevada Reno
1664 N. Virginia St, MS258
Reno, NV 89557
(775) 331-5582
norris@unr.edu

Prepared for the 74th Highway Geology Symposium, August, 2025

Disclaimer

Statements and views presented in this paper are strictly those of the authors, and do not necessarily reflect positions held by their affiliations, the Highway Geology Symposium (HGS), or others acknowledged above. The mention of trade names for commercial products does not imply the approval or endorsement of HGS.

Copyright Notice

Copyright © 2025 Highway Geology Symposium (HGS)

All Rights Reserved. Printed in the United States of America. No part of the publication may be reproduced or copied in any form or by any means – graphic, electronic, or mechanical, including photocopying, taping, or information storage, and retrieval system – without prior written permission of the HGS. This excludes the original author(s).

ABSTRACT

The shape of sand particles is typically characterized by the parameter, roundness, using one of the available comparison charts provided by sedimentary petrologists. Particle shape is attributable to features seen when viewing the particle as a whole. Surface roughness, on the other hand, refers to the features that exist at a level smaller than those contributing to particle shape. Shape features are the result of their original form on particles as released from the parent rock and the cumulative history of abrasion the particles undergo through the different environments through which the particles pass. Surface roughness is a function of the mechanical/chemical action of the last environment in which the particles reside. While the interaction of the particles' shape features contributes to volumetric dilatancy during shearing, surface roughness features contribute to a non-volumetric component of dilatancy as the surface of the particles' shape features slide over that of opposing particles. The objective of this paper is to establish separate components of the peak drained triaxial test friction angle attributable to particle shape versus that attributable to surface roughness. For that purpose, triaxial tests were performed on up to four uniform size fractions of quartz particles from seven different natural sands: two beach sands (high versus low wave action), two eolian sands (desert versus coastal dune sand), two river sands (poorly versus well graded sand) and a diagenetic sand. Drained tests were performed at three levels of confining pressure over a range in relative density, 144 tests in total.

INTRODUCTION

That part of the drained triaxial test peak friction angle attributable to the microscopic surface roughness on sand particles, distinct from that of features that constitute the particle's shape, has yet to be established. The shape of sand particles is a function of their original shape as released from the parent rock, plus the cumulative history of abrasion through one or more geologic environments through which the particles travel. On the other hand, the microscopic roughness on the surface of the particle shape features is a function of the mechanical/chemical action of the last environment in which the sand particles reside.

The up and down motion as the surface of one particle's shape features rides up and over the surface of the shape features of an opposing particle, during shear in a drained triaxial test, lends to a non-volumetric component of dilatancy. At the same time, the interaction of the shape features that occurs between particles is reflected in a volumetric component of dilatancy. Norris et al. (*1*) provide a basis for understanding the contribution to the drained friction angle of surface roughness beyond that of the mineral-to-mineral interaction of particle surfaces.

The same paper indicates the means for distinguishing the relative size features that are surface roughness, from the range in size features that constitute the particle shape. Scanning electron microscope photographs from Norris (*2*) showing the surface roughness attributable to particles from different geologic environments appear in the textbook by Mitchel (*3*).

Particle shape has traditionally been characterized using comparison charts of Krumbein (*4*), Pettijohn (*5*), Russel and Taylor (*6*) or Powers (*7*) of images of different roundness values. On the other hand, a geotechnical engineering parameter for the purpose of evaluating the contribution of surface roughness to the drained friction angle has only recently been provided (*1*, based on Norris, *2*). It is the intent here, to review shape and surface roughness parameter definitions, and to establish functional relationships to the separate components of the drained friction angle they represent. Data from 144 "frictionless" (i,e, lubricated end) cap and base tests undertaken on 18 different uniform size quartz fractions from seven natural sands (two each of river, beach and dune sand and a separate diagenetic sand) was used to obtain such relationships.

SANDS COLLECTED AND PREPARED FOR EVALUATION AND TESTING

Of the different geologic environments in which sands are found, according to Folk (*8*), it is river channel, beach and eolian sands that have less than 5% clay. Since clay particles adhering to the surface of sand particles obscure the frictional effect of the particles' natural surface roughness, it is these type sands that were selected for study. From work of sedimentary petrologists based on scanning electron microscopic viewing of quartz particles (see *2* citing ten such references), it has been ascertained that a cause-effect correspondence exists between the mechanical and/or chemical action of natural environments and the surface roughness patterns on particles found in these environments. Furthermore, there are differences between high versus low wave energy beach sands and desert versus coastal dune sands, while river sand particles are supposedly devoid of surface roughness (though not the coarsest size river sand particles, *2*, *9*). Hence two differing beach and two differing eolian sands were collected for study, as well as a poorly and a well graded, river channel sand. Since Ottawa sand, a diagenetic sand from the

Saint Peter sandstone deposit, has been used in numerous classical geotechnical studies, a similar diagenetic sand was added to the current study.

Six tons each of the sands, except the bagged diagenetic sand, were collected from their natural environment prior to any aggregate processing. Table 1 lists the environment, subtype, locality, property manager and abbreviation employed for each sand. The sands were sieved to obtain up to four uniform sizes: material passing the U.S. # 7 sieve and retained on the U.S. # 8 sieve, U.S. 18-20, U.S. 45-50, and U.S. 120- 140. The ratio between each size fraction and the next lower fraction is 2.83, while the Uniformity Coefficient, $Cu = D_{60}/D_{10}$, of each size fraction is 1.18.

All sieved fractions (except the pure quartz Ione and Gopher sand fractions) were then subject to heavy media separation to collect just the quartz particles. After an acetone rinse to remove the remnants of the heavy media, all material fractions were then boiled in hydrochloric acid for 30 minutes (or more for the Prattco sand fractions) and then ultrasonically cleaned in different small weight batches (depending on the particular size fraction) for two minutes. Greater detail of the heavy media separation and operations needed to clean the different quartz fractions of any heavy media or surface coating and adhering clay (or other) particles is given in Norris (*2*). Unfortunately, unsuccessful attempts to limit non-quartz minerals to less than 10 percent in the M and BR 45-50 size fractions resulted in their exclusion from further use.

Table 1 - Sands Employed

Environment	Subtype	Locality[+]	Property Manager	Abbreviation
Beach	High Energy Wave Low Energy Wave	Felton Monterey Bay	PCA[++] (Felton Plant) PCA (Lapis Plant)	F for Felton M for Monterey
Eolian	Coastal Dune Desert Dune	Monterey Bay Kelso	PCA (Prattco Plant) Mr. Roy Parker	P for Prattco K for Kelso
River Channel /Primary		Ione Bear River	Owens-Illinois Joe Chevreaux	I for Ione BR for Bear River
Diagenetic		Le Seur, Minn	Gopher Silica	G for Gopher

[+] All localities are in California except for the diagenetic source.
[++] PCA is an abbreviation for Pacific Cement and Aggregate.

PARTICLE SHAPE AND ITS EVALUATION

Evaluation of particle shape of bulky and elongated (non-platy) particles in geological endeavors has traditionally been limited to two parameters, sphericity (ψ) and roundness (ρ). Both definitions rely on the observation and assessment relative to the maximum projected image of the particles spread out on a flat surface. Figure 1 provides the definition of sphericity (ψ) and roundness (ρ) after Wadell (*10*).

While it would be extremely time consuming to evaluate ψ and ρ from a photograph of a given particle and then average those values from a number of particles, comparison charts provide a semi accurate capability. Figures 2 and 3 are what were used here for such assessment of an average value for 100 photographed particles of each of the 18 quartz fractions. Note that there are other charts for roundness beside the Krumbein chart, but the Krumbein chart offers the greater number of sets of images. Other sets provide images related to descriptive adjectives (well rounded, rounded, subrounded, subangular, angular, very angular).

Prior to the adoption of the Krumbein chart, a study of the use of the Krumbein versus Russel & Taylor versus Pettijohn charts, was undertaken. (It should be noted that the Pettijohn chart uses a select number of the Krumbein images grouped in categories of angular, subangular, etc.). Once the Krumbein chart was adopted, studies were made regarding a) the number of particles that should be viewed and b) differences in values observed at different times of viewing (one week apart, and one year later). All values employed in the current study were assessed in a short span of time using 100 photographed and numbered particles.

Figure 4 provides a plot of the sphericity value versus the roundness value of the 18 fractions. Accordingly, it was deemed that with some, but an acceptable degree of error, only one shape parameter need be used to correlate with the results of the peak drained friction angle. Given the greater spread/range of the roundness values, roundness was chosen as the more sensitive shape parameter to use. This is borne out in the R^2 value of e_{max}, e_{min} and $e_{max} - e_{min}$ variations with ρ as compared to the same variations with ψ.

Table 2 provides the values for the shape parameters as well as the surface roughness, n, value (to be introduced subsequently) and the maximum and minimum void ratio values of the 18 quartz size fractions. While the sphericity chart yields a two significant digit value for a particle, and the roundness chart, a single significant digit, three significant digit assessments are shown in Table 2. Thus, the last two significant digits, in the case of roundness, should be viewed as how many of the 100 particles are closer to the first significant digit value versus the next higher first significant digit value. For instance, a ρ value of 0.332 implies that 68 of 100 particles are closer to 0.3, while 32 are closer to 0.4. (A similar interpretation can be made regarding the sphericity value.)

In regard to the use of the Krumbein chart, there was an ambiguity that arose. What is noticeable is that with smaller, sharper corners, there is room for more such corners on the peripety of the Krumbein particles. Therefore, it was decided to undertake a separate evaluation using the Krumbein chart relying not so much on the sharpness of the corners of the 100

particles, but on the frequency or number of corners. Table 2 provides separate columns of assessed values of ρ o Table 2 provides the values for the shape parameters as well as the surface roughness, n, value

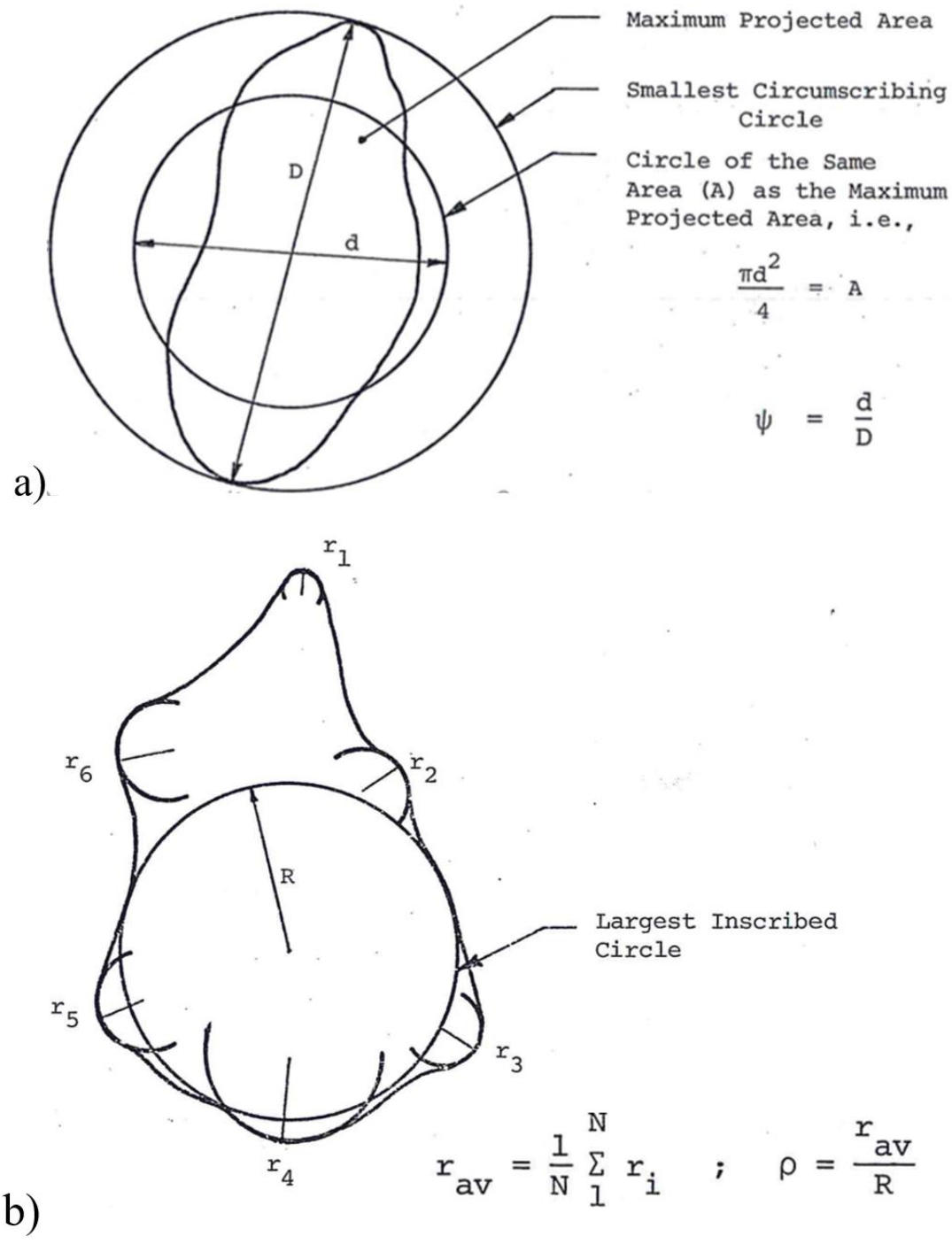


Figure 1 - Particle a) Sphericity, ψ and b) Roundness, ρ, Definitions after Wadell (*10*)

(to be introduced subsequently) and the maximum and minimum void ratio values of the 18 quartz size fractions. of the 18 quartz fractions: that based on the strict or original definition of roundness and the alternative version corresponding to the frequency or number of corners. It is this alternative version that was adopted as the measure of roundness, ρ, used in the current

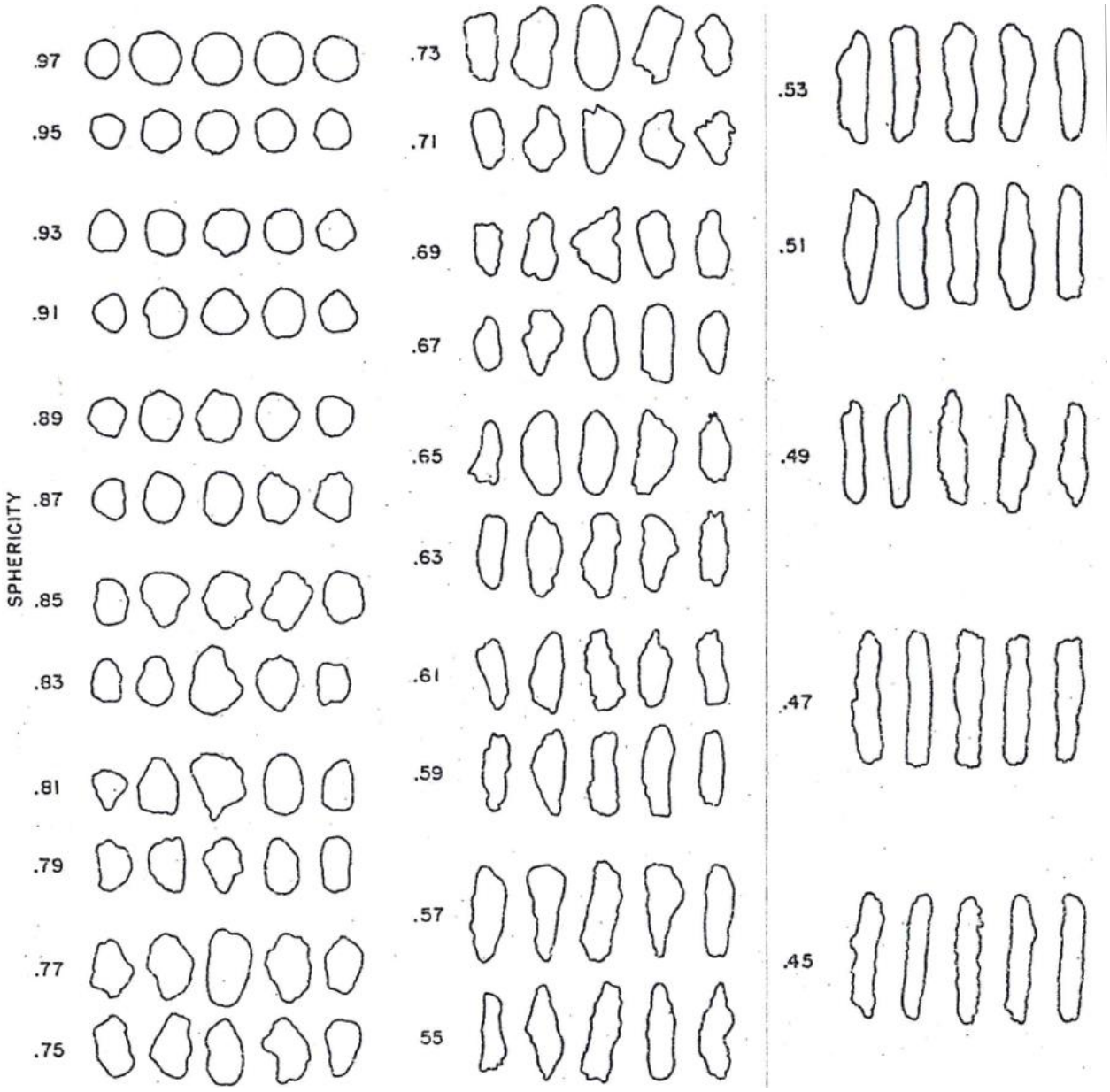


Figure 2 - Sphericity, ψ, Comparison Chart After Rittenhouse (*11*)

study, though in fact it is really not a measure of the sharpness of the particle's corners but the number/frequency of them. (This alternate ρ is more in keeping with the consideration of the contribution of surface roughness features to the friction angle, as presented subsequently.)

Furthermore, there is a better correlation of both maximum and minimum void ratios (as well as the sphericity value of Fig. 4) with this alternate version of “roundness”.

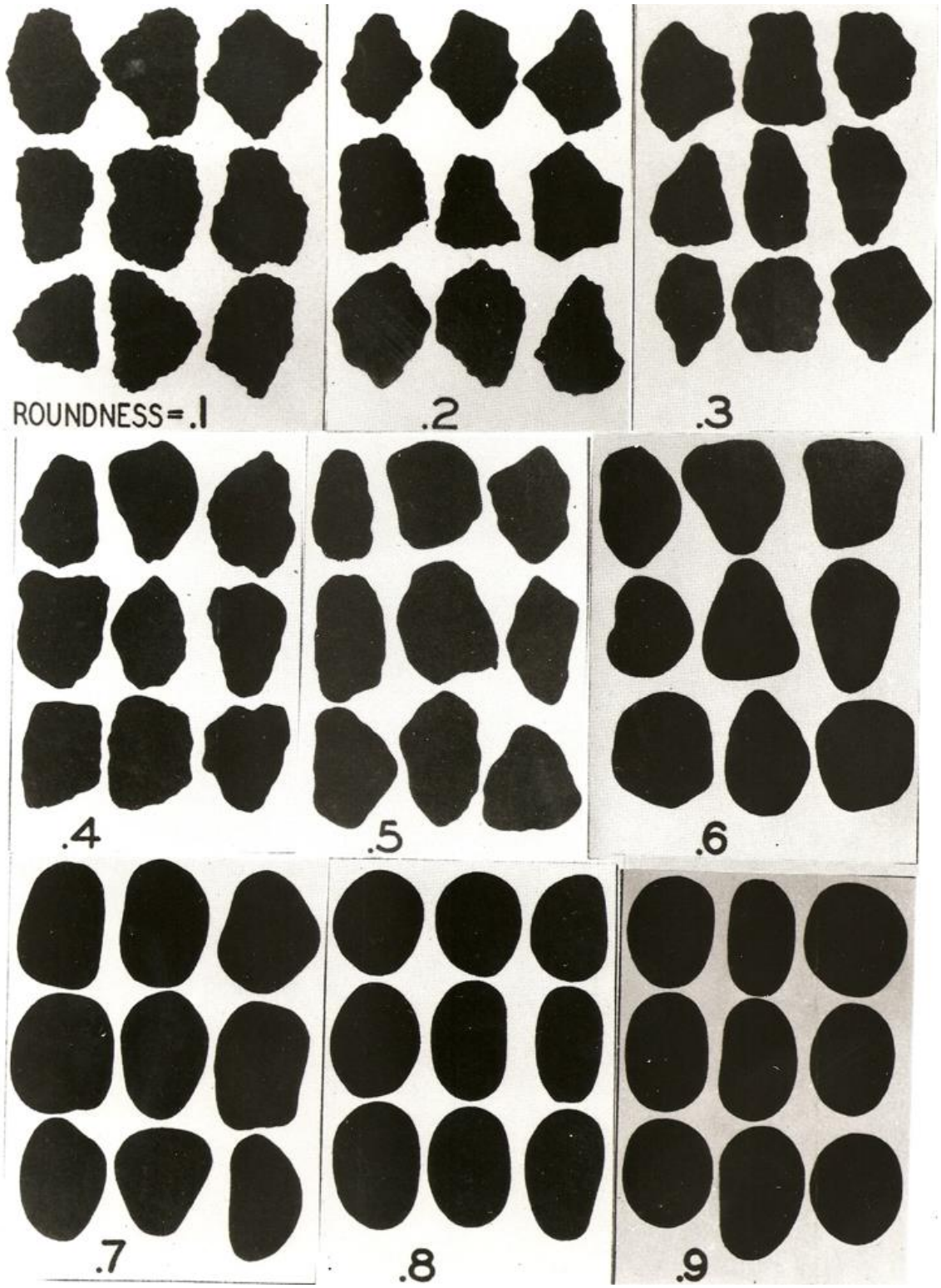


Figure 3 - Roundness, ρ, Comparison Chart Images After Krumbein (*4*)

Table 2 - Characteristics of Sands Tested

Material	ψ	ρ_{orig}	ρ_{alt}	% Diff in ρ's	n	e_{min}	e_{max}
7-8 M	0.835	0.610	0.612	0.3	0.03	0.489	0.720
F	0.831	0.491	0.496	1.0	0.03	0.540	0.820
BR	0.810	0.423	0.451	6.2	0.03	0.544	0.843
18-20 G	0.853	0.665	0.665	0.0	0.03	0.471	0.723
M	0.827	0.459	0.462	0.6	0.03	0.539	0.811
F	0.820	0.309	0.344	10.2	0.02	0.563	0.884
BR	0.806	0.215	0.287	25.1	0	0.588	0.888
45-50 G	0.845	0.636	0.636	0.0	0.03	0.486	0.733
K	0.821	0.442	0.454	2.6	0.04	0.566	0.805
P	0.796	0.347	0.379	8.4	0.04	0.596	0.892
F	0.806	0.274	0.289	5.2	0	0.654	1.002
I	0.800	0.283	0.291	2.7	0	0.705	1.049
120-140 G	0.826	0.556	0.559	0.5	0.01	0.539	0.799
K	0.775	0.461	0.461	0.0	0.04	0.638	0.894
P	0.762	0.315	0.332	5.1	0.04	0.680	1.012
I	0.780	0.288	0.313	8.0	0	0.733	1.104
BR	0.766	0.225	0.251	10.4	0	0.814	1.26
F	0.755	0.215	0.236	8.9	0	0.856	1.36

ρ_{orig} was used in Fig. 4

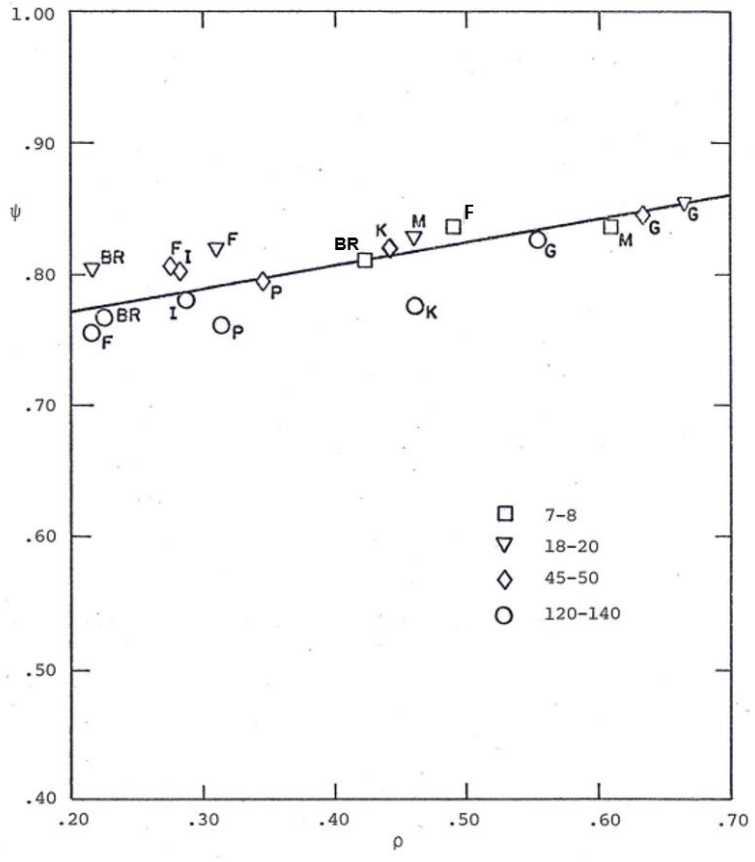


Figure 4 - Correlation of Sphericity (ψ) with Roundness (ρ) for the Quarts Sand Fractions

SURFACE ROUGHNESS

Sedimentary petrologists have studied surface roughness (that they refer to as surface texture) on quartz sand particles from different environments using the scanning electron microscope (SEM). However, their catalogue of the form of roughness for purposes of correlation to geologic environment is not readily useful for studying the effect of roughness on its contribution to the peak friction angle. For one thing, sedimentary petrologists limited SEM studies to particles of size ½ to 1 mm and magnification to 1000x to 10,000x. The magnification needs to vary relative to the particle diameter (d), i.e. $d/10^2$ to $d/10^4$ (level 2 features) and $d/10^4$ to $d/10^6$ or 100 Angstroms (level 3 features). The 100 Angstrom level is taken to delineate the level below which the surface is perfectly smooth. The 100 Angstrom value occurs at the boundary between level 2 and level 3 features of the 120-140 size fraction, signifying there is no level 3 roughness range for that size quartz fraction. Shape, or rather shape features, fall in the range of d to $d/10^2$ or level 1 features. Fortunately, roughness features, if they exist, were found in only one level of roughness, not both, of all the size fractions and thus required only one surface roughness parameter (the non-zero value of n_2 or n_3 then designated as n).

Norris (*2*) [and to a lesser degree, Norris et al. (*1*)] provides the full background for roughness evaluation. For purpose of brevity, consider here just the following. At the level of SEM roughness in which features appear, consider the horizontal movement of one surface over a copy of itself as shown in Fig. 5. The up and down movement of a fixed point on one surface as that surface is drawn horizontally across the other constitutes the "effective path" which has a length ℓ. The surface roughness parameter, n, is defined here as

$$n = (\ell - x)/x \qquad (1)$$

where x is the horizontal component of ℓ. See Fig. 6.

Consider, as an experiment involving the two matching sawtooth profile quartz blocks shown in Fig. 7a. When the upper block is displaced horizontally relative to the lower, as indicated in Fig. 7b, the corresponding shear force that drives it varies as shown in Fig. 7b. Note that the asperity angle is given as $i_{2\text{ or }3}$. The contribution of such roughness to the resulting friction is

$$\Delta\phi_{2\text{ or }3} = \tan^{-1}\{[\tan(\phi_\mu + i_{2\text{ or }3}) + \tan(\phi_\mu - i_{2\text{ or }3})]/2\} - \tan^{-1}[\tan(\phi_\mu)] \qquad (2a)$$

where ϕ_μ is the mineral-to-mineral friction angle of quartz, taken to be 25°. In the above case, note that the effective path is identical to the sawtooth surface profile.

By contrast, consider two effective paths shown in Fig. 8a and 8b. The effective path in Fig. 8a is identical to the sawtooth profile of multiple/continuous asperities of Fig. 7a, while Fig. 8b is the effective path of an isolated asperity profile. This single asperity of Fig. 8b takes up 1/3 of the horizontal component of the effective stress path shown. Consequently, its contribution to friction, $\Delta\phi$, would be

$$\Delta\phi = \tan^{-1}\{[2\tan(\phi_\mu) + \tan(\phi_\mu + i) + \tan(\phi_\mu - i) + 2\tan(\phi_\mu)]/6\} - \tan^{-1}[\tan(\phi_\mu)] \qquad (2b)$$

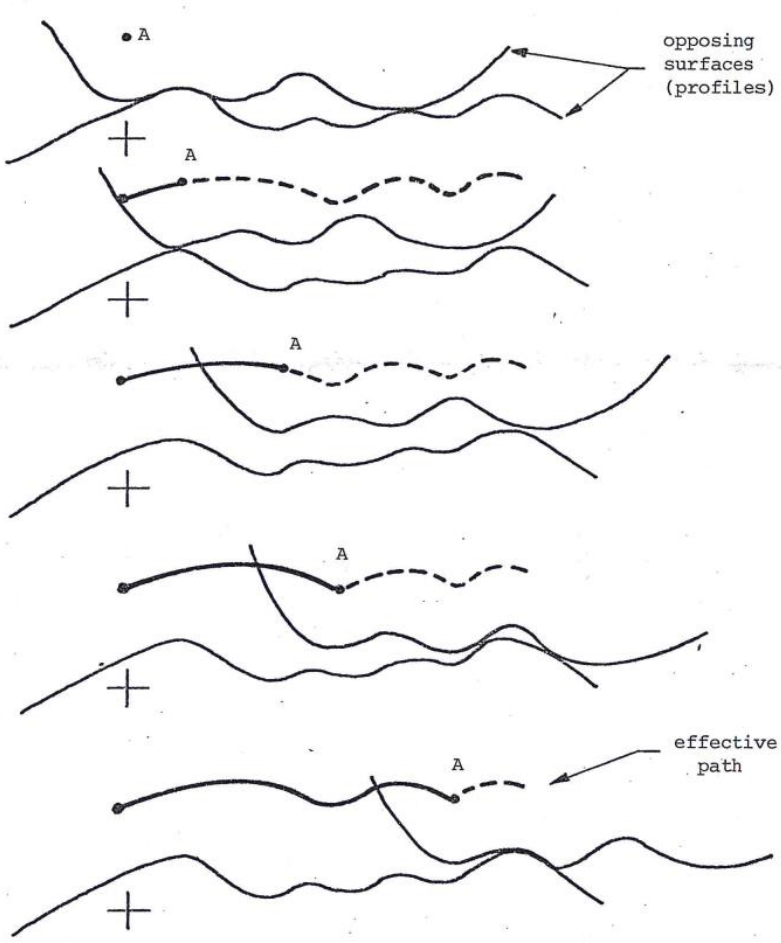
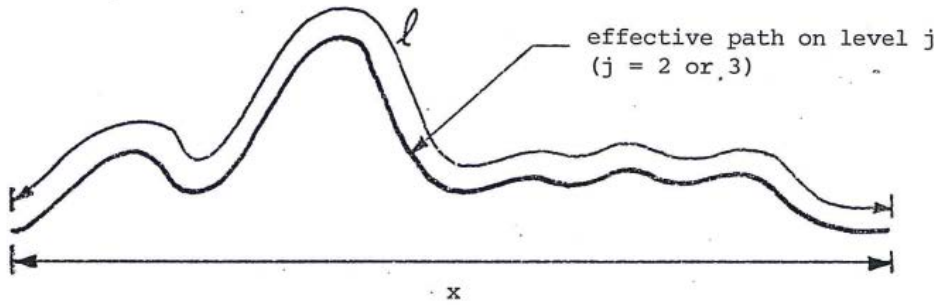


Figure 5 - The Establishment of the Effective Path of Horizontal Shear Movement



$$n_j = \frac{\ell - x}{x} \quad ; \quad j = 2 \text{ or } 3$$

Figure 6 - Visualized Definition of Surface Roughness Value n (j = 1 refers to Shape Features)

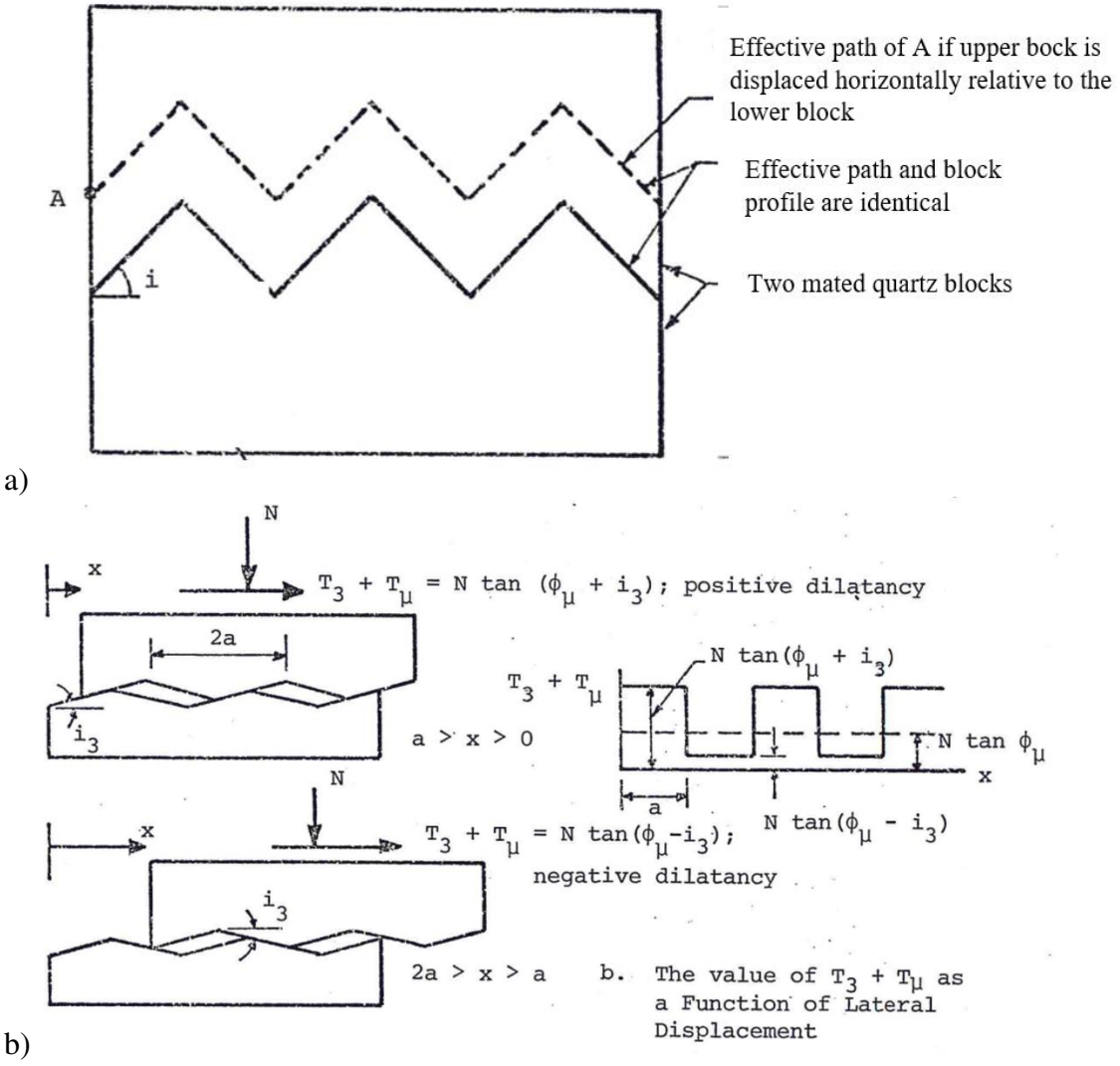


Figure 7 - a) Two Matched Sawtooth Quartz Blocks of Asperity Angle i Showing the Effective Path of a Point A When the Upper Block is Displaced Laterally and b) the Variation in Shear Force Required Given the Mineral-to-Mineral Friction Angle of the Quartz, ϕ_μ.

The $\Delta\phi$ of Fig. 8a is the same as that given by Eq. 2a. On the other hand, the respective surface roughness n values of Fig. 8a and Fig. 8b are

$$n = 1/\cos i_{8a} - 1 \qquad \text{for Fig. 8a} \qquad (3a)$$

and

$$n = (1 + 1/\cos i_{8b} + 1)/3 - 1 \qquad \text{for Fig. 8b} \qquad (3b)$$

Table 3 and Fig. 9 provide a comparison of the n and $\Delta\phi$ values for the effective paths of Fig. 8a versus 8b, of the multiple versus the isolated asperity. For the same height and sharpness or i

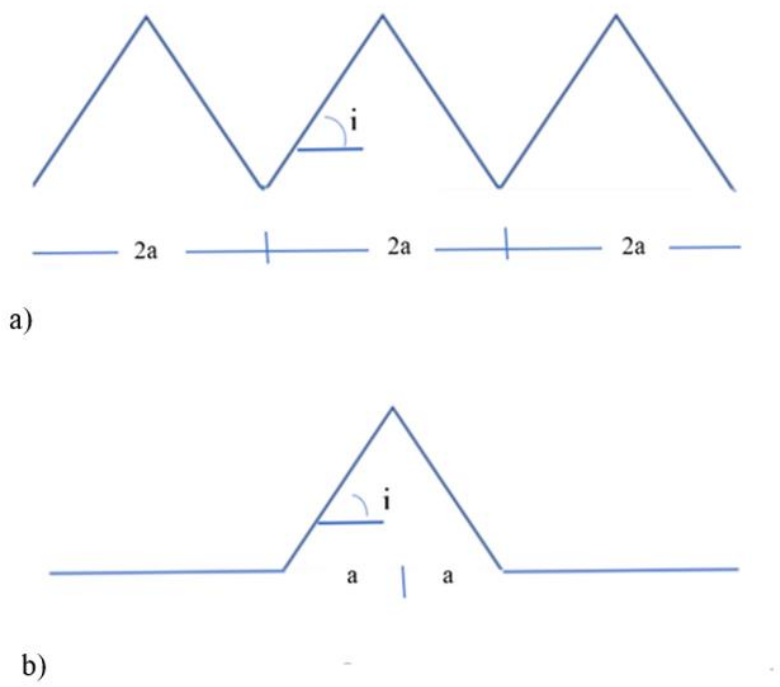


Figure 8 - Comparison of Two Effective Paths of Base Angle i

value of 18° of the asperity base angle, note the highlighted 8a and 8b data points on the respective curves of Fig. 9 and in Table 3. The difference in $\Delta\phi$ is 1.86° (2.818 – 0.9547). On the other hand. for the same n, but i = 30° for case 8b, note a difference in $\Delta\phi$ of 0.30° (3.116 - 2.818). This signifies that it is the frequency/number of asperities rather than their sharpness that is the more dominant factor. These last statements lend support to the use of the alternate version of the roundness shape parameter, i.e. the number or frequency of the corners of the Krumbein comparison chart images is more important than the sharpness/roundness, r_{av}, of the corners of the shape features.)

The reader will note that Fig. 9 and Table 3 also provide an assessment of $\Delta\phi$ versus n for the mineral-to mineral friction angle of 22.5° for water saturated quartz, different from its dry state angle of 25°. (Wang X L, et al., 2014 give a range of 22 to 24.5° for saturated quartz.) This lower value would be more consistent with the triaxial tests considered here because volumetric strain was assessed based on the burette measured movement of water in and out of the triaxial test sample. Of particular note is that at n = 0.04, $\Delta\phi$ = 1.95° (Fig. 9 saturated quartz slope of 48.646 x 0.04). This value will be compared with that from the test data later.

The pages in Mitchell (*3*) show a few of the Norris (*2*) SEM photographs of surface roughness (from the geologic environments with minimal clay content) covering the upper (n_2) and lower (n_3) ranges of possible surface roughness, from which n values were assessed.

Table 3 - Values of n and Δϕ of Fig. 8a vs 8b

		degrees	radians						
	ϕ_μ (°)	25	0.43633						
	$\phi_\mu + i$ (°)	43	0.75049		tan ($\phi_\mu + i$)	0.93252			
	$\phi_\mu - i$ (°)	7	0.12217		tan ($\phi_\mu - i$)	0.12278			
	i (°)	18	0.31416		tan ϕ_{eff}	0.52765			
	tan i	0.32492				degrees	radians		
					ϕ_{eff} (°)	27.8184	0.48552		
					Δϕ (°)	2.81836			
	Case 8a								
	i (°)	0	5	8.1	11.5	14	16	18	20
	n	0	0.00382	0.01008	0.02049	0.03061	0.0403	0.05146	0.06418
$\phi_\mu = 25°$	Δϕ (°)	0	0.2045	0.54115	1.10577	1.66041	2.19571	2.81836	3.53489
$\phi_\mu = 22.5°$	Δϕ (°)	0	0.18166	0.4807	0.98227	1.475	1.95062	2.50393	3.14082
	Case 8b								
	i (°)	0	5	10	20	25	27	30	18
	n	0	0.00127	0.00514	0.02139	0.03446	0.04078	0.05157	0.01715
$\phi_\mu = 25°$	Δϕ (°)	0	0.06824	0.27814	1.20272	1.99872	2.40111	3.11626	0.95474

In the subjective assessment of l (in Eq. 1) from the SEM photographs of the 18 size quartz fractions, the envisioned horizontal movement of one SEM surface relative to its match was sketched and n evaluated from it. Such work yielded only single significant digit differences in n values of 0.01, 0.02, 0.03 or 0.04 on either the upper or lower surface roughness level, versus 0 for no features (i.e. no roughness). The n = 0.04 value, the greatest surface roughness value of all the quartz sand fractions was attributable to the desert and coastal dune sand size fractions (45-50 and 120-140 sizes). The n = 0 value, was attributable to the 18-20 and finer river sands (BR and I) and the 45-50 and 120-140 sizes of the Felton beach sand. Notably, the n value of the coarse fraction of the BR river sand was not 0.

The collective set of assessed n values is given in Table 2.

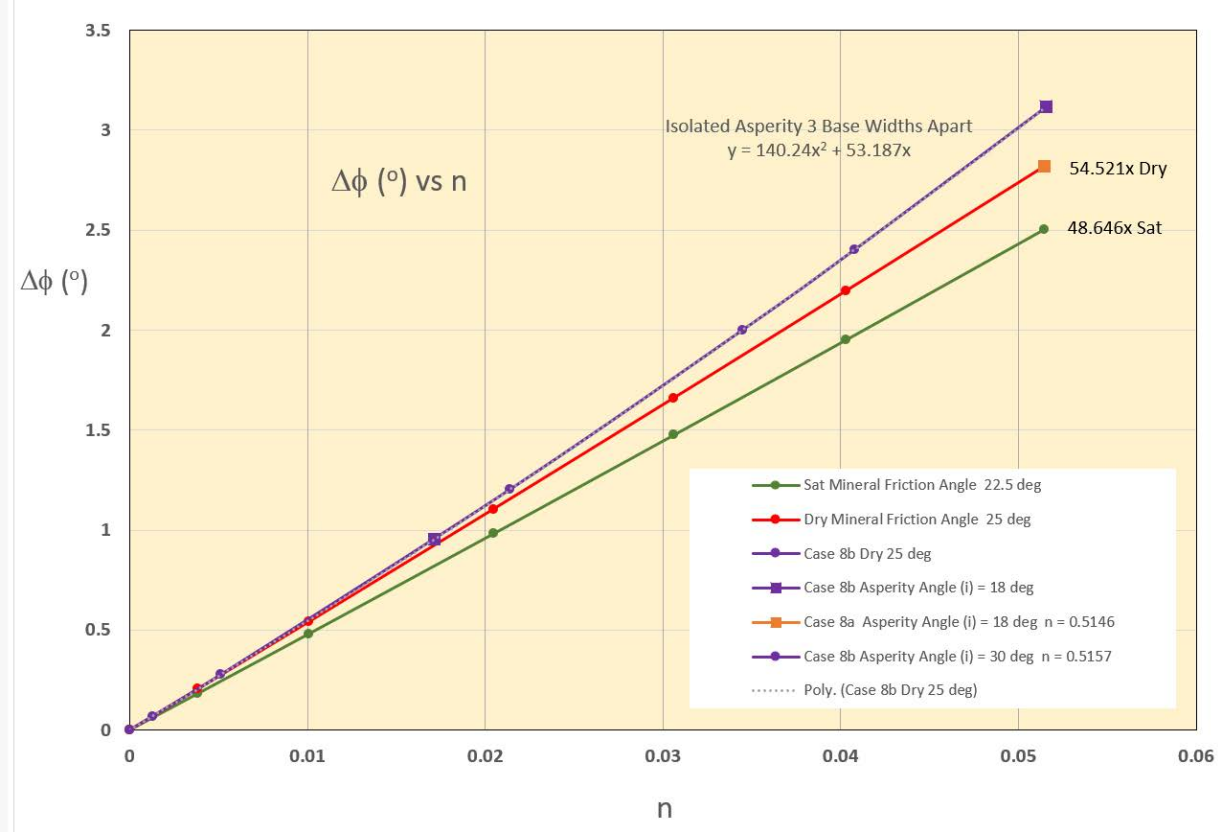


Figure 9 - The Theoretical Relationship of the Contribution to Friction Angle, Δϕ, as a Function of Surface Roughness, n

PEAK STRENGTH DUE TO SURFACE ROUGHNESS VERSUS PARTICLE SHAPE FROM THE TRIAXIAL TEST DATA

Table 4 provides (in separate column groups by confining pressure, σ_3, of 0.425, 1.20, and 3.40 kgf/cm^2) the peak friction angle (ϕ) data along with their associated material source and size (soil type), relative density (Dr), roundness (ρ) and surface roughness (n) ordered vertically by surface roughness groups (0, 0.01, 0.02. 0.03 and 0.04). A modified peak friction angle ($\phi_{n=0}$) appears in the last column of each confining pressure group. Such value is the peak ϕ multiplied by (1-n), i.e.

$$\phi_{n=0} = \phi\,(1- n) \qquad (4a)$$

or $$\phi_{n=0} = \phi - \Delta\phi \quad \text{where} \quad \Delta\phi = n\,\phi \qquad (4b)$$

Basically, the modified friction angle, $\phi_{n=0}$, is an assessment of ϕ with the surface roughness component $\Delta\phi$ (= n ϕ) removed, or a $\phi_{n=0}$ converted to an equivalent ϕ of surface roughness equal to zero. The intent is to establish $\phi_{n=0}$ values that are only a function of particle shape, ρ. From such collection of $\phi_{n=0}$'s, their dependence on ρ can then be assessed independent of surface roughness.

Table 4 - Test Dr, ρ, n and Peak Friction Angle at σ_3 of 0.425, 1.20 and 3.40 kgf/cm^2 Pressures

σ'3 kgf/cm² = 0.425						
Test	Soil type	D_r(%)	ρ	n	Peak ϕ (°)	Modified Peak ϕ(1-n)°
40	BR 18-20	28	0.287	0	39.4	39.4
41	BR 18-20	86	0.287	0	42.9	42.9
75	I 45-50	50	0.291	0	39.7	39.7
76	I 45-50	97	0.291	0	44.3	44.3
83	F 45-50	29	0.289	0	39.0	39.0
84	F 45-50	48	0.289	0	39.7	39.7
85	F 45-50	98	0.289	0	44.3	44.3
119	I 120-140	29	0.313	0	39.0	39.0
120	I 120-141	51	0.313	0	39.1	39.1
121	I 120-140	101.5	0.313	0	44.7	44.7
128	BR 120-140	20.5	0.251	0	40.0	40.0
129	BR 120-140	52	0.251	0	41.4	41.4
136	F 120-140	25	0.236	0	41.1	41.1
137	F 120-140	43.5	0.236	0	43.6	43.6
138	F 120-140	103	0.236	0	48.6	48.6
			0.278			
92	G 120-140	29	0.559	0.01	36.5	36.1
93	G 120-140	56.5	0.559	0.01	37.5	37.1
94	G 120-140	97	0.559	0.01	41.7	41.3
33	F 18-20	46	0.344	0.02	38.5	37.7
34	F 18-20	89.5	0.344	0.02	43.6	42.7
1	M 7-8	20	0.612	0.03	36.4	35.3
2	M 7-8	76	0.612	0.03	42.3	41.0
7	F 7-8	26	0.496	0.03	37.4	36.3
8	F 7-8	83	0.496	0.03	42.3	41.0
13	BR 7-8	24.5	0.451	0.03	37.7	36.5
14	BR 7-8	88.5	0.451	0.03	42.5	41.2
19	G 18-20	45.5	0.665	0.03	33.0	32.0
20	G 18-20	89	0.665	0.03	38.5	37.3
26	M 18-20	36	0.462	0.03	40.6	39.4
27	M 18-20	94	0.462	0.03	44.5	43.2
47	G 45-50	28.5	0.636	0.03	35.2	34.1
48	G 45-50	61	0.636	0.03	37.4	36.3
49	G 45-50	97.5	0.636	0.03	40.9	39.6
			0.560			
56	K 45-50	21.5	0.454	0.04	39.4	37.8
57	K 45-50	56	0.454	0.04	41.7	40.0
58	K 45-50	100	0.454	0.04	43.5	41.8
65	P 45-50	23	0.379	0.04	39.5	38.0
66	P 45-50	54	0.379	0.04	41.6	40.0
67	P 45-50	95	0.379	0.04	43.9	42.1
101	K 120-140	18	0.461	0.04	41.1	39.4
102	K 120-140	67	0.461	0.04	44.0	42.3
103	K 120-140	100.5	0.461	0.04	45.3	43.5
110	P 120-140	24.5	0.332	0.04	39.3	37.7
111	P 120-140	68	0.332	0.04	43.3	41.5
112	P 120-140	107	0.332	0.04	47.4	45.5
			0.407			

σ'3 kgf/cm² = 1.20						
Test	Soil type	D_r(%)	ρ	n	Peak ϕ (°)	Modified Peak ϕ(1-n)°
42	BR 18-20	39	0.287	0	37.5	37.5
43	BR 18-20	42	0.287	0	37.8	37.8
44	BR 18-20	87	0.287	0	41.8	41.8
77	I 45-50	33	0.291	0	36.7	36.7
78	I 45-50	45.5	0.291	0	36.7	36.7
79	I 45-50	96	0.291	0	41	41.0
86	F 45-50	26	0.289	0	36.4	36.4
87	F 45-50	50	0.289	0	37.8	37.8
88	F 45-50	98	0.289	0	42.0	42.0
122	I 120-140	25.5	0.313	0	34.9	34.9
123	I 120-140	51	0.313	0	36.4	36.4
124	I 120-140	100	0.313	0	41.9	41.9
130	BR 120-140	26.5	0.251	0	36.0	36.0
131	BR 120-140	60	0.251	0	39.8	39.8
132	BR 120-140	100	0.251	0	43.8	43.8
139	F 120-140	24.5	0.236	0	37.7	37.7
140	F 120-140	50	0.236	0	39.8	39.8
141	F 120-140	105	0.236	0	45.9	45.9
95	G 120-140	28	0.559	0.01	32.6	32.3
96	G 120-140	50	0.559	0.01	34.5	34.1
97	G 120-140	103	0.559	0.01	39.9	39.5
35	F 18-20	48	0.344	0.02	37.0	36.3
36	F 18-20	57.5	0.344	0.02	37.5	36.8
37	F 18-20	91	0.344	0.02	41.0	40.2
3	M 7-8	18	0.612	0.03	34.7	33.7
4	M 7-8	85	0.612	0.03	39.0	37.8
9	F 7-8	24	0.496	0.03	35.4	34.3
10	F 7-8	88	0.496	0.03	40.6	39.4
15	BR 7-8	24	0.451	0.03	35.7	34.6
16	BR 7-8	87	0.451	0.03	40.1	38.9
21	G 18-20	42.5	0.665	0.03	31.3	30.4
22	G 18-20	60.5	0.665	0.03	34.0	33.0
23	G 18-20	102	0.665	0.03	37.9	36.8
28	M 18-20	48.5	0.462	0.03	37.4	36.3
29	M 18-20	63	0.462	0.03	39.5	38.3
30	M 18-20	95.5	0.462	0.03	41.8	40.5
50	G 45-50	32	0.636	0.03	33.7	32.7
51	G 45-50	58	0.636	0.03	35.9	34.8
52	G 45-50	89	0.636	0.03	37.7	36.6
59	K 45-50	24	0.454	0.04	37.0	35.5
60	K 45-50	52.5	0.454	0.04	38.8	37.2
61	K 45-50	99	0.454	0.04	41.2	39.6
68	P 45-50	24	0.379	0.04	36.8	35.3
69	P 45-50	56	0.379	0.04	38.6	37.1
70	P 45-50	96	0.379	0.04	41.9	40.2
104	K 120-140	25	0.461	0.04	38.7	37.2
105	K 120-140	67	0.461	0.04	42.4	40.7
106	K 120-140	105.5	0.461	0.04	43.8	42.0
113	P 120-140	22.5	0.332	0.04	37.4	35.9
114	P 120-140	71	0.332	0.04	41.1	39.5
115	P 120-140	103	0.332	0.04	44.0	42.2

σ'3 kgf/cm² = 3.40						
Test	Soil type	D_r(%)	ρ	n	Peak ϕ (°)	Modified Peak ϕ(1-n)°
45	BR 18-20	34	0.287	0	35.8	35.8
46	BR 18-20	85	0.287	0	39.2	39.2
81	I 45-50	52	0.291	0	34.7	34.7
82	I 45-50	99.5	0.291	0	38.4	38.4
89	F 45-50	31.5	0.289	0	34.7	34.7
90	F 45-50	50	0.289	0	35.4	35.4
91	F 45-50	98	0.289	0	40.2	40.2
125	I 120-140	28.5	0.313	0	32.6	32.6
126	I 120-140	55	0.313	0	34.2	34.2
127	I 120-140	105	0.313	0	37.6	37.6
133	BR 120-140	32	0.251	0	34.8	34.8
134	BR 120-140	49.5	0.251	0	35.7	35.7
135	BR 120-140	102.5	0.251	0	41.3	41.3
142	F 120-140	25	0.236	0	35.5	35.5
143	F 120-140	47	0.236	0	37.0	37.0
144	F 120-140	103.5	0.236	0	43.3	43.3
98	G 120-140	21	0.559	0.01	31.0	30.7
99	G 120-140	66	0.559	0.01	34.4	34.1
100	G 120-140	91.5	0.559	0.01	36.5	36.1
38	F 18-20	46	0.344	0.02	34.4	33.7
39	F 18-20	89.5	0.344	0.02	38.6	37.8
5	M 7-8	16.5	0.612	0.03	33.0	32.0
6	M 7-8	74	0.612	0.03	36.5	35.4
11	F 7-8	30	0.496	0.03	33.3	32.3
12	F 7-8	88	0.496	0.03	36.7	35.6
17	BR 7-8	42	0.451	0.03	34.1	33.1
18	BR 7-8	83	0.451	0.03	37.6	36.5
24	G 18-20	45.2	0.665	0.03	30.5	29.6
25	G 18-20	96	0.665	0.03	34.9	33.9
31	M 18-20	28	0.462	0.03	34.8	33.8
32	M 18-20	93	0.462	0.03	39.8	38.6
53	G 45-50	29	0.636	0.03	32.1	31.1
54	G 45-50	54	0.636	0.03	34.4	33.4
55	G 45-50	96.5	0.636	0.03	37.7	36.6
62	K 45-50	23.5	0.454	0.04	34.5	33.2
63	K 45-50	55	0.454	0.04	37.1	35.6
64	K 45-50	94	0.454	0.04	38.9	37.3
71	P 45-50	21.5	0.379	0.04	34.1	32.7
72	P 45-50	53	0.379	0.04	36.4	34.9
73	P 45-50	93	0.379	0.04	39.4	37.8
107	K 120-140	21	0.461	0.04	36.1	34.7
108	K 120-140	66	0.461	0.04	40.4	38.8
109	K 120-140	111	0.461	0.04	43.2	41.5
116	P 120-140	26.5	0.332	0.04	35.9	34.5
117	P 120-140	60	0.332	0.04	38.6	37.1
118	P 120-140	107.5	0.332	0.04	43.0	41.3

While the theoretical Δϕ (°) (= 44.646 n) given for saturated quartz in the last section is dependent on n, the Δϕ of Eq. 4b is instead, dependent on ϕ and n. At n = 0.04, the theoretical Δϕ is 1.95°, while Δϕ of Eq. 4b yields 1.95° when ϕ = 48.75°. The value of Δϕ of Eq. 4b is lower for lesser values of ϕ.

Figure 10 is a plot of $\phi_{n=0}$ versus Dr for various groupings of ρ values from the 0.425 kgf/cm^2 confining pressure data, while Fig. 11 is a simplification based on the average values of ρ (0.278, 0.407 and 0.560) associated with the n = 0, 0.04 and 0.03 groupings for the 0.425 kgf/cm^2 pressure of of Table 4. With the variation of $\phi_{n=0}$ for ρ = 0.278, 0.407 and 0.559 at Dr values of 20, 60 and 100% from Fig. 11, a plot of $\phi_{n=0}$ versus ρ for these Dr values is constructed. See Fig. 12. The polynomial trendline equations for the expressions yield coefficients for the x^2 and x terms and the constant that can be plotted versus the Dr values yielding plots shown in Fig. 13. A universal equation for $\phi_{n=0}$ as a function of Dr (%) and ρ can then be established for the 0.425 kgf/cm^2 confining pressure using the coefficient and constant equations for Dr. Such expression is given as Eq. 5 with Dr in % yielding $\phi_{n=0}$ in degrees.

$$\phi_{n=0} = (0.159\ Dr - 19.893)\ \rho^2 - (0.1198\ Dr - 2.3477)\ \rho + (0.0987\ Dr + 38.17) \qquad (5)$$

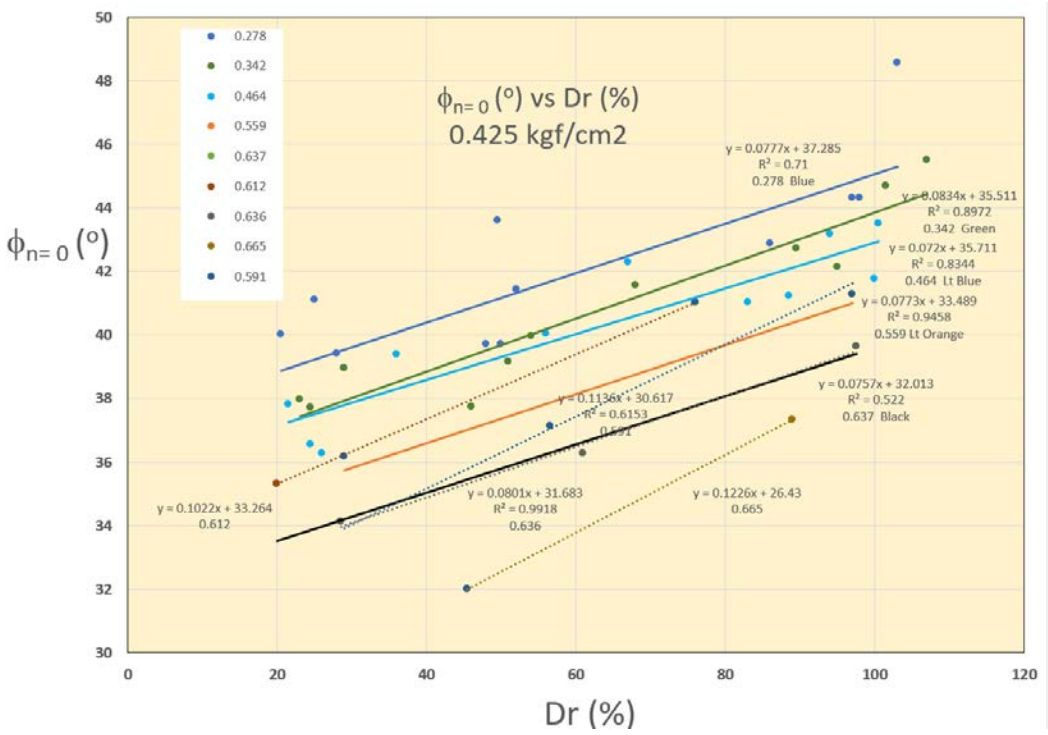


Figure 10 - Variations of $\phi_{n=0}$ Versus Dr for Different Groupings of ρ of Table 4, 0.425 kgf/cm²

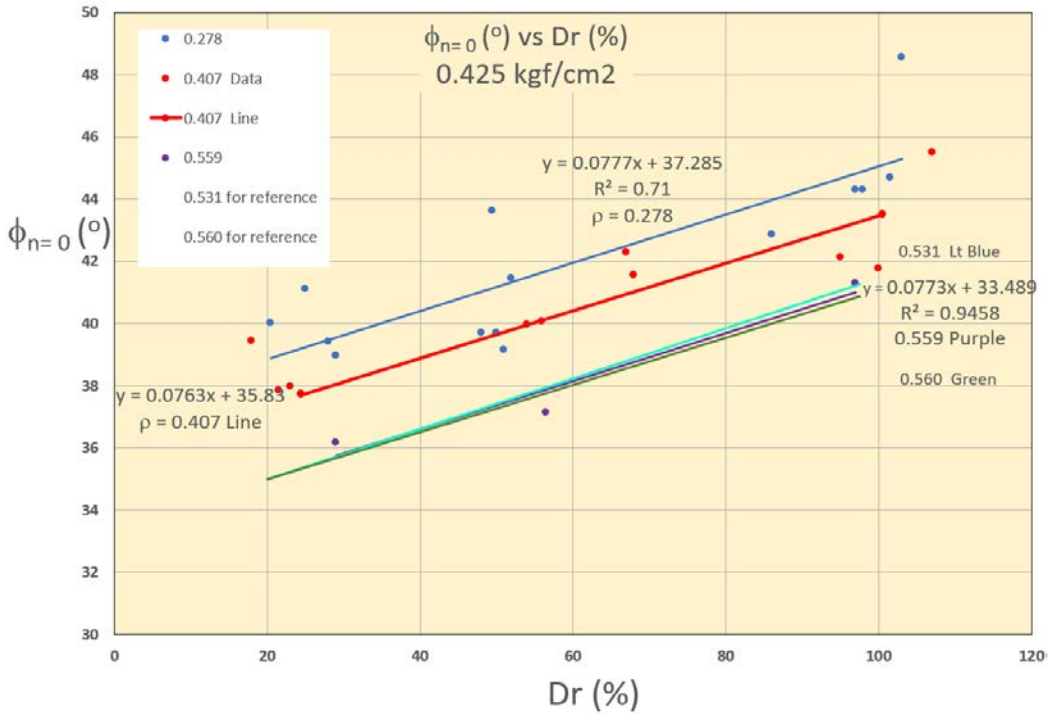


Figure 11 - Simplified Variations of $\phi_{n=0}$ Versus Dr for Average ρ Values (0.278, 0.407, 560)

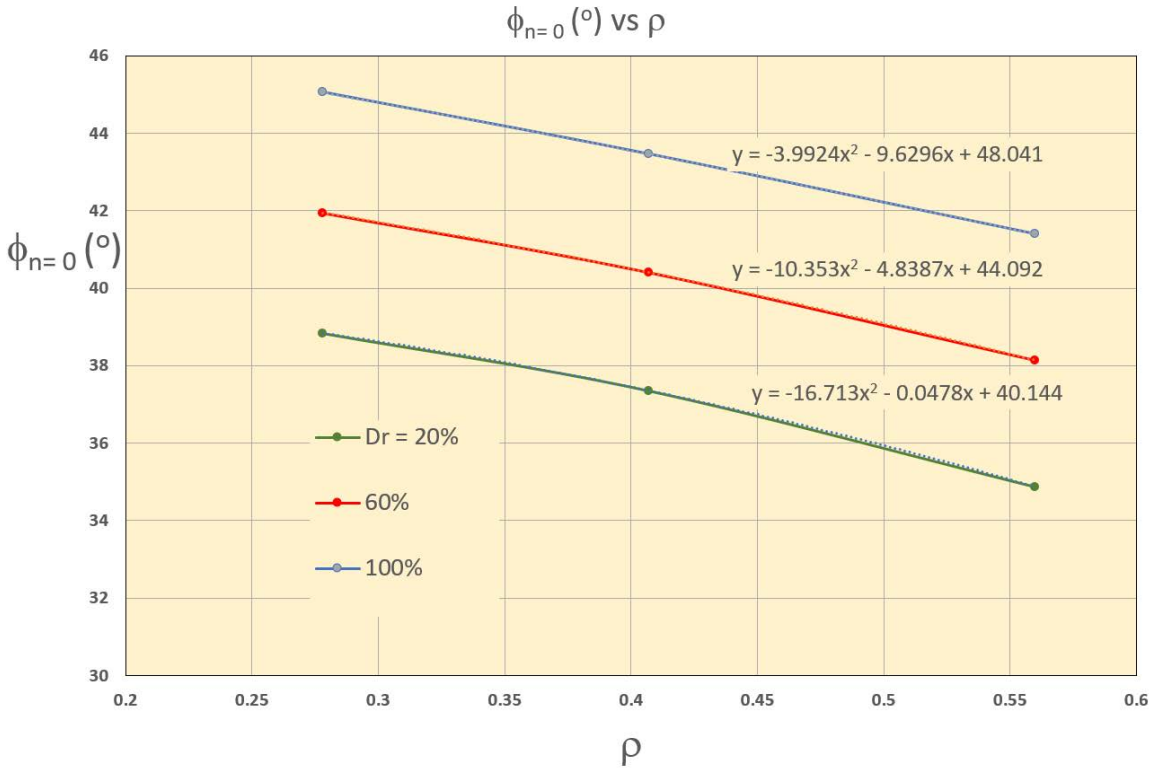


Figure 12 - Variation in $\phi_{n=0}$ Versus ρ for Dr = 20, 40 and 100%, 0.425 kgf/cm²

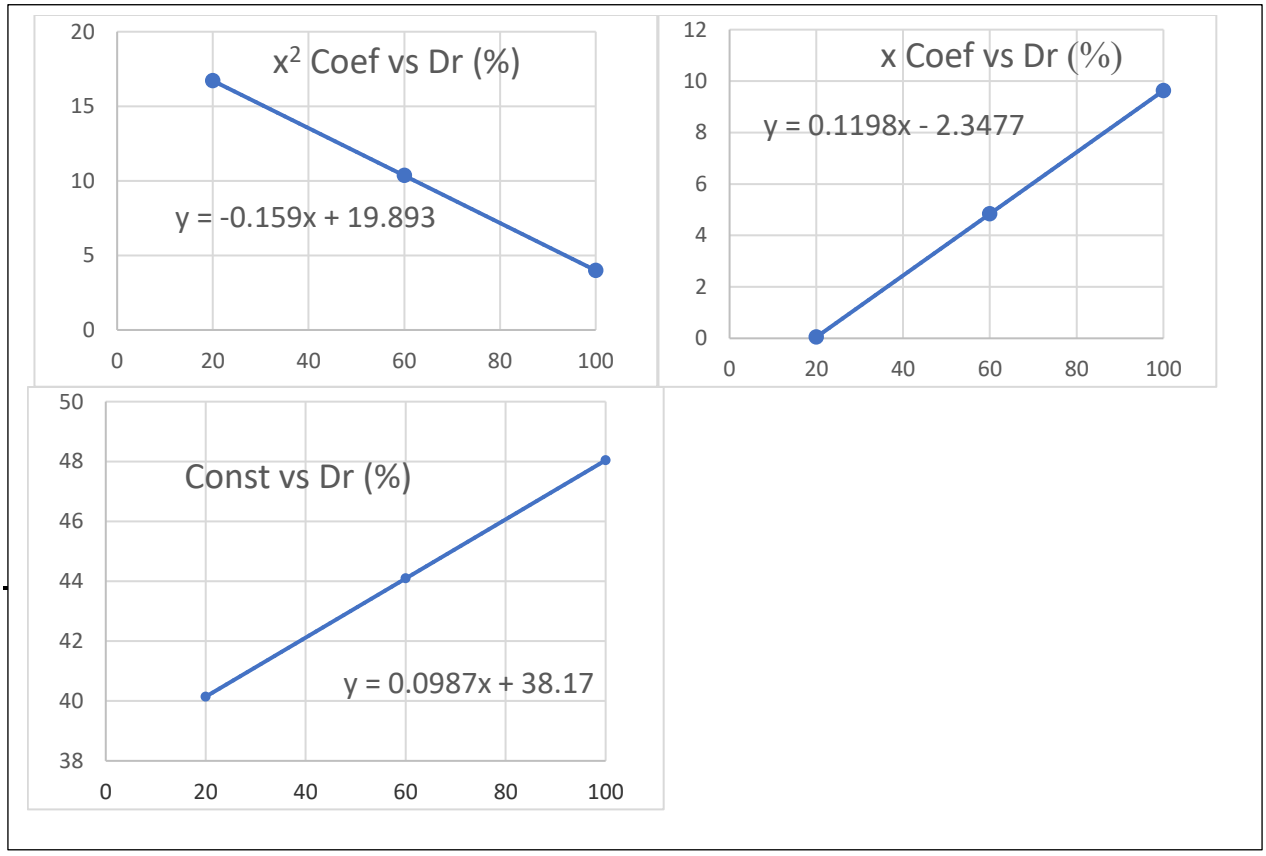


Figure 13 - Variations in Coefficients of x^2 and x Terms and Constant with Dr Based on the Dr = 20, 60 and 100% Equations of Fig. 12

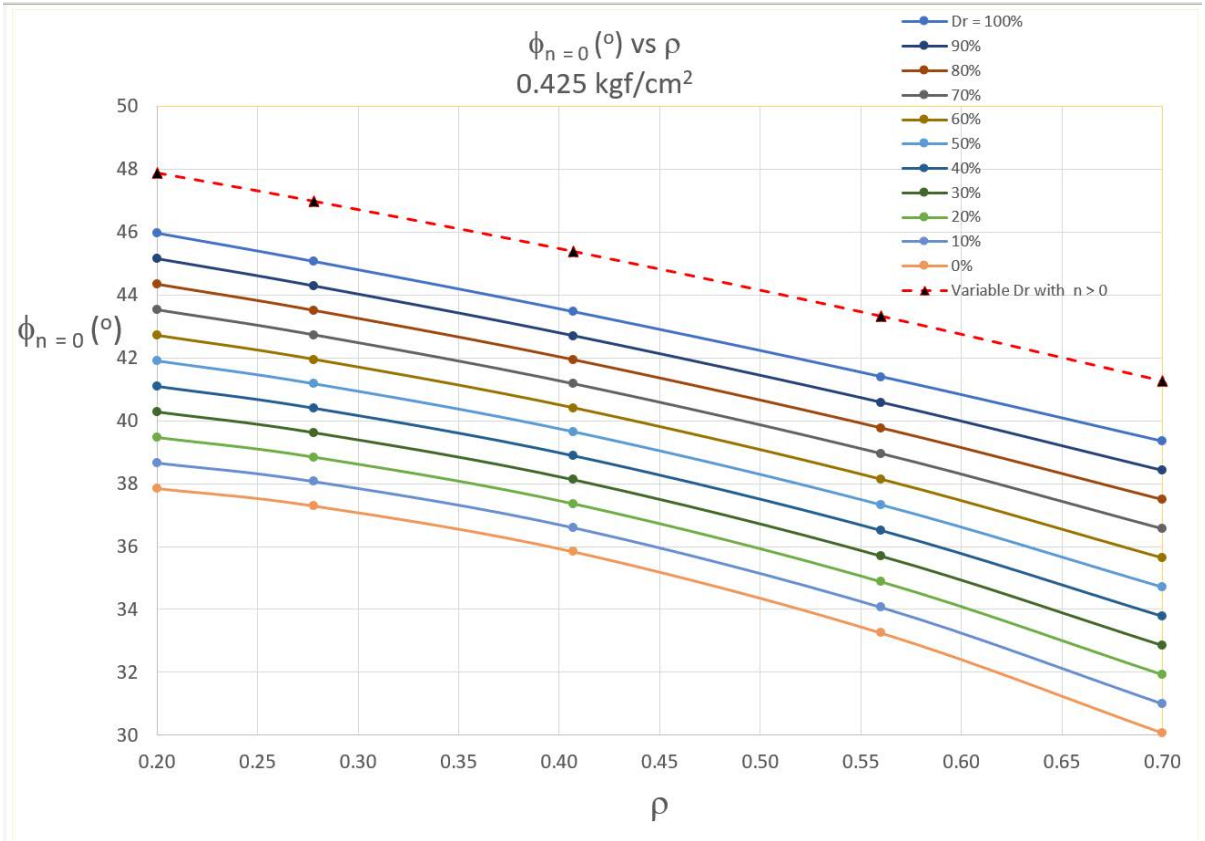


Figure 14 - Variation in $\phi_{n=0}$ with ρ for Different Dr Based on Eq. 5 for 0.425kgf/cm² Confining Pressure

Figure 14 is a plot using Eq. 5 of $\phi_{n=0}$ versus ρ for successive values of Dr. There is a line at the top showing the Dr =100% $\phi_{n=0}$ line with a $\Delta\phi$ corresponding to a surface roughness of n = 0.04 added back in. Based on Eq. 4, the peak secant ϕ (ϕ_n) with a given roughness, n, for $\phi_{n=0}$ evaluated from Eq. 5 is then

$$\phi_n = \phi_{n=0}/(1- n) \quad (6a)$$

It can be shown that Eq. 6a can also yield the following version of ϕ_n,

$$\phi_n = \phi_{n=0}(1+ n + n^2 + n^3 + n^4 + n^5 + n^6 +.....) \quad (6b)$$

It is noted that rather than undertake independent assessments to determine the type curves of Fig. 14 for the 1.20 and 3.40 kgf/cm^2 test data, it was decided to first try the same equations (5 and 6) on the 1.20 and 3.40 kgf/cm2 confining pressure tests. The only modification needed was to offset/subtract 2.5° from ϕ_n for the 1.20 tests and 4.5° for the 3.40 tests$^+$. Such confining pressure effect is shown by Norris (*12*) relative to the same tests considered here.
Equations 5 and 6 have been used, with the values of Dr, ρ and n of Table 4, to assess ϕ_n to compare with the listed secant ϕ values. Table 5 reports the average and maximum (absolute) difference in ϕ, and the average and maximum percent difference in ϕ for each confining pressure.

Based on the results noted in Table 5, it is suggested that Eqs. 5 and 6 are sufficient for use relative to all confining pressures provided that the appropriate offset is applied. The offset for any confining pressure, based on the 0, 2.5 and 4.5° for the 0.425, 1.20 and 3.40 kgf/cm^2 values used here, can easily be assessed.

Table 5 - Comparison of Test ϕ vs Equation 5$\phi_{n=0}$ with n Added

Test ϕ (°) vs $\phi_n=\phi_{n=0}/(1-n)$°	$\phi_{n=0}/(1-n)$ 0.425 kgf/cm2 Abs Diff (°)	0.425 kgf/cm2 % Error	1.20 kgf/cm2 Abs Diff (°)	1.20 kgf/cm2 % Error	3.40 kgf/cm2 Abs Diff (°)	3.40 kgf/cm2 % Error
Ave	1.0	2.5	0.9	2.4	1.1	3.0
Max Difference°	3.3	10.1	2.8	7.2	2.9	8.2

DISCUSSION/CONCLUSIONS

The presentation given here has attempted to define a geotechnical parameter for surface roughness (n) to help investigate the contribution of surface roughness to the peak secant friction angle separate from particle shape. Frictionless cap and base tests on 18 uniform quartz sand fractions from seven natural sands were employed in the investigation. Particle shape was assessed using the Krumbein images but with more attention paid to the number of corners than their sharpness. Surface roughness, n, was rather subjectively evaluated from scanning electron photographs taken over a range of magnifications relative to the particle diameter. Despite the single digit accuracy of assessed n values, assessing the equivalent peak friction angle devoid of surface roughness, $\phi_{n=0} = \phi\ (1- n)$, yielded data that could be successfully assessed as a function of relative density (Dr) and particle shape (ρ), i.e. Eq. 5, and with offset as a function of confining pressure. Such $\phi_{n=0}$ value could then have the roughness contribution added back in. Table 5 proports to the validity of Eqs. 5 and 6.

While not strictly employed, the theoretical assessment of the contribution of surface roughness (Eq. 2a) to the peak friction angle as a function of an envisioned effective paths in the form of asperities (of angles i) provided support to the Δϕ assessed from the triaxial test data (Eq. 4b). Equation 2a depends on n alone while Eq. 4b depends on n and ϕ.

Now consider the limitations of the current work. The results are specific to quartz material, devoid of other constituent surface coatings. The results do not consider grain size distribution and possible fabric (aligned particle) variations.

As noted, it is the desert and coastal dune sands (45-50 and lesser size) that exhibit greater surface roughness (n = 0.04). The river sands (!8-20 and lesser size) are perfectly smooth (n = 0) along with 45-50 and 120-140 Felton beach sand. All n = 0 materials exhibited ρ values less than 0.313. All larger size particles (7-8) exhibited roughness (n = 0.03). Unfortunately, because heavy media separation was unsuccessful in limiting non-quartz material to less than 10% of the BR and M 45-50 size fractions, they were excluded from the triaxial test program.

REFERENCES

1. Norris, G., S. Elfass, and H-J. Yang, Internal Friction as a Function of Surface Roughness, *Proc. of the 43rd Engineering Geology and Geotechnical Symposium*, Las Vegas, Nevada, 2011, pp. 412-420.

2. Norris, G., The Drained Shear Strength of Uniform Quartz Sand as Related to Particle Size and Natural Variation in Particle Shape and Surface Roughness, Ph.D. Thesis, University of California, Berkeley, 1977.

3. Mitchell, J.K., *Fundamentals of Soil Behavior*," Second Edition, John Wiley & Sons, Inc., N.Y., 1993, pp. 61-64, 372.

4. Krumbein, W.C., Measurement and Geological Significance of Shape and Roundness of Sedimentary Particles, *Journal of Sedimentary Petrology*, Vol. 11, No. 2, 1941, pp. 64-72.

5. Pettijohn F.J., Sedimentary Rocks, 2nd Edition, Harper, New York, 1957.

6. Russell, R.D., and R.E. Taylor, Roundness and shape of Mississippi River sands." *Journal of Geology*. Vol. 45, No. 3, 1937, pp. 225–267.

7. Powers, M.C., A New Roundness Scale for Sedimentary Particles, *Journal of Sedimentary Petrology*, Vol. 23, No. 2, 1953, pp. 117-119.

8. Folk, R.L., Petrology of Sedimentary Rocks, Syllabus for Course 370K, 383L, 383M. University of Texas, Austin, 1965.

9. Norris, G., The Characteristic Friction Angle, Its Determination and Use, *Proc. 70th Highway Geology Symposium, Portland, Oregon.* Paper 14, 2019, 16 pp.

10. Wadell, H., Volume, Shape and Roundness of Quartz Particles,. *Journal of Geology*, Vol. 43, 1935, pp. 250-280.

11. Rittenhouse, G.A., Visual Method of Estimating Two Dimensional Sphericity, *Journal of Sedimentary Petrology*, Vol. 13, No. 2, 1943, pp. 79-81.

12. Norris, G., Recent Applicable UNR Geotechnical Research, *Proc of 73rd Highway Geology Symposium,* Lawrence, Kansas. Paper 14, 2024, 30 pp.

Blasting Design that Ensures Back-Slope Stability
How and why - There is a Need to Provide Specifications and Oversight that Protects the Final Slope

Daniel B Conn
Fragmentation Efficiency Services, Inc.
215 South Main St.
Zelienople, PA 16063
(412)-855-7423
dconn@kesco-fes.com

Prepared for the 74th Highway Geology Symposium, August, 2025

Acknowledgments

The author would like to thank the individuals/entities for their contributions to the work described:

Highway Geology Symposium
Dr. Calvin J. Konya
Peter Ingraham, P.E.

All the great geologists and geotechnical engineers that motivated us on past projects.

Disclaimer

Statements and views presented in this paper are strictly those of the authors, and do not necessarily reflect positions held by their affiliations, the Highway Geology Symposium (HGS), or others acknowledged above. The mention of trade names for commercial products does not imply the approval or endorsement of HGS.

Copyright Notice

Copyright © 2025 Highway Geology Symposium (HGS)

All Rights Reserved. Printed in the United States of America. No part of the publication may be reproduced or copied in any form or by any means – graphic, electronic, or mechanical, including photocopying, taping, or information storage, and retrieval system – without prior written permission of the HGS. This excludes the original author(s).

ABSTRACT

Traditional blasting practices will damage the final slopes for new cut and widening infrastructure projects. The downstream costs and increased liability are appreciable and can be avoided.

Fragmentation Efficiency Services, Inc. (FES) and KESCO have been engaged in every aspect of explosive manufacturing, use, and consulting for close to 70 years and may be in a unique position to frame and change how Owners and highway geologists understand and manage this problem. In one project, a 2003 United States Army Corps project in Grundy, Virginia, the initial blasting subcontractor was dismissed, and KESCO was contracted to execute two forms of precision presplitting. The net result was stable, and undamaged, final slopes in both a very weak shale and in the massive high compressive strength sandstone. These formations will be on display when we take our field trip through West Virginia. As our evolution as both a contractor and consultant evolved, FES was contracted more often to provide consulting for the specifications draft and oversight. One example was for the Vermont Agency of Transportation's Route 9 slope construction project.

This presentation has two distinct focuses:

First, we will show why there is a clear disconnect between what blasters are trained and contracted to do and what owners want and need.

Then, we will also outline design and oversight practices that must be included in project specifications and a request for pricing.

INTRODUCTION

First, we must recognize a disconnect between what is a blasters priority and what owners and engineers need. This is accomplished by looking back on history and considering certain industry facts:

What was the motivation behind the invention of explosives?

Initially black powder and gun powder were designed for weapons propulsion and sky bursts so that the enemy could be identified at night. It was then discovered that explosives functioned as an excellent tool for breaking rock. Today, we equate that finely fractured rock improves excavation cycle time and/or crusher throughput. In fact, muck pile gradation is part of most subcontracts.

How are blasters educated, trained, and certified?

Blasters are certified by state agencies and tasked with handling explosive products legally, safely, and to do no harm to the public. Blasters are primarily trained by explosives manufacturers and blasting contractors to break rock.

Is training provided for blasters to protect final slopes on infrastructure projects?

This training is not a focus when blasters are educated. After reviewing this paper, you may be able to ask questions that will verify that this connection to your goals is lacking.

Field interactions with engineers and project geotechnical reports have identified slope damage caused by the blasting practices during the initial highway slope construction. The root causes of this ongoing issue are identifiable. Blasting techniques are much to blame. This problem may be overcome through education and design of projects, blasting specifications and oversight. This position is not intended to direct blame but leads us to a question. Is it our intent to shift the risk of slope failure on the construction and blasting contractor, or could we motivate better outcomes through geology education of blasters and drafting specifications that lead the blasting firm to address geologic realities in their blast designs?

Therefore, specifications for blast designs must be tailored to redirect the blasters' consideration of project geology site realities and to include slope protection blast engineering requirements. What Owners want and need is for slope debris maintenance to be pushed out and low, and for slope failure liability connected to means and methods to be minimized and have design and specifications evidence.

OVERVIEW:

How Do Blasters Think – What is their Hierarchy of Priorities?

We have established that blasters' regulatory requirements include the protection of people, structures, and other items from damage caused by blasting operations. Therefore, addressing flyrock, excessive vibration, and air over-pressure are among the first priorities of the blast design process. After this, designing for fragmentation expectations become the focus of the design process. Slope protection does not carry equal weight in this process.
So, let us dig a little deeper into the fragmentation and liability management process and demonstrate how these weighted design factors can result in increasing the likelihood that final slope damage will occur.

If a blaster wants to improve fragmentation, the first instinct is to increase the pounds of explosives, or **powder factor,** which is a ratio of the pounds of explosives per target cubic yard. An advanced explosives engineer should study powder factors on a cross-sectional plane, on a single borehole level, and on a global basis across the entire blast bench. Simply stated, more explosives = better fragmentation! However, the goal of better fragmentation should have limitations as we get next to the final slope. *Are more pounds better when located next to the final slope?*

Presplit hole loads are a good place to examine whether the amount of explosive loaded is excessive. The design explosives engineer should consider whether commercially available presplit explosives are the correct load per foot for the boreholes located at the intersection of the final design slope. It has been proven by Dr. Calvin J. Konya and others that in most cases where commercially available packaged presplit load is used, that the energy is somewhere between 65% to 85% more than is required to induce a neat plane between holes in a row.

Another factor is the delay in timing between rows. In most geologic formations, **fast initiation timing** improves fragmentation! Fast timing can be a relative term but for this discussion, we will define it as 5 to 10 milliseconds of delay per foot of true burden between rows of holes. However, this fast timing next to the wall will increase pressure against the back slope. In some cases, the geological structure is massive and/or consisting of a high compressive strength formation and therefore can withstand the pressure confined when delay time does not permit rock movement for relief. Often, the strength, or structure, of the rock can withstand little gas pressure at the slope interface.

In the 1980s non-electric detonators were introduced and adopted by the blasting community at large. The motivation was both costs saving through reduced inventory elements and simplicity of use. The net result of this non-electric initiation introduction was simplified application and faster blast detonation. Typical bench delay timing became extremely fast.

Finally, **confinement** is essential to fragmentation and, in some cases, expended burdens the face are used to ensuring that blasted rock remains on the bench. Simply put, confinement is necessary to ensure that the explosive energy is most efficiently used to break rock. As we shall

illustrate, confinement is a function of not just the top stemming length, but also is defined by the true borehole burden, the borehole stiffness ratio, and the geometry of the overall cut height to width ratio.

While these items are considered by the blaster to achieve their fragmentation goals seldom, if ever, are they considered as a function of slope pressure and the potential for rock destabilization beyond the design template.

Blast Design Features That Must Be Addressed in Ensuring That the Final Slope is Protected

There are many essential components of a blast design that ensure the final slope is protected against the harmful effects of the confined pressures created during the explosion process. The following components are critical elements to enlighten project owners and their engineers to protect the final slope from damage.

1. Incorporation of the bedding orientation, other formation discontinuities, and properties into blast design.
2. Method of perimeter control.
3. Powder factor.
4. Confinement of the explosive energy in the pre-shearing process and in the boreholes next to the final slope.
5. Individual borehole stiffness ratio.
6. Overall bench geometry stiffness ratio as defined by the depth of the cut and the width of the bench as measured perpendicular to the final slope.
7. Delay timing in milliseconds per foot of true burden measured against a perpendicular axis connected to the final wall.
8. Slake durability differential as measured against the unique load explosive pressures.
9. Test blasting validation of the explosives engineering designs.

We will address these components in more detail.

Geotechnical Report Connection

Incorporation of the bedding orientation, other discontinuities, and properties of the site geology can have a significant impact on the customization of a blast plan. We are not certain whether all stakeholders assume that these geological components are addressed in the site-specific blast plan. Owners and engineers must ensure that they are used. The project specifications should identify this requirement and request specific documentation on how the two sciences are connected in the blasting plan. It would be beneficial to require a specific topic meeting prior to submission of the blasting plan to incorporate specific geologic information.

Perimeter Control

Perimeter control is a full range topic addressed in most blasting manuals and project specifications. Perimeter control techniques include line drilling, presplitting, trim blasting, buffer blasting, and cushion blasting. Often, these terms are misused, or not significantly understood by the owner. On most projects, the limitations for the use of these techniques are not defined.

Precision presplitting has been presented at previous HGS meetings, and should be mandated in all slope excavation projects due to the risk hazards associated with slope failure and subsequent potential impacts to the traveling public. Specified precision presplitting parameters should address the cut geological structure and rock strength. Precision presplitting uses explosive load weights that range from 65% to 85% less than the lightest cartridges manufactured for presplitting. Testing of a full range of borehole spacings and loads should be required. All project stakeholders should agree to the final design.

Other perimeter control techniques should be utilized to control the impact of blast holes within thirty feet of the final slope. These tools include the use of buffer holes, increased stiffness ratios, increased delay timing to allow sufficient rock movement, and reducing the overall bench geometry ratio where there is uncertainty of rock movement relief.

Powder Factor

Increasing the *explosive powder factor* (defined as pounds per target cubic yard) is the surest way to improve fragmentation. Explosives are the cheapest way to size rock as steel has always been more expensive than blasting products. Also, increasing the powder factor in areas outside the slope impact zone can aid in muck pile movement and assist in relieving pressure against the back wall. The powder factor is not often reduced as the boreholes get closer to the final slope. It is common for the blasting firm to communicate that the presplit weight must be large enough to move, or break, the rock in front of the slope. This is a sure sign that the blaster does not understand the physics of pre-shearing and the needs of the owner, thus not prioritizing the needs of the owner. And when the contractor is required to reduce the pounds per cubic yard next to the slope, they will complain about the oversize of the muck pile. The owner and engineer must design specifications that clearly state the rock size next to the slope will never define how the presplit or adjacent production holes are loaded.

Confinement

Confinement makes the rock fragmentation process work. Without confinement, explosive energy would simply burst out of the top of a blast hole and do-little work. It can also be said that too much of anything can degrade the intended outcome. Blast energy confinement can be found in many of the design variables of a blast. When solid explosives detonate, there are two forms of energy that get the intended fragmentation work accomplished.
As the reaction front travels through an explosive, a shock wave is transmitted into the surrounding rock mass but does not appreciably break the rock. Immediately following the full

chemical transformation, a large volume of gas exerts tremendous pressure that does the work of moving the mass and breaking the rock.

When considering confinement in the pre-shearing process, we want all the shear wave components to perform the work of creating the plane connecting holes, and we want none of the gas to displace or break the rock. Therefore, little confinement is desirable. Hence, sand is recommended as stemming material for precision presplitting. And we recommend less than 3 feet of sand stemming is used in the pre-shear boreholes.

In the mass rock area of the blasting bench, confinement is most often defined by the burden and stemming. The stemming material type and the depth of burial must be sufficient to eliminate flying debris and use the available energy in the most efficient manner. Simple borehole confinement/stemming depth ratio do normally range from 70% to 120% of true burden. Sometimes, the stemming ratios are increased to address hard rock at the bottom of a borehole or to lighten the pounds per delay, thus decreasing the potential for high vibrations.

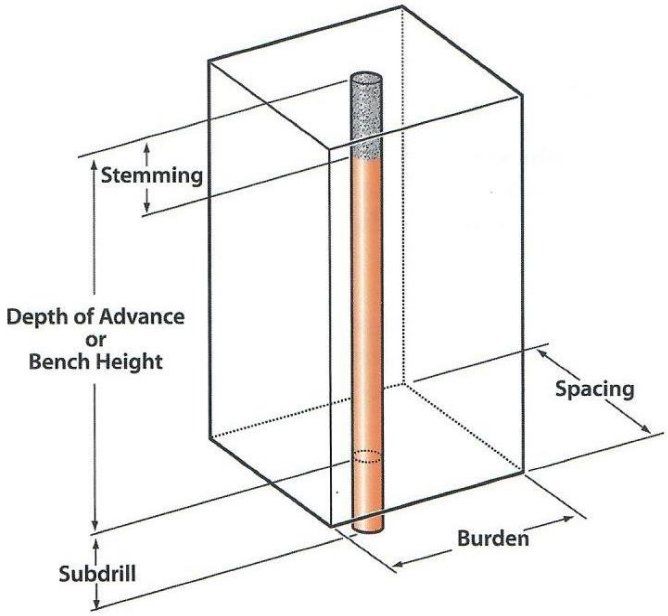


Figure 1 - Diagram of a Typical Blast Hole. Blast design dimension (*2*)

The burden is defined as the distance to a known face or to relief created by stemming, or delay timing in creating new faces as the blast moves through the detonation sequence. Assessment of the true burden of any borehole on the blast bench should involve thorough examination of all explosive engineering design factors. Often, the confinement components that could impact the amount of pressure realized at the final slope interface that are not considered in the design process include the stiffness ratio, muck pile build up generated by quick delay timing, and low overall bench geometry ratio.

Stiffness Ratio

Construction component stiffness is studied by engineering majors around the globe. This concept is essential in defining the strength of a support structure in relation to its length. As far as this author knows, Dr. Calvin J. Konya's Book entitled, Rock Blasting and Overbreak Control, was the first to attach this ratio to blasting burdens and define acceptable and outstanding parameters. The stiffness ratio of any borehole is defined as the propensity for this borehole flex or to move along the burden axis. The ability of the rock mass to move in a desired direction is greater if the depth to burden ratio is higher than a 3 to 1 ratio. If this ratio is 1 to 1 or less, there should be an expectation of cratering or excessive pressure in all directions surrounding a borehole location.

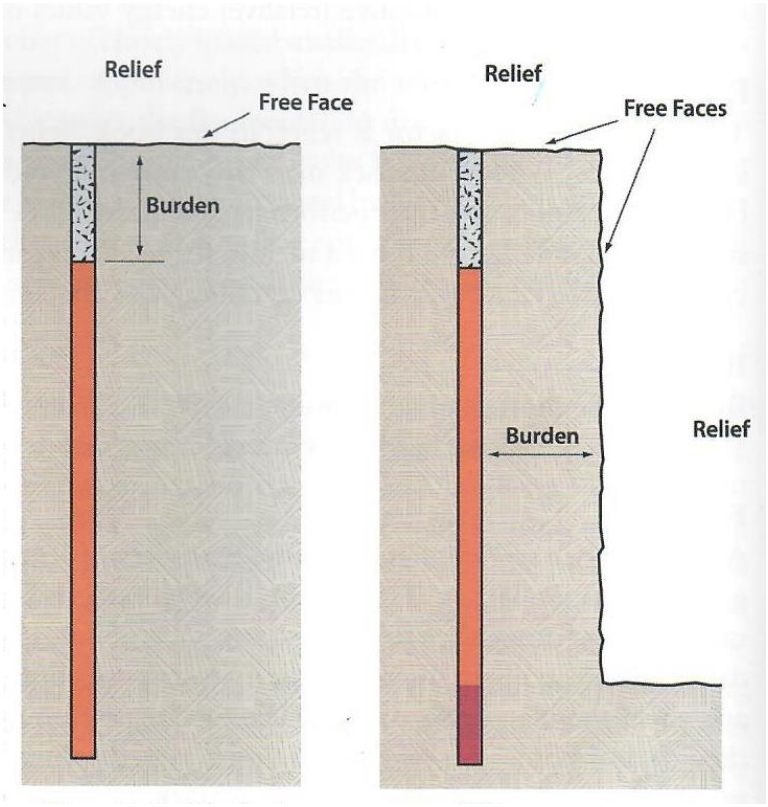


Figure 2 - Confined Blasthole and Relief (*2*)

The stiffness ratio of all boreholes near a final slope should be high enough to ensure movement and relief away from the slope and should accurately address the geology.

The selection of the burden in front of any hole, or row of holes, should consider stiffness ratio first. Then, the borehole diameter, charge diameter, and exact placement are determined using calculations that include the rock and explosive product specific gravity. Below you will find the burden determination chart found in Dr. Konya's book.

BURDEN ESTIMATE (IN FEET)

CHARGE DIAMETER (INCH)	DENSITY RATIO (DR) DENSITY OF EXPLOSIVE / DENSITY OF ROCK						
	0.20	0.30	0.40	0.50	0.60	0.70	0.80
1.25	2.3	2.6	2.9	3.1	3.3	3.5	3.7
1.50	2.8	3.2	3.5	3.8	4.0	4.2	4.4
1.75	3.2	3.7	4.1	4.4	4.6	4.9	5.1
2.00	3.7	4.2	4.6	5.0	5.3	5.6	5.8
2.25	4.1	4.7	5.2	5.6	6.0	6.3	6.6
2.50	4.6	5.3	5.8	6.3	6.6	7.0	7.3
2.75	5.1	5.8	6.4	6.9	7.3	7.7	8.0
3.00	5.5	6.3	7.0	7.5	8.0	8.4	8.8
3.25	6.0	6.9	7.5	8.1	8.6	9.1	9.5
3.50	6.4	7.4	8.1	8.8	9.3	9.8	10.2
3.75	6.9	7.9	8.7	9.4	10.0	10.5	11.0
4.00	7.4	8.4	9.3	10.0	10.6	11.2	11.7
4.25	7.8	9.0	9.9	10.6	11.3	11.9	12.4
4.50	8.3	9.5	10.4	11.3	12.0	12.6	13.2
4.75	8.8	10.0	11.0	11.9	12.6	13.3	13.9
5.00	9.2	10.5	11.6	12.5	13.3	14.0	14.6
5.25	9.7	11.1	12.2	13.1	13.9	14.7	15.4
5.50	10.1	11.6	12.8	13.8	14.6	15.4	16.1
5.75	10.6	12.1	13.3	14.4	15.3	16.1	16.8
6.00	11.1	12.7	13.9	15.0	15.9	16.8	17.5
6.25	11.5	13.2	14.5	15.6	16.6	17.5	18.3
6.50	12.0	13.7	15.1	16.3	17.3	18.2	19.0

INSTRUCTIONS FOR USE OF THE TABLE:

1. Divide density of explosive by density of rock to determine density ratio (DR)
2. Find density ratio in table, find charge diameter in column 1
3. Find where both vertical column and horizontal row intersect and read burden in feet

Figure 3 - Burden Estimate Konya, C. J. (*1*). Rock blasting and Overbreak Control. U.S. Dept. of Transportation, Federal Highway Administration, National Highway Institute

Overall Bench Geometry

The diagram below is from the 18th edition of the ISEE Blasters Handbook and shows the potential for energy transmission beyond the intended backwall.

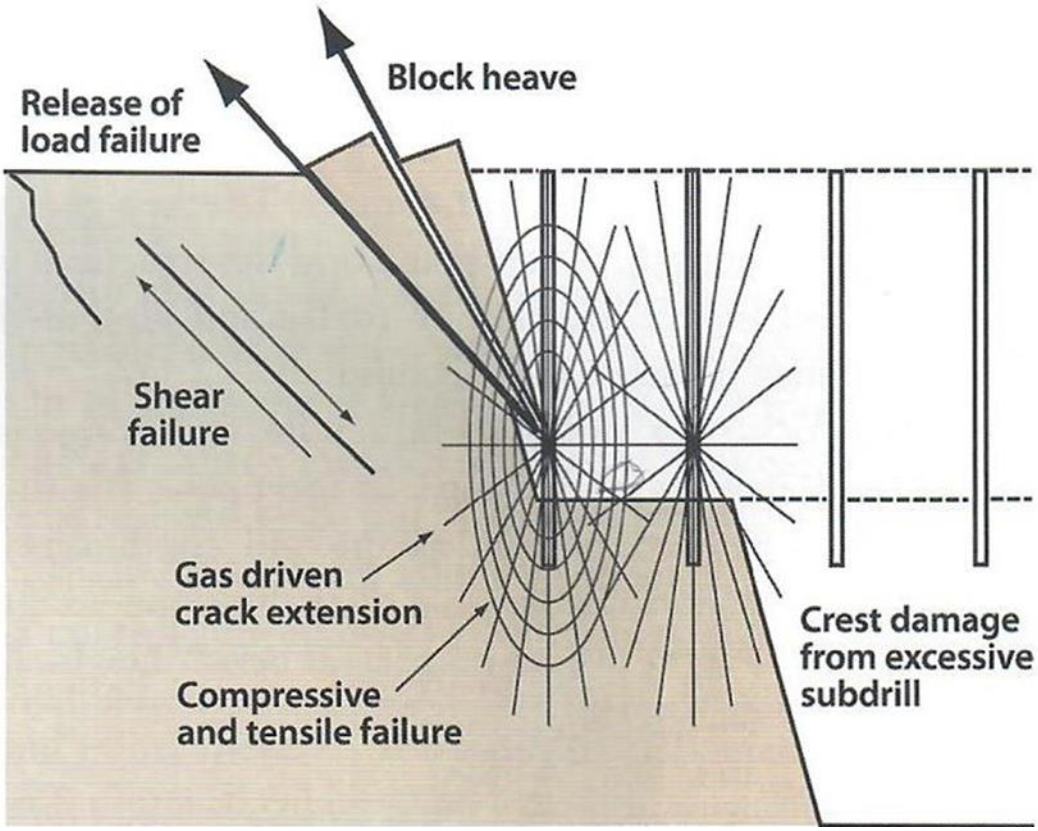


Figure 4 - Potential for energy transmission beyond the intended backwall (*2*, Figure 31.15)

The *overall bench geometry ratio* is like the concept of borehole stiffness ratio. Simply stated, rock/muck located next to a final slope cannot move during the detonation process if the ratio of the bench width is much greater than the cut depth stated. This concept can be seen as connected to the desired post detonation muck pile profile. The desired muck pile profile is most often connected to the type and operational limitations of excavation equipment. However, what infrastructure owners and engineers need has no connection to a desired muck pile profile. What is most desirable is for the mass rock next to the slope to have sufficient relief so that swelling forces and rock movement is in the direction perpendicular to the final slope axis. When a blast is designed correctly, this movement can be clearly viewed in post blast video analysis.

Fragmentation Efficiency Services has developed a series of diagrams and a moving storyline that may better illustrate the pressure problem that develops if the width of the bench does not allow for the rock next to the slope to move.

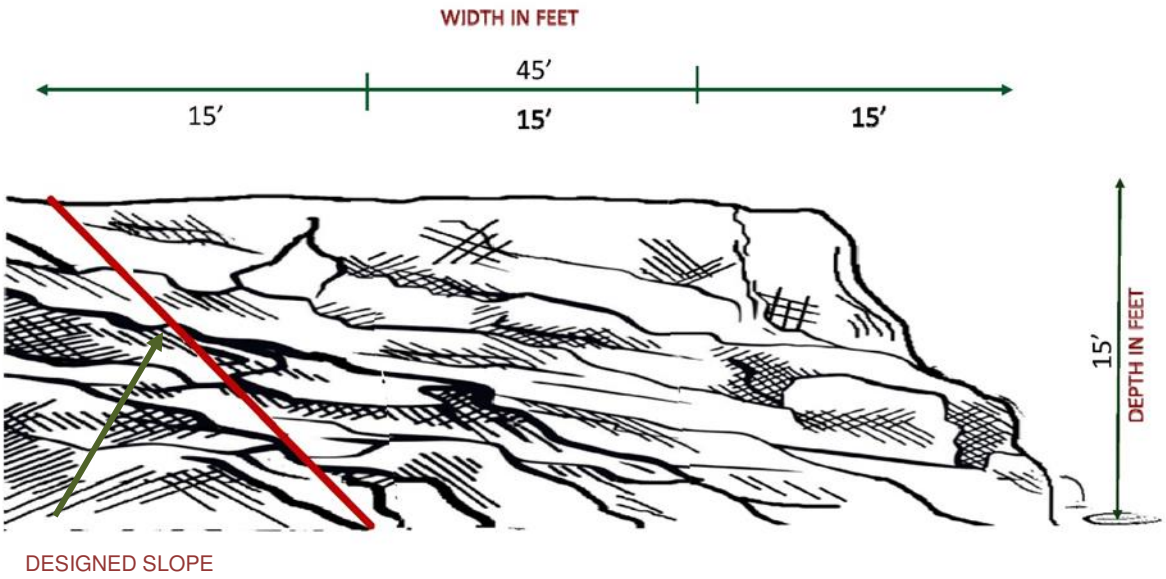


Figure 5 - Overall Bench Geometry

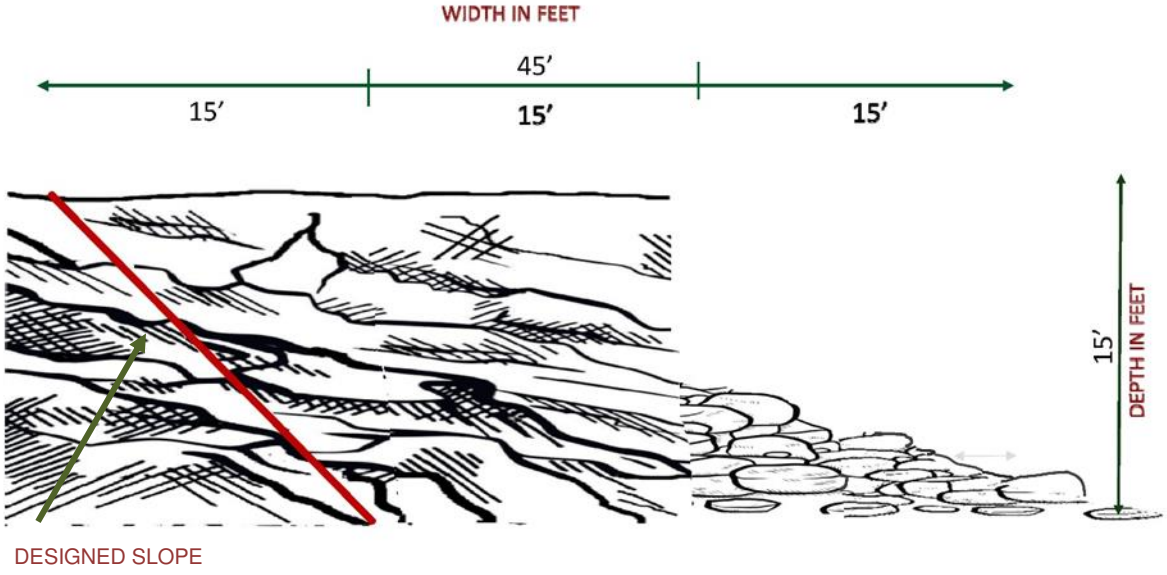


Figure 6 - Overall Bench Geometry

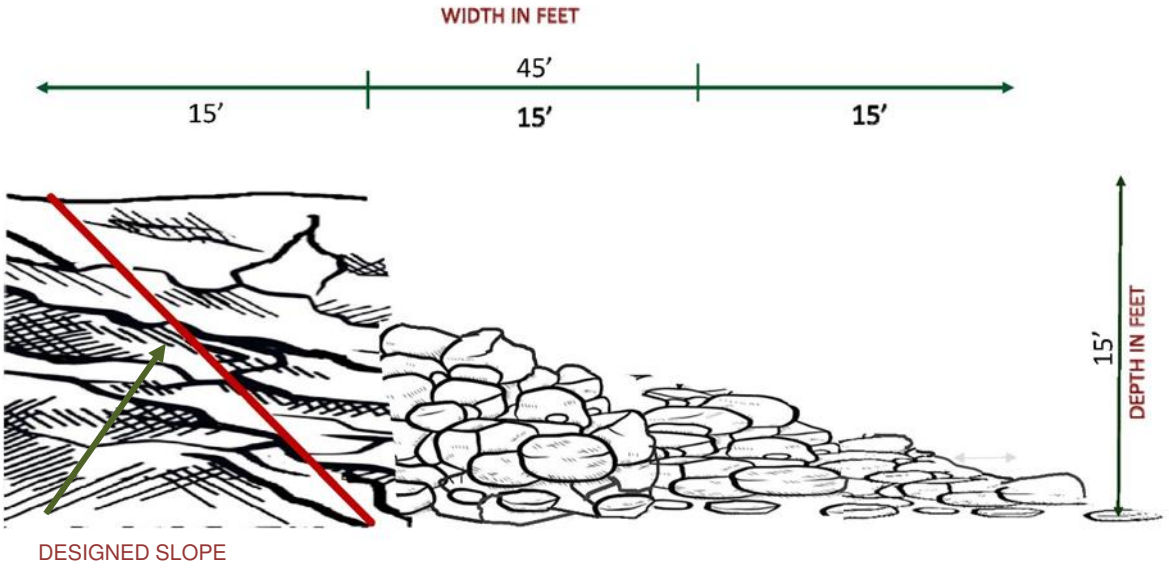


Figure 7 - Overall Bench Geometry

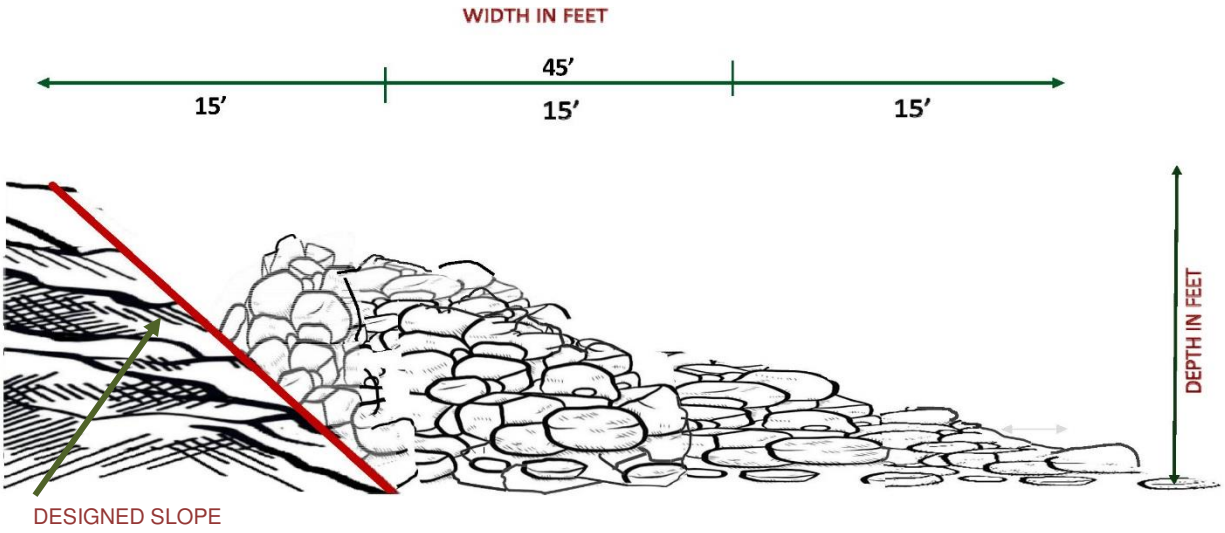


Figure 8 - Overall Bench Geometry

During highway development through cuts the blasting depth is most often defined or confined to the efficient reach length of an excavator. Fifteen feet bench heights are quite common. We see this as a shallow bench, and if the stiffness ratio concepts are considered, it would limit the true burden of any blasthole to 7.5 feet. Five feet of burden would better promote movement perpendicular to the slope.

In the same manner this bench height should reduce the width of blasting of the cut near the slope to 25 to 45 feet. If this bench width is unachievable or undesirable, then the powder factor, timing, and coupling design should be reduced. Expectations of a larger rock size next to the slope should be a given parameter.

In our experience, stiffness ratio as it pertains to the overall bench geometry is rarely, if ever, considered in blast engineering. This is unfortunate as this dismissal can promote wall damage. In close proximity of the final slope, blast cost and schedule should not be the primary design driver.

Delay Timing

Many decades have been devoted to the study of all things connected to blast initiation. These studies included detonator accuracy influence on both fragmentation and rock movement. We have long engineered our *blast delay timing* to have definable impact on verified rock movement and vibration control. It is this latter study component that could have a positive impact on the pressures realized at the final slope interface.

Delay timing, measured as the milliseconds per foot of true burden, should be implemented using site geology parameters and other explosive engineering design variables as guides. The timing near the final slopes should be sufficient to ensure that movement in a direction perpendicular to the slope axis is facilitated. Sufficient timing can, and should be, verified through video analysis.

Once again, fast timing enhances fragmentation by increasing confinement and can improve secondary breakage through repeated rubble impacts. And fast timing became more common with the introduction of non-electric detonators with their “out of the box” millisecond delay standards. We have witnessed so many occasions where 17, 42 and 59 milliseconds are used between blast rows regardless of the burden, stiffness ratio, or powder factor. Electronic detonators offer greater flexibility for customized delay timing but are rarely used in roadway construction due to the cost increase.

Fast delay timing can be beneficial in breaking rock, but the timing must be significantly slowed where necessary to accommodate relief next to the final slope.

Slake Durability Consideration.

Slake durability is a measure of rock strength and potential for differential weathering thus creating overhangs. Figure 9 Kentucky Department of Transportation Route 321 shows why overhangs are a problem. The overhangs may start out as inconsequential but over time weathering difference will widen the gap and can develop into a geotechnical hazard.

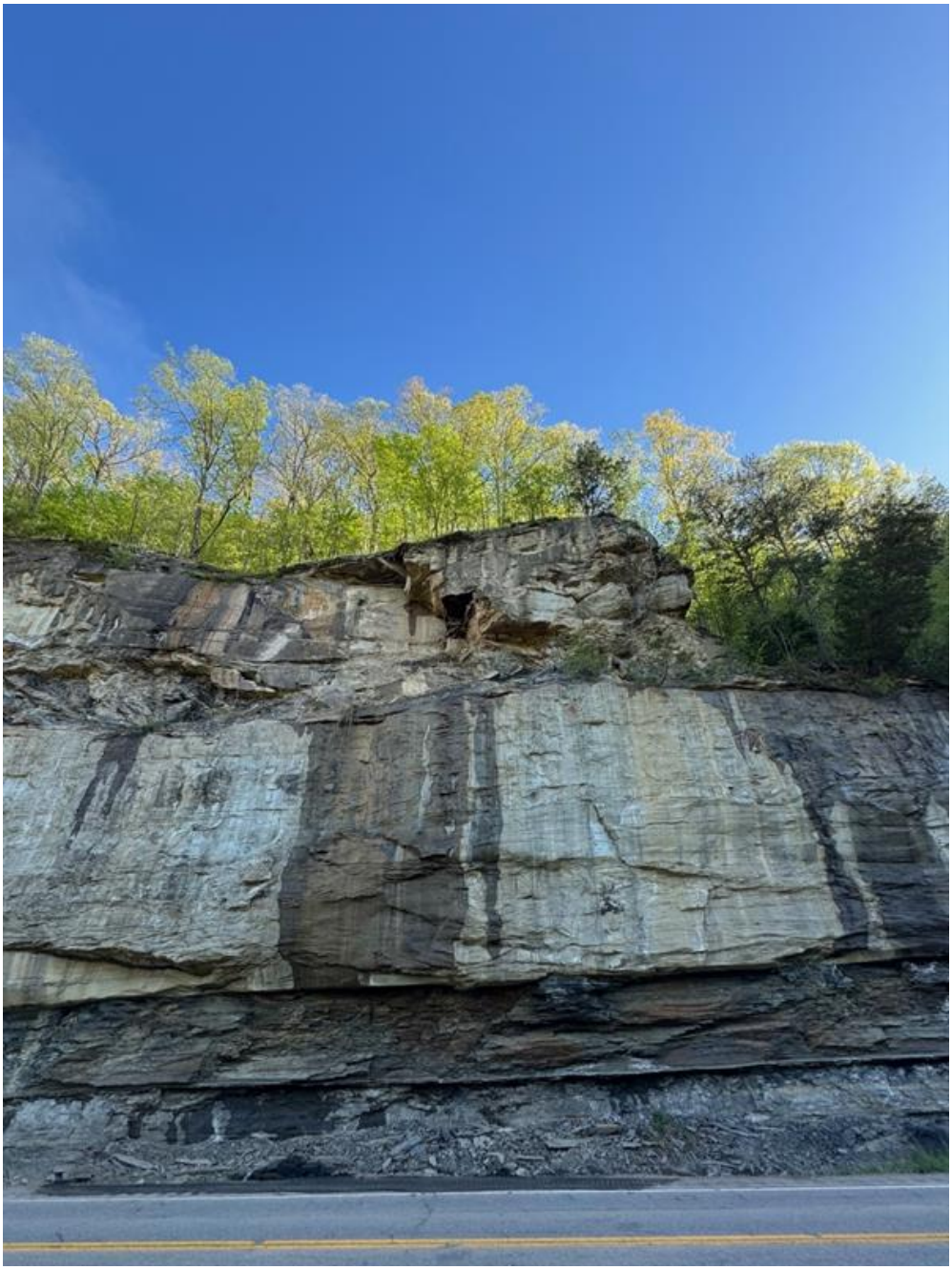


Figure 9 - Kentucky Department of Transportation Route 321

The geo hazard issue can be greatly truncated or acerbated, by the blaster's attention of borehole loading and delay timing. The explosive load and coupling strategy must be changed in weak rock zones for holes at or near the final slope. Decking is wise throughout the bench blast. Decking, or differential loading, is essential near the final slope when rock strength varies.

This concept circles back to our first requirement of an intense site geology study and contractor evidence of connection to a sophisticated blast design.

Test Blasting:

Test blasting as part of the field oversight process must also be required. The project specifications should define test blasting as an example of all probable means and methods and the owner should have considerable weight in selecting the final methods to be used for blasting near the slope. A consultant could assist the Owner in this decision and minimize liability. If oversight is not allowed in this phase of blast design, then previous experience shows that the contractor will utilize low-cost possibilities exclusively.

Other Consideration:

Other design variables that could positively impact owner satisfaction include sequencing of blasting operations and decoupled charges. The pre-shearing operation should always be completed in advance of production drilling and blasting. If this is impossible, then the presplit load design must have no impact on the boreholes used to break and move the rock in front of the face. Decoupling is an advanced method of controlling the time and amount of pressure surrounding the borehole. Decoupling is also effective in reducing debris movement from an open face near existing infrastructure components. Decoupling can also be a technique used to lighten the powder factor in buffer holes while also distributing available energy uniformly across the borehole cross section.

Also, video analysis of all blasting operations and slope inspection should be part of the project requirements. Drone views are very useful. Ground based views are helpful when overhanging features are present.

CONCLUSION

After decades of experience, we recommend an overhaul of traditional blasting specifications. Primarily, the focus of rock fragmentation gradation as the primary goal in blast design when working next to a final slope must be discouraged by owners. Blast design criteria that will ensure the final slope is left undamaged by blasting operations have been outlined in this presentation. All these items should be included in the project's blasting specifications. This can be accomplished by outlining the project goals and explosives engineering variables that must be included in the blast plan and would not include specific means and methods. These are engineering concepts and not actual empirical definitions.

Owners, geotechnical engineers, and field oversight personnel must have sufficient education so that they are comfortable in their accountability roles. Professionals who draft specifications and those who have blasting scope oversight in the field must have a thorough understanding of these critical explosive engineering design factors. It is common for the blasting subcontractor to point to geological issues as having an absolute connection to slope damage. We have proven that this is the most cases it is the blaster that has not thoroughly considered indigenous geology.

Slope failure has the kinetic potential to cause significant harm. All stakeholders must recognize this hazard and act. Great outcomes and lower downstream costs are achievable.

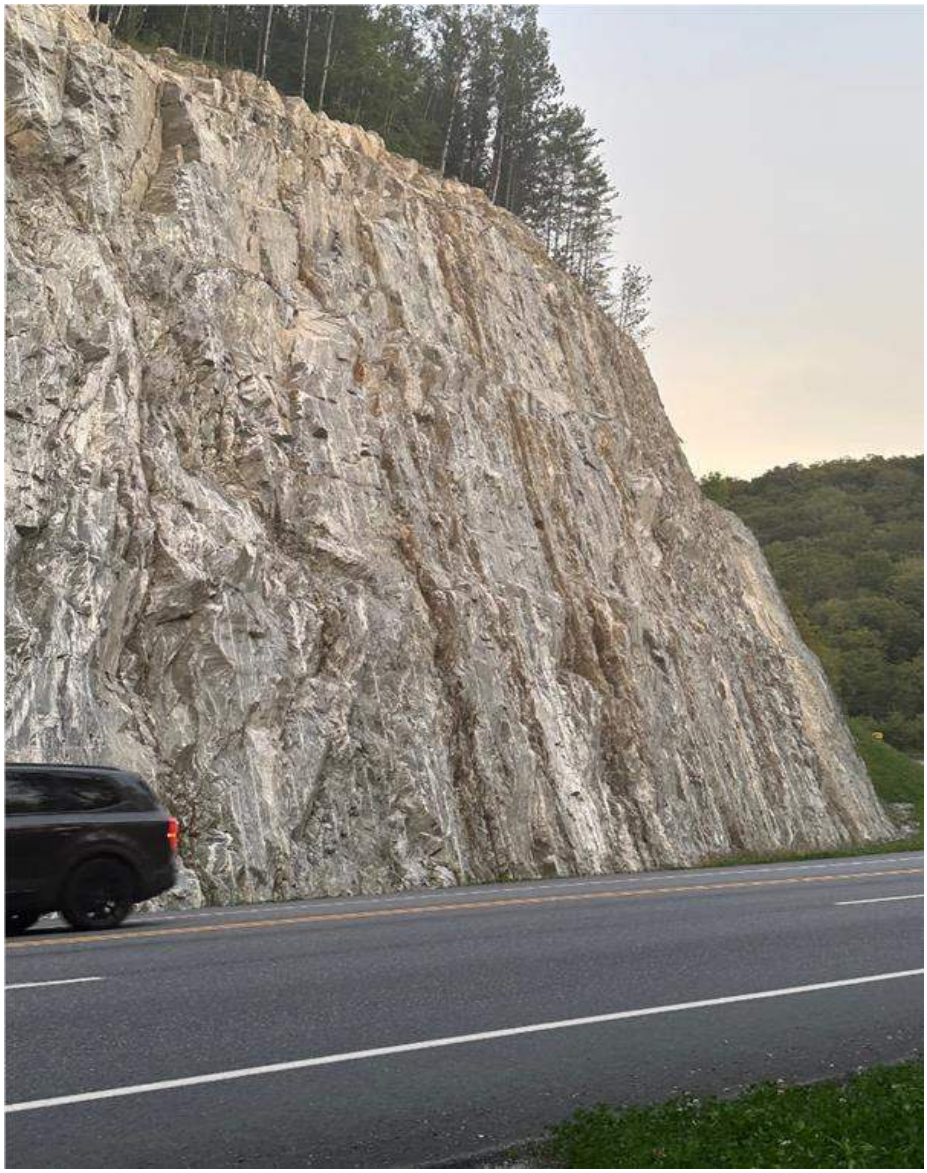


Figure 10 - Vermont Agency of Transportation's Route 9 Woodford VT, slope construction project

REFERENCES

1. Konya, C.J., Rock blasting and Overbreak Control. U.S. Dept. of Transportation, Federal Highway Administration, National Highway Institute, 2008.

2. Stiehr, J.F., ISEE Blasters Handbook, 18th Edition, International Society of Explosives Engineers, 2011.

Paw Paw Trail Slope Stabilization - Chesapeake & Ohio Canal National Historic Park

Nick H. Strater, P.G.
Brierley Associates
167 S. River Road, #8
Bedford, NH, 03110
(603) 918-0606
nstrater@brierleyassociates.com

Bob Stier
Drill Tech Drilling & Shoring
P O Box 1846
Cockeysville, MD 21030.
(410) 598-1933
bob.stier@drilltechdrilling.com

Joeseph Reed, P.E CFM
National Park Service
142 W. Potomac St.
Williamsport, MD 21795
(240) 291-6612
Joseph_reed@nps.gov

Brian C. Dorwart, P.E., P.G.
Brierley Associates
167 S. River Road, #8
Bedford, NH, 03110
(617) 510-8090
bdorwart@brierleyassociates.com

A. James Duffy, P.G.
Brierley Associates
167 S. River Road, #8
Bedford, NH, 03110
508-919-8650
jduffy@brierleyassociates.com

Prepared for the 74th Highway Geology Symposium, August, 2025

Disclaimer

Statements and views presented in this paper are strictly those of the authors, and do not necessarily reflect positions held by their affiliations, the Highway Geology Symposium (HGS), or others acknowledged above. The mention of trade names for commercial products does not imply the approval or endorsement of HGS.

Copyright Notice

Copyright © 2025 Highway Geology Symposium (HGS)

All Rights Reserved. Printed in the United States of America. No part of the publication may be reproduced or copied in any form or by any means – graphic, electronic, or mechanical, including photocopying, taping, or information storage, and retrieval system – without prior written permission of the HGS. This excludes the original author(s).

ABSTRACT

The Paw Paw Slope Stabilization Project is located in one of the most remote portions of the Chesapeake & Ohio Canal National Historical Park (CHOH), immediately adjacent to the historic Paw Paw Tunnel in western Maryland. The steep rock slopes on both sides of the canal have long plagued the Park with instability, including a significant rockslide in 2016, which closed the CHOH Towpath Trail, and destroyed a popular pedestrian boardwalk.

Utilizing a design-build contracting approach, the National Park Service teamed with Drill Tech and Brierley Associates to design and complete stabilization of 1,000 linear feet of rock slopes located on both sides of the canal, removal of the May 2016 rockslide debris field, and construction of a new boardwalk. The goal of the project was to improve park safety and access, while preserving the natural appearance of the site, and protecting sensitive historic features.

During site mobilization it was discovered that a second, previously undetected large rockslide was imminent, requiring immediate removal and adding additional challenges to the project from the standpoint of access and safety. Innovative slope stabilization methods included top-down excavation and rope-access scaling, site-specific spot and pattern rock anchors, use of pinned steel mesh, and placement of sculpted steel reinforced concrete buttresses.

HISTORY AND BACKGROUND

As early as 1820, the State of Virginia began to conduct land surveys between the Potomac River and the southern branches of the Ohio River for development of a continuous waterway to improve the flow of trade, including coal, lumber and agricultural goods. Constructed by the C&O Canal Company between 1828 and 1850, the Chesapeake & Ohio (C&O) Canal was one of the first largescale civil works projects funded by the U.S. Government, with supplemental funds provided by Maryland and Virginia.

The C&O Canal's navigational system stretched along the Potomac River for 184.5 miles from Washington, D.C. to Cumberland, Maryland. Collectively, the canal's navigational system was comprised of 74 lift locks, seven dams, over 168 culverts, 1 wooden and 11 stone aqueducts, an overall change in elevation of 605 feet, and included one tunnel (Paw Paw Tunnel) that carried the canal through a mountain. The canal would operate from about 1831 to 1924.

The Paw Paw Tunnel was constructed by the C&O Canal Company in lieu of building over 6.7-miles of canal along the Potomac River. The tunnel is approximately 3,118 LF long, 25-feet wide, brick-lined, and included open cuts through the interbedded shale and siltstone bedrock to establish the tunnel portals. Although it was originally anticipated to only take 2 years to construct this section of the canal, due to labor shortages, outbreaks of disease, work stoppages, and the arduous nature of the work, the project took 14 years with a construction duration that extended between 1836 and 1850. Following completion, the canal remained operational for 74 years until 1924. Today, it endures as a pathway for discovering historical, natural, and recreational treasures and serves as an important tourist destination. The original canal towpath, located on the east side of the canal, now serves as an active pedestrian and biking trail. It is estimated that approximately 250,000 annual visitors (many with heavily loaded bicycles) traverse through this area.

The Project vicinity is located in one of the most remote portions of the Chesapeake & Ohio Canal National Historical Park (CHOH), approximately 155 river miles upstream of Washington, DC, in Oldtown, Maryland. The Chesapeake & Ohio Canal National Historical Park is a U.S. Department of Interior, National Park Service (NPS) unit. Details of the project area are included in Figure 1 below. This region is notorious for having limited communication coverage and difficult rescue capability.

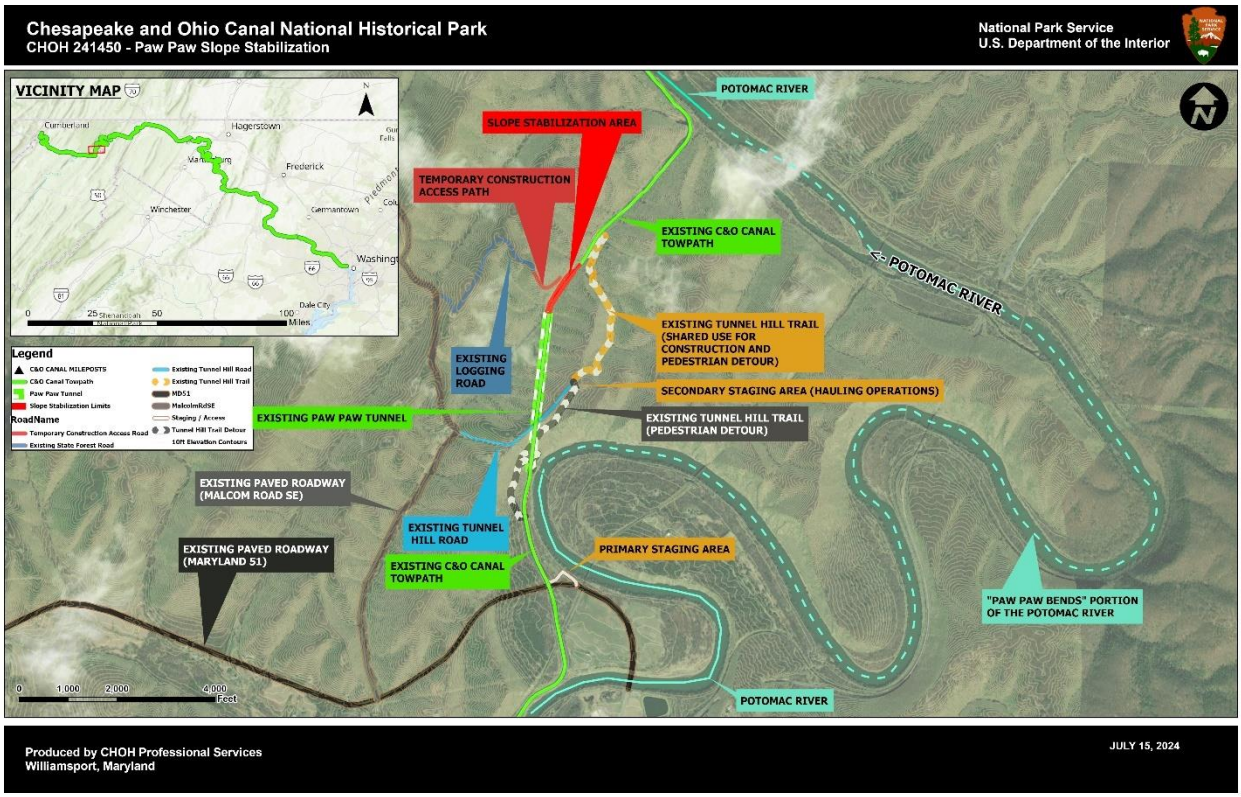


Figure 1 - Chesapeake & Ohio Canal National Historical Park Regional and Project Area

The canal area to the north of the tunnel is bordered and constrained by steep bedrock slopes, which have a long history of instability, presenting safety concerns to park visitors. There have been multiple rockslide events that have occurred since the canal's completion in 1850. Previous ad hoc efforts stabilization methods have included scaling, placement or bolts and loose mesh above the towpath. Photos showing the North Portal of the Paw Paw Tunnel are included in Figure 2 and slope 1950's era slope stabilization in Figure 3.



Figure 2 - North Portal Paw Paw Tunnel, 1890



Figure 3 - Rock Bolting and Scaling by NPS in 1950's, Eastern Slope

A significant rockslide was released from the western slope in 2016, filling the canal and damaging the wooden towpath trail boardwalk leading to the tunnel. Images of the 2016 rockslide are included in Figure 4 and shown in aerial footage in Figure 5.



Figure 4 - Images of 2016 Rockslide, taken 2021

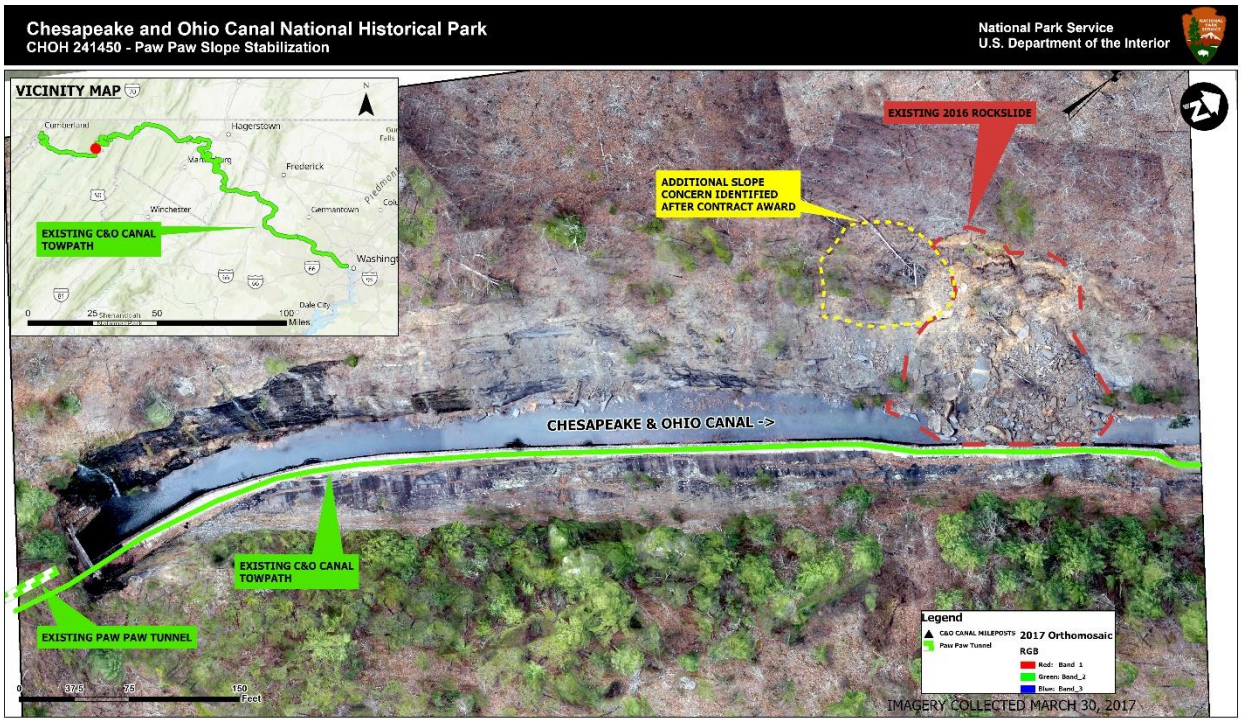


Figure 5 - Drone Photograph of Western Slope Circa 2017

In 2021, a design-build contract was awarded to Drill Tech Drilling and Shoring, Inc. (DTDS) to remove the 2016 slide debris, stabilize the adjacent slopes and replace the wooden boardwalk. The extent of the planned remediation extended from the north tunnel portal approximately 1,000-ft to the north as shown in Figure 5. The engineer of record for the design-build team was

Brierley Associates (Brierley). Construction management and onsite inspection was provided by Gannett Fleming. Overall contract administration was done by the National Park Service's Denver Service Center, and technical services prior to and during construction were provided by NPS Ohio Canal National Historical Park personnel.

SITE GEOLOGY

The project vicinity is located within the heart of the Valley and Ridge Physiographic Province. The bedrock in this area includes Ordovician to Mississippian marine and terrestrial sedimentary lithologies that were deposited within the Appalachian Basin and subsequently deformed during the late Paleozoic Allegheny Orogeny.

The rock slopes within the work area are comprised of moderately bedded shale, siltstone, and sandstone of the Upper Devonian Brallier Shale (Formation) which represent ancient submarine turbidity flow deposition (*1*). The bedrock has been folded, resulting in an anticlinal structure. The axis of the anticline is located immediately above the north tunnel portal and within the eastern rock slope bordering the work area, and trends approximately northeast-southwest, consistent with the broader Valley and Ridge trends. Flexural slip movement during folding resulted in slickensided bedding surfaces, and a distinct axial cleavage which trends northeast-southwest, and dips at steep angles to the northwest.

Within the work area, the bedding of the bedrock dips to the northwest, which encourages planar sliding failure of blocks on the southeast slope. A conjugate joint set dips to the southeast, which results planar sliding failure of blocks on the northwest (opposite) slope. This pattern can be seen in Figure 6. This conjugate joint set was determined to be the cause of the 2016 slope failure. In addition, a concentration of cleavage joints results in spalling and toppling failures along the upper portions of the southwest slope, and near the tunnel portal.

DESIGN

A schematic design was developed for the original design-build request-for-proposal by the NPS with the help of consulting services from Vanasse Hangen Brustlin, Inc. (VHB) and Terracon. As part of the schematic design development, a slope stability risk assessment was developed to prioritize 13 different discrete rockfall (RF) areas within the project area. These RF areas were carried through the subsequent stages of the design/construction and used to determine appropriate treatments and prioritizations.

After an intensive site reconnaissance Brierley developed a comprehensive slope remediation design that would include a combination of scaling (rock removal), pattern and spot bolts, pinned mesh, water control measures (internal drains and surface swale improvements), and anchored shear buttresses. A distinct remediation approach was developed for each RF zone, specific to the surface morphology, structural geology and previous slope behavior in that area.

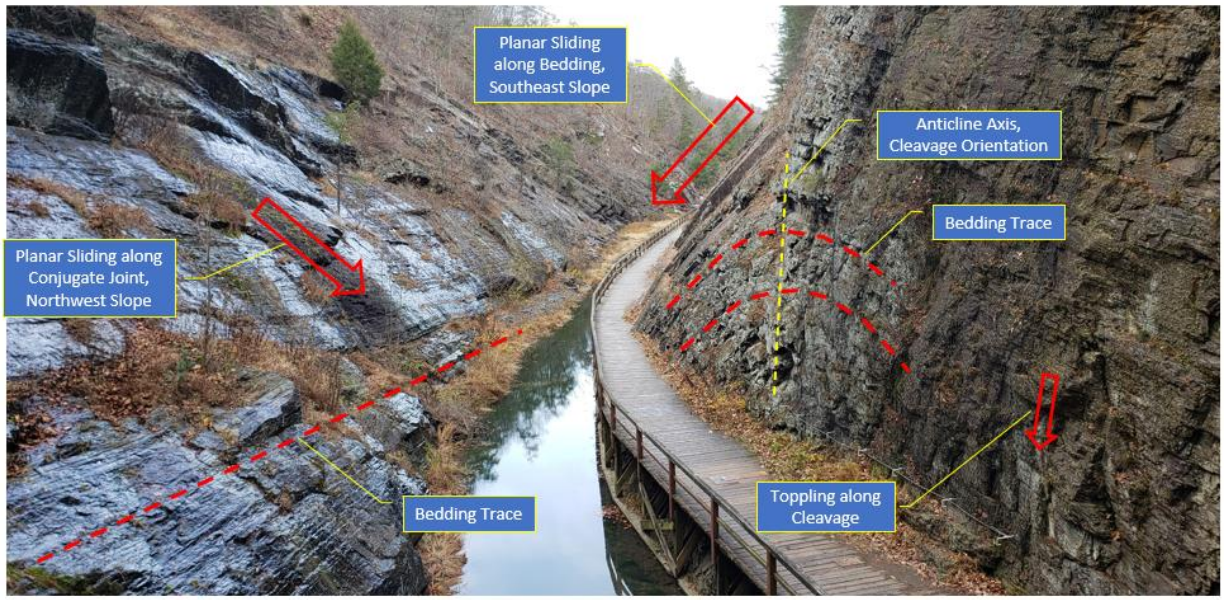


Figure 6 - Structural Geology and Rock Slope Failure Elements within the Canal, Facing North (Preconstruction)

Following a scaling program and removal of the 2016 slide debris, isolated rock blocks would be supported by spot anchors, whereas laterally extensive rock slabs would be addressed through application of a pattern anchor system. In each case the anchor design was developed to accommodate the individual block or slab size and slope geometry, and localized testing of anchors was completed to confirm capacity. For areas where upslope anchor installation might be problematic, anchored shotcrete shear buttresses were designed to provide supplemental support of both blocks and slabs. A variety of shear block designs were developed in advance to facilitate selection in the field during construction. Rock drains were included in the remedial design to reduce hydrostatic loading of the rock mass.

A pinned mesh concept developed for the upper portions of the southwest slope, and for a near-vertical section of the rock slope adjacent to the north tunnel portal, where pedestrians often stop for photographs, or to rest after completing the tunnel hike on the wooden boardwalk below. The mesh was intended to reduce rockfall potential caused by spalling and toppling of smaller blocks along the pervasive cleavage joints exposed in this area.

During initial site reconnaissance, an active rockslide was identified to the immediate south-southwest of the 2016 failure (Figures 5 and 7). The active slide was estimated to be about 125-ft (measured along slope) by 65-ft (measured up and downslope) in plan dimensions, and approximately 5 to 10 feet thick. The upslope limit of the active slide was defined by a tension crack and down drop scarp, and field measurements suggested that this mass had already moved downslope by about 1 to 3 feet. Given its size and degree of apparent movement, in-place stabilization of the active rockslide mass was not considered practical, safe or cost-effective, and a plan for removal was developed.



Figure 7 - Aerial Closeup of Active Rockslide, Adjacent to 2016 Rockslide.

PRECONSTRUCTION

Drill Tech Drilling & Shoring, Inc. (DTDS) could not start construction until the entire design was completed by Brierley and environmental permits from Maryland Department of the Environment (MDE) and U.S. Army Corps of Engineers (USACE) were obtained by DTDS with the assistance of KCI Technologies, Inc. DTDS also performed additional slope monitoring of the active slide area during the design and permit acquisition phases to track movement. Threshold stop work movement limits were established to ensure the safety of personnel working in this area.

Preservation of existing historic features throughout the Project site were critical to all parties. These included stone masonry placed during original canal construction, barge rope drag grooves (burn marks) within the adjacent rock mass, and the brick lining of the tunnel. Sauls Seismic, LLC performed preconstruction assessment of all existing historic features along the existing 3,118-foot-long Paw Paw Tunnel, approximately 4 miles of canal towpath and Tunnel Hill Trail, which would be used for equipment access. Solar-powered seismographs were installed at each of the Paw Paw Tunnel portals and at the midway point of the tunnel and continually monitored vibration and air overpressures. Automated alerts were disseminated via email if vibrations and/or air overpressure were detected above the thresholds of concern.

ROCK SLOPE SCALING

The project required over 110,000 SF of rock slope scaling and the removal of trees and vegetation. Slope preparation also required removal of 5,000 SF of pre-existing draped mesh

near the tunnel portal, which was judged to be ineffective. All scaling and removals were completed via rope access utilizing Society of Professional Rope Access Technician (SPRAT) certified workers (Figure 8). DTDS estimated approximately 500 CY of rock was removed from the slopes during the scaling process. The scaled material was removed from the site during the removal of the existing (2016 slide) slide material which was estimated by DTDS at approximately 2,900 CY. Materials removed were trucked from the site for disposal using the adjacent Tunnel Hill Trail.

ROCK ANCHORS

Installation of pattern and spot anchors began immediately following completion of scaling, using criteria established during design based on dimension of the rock (thickness, width) and angle of failure plane. The majority of the pattern anchors consisted of 8-ft long #10 galvanized threaded steel bars placed on an 8-ft x 8-ft pattern. While the design called for resin encapsulation of the bolts some of the anchors required cement encapsulation due to the weathered nature of the bedrock. Spot anchors consisted of 10 to 20-ft long, #10 galvanized threaded bars. It was originally envisioned that the anchors would be installed utilizing a long-reach Pegasus Drill staged at the bottom of the canal. However, due to the unforeseen active slide, staging of this drill at the toe of most of the slope was considered risky. The majority of the anchors were instead installed utilizing wagon drills with rope access and rope access drill technicians (Figure 8). In all DTDS installed over 10,000 LF of anchors during construction.



Figure 8 - Scaling and Rock Anchor Installation by Rope Access and Wagon Drill, Typical.

PINNED MESH

The design – build contract concept design envisioned rockfall protection mesh in the areas on the east side of the canal, above the towpath boardwalk, although not adjacent to the north tunnel portal. After detailed analysis by Brierley it was determined that additional rockfall protection

mesh would be required in this area to control long-term spalling of rock along the existing cleavage. The height of the bottom of the rockfall mesh was carefully coordinated to try to limit accessibility for unauthorized climbing of it by park visitors while balancing the need to mitigate the potential for spalling rock to endanger the traveling public. A minimum height of about 6-ft was applied for this purpose. A pinned Geobrugg Tecco® mesh was utilized and colored with powder coating to blend into the existing geology to minimize the visual impact. The mesh was "pinned" in place using 8-ft long #10 galvanized threaded steel bars. Over 30,000 SF of Tecco® mesh was installed by rope access drill technicians (Figure 9).



Figure 9 - Placement of pinned Geobrugg Tecco® Mesh.

SLIDE REMOVAL

A principal scope item of the design-build contract was removal and stabilization of the 2016 rockslide in area located on the west side of the canal, having an estimated area of approximately 7,000 SF and an in-place volume of about 2,600 CY. Once the slide material was removed spot and pattern rock anchors would be installed for long term stabilization. However, removal of the 2016 rockslide was complicated by the discovery of the active slide to the south (Figures 5 and 7). As noted, due to its size and unstable nature, it was determined that removal of the active slide would be required. A supplemental survey completed by DTDS determined that the 2016 and active slide had a combined area of approximately 27,000 SF, and that 10,000 CY on in-situ of material would need to be removed.

Initially controlled blasting was considered the safest and quickest way to remove the active slide and blast plan was developed by DTDS and Beckley Drilling and Blasting (BDB). This would involve drilling a series of angled blast holes upslope of the active slide, parallel to and below the

estimated slide failure plane. A new access path was pioneered into this area by DTDS in cooperation with NPS and the State of Maryland by using a portion of an existing logging road through Green Ridge State Forest and NPS lands (see Figures 1 and 10). To facilitate access, materials were also mobilized by helicopter. Unfortunately, the drill holes encountered zones of poor-quality, weathered bedrock and would not remain open, and the plan to complete the blasting was abandoned.

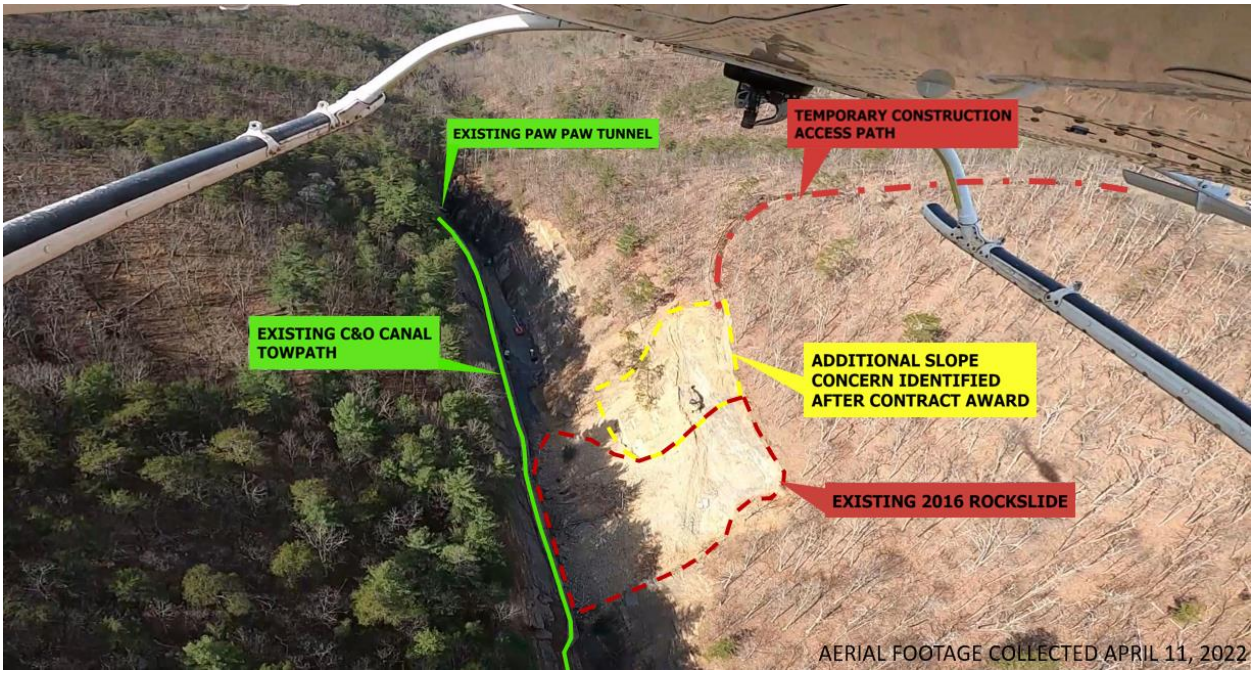


Figure 10 - Aerial View of Temporary Access Path Installation.

After close coordination with Brierley, NPS, and DTDS, it was decided to mechanically remove the active slide material rock utilizing excavators and breakers. To access the active slide from the north, switchbacks were installed on the western rock slope utilizing existing slide materials and scaled rock to allow the excavators to reach the upper limits of the slide (Figure 10). Given the magnitude of this effort, this became the critical path of the project and extended the schedule. Stabilization of the underlying slope was completed using wagon drills concurrent with slide material removal. DTDS estimated that about 13,000 CY of rock was removed from the slide area, downsized and removed from the site.

SHEAR BLOCKS

The lateral and upslope extent of the exposed rock slabs on the western rock slope necessitated the installation of shear blocks to provide additional support. The original schematic design included in the request for proposal (RFP) envisioned large, discrete cast-in-place steel reinforced concrete wedges spaced at regular intervals. As an alternative, Brierley developed a shear block design consisting of anchored, hand sculpted shotcrete with welded wire mesh and drainboards to reduce the buildup of hydrostatic pressures.

A water-based was incorporated to match the color of the native rock mass. The combined staining and sculpting resulted in shear blocks that blended so well into the adjacent geology that some visitors had difficulty identifying their locations. The sculpted and stained shotcrete was utilized on the remainder of the shear blocks with great success, minimizing the impact to the cultural landscape. Examples of finished shear blocks are shown in Figure 12.



Figure 11 - Establishment of Switchbacks and Removal of Additional New and 2016 Rockslide.

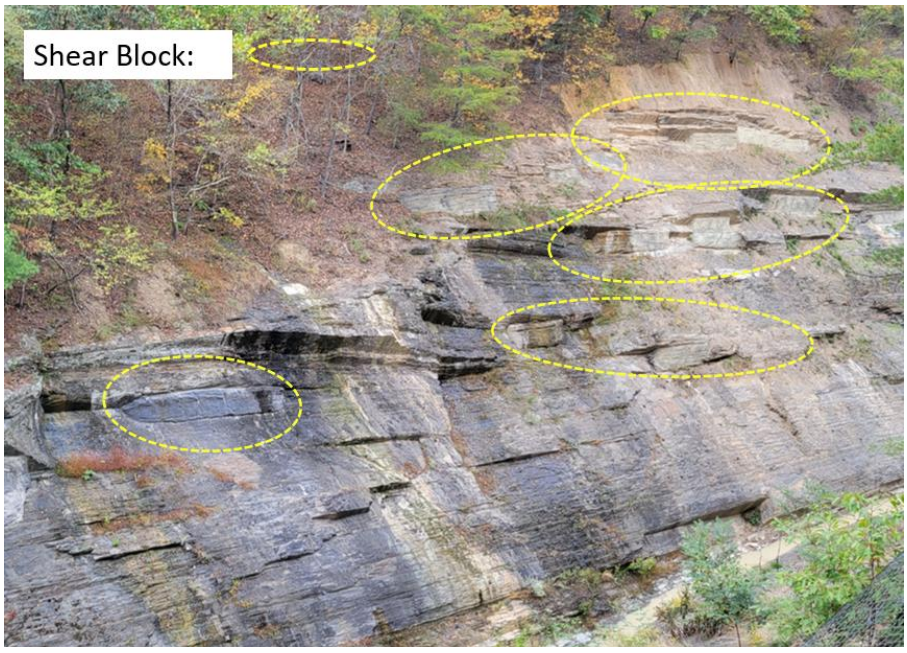


Figure 12 - Location of Finished Shear Blocks.

BOARDWALK

The design-build contract called for the demolition and re-installation of an approximately 700-foot-long wooden boardwalk connecting the portal of the tunnel to the rock towpath to the north of the site. Boardwalk construction occurred at the end of the project, once stabilization of the adjacent slopes was completed. The boardwalk design met the most recent codes and standards, most notably installing the vertical support posts on 8-foot centers with proper cross and angle braces. Greenway Bridge Company, the boardwalk subcontractor, was required to cut each of the deck boards within a tight tolerance to match the uneven rock face along the length of the boardwalk (Figure 13). Close coordination and adaptive design were required to avoid damaging the historic features that were to remain, including the rope burns in the rock face and the historic remnant of the towpath that was exposed at the southern end of the boardwalk. The final boardwalk construction was completed with no quality issues and to the satisfaction of the entire team.



Figure 13 - Finished Towpath Boardwalk

Conclusion

The Paw Paw Slope Stabilization Project advanced to the point of being able to reopen the park's primary trail system (C&O Canal Towpath/Boardwalk) in 1,066 days after award of the design-build contract. Throughout construction, the project team had to remain adaptive to the constraints of the project while maintaining a sensitivity and awareness to both the natural & cultural resources as well as the engineering. Overcoming logistical hurdles, technical challenges, and including measures to minimize impacts to the exceptionally rare resources in the project areas; the project team successfully delivered a project to stabilize the slopes on both sides of the canal for the approximately 1,000-LF of the North approach to Paw Paw Tunnel and in doing so preserved it for the current and future generations. Visitors can continue to visit the storied and historic Chesapeake & Ohio Canal and the notable Paw Paw Tunnel to not only learn more about the historic engineering of this marvel but also the fascinating geology that makes this setting so unique. This project exemplifies the potential of the design-build model for sites with challenging and varied conditions. Pre-construction conditions are included below to compare to the post-construction product (Figures 14 and 15).



Figure 14 - Paw Paw Slope Stabilization Project – Facing North at the 2016 Rockslide (November 2020 on left and October 2023 on right).



Figure 15 - Paw Paw Slope Stabilization Project – Facing at the 2016 Rockslide (May 2021 on left and October 2023 on right).

REFERENCES

1. Southworth S., D. Brezinski, R. Orndorff, J. Repetski, and D. Denenny, *Geology of the Chesapeake and Ohio Canal National Historical Park and Potomac River Corridor, District of Columbia, Maryland, West Virginia, and Virginia,* U.S.G.S Professional Paper 1961, 2008.

ATTERO:
A New Design Tool for Rockfall Attenuator Performance

Tim Shevlin, PG
Geobrugg NA, LLC
Salem, OR 97302
503-423-7258
Tim.shevlin@geobrugg.com

Remo Dudler
Geobrugg, AG
Romanshorn, Switzerland
Remo Dudler@geobrugg.com

Prepared for the 74th Highway Geology Symposium, August, 2025

Disclaimer

Statements and views presented in this paper are strictly those of the authors, and do not necessarily reflect positions held by their affiliations, the Highway Geology Symposium (HGS), or others acknowledged above. The mention of trade names for commercial products does not imply the approval or endorsement of HGS.

Copyright Notice

Copyright © 2025 Highway Geology Symposium (HGS)

All Rights Reserved. Printed in the United States of America. No part of the publication may be reproduced or copied in any form or by any means – graphic, electronic, or mechanical, including photocopying, taping, or information storage, and retrieval system – without prior written permission of the HGS. This excludes the original author(s).

ABSTRACT

Rockfall attenuators are passive rockfall protection solutions that have been utilized for decades and are often described by other names. Previously, the instrument of the experienced geohazard practitioner, the use of Rockfall Attenuators, has become more popular among general practitioners. To date, there are no formal solutions to attenuator design. There are no guidelines for testing and validating the attenuator performance, as there are for traditional rockfall barriers. Nor is there an accepted guideline like there is for classic draped mesh performance.

Attenuators present a very complex design challenge wherein they do not stop the rockfall but rather change the trajectory and moderate the velocity to varying degrees. These two design parameters are highly difficult to predict due to site, rockfall, and attenuator system variability. The performance is a complex interaction of the rock and attenuator net, the rock and the ground as the rock moves under the net, and the attenuator net and the ground, in the common case where the attenuator net lies on the ground.

Geobrugg presents a new design tool called ATTERO that is based on kinetics to estimate the performance of rockfall attenuator systems. The kinetic model considers the interaction between the rock and a hanging attenuator net; the model performance is validated from the results of a 3-year full-scale testing program. This paper summarizes the testing of Geobrugg's ATT systems and presents the ATTERO model.

INTRODUCTION

Rockfall attenuators are passive rockfall protection solutions that have been utilized for decades. Previously, the instrument of the experienced geohazard practitioner, rockfall attenuators have become more popular among general practitioners. A rockfall attenuator system combines posts from a flexible rockfall barrier elevating a standard unsecured drapery that lies on the slope, often called the attenuator tail. Although attenuators utilize posts and nets of a traditional rockfall barrier, an attenuator has an open, draped tail allowing rocks to pass through and exit to a designated collection area.

Attenuator systems have been called deflector nets, post-supported drapes, hybrid barriers, hybrid drapery, Type 2 Slope Protection (per Washington DOT), and hanging nets (*1*,*2*,*3*,*4*,*5*). While the literature generally uses all these names synonymously, others like to split attenuators and hybrid rockfall barriers further, where hybrid rockfall barriers use all the components of a standard rockfall barrier (posts, nets, top, bottom, and transmission support rope, and mechanical friction brakes), but having an extended, long net between the top and bottom ropes compared to the net length of a standard flexible barrier (*6*).

We subscribe to the modern term rockfall attenuator and define it as a completely free attenuator tail/ drape where there are no bottom or side support ropes, with the mesh secured to a top rope elevated off the ground by a series of posts. This precise description can be found in the literature, being called both Hybrid Drapery and Hybrid Barrier System (*1*,*2*,*3*).

Attenuators present a very complex design challenge wherein they do not stop the rockfall but rather change the trajectory and moderate the velocity to varying degrees. These two design parameters are highly difficult to predict due to site, rockfall, and attenuator system variability. The performance is a complex interaction of the rock and attenuator net, the rock and the ground as the rock moves under the net, and the attenuator net and the ground, in the common case where the attenuator net lies on the ground.

To date, there is no formal industry agreement on the successful performance criteria of an attenuator system or solutions/ boundaries to attenuator design. There are no guidelines for testing and validating the attenuator performance, as there are for traditional rockfall barriers (*7*,*8*). Nor is there an accepted guideline like there is for classic draped mesh performance (*9*).

The lack of guidance and agreement on the performance of rockfall attenuators creates uncertainty about what a successful outcome is for a rockfall attenuator. Often, practitioners request and specify attenuators with energy, as they do with traditional flexible rockfall barrier systems. The energy rating for rockfall barriers is the maximum energy that was successfully retained during the certification test. Assigning an energy rating to rockfall attenuators, which are not intended to stop rocks, is unclear and inappropriate.

In the case of an attenuator, is the practitioner asking for the attenuator to stop the energy requested? Not be damaged by the requested energy? Reduce the impact energy by the requested energy, regardless of the initial impact energy? Due to the variability of rockfall

attenuators and sites where they are applied, none of the scenarios described above are currently predictable and may never be possible.

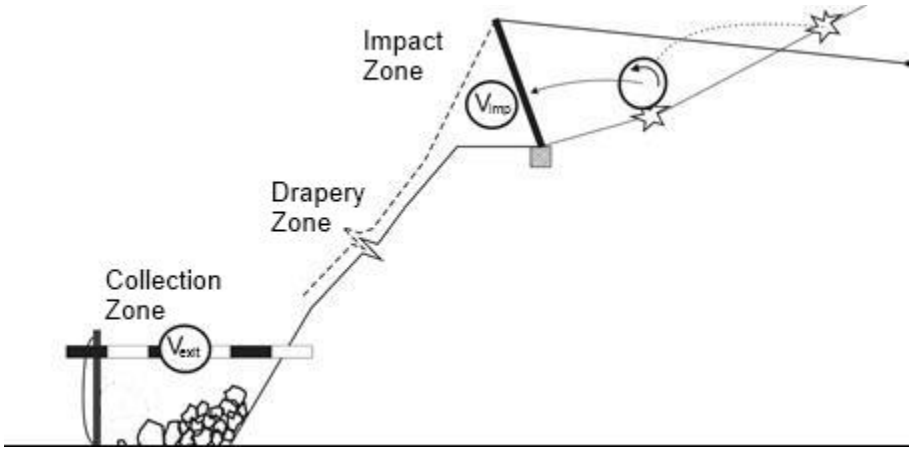


Figure 1: Sketch of typical post supported attenuator system Vimp = impact velocity; Vexit = exit velocity (*10*).

Testing

Flexible Rockfall Barriers

Rockfall mitigation dates back hundreds of years and can be linked to the period of building the first railroads in mountainous areas in Europe (*11*). Early rockfall protection barrier systems did not have known energy capacity, leading to the first field tests starting in Switzerland in the 1960s and continuing through today. Additional full-scale barrier field tests were conducted by the California Transportation Authority (*12*) and Brugg in 1989 in Big Sur, California, and then in 1992 in Switzerland (*11*). Decades of full-scale tests at different test site geometries and according to different procedures led to a series of data and information that are not easy to compare (*13*).

This was resolved in 2001 when a permanent, modern test site in Walenstadt, Switzerland, was brought online, allowing repeatable, controlled testing, and it is still in use today. At the same time, the *Guideline for the approval of rockfall protection kits* was published by the Swiss Agency for the Environment, Forests and Landscape (SAEFL) and the Swiss Federal Research Institute (WSL). This guideline requires a stringent field test and approval, allowing direct comparison of different rockfall barriers where the barrier must meet limit values. In 2009, another guideline, the *ETAG 027: Guideline for European Technical Approval of Falling Rock Protection Kits* (*7*), became valid. In 2018, ETAG 027 was replaced by the *EAD 340059-00-0106: Falling Rock Protection Kits* (*8,14*).

Attenuator Testing

With this long history of testing flexible rockfall barriers, the full-scale testing of rockfall attenuators came naturally. The paper *Raised Draperies: Defining Hybrid Barriers and Attenuators by Application* by John Duffy provides summaries of various full-scale attenuator tests performed over the past two decades. Attenuator testing was performed in Italy by IGOR Paramassi (2007); comprehensive testing by the Colorado Department of Transportation (2009); in Switzerland, a joint testing between Geobrugg and the WSL (2010); Canadian Attenuator Tests at Nicolum Quarry (2015–2017) by Geobrugg, LLC and Wyllie & Norrish Rock Engineers, Ltd. in Canada. All of these research programs tested different attenuator systems and net geometries, plus impact conditions varied significantly from using concrete blocks rolling across a weathered slope with vegetation, to concrete blocks dropped and rolling across constructed ramps, to natural and concrete blocks dropped onto hard bedrock slopes, not forgetting variations in slope angles and other conditions. These test facilities and programs generally allowed block impacts ranging from 100 to 500 kJ, with many more lower energy impacts and a few one-time larger impacts (*5*,*15*,*16*,*17*,*18*). Other unpublished attenuator tests are known to have additional interesting results and variability.

Geobrugg Nicolum Testing

The joint testing program to measure and validate the performance of rockfall attenuator systems was conducted from 2015 to 2017 by Wyllie & Norrish Rock Engineers, Ltd. in Canada and Geobrugg, LLC. The testing took place at the Nicolum Quarry near Hope, British Columbia, Canada, owned by the British Columbia Ministry of Transportation and Infrastructure (MoTI), which also used it for their own attenuator testing in the 1990s. Geobrugg's full-scale testing was documented with high-speed cameras, a data acquisition system, load cells, accelerometer, and gyroscope rock motion sensors inside steel reinforced concrete cubes. The initial round of testing conducted 26 tests during January and February of 2015. The initial testing validated the suitability of the site and identified extensive improvements that were made before the next round of testing in January of 2016, where 84 rocks were rolled. A third and final round of testing took place in 2017, where another 39 impacts were recorded. A total of over 200 rocks were rolled at the Nicolum quarry over the three test phases. All of Geobrugg's primary meshes (DELTAX, TECCO, SPIDER, Rolled Cable Nets, and ROCCO ring nets) were tested.

As summarized in Wyllie and Shevlin (*19*) the Nicolum Testing attempted to address future work cited in the above-mentioned studies:

- Attenuator design needs to consider how these systems work in conjunction with the terrain in which they are installed (*15*,*20*).
- Choice of netting properties (weight, length, and mesh size) that are tailored to terrain properties (slope angle, surface roughness, and material), and expected rockfall.
- Hazards (shape, size, and velocities) are the challenging decisions the rockfall engineer must face.

- Tests that focus on natural rockfall trajectories with both translational and rotational energy components are necessary over testing performed on inclined ropeways with no rotational energy velocity to the block (*15*,*16*).
- Attaining natural rockfall impacts into attenuator systems at energies higher than 100 ft.-tons (270 kJ) to 184 ft.-tons (500 kJ) (*2*).
- Evaluation of (a) how the attenuator absorbs the initial impact in the "fence" portion of the system, and (b) how the "tail" portion of the system contributes to the further attenuation of the kinetic energy of the rockfall blocks as they pass through the system (*16*,*21*).

The testing carried out at the Nicolum test site has provided very valuable information on the loading of the attenuator systems, the attenuation processes, and rock motion dynamics. This data led to an initial attenuator design tool that has been succeeded by the ATTERO kinetic model.

Attenuator Performance

The published literature about rockfall attenuators generally describes that the rockfall trajectory is changed, and many sources say that rockfall energy is attenuated, although without any specific values. It was notably stated:

- Rockfall attenuator systems, also known as hybrid rockfall barriers or hanging nets….do we know how they work, do we know what should be specified to have the intended rockfall mitigation? What is the mitigation strategy? Is the expectation to slow the rock down or stop the rock? (*19*).

- But what do we really know about their performance and capacity? There is risk associated with expanding systems that are installed based only on past experience if a practitioner wants to apply the same type of system to a case with larger or heavier rockfall and does not know the actual capacity of wire mesh and attenuator system (*5*).

To date, published attenuator testing and modeling have only demonstrated that attenuators withstand impacts up to relatively low initial rockfall impacts around 500 kJ, and to our knowledge, none have reported any energy attenuation magnitude. Most reports state that rockfall trajectories were changed, sometimes rocks stopped before exiting, while other impacts result in rocks exiting the attenuator. The published literature has not clearly developed a procedure for estimating the rockfall exit energy/ velocity of the unstopped rockfall or provided specific rockfall end locations after exiting. And attenuator certification guidelines have not yet been established.

ATTERO

Geobrugg's ATTERO software allows some insight into attenuator behavior. The practitioner defines the site-specific attenuator geometries and rockfall impact scenarios

(velocities, mass, and impact angle) and evaluates the change of the rockfall trajectory from a suite of Geobrugg's standard attenuator systems.

The model describes the interaction between a falling rock and a flexible attenuator net in a simplified, two-dimensional space (Figure 2a). The rock-slope interactions are neglected, and the mesh-slope interaction can be accounted for by modeling mesh-slope friction.

It focuses specifically on the moment the rock first hits the net and continues until it exits it again. To achieve this, the model uses six first- and second-order differential equations based on Newton's laws of motion (Figure 2b). These equations define how the rock moves horizontally, vertically, and rotates during the entire interaction.

The net is partially treated like a physical pendulum. This helps to simulate how the net swings and behaves from the rock impact. The model includes the movement of the net both above and below the rock, but it does not consider the final wrap-up of the rock in the net.

The model also considers how friction and rock shape influence the interaction. Rock shape is considered where angular rocks create more force due to their edges hooking onto the net. This effect is described with a shape factor and an additional time-based force function. These forces are then split into vertical and horizontal components, making it possible to calculate the total stress on the net.

This model's main purpose is to predict the forces acting on the mesh, which is key for designing rockfall attenuator systems. Table 1 shows the overall agreement of the calibrated model with the full-scale Nicolum test data. The model allows practitioners to simulate different rock shapes and impact scenarios without relying only on expensive field tests.

Table 1: Calibrated kinetic model comparison to Nicolum test data.

Dynamic Parameter	Agreement, %
Flight Time	88%
Net Deflection	82%
Reversal of Rotation	98%
Forces in support ropes	75%

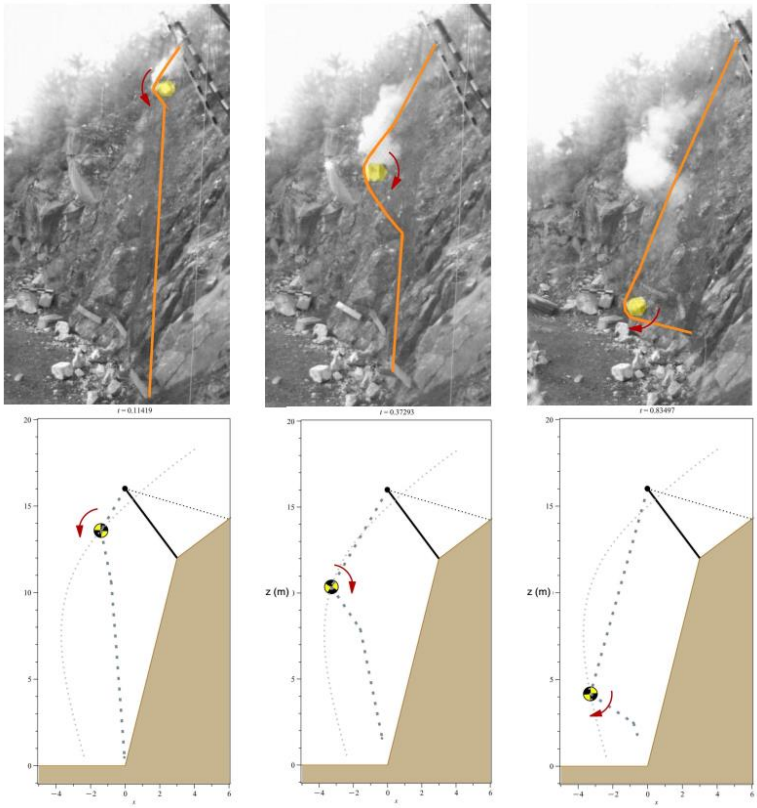


Figure 2a: (a) 0.12 sec after impact (test) (b) 0.38 sec after impact (test) (c) 0.83 sec after impact (test) - Frames of the high-speed footage of test T092, rock stays in contact with the net over the whole flight period. Orange: Position/deflection of the net, the rotation of the rock changes according to the red arrow, wrap up at the end of the attenuation process (d) 0.12 sec after impact (simulation) (e) 0.38 sec after impact (simulation) (e) 0.83 sec after impact (simulation) - Frames of the simulation at the same time steps.

$$\frac{d}{dt}x_n(t) = u_n(t) \tag{1}$$

$$m_s \cdot \frac{d}{dt}u_n(t) = S_x(t) \tag{2}$$

$$\frac{d}{dt}z_n(t) = v_n(t) \tag{3}$$

$$m_s \cdot \frac{d}{dt}v_n(t) = S_z(t) \tag{4}$$

$$J_s \cdot \frac{d}{dt}\omega(t) = M_s(t) \tag{5}$$

$$J_p(t) \cdot \frac{d^2}{dt^2}\varphi(t) = M_p(t) - k \cdot \frac{d}{dt}\varphi(t) \tag{6}$$

Figure 2b: First and second order differential equations that describe the general kinetics of the rock net interaction. x_n = coordinates in x direction, z_n = coordinates in z direction, u_n = velocity in x direction, v_n = velocity in z direction, m_s = rock mass, S_x = force in x direction, S_z = force in z direction, J_s moment of inertia rock, Omega = angular velocity rock, M_s = torque rock, J_p moment of inertia, Phi = angular velocity pendulum, M_p = Torque pendulum, K = damping coefficient

CONCLUSIONS

Numerous full-scale tests of attenuators have been conducted, and very good data has been collected. All performance data is unique to one site and generally uses one-size attenuator geometry. The application of attenuators for rockfall mitigation is very site-specific due to the endless variability of attenuator sizes and slope conditions.

To date, there is no formal industry agreement on the successful performance criteria of an attenuator system or solutions/ boundaries to attenuator design. There are no guidelines for testing and validating the attenuator performance, as there are for traditional rockfall barriers (SAEFL, ETAG, EAD). Combine this with the variability of rockfall dynamics, where simulations present a probability of results based on statistical models. Furthermore, recognize the fact that the attenuation process is a combination of rock into mesh, rock into slope, and mesh interacting with the slope as the rock moves the mesh.

Due to the variability of rockfall dynamics and attenuator geometries, it could be the case that full-scale certification testing similar to what we do for standard flexible rockfall barriers is unproductive and not cost-effective. The ATTERO model is a first step in providing practitioner guidance in the performance of attenuator systems.

REFERENCES

1. Badger, T.C., J.D. Duffy, F. Sassudelli, P.C. Ingraham, P. Perreault, B. Muhunthan, H. Radhakrishnan, O.S. Bursi, M. MolinarI, and E. Castelli, Hybrid Barrier Systems for Rockfall Protection, in A. Volkwein et al. (eds) *Proceedings from the Interdisciplinary Workshop on Rockfall Protection, Morschach, Switzerland*, 2008. pp. 10-12.

2. Badger T.C. and J.D. Duffy, 2012, Drapery Systems In *Rockfall: Characterization and Control* Transportation Research Board, National Academy Press, Washington, D.C., 2012. pp 554-576.

3. Turner, A. K., and R. L. Schuster, (Eds.) *Rockfall: Characterization and Control*. Transportation Research Board, National Academies Press, Washington, D.C., 2012. https://doi.org/10.17226/27824

4. Andrew, R.D., R. Barttingale, and H. Hume, *Context Sensitive Rock Slope Design Solutions*, Publication FHWA-CFL/TD-11-002. Federal Highway Administration, Central Federal Lands Highway Division, Lakewood, CO, 2011.

5. Duffy, J. D., *Raised Draperies – Defining Hybrid Barriers and Attenuators by Application*. Presented at the 72nd Highway Geology Symposium, August 14–17, 2023, Tacoma, Washington. Available online.

6. Bichler, A. and Stelzer, G., A fresh approach to the hybrid/attenuator rockfall fence, *Landslides and Engineered Slopes: Protecting Society through Improved Understanding* edited by Eberhardt et al. Proceedings of the 11th Annual Symposium on Landslides and Engineered Slopes, Banff, Canada, 3-8 June 2012, Taylor and Francis Group, London, 2012, pp. 1209-1214.

7. EOTA (European Organisation for Technical Approvals), *ETAG 027: Guideline for European Technical Approval of Falling Rock Protection Kits*. Brussels: EOTA, 2008. Retrieved from http://www.eota.be

8. EOTA (European Organisation for Technical Assessment), *EAD 340059-00-0106: Falling Rock Protection Kits*. Brussels: EOTA, 2018. Retrieved from http://www.eota.be

9. Muhunthan, B., S.Shu, N. Sasiharan, O.r A. Hattamleh, T. C. Badger, S. M. Lowell, and J. D. Duffy, Design guidelines for wire mesh/cable net slope protection, *Report N. WA-RD* 612, 2005.

10. Mumma, S., Research into and Application of Attenuator Rockfall Protection Systems, *Proceedings, 63rd Highway Geology Symposium,* Redding, CA, May 2012.

11. Spang, R. M., and R. Bolliger, *From the timber fence to the high-energy net: Developments in rockfall protection from the origins to the present*, Paper presented at the Geobrugg Jubilee Conference, Bad Ragaz, Switzerland, 2001.

12. Kane, W. F., and J. D. Duffy, *Brugg Low Energy Wire Rope Rockfall Net Field Tests* (Technical Research Report 93-01), Department of Civil Engineering, University of the Pacific, Stockton, CA, and California Department of Transportation, San Luis Obispo, CA, 1993.

13. Peila, D., and C. Ronco, *Design of reinforced ground embankments used for rockfall protection*. Natural Hazards and Earth System Sciences, 9(4), 2009, pp. 1189– 1199. https://doi.org/10.5194/nhess-9-1189-2009

14. Volkwein, A., W. Gerber, J. Klette, and G. Spescha, Review of Approval of Flexible Rockfall Protection Systems According to ETAG 027. *Geosciences, 9*(1), 2019, p. 49. https://doi.org/10.3390/geosciences9010049

15. Arndt, B., T. Ortiz, and K, Turner, *Colorado's Full-Scale Field Testing of Rockfall Attenuator Systems*, Transportation Research Circular E-C141, Transportation Research Board, October 2009.

16. Glover, J., A. Volkwein, F. Dufour, M. Denk, and A. Roth, Rockfall attenuator and hybrid drape systems - design and testing considerations. In: *Third Euro-Mediterranean Symposium on Advances in Geomaterials and Structures. Third Edition*, *Djerba*, 2010. pp. 379-384.

17. Shevlin, T., D.C. Wyllie, J.M.H. Glover, and C. Wendeler, Development of design method for rockfall Attenuators, NASL Roanoke, VA, June 4-8, 2017.

18. Hofmann, H., and T. Shevlin, *Advances in Rockfall Protection: A Preliminary Design Tool for Attenuators Estimating Rockfall Kinetic Energy as a Function of Rock Mass*, Presented at the 70th Highway Geology Symposium (HGS), Roanoke, VA, October 2019.

19. Wyllie D.W. and T. Shevlin, 2015, Attenuators for controlling rockfall: Do we know how they work? Can we specify what they should do?, *Proceedings, 66th Highway Geology Symposium,* Sturbridge, MA, September 2015.

20. Glover, J., A. Volkwein, W. Gerber, and M. Denk, Design criteria for rockfall attenuating systems. [Abstract] *Geophys. Res. Abstr.* 13: EGU2011-13273, 2011.

21. Eliassen, T.D., *Evaluation of Hybrid Rockfall Barrier/Drape System Initial Report Experimental Features*, Report 2011-1, Reporting on Work Plan 2008-1, Vermont Agency of Transportation, 2011.

Optical and Acoustic Televiewer Logging in Competent and Unstable Rock

Jorgen Bergstrom, P.G., P.Gp.
Collier Geophysics
889 Franklin Gateway SE, Suite 104
Marietta, Georga 30067
(770) 543-8444
jbergstrom@colliergeophysics.com

Prepared for the 74th Highway Geology Symposium, August, 2025

Disclaimer

Statements and views presented in this paper are strictly those of the authors, and do not necessarily reflect positions held by their affiliations, the Highway Geology Symposium (HGS), or others acknowledged above. The mention of trade names for commercial products does not imply the approval or endorsement of HGS.

Copyright Notice

Copyright © 2025 Highway Geology Symposium (HGS)

All Rights Reserved. Printed in the United States of America. No part of the publication may be reproduced or copied in any form or by any means – graphic, electronic, or mechanical, including photocopying, taping, or information storage, and retrieval system – without prior written permission of the HGS. This excludes the original author(s).

ABSTRACT

Optical and acoustic televiewer geophysical logging is common in transportation projects to gather valuable information about subsurface conditions such as rock mass quality and the orientation of discontinuities that may influence stability. Televiewer logging facilitates the determination of the dip and strike of bedding planes and foliation, that is crucial for understanding the geological structure and anisotropy of the rock mass. It also serves as a tool for orienting recovered core samples by providing a visual reference for matching features. The high resolution of televiewer logs allows for the detection of thin beds, veins, and other small-scale features that might be overlooked by other logging methods, and it can reveal indicators of fluid flow, such as mineral precipitation or staining. Furthermore, it allows for detailed mapping of natural fractures, drilling-induced fractures, and other discontinuities, and aids in assessing rock mass quality by identifying discontinuities and weathered zones with the orientation of these planar features accurately determined.

Using these tools, engineers can assess the integrity and quality of rock masses and other features that may affect the stability and performance of transportation structures. This paper includes case studies using acoustic and optical televiewers to assess rock integrity at proposed rock cuts and bridge abutments. Televiewer logging in unstable rock using a drilling/grouting/re-drilling technique is also reviewed.

HISTORY OF TELEVIEWER LOGGING

The development of the televiewer logging tools marks a significant evolution in borehole imaging technology, progressing from early, rudimentary methods to advanced, high-resolution systems used today.

A pivotal development occurred in the late 1960s with the introduction of the first acoustic televiewer (ATV) by Mobil. The ATV uses acoustic waves to create an image of the borehole wall based on the amplitude and travel time of reflected signals. The ATV provides a magnetically oriented, pseudo-image that can reveal fractures and other features, marking a significant step beyond direct optical methods, especially in fluid-filled boreholes where optical visibility is limited. The first generation of optical televiewers (OTV) was launched in 1999. These tools provide high-resolution, magnetically oriented, color images of the borehole wall, offering a direct visual representation akin to a virtual drill core, particularly valuable in air-filled or clear fluid-filled boreholes.

Since the early 1990s, there has been a considerable increase in the use of televiewers, driven by the demand for higher resolution images, faster data acquisition rates, and the advent of slimline logging systems. Modern televiewers incorporate sophisticated digital recording techniques, advanced beam focusing, increased dynamic range, and built-in high-precision orientation sensors (three-axis magnetometers and accelerometers) for accurate image orientation. Software for processing and interpreting televiewer data has also evolved significantly, with advanced 2D and 3D imaging packages offering corrections for borehole conditions and automated structural analysis algorithms.

Today, both ATV and OTV are considered mainstream tools for borehole logging in rock, providing invaluable information about lithology, structures, and fractures within boreholes across a wide spectrum of applications, from petroleum and mining to geotechnical and environmental studies. The technologies continue to advance, with ongoing developments focused on enhancing image resolution, operational efficiency, and interpretive capabilities.

OPTICAL TELEVIEWER

The OTV log is a sophisticated borehole imaging technique that delivers a continuous, high-resolution, oriented, true-color digital image of the borehole wall. This method relies on optical principles to directly visualize the borehole wall, offering a wealth of detailed information about the geological and structural characteristics of the formations intersected by the borehole. A high-resolution digital camera, often paired with a wide-angle or fisheye lens and a reflective conical or hyperbolic mirror, captures an oriented 360-degree panoramic view of the borehole circumference (Figure 1).

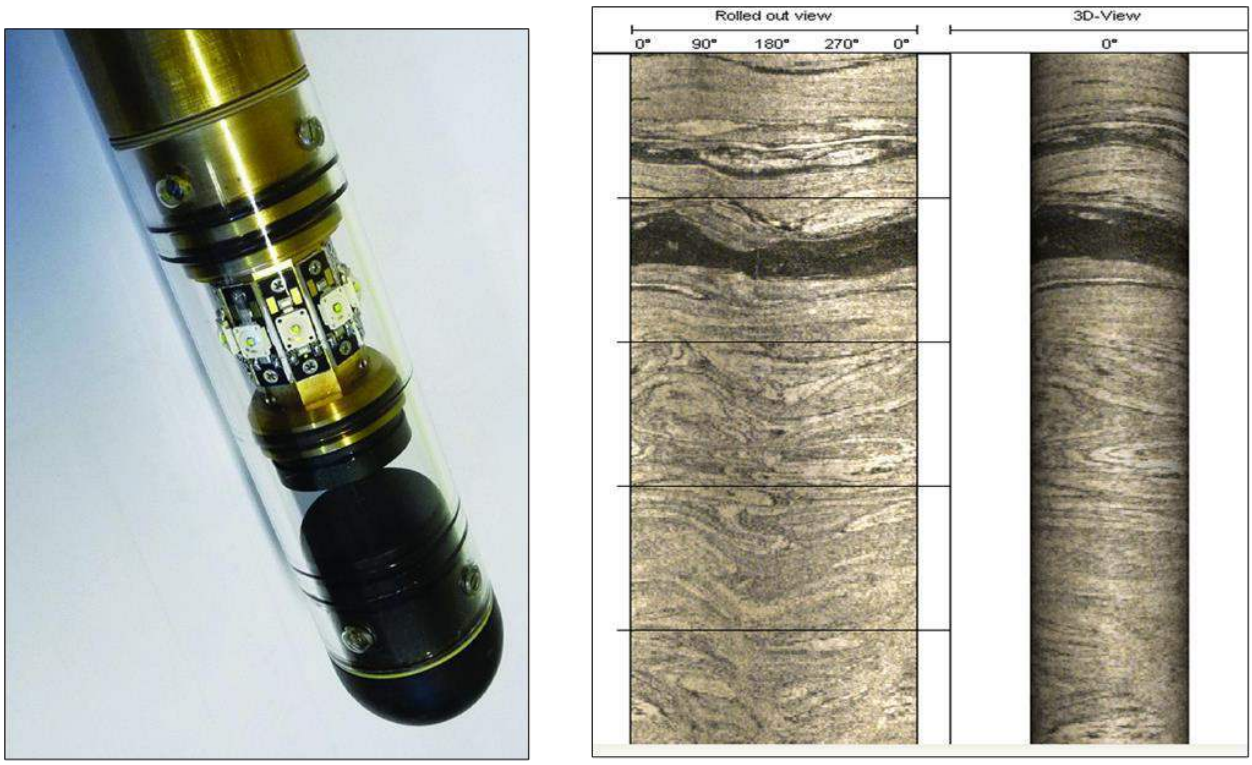


Figure 1 - Optical Televiewer

OTV tools integrate a three-axis fluxgate magnetometer and three accelerometers. These sensors continuously monitor the tool's spatial orientation within the borehole, specifically its azimuth and inclination. This orientation data is paramount for accurately aligning the captured images with respect to true orientation and vertical depth. In environments with magnetic interference, a borehole deviation survey with gyroscopic sensors can be conducted to maintain accurate orientation.

Despite its numerous advantages, OTV logging has limitations. The most significant is its requirement for a clear borehole fluid, if the borehole is fluid-filled. Turbid or opaque fluids severely impede light penetration and render the image unusable. Also, the presence of coatings on the borehole wall, such as drilling mud cake or mineral precipitates, can obscure the underlying formation and degrade image quality.

A typical vertical sample interval for the OTV logging is approximately 0.01 feet, and a typical horizontal scan density is approximately 360 points per revolution. A typical logging rate with a modern system is approximately 10 feet per minute.

ACOUSTIC TELEVIEWER

ATV logging produces a high resolution, magnetically oriented digital image of the borehole wall to map the location and orientation of intersecting fractures, foliations, and lithologic contacts. The ATV emits a rotating, narrow, acoustic beam that is reflected off the

borehole wall. Using acoustic energy in the mega-hertz range, the ATV measures the acoustic impedance of the borehole wall and the two-way travel time of the transmitted signals (Figure 2).

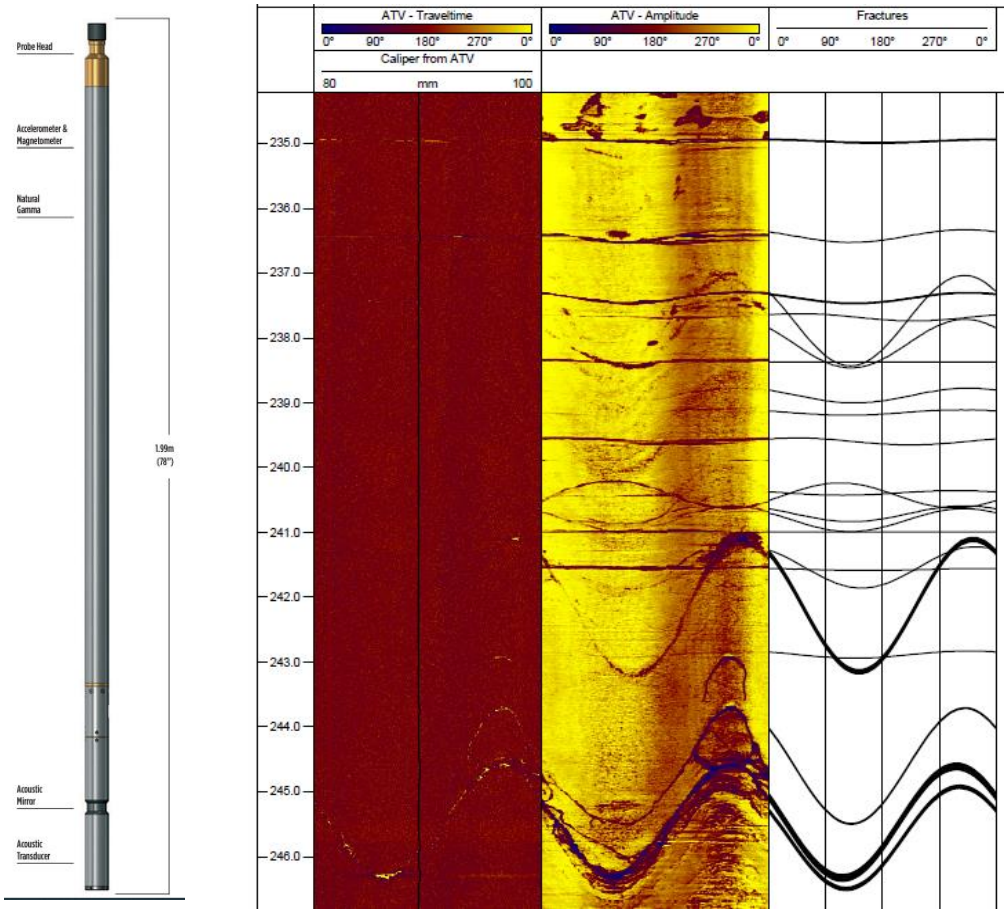


Figure 2 - Acoustic Televiewer

Major differences in travel time and reflection amplitudes from background values are seen as anomalous features. Both datasets are useful for identifying the location and orientation of fractures. The amplitude of the reflected signal will decrease at the location of fractures and the travel time will increase. The travel time data can also be used for developing a high-resolution caliper log for a more comprehensive analysis of fractures. ATVs can only be used in fluid filled boreholes. However, the fluid does not have to be optically clear for the method to work.

When operating the ATV, a "time window" is set based on the borehole diameter. The time window is the time interval in which the ATV instrument searches for an echo from the borehole wall. For smaller increases in borehole diameter around fractures and sections of weaker rock, the ATV typically records an accurate borehole diameter (correlates well with three-arm caliper data). However, if borehole openings are much larger than the borehole diameter, the echo from the borehole wall may fall outside the time window, or be too weak to be detected. In these situations, borehole diameters recorded with ATV may be inaccurate.

Similar to the OTV log, borehole deviation data, recorded from built-in three-component magnetometer and accelerometers, are used to provide the corrected orientation and shape of the imaged features. In situations with magnetic rock minerals or steel casing, gyroscopic borehole deviation data can be used in lieu of the internal ATV deviation data. Correcting for borehole deviation allows calculation of actual dip direction and dip angle of imaged planar features and true vertical depth. Discontinuities imaged with the ATV include open or filled fractures, foliation, mineralization, weathered zones, and rock fabric.

A typical vertical sample interval for the ATV logging is approximately 0.01 feet, and a typical horizontal scan density is approximately 200 measurements per revolution. A typical logging rate with a modern system is approximately 10 feet per minute.

DATA PROCESSIING

The circular, 360-degree OTV and ATV images are flattened into two-dimensional, continuous image logs. These unwrapped images effectively portray the borehole wall as if it were laid out in a planar format. The accompanying orientation data ensures that every point on this unwrapped image is correctly positioned azimuthally, preserving the true bearing of features observed. Throughout the logging process, the images are precisely correlated with the depth of the tool, yielding a continuous log with a high degree of vertical resolution. To enhance the visibility of subsurface features, various image processing techniques are routinely employed. These may include adjustments to brightness, contrast, and color balance, as well as the application of filters designed to minimize noise and tool decentralization. Other processing steps involve adjustments for magnetic declination and borehole deviation, and depth correction. Synthetic caliper logs from the ATV travel time data are also typically calculated.

DATA INTERPRETATION

Interpreting borehole televiewer data involves the systematic identification of features present on the borehole wall images. Although modern software tools do include automated image analysis, manual reviews and edits are still necessary for correct interpretation. Planar features, such as fractures, bedding planes, foliation, and lithological contacts, are frequently encountered and are characterized by their sinusoidal traces on the unwrapped image. The specific geometry of these sinusoids directly reflects the dip and dip direction of the corresponding planar structure. Open fractures often exhibit lower acoustic reflectivity in ATV data or a visible aperture in OTV logs, while filled or healed fractures may present different characteristics depending on the nature of the infilling material.

Bedding and foliation typically manifest as more continuous, often sub-parallel sinusoidal patterns, indicative of changes in rock composition or fabric. Abrupt changes in image texture or color in OTV logs, or in acoustic impedance in ATV logs, that follow a sinusoidal pattern signify planar boundaries between different rock types. In addition to planar features, non-planar features such as borehole breakouts, vugs, cavities, and zones of borehole wall rugosity or washouts are also identified.

Once features have been identified, a detailed characterization follows, focusing on their specific attributes. For planar features, the dip, which is the angle of inclination from the horizontal, and the dip direction, which is the azimuth towards which the feature dips, are determined by fitting a sinusoidal curve to the feature's trace on the unwrapped image. In the case of fractures, televiewer data can provide a direct visual estimate of the aperture or opening width (Figure 3).

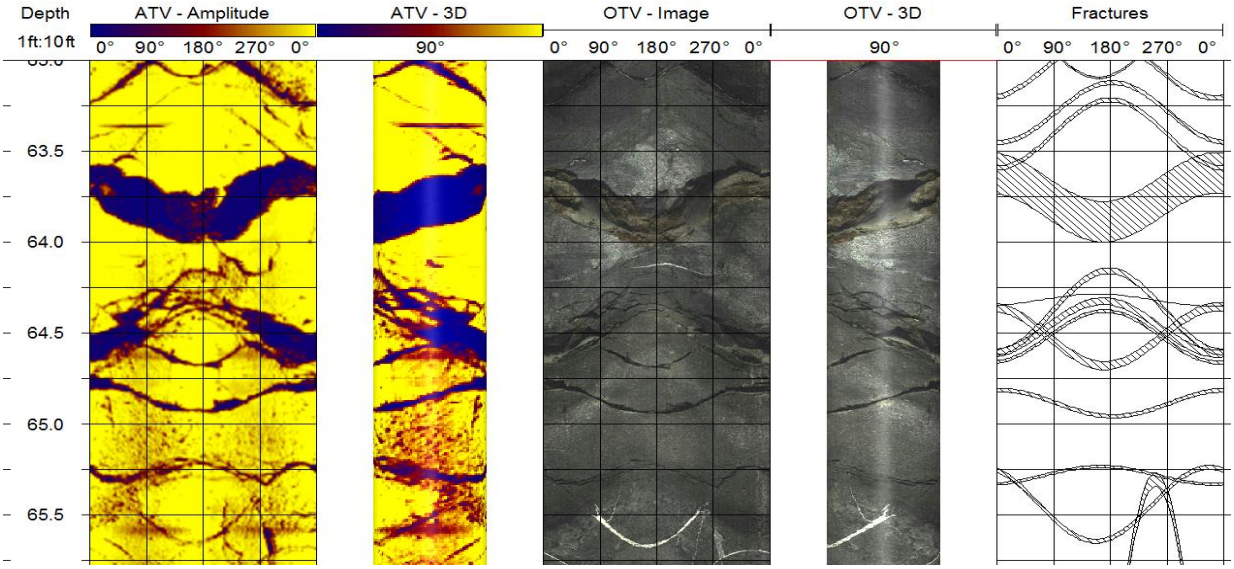


Figure 3 - ATV and OTV Data Interpretation

The final stage involves the analysis and interpretation of the characterized features to extract meaningful geological, structural, and geotechnical insights. Structural analysis often involves plotting the orientation data of planar features on stereonets and rose diagrams to identify dominant structural trends, joint sets, and potential planes of weakness. The orientation and characteristics of borehole breakouts can be used to infer the direction of principal horizontal stresses. Lithological interpretation is enhanced by integrating OTV and ATV data with other borehole logs and geological knowledge.

CASE STUDY 1: NC-88 WIDENING AND REALIGNMENT, WEST JEFFERSON, NORTH CAROLINA

A section of the NC-88 Widening and Realignment project was going through mountainous areas with significant planned rock cut slopes. Creating steep rock cut slopes inherently introduces the risk of instability, and the inherent weaknesses within the rock mass (discontinuities like joints, faults, and bedding planes) can lead to rockfalls, slides, and other slope failures, posing significant safety hazards to construction workers and future road users.

The geotechnical investigation for this NCDOT project was led by HDR. As part of their investigation, HDR conducted roadside geological mapping of the exposed rock outcrops adjacent to the proposed route. In an area where the proposed alignment deviated significantly

from the current road alignment, a 130-foot angle bore was oriented along the proposed alignment to supplement the roadside mapping. The angle bore was drilled 20 degrees from vertical, and oriented to the southwest in order to intercept high-angle joint sets and to pin down the persistence/spacing of high-angle joint sets truncating planar and wedge features related to foliations in the amphibolite/schistose gneiss rock mass. Televiewer logging of the bore was then added to enhance mapping and to gather critical data to assess the potential for specific failure mechanisms, inform slope design, and refine risk assessments.

For this project, a Robertson GEO borehole logging system was used to collect geophysical logging data. OTV data was collected for the entire length of open hole, and ATV data was collected for the submerged portion of the borehole (112-130 feet). All data was reviewed for quality and accuracy in the field. Fractures and lithological features were interpreted through a complete analysis of both logs. Dip and dip direction were picked from OTV and ATV data and were adjusted to true orientation based on borehole deviation and magnetic declination. Summaries of fracture data were provided as rose diagram and lower hemisphere stereonet (Schmidt) plots. Fracture and foliation data were also provided in tabular format with apparent depth, approximate vertical depth, dip direction, dip angle, and approximate aperture for each fracture.

Based on the results of these studies, HDR adjusted the proposed alignment, since the orientation of fracture and foliation planes would have made it difficult to construct stable slopes at reasonable cut angles. The initial and final proposed road alignments, and a fracture Rose diagram derived from the OTV and ATV data interpretation is shown in Figure 4.

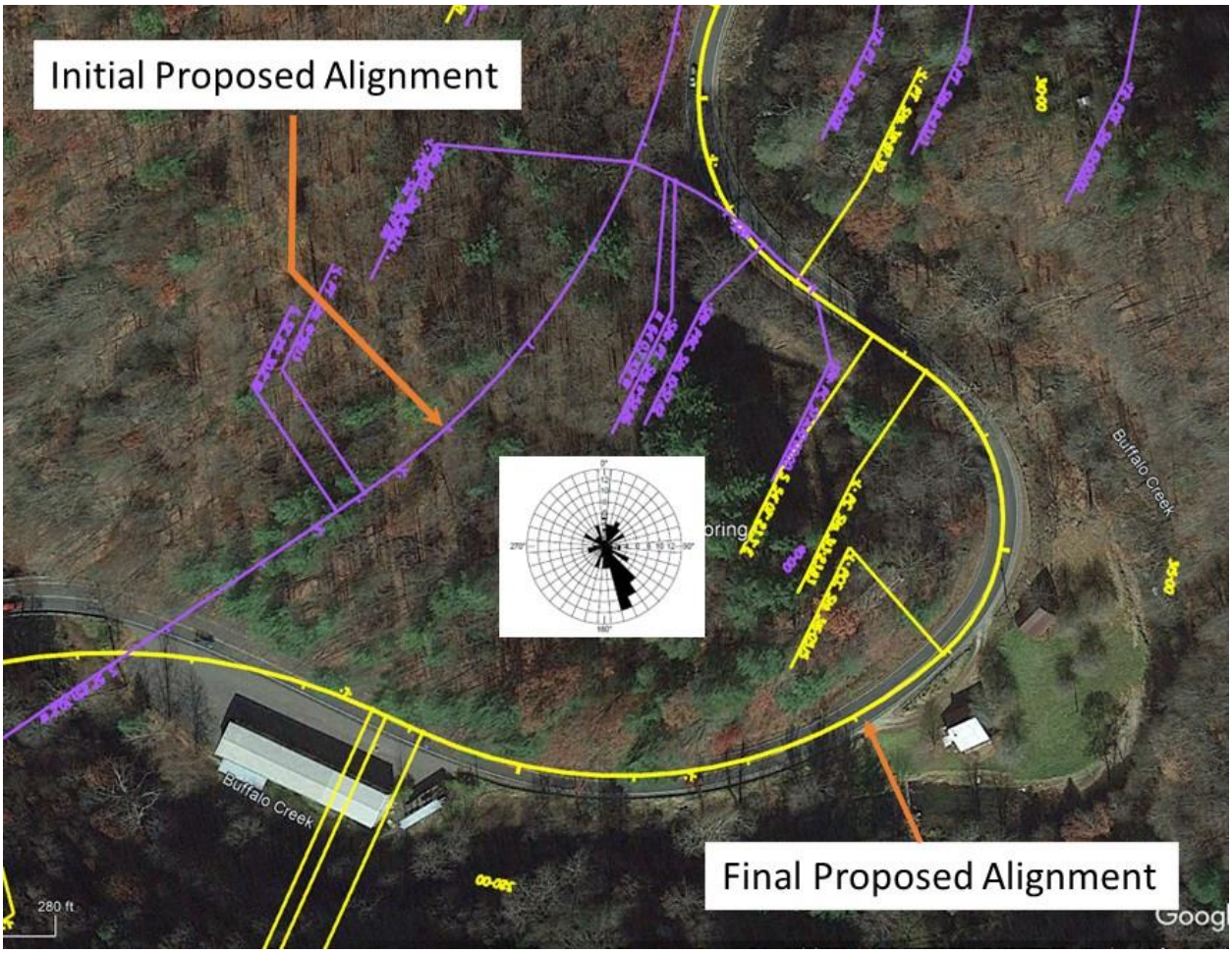


Figure 4 - Adjusted Prpoposed Alignment

CASE STUDY 2: PROPOSED NEW BRIDGE FOR THE TH 53 RELOCATION, VIRGINIA, MINNESOTA

The Thomas Rukavina Memorial Bridge in Virginia, Minnesota, was constructed to relocate a 3.2-mile segment of TH 53 due to the expansion of the Rouchleau Mine Pit. The necessity for this relocation stemmed from a 1960 agreement where the MNDOT agreed to move the highway if mining companies intended to mine beneath it after 1987. Following notifications from two landowners in 2010 about their mining intentions, the state had until 2017 to complete the relocation. The project presented significant geotechnical challenges, including rock and soil slope stability concerns and the need for rockfall protection during construction and for the completed bridge piers.

Two phases of drilling were conducted to assess geotechnical characteristics of the bedrock at the two bridge abutment locations. In total, 17 angled boreholes were completed and were logged with OTV, ATV, and 3-arm caliper using a Mount Sopris logging system. At this site, there were two challenges for the logging program. First, poor rock quality created problems

with maintaining open bedrock intervals, and second, magnetic interference with the directional sensors on the televiewer tools from the iron formation.

The first challenge was mitigated by using a drilling-grouting-re-drilling (DGR) approach. DGR is a specialized methodology employed in geotechnical investigations to ensure the successful acquisition of high-quality televiewer logs, particularly when encountering challenging ground conditions that lead to borehole instability or hinder the use of downhole tools. This method is not a standard procedure for all boreholes but is reserved for situations where conventional drilling results in conditions unsuitable for effective televiewer logging. With a stable and accessible borehole achieved through the DGR process, the televiewer tools can be deployed to acquire detailed images of the borehole wall. The benefits of using DGR for televiewer logging include improved log quality due to the stable and uniform borehole wall, a reduced risk of expensive tools getting stuck, increased reliability of the acquired data, and the ability to obtain logs in formations that would otherwise be too challenging to log effectively (Figure 5).

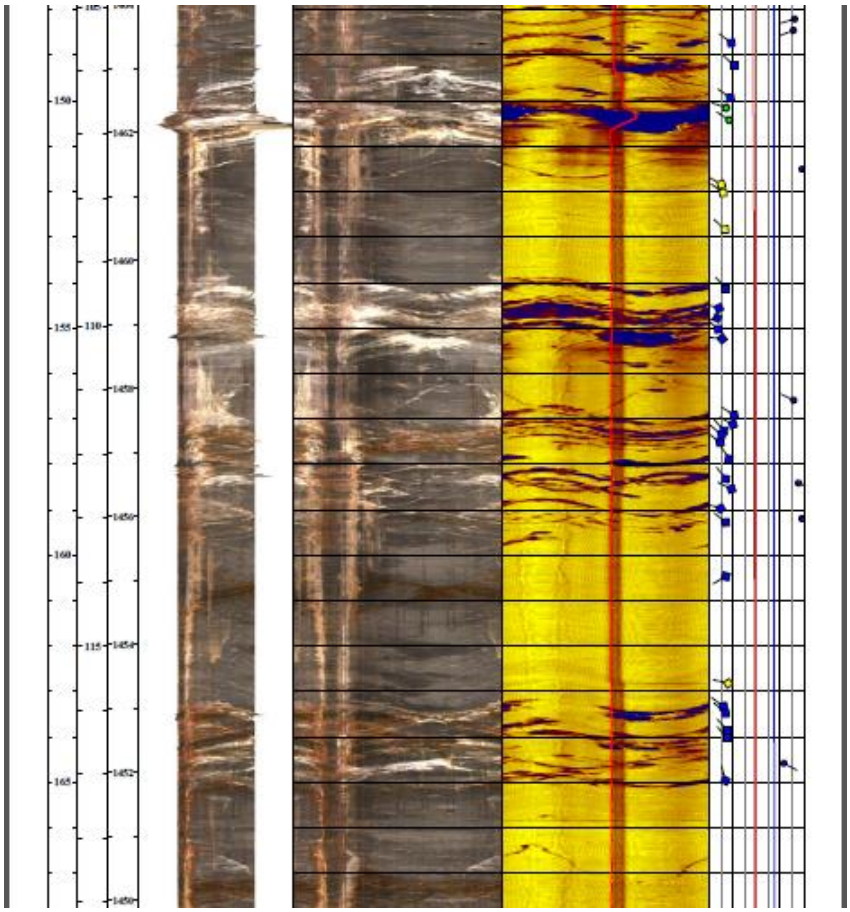


Figure 5 - OTV and ATV Data at DGR Borehole

The second challenge was addressed by adding gyroscopic deviation logging to the log suite. Gyroscopic borehole deviation logging provides a precise, non-magnetic method for determining the path of a borehole by continuously measuring its inclination and azimuth with

depth. Utilizing the principle of a gyroscope, which maintains its orientation in space, these tools can accurately survey boreholes even in environments where magnetic interference is significant, such as within steel casing, drill pipe, or in formations containing magnetic minerals. Summaries of fracture data were provided as rose diagram and lower hemisphere stereonet (Schmidt) plots. Fracture and foliation data were also provided in tabular format with apparent depth, approximate vertical depth (calculated from inclination estimated by tool sensors), azimuth (dip direction), dip angle, and approximate aperture for each fracture.

The geotechnical investigation including the geophysical borehole logging program informed the bridge design and construction. The bridge was completed on time in September of 2017. The bridge features a three-span plate girder design supported by two intermediate piers. These piers rest on groups of 30-inch diameter micropiles drilled up to 175 feet deep into the Biwabik Iron formation bedrock. The abutments use rock-bearing spread footings, with tie-back anchors to mitigate lateral forces on the tall piers. Standing approximately 204 feet above the water, it holds the distinction of being the tallest bridge in Minnesota, with a total length of about 1,125 feet.

CONCLUSIONS

This paper highlights the significant role of OTV and ATV geophysical logging in transportation projects, providing detailed insights into subsurface rock mass characteristics and discontinuity orientations critical for stability assessments. The evolution of televiewer technology has equipped engineers with invaluable capabilities for visualizing and analyzing borehole conditions. These tools enable the accurate determination of the dip and strike of planar features, the orientation of recovered core, the identification of subtle geological features, and potential indicators of fluid flow. Furthermore, the ability to map natural and drilling-induced fractures and assess rock mass quality through discontinuity analysis underscores the utility of televiewer logging in geotechnical investigations.

The case study of the NC-88 Widening and Realignment project effectively demonstrates how televiewer logging, integrated with roadside geological mapping, can influence critical project decisions such as road alignment. The detailed fracture and foliation data obtained from the angled borehole allowed engineers to identify unfavorable geological conditions, leading to an adjustment of the proposed alignment to mitigate potential slope instability. This proactive use of televiewer data underscores its value in minimizing risks and optimizing design in challenging mountainous terrain.

The second case study focused on the TH 53 Relocation Bridge. OTV and ATV logging for this project encountered challenges related to poor rock quality and magnetic interference from the iron formation. The successful application of the DGR technique demonstrated an effective method for obtaining high-quality televiewer logs in unstable borehole conditions. Additionally, the integration of gyroscopic borehole deviation logging provided accurate orientation data in the presence of magnetic interference, ensuring the reliability of the fracture and foliation analyses. The comprehensive geotechnical investigation, including the advanced borehole logging program, directly informed the bridge's foundation design, contributing to the timely and successful completion of this critical infrastructure project.

These case studies collectively emphasize the indispensable contribution of OTV and ATV logging in transportation geotechnics. By providing detailed, oriented imagery and quantitative data on subsurface discontinuities and rock mass quality, these geophysical techniques empower engineers to make informed decisions regarding alignment, slope design, foundation engineering, and risk assessment, ultimately leading to safer, more cost-effective, and sustainable transportation infrastructure. The continued advancements in televiewer technology and data processing methods promise even greater accuracy and efficiency in future geotechnical investigations.

Integrated Approaches to Landslide Monitoring and Interpretation: Remote Sensing, Field Investigations, and Geomorphic Terrain Analysis in Yellowstone National Park, Montana and Wyoming

Kristofer Hornsby, CEG, PG
BGC Engineering
Suite 300 – 600 12th Street
Golden, CO 80401
720-617-1868
khornsby@bgcengineering.ca

Brian Collins, PE
BGC Engineering
Suite 300 – 600 12th Street
Golden, CO 80401
720-647-6210
bcollins@bgcengineering.ca

Eric Lim, PE, GE
Western Federal Lands Highway Division
610 East Fifth Street
Vancouver, WA, 98660
360-619-7826
eric.lim@dot.gov

Prepared for the 74th Highway Geology Symposium, August, 2025

Disclaimer

Statements and views presented in this paper are strictly those of the authors, and do not necessarily reflect positions held by their affiliations, the Highway Geology Symposium (HGS), or others acknowledged above. The mention of trade names for commercial products does not imply the approval or endorsement of HGS.

Copyright Notice

Copyright © 2025 Highway Geology Symposium (HGS)

All Rights Reserved. Printed in the United States of America. No part of the publication may be reproduced or copied in any form or by any means – graphic, electronic, or mechanical, including photocopying, taping, or information storage, and retrieval system – without prior written permission of the HGS. This excludes the original author(s).

ABSTRACT

In June 2022, a significant rain-on-snow event in the high elevations of northern Yellowstone National Park led to flooding and bank erosion severely damaging the North Entrance Road along the Gardner River. In the immediate aftermath, the National Park Service (NPS) and Western Federal Lands Highway Division (WFLHD) rehabilitated the previously unpaved Old Gardiner Road between Gardiner, Montana and Mammoth, Wyoming as an emergency and temporary roadway replacement for the North Entrance Road. NPS and WFLHD are working on the design of a permanent alignment. The Old Gardiner Road crosses multiple large, deep-seated landslide complexes. WFLHD and Jacobs/BGC Engineering have completed site investigations, including geomorphic terrain mapping, deep geotechnical boreholes with instrumentation (Shape Accel Arrays and vibrating wire piezometers) and telemetry, radiocarbon geochronology, geologic interpretation, and remote sensing (lidar change detection and interferometric synthetic aperture radar analysis). This paper summarizes the results of these data sets, explains how integrating these data enhances the interpretation of landslide movement, and describes how these findings can inform decisions on alignment and grade selection for roadway design.

INTRODUCTION

The North Entrance Road in Yellowstone National Park (Figure 1) crosses multiple large, deep-seated landslide complexes and earthflows. Western Federal Lands Highway Division (WFLHD) and Jacobs/BGC Engineering have completed site investigations, including terrain mapping, boreholes with instrumentation, laboratory testing, geologic interpretation, and remote sensing (lidar change detection and Interferometric Synthetic Aperture Radar (InSAR) analysis). This paper summarizes the results of these data sets, explains how integrating these data enhanced the interpretation of landslide movement, and describes how these findings can inform decisions on alignment and grade selection for roadway design.

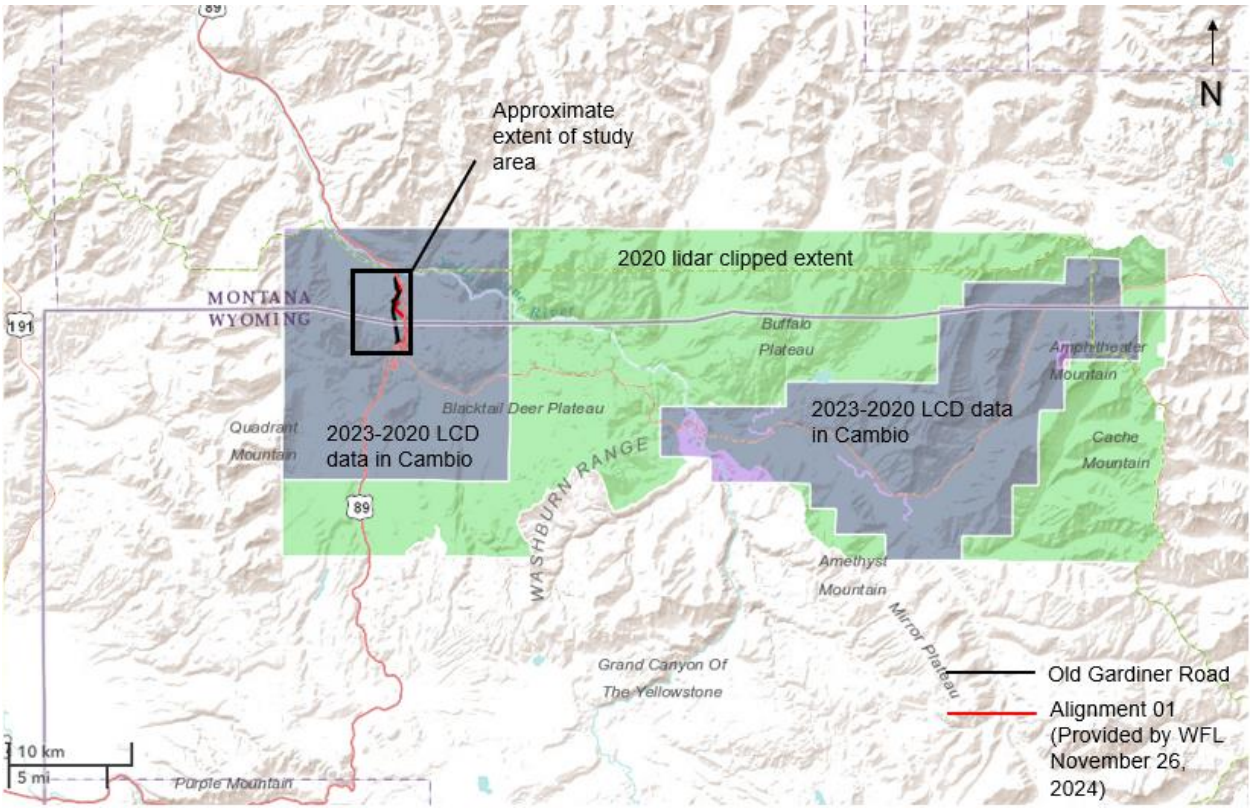


Figure 1 – Map of Northern Yellowstone National Park Illustrating Location of this Study.

JUNE 2022 FLOODING

In late May and early June 2022, parts of the Absaroka Range and Beartooth Mountains had over 140 percent of the average snowpack; from June 9 to June 13, an atmospheric river dropped 2 to 5 inches of rain in northern Yellowstone National Park, for a combined total of 4 to 9 inches of total water equivalent precipitation (*1*). The precipitation caused a 500-year flood event for some rivers and creeks in northern Yellowstone National Park that resulted in damage to critical transportation infrastructure.

NORTH ENTRANCE ROAD BACKGROUND

The North Entrance Road provides access to Yellowstone National Park from Gardiner, Montana, to Mammoth, Wyoming, along an approximately 5-mile-long alignment. Erosion caused by the Gardner River during the June 2022 flooding destroyed several sections of the North Entrance Road in the Gardner River Canyon (Figure 2). To restore access between Gardiner and Mammoth, the Old Gardiner Road, which at the time was a seldom-used single-lane gravel bypass, was widened to two lanes and paved to carry the high volume of employee and visitor traffic that uses this access to the park daily. The rehabilitated Old Gardiner Road has little to no shoulders, steep grades, and sharp curves. Rehabilitation of this road was done as an emergency measure, and its use is intended to be temporary until a permanent alignment can be selected and constructed. The NPS and WFLHD are in the process of evaluating alternative alignments that satisfy modern geometric design criteria and avoid the risk of flood damage in the Gardner River Canyon.

The Old Gardiner Road is routed across east to northeast-facing slopes, upslope (west) of the Gardner River (Figure 2). The slopes are mantled by deep-seated landslide complexes characterized by hummocky topography, arcuate scarps, toe deposits, sag ponds, and earthflow morphology, and discrete lateral margins. The landslides have previously been identified and mapped, most recently by Dewey et al. (*2*) and Pierce et al. (*3*), as part of work to support the National Park Service identify geohazards along potential alternative road alignments. These authors numbered the landslides from north to south and we followed this established numbering system and nomenclature. We completed detailed geomorphic mapping of geohazards along the North Entrance Road and Old Gardiner Road, including landslides, earthflows and debris flow hazards (Figure 2).

Based on observations of landslide deposits overlying Pinedale glaciation flood deposits, Dewey et al. (*2*), concluded that landsliding on the slopes above the Gardner River likely initiated post-Pinedale Ice Age deglaciation, approximately 12,000 to 13,000 thousand years ago (ka). They inferred that initial landsliding likely occurred before the climate became drier than modern conditions around approximately 11.5 ka (*2*). Additionally, Nicholas (*4*) calculated surface roughness using the average deviation of the slope along the northern 8 landslides and concluded that only landslide 7 (Slide Lake landslide) and the upper portion of landslide 5 were active. Measured landslide movement rates, the spatial extent of active movement, and age dating of the landslide deposits was not quantified. Below we provide remote sensing, lidar-based mapping, and instrumentation results to provide insights into Holocene landslide activity.

LANDSLIDE CHARACTERIZATION

Surface characterization of the landslides included desktop studies, geomorphic terrain mapping, and remote sensing, including lidar change detection and Interferometric Synthetic Aperture Radar (InSAR) analysis. Subsurface characterization included deep (up to 400 feet) boreholes with instrumentation, laboratory testing (material properties and geochronology), integrating these data into a 3D geologic model, and data interpretation.

Geomorphic Characterization and Remote Sensing Methods

Parkwide 1-meter resolution lidar data collected by the U.S. Geological Survey (USGS) 3D Elevation Program (3DEP) in fall 2020 (*5*) was used to create lidar derivates including hillshade, slope shade, and aspect maps for delineating geomorphic features. We mapped the lateral extents and relative relationships of landslides including the previously mapped earthflows.

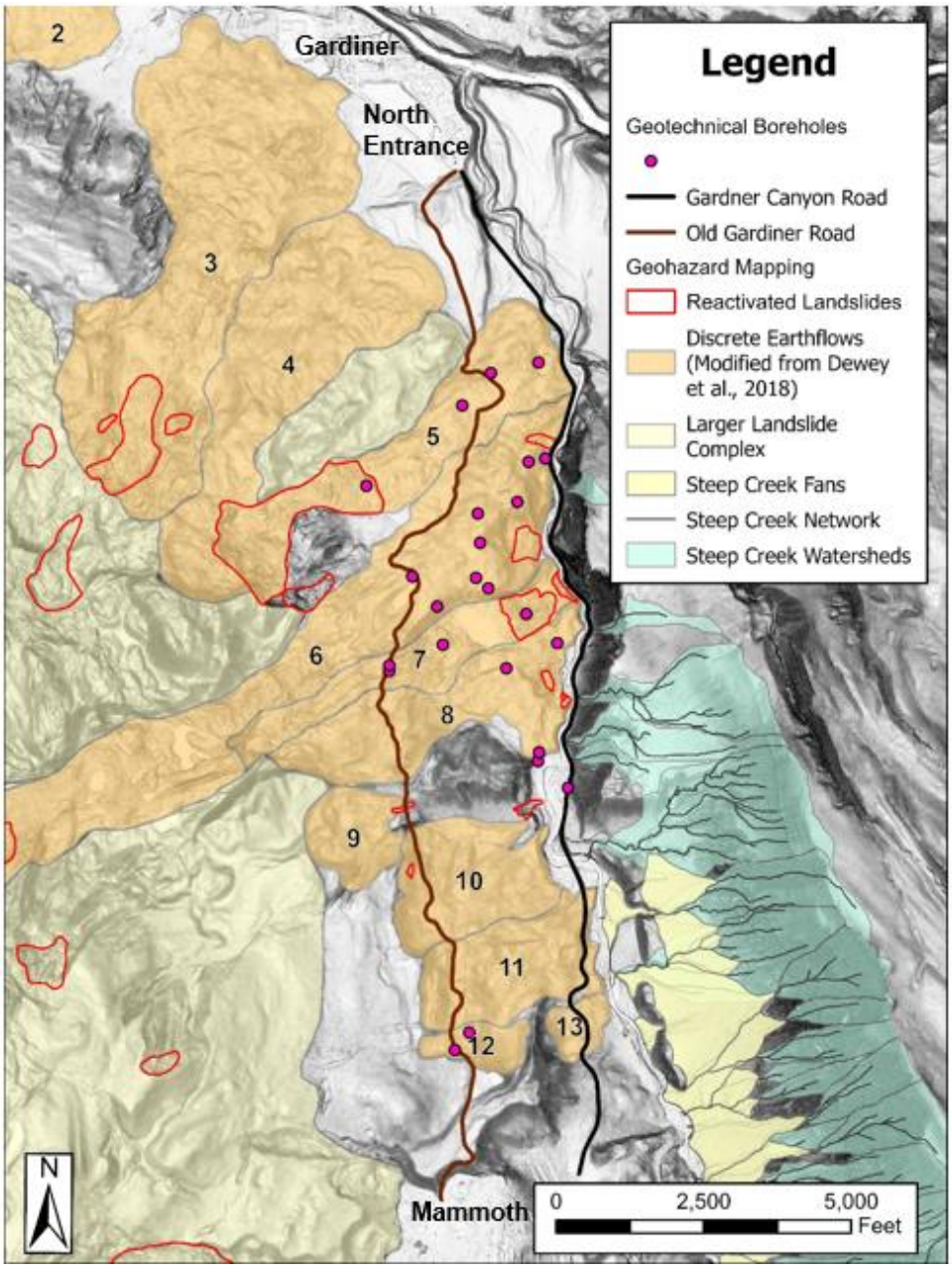


Figure 2 – Geohazard Mapping of North Entrance Road Corridor.

Field Mapping

Site geologic data were compiled onto a GPS-enabled iPad. Base layers included georeferenced geologic maps (*3*), 2020 lidar-derived hillshade digital elevation model, and InSAR analysis data. The mapping team used these data to field check landslide boundaries, geologic contacts, and to visit various areas with differing geomorphic expressions including hummocky terrain, uphill-facing slopes, mapped areas with different reported landslide activity rates and relative recency, upslope source areas, and exposed landslide toes in the Gardner River Canyon. Geologic orientation data were obtained using a Brunton compass. The mapping team also visited proposed borehole locations to evaluate logistics for drilling, observe conditions associated with proposed alignments, and evaluate proposed borehole depths.

Remote Sensing

Lidar Change Detection

Lidar change detection (LCD) involves using lidar datasets to capture high-resolution data of the same ground surface over time, allowing for measurement of topographic changes at approximate detection scale ranges of 3 to 12 inches. This method can identify active landslides by detecting shifts in 3D terrain data resulting from ground displacements, which can be indicative of landslide activity.

The lidar data used in this study were procured by the USGS (September 2020 data) and YNP (September 2023 data) and provided to BGC. BGC clipped the data extents to the Northeast Entrance Road corridor and nearby basins and slopes of interest. The data were provided as bare-earth point clouds with average point densities of approximately 1 point per square foot (10 to 15 pts/m2). Note that bare-earth point density can be influenced by several factors, including steep slope angles, vegetation density, snow cover, leaf conditions, data collection parameters, and post-processing methods used to generate the bare-earth model.

The approach used to conduct the lidar change detection involved aligning datasets using an iterative closest point (ICP) algorithm, conducting a three-dimensional (3D) change measurement between the two bare-earth point cloud datasets, and determining the limit of detectable change (LoD) with a statistical confidence of 95% ($LoD_{95\%}$). The LoD calculated for the 2020 vs. 2023 comparison in the Mammoth to Gardiner region was approximately +/- 0.33 ft (0.10 meters) to +/- 0.16 ft (0.05 meters) based on multiple LoD estimates at different locations. The change detection results are presented as color-contoured data illustrating the 3D change measurement between the two datasets, where the model differences are greater than the $LoD_{95\%}$.

InSAR

Satellite-derived InSAR is a remote sensing technology that can detect and monitor surface displacement with millimeter-level precision at locations where a recurring reflective surface can be observed in the time series data. Given the availability of several years of archived data, InSAR data can be used to provide insights into observable ground movement over the earth, including i) the 1-D line-of-sight displacement timeseries for the ascending and descending satellite orbit geometries, and ii) the 2-D (vertical and east-west) components of the

resolved displacement vectors where both ascending and descending measurement points are available.

When viewing InSAR results, regions without InSAR measurement points indicate an absence of recurring data in that region, and an absence of data does not necessarily indicate movement is not occurring. A consideration when using InSAR data is that measurements are one-dimensional displacements along the satellite line of sight (LoS) and, therefore, the reported displacements only represent the component of the true slope displacement in the LoS direction (i.e., InSAR measurements may underestimate the real landslide displacement magnitude, even greatly, and will not overestimate it). The measurable displacement is therefore dependent on the orientation of movement of the slope of interest relative to the satellite LoS.

BGC subcontracted the InSAR data service provider TRE Altamira to perform InSAR analyses for snow-free periods of Sentinel 1 satellite data in 2024 for park-wide data acquired between May 2017 and July 2024. BGC analyzed descending InSAR data between 2017 and 2024 and descending, ascending, and east-west InSAR data between 2017 and 2021 to delineate areas of measurable slope displacement and calculate landslide movement rates. The InSAR data images were collected approximately every 12 days over the study periods.

Site Investigations and Instrumentation

The geotechnical investigations completed for the North Entrance Road project have included 23 geotechnical boreholes to date (Figure 2). The soil deposits and bedrock units encountered were logged to characterize subsurface materials. Interpretations were made of the depositional setting of soil units, potential landslide failure surfaces, bedrock formations, and bedrock faults.

Geotechnical instrumentation includes vibrating wire piezometers (VWPs) to monitor subsurface groundwater levels and vertical ShapeArrays™ (SAAVs) installed in 2.75-inch outside diameter slope inclinometers (SI) casing to measure potential subsurface lateral ground displacement. Eight boreholes with instrumentation were completed in 2023 (BH22-01 to BH22-06; BH22-08 to BH22-10) and 13 additional instrumented boreholes were completed in 2024 (BH24-01 to BH24-11; BH24-13, and BH24-14). The 2023 boreholes were drilled to depths ranging from 51.5 feet to 286.0 feet, and the 2024 boreholes were drilled to depths between 65.5 and 401.8 feet.

RESULTS

Soil deposits and bedrock units were logged to characterize subsurface material properties and interpretations, including the depositional setting of soils, potential landslide failure surfaces, buried organic material, bedrock formation, and bedrock faults to inform potential landslide depths. Poorly sorted landslide deposits, typically consisting of subangular to angular gravel to cobble-sized clasts of predominantly Absaroka volcaniclastic and Landslide Creek Formation sedimentary clasts within a clayey to silty soil matrix were encountered. The landslide deposits were typically encountered overlying sedimentary bedrock; however, landslide deposits were also found to locally overlie glacial till, glaciolacustrine, and fluvial deposits. The

glacial and fluvial deposits were generally interpreted to be below the depth of landslide movement. Potential landslide failure/slip planes were interpreted where observations of planar to curved discontinuities with slickensided or polished surfaces were observed, typically within high plasticity clay units. In most boreholes, multiple slickensided and clayey zones were observed, as well as fine-grained silt and clay deposits, interpreted to be sag pond lacustrine deposits, indicating multiple generations of landslide activity and deposition. In some instances, buried organic material, including wood debris, was observed near potential failure surfaces.

Geochronology

Radiocarbon samples from detrital charcoal and wood were collected from the boreholes to provide context for the timing of landslide activity. It is important to note that charcoal samples may undergo multiple phases of deposition, exhumation, and transportation, providing a radiocarbon age that is inherently older than the age of the deposit from which the sample was collected and is considered a maximum age.

Near the basal plane of Landslide #8 (Figure 2), wood collected from depths of 106.5 and 109 feet below the ground surface yielded ages of approximately 6900 and 7300 calendar (cal) years before present (BP), respectively. We observed slickensides along a planar surface at 109.5 feet and interpreted this to be the basal slip plane with landslide deposits overlying 11 feet of alluvium over Cody Shale bedrock at 118.0 feet. At the Floating Block Landslide (Landslide #6), wood collected at 100.3 feet in BH24-07 yielded ages of approximately 12,100 and 12,300 cal years BP at a depth of 174.4 feet. A slip plane was observed at a depth of 168.0 feet and the basal slip plane may be below the final borehole depth of 265.9 feet. At Landslide #5 detrital charcoal collected at a depth of approximately 21 feet yielded an age of approximately 10,200 cal years BP and detrital charcoal collected at 58.8 feet had an age of approximately 19,200 cal years BP. At the Slide Lake Landslide (Landslide #7) detrital charcoal collected from a stream bank exposure at the toe of the landslide yielded an age of approximately 3400 cal years BP. This sample was collected above a nested slip plane that was approximately 10 feet above the basal slip plane. We interpreted that these landslide deposits are a shallower landslide that is likely younger than the initial Slide Lake Landslide deposits.

The radiocarbon results support the Dewey et al. (*2*) interpretation that landsliding may have initiated shortly after deglaciation of the Gardner Valley approximately 12,000 to 13,000 years BP. The results also indicate that landslide activity is more temporally complex, with multiple generations of younger landslide activity, and that the age of individual landslides is variable. The age results also indicate that younger, reactivated landslides have occurred along the toe of the slopes near the Gardner River.

Instrumentation

To date, SAAs have measured displacement from Shape Accel Arrays (SAAs) that we interpret to be consistent with landslide movement in three boreholes in Landslide #5. The measured displacements are consistent with borehole logging and initiate proximal to where potential failure planes were observed during borehole logging (Figure 3). The largest cumulative displacements have been measured in BH24-06 where cumulative displacement

between November 2024 and May 2025 exceeded 0.25 inches at a depth of 140 feet (Figure 3). Each borehole has its own data acquisition station that collects the VWP and SAA data and uses cellular telemetry to transmit the data to BGC. The data is hosted on a GIS-based website (Cambio) that allows integrated interpretation of the subsurface data with remote sensing results and other GIS data sets.

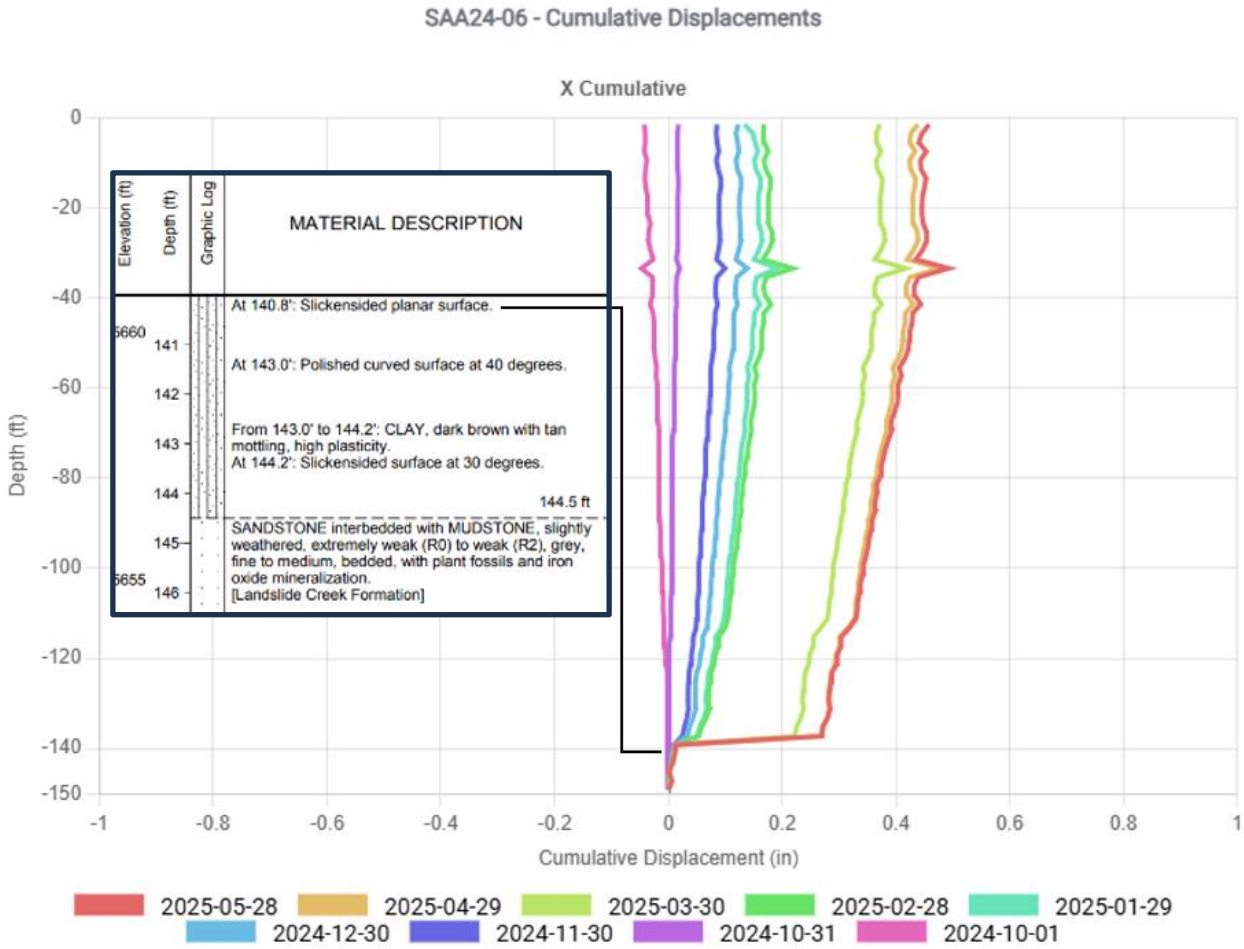


Figure 3 –SAA 24-06 Cumulative Displacement Plot Between October 2024 and May 2025 with the BH24-06 borehole log from 140 feet to 146 feet. Note the larger increase in displacement between January 2025 and March 2025.

Remote Sensing

The results of the 2020 to 2023 LCD analysis, 2017 to 2024 descending InSAR, and 2017 to 2021 descending, ascending, vertical, and east-west InSAR analysis indicate that Landslide #5, Landslide #6 (Floating Block Landslide), and the lower portion of Landslide #8 (Figure 2) are active and creeping at very slow to extremely slow to rates (*6.7*). The LCD results indicate more broad areas of movement along the toe of the slopes near the limit of detection that encompass some discrete landslides along the Gardner River (Figure 4) with greater rates of movement that are slow to very slow (*7*) and may move more rapidly during shorter time scales

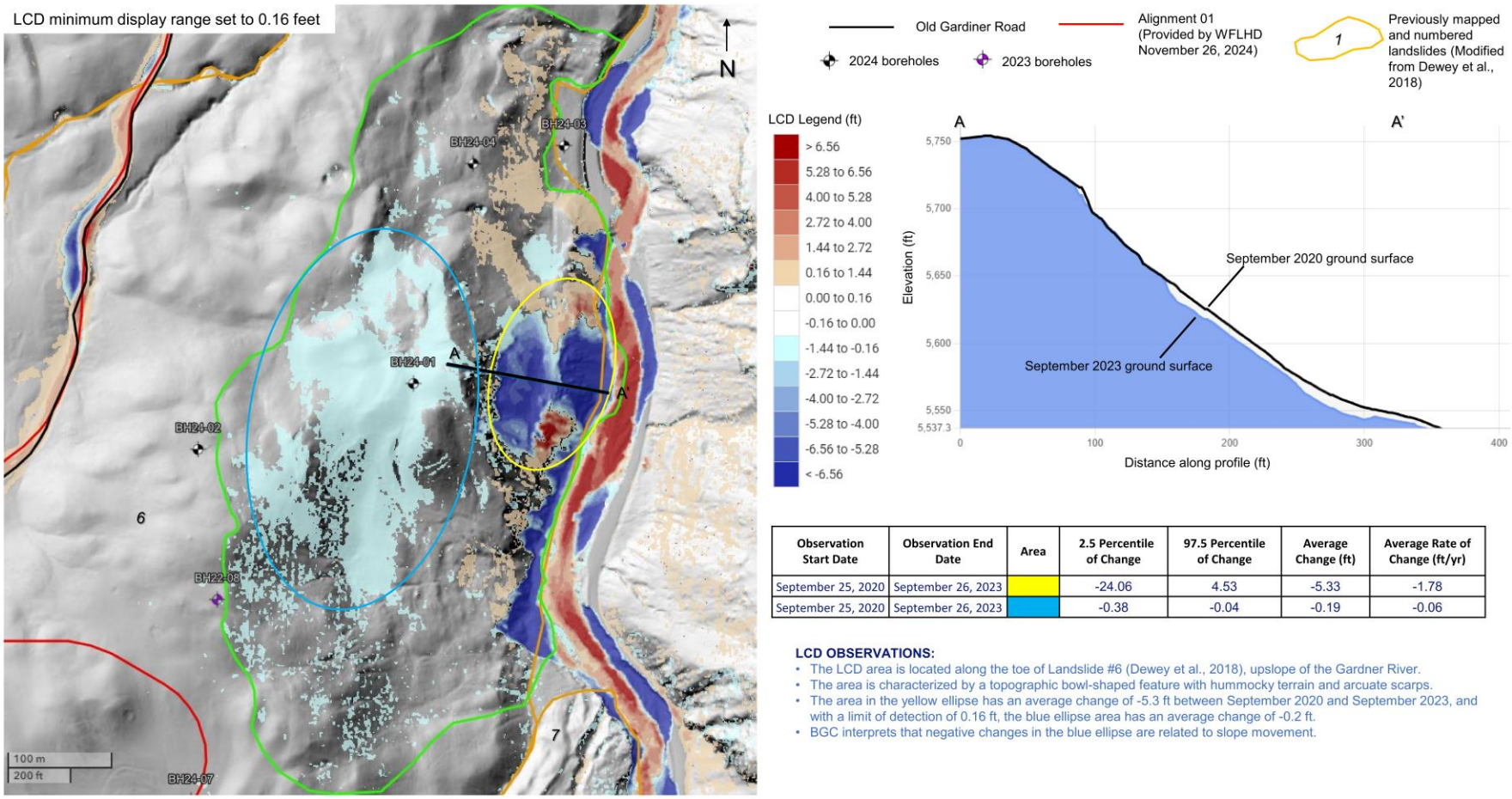
than resolvable between lidar datasets because movement rates are averaged over the 2020 to 2023 time span.

While the LCD data shows higher rates of change concentrated along the toe of the landslides, the InSAR data indicates that larger areas of creeping movement are present further upslope within the landslides (Figures 5 and 6). These data indicate that most of the area north of Slide Lake, including Landslides #2 to the southern margin of the Slide Lake Landslide (Landslide 7) are actively creeping. The highest rates of movement observed in the 2017 to 2024 InSAR analysis are within Landslide #5, which has movement rates that are highest near the headscarp and gradually decrease downslope (Figure 7).

Landslide movement near the toe of the slopes may be accelerated by erosion from the 2022 flood event along the Gardner River. Ongoing slope movement and erosion of the toe could cause the observed areas of movement to retrogress and extend past the delineated lateral margins.

Subsurface Cross Sections

The field mapping observation, remote sensing analysis results, site investigation and instrumentation data, and geochronology results were used to create interpretive cross-sections at select locations in the landslide complex. Figure 8 is an example cross-section through Landslide #5. The ground surface in Figure 8 is from the digital elevation model based on the 2023 lidar data. The colored circles and triangles on the ground surface are LCD and InSAR analysis results, respectively, along the location of the cross-section. The simplified borehole stick logs shown on the cross-section include the material type and geologic unit. The average displacement rate recorded is plotted at elevations where landslide displacement is evident in the SAA and observed groundwater levels in the VWPs are reported. The cross sections present the interpreted contact between the landslide deposits and the underlying bedrock and alluvial deposits. Although the number of boreholes is limited considering the scale of the landslides, combining data sets and geologic interpretations partially overcomes this shortcoming. Presenting all the data sets in one cross-section allows for an improved interpretation of the landslide that can inform geotechnical design of project elements.

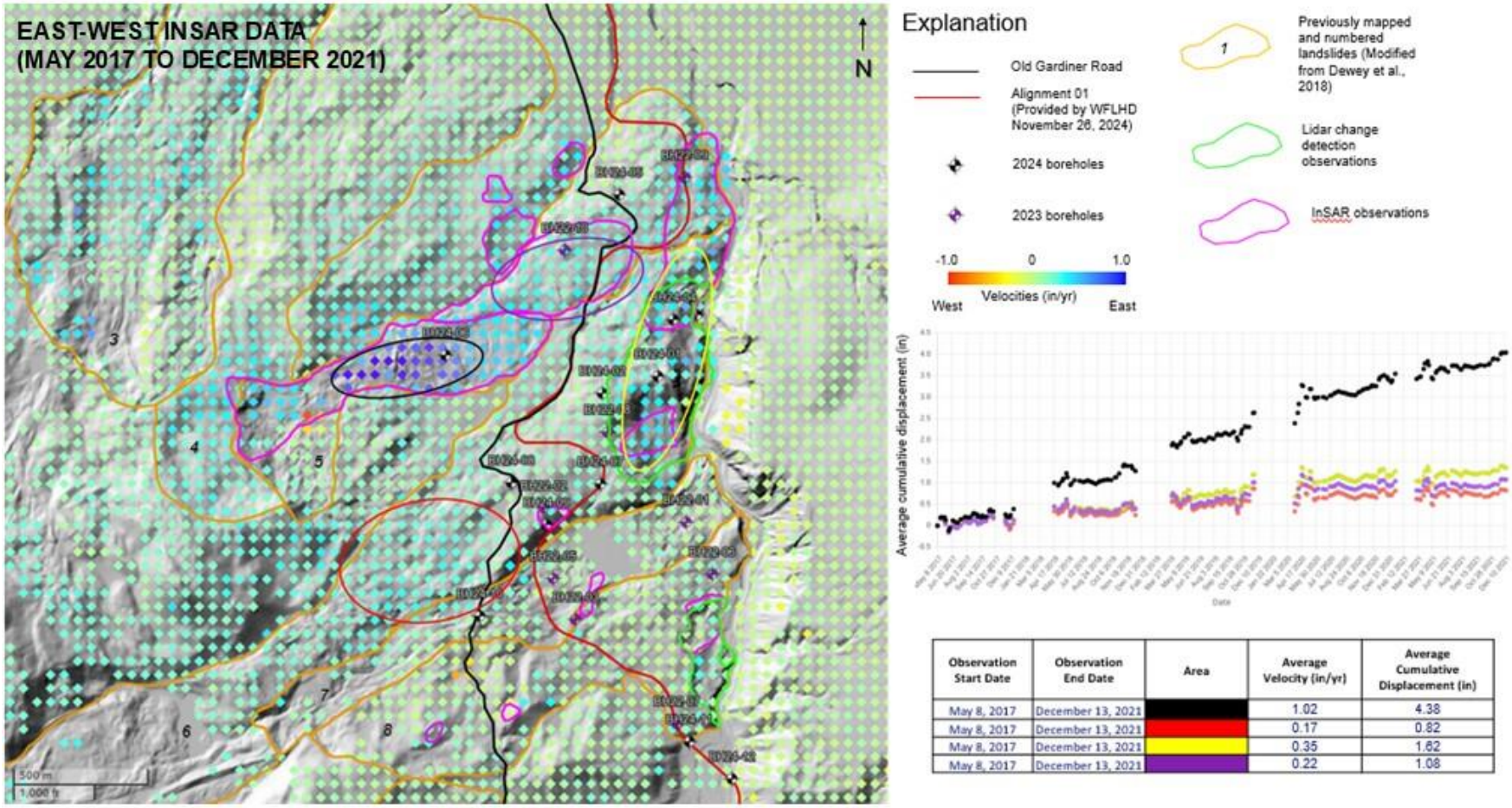


Observation Start Date	Observation End Date	Area	2.5 Percentile of Change	97.5 Percentile of Change	Average Change (ft)	Average Rate of Change (ft/yr)
September 25, 2020	September 26, 2023		-24.06	4.53	-5.33	-1.78
September 25, 2020	September 26, 2023		-0.38	-0.04	-0.19	-0.06

LCD OBSERVATIONS:

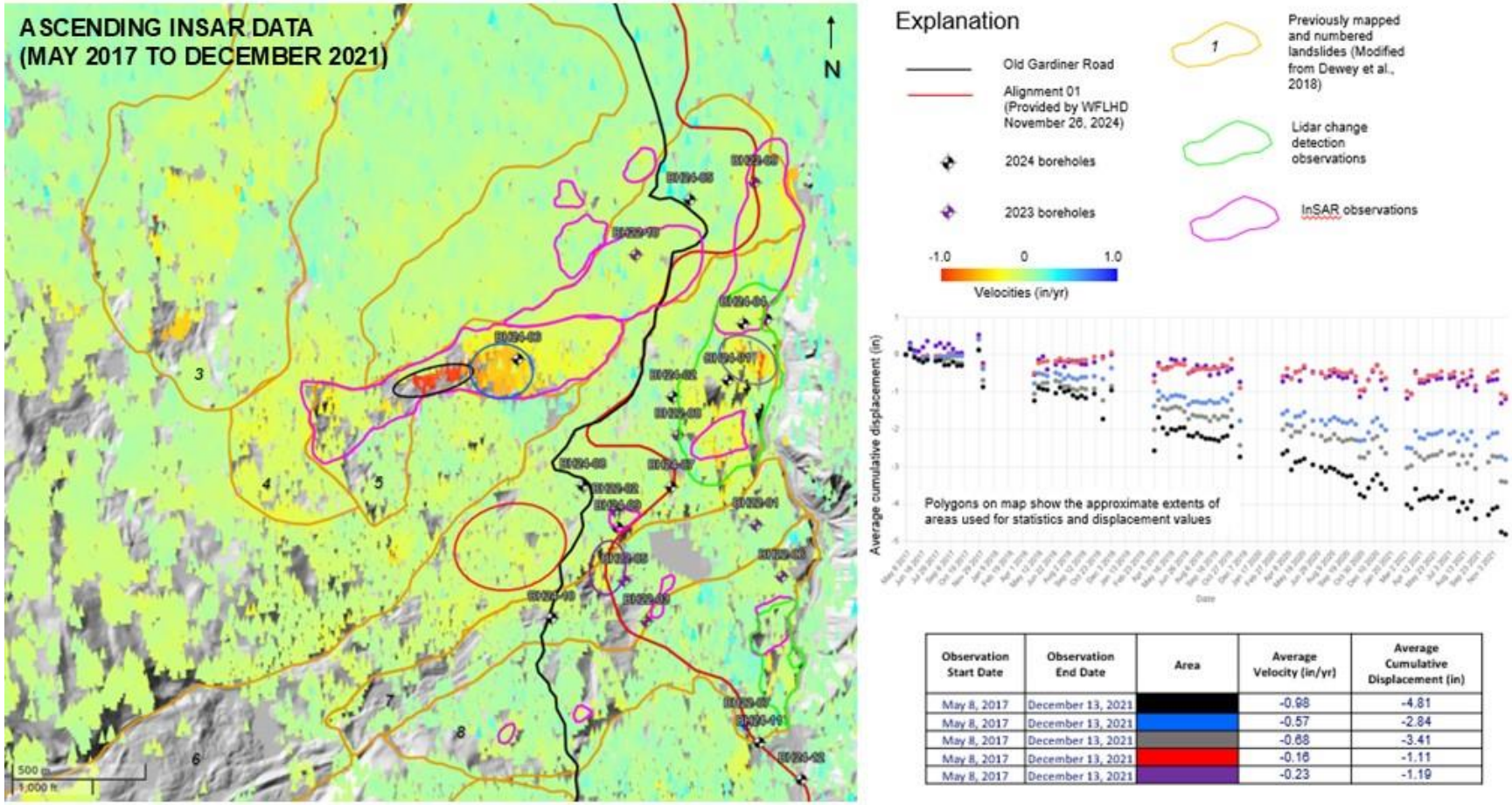
- The LCD area is located along the toe of Landslide #6 (Dewey et al., 2018), upslope of the Gardner River.
- The area is characterized by a topographic bowl-shaped feature with hummocky terrain and arcuate scarps.
- The area in the yellow ellipse has an average change of -5.3 ft between September 2020 and September 2023, and with a limit of detection of 0.16 ft, the blue ellipse area has an average change of -0.2 ft.
- BGC interprets that negative changes in the blue ellipse are related to slope movement.

Figure 4 – Lidar change detection results between September 2020 and September 2023 along the toe of Landslide #6 (*6*). The image on the left is from Cambio Earth Systems and shows lidar change detection with blue colors indicating negative topographic change and red color indicating positive topographic change. The minimum display range is set to 0.16 feet. The profile on the right shows the topographic surface from 2020 (blue) and from 2023 (black).



Observation Start Date	Observation End Date	Area	Average Velocity (in/yr)	Average Cumulative Displacement (in)
May 8, 2017	December 13, 2021		1.02	4.38
May 8, 2017	December 13, 2021		0.17	0.82
May 8, 2017	December 13, 2021		0.35	1.62
May 8, 2017	December 13, 2021		0.22	1.08

Figure 5 –East-West InSAR Data collected between May 2017 and December 2021 in the area north of Slide Lake (*6*). The blue colors indicate eastward movement relative to the satellite. Note the broad region of measurable movement that extends from Landslide #3 south to Slide Lake. The plot on the right shows average cumulative displacements over time within the oval polygons shows on the image in the left. The largest displacements were measured within the black oval polygon in the area that includes BH24-06.



Observation Start Date	Observation End Date	Area	Average Velocity (in/yr)	Average Cumulative Displacement (in)
May 8, 2017	December 13, 2021		-0.98	-4.81
May 8, 2017	December 13, 2021		-0.57	-2.84
May 8, 2017	December 13, 2021		-0.68	-3.41
May 8, 2017	December 13, 2021		-0.16	-1.11
May 8, 2017	December 13, 2021		-0.23	-1.19

Figure 6 –Ascending InSAR Data collected between May 2017 and December 2021 in the area north of Slide Lake (*6*). The yellow to red colors indicate movement relative to the satellite. Note the broad region of measurable movement that extends from Landslide #3 south to Slide Lake. The plot on the right shows average cumulative displacements over time within the oval polygons shown on the image in the left. The largest displacements were measured within the black oval polygon in the area that includes BH24-06.

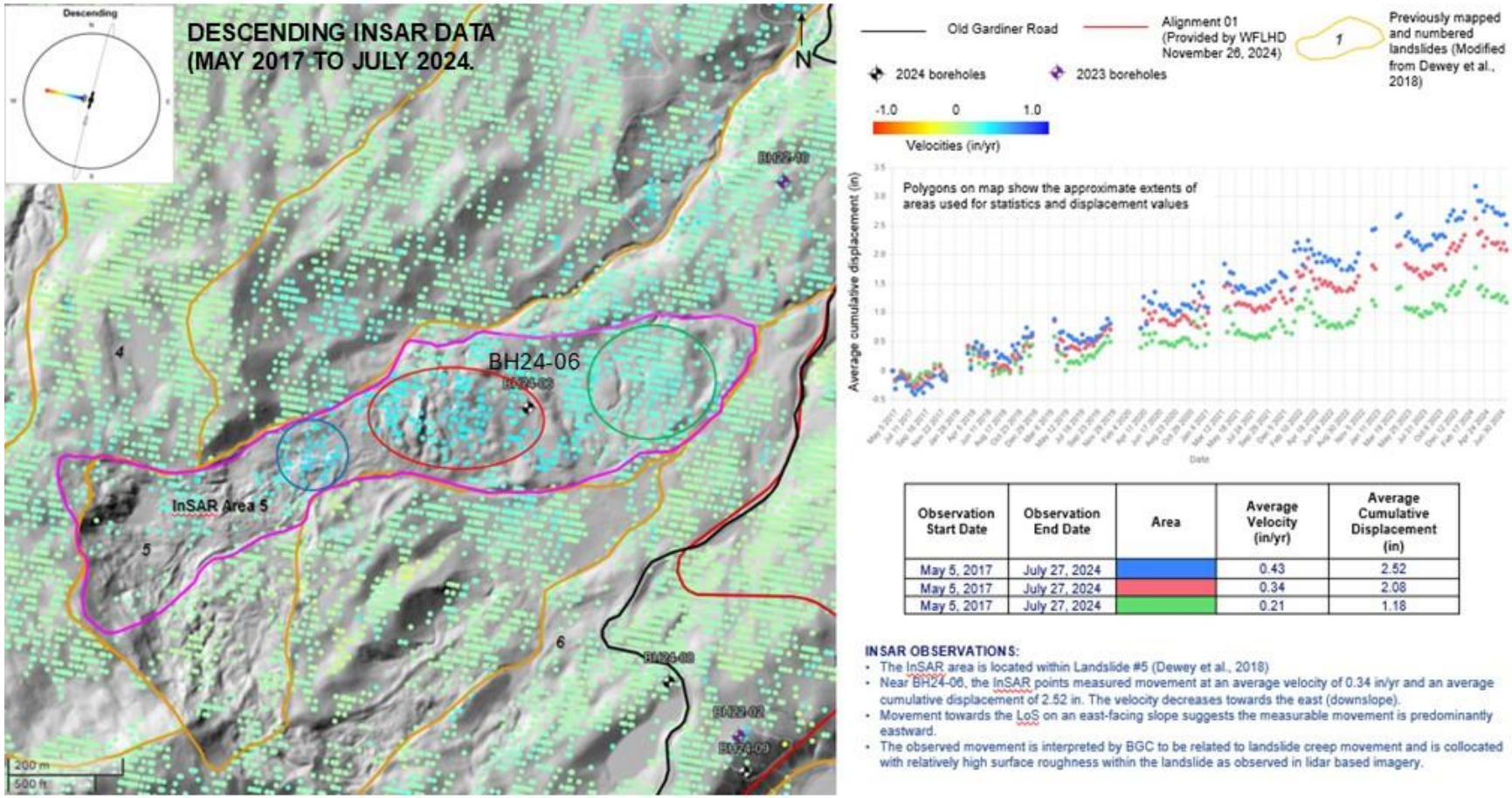


Figure 7 –Descending InSAR Data between May 2017 and July 2024 in the active area within Landslide #5 (*6*). The blue colors indicate movement. The plot on the right shows average cumulative displacements over time within the oval polygons shown on the image in the left. The measured displacement decreases towards the east.

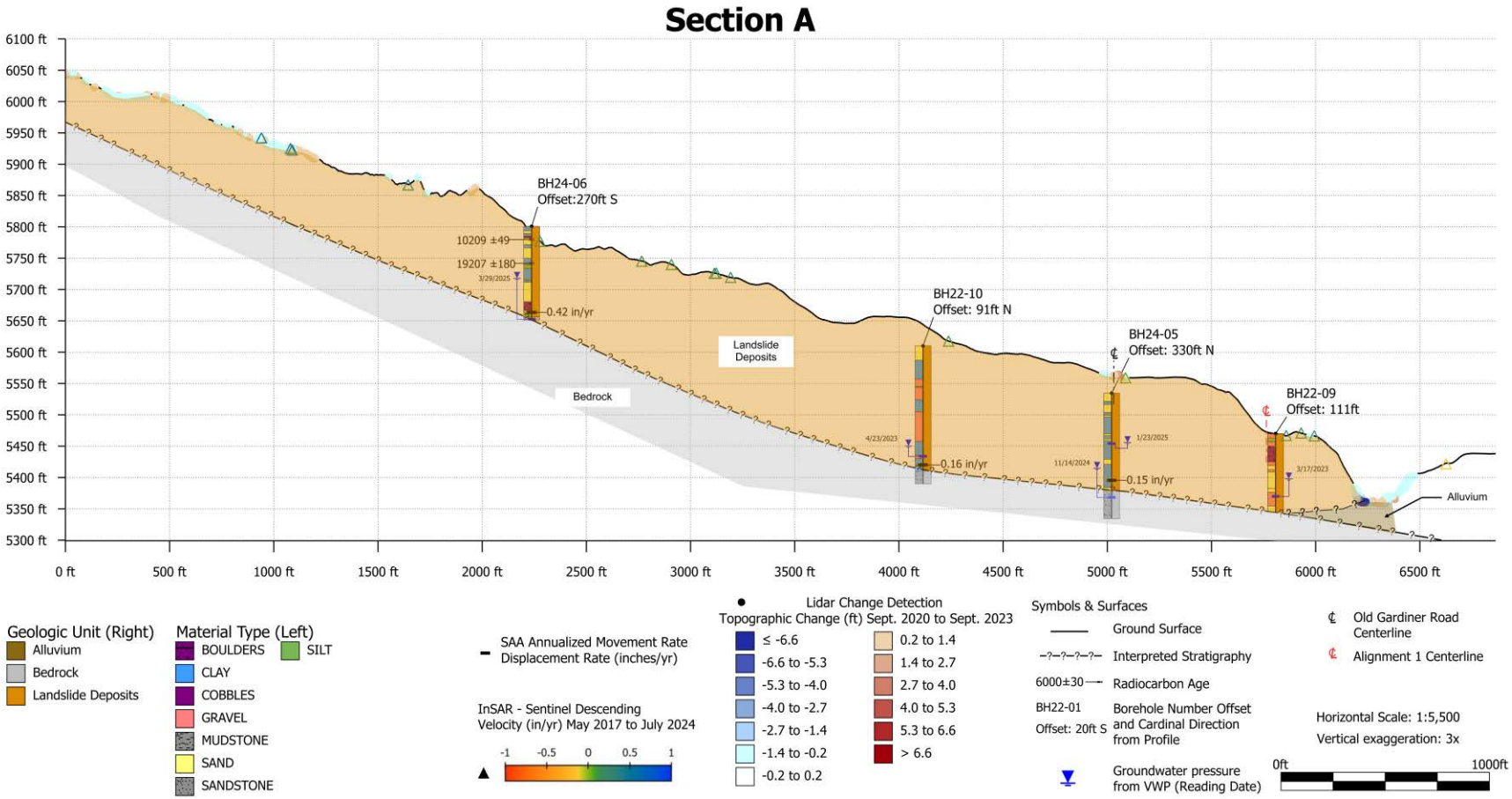


Figure 8 – Geologic Cross-Section Through Landslide #5.

SUMMARY AND CONCLUSIONS

This study utilized traditional geologic mapping and subsurface characterization methods along with innovative subsurface deformation instrumentation and remote sensing methods to characterize a landslide complex on the Mammoth to Gardiner permanent road project in Yellowstone National Park. This integrated approach provided robust evidence of large-scale active creeping landslides that informed the alternative roadway alignment selection process.

Different remote sensing methods better captured different rates and types of landsliding observed on the project site. LCD uses high-resolution digital elevation models to indicate the movement over the area of interest that has occurred between two specific points in time; whereas, InSAR analysis provides a general trend of movement at specific points over the period of available imagery. The LCD results for the North Entrance Road corridor generally provided a more reliable indication of the more localized and very slow to slow landslide movement (*7*) that occurred at the toe of the earth flows along the Gardner River Canyon as a result of the 2022 Flooding. The InSAR analysis proved to be a more reliable indication of the very slow to extremely slow (*7*) creeping movement observed at various locations within the earth flow landslide complex. Detailed borehole logging and soil characterization provided critical context for understanding instrumentation data and the landslide movement mechanism. Measured subsurface displacement in SAAs was often coincident with observations of slickensides in borehole logs and typically in zones of high plasticity bentonitic clay.

The integration of these data provides an improved geologic understanding of the extent and movement rates across a landslide complex and is crucial to informing the selection of roadway alignments and decisions to improve resilience in geotechnical design. Conventional practice for subsurface investigations requires a waiting period to drill borings, install downhole instrumentation, and wait for movement data to help inform movements over discrete boring locations. The addition of remote sensing techniques greatly accelerated the investigation process in this emergency response project by providing an immediate data set from the last several years. The InSAR data was particularly helpful in delineating the more active landslide areas, which helped in the selection of exploration locations and road alignment alternatives.

REFERENCES

1. Chase, K.J., D. Dutton, W.B. Hamilton, S.A. Siefken, C. Vander Voort, C., and A. Whiteman, *June 2022 Floods in the Upper Yellowstone River Basink,* U.S. Geological Survey Fact Sheet 2024–3035, 2024, 6 p., https://doi.org/10.3133/fs20243035.

2. Dewey, C.S., K.L. Pierce, and G.E. Nicholas, Geological Studies on the North Entrance Road: Phase 3 – Collaboration on Alternatives for the Road Corridor, Slickenside Consulting, LLC, 2018.

3. Pierce, K.L., C.S. Dewey, and G.E. Nicholas, Surficial Geologic Map Involving the Roads Between Gardiner, Montana and Mammoth, Wyoming, 2018.

4. Nicholas, G.E., Landslide Morphology and Its Insight into the Timing and Causes of Slope Failure: Case Study of Post-Glacial Landslides in Yellowstone National Park, 2018.

5. U.S. Geological Survey (USGS), 1222, 2020 LiDAR. USGS Original Project Resolution WY_YellowstoneNP_2020_D20 12TWQ350375: U.S. Geological Survey, 2021.

6. BGC Engineering USA Inc., *Geotechnical Memorandum GM5824, Mammoth to Gardiner Remote Sensing Interpretations.* Prepared for Western Federal Lands Highway Division, Federal Highway Administration, FHWA, 2025.

7. Cruden, D.M. and D.J. Varnes, Landslide Types and Processes, Special Report, Transportation Research Board, National Academy of Sciences, 247, 1997, pp. 36-75.

Engineering Assessment of Field Data from A Unique Drive Point Method

Paritosh Chataut
Graduate Student
Department of Civil and Architectural Engineering and Construction Management
University of Wyoming
1000 E. University Avenue, Laramie, Wyoming, 82071
pchataut@uwyo.edu

Keely Wolf
Graduate Student
Department of Mathematics and Statistics
University of Wyoming
1000 E. University Avenue, Laramie, Wyoming, 82071
kwolf6@uwyo.edu

Kam Ng, P.E., Ph.D., M. ASCE (Corresponding author)
Professor
Department of Civil and Architectural Engineering and Construction Management
University of Wyoming
1000 E. University Avenue, Laramie, Wyoming, 82071
kng1@uwyo.edu

Shaun S. Wulff, Ph.D.
Professor
Department of Mathematics and Statistics
University of Wyoming
1000 E. University Avenue, Laramie, Wyoming, 82071
wulff@uwyo.edu

Taylor Ree, P.G.
Principal Geologist
Wyoming Department of Transportation
5300 Bishop Blvd., Cheyenne, WY 82009-3340
taylor.ree@wyo.gov

Prepared for the 74th Highway Geology Symposium, August, 2025

Acknowledgments

The authors express their gratitude to the research supports from the Wyoming Department of Transportation.

Disclaimer

Statements and views presented in this paper are strictly those of the authors, and do not necessarily reflect positions held by their affiliations, the Highway Geology Symposium (HGS), or others acknowledged above. The mention of trade names for commercial products does not imply the approval or endorsement of HGS.

Copyright Notice

Copyright © 2025 Highway Geology Symposium (HGS)

All Rights Reserved. Printed in the United States of America. No part of the publication may be reproduced or copied in any form or by any means – graphic, electronic, or mechanical, including photocopying, taping, or information storage, and retrieval system – without prior written permission of the HGS. This excludes the original author(s).

ABSTRACT

Site investigation (*SI*) is an important part of the engineering design and construction of highway infrastructure. The Drive Point (*DP*) method, as a unique *SI* technique, has been utilized by the Wyoming Department of Transportation in most highway projects since the 1960s. This *DP* method involves driving a 1¾-inch hollow steel rod with a 2-inch solid conical tip into the ground and recording the number of blows required for each foot of penetration. The *DP* blow counts provide a "continuous" profile of the relative denseness of the subsurface. This paper presents an engineering assessment of the amassed *SI* data and a proposed method for correcting *DP* blow counts. *DP*, Standard Penetration Test (*SPT*), geotechnical and pile driving data from 86 bridge projects, including dynamic load test data of 68 test piles has been compiled. This study shows that the measured *DP* blow count is influenced by the corresponding overburden stress. Adopting the methodology developed for *SPT* N-values, a more advanced method considering both statistical and engineering criteria is proposed to correct *DP* values for the overburden effect in term of the effective vertical stress. Geomaterials were categorized based on the Unified Soil Classification System and denseness, and a reference effective vertical stress of 2 kips per square foot (ksf) was selected to improve *DP* correction. The methodology for *DP* correction is demonstrated for silty sand SM with medium density. A mathematical expression for a *DP* correction factor (C_{DP}) in terms of effective vertical stress was proposed. The proposed method was validated by evaluating the consistency of the corrected *DP* values.

INTRODUCTION

Site investigation (*SI*) is an important component of the engineering design and construction of highway infrastructure. *SI* involves the use of various laboratory tests conducted on representative soil samples, as well as in-situ methods. The Drive Point (*DP*) method is a unique in-situ *SI* technique that has been employed by the Wyoming Department of Transportation (WyDOT) in most highway projects since the 1960s. This *DP* method involves driving a 1¾-inch hollow steel rod with a 2-inch solid conical tip into the ground and recording the number of blows required for each foot of penetration. This driving is performed using a standard weight of 140 lbs. and 30 inches for the hammer drop height. WyDOT currently utilizes an automatic hammer with average efficiency of 90% for this operation (*1*). Figure 1 shows a 2-inch diameter steel *DP* cone.



Figure 1 - A 2-inch diameter steel drive point

The *DP* blow counts provide a continuous profile of the relative denseness of the subsurface. Standard penetration test (*SPT*), as one of the commonly used in-situ test methods, is often conducted at about 5 ft. intervals and can only provide a discrete snapshot of the subsurface condition. Furthermore, the *DP* method is more suitable than other continuous subsurface methods, such as the cone penetration test (*CPT*) in subsurface conditions with boulders, cobbles, and hard gravels. However, the measured *DP* blow counts cannot be directly used to estimate the subsurface soil properties such as friction angle and unit cohesion. The current study has demonstrated that the measured *DP* blow counts depend on the overburden stress at which the *DP* test was conducted. Therefore, to correlate the *DP* blow counts with in-situ soil properties, standardization of the *DP* method in terms of a reference overburden stress is necessary. This study performs this standardization for overburden pressure in terms of effective vertical stress. Previous studies on similar in-situ *SI* methods, such as the *SPT* and the Texas

Cone Penetration (*TCP*) test, have also highlighted the need for standardization with respect to effective vertical stress (*2*,*3*). Departments of Transportation (*DOTs*) in the U.S. commonly use *SPT* blow count corrected for effective vertical stress, $(N_1)_{60}$ to predict soil properties such as friction angle and unit weight (*4*,*5*). This standardization is achieved by multiplying the measured blow counts by an overburden correction factor, namely C_N. The correction factor C_N is a function of the reference effective vertical stress and the effective vertical stress at which the test is conducted, as defined by Equation 1.

$$C_{\mathrm{N}} = \frac{\text{SPT or TCP blows at the reference effective vertical stress}}{\text{SPT or TCP blows at the required effective vertical stress}} \quad \text{(Eq. 1)}$$

To use this equation, a relationship between the measured blow counts and the corresponding effective vertical stress is required. Researchers have developed various mathematical expressions to establish such relationships for *SPT* and *TCP* tests (*2,3*). Table 1 provides a summary of some existing C_N relationships available for *SPT* and *TCP* tests. It can be observed that a reference effective vertical stress of about 2 ksf was commonly adopted. The reference effective vertical stress of 2 ksf was selected for *SPT* normalization because many existing design charts and graphs were already adopted for foundations when researchers began developing *SPT* correction factors. These design charts were developed using *SPT* data collected from soil layers at shallow depths. By standardizing the *SPT* N-value to a reference vertical stress corresponding to a shallow depth at which *SPT* data were collected, these available design charts could be used for soil layers at different effective stresses without requiring new empirical correlations (*6*). Bazaraa (*6*) adopted the design chart developed by Terzaghi (*7*) (Figure 2) for designing shallow foundation based on settlement criteria. This chart was developed using *SPT* N-values collected from soil layers under a specific effective vertical stress. To use this chart with *SPT* N-values collected at various effective vertical stresses, the N-values must be normalized to the same effective vertical stress at which the design chart was developed. However, the effective vertical stress corresponding to the soil layers from which Terzaghi collected the *SPT* data were not known. Bazaraa (*6*) proposed a methodology to determine the effective vertical stress at which Terzaghi's *SPT* data were collected in the development of the design chart shown in Figure 2. This methodology involved comparing the relationship between relative density and *SPT* N-value based on Terzaghi's data with the same relationship from data where the corresponding effective vertical stress is known. However, the exact relative density versus *SPT* N-value relationship for Terzaghi's data was also not known. The only available information was the relationship between *SPT* N-value and soil denseness as shown in Table 2. To convert this denseness classification into relative density, definitions from various researchers were used; one such definition, proposed by USBR (*8*), is presented in Table 3. Integrating Tables 2 and 3, Bazaraa (*6*) developed a relationship between *SPT* N-values and relative density as shown in Table 4, and the derived relationship is plotted in Figure 3. Using the same methodology, Bazaraa (*6*) developed similar relationships using definitions proposed by Burmister (*9*) and Meyerhof (*10*). Bazaraa (*6*) then compared the *SPT* N-value versus relative density curves in Figure 3 for the three methods (USBR, Burmister, and Meyerhof) with field-measured relationships established by Gibbs & Holtz (*11*) and Wu (*12*). Since the curve derived from Terzaghi's data fell between those of Gibbs & Holtz and Wu, Bazaraa (*6*) concluded that the effective vertical stress corresponding to Terzaghi's *SPT* data likely matched the average of these field measurements. Gibbs collected *SPT* N-values at effective vertical stresses between

0.94 ksf and 1.92 ksf, while Wu's data were collected at effective vertical stresses between 0.5 ksf to 3.0 ksf; The average effective vertical stress of the field measured data was 1.5 ksf that was adopted by Bazaraa (*6*). Later, Peck proposed a C_N relationship for *SPT* based on Bazaraa's work while using a reference effective vertical stress of 2 ksf (*13*,*14*). Since then, 2 ksf has been widely adopted by researchers (*2*) and engineers (*4*,*5*) as an industry standard (Table 1).

The present study indicated that the effect of effective vertical stress on *DP* blow count depends on the soil type and denseness. Thus, separate correction factor equations have been developed based on Unified Soil Classification System (*USCS*) soil classification and denseness. The adopted methodology will be demonstrated for silty sand SM with medium density.

Table 1- Overburden correction factor equations for SPT and TCP methods

Reference	C_N	Reference effective vertical stress	Reference effective vertical stress in ksf
Peck et al. (1974) (*13*)	$0.77log\frac{20}{\sigma_v'}$	1 tsf	2.00
Skempton (1986) (*15*)	Fine grained sand: $\frac{2}{1+\sigma_v'}$ Coarse grained sand: $\frac{3}{2+\sigma_v'}$	1 kg/cm^2	2.05
Liao and Whitman (1986) (*2*)	$\sqrt{\frac{1}{\sigma_v'}}$	1 tsf	2.00
Moghaddam et al. (2017) (*3*)	$\left(\frac{100}{\sigma_v'}\right)^{0.73}$	100 kPa	2.09

Table 2- Relationship between SPT N value and soil denseness proposed by Terzaghi (*7*)

SPT N value	Soil denseness
0-4	Very loose
4-10	Loose
10-30	Medium
30-50	Dense
50	Very dense

Table 3- Relationship between soil denseness and relative density as per USBR

Soil denseness	Relative density
Very loose	Below 15
Loose	15-35
Medium	35-65
Dense	65-85
Very dense	Over 85

Table 4- Relationship between SPT N value collected by Terzaghi and relative density based on USBR definition	
SPT N value	Relative density
0	0
4	15
10	35
30	65
50	85

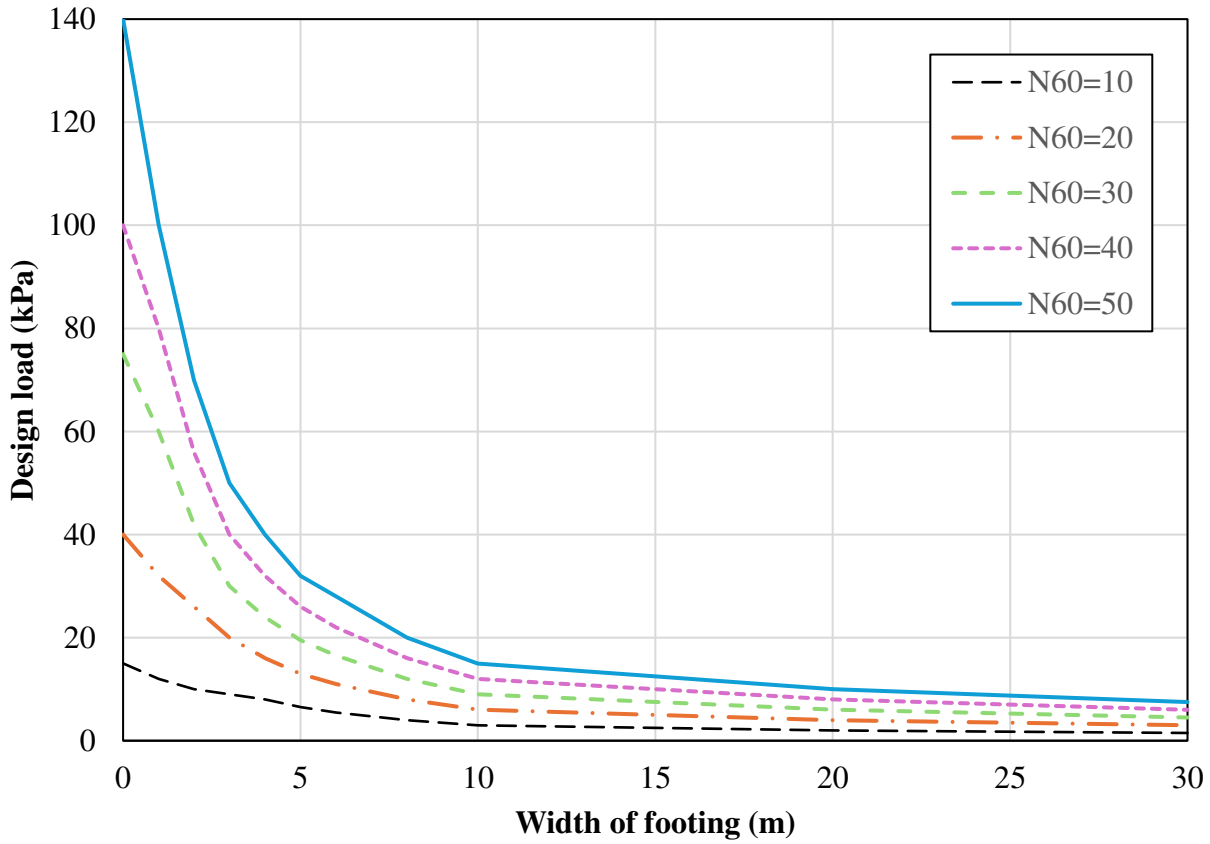


Figure 2 - Design Chart developed by Terzaghi to design shallow foundation based on SPT N value

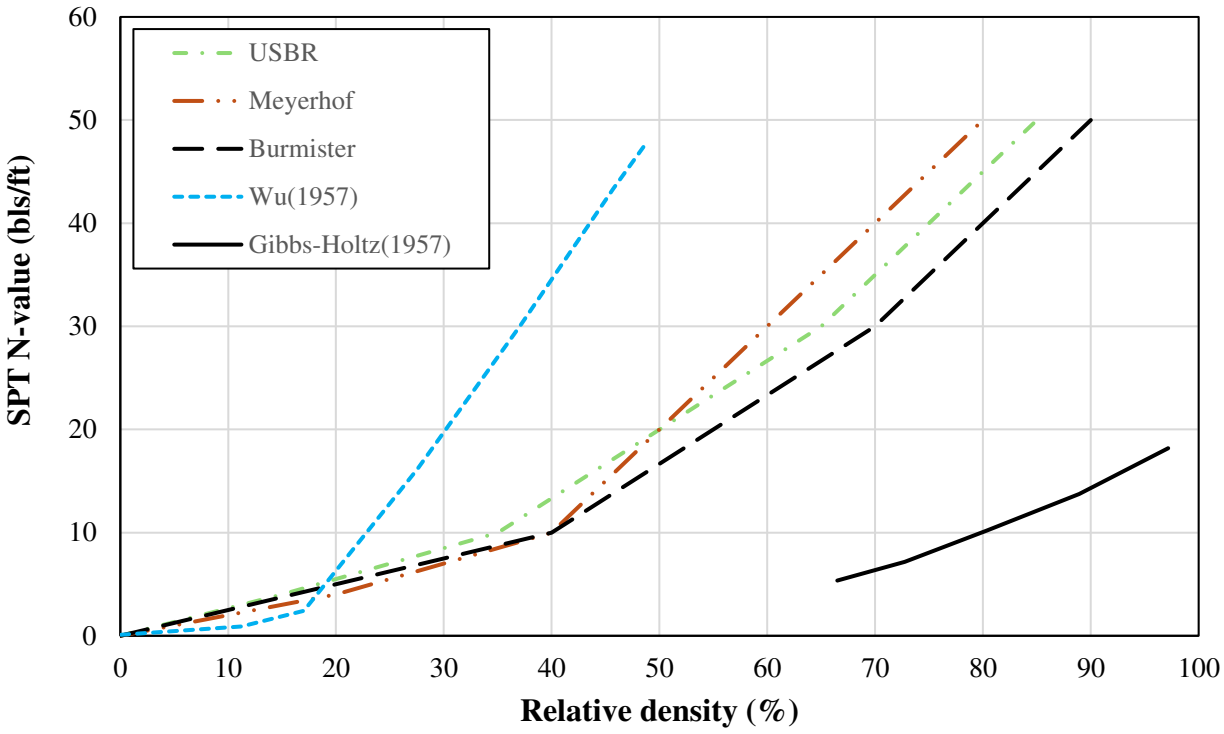


Figure 3 - Comparison of SPT verses relative density relation obtained from Terzaghi's data and field measured data

METHODOLOGY

Database preparation

DP, *SPT*, geotechnical, and pile driving data from 86 bridge projects were compiled and assessed. *DP* data were obtained from two sources. First, the *DP* data were collected from drill logs for projects where such logs were available. Figure 4a shows the drill log for the *SI* station 397+55, 35'Rt. of bridge project I806209 in Wyoming. The *DP* blow count data were provided under the heading "Drive Point". For the remaining projects where drill logs were not available, *DP* data were determined from the *DP* driving logs provided in the project plan documents. Figure 4b shows an example of *DP* driving logs provided in the plan for the same project. Figure 4c illustrates the digitization process used to determine *DP* data from *DP* driving logs. This digitization was performed using online application called PlotDigitizer. This application allows the user to extract data from an image or graph and uploaded a picture of *DP* driving log. After this, X-axis and Y-axis were defined in the program. For defining the X-axis, blue circular markers were placed at the 20 and 200 labels on the X-axis of the *DP* driving log, and the corresponding values were entered into the software. The Y-axis was defined in a similar manner using the red circular markers. The *DP* data were extracted by clicking various data along the *DP* driving line. These extracted points are shown by the white circular markers in Figure 4c. *DP* values obtained through digitization process were interpolated to obtain *DP* values at one foot interval using R program. Validation of this digitization and interpolation process was performed by comparing the *DP* data obtained from the digitization process for three *SI* stations of project

I806209 with the DP data of the corresponding *SI* stations available in the drill logs. Table 5 compares the digitized and interpolated *DP* data with the measured *DP* values from the borelogs at the *SI* station 397+55. As the *DP* values near the ground surface shows higher error due to the sensitivity of digitizing small *DP* values, *DP* values corresponding to less than 125 psf effective vertical stress were not considered in regression analysis.

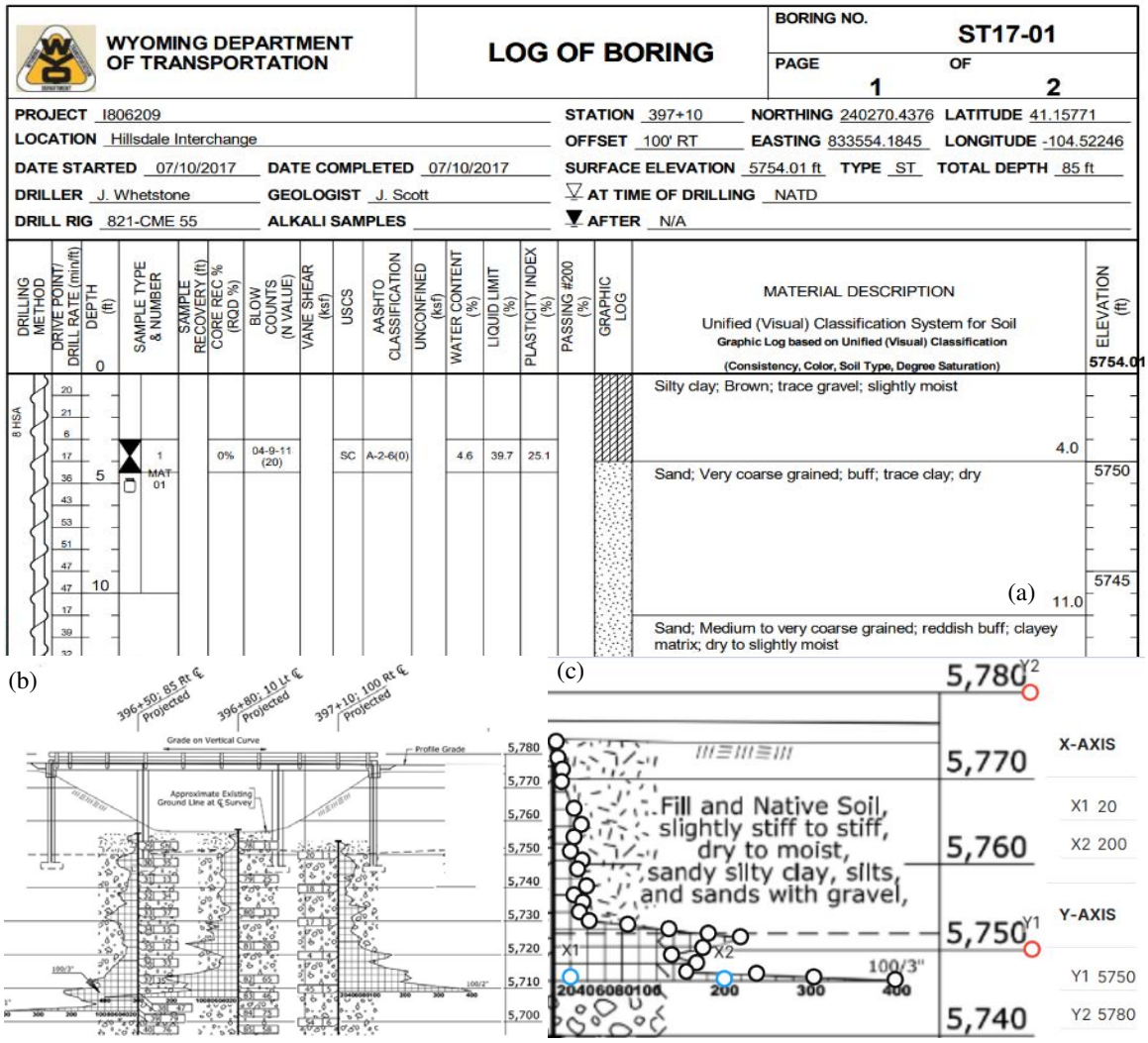


Figure 4 - a) DP data available in the project drill log, b) DP driving logs available in plan, and c) digitization process to determine DP data for bridge project I806209 in Wyoming

Table 5- Validation of digitization and interpolation process

Values from Digitization		Values after interpolation		Values from borelog		
Elevation ft	DP from digitization	Elevation ft	DP bls/ft	Elevation ft.	DP bls/ft	Percent Error %
5774.68	0.00	5774.4	2	5774.4	0	
5773.76	6.78	5773.4	7	5773.4	5	-40.0
5771.51	9.69	5772.4	9	5772.4	6	-50.0
5769.90	11.63	5771.4	10	5771.4	9	-11.1
5768.44	17.44	5770.4	11	5770.4	11	0.0
5766.54	25.19	5769.4	14	5769.4	11	-27.3
5764.59	33.43	5768.4	18	5768.4	16	-12.5
5763.32	25.67	5767.4	22	5767.4	19	-15.8
5761.61	20.83	5766.4	26	5766.4	25	-4.0
5760.44	33.91	5765.4	30	5765.4	27	-11.1
5759.41	30.03	5764.4	32	5764.4	33	3.0
5757.46	39.72	5763.4	26	5763.4	26	0.0
5756.44	27.61	5762.4	23	5762.4	23	0.0
5755.46	35.36	5761.4	23	5761.4	20	-15.0
5754.49	32.46	5760.4	34	5760.4	35	2.9
5753.51	42.15	5759.4	30	5759.4	29	-3.4
5753.12	62.49	5758.4	35	5758.4	34	-2.9
5752.93	92.04	5757.4	39	5757.4	39	0.0
5752.44	131.76	5756.4	28	5756.4	25	-12.0
5752.05	166.16	5755.4	35	5755.4	35	0.0
5751.80	200.55	5754.4	33	5754.4	31	-6.5
5751.51	218.96	5753.4	48	5753.4	42	-14.3
5750.73	199.58	5752.4	135	5752.4	125	-8.0
5749.95	166.64	5751.4	216	5751.4	220	1.8
5749.41	139.52	5750.4	186	5750.4	190	2.1
5748.93	153.08	5749.4	140	5749.4	135	-3.7
5748.54	165.67	5748.4	164	5748.4	168	2.4
5747.56	155.02	5747.4	174	5747.4	154	-13.0
5747.17	200.07					
5747.07	238.82					
5746.88	283.39					
5746.68	332.32					
5746.39	398.20					

Calculation of effective vertical stress

The effective vertical stress of soil (σ_v') at various depths (h) corresponding to different *DP* blow counts was calculated using Equation 2. Using the groundwater table (*GWT*) elevation at the time of the *SI* and the soil unit weight (either moist unit weight γ_{moist} or saturated unit weight $\gamma_{saturated}$), the effective unit weight (γ') was calculated accordingly for layer i.

$$\sigma_v' = \sum \gamma'_i h_i \quad \text{(Eq. 2)}$$

where $\gamma' = \gamma_{moist}$ for the soil layer above *GWT*, and $\gamma' = \gamma_{saturated} - \gamma_w$ for soil layer below *GWT*.

Determination of overburden correction factor

The overburden correction factor for *DP* (C_{DP}) was developed based on *DP* and the corresponding effective vertical stress data. The mathematical expression for C_{DP} is presented in Equation 3. This method was adopted using the approach developed for SPT and CPT test. Our current study has shown that the effect of effective vertical stress on DP depends on the soil type and denseness. The available *DP* data were classified based on the *USCS* according to ASTM D2487-17 (*16*) and further categorized based on denseness as per Terzaghi et al. (*7*). $(N_1)_{60}$ values were used here to classify soil based on SPT data collected at various effective vertical stresses. Table 6 presents the classification criteria for categorizing soils according to denseness based on the corrected SPT N-values for coarse-grained soils.

Table 6- Classification of coarse-grained soils based on corrected SPT N-values

$(N_1)_{60}$	Denseness
0-4	Very loose
>4-10	Loose
>10-30	Medium
>30-50	Dense
>50	Very dense

Using this database, regression analysis was performed between the *DP* values and the corresponding effective vertical stress. The steps of the analysis were conducted as described below. Using the C_{DP} values obtained using Equation 3, corrected *DP* (DP_c) were calculated using Equation 4:

$$C_{DP} = \frac{\widehat{DP}(\sigma'_{ref})}{\widehat{DP}(\sigma'_v)} \quad \text{(Eq. 3)}$$

$$DP_C = DP \times C_{DP} \quad \text{(Eq. 4)}$$

where, $\widehat{DP}$ represents the predicted *DP* value, σ'_v is the effective vertical stress, and σ'_{ref} is the reference effective vertical stress adopted as 2 ksf. The correction process involved the following steps:

(1) Examine available data for *USCS* classification and density.
(2) Determine which *USCS* classes can be combined to yield similar $\widehat{DP}(\sigma'_v)$.
(3) Select a regression model to obtain $\widehat{DP}(\sigma'_v)$.
(4) Compute C_{DP} and use that value to obtain DP_c.
(5) Verify that DP_c is relatively constant across σ'_v.

A variety of regression models were evaluated to develop the prediction equations. Table 7 summarizes the forms of the prediction equations that were considered, where $\hat{\beta}_0$ and $\hat{\beta}_1$ are the estimated model parameters that define the mathematical relationship between σ'_v and predicted *DP* blow counts.

Table 7- Functional forms of the prediction equations	
Regression Model	**Functional Form**
Power	$\widehat{DP} = \hat{\beta}_0 \sigma_v^{'\,\hat{\beta}_1}$
Exponential	$\widehat{\mathrm{DP}} = \hat{\beta}_0 e^{\hat{\beta}_1 \sigma_v^{'}}$
Reciprocal	$\widehat{\mathrm{DP}} = \frac{\sigma_v^{'}}{\hat{\beta}_0 + \hat{\beta}_1 \sigma_v^{'}}$
Natural Logarithm	$\widehat{\mathrm{DP}} = \hat{\beta}_0 + \hat{\beta}_1 ln(\sigma_v^{'})$
Linear	$\widehat{\mathrm{DP}} = \hat{\beta}_0 + \hat{\beta}_1 \sigma_v^{'}$

Regression model performance was evaluated using the following criteria:

- The average sum of squares of the corrected drive point values from the average of all the corrected drive point values (DP_c), denoted as *SSM*, provided a measure of goodness-of-fit between how well the model explained variation in the data (*17*).

- The cross-validated sum of squares, denoted as SSM_{CV}, is calculated using leave-one-out cross-validation (*LOO-CV*) (*18*). For each observation, the model was refit using all other data (training data), a DP_c value is predicted for the left-out observation (test data), and the corresponding *SSM* was calculated.

- The GAM-smoothed sum of squares (SSM_{GAM}) was obtained by fitting a Generalized Additive Model (*GAM*) with a smooth spline to the relationship between σ_v' and the DP_c values (*17*). This approach estimated a smoothed trend in the $\mathrm{DP_c}$ values. The smoothed predictions were then used to calculate the *SSM*.

- The GAM-cross validated smoothed sum of squares, denoted as $SSM_{GAM,\,CV}$, was computed by first applying a *GAM* with a smooth spline to the relationship between σ_v' and the cross-validated DP_c values (*17*). This approach estimated a smoothed trend in the leave-one-out DP_c values. The smoothed predictions were then used to calculate the *SSM*

- Akaike Information Criterion (*AIC*) values were used to compare the relative fit of the different regression models, with lower *AIC* values indicating a better balance between model fit and complexity (*17*).

Different weightings were assigned to these criteria based on engineering and statistical assessments. Each fitted model was assessed using the metrics defined above: *AIC, SSM,* SSM_{CV}, SSM_{GAM}, and $SSM_{GAM,CV}$. For each of these metrics, the prediction equations were ranked from 1 to 5, with the lowest values receiving the highest rankings. To summarize overall model performance in a single value, a weighted average of the ranks was calculated. The rankings helped in formulating about the weights on the individual criteria. The weights were assigned as follows: 0.4 for *SSM*, 0.3 for *AIC*, and 0.1 each for SSM_{CV}, SSM_{GAM}, and $SSM_{GAM,CV}$. *SSM* was

assigned the highest weight of 0.4, as it reflected the consistency of DP_c values across varying σ_v', which was the primary objective of the correction process. *AIC* received a weight of 0.3, for the importance in balancing model fit and model complexity. The remaining criteria SSM_{CV}, SSM_{GAM}, and $SSM_{GAM,CV}$ were each assigned a weight of 0.1, as they provided insights, but were considered secondary in importance relative to overall consistency and fit. These weighting assignments prioritized models that exhibited low variability after correction and best model fit while also considering smoothness and cross-validated performance. The model with the lowest weighted average was selected, representing the best overall balance across all evaluation criteria. Individual ranks were also provided in order to easily accommodate other weighting schemes.

RESULTS

After reviewing the available data by the *USCS* and density classifications, the second step in the overburden pressure correction process involved grouping *USCS* classifications based on similarities in drive point as a function of effective vertical stress, $\widehat{DP}(\sigma_v')$. To determine which classes could be combined, analysis of variance (*ANOVA*) techniques were applied (*17*). This approach allowed for simplification of the modeling process and increased sample sizes within each *USCS*–density combination in order to improve the fitting of the final regression models. Tables 8 and 9 show the groupings before and after consolidation for coarse-grained sand classifications, and the available sample sizes.

Table 8- Original coarse-grained sand USCS/density classification combinations

Classification	SC	SC-SM	SM	SP	SP-SM	SW	SW-SM	SP-SC
Dense	421	11	438	84	165	74	35	0
Loose	108	30	354	44	92	27	21	0
Medium	597	118	665	197	396	138	56	6
Medium(Fill)	0	0	125	0	0	0	0	0
Very dense	116	21	403	175	189	45	96	16
Very Loose	0	0	36	0	15	0	0	0

Table 9- Coarse-grained sand USCS/density classification combinations after performing ANOVA.

Classification	SC+SC-SM+SW	SM	SP-SM	SW-SM+SP+SP-SC
Dense	506	438	165	119
Loose	165	354	92	65
Medium	853	665	396	259
Medium (Fill)	0	125	0	0
Very dense	182	403	189	287
Very Loose	0	36	15	0

After defining *USCS* groups and corresponding density classifications, each unique combination was analyzed individually. Before fitting models, linear regression was performed to each unique combination involving *USCS* group and density classification. Outliers were identified using standardized residuals compared against a Bonferroni-adjusted critical value from the *t*-distribution (*17*). Engineering assessment of the outliers identified through this

statistical process was performed. The underlying causes of these outliers were identified through this engineering assessment, and further analysis was conducted after removing the identified outliers.

The development of the correction equation process is demonstrated here based on *USCS* SM with medium density. This soil group has 665 total observations. Based on the statistical analysis, seven of these observations were identified as outliers. An engineering assessment was conducted and determined that these outliers corresponded to elevations where sudden changes in subsurface denseness, making soil classification based on *SPT* criteria difficult. This condition is illustrated by the following example (Table 10): as part of the *SI* for a bridge constructed over a BNSF railway line under project N345093, a *DP* test was conducted at *SI* station 190+35, 38' Lt. At this location, an *SPT* test conducted at elevation 3873 ft, and the soil classification provided in the plan indicated a medium dense SM soil layer. However, *DP* values showed a sharp increase from elevations 3873 ft to 3872 ft, making it challenging to classify the soils at 3872 ft and 3871 ft based on the *SPT* data at 3873 ft. As a result, the *DP* data at these lower elevations appeared as outliers in the statistical analysis. Further analysis was conducted using 658 observations after removing the seven identified outliers.

Table 10- Engineering assessment of outliers based on project N345093

DP bls/ft	Soil layers	USCS	Elevation ft	σ'_v lbs/ft^2	SPT bls/ft		Classification
					N	$(N_1)_{60}$	
126	Soft to very stiff, sandy to fat clay with isolated gravel and gypsum layers with caliche stringers; dry to moist		3877	5659.58			
139			3876	5587.98			
128			3875	5516.38			
128			3874	5444.78			
177		SM	3873	5373.18	22	22.15	Medium
261			3872	5301.58			
295			3871	5229.98			

Table 11 compares the five prediction equations using the evaluation criteria: *AIC, SSM,* SSM_{cv}, SSM_{GAM}, and $SSM_{GAM,CV}$.Each fit was ranked for each criterion with the lowest values ranked more favorable, and a weighted score was calculated using assigned preferred weights. The exponential model had the lowest weighted average (1.6) and was selected as the best fit for this group.

Table 11- Comparison of regression models											
Model	a. AIC	b. SSM	c. SSM_{CV}	d. SSM_{GAM}	e. $SSM_{GAM,CV}$	Ranking based on criteria					Weighted average
						a	b	c	d	e	
exponential	6125.44	314.84	315.68	11.44	11.58	1	1	1	4	4	1.60
reciprocal	6128.56	338.05	338.88	0.25	0.23	2	2	2	1	1	1.80
Power	6132.68	342.77	344.08	0.35	0.39	3	3	3	2	2	2.80
Linear	6137.88	360.61	361.57	2.42	2.52	4	4	4	3	3	3.80
Log	6266.83	4982.74	4112.55	1202.82	1069.70	5	5	5	5	5	5.00

Criteria a, b, c, d, and e corresponds to AIC, SSM, SSM_{CV}, SSM_{GAM}, and $SSM_{GAM,CV}$ respectively

The selected prediction equation for SM with medium density was based upon the exponential model, described by Equation 5.

$$\widehat{\mathrm{DP}} = 12.55 \times \mathrm{e}^{0.36\sigma'_{\mathrm{v}}} \quad \text{(Eq. 5)}$$

$$\widehat{\mathrm{DP}}(\sigma'_{\mathrm{ref}}) = 12.55 \times \mathrm{e}^{0.36\times 2} \quad \text{(Eq. 6)}$$

$$\mathrm{C_{DP}} = \frac{\widehat{\mathrm{DP}}(\sigma'_{\mathrm{ref}})}{\widehat{\mathrm{DP}}(\sigma'_{\mathrm{v}})} \quad \text{(Eq. 7)}$$

$$\mathrm{C_{DP}} = \frac{12.55 \times \mathrm{e}^{0.36\times 2}}{12.55 \times \mathrm{e}^{0.36\sigma'_{\mathrm{v}}}} \quad \text{(Eq. 8)}$$

$$\mathrm{C_{DP}} = \frac{25.78}{12.55 \times \mathrm{e}^{0.36\sigma'_{\mathrm{v}}}} \quad \text{(Eq. 9)}$$

$$\mathrm{C_{DP}} = \frac{2.05}{\mathrm{e}^{0.36\sigma'_{\mathrm{v}}}} \quad \text{(Eq. 10)}$$

The expression for C_{DP} was obtained from the above Equations 5 to 10. Effective vertical stress of 2 ksf was considered as the reference to calculate the value of $\widehat{DP}(\sigma'_{ref})$ in Equation 6. Using this value and the prediction equation described by Equation 5, the expression for C_{DP} was obtained using Equation 7. Equation 10 provided the obtained mathematical expression for C_{DP}. Figure 5 shows the scatter plot for available data with the prediction Equation 5 from the exponential regression model. Figure 6 shows the graph for obtained overburden correction factor.

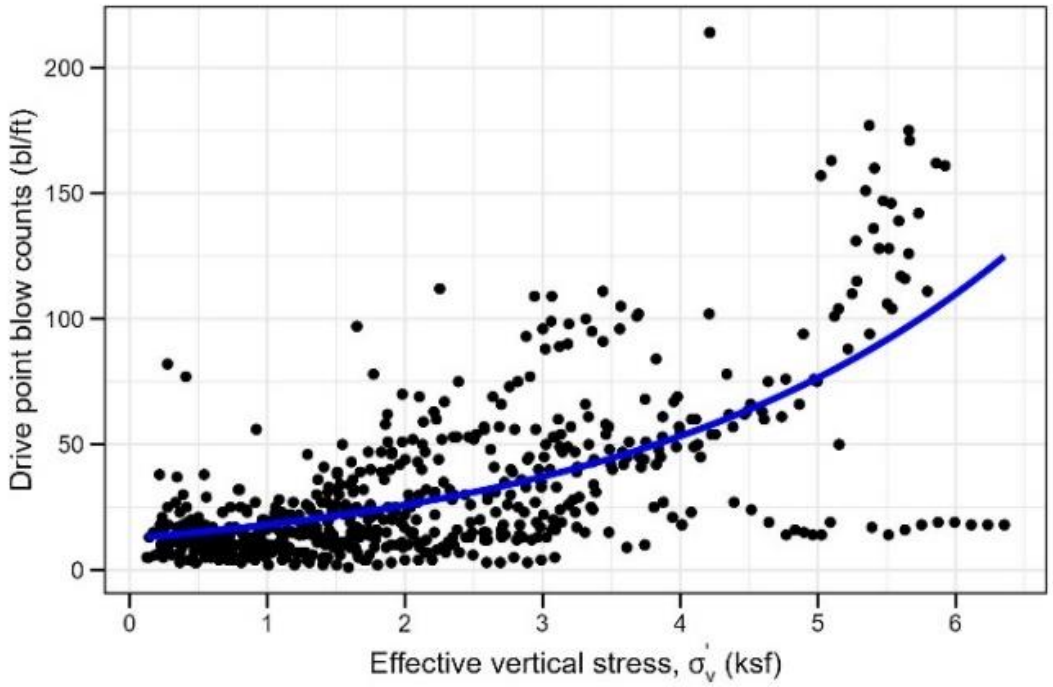


Figure 5 - Scatterplot of effective vertical stress and drive point along with the fitted curve from the exponential regression model

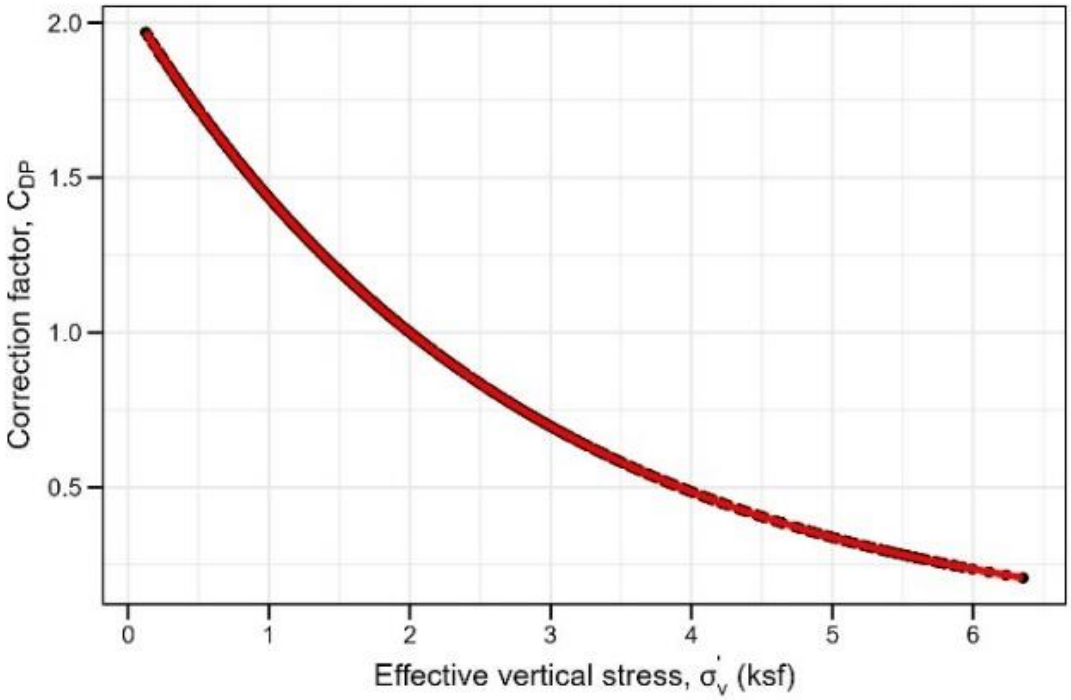


Figure 6 - C_{DP} values as a function of effective vertical stress

The validation of the obtained C_{DP} was performed by evaluating the consistency of the corrected *DP* values across various effective vertical stresses. Figure 7 displays the corrected *DP* values (DP_c) plotted against the effective vertical stress. The dashed orange line represents the mean corrected *DP*, while the solid green line shows the smoothed trend fitted using a

Generalized Additive Model (*GAM*) (17). Figure 8 presents the cross-validated DP_c values obtained from leave-one-out cross-validation (*LOO-CV*). These values are plotted against effective vertical stress. The orange dashed line again indicates the mean cross validated corrected *DP* (*CV-*DP_c), while the solid purple line shows the smoothed trend applied to the cross-validated points. A total of 658 original and 658 cross validated DP_c observations were available.

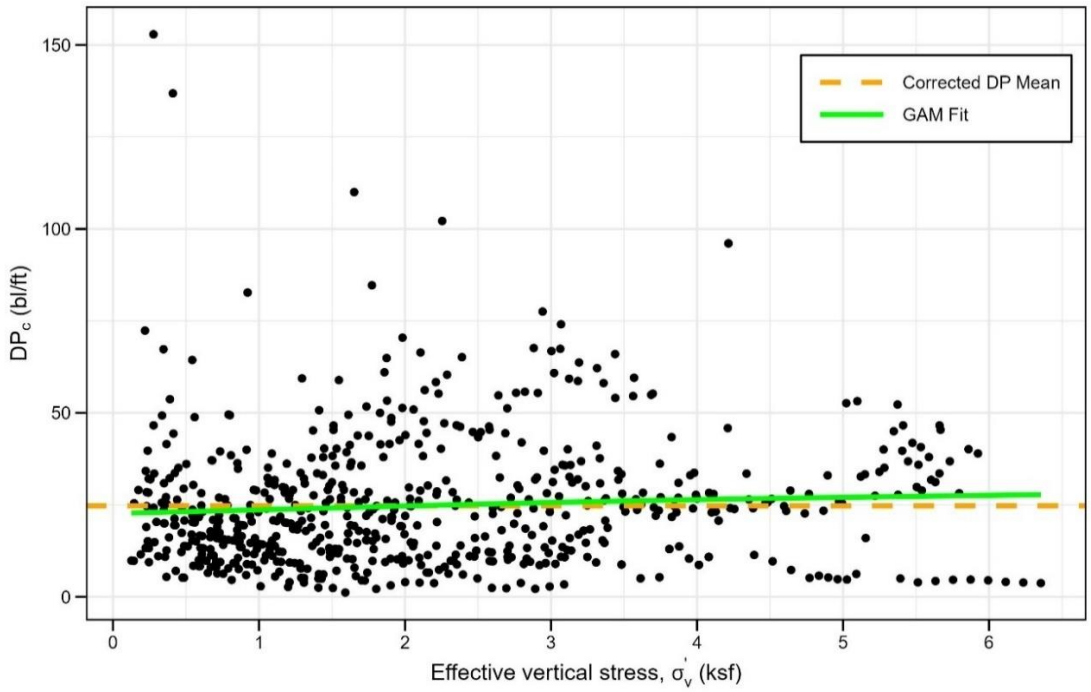


Figure 7 - Corrected DP values across effective vertical stresses in ksf for original data

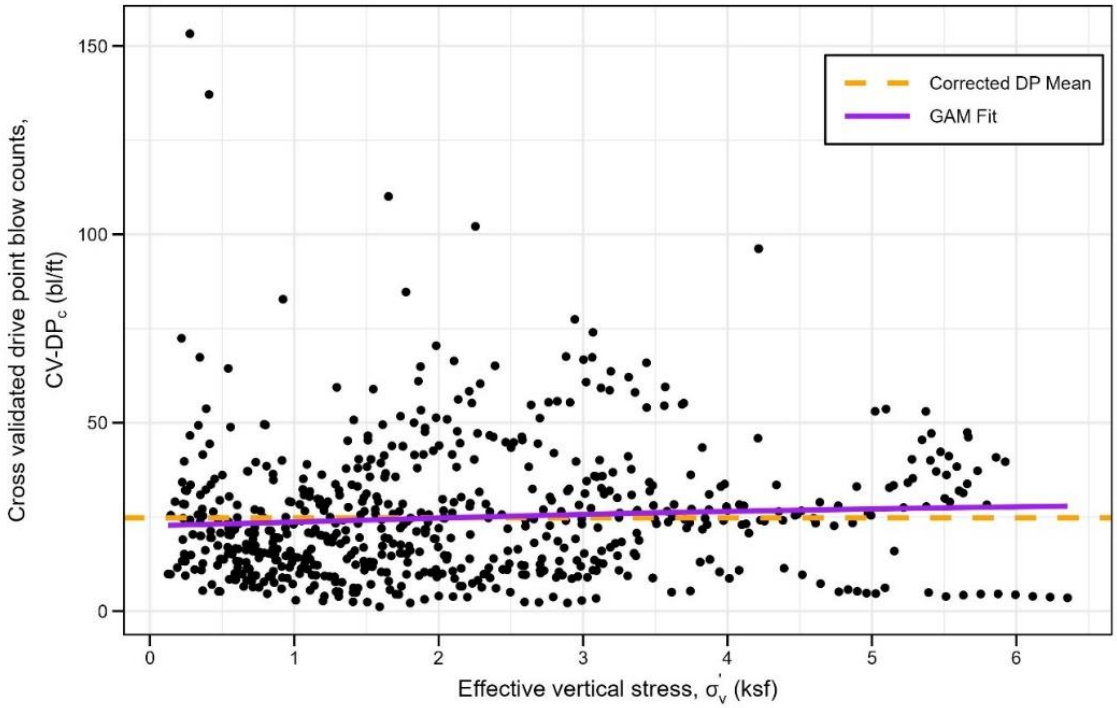


Figure 8 - Corrected DP values across effective vertical stresses in ksf for cross validated data

The use of LOO-CV in Figure 8 ensures that each corrected *DP* value was predicted without including the corresponding observation in the model, providing an unbiased validation of model performance (*18*). From Figure 7 and Figure 8, it can be observed that corrected *DP* remain relatively stable across relative stress, indicating that the overburden correction effectively standardized the measured *DP* blow counts. Thus, by using the proposed method, the measured *DP* blow counts can be standardized for overburden pressure in terms of σ_v'. The obtained C_{DP} has been compared with the C_N obtained for *SPT* and *TCP* methods in Figure 9. Our current study has shown that measured *DP* blow depends on the corresponding effective vertical stress value and shows an increasing trend. Therefore, to normalize these *DP* blow counts to a reference effective vertical stress of 2 ksf, C_{DP} less than 1 should be applied when the effective stress exceeds 2 ksf. Similarly, for effective stresses below 2 ksf, C_{DP} values greater than 1 should be used. This trend is shown by our proposed C_{DP} value and is consistent with the C_N developed for various *SPT* and *CPT* methods. Moreover, the C_{DP} values at different effective stresses are comparable to C_N values developed for the *SPT* and *CPT* methods. The obtained DP_c values will be utilized to develop correlations with soil properties such as friction angle, cohesion, and undrained shear strength. In addition, the DP_c will be used for predicting driven pile resistances.

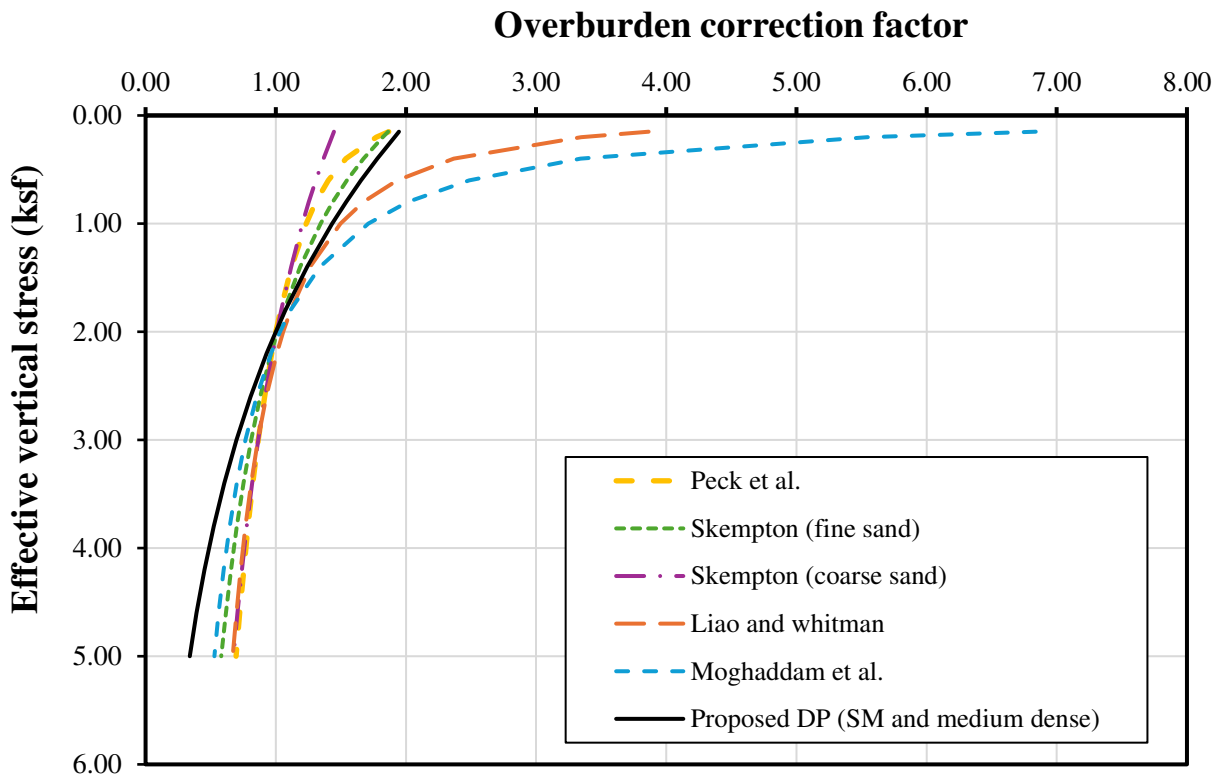


Figure 9 - Comparison of proposed overburden correction with various overburden correction factors developed for SPT and TCP test

SUMMARY AND CONCLUSION

The overburden correction factor was developed for the *DP* method. This study leads to the following conclusions:

(1) The *DP* blow count depended on the corresponding effective vertical stress. Therefore, standardization of the *DP* blow count to a reference effective vertical stress was necessary before using these values to predict in-situ soil properties.

(2) The relationship between *DP* blow count and effective vertical stress varied depending on the *USCS* classification and denseness of the soil. Accordingly, the available *DP* data were categorized based on these criteria. The *ANOVA* was used to group *USCS* soil types that were homogeneous in terms of *DP* and effective vertical stress.

(3) Regression analysis was performed for each soil group, and the corresponding overburden correction factors were developed in term of effective vertical stress. This process was demonstrated using the example of *USCS* soil type SM (silty sand) with medium density.

(4) The *DP* values, after standardization for overburden, were relatively stable across varying effective vertical stress, which confirmed the effectiveness of the proposed standardization method in accounting the effect of overburden pressure on *DP*.

REFERENCES

1. Hannigan, P.J. and A.M. Klesney, GRL report on energy measurement for dynamic penetrometers, standard penetration tests (SPT), Report prepared for Wyoming department of transportation, 2017.

2. Liao, S.S.C. and R.V. Whitman, Overburden correction factors for SPT in sand, *Journal of Geotechnical Engineering* vol. 112(3),1986, pp. 373–377.

3. Moghaddam, R.B., et al. Hammer efficiency and correction factors for the TxDOT Texas cone penetration test, *Geotechnical and Geological Engineering*, vol. 35 (5), 2017, pp. 2147–2162.

4. Texas Department of Transportation, Geotechnical Manual - LRFD. Bridge Division, 2024.

5. California Department of Transportation, Caltrans geotechnical manual (soil correlations), 2021.

6. Bazaraa, A.R.S.S, *Use of the Standard Penetration Test for Estimating Settlements of Shallow Foundations on Sand*, Ph.D. Thesis. University of Illinois, Urbana, 1967.

7. Terzaghi K., R.B. Peck, and G. Mesri, *Soil mechanics in engineering practice*, 3rd ed. New York: John Wiley & Sons, 1996.

8. Gibbs, H.J. and J. Merriman, *Progress Report of Research on the Penetration Resistance Method of Subsurface Exploration*, Earth Laboratory Report No. EM-314, Report prepared for U.S Bureau of Reclamation, 1952

9. Burmister, D. M., The Importance and Practical Use of Relative Density in Soil Mechanics, In Conference Proceedings: *ASTM International* vol. 48, 1948, pp. 1249–1268.

10. Meyerhof, G.G., Penetration Tests and Bearing Capacity of Cohesionless Soils, In Conference Proceedings: *ASCE.* vol. 82,1956. pp. 19.

11. Gibbs, H.J. and W.G. Holtz, Research on Determining the Density of Sands by Spoon Penetration Testing. In Conference Proceedings: *Fourth International Conference on Soil Mechanics and Foundation Engineering*, London, Vol 1, 1957, pp 35 - 39.

12. Wu, T.H., Relative Density and Shear Strength of Sands, In Conference Proceedings: *ASCE.* vol. 83,1957. pp. 23.

13. Peck, R. B., W.E. Hanson, and T.H. Thornburn, *Foundation Engineering*, 2nd ed. New York: John Wiley & Sons, 1974.

14. Deger, T.T., *Overburden Stress Normalization and Rod Length Corrections for the Standard Penetration Test (SPT),* Ph.D. Thesis, University of California, Berkeley, 2014.

15. Skempton, A.W., Standard penetration test procedures and the effects in sands of overburden pressure, relative density, particle size, ageing, and overconsolidation. *Géotechnique*, vol. 36(3), 1986, pp. 425-447.

16. ASTM D2487-17: Standard practice for classification of soils for engineering purposes (Unified Soil Classification System), ASTM International, January 2018.

17. Faraway, J. J., *Extending the Linear Model with R*, 2nd ed., Chapman and Hall/CRC, 2016.

18. James, G., D. Witten, T. Hastie, and R. Tibshirani, *An Introduction to Statistical Learning with Applications in R*, Springer Texts in Statistics, Springer, 2013.

Enhancing Risk Management in Transportation Geotechnics Through Standardized Data Collection

Declan Vanderhor
TabLogs Inc. 1615 Platte St,
(Level 2, The Circa Building)
Denver, CO 80202
(720) 720 3609
declan@tablogs.com

Prepared for the 74th Highway Geology Symposium, August, 2025

Disclaimer

Statements and views presented in this paper are strictly those of the authors, and do not necessarily reflect positions held by their affiliations, the Highway Geology Symposium (HGS), or others acknowledged above. The mention of trade names for commercial products does not imply the approval or endorsement of HGS.

Copyright Notice

Copyright © 2025 Highway Geology Symposium (HGS)

All Rights Reserved. Printed in the United States of America. No part of the publication may be reproduced or copied in any form or by any means – graphic, electronic, or mechanical, including photocopying, taping, or information storage, and retrieval system – without prior written permission of the HGS. This excludes the original author(s).

ABSTRACT

Risk management in transportation geotechnics relies heavily on the quality and consistency of subsurface data. Traditional borehole logging methods, often paper-based or manually transcribed, introduce variability that can lead to inconsistent interpretations, data silos, and increased project uncertainty. As infrastructure projects become more complex, ensuring standardized, reliable geotechnical data collection is essential for effective risk assessment and decision-making.

This paper explores how structured digital workflows and standardized data collection methods improve geotechnical risk management in transportation projects. By implementing consistent logging procedures, engineers can reduce variability in soil and rock classification, enhance predictive modeling for slope stability, and improve integration with geotechnical risk assessment frameworks. The ability to standardize logging practices across teams also supports regulatory compliance and long-term geotechnical asset monitoring.

Using case studies from recent transportation projects, this paper will demonstrate how standardized borehole data collection reduced data variability by over 60%, improved hazard detection accuracy, and accelerated data availability for decision-making. The discussion will also address challenges such as data validation, training field staff, and integrating standardized logs into GIS and geotechnical modeling tools.

By adopting structured data collection methods, transportation geotechnical engineers can significantly reduce uncertainty, improve collaboration, and enhance the reliability of risk assessments, ultimately leading to safer and more resilient infrastructure.

INTRODUCTION

The transportation sector is experiencing unprecedented demands due to aging infrastructure, climate change, and increasing urbanization. In such a context, geotechnical risk management becomes a cornerstone of safe and resilient infrastructure development. At the heart of effective risk management lies the quality and consistency of subsurface data. Unfortunately, conventional borehole logging practices—often reliant on paper forms or manually inputted digital records—are prone to errors, misinterpretation, and inefficiencies. This paper presents an in-depth analysis of how standardized, digital borehole data collection enhances geotechnical risk management in transportation projects. Through structured workflows, engineers can significantly reduce uncertainty, increase interoperability, and make better-informed decisions (*1*,*2*).

BACKGROUND AND OBJECTIVES

Borehole logging is a foundational practice in geotechnical investigations, serving as a primary source of data for ground characterization, design parameters, and risk analysis. However, inconsistencies in logging methodologies—ranging from varied classification systems and terminology to subjective interpretations—frequently result in data sets that are incompatible or difficult to compare across teams or project phases. This variability is particularly problematic in transportation projects, which often span large geographical areas, involve multiple contractors, and demand tight timelines for delivery.

Numerous industry reports have highlighted that inconsistent and unreliable ground investigation data has been a contributing factor to delays, rework, and even structural failures in transport infrastructure (*3*,*4*). For instance, the UK's Transport Infrastructure Efficiency Strategy (TIES, *5*) noted that standardization in data formats and processes could unlock significant cost savings by reducing duplication and avoiding costly remedial works.

Additionally, the Geotechnical Asset Management initiatives (*6*) undertaken by agencies like Highways England and the U.S. Federal Highway Administration stress that high-quality, repeatable ground investigation data is critical for long-term risk modeling, slope stability forecasting, and structural health monitoring.

Digitalization offers a pathway to overcome these longstanding inefficiencies. Structured digital workflows—particularly those aligned with data standards such as AGS and DIGGS—are enabling the geotechnical community to collect, validate, share, and analyze subsurface data more efficiently. The use of drop-down classifications, real-time digital input, GPS-tagged logs, and embedded validation rules is reducing the room for subjectivity and error in field data collection.

Ultimately, the transition to standardized digital borehole logging is about more than just speed—it's about improving confidence in geotechnical decisions and ensuring infrastructure resilience from the earliest phases of project planning through to operation and maintenance.

The key objectives of this paper are:

- To identify the limitations of traditional borehole logging methods in the context of transportation geotechnics.
- To examine how standardized digital workflows enhance the consistency and reliability of geotechnical data.
- To evaluate case studies demonstrating the benefits of such standardization.
- To discuss implementation challenges and strategies for overcoming them.

TRADITIONAL PRACTICES AND THEIR LIMITATIONS

Traditional borehole logging involves the manual recording of soil and rock descriptions in the field. These logs are later digitized, often inconsistently, by different personnel. The limitations include:

- Human error during transcription: Manual data entry in geotechnical logging is inherently prone to human errors, which can compromise data quality and reliability. A 2022 study by Russo et al. (*7*) highlighted that common errors in geotechnical core logging—such as misidentification of discontinuities and incorrect assessments of rock quality—are often due to insufficient or incorrect logging procedures and low skill levels among personnel. These errors can lead to conservative or overly optimistic analyses, impacting the design and safety of engineering projects.
- Subjective interpretations of soil classifications: The reliance on personal judgment during field logging leads to inconsistent identification of soil and rock types. Variability in classification across teams and regions is a known problem, and digital templates with standardized dropdown classifications have been proposed to reduce this subjectivity (*8*).
- Non-uniform terminology and units, leading to confusion: Without standardized vocabulary or measurement units, logs may be interpreted differently by stakeholders. This not only leads to miscommunication but can also delay reporting and model calibration (*8*).
- Difficulty in integrating with GIS and modeling tools due to non-standard formats: Traditional paper-based or unstructured digital logs often require significant reformatting to be compatible with GIS or modeling software. This lack of interoperability results in lost time and limits the ability to use geotechnical data for advanced analysis or visualization (*9*).
- Challenges in long-term data storage and retrieval: Paper records are vulnerable to degradation, loss, or damage, and inconsistent digital archiving makes data retrieval difficult over the lifecycle of a project. This severely limits historical comparison and longitudinal analysis (*2*).

These shortcomings introduce significant variability, complicating efforts to build accurate geological models and hindering effective risk management.

DIGITAL WORKFLOWS AND STANDARDIZATION

Standardized digital borehole logging tools enable field personnel to collect data in real-time using structured templates aligned with industry standards (e.g., AGS, DIGGS). These platforms ensure:

- **Uniform data structures** across all logs.
- **Drop-down classifications** to minimize variability.
- **Automated error checking and validation.**
- **Immediate availability** of data for stakeholders.

As Ioannides and Papadopoulos (*1*) highlight, the adoption of digital workflows in geotechnical engineering enables improved transparency, faster turnaround of design iterations, and enhanced team-wide access to critical information. Their findings reinforce that cloud-based environments and real-time data sharing not only reduce redundancy but also establish a collaborative culture of accuracy and efficiency across project lifecycles.

This is echoed in the work of Tian and Wang (*2*), who emphasize the role of data-centric geotechnics, digital twins, and data-driven modeling in systematically integrating prior knowledge, site-specific observations, and domain expertise across all stages of a geotechnical project. The digitization process also facilitates easier integration with Geographic Information Systems (GIS), Building Information Modeling (BIM), and risk modeling platforms.

El-Gohary and Mohamed (*10*) further support these insights by demonstrating how statistical digital analysis can optimize geotechnical parameter identification through data-driven workflows. The digitization process also facilitates easier integration with Geographic Information Systems (GIS), Building Information Modeling (BIM), and risk modeling platforms.

Goodbody (*4*) highlights that cloud technology enables seamless collaboration by giving field and office personnel simultaneous access to data, enhancing transparency, speeding up decision-making, and reducing rework. As multiple experts pointed out, this “single source of truth” dramatically improves the efficiency of data management and ensures that all stakeholders are aligned in real time.

Experts from Topcon and Atkins (*11*) emphasize that interoperability and data accessibility are central to modern geotechnical workflows, especially when dealing with large volumes of data collected via field instruments and sensors. These points further strengthen the rationale for standardized digital borehole logging systems integrated with cloud-based geotechnical platforms.

CASE STUDIES

Case Study 1: Slope Stability Monitoring in Norway Using Digital Twin Technology

In Norway, researchers developed and implemented a digital twin framework to monitor slope stability along critical highway infrastructure. The project combined real-time

sensor data with predictive modeling tools powered by artificial intelligence to monitor landslide-prone areas. The digital twin was continuously updated with live field data, enhancing the accuracy and responsiveness of slope failure predictions. This proactive approach allowed for early detection of hazardous conditions and supported more precise risk mitigation strategies. This case (*12*) reinforces the thesis that standardized digital workflows and structured data collection enable continuous monitoring and adaptive geotechnical modeling, ultimately leading to safer infrastructure and better-informed decisions.

Case Study 2: Shenzhen Metro Line 14 – Integrated Digital Management

The construction of Shenzhen Metro Line 14 in China (*13*) showcased how standardized digital workflows and data integration can improve large-scale urban infrastructure projects. The project team implemented a comprehensive digital twin environment that connected GIS, BIM, and construction data into a single platform. Using standardized templates and structured digital logs, contractors across disciplines were able to contribute to a unified digital ecosystem. This facilitated real-time collaboration, reduced the need for repetitive re-logging or manual data transfers, and improved traceability. The implementation of digital workflows enabled smoother project execution, enhanced stakeholder communication, and streamlined risk management efforts. This example validates the core message of this paper: that adopting standardized digital data practices enhances collaboration, improves data integrity, and increases project efficiency, particularly in transportation geotechnics.

RESULTS AND LESSONS LEARNED

Across both case studies and broader industry observations, the adoption of standardized data collection in transportation geotechnics yielded several benefits:

- **Reduction in data variability** by over 60% compared to manual logs.
- **Faster data processing times**, improving decision-making timelines.
- **Improved confidence** in geotechnical models due to consistent inputs.
- **Enhanced collaboration** across multidisciplinary teams.
- **Easier compliance** with regulatory documentation requirements.

Beyond consistency and speed, digital geotechnical workflows enable the use of advanced technologies such as automated generative design and virtual reality. These allow engineers to model, analyze, and refine structural solutions in real-time, dramatically improving efficiency and safety training (*2*,*14*). Furthermore, statistical tools such as correlation matrices and regression models have been shown to enhance parameter interpretation, enabling more accurate and replicable outcomes (*10*). Lessons learned include the importance of: Lessons learned include the importance of:

- User training to ensure proper use of digital tools.
- Change management strategies to transition teams from legacy methods.
- Feedback loops for continuous improvement of digital templates.

Practical case studies such as the Slope Stability Monitoring in Norway and the Shenzhen Metro Line 14 show how digital workflows and cloud-based systems lead to better

ground understanding, streamlined data sharing, and even design simplifications that reduced construction costs (*4*). These real-world implementations reinforce the broader benefits of digital standardization for data accuracy, collaboration, and client value.

IMPLEMENTATION CHALLENGES

Despite the benefits, Ioannides and Papadopoulos (*1*) acknowledge that digital transformation requires overcoming institutional inertia and skill gaps. Their study found that successful implementation often hinges on clear knowledge of software tools, strong cross-departmental communication frameworks, and a long-term digital strategy supported by leadership.

- **Resistance to change** from experienced personnel accustomed to paper-based methods.
- **Initial setup costs**, including hardware and software acquisition.
- **Data migration** from legacy systems.
- **Ensuring data security and redundancy.**

Tian and Wang (*2*) further highlight the challenge of working with "small and ugly" data typical in geotechnics, which requires new approaches like data-driven methods and machine learning supported by project-specific training databases. These challenges can be mitigated through targeted training programs, stakeholder engagement, and selecting scalable, user-friendly digital platforms.

Despite its benefits, the path to digital transformation in geotechnics is often hindered by resistance to change and variable levels of digital maturity across the supply chain. As noted by GEL and Mott MacDonald professionals, cultural adaptation, staff upskilling, and cross-software compatibility remain significant hurdles (*4*).

The article also echoes the importance of clear communication and training, noting that appointing internal ‘cloud champions’ and developing onboarding strategies are vital to overcoming friction during migration to digital systems.

FUTURE DIRECTIONS

Looking ahead, the integration of standardized borehole data with advanced technologies such as artificial intelligence (AI), machine learning, and remote sensing will further revolutionize geotechnical risk management. Predictive analytics based on consistent, high-quality data will enable:

- Real-time hazard identification.
- Automated anomaly detection.
- Enhanced lifecycle management of transportation infrastructure.

Echoing industry-wide trends, Ioannides and Papadopoulos (*1*), Tian and Wang (*2*), and El-Gohary and Mohamed (*10*) foresee that emerging technologies like virtual reality, generative modeling, and interactive cloud platforms will continue to redefine the way

geotechnical data is collected, processed, and applied. These tools are rapidly becoming not just enhancements, but necessities in high-stakes, multidisciplinary projects. Standardization will also support the development of national and international geotechnical data repositories, promoting transparency and long-term resilience planning.

As Goodbody (*4*) notes, the integration of geotechnical digital twins, automated monitoring systems, and machine-learning-ready data ecosystems is becoming essential to future geotechnical risk strategies.

CONCLUSION

Standardized digital data collection methods are transforming risk management in transportation geotechnics. By minimizing variability, enhancing data usability, and supporting integration with modeling and GIS tools, standardized logging enables more accurate assessments and proactive risk mitigation. While implementation presents challenges, the long-term benefits in terms of safety, efficiency, and reliability make the transition not only worthwhile but essential for modern infrastructure development. As infrastructure demands grow in complexity, the role of consistent and reliable geotechnical data will only become more critical. Engineers and project managers are encouraged to embrace standardized digital workflows to future-proof their projects and contribute to a safer built environment.

REFERENCES

1. Ioannides, M., and K. Papadopoulos, Digital transformation in geotechnical engineering, *Proceedings of the 10th International Symposium on Field Measurements in Geomechanics* (FMGM 2022), International Society for Soil Mechanics and Geotechnical Engineering (ISSMGE), 2022. https://www.issmge.org/uploads/publications/51/126/347_F_digital_transformation_in_geotechnical_engineering.pdf

2. Tian, Y., and L. Wang, Digital transformation and machine learning for geotechnical engineering: A framework and case study, *Computers and Geotechnics*, 157, 105283, 2023. https://www.tandfonline.com/doi/full/10.1080/17499518.2023.2278136#abstract

3. AGS, Digital transformation in ground engineering: Hopes and fears. Association of Geotechnical and Geoenvironmental Specialists, 2021. https://www.ags.org.uk/2021/07/digital-transformation-in-ground-engineering-hopes-and-fears/

4. Goodbody, A., *Embracing digitalisation in geotechnics*, New Civil Engineer, 2021, Retrieved from https://www.newcivilengineer.com/in-depth/embracing-digitalisation-in-geotechnics-09-09-2021/

5. Transport Infrastructure Efficiency Strategy (TIES), Published by the UK Infrastructure and Projects Authority (IPA), 2017. https://www.gov.uk/government/publications/transport-data-strategy-innovation-through-data

6. Daly, T., S. Carluccio, D. Bhanderi, D. Patterson, C. Power, and J. Codd, Use of Geotechnical Asset Data Within Highways England: The Journey so Far and the Future. In: A. Correia, J. Tinoco, P. Cortez, and L. Lamas, (eds), *Information Technology in Geo-Engineering. ICITG 2019,* Springer Series in Geomechanics and Geoengineering. Springer, Cham, 2022. https://doi.org/10.1007/978-3-030-32029-4_68

7. Russo, A, E. Montiel, and E. Hormazabal, Impact of the typical errors in geotechnical core logging for geomechanical design in large caving mines, in Y. Potvin (ed.), *Caving 2022: Proceedings of the Fifth International Conference on Block and Sublevel Caving*, Australian Centre for Geomechanics, Perth, 2022, pp. 1319-1334, https://doi.org/10.36487/ACG_repo/2205_92

8. Palmström A., RMi – a rock mass characterization system for rock engineering purposes. PhD thesis, Oslo University, Norway, 1995, 400 p. https://www.rockmass.net/phd/chapter3.pdf

9. Brown, J., D. Ruston, H. Cole, and B. Bruce, Geospatial data integration for geotechnical site characterisation. ESRI Petroleum GIS Conference, 2017. https://proceedings.esri.com/library/userconf/petrol17/papers/petrol_09.pdf

10. El-Gohary, F. S. M., and A. M. A. Mohamed, A. M. A., Digital transformation solution for identification of geotechnical parameters using statistical data analysis, *Scientific Journal of Engineering Research*, 5(3), 2021, pp. 59–70. https://journals.ekb.eg/article_214155_312eba0f87511dae90b50761e998381a.pdf

11. Lowries, R., A. Wu, and F. Hamidi, 2025). Connected Geotechnical Workflows Enable Dynamic Communication Mitigating Cost Pressures and Project Risk. In: C. Rujikiatkamjorn, J. Xue, B. Indraratna (eds), *Proceedings of the 5th International Conference on Transportation Geotechnics (ICTG) 2024*, Volume 3, ICTG 2024, Lecture Notes in Civil Engineering, vol 404, 2025, Springer, Singapore. https://doi.org/10.1007/978-981-97-8221-5_34

12. Xu, J. and Y. Zhang, AI-Powered Digital Twin Technology for Highway System Slope Stability Risk Monitoring, *Geotechnics* 5, no. 1:19, 2025. https://doi.org/10.3390/geotechnics5010019

13. Li, D., J. Wang, and K. Chen, Research on Integrated Management of Urban Rail Transit Project Based on Digital Twin. In: H. Guo, D. Fang, W. Lu, and Y. Peng (eds), *Proceedings of the 26th International Symposium on Advancement of Construction Management and Real Estate*, CRIOCM 2021. Lecture Notes in Operations Research. Springer, Singapore, 2022. https://doi.org/10.1007/978-981-19-5256-2_75

14. Dicu, A., and C. Simion, Digitization in geotechnical engineering - from concepts to applied practices, *Solid State Phenomena*, 2021, pp. 320, 337–342.

Subsidence Geohazard Investigations Using Geophysical Methods

Stan Smith
Collier Geophysics
7711 6th Avenue, Suite G
Lakewood, Colorado 80214
(720) 487-9200
ssmith@colliergeophysics.com

Prepared for the 74th Highway Geology Symposium, August, 2025

Acknowledgments

The author would like to thank the individuals for their contributions in the work described

Jorgen Bergstrom,
Collier Geophysics
(943) 300-9009
jbergstrom@collierconsulting.com

Doug Laymon,
Collier Geophysics
(512) 851-8740
doug@collierconsulting.com

Roy Bowling
Collier Geophysics
((720) 487-9200
roy@collierconsulting.com

Disclaimer

Statements and views presented in this paper are strictly those of the authors, and do not necessarily reflect positions held by their affiliations, the Highway Geology Symposium (HGS), or others acknowledged above. The mention of trade names for commercial products does not imply the approval or endorsement of HGS.

Copyright Notice

Copyright © 2025 Highway Geology Symposium (HGS)

All Rights Reserved. Printed in the United States of America. No part of the publication may be reproduced or copied in any form or by any means – graphic, electronic, or mechanical,

including photocopying, taping, or information storage, and retrieval system – without prior written permission of the HGS. This excludes the original author(s).

ABSTRACT

Sinkholes and subsidence can appear throughout the nation's highway system and are surface expressions of loss of subsurface support. These can be formed by geologic conditions, while others can be attributed as anthropogenic or human-made in nature. Geophysics can provide insight into their existing location and determine potential continued risk to surface conditions. Evaporite formations are susceptible to dissolution that can lead to collapse into a sinkhole, while mine working experiencing roof failures can also propagate toward the subsurface.

Subsidence and sinkhole features are a geohazard of concern in highway right-of-way due to their potential detrimental effect to highway projects. Subsurface imaging using geophysical methods such as electrical resistivity tomography (ERT) and seismic refraction tomography (SRT) can be useful when mapping these features to address highway engineering and construction related concerns. With differing conditions contributing to highway distress, it is important to consider which geophysical technique(s) to select to investigate the area of concern. Case studies will be presented to illustrate effective application of the appropriate techniques.

SINKHOLE FORMATION

In their Glossary of Geologic Terms, the National Park Services defines a sinkhole as “A circular, commonly funnel-shaped depression in a karst area with subterranean drainage.” This paper covers more than karst terrain. Additional subsidence conditions include evaporite dissolution and other water-soluble rocks. Mechanisms for subsidence and sinkhole formation are shown in Figure 1. Subterranean mines collapse over time as their roofs fail, shown in Figure 2.

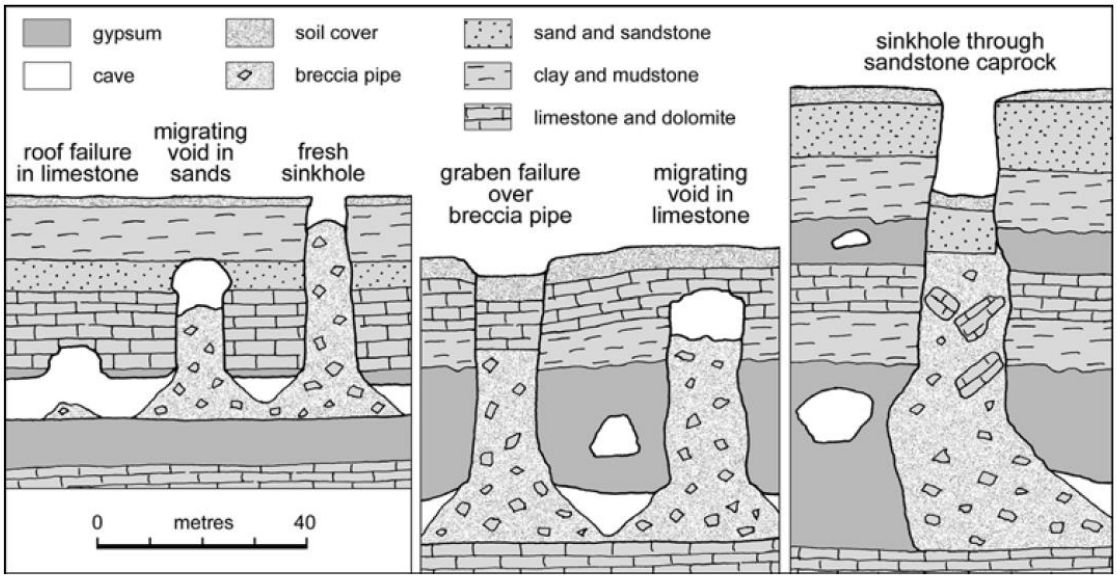


Figure 1 - illustrates formation of sinkholes in a few geologic settings. These scenarios diagram how cavities work to the surface expression of the feature. (*1*) From Herrick, C.G., Sandia National Laboratories.

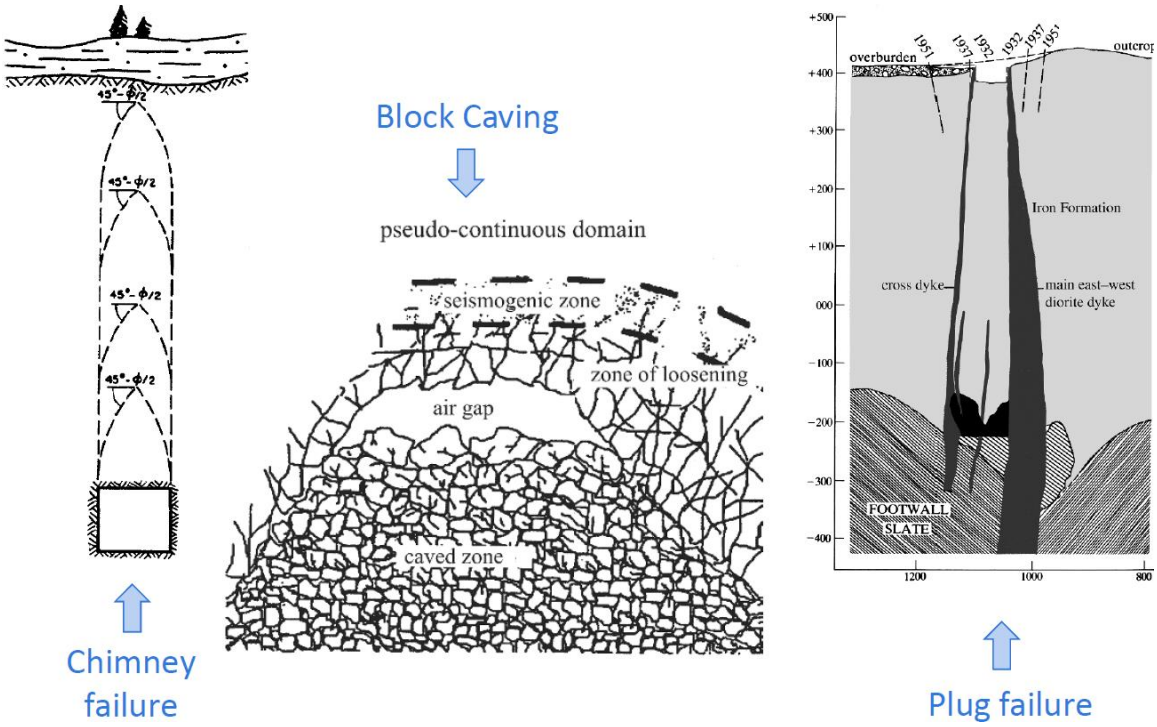


Figure 2 - shows diagrams of several types of caving. Abandoned mining workings commonly lead to geohazards. (*1*) From Herrick, C.G., Sandia National Laboratories.

Changes in groundwater levels can cause sinkholes. Heavy precipitation, including heavy rain and flooding events, can lead to sinkhole formation. Human-caused water leaks and sewer line failures also can be root causes of subsidence. Abandoned mine workings, as shown in Figure 2, roof collapse can be affected by nearby earthwork such as excavating and drilling activities. There are myriad conditions that lead to the surface expression of these geohazards.

APPLICATION OF GEOPHYSICAL METHODS

Subsurface imaging using geophysical methods such as electrical resistivity tomography (ERT) and seismic refraction tomography (SRT) can be useful when mapping these subsidence and sinkhole features to address highway engineering and construction related concerns. Additional geophysical methods applicable to detection and location of potential voids include, but are not limited to:

Electrical Imaging:

- Frequency-domain Electromagnetic (FDEM),
- Time-domain Electromagnetic (TDEM)
- Ground Penetrating Radar (GPR)

Seismic Methods:

- Surface Waves - Multichannel Analysis of Surface Waves (MASW)
- Seismic Reflection

Microgravity

There are ASTM guidelines and standards for these geophysical methods. See Figure 3.

ASTM guidelines and standards for subsurface geophysical investigations

Geophysical Method	ASTM Guide or Standard
Standard Guide for Selecting Surface Geophysical Methods	D6429
Seismic Refraction	D5777
Seismic Reflection	D7128
Electrical Resistivity	D6431
Geophysical Method	**ASTM Guide or Standard**
Time-domain electromagnetic	D6820
Ground-penetrating radar	D6432
Microgravity	D6430

Source: Sirles (2006)

Figure 3 - indicates ASTM Guidelines and Standards for Geophysical Methods. (*2*)

Publications such as USACE EM-1110-1-1802 are available to assist engineers when determining which geophysical method to use. Figure 4 is the matrix from the USACE. FHWA has also published the Application of Geophysical Methods to Highway Related Problems which includes overviews of various methods and applications, this includes detecting voids and sinkholes.

Table 2-1
Decision Matrix of Surficial Geophysical Methods for Specific Investigations

	Lithology	Top of Bedrock	Rippability	Detection of Water Surface	Fault Detectio	Suspected Voids or Cavity Detection	In Situ Elastic Moduli (Velocities)	Material Boundaries, Dip, ...	Linear Subsurface Water Conduits	Landfill Boundaries	Large Ferrous Bodies-Tanks	Conductive Bodies, Ores, Plumes, ...
Seismic Refraction	S	W	W	S	S		W	S				
Seismic Reflection	S	S	S		S	S		W				
SP									W			S
DC Resistivity	S	S		S	S	S		S		W	S	S
Electro-Magnetics					S			S	W	S	S	W
Ground Penetrating Radar		S		S	S	S		S	S	S	S	
Gravity					S	S		S				
Magnetics					S					W	W	

W - works well in most materials and natural configurations.
S - works under special circumstances of favorable materials or configurations.
Blank - not recommended.

Figure 4 - Table of Decision Matrix of Surficial Methods for Specific Investigations presents a few methods for suspected voids or cavity detection. (*3*) From USACE EM 1110-1-1802, pg 2-4, 1995.

In addition to selecting the method(s) to be used there are physical considerations to consider. A tradeoff exists between resolution and depth of penetration. For example, with GPR high frequency antennas are used to detect small targets, but those frequencies are quickly attenuated. As a result, the high resolution GPR is only effective at shallow depths of penetration. In contrast, lower frequency GPR signals can penetrate much deeper but will not image small targets like the high frequency data. The same is tradeoff exists with seismic data. With EM data the lower frequencies also penetrate deeper.

For tomographic techniques, sensor spacing plays a key role in the resolution and depth of investigation. Shorter sensor spacing improve near surface resolution; therefore, investigating shallow bedrock requires a smaller distance between geophones. The length of the profile line influences the maximum depth of investigation. Geophones spread over a longer line length produce deeper depths of investigation.

Electrical resistivity and ground conductivity methods can provide indications of the soil and rock types surveyed. For example, clay soils are more resistive than sands and gravels and the method helps to distinguish between those soil types. Refer to Figure 5, which presents the resistivity of various soil and rock types. The presence of air-filled voids can present as highly resistive zones as can be seen in Figure 6. While in the same figure, low resistivity zones can indicate water- or clay-filled voids.

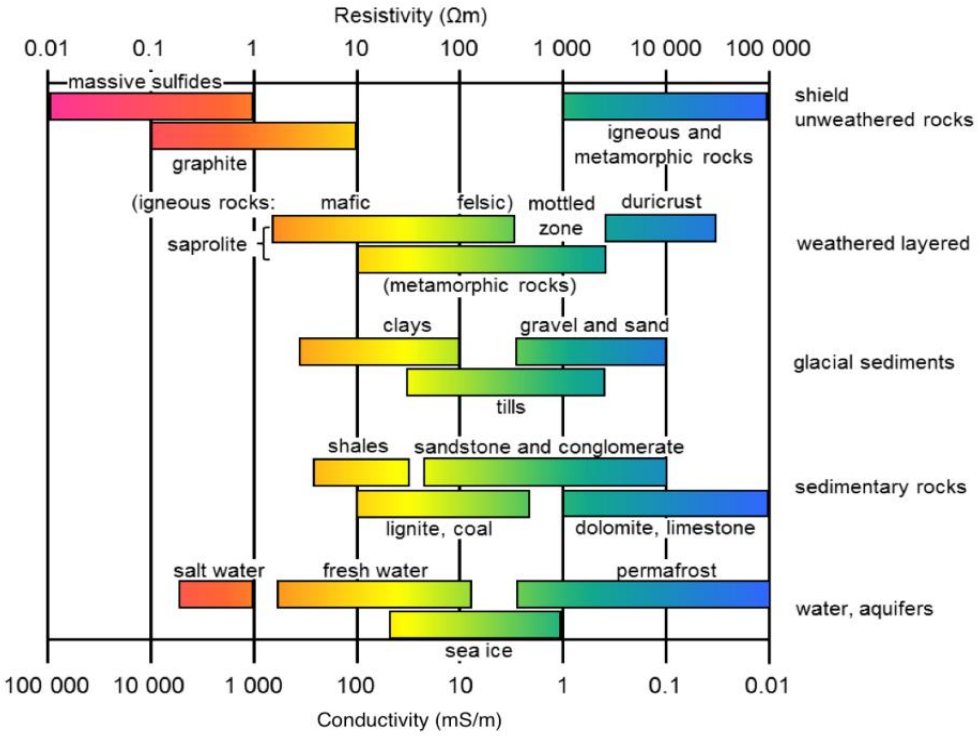


Figure 5 - is a plot of earth materials showing the materials range of resistivity (top axis) and its inverse ground conductivity (bottom axis).

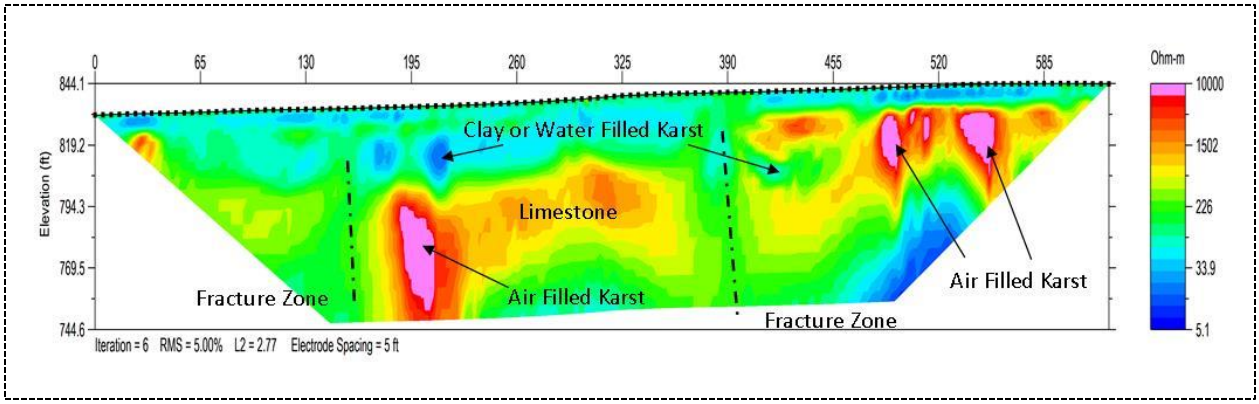
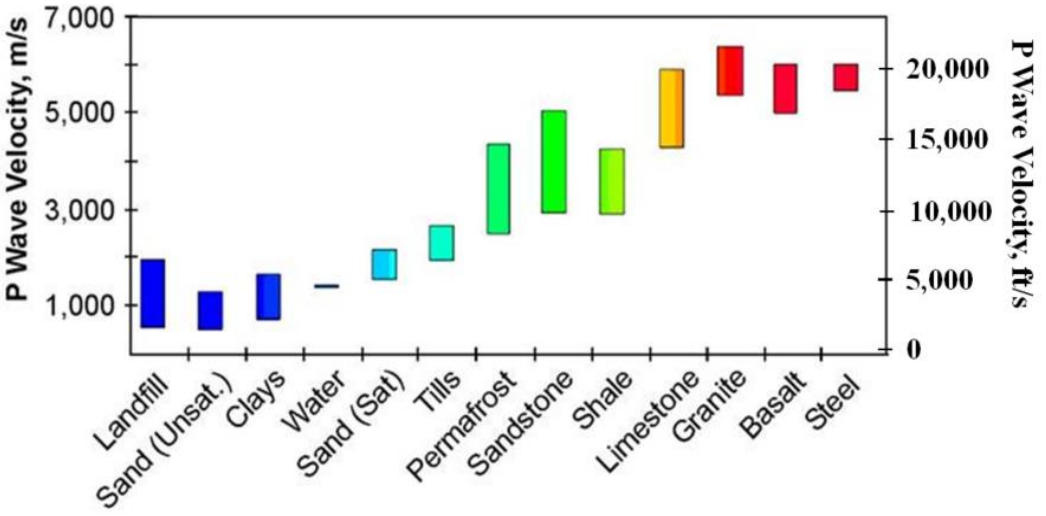


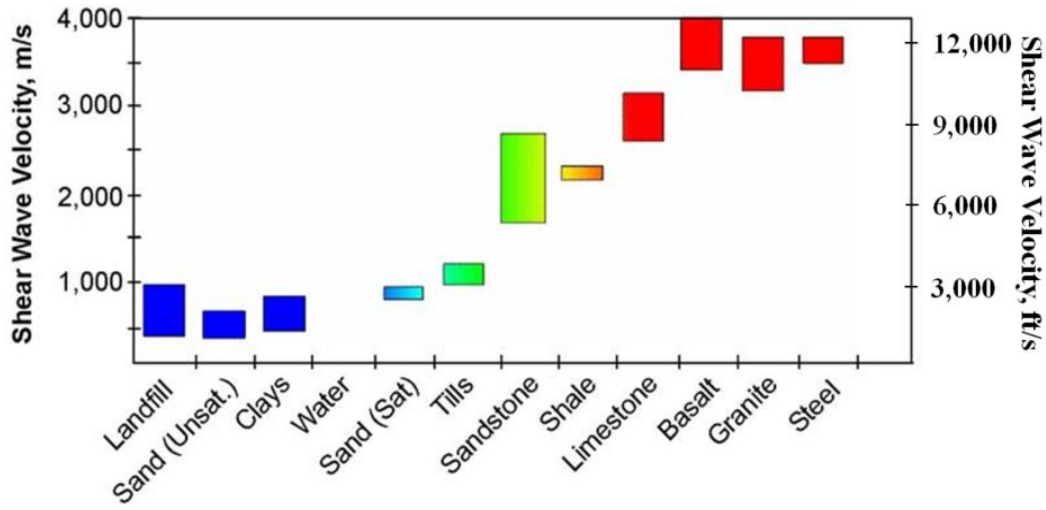
Figure 6 - Using electrical resistivity to map karst features using tomographic analysis. By means of 2D interpretations, the successful identification of the extent of cave and other possible caves in the area.

It is important to note that electrical methods may work well in electrically conductive materials that are not conducive to good GPR results, such as clay soils. GPR works well in resistive materials like sandy soils.

Seismic data can be analyzed to provide an idea of the material's moduli. The compressional wave, or P-wave, velocity is controlled by the materials bulk compressibility (or bulk modulus). While the shear wave, or S-wave, is controlled by the material's shear strength (or shear modulus). Figure 7 plots some of those parameters for various soil and rock types. Geophysicists have been employing these relationships to determine in situ subsurface parameters indirectly (vs. laboratory, or direct methods).



Related to: **Bulk Compressibility (*Bulk Modulus)***



Related to: **Shear Strength (*Shear Modulus)***

Figure 7 - presents two (2) graphs depicting seismic velocities for a range of earth materials. Compressional and shear waves provide moduli data.

CASE STUDIES

A geophysical survey was conducted using GPR to locate shallow mine workings in Wyoming where the existence of subsurface shallow coal mine workings posed a subsidence risk to a residential area. The objective of the investigation was to map potential voids beneath pavement, up to 15 feet deep below the ground surface. This was accomplished by acquiring GPR on the subdivision roads. Figure 8 shows profiles with areas of voids or loss of support circled. In this

case the soil properties were conducive to GPR investigations and subsurface voids were located.

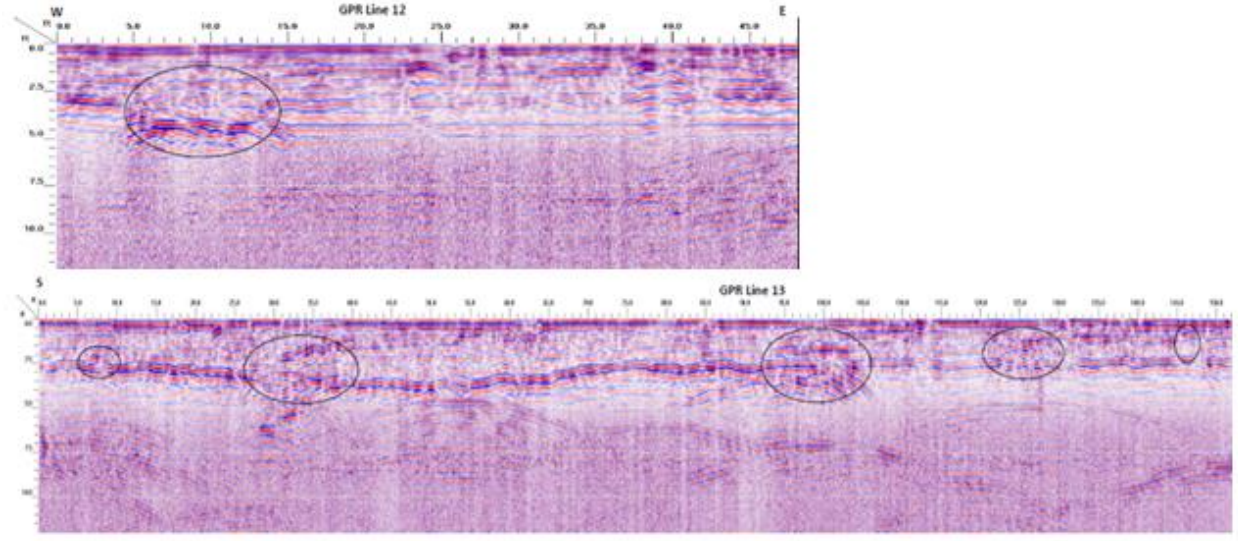


Figure 8 exhibits void-like GPR returns in the areas circled.

In a second example, a near surface karst investigation was performed for the National Parks Service at Carlsbad Caverns National Park in Carlsbad, NM. The survey was conducted for pre-utility construction and planning purposes. This investigation employed GPR, FDEM, and ERT to produce maps of potential risk related to karst. (Refer to Figure 9. Figure 10 shows GPR

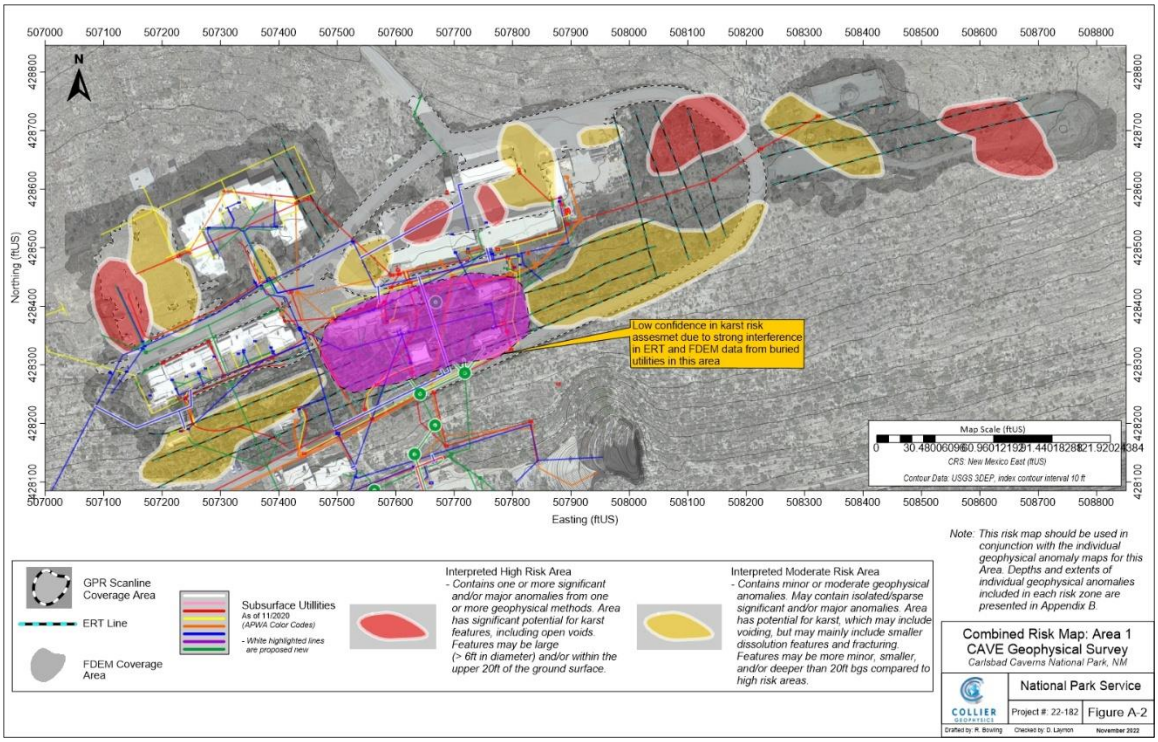


Figure 9 - shows a risk assessment presented in map form. It was produced from ERT and GPR surveys data. Anomalies shown in both data lead to higher risk to future SUE projects.

profiles where anomalous areas were identified. These can be interpreted as fractured rock, cavaties, or voids. Figure 11 presents a series of 2D ERT profiles. Very resistivite areas are possible air-filled voids. While the areas of low resistivity indicate highly weathered limestone, shale, or potential clay-filled solution zone. Increased confidencee with the interpretation of the subsurface conditions was provided by implementing multiple geophysical methods.

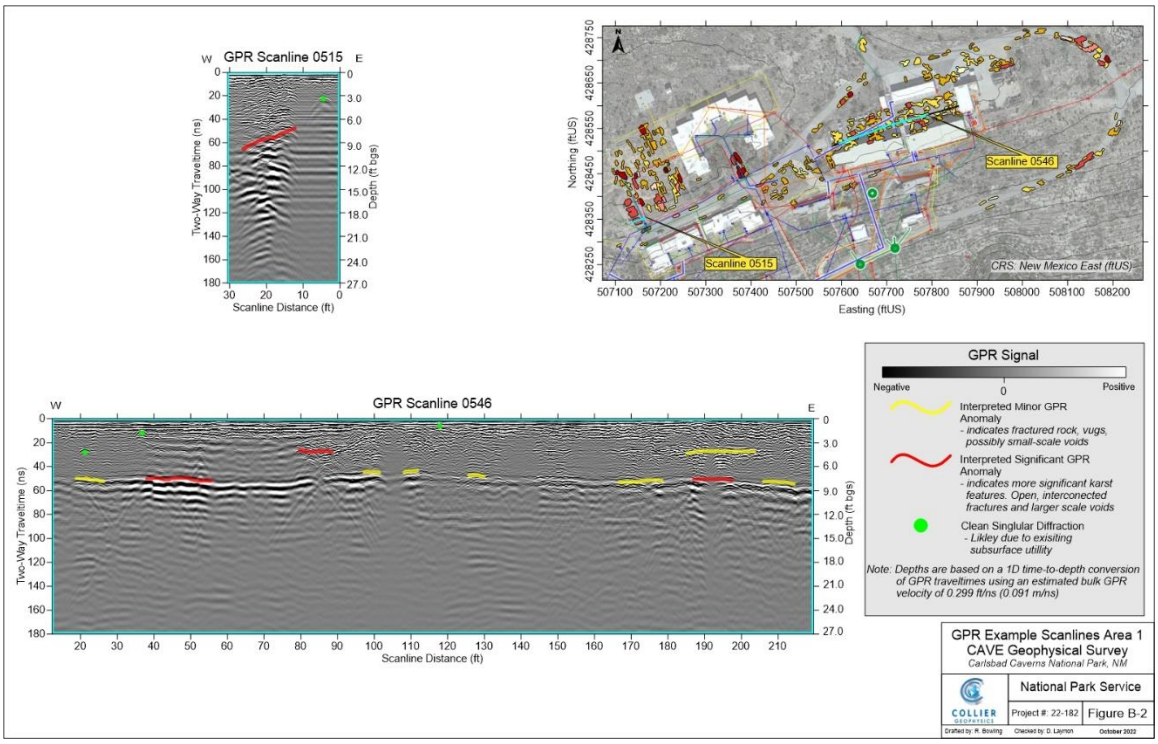


Figure 10 - exhibits void-like GPR returns in the areas circled.

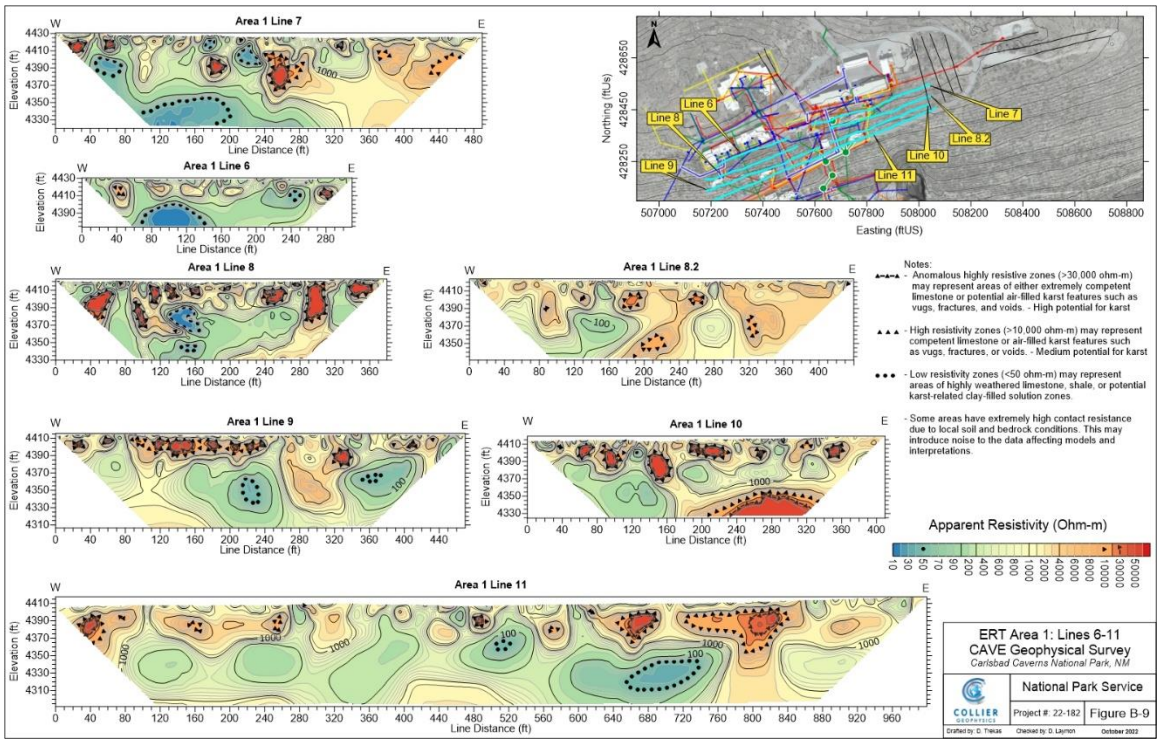


Figure 9 - shows a series of 2D ERT profiles. Very resistivity areas are possible air-filled voids. While the areas of low resistivity indicate highly weathered limestone, shale, or potential clay-filled solution zone.

A third case study is sinkhole remediation on the Chilhowee Dam in Tennessee. The purpose of the survey was to investigate a subsidence expression near the dam. Figure 11 is a 3D velocity model of the area of concern. SRT detected a low velocity, or “weakened” zone, which is less dense. A 120-channel seismic survey with 10-foot separation between geophones meant the

depth of investigation was roughly 60 feet. Refer to Figure 12. SRT proved quite useful to identify an area of significant concern.

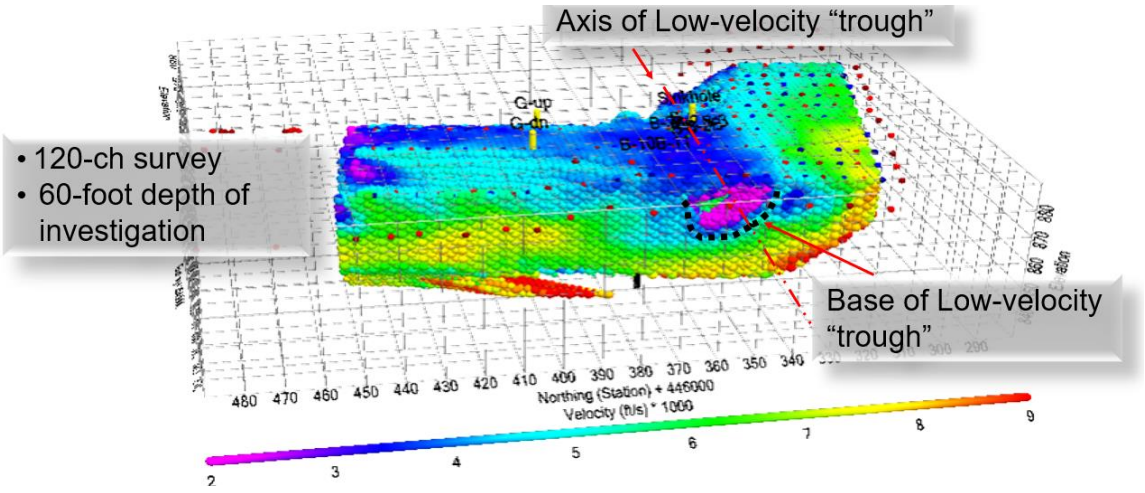


Figure 11 - shows a map of collapse feature on the Chilhowee Dam with SRT. The volume indicates a low-velocity region which is a region of preferential flow in the structure.

CONCLUSION

Geophysical methods have been successfully used to detect sinkholes and loss of support for highway engineering projects. Correctly selecting the proper approach and optimal survey parameters enhances the likelihood of detection and provides improved detection results. Understanding how geophysical data relate to the subsurface material provides the basis for modeling and interpretation. Risks due to subsidence geohazards can be analyzed during planning and pre-construction phases of a project. In addition, geophysical methodologies can indicate potential future issues resulting from subsurface voids. Finally, when using a multiple method approach, analyzing corroborative data across differing methods can greatly increase the confidence in the interpretation of these data.

REFERENCES

1. Herrick, C.G., *Sinkhole Formation*, Sandia National Laboratories, SAND2012-10178P, Sinkhole Overview, 2012, p. 2.

2. Application of Geophysical Methods to Highway Related Problems, Federal Highway Administration, Publication Number FHWA-IF-04-021, 2003, 742 pp.

3. Geophysical Exploration for Engineering and Environmental Investigations, U.S. Army Corps of Engineers, Engineer Manual 1110-1-1802, Publication Number 301-394-008, 1995, 208 pp.

a. Applied Geophysics, W.M. Telford, L.P. Geldart, and R.E. Sheriff, Cambridge University Press, 1990

b. Hoover, R.A., Geophysical Choices for Karst Investigations, 9th Multidisciplinary Conference on Sinkholes & the Engineering and Environmental Impact of Karst. Huntsville Alabama, 2003, 10 pp.

*References a-b are not cited in the body of text.

SlipStik: A Low-Cost Solution for Shallow Landslide Monitoring in Remote and Difficult-to-Access Terrain

Dugan, Brett M.
Pillar Innovations
104 Corporate Drive
Morgantown, WV 26501
304-376-8042
brettdugan@pillarinnovations.com

Ladavat, Steve M.
WSP
5500 Brooktree Rd, Suite 102
Wexford, PA 15090
412-605-7672
steven.ladavat@wsp.com

Lloyd, Jeffrey D.
WSP
428 Dow Hwy
Eliot, ME 03903
207-653-9641
jeffrey.lloyd@wsp.com

Robertson, Zachary J.
WSP
5500 Brooktree Rd, Suite 102
Wexford, PA 15090
724-553-9670
zachary.robertson@wsp.com

Fela, Dennis J.
WSP
5500 Brooktree Rd, Suite 102
Wexford, PA 15090
724-814-0394
dennis.fela@wsp.com

Hogue, Michael H
Pillar Innovations
104 Corporate Drive
Morgantown, WV 26501
240-727-6601
michaelhogue@pillarinnovations.com

Prepared for the 74th Highway Geology Symposium, August, 2025

Disclaimer

Statements and views presented in this paper are strictly those of the authors, and do not necessarily reflect positions held by their affiliations, the Highway Geology Symposium (HGS), or others acknowledged above. The mention of trade names for commercial products does not imply the approval or endorsement of HGS.

Copyright Notice

Copyright © 2025 Highway Geology Symposium (HGS)

All Rights Reserved. Printed in the United States of America. No part of the publication may be reproduced or copied in any form or by any means – graphic, electronic, or mechanical, including photocopying, taping, or information storage, and retrieval system – without prior written permission of the HGS. This excludes the original author(s).

ABSTRACT

SlipStik is a low-cost, customizable, slope monitoring device designed to be installed without the use of motorized assistance (drill rig), making it particularly suited for remote locations with difficult access. Originally developed for linear infrastructure (such as pipelines), this emerging technology leverages manual dynamic cone penetrometer installation methods and the ability to utilize remote monitoring technology to provide near real-time data on the depth, direction, and magnitude of subsurface displacement. This information allows operators and engineers to determine whether critical infrastructure such as roads, bridges, dams, or pipelines, are being impacted by slope movement.

This paper explores the application of SlipStik technology in slope monitoring, including detailing applications in which SlipStik will enable cost effective slope monitoring with the ability to be deployed quickly in a highway setting. Monitoring data will be presented alongside an estimate of effort required for various existing monitoring strategies. The benefits and limitations of SlipStik technology relative to conventional slope monitoring methods will be discussed, highlighting its potential as an accessible and cost-effective option for monitoring displacement across varying applications for linear infrastructure and beyond.

INTRODUCTION

Shallow landslides are a persistent geohazard throughout the Appalachian Basin, where the interplay of geology, topography, lithology, and climate creates conditions highly susceptible to slope movement. These landslides typically involve the downslope movement of surficial materials—often less than twenty feet thick—along shear surfaces that develop at the interface between overburden soils and underlying bedrock. In much of the basin, this configuration is typified by clay-rich colluvium or residuum overlying weathered shale, siltstone, claystone and other sedimentary strata.

The shallow nature of these failures is produced by the limited amounts of overburden present on slopes and they are developed by the mechanical contrast between the overlying clayey soils and the underlying bedrock, which acts as a preferential slip plane under loading. Saturated conditions can add to this driving load and intense rainfall events, increasingly frequent due to climatic shifts, rapidly elevate pore water pressures in the overlying soil, reducing effective stress and triggering slope instability. Freeze-thaw cycles further exacerbate this process by promoting soil loosening, fissuring, and progressive weakening of the soil-bedrock contact.

These landslides pose significant risks to linear infrastructure, including roads, railroads, bridges, pipelines, and dams, which often traverse or are constructed along the region's steep terrain. The cumulative impact of shallow landslides includes not only direct structural damage but also long-term maintenance burdens and service disruptions.

The SlipStik was developed to provide an alternative or complement to traditional geotechnical instrumentation (i.e. slope inclinometers) and provides comparable subsurface information in these types of shallow failures. Traditional inclinometer installation can be costly and requires the use of a drill rig for installation and manual readings to be taken. When installed with a Dynamic Cone Penetrometer (DCP) and paired with a remote monitoring unit, the SlipStik installation process by using a DCP can provide subsurface data that can be correlated to SPT values and collect near real-time data on subsurface displacement without the need to send staff back to the site (*1*). Additionally, hand soil augers can be advanced adjacent to SlipStik installation locations to allow for soil samples to be collected and therefore soil lab testing to be performed. The ability to install the SlipStik without using a drill rig negates the need for access roads to be created and as a result it can be deployed quickly in difficult to access areas and in many cases without the need for environmental permitting processes and the associated costs. This also makes it a valuable tool for emergency response monitoring.

It is common for landslide threats, once identified, to be classified, measured, and monitored before mitigation measures are pursued. The SlipStik is intended to facilitate in situ monitoring of landslide hazards and provide accurate and nearly instantaneous indication of landslide movement. The use of this tool, or other similar products on the market, allows owners to reduce the potential for landslide impact, to reduce the consequence of potential accidents by temporarily changing the use of the infrastructure asset (closing lanes or road), and to gather engineering data that can be used in the mitigation of the landslide threat [2]. The SlipStik device is

intended to monitor the depth of the failure plane, the direction of soil movement, and the magnitude of movement. Installation of the SlipStik provides owners with a vertical column of two-dimensional soil movement with six-inch vertical resolution. This is similar to other conventional products on the market like in-place inclinometers, IPIs, and Shape Arrays, allowing owners and engineers to quickly understand the data generated by the SlipStik.

While traditional instrumentation provides operators with reliable data pertaining to landslide movement, the installation of landslide monitoring instrumentation can be a challenging process. The installation of a traditional inclinometer (casing) requires a drill rig and frequently other support equipment like excavators and bulldozers. Although access for a drill rig along an existing roadway is straightforward, landslides often extend far off the road and providing geotechnical information and installation of landslide monitoring instrumentation can frequently be very difficult. This mobilization presents challenges to owners that require landowner agreements, environmental permits and steep slope safety planning as well as other miscellaneous challenges associated with traversing equipment through landslide prone terrain. SlipStik is intended to simplify the installation process over traditional solutions allowing owners to be agile in their response to the identification of threats. The monitoring system was developed to be installed using only hand tools to avoid the challenges that accompany heavy equipment mobilization. An example installation schematic is referenced below in Figure 1.

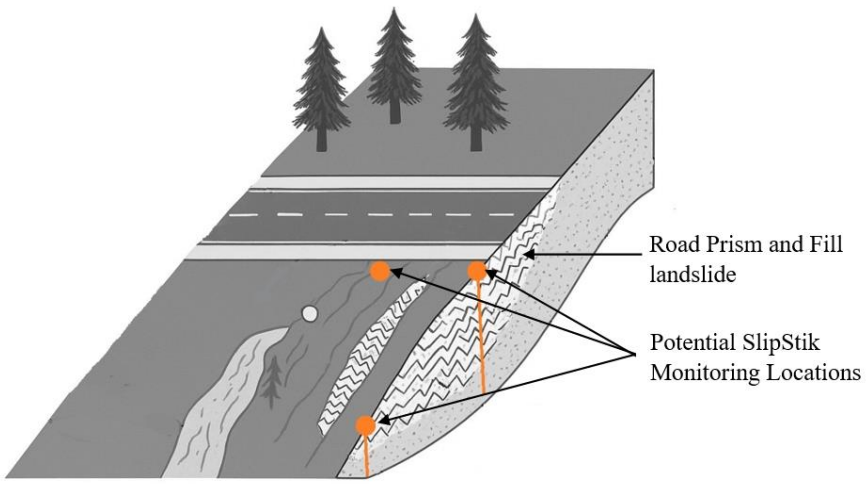


Figure 1 - Provides a schematic view of instrumenting SlipStik Sensors on a landslide impacting a roadway. Barriers like guardrails may drive the need to install DCP driven instrumentation solutions rather than drilled borehole solutions.

This paper will introduce SlipStik, a product that will soon be available for geotechnical monitoring highlighting scenarios in which the installation and monitoring of SlipStiks can enhance owners' monitoring capabilities.

SLIPSTIK OVERVIEW

The SlipStik functions similarly to an in-place inclinometer. The technology leverages its onboard inertial measurement unit to accurately monitor the acceleration of gravity in the A (downslope) and B (cross slope) direction. Angles as referenced from the plumb direction are then inferred from the portion of gravity measured. Upon installation of the SlipStik assembly, the initial angles recorded are set as baselines for each segment in each direction. As new readings are taken, the device subtracts the baseline readings from the respective current readings to provide the current change in angle in reference to the installed angle. This angle uses trigonometric relationships to determine displacement given a fixed bay length of six inches as shown in Figure 2.

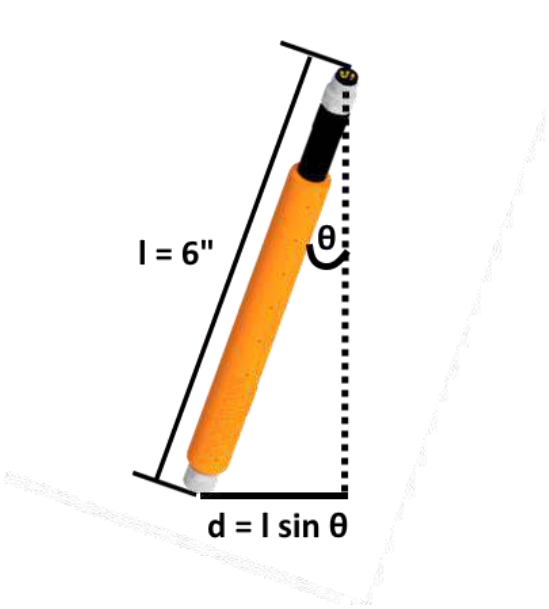


Figure 2 - Demonstrates the trigonometric relationship between the respective axis's label and the displacement in that direction as it applies to SlipStik

Once the displacement for each segment has been calculated, displacements in the same axis can be summed starting at the bottom in this bottom referenced technology to the segment of interest to calculate a total displacement at that height. This is represented in Equation 1 where d represents individual displacements and Dn is the cumulative displacement (*2*).

Equation 1 Cumulative displacement calculation that sums all displacements in a single direction to determine total displacement at a respective depth.

$$D_n = \sum_{i=1}^{n} d_i$$

Cumulative displacements are often graphed in both the A and B directions to provide easy interpretation of failure plane depth, with up to six inch depth resolution and relative displacement at depths of interest. Finally, the vector can be composed from its A (downslope) and B (cross slope) components to a function providing both magnitude and direction of the measured movement.

The SlipStik system is comprised of the following components: the SlipStik segment, the anchor, and the vault. The SlipStik segment is an encapsulated printed circuit board assembly that when interconnected acts as the sensors of the assembly. The anchor provides an immobile reference point that serves as the basis for displacement calculations of the above SlipStik segments. The vault serves as an enclosure for ancillary systems including bus translators, data logging, and wireless telemetry supporting systems as shown in Figure 3.

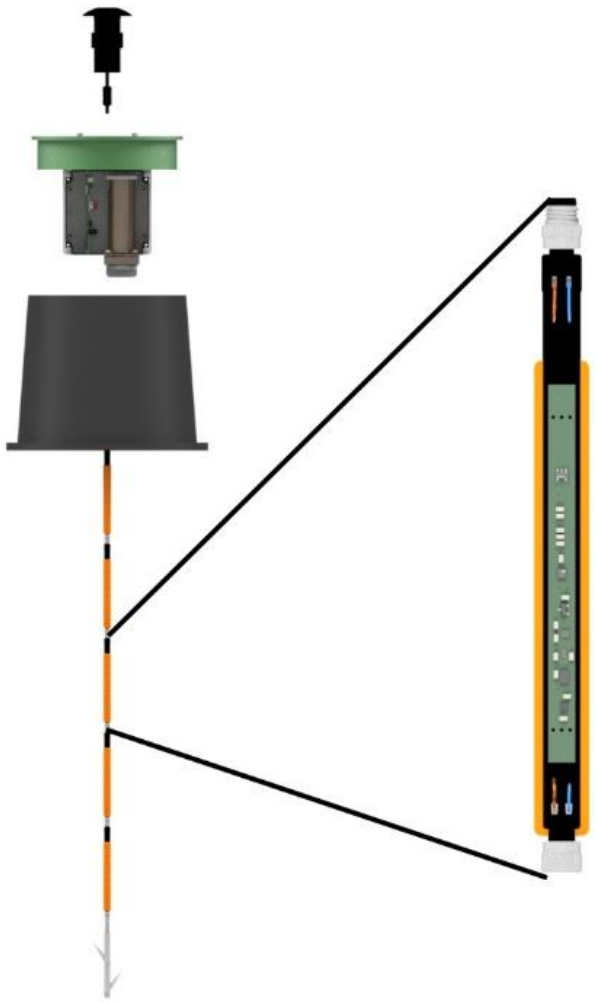


Figure 3 - This figure provides an overview of a SlipStik assembly starting with the vault section at the top, continuing to the interconnected SlipStik segments and concluding with the anchor section at the bottom of the assembly. A detailed cutaway view of a segment is also shown on the right.

The installation method is the primary differentiator between the SlipStik and conventional forms of instrumentation. The SlipStik is designed to have clearance within the Wildcat DCP by Triggs Technologies as shown in Figure 5. The Wildcat DCP utilizes a slide hammer with a known force to drive a lost point into a vertical column of soil. As this vertical point is being driven, the force required to drive the point a specified distance is tracked to enable the inference of in-situ soil strength and compaction characteristics. When site geology permits, this technique is much less invasive than deploying drill rigs to installation locations and provides considerable savings in not only direct installation cost but also with landowner access and permitting constraints. The agile installation process is backpack based and can be implemented as soon as the one call utility locate process is complete. This enables geotechnical engineers to collect data and enable alerts on nascent threats almost as soon as they are discovered.



Figure 4 - Details a DCP being driven to refusal. This underscores the portability of the installation method. In this instance the DCP reached refusal at 18 feet.

The SlipStik segment is the heart of the SlipStik technology. It acts as the sensor to provide measurements of soil displacement. The segment contains a custom designed printed circuit board assembly. The assembly is a single layer and measures ¼” x 3”. This small footprint

is dictated by the size requirements of existing DCP dimensions and provides room for ingress and mechanical protective layers. The board is single layer to promote a cost-effective solution. The board is comprised of a digital data bus, non-volatile memory, an analog switch, a temperature sensor, and an Inertial Measurement Unit (IMU). The data bus allows for digital communication between segments and the vault. This allows flexibility in the information that can be contained in the digital communication transmission, flexibility in the number of segments that can be connected, as well as avoidance of electromagnetic related noise and error on the sensor readings. Non-volatile memory (EEPROM) on each segment allows precision calibration data to be stored exclusively to each segment and applied during sensor measurement. Each board also holds an analog switch, giving it the ability to control power and data bus supply to the next segment linked below it. In the case of any failures that may be associated with external forces, this will allow segments below the point of failure to stay powered down so that the remainder of the assembly can still operate and take readings correctly. Finally, the IMU is comprised by a MEMS three axis accelerometer, gyroscope, magnetometer and temperature sensor. The accelerometer is the primary sensor in the landslide monitoring application while the remaining sensing technologies are used in filtering for accurate and stable readings. The IMU's static gravitational readings on each axis are converted to degrees of pitch and yaw tilt relative to the gravity vector.

With casingless installation being central to the operation of SlipStik, ingress protection and mechanical protection are then required to enable the technology's reliable operation in a slide. As a first step to cost effective ingress protection, a hot melt undermold is applied to the PCBA. This undermold seals the board and its connection to the electronic connectors providing a complex leak path that resists water and dust ingress to IP68. This undermold also serves as a protective layer to the electronic components for the high pressure injection molding process. Finally, the undermold also acts as a discrete pivot point ensuring that the trigonometric relationship accurately represents displacement based on the idealized calculations. Accurate bay lengths and infinitesimal pivot points are accounted for in the calculation. The design of the undermold is aimed to minimize real world error. Finally, the overmold is designed to minimize flex imposed by differential movement and the forces imposed on the SlipStik assembly on the PCBA. This is achieved with a proprietary high pressure injection molding process and material that encapsulates the bottom connector to the neck of the segment where the overmold terminates at the designed pivot point.

Another requirement for the casingless installment is rotational alignment of the individual SlipStik segments. Traditional inclinometers rely on grooves cut in their casings. Typically, the inclinometers utilize wheels or other mechanical features to ensure that the inclinometers' directions are coupled to the casing grooves. SlipStik leverages a casingless technology and thus relies on the individual segment connector's asymmetric connector pinout that ensures segment alignment between subsequent SlipStik segments.

A suitable anchor is required for this bottom referenced technology to ensure that the bottom portion of the SlipStik assembly is immobilized in competent material. This fixed reference point (datum) must be installed beneath the active displacement zone to ensure stability

and allow accurate displacement calculations (*3*). This anchor, in this case, is dimensionally constrained by the installation requirements of the DCP installation method. Its folded dimension cannot exceed a ½" diameter footprint. A laser cut stainless steel multi-barbed assembly has been developed to ensure a drag free insertion in the DCP with deployable barbs with a designed holding strength greater than the breaking strength of the SlipStik assembly in the various materials in which SlipStik will be installed.

At the top of the SlipStik assembly resides the vault, an at grade enclosure designed to house the data acquisition system, telemetry or logging solutions, and battery power sources. The primary component of the SlipStik vault is the node. This custom PCBA is responsible for orchestrating the successful operation of all electronic SlipStik functions. The node operates at low levels of current draw (milliamps) while sampling and processing data and employs a dynamic deep-sleep system (microamps) while idle. The battery system in the vault leverages lithium iron phosphate chemistries to support robust performance among the extreme temperature ranges that it is associated with. The battery system is designed to function for greater than 1 year with readings being taken and stored in fifteen minute intervals. The vault has been designed with ease of maintenance in mind and provides a means for a toolless battery change with a quarter turn battery lid. The vault also acts as a master to the SlipStik segments, powering up and initiating readings in accordance with its cloud or local configurable reading frequency rates. The SlipStik node handles the data bus conversion and prepares the readings for logging or wireless transmission. In the case of telemetry enabled systems, a quarter watt 900 MHz wireless meshing radio system is used to transmit the readings to a centralized cloud connected device enabling ingestion to a web-based monitoring platform. The meshing radio system relies on an optimized antenna design that can reliably transmit data packets about 400 feet. This creates a localized sensor network with a single data plan required for near real time monitoring of an entire site. This also provides a means to monitor areas that have poor cell and satellite signal by locally transmitting the readings to a location with reception. If near real time notification is not required for the site, local storage of historical readings is accomplished within the node and the storage capacity exceeds the usable life of the instrument.

DATA VALIDATION

To validate the measurement performance of the newly developed SlipStik technology, the development team pursued an iterative approach of lab-based landslide simulations, field landslide simulations and actual installation in active slides.

As a first step in testing, the sensor assembly simulated a translational movement on an inclinometer casing in a laboratory. Traditional in-place inclinometers were installed in the inclinometer casing in two foot intervals. An assembly of SlipStik prototypes were coupled to the exterior of the casing. Finally, as a truthing mechanism, an extensometer, or string potentiometer, was installed to directly measure the translational displacement of the casing at the respective height. As shown in Figure 5, both the SlipStik and the In-Place Inclinometer closely mimicked the measured displacement of the assembly.

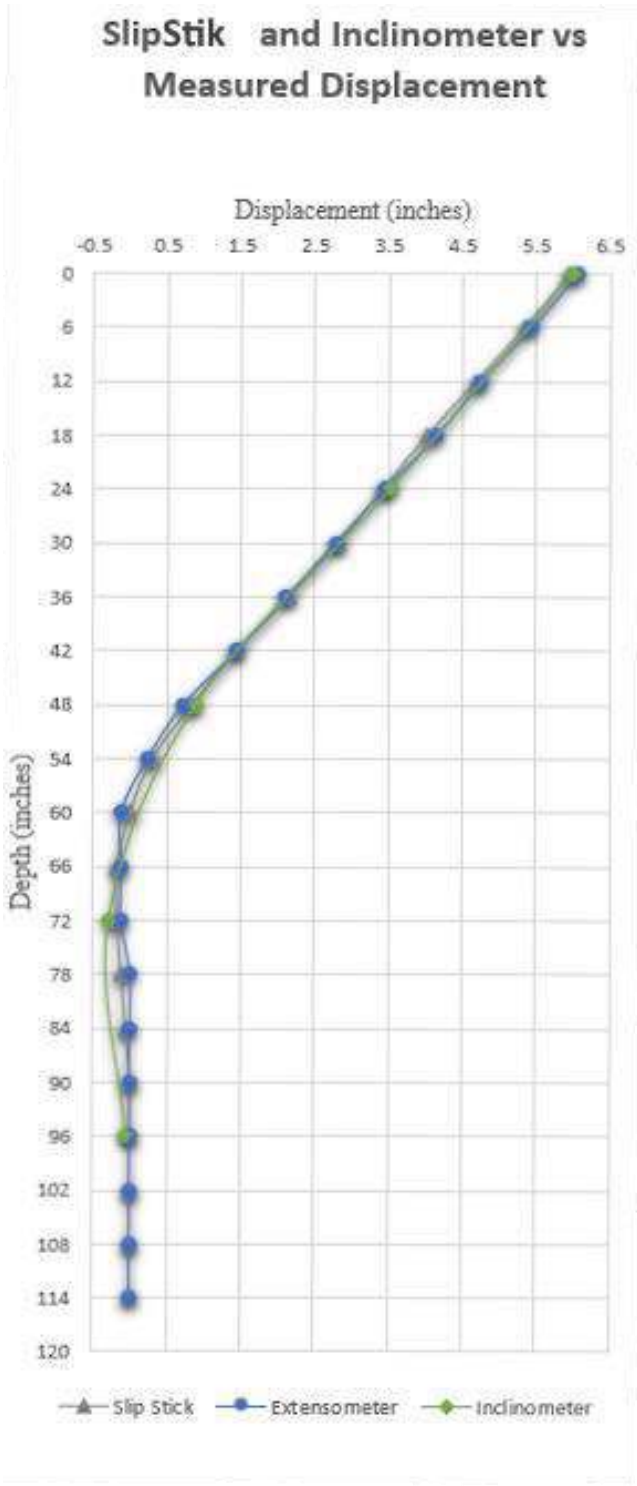


Figure 5 - Shows a lab-based comparison of a SlipStik assembly as compared to an In-Place Inclinometer. An extensometer was also used to directly measure displacement in six-inch intervals.

The most notable difference between the in-place inclinometers and the SlipStik is the resolution of depth measurements. This is a consequence of the difference in bay lengths between the technologies. In-place inclinometers are available in as short as two-foot bay lengths while the SlipStik is only currently available in six-inch bay lengths. This short bay length design is a consequence of the low-cost design target of SlipStik and the focus on precisely determining the failure plane depth when monitoring landslides. In the ten-foot lab-based landslide simulation, the failure plane was directly measured by the extensometer at 57 inches; as seen in Figure 5, the SlipStik reported its lowest deviation from zero at the depth of 54 inches. The in-place inclinometer, in contrast, shows its deepest displacement at a depth of 48 inches. This resolution difference requires the use of engineering judgment to infer how discrete the failure plane is and at what depth it is occurring. It should be noted that, in the presence of a borehole installed instrument, other technologies are available to ascertain more comprehensive information about the failure plane including manual inclinometer readings. This is a labor and cost intensive practice in comparison to remotely monitored instruments.

Accuracy was also analyzed for SlipStik to ensure that displacement measurements of the landslide can be relied upon. For the purposes of this comparison, measurements were compared at the top of the inclinometer casing. As can be seen in Table 1 (*4*), SlipStik measurements were within 3/16” of actual extensometer measurements. The mean error for SlipStik in our lab-based testing was about 0.1”. It should be noted that this test was executed in a controlled environment in essentially isothermal conditions. MEMS technologies are known to have temperature induced deviations. This test was not intended to confirm compensation for temperature effects. It should be noted that in-place inclinometer error was higher than expected. It is believed some of the error accumulated in the in-place inclinometer measurements is a consequence of large displacements applied over the short, by comparison, height of the test fixture. For this reason, SlipStik accuracy was benchmarked based on datasheet specifications of traditional technologies rather than the results of this test. This lab testing confirmed that the product met requirements intended to mimic accuracies of traditional technologies and was suitable to move onto field testing (*4*).

Table 1

Displacement Test Results 10 Feet Above Datum (Inches)

Extensometer	**SlipStik**		**Inclinometer**	
Displacement	**Displacement**	**Error**	**Displacement**	**Error**
1.4369	1.4404	0.0035	1.2683	0.1686
2.9519	2.8820	0.0699	2.5390	0.4129
4.6632	4.5063	0.1569	3.8064	0.8568
6.0577	5.8926	0.1651	6.0111	0.0466

After promising laboratory testing with the prototype was achieved, the team moved to test in the field by simulating a landslide. This test was particularly significant because a key feature of SlipStik's design is its casingless topology, which enables easy installation; a method that differs markedly from most other soil displacement monitoring technologies. A landslide simulation test was the most prudent way to verify design assumptions translated to accurate field monitoring. To simulate, loose sandy soil was mounded approximately 20 feet by 20 feet at the base and 10 feet high as shown in Figure 6. The team then installed a SlipStik to a depth of about 9.5 feet into the mound using DCP methods. Finally, a backhoe was used to simulate 4 incremental soil movements of two inches of surface movement with a failure plane at approximately 40-60 inches.



Figure 6 - Shows the forced translational movement landslide simulation. This simulation confirmed engagement of the casingless technology in soil as ground truthed with a physical measurement.

The SlipStik was actively streaming data to the cloud while the simulation was in progress and the surface movements were truthed with a tape measure from a reference monument to the datum point on the SlipStik vault. The results of the simulation directly confirmed the surface measurements as shown in Figure 7.

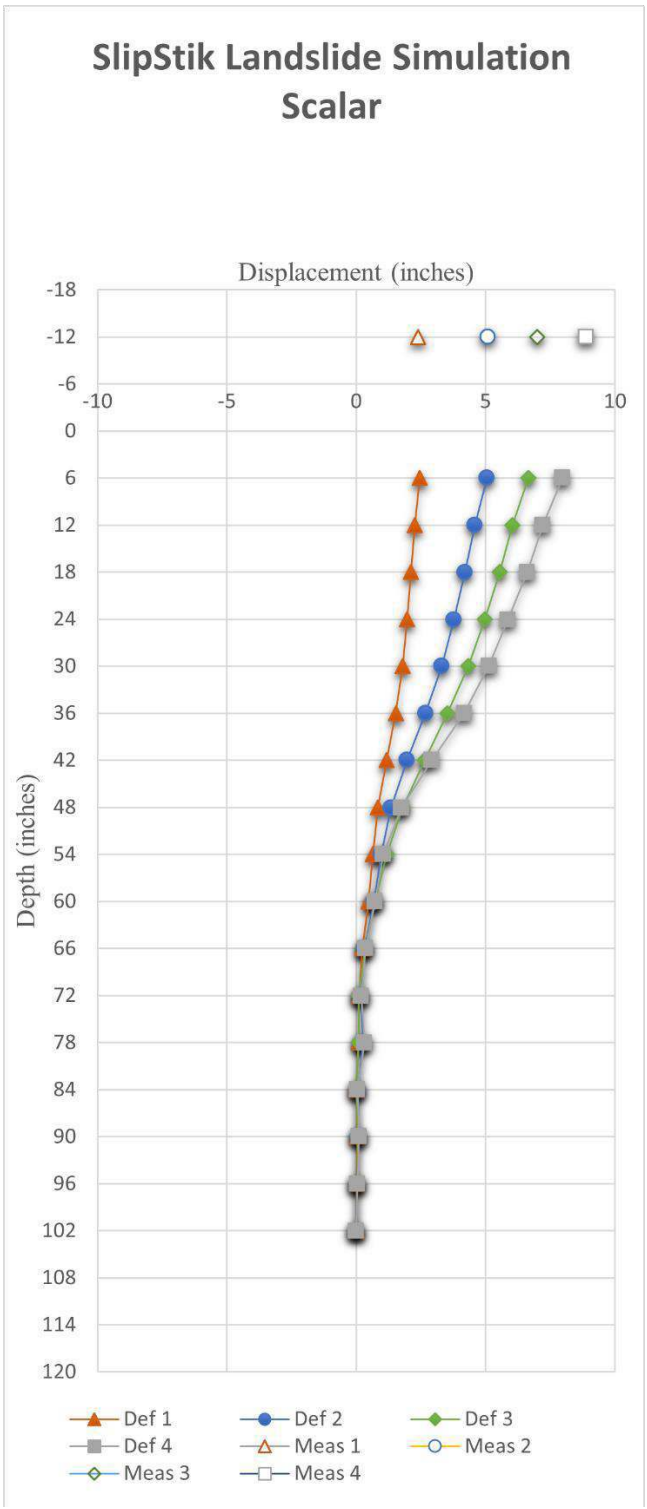


Figure 7 - Shows the iterative forced 2-inch surface translational movements (Def 1 - Def 4). The hollow shapes represent surface measurements for the corresponding deformation.

With successful field landslide simulation results, the team took steps in field verifying the SlipStik is a viable monitoring technology by installing it alongside linear infrastructure in an active landslide. This would confirm installation methods are viable in typical shallow landslides, test real world reliability of the system and be provide a basis of field comparison to actively monitored sites and the data from boring logs associated with previous instrumentation installation. A total of five SlipStik assemblies were installed at two different sites. At the first site, as shown in Figure 8 installations were driven to about 18.5' deep into weathered bedrock. This DCP installation took about one hour per borehole. The depth of DCP refusal coincided with weathered bedrock depth as determined from previous site boring activities. At the subsequent site three assemblies were driven to refusal at seven feet. No boring information was available, but the installation depth was expected based on geotechnical engineering judgment.



Figure 8 - Installation technicians inserting the SlipStik assembly into the DCP during a site installation.

Within weeks of installation, monitoring of the SlipStik assemblies confirmed failure plane depths as determined by nearby instrumentation and boring data. Distinctive failure planes were observed with abrupt movements occurring shortly after rain events. As seen in Figure 9, in a vertical displacement graph of the A-axis, a very discrete failure plane was observed at 36" deep (24" below the top of the SlipStik, which was 12" below grade in the vault). This failure plane displayed soil movement occurring almost exclusively between the third and fourth SlipStik segments. Weekly multi-inch displacements were recorded with as high as three-inch displacements accruing after rain events.

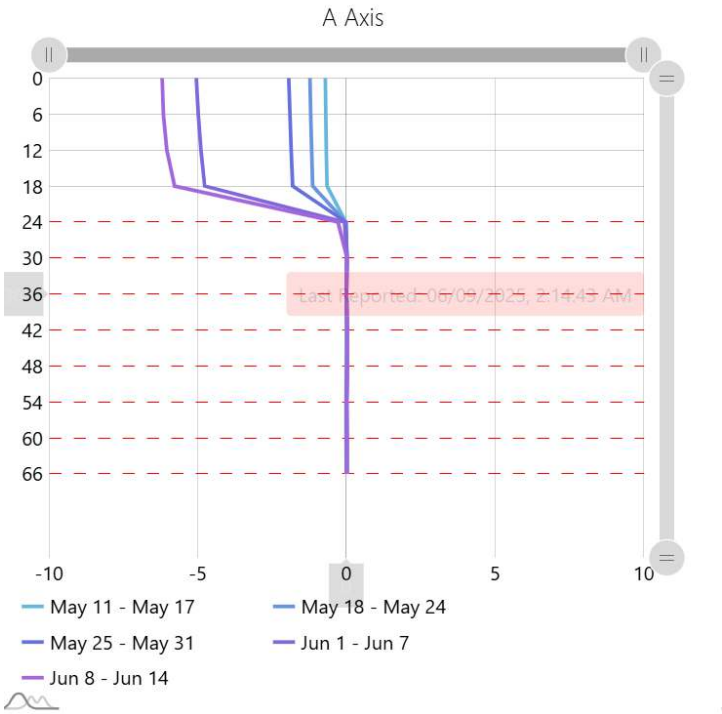


Figure 9 - A vertical displacement graph showing a failure plane at a depth of 24 inches on the SlipStik. After approximately seven inches of displacement, the fifth segment became unresponsive, indicating that it was likely damaged by the large magnitude of soil movement.

HIGHWAY MONITORING APPLICATIONS

The goal for the development of the SlipStik was to create an automated landslide monitoring system that could be installed by hand without the need for a drill rig, making it especially useful for instrumenting remote landslides that are difficult to access such as along pipeline and power transmission right of ways. It is this ease of installation that also makes the SlipStik well suited for a variety of transportation related uses.

In many instances when responding to a newly developed geotechnical issue on a roadway, such as a landslide, a drill rig must be mobilized to the site in order to get subsurface data. This may be practical in many instances, but the SlipStik is envisioned to be another tool in the toolbox of owners and engineers to quickly establish an understanding of the subsurface and start collecting data as soon as possible.

Emergency Response

SlipStik technology is well suited for emergency response to highway slides due to its rapid deployment with just a trained team of two technicians. Pending site accessibility, a team

can typically install four or more SlipStiks in a standard workday. Rapid deployment allows stakeholders to obtain important engineering mitigation design parameters quickly such as DCP soil strength data, failure plane depth, and rate of movement. The ability to freely move around the site to install SlipStiks allows for monitoring locations away from established vehicle access points such as the toe of an embankment. This results in an accelerated engineering design schedule that is typically held up by traditional geotechnical drilling coordination and steep slope accessibility.

Speed of deployment will be dependent primarily upon execution of a One-Call. Installations can typically be completed in as few as 48 to 72 hours immediately following the clearing of the One-Call ticket. In cases where the owner deems it necessary, further acceleration of installation timeframes can be achieved by placing an emergency One-Call.

Low-Cost Monitoring and Public Safety

SlipStik can be deployed in slide-prone areas as an early warning system or in areas with active slope stability issues that are awaiting funding for mitigation. Remote monitoring allows stakeholders to track slide movement rate and depth on a near real-time basis, which can lead to better informed public safety decisions such as road closures. SlipStik's hand installation also eliminates the need for geotechnical drill access on steep slopes which often requires winching plans, lane closures, and worker safety concerns, significantly reducing the cost of system installation. The total installation and support cost of three SlipStik landslide monitoring devices and an associated remote monitoring unit, RMU, system is a fraction of the cost compared to the installation of three traditional inclinometer monitoring casings. The cost savings are due to the lack of a need for a geotechnical drilling subcontractor, traffic control, drill rig access grading and winching, drill inspection, permitting and landowner agreements, and subcontractor coordination fees. Drill rig installation costs are situationally dependent, but SlipStik installation cost will be generally consistent between sites, assuming the geology is suitable for DCP based installation. This ultimately leads to varying levels of installation-based savings. In general, DCP based SlipStik installation will provide significant savings, with highly constrained sites driving more extreme levels of savings and overall monitoring feasibility.

Horizontal applications- bridge sagging, rail monitoring

The technology in the SlipStik allows for flexibility beyond typical vertical installation. The sensor technology can be installed at any orientation/angle which allows for applications on horizontal or angled surfaces/structures. The small footprint allows for installation in tight spaces or in difficult to reach locations. In horizontal applications, the SlipStik can be laid in shallow trenches or integrated into engineered fills to monitor differential settlement, lateral spreading, or ground movement that may impact buried infrastructure such as bridge foundations approach slabs, railroad track monitoring, embankments, and retaining walls. This could allow for near real-time data collection at the point of concern such as roadway surface where the effects of slope movement are realized. The data can be combined with traditional in-slope applications to help build a better model of the conditions affecting the roadway or other linear structures.

Limitations

Some limitations were identified during the findings. Hand installation is best suited to areas where manual tools like the Dynamic Cone Penetrometer (DCP) can be used to reach the target depth. Soils that are coarse-gravel or highly heterogeneous with cobbles may pose challenges to manual installation. The maximum depth achievable is currently limited by the reach of the DCP or a maximum of 40 SlipStik segments (20 feet). Work is underway to allow for greater depth by increasing the maximum number of SlipStik segments. The first production units will be limited to installation within shallow landslides of more fine grained and homogeneous soils.

Future Improvements

As the SlipStik is field tested in varying scenarios over the coming months, the team is working to refine its capabilities and look to future applications. The incorporation of pressure sensors into SlipStik segments represents a possible step forward in their ground monitoring scope. By coupling inclination measurements with localized pressure data, such systems could offer a multidimensional view of stress distributions and deformation behavior. This would allow the user to measure local pore water pressure without the need for a second DCP or borehole based installation.

At the time of this paper, development is underway to provide the technology higher-resolution monitoring. The goal of SlipStik was a low-cost, agile and rapidly deployed technology without a focus on high accuracy and precision. Over the course of development, the team has become aware of a desire for high accuracy. The creation of high-precision variants with high resolution could expand their applicability into areas where high-precision monitoring is required. The SlipStik segment's digital bus design provides high technical feasibility for this change. A printed circuit board footprint and layout change with corresponding firmware changes would be required to complete this variation.

The development of a modular adapter capable of retrofitting existing inclinometer casings with updated SlipStik components offers a practical pathway to modernization. This adapter could feature universal mounting designs and plug-and-play data interfaces. Through such modularization, legacy systems could be seamlessly integrated into smart infrastructure networks, extending their operational lifespan.

CONCLUSION

In conclusion, SlipStik will be a complementary technology to existing instrumentation to extend owners' ability to instrument geologic hazards and protect life, the environment and property. With the SlipStik's ease of installation and minimal footprint, the SlipStik can help provide slope monitoring in previously inaccessible locations in a cost effective and rapid manner. Primarily, SlipStik will enable owners to monitor shallow landslides and their respective plane depths and the magnitude and direction of soil movement in applications where the following constraints are of concern:

- Budget
- Agile installation
- Off right of way features of concern (toes, scarps, steep embankments, etc.)
- Minimization of environmental impact

With this addition to owners' suite of existing monitoring technologies, multi-faceted monitoring systems will be able to be configured to further minimize the risk of operating linear assets through landslide prone or temporarily stabilized construction areas.

REFERENCES

1. Ampadu, S., F.K. Boadu and F.J.F A. Ayeh, Deriving SPT N-Values from DCP Test Results: The case of Foundation Design in a Tropical Environment, *Goetechnical and Geological Engineering*, no. August, 2018.

2. ASTM D6230-21e1 Standard Practices for Monitoring Earth or Structural Movement Using Inclinometers, 2021.

3. Macahan, G. and V. Bennett, Transportation Research Circular, *Use of Inclinometers for Geotechnical Instrumentation on Transportation Projects State of the Practice*, October 2008.

4. Dugan, B., C. Johnson, J. Lloyd, J. Taylor, D. Fela and S. Ladavat, Slip Stick – Innovative Advancement in Subsurface Ground Movement Monitoring, *ASME IPC Volume 4: Geohazards Management and Strain-Based Design and Assessment*, 2024.

Geohazard Decision Support: Leveraging AI and Satellite Data for Infrastructure Resilience

Randy Post, PE
WSP USA Inc.
177 N. Church Ave., Ste. 1105
Tucson, AZ 85701
520-888-8818
randy.post@wsp.com

Winston Wade, PEng.
WSP Canada Inc.
840 Howe St
Vancouver, BC V6Z 2L2, Canada
+1 604-296-2811
winston.wade@wsp.com

Prepared for the 74th Highway Geology Symposium, August, 2025

Acknowledgments

The work described in this paper has been a collaborative effort between a global group of WSP colleagues. It has been supported at very high levels in our organization, and we are grateful. The following alphabetical list of people we wish to acknowledge and thank for their efforts is by no means exhaustive.

Syed Haider Ali – WSP Canada
Mark Easton – WSP UK
Nicky Jennings – WSP Canada
John Kreft – WSP New Zealand
Jazz Pabla – WSP Canada
Anna Robak – WSP Canada
Cheryl Trent – WSP Canada

We also acknowledge the support and effort of our technology partners, Planet Labs and UrbanLogiq. Without them, this project would not be possible.

Disclaimer

Statements and views presented in this paper are strictly those of the authors, and do not necessarily reflect positions held by their affiliations, the Highway Geology Symposium (HGS), or others acknowledged above. The mention of trade names for commercial products does not imply the approval or endorsement of HGS.

Copyright Notice

Copyright © 2025 Highway Geology Symposium (HGS)

All Rights Reserved. Printed in the United States of America. No part of the publication may be reproduced or copied in any form or by any means – graphic, electronic, or mechanical, including photocopying, taping, or information storage, and retrieval system – without prior written permission of the HGS. This excludes the original author(s).

ABSTRACT

Transportation infrastructure is increasingly vulnerable to geohazards such as landslides, debris flows, and rockfalls, risks that are amplified by climate change and aging assets. Traditional approaches to geohazard management often rely on static hazard maps and reactive interventions, which can fall short in addressing the dynamic and interconnected nature of these threats. This paper presents a modern, data-driven framework for geohazard risk management that integrates satellite-based Earth observation, machine learning, and geotechnical expertise into a comprehensive Decision Support System (DSS).

We describe a Geotechnical Asset Management (GAM) approach that quantifies hazard likelihood, infrastructure exposure, and consequence to support risk-informed decision-making across large transportation networks. By leveraging high-resolution satellite data from sources such as Planet Labs and Sentinel, combined with Random Forest machine learning models, we generate climate-informed risk profiles that support both real-time operations and long-term capital planning. These insights are translated into actionable tools such as Trigger Action Response Plans (TARPs) or programmed mitigation projects, enabling infrastructure owners to proactively manage risk through targeted monitoring, mitigation, and resource allocation.

Case studies from New Zealand and Colorado demonstrate the practical application of this methodology. In New Zealand, a near real-time rockfall risk management system has enabled preemptive road closures and resource deployment. In Colorado, a corridor-wide risk assessment on State Highway 133 led to prioritized mitigation investments that significantly reduced risk exposure relative to cost.

Rather than replacing traditional engineering, this approach enhances it, providing a scalable, transparent, and adaptive system that evolves with new data and changing conditions. By embracing uncertainty and integrating diverse data sources, geotechnical professionals can better support infrastructure resilience, safety, and cost-effectiveness in the face of growing environmental challenges.

INTRODUCTION: ENGINEERING AT THE EDGE OF RISK

Making persuasive arguments for investment in infrastructure affected by geohazards such as floods and landslides is often undermined by limited knowledge and high uncertainty around the design conditions. Current priorities are frequently driven by reactive decisions, fixing failed infrastructure or applying a “worst-first” mentality that addresses only the most obvious issues while overlooking future risks or broader system performance. Sometimes this is out of financial necessity. However, by leveraging the full range of available observational data and analytical methods, we can better understand where and how to manage risk. Our goal is to lower the operational costs of roads while increasing the safety and utility of infrastructure assets.

Our current philosophy is rooted in decades of applied geohazard management. We continuously seek to reduce uncertainty, provide robust guidance for infrastructure investment, and elevate non-structural and adaptive strategies alongside traditional engineering solutions. By doing so, we improve our ability to manage risk safely, cost-effectively, and transparently, without relying solely on worst-case assumptions.



Figure 1 - Rockslide on I-70 illustrates the challenges faced by owners to manage geohazard risk. (courtesy of Colorado DOT)

Our approach brings together operational insights from maintenance staff and asset managers, technical knowledge from subject matter experts, and emerging observational datasets from Earth observation satellites. It also incorporates the dynamic learning capacity of machine learning models. Together, these components support a comprehensive risk management system that includes operational responses (e.g., road closures), maintenance prioritization, mitigation design, construction, and monitoring.

To deliver real value, however, we must also align this technical capability with what infrastructure owners and clients actually need: clear risk information, actionable options, and tools that allow them to prioritize across large networks with limited budgets.

WHAT OWNERS AND CLIENTS REALLY NEED

Owners and agencies responsible for geohazard-prone infrastructure increasingly require a clear, structured understanding of where their assets intersect with hazard exposure, how likely failures are, what consequences they carry, and what proactive options are available. These decisions rely not just on engineering feasibility, but also on cost-effectiveness, resiliency, and residual risk post-intervention. Even where quantitative risk assessments exist, decisions still depend on expert input, as tools for network-wide geohazard optimization remain limited. Many organizations lack a complete hazard inventory or manage risks with basic spreadsheets, GIS maps, and information deficiencies that are not adequate to justify investment across large portfolios with limited budgets.

A **Geotechnical Asset Management (GAM)** approach addresses these challenges by providing a repeatable, scalable framework that links hazard information with infrastructure value, risk, and intervention options. Key components of a GAM system include:

Asset and Hazard Inventory: Identify and map where geotechnical hazards intersect with critical infrastructure across the region, establishing a baseline for exposure.

Quantified Risk Assessment: Evaluate the likelihood and potential consequences of hazard impacts, translating geotechnical threats into measurable community and infrastructure risks.

Mitigation and Monitoring Options: Develop practical and site-specific responses, including both structural mitigation measures and monitoring strategies to manage uncertainty.

Prioritization for Action: Rank interventions based on risk reduction, cost-effectiveness, and safety benefits to support defensible decision-making and long-term planning.

Benchmarking Versus Competing Funding Needs: Owners always have more problems than they have resources to deal with them. The system must allow an “apples to apples” comparison of risk, often in terms of financial risk exposure over some time period, so funding for geohazard risk reduction can compete for resources with other project and operational needs.

Iterative Improvement: Continuously refine the framework using updated hazard data, asset changes, and monitoring results to ensure adaptive and resilient management over time. By using this asset-based, risk-informed, and lifecycle-driven approach, owners can prioritize funding not just based on what’s broken, but on where it is most cost-effective to act now to reduce future failures.

Unfortunately, many existing approaches stop at identifying hazards or assigning qualitative risk levels. While helpful for awareness, these methods often fall short in informing investment decisions, scheduling interventions, or understanding how cascading hazards unfold under changing weather or climate conditions. That's where a shift from static maps to dynamic risk quantification becomes critical.

FROM HAZARD MAPS TO QUANTITATIVE RISK ASSESSMENT

Many practitioners rely on geohazard susceptibility maps that provide relative hazard scores based on topography, geology, vegetation, and other factors. While useful for screening, these products rarely offer the quantitative depth or spatial precision needed to support operational, financial, or emergency response decisions. They identify where a hazard might exist, but not how likely it is to occur, what it might cost, or what actions are most effective to manage it.

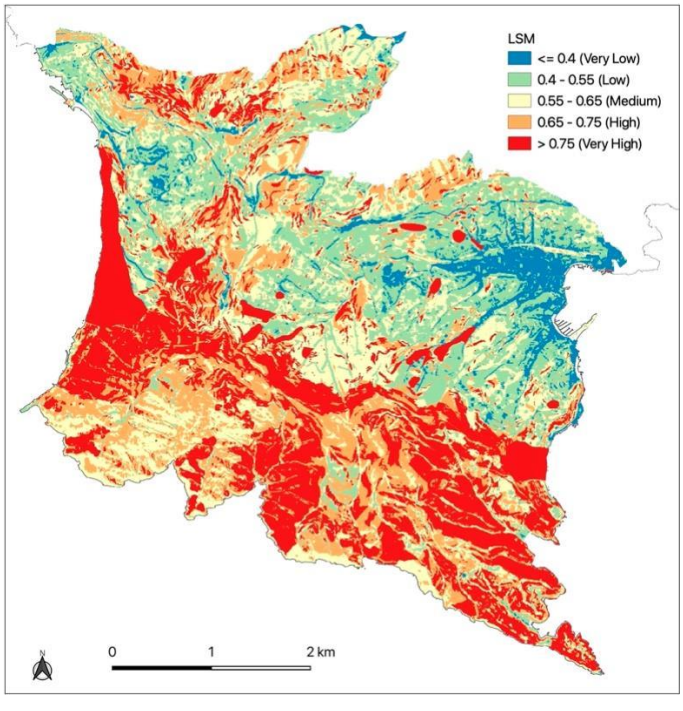


Figure 2 - Example of landslide susceptibility map. While useful for understanding geographic distribution of landslide-prone areas, is of limited use for decision making (from *1*)

Our approach shifts from static susceptibility mapping to a fully quantitative, risk-based framework that explicitly integrates hazard likelihood, infrastructure exposure, and consequence. Using advanced weather modeling and machine learning, we link observed or predicted climate variables, such as precipitation intensity, freeze-thaw cycles, and soil moisture dynamics, to hazard occurrence. This enables the generation of location-specific, climate-informed risk profiles with daily resolution for both real-time operations and long-term capital planning.

At the core of this methodology is a continuous hazard quantification process that translates climate forcing variables into predictive indicators of slope failure, debris flows, or

other geotechnical hazards. Triggering mechanisms such as rainfall, antecedent soil saturation, and freeze-thaw are modeled using bias-corrected weather data and high-resolution inputs (e.g., Planet Labs soil moisture imagery). By including climactic triggering mechanisms, the methodology allows evaluation of climate change scenarios. In seismically active areas, earthquake ground motion thresholds can also be incorporated to account for non-climatic triggers.

These data-driven insights support the development of Trigger Action Response Plans (TARPs), enabling asset managers and emergency planners to define specific thresholds for road closures, evacuation protocols, or intensified monitoring. Over time, these thresholds are refined as more data become available, forming a feedback loop between predicted hazard potential and actual site behavior.

This AI-enhanced process addresses major gaps in traditional workflows:

- **Data scarcity**, particularly in distributed or unmonitored hazard zones;
- **Manual inefficiencies** in processing large volumes of field or satellite data;
- **Trigger uncertainty**, where weather–hazard relationships exist but are not yet statistically validated or calibrated.

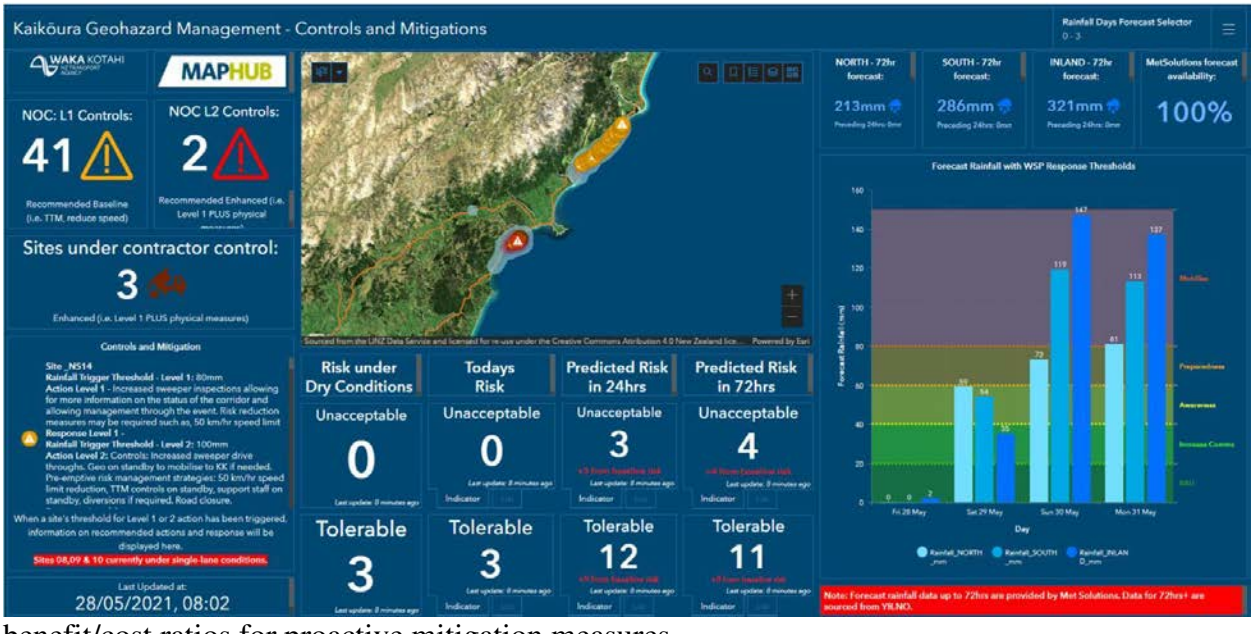
By incorporating these advances into a Decision Support System (DSS), geotechnical asset managers gain access to a living, learning tool that evolves with the landscape and climate. The result is a more reliable foundation for justifying investments, prioritizing interventions, and improving safety across large networks of exposed infrastructure.

DSS AND RISK RANKING FOR GEOHAZARD INVESTMENT

Building on this foundation, WSP's collaboration with Waka Kotahi – New Zealand Transport Agency (NZTA) exemplifies the practical application of these principles. Following the 2016 Kaikōura earthquake, which triggered an estimated 10,000 landslides and caused extensive damage to transportation infrastructure, WSP developed a near real-time rockfall risk management system (*2*). This system leverages live data and geotechnical expertise to provide current and predicted geohazard risk estimations, enabling timely operational decisions and proactive maintenance. By integrating slope movement observation data, traffic volume, and rainfall forecasts, the system forecasts near-term changes in slope failure risk, demonstrating the potential for broader application in geohazard risk management. This system has been successfully used as a DSS by NZTA for operational risk management to pre-position resources, and to conduct partial or complete road closures in advance of potential landslide activities. This approach not only enhances immediate response capabilities but also contributes to long-term resilience by continuously refining risk assessments with new data.

Geohazard risk assessment is not only important at the operations level, but also at the planning level. Agencies need help assessing risk at a corridor or network level to prioritize where to focus their resources for monitoring or mitigation. WSP demonstrated how to perform this successfully with work on Colorado State Highway (SH) 133 (*3*).

Highway safety, mobility, and maintenance efforts on SH 133 between Carbondale and Paonia, Colorado, are severely impacted by rockfall, debris flows, landslides, avalanches, and the occasional sinkhole. The study implemented a risk-based geohazard management approach commissioned by the Colorado Department of Transportation (CDOT). It evaluated geohazard sites from an asset management perspective, considering quantitative risk, life-cycle costs, and



benefit/cost ratios for proactive mitigation measures.

Figure 3 - The dashboard DSS for NZTA allows operational decisions to be made based on forecasted weather conditions and existing site knowledge.

A total of 300 geohazard sites were inventoried, and 125 sites were subjected to quantitative risk assessment. The assessment considered event likelihood, consequence analysis, and annual risk exposure in terms of safety, mobility, and maintenance impacts. Conceptual mitigation options with preliminary cost estimates were prepared for 50 of the highest risk sites, allowing for benefit-cost ratios to be computed to allow CDOT to select projects that produced the best return-on-investment (ROI). Based on the findings, five mitigation projects were undertaken, representing 21 sites that have been mitigated or are addressed with shelf-ready construction plans. This work has ultimately resulted in an approximate $18.5 million reduction in risk exposure compared to $16.8 million in construction costs.



Figure 4 - The Nettles Cut on Colorado SH 133 had a history of major rockfall events prior to stabilization

With the ability to forecast hazard likelihood and cost, the next frontier is selecting the right computational methods to make sense of the growing volume of environmental data. That's where machine learning (specifically, Random Forest) offers a practical path forward for engineers seeking scalable, interpretable, and proven tools for geohazard prediction.

AI AND MACHINE LEARNING IN GEOHAZARDS

Undoubtedly, one of the most persistent challenges in integrating machine learning (ML) into engineering practice is the concern over "black box" models and the lack of established precedence in applied geotechnical workflows. Despite these concerns, recent advancements in ML, particularly the application of **Random Forest (RF)** algorithms, offer significant opportunities for improving geohazard susceptibility assessment and forecasts, especially in data-limited environments.

Traditional modeling approaches often rely on simplifying assumptions and deterministic rules, which can constrain their utility when facing the complex, nonlinear interactions inherent to geohazard processes. As a result, while these models may produce useful predictions, they often fail to capture underlying mechanisms or miss key dependencies due to data scarcity, computational limitations, or incomplete process understanding (*4,5*).

By contrast, ML-based methods, especially ensemble approaches like RF, are well-suited for capturing complex interactions across diverse datasets, even when the physics are partially known or poorly constrained. RF models have been shown to outperform simpler statistical or rule-based models in numerous geohazard contexts. For example, RF models excel in combining heterogeneous inputs such as slope, land cover, rainfall, and soil type to generate susceptibility scores and rank hazard likelihood.

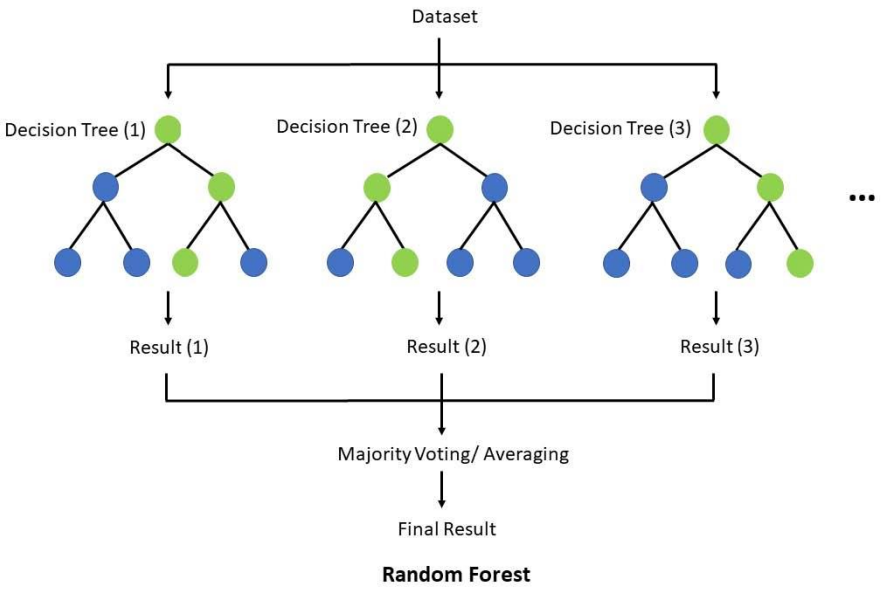


Figure 5 - Random Forest Model schematic showing multiple decision trees (from *6*)

Unlike neural networks that require large training datasets and are often viewed as opaque, Random Forest brings balance of accuracy and interpretability. It can identify the most influential predictors in a model, offering engineers clear insight into which environmental variables are driving hazard potential. This interpretability, combined with its robustness to noisy or incomplete data, makes Random Forest (RF) particularly well-suited for operational applications where decisions must be defensible, transparent, and communicable across technical, managerial, and policy-making audiences.

It is our opinion that the integration of RF models into our regional assessment and awareness of Geohazards enables a practical and scalable addition to traditional approaches. Enabling practitioners to integrate ML insights into decision-making without abandoning the engineering principles they rely on.

REMOTE SENSING AND DATA-DRIVEN OPPORTUNITY

Ideally, geotechnical engineers and geologists would physically visit and characterize all the geohazard sites in an owner's inventory. While this is impractical, if not impossible, remote sensing can be a useful tool to fill that data gap, and direct our limited geohazards engineers to the most imminent and or critical locations. This opportunity has been underutilized in practice. The exponential growth of satellite-based data collection systems has reshaped the landscape of geohazard monitoring and infrastructure planning. Missions such as those deployed by Planet Labs, along with open-source satellite data sources like Sentinel and Landsat, provide a wealth of geospatial and temporal data that has enabled unprecedented capabilities in monitoring, forecasting, and managing geohazards.

The initial phase of our methodology addresses the significant challenges arising from limited direct observational data, especially within regions characterized by complex terrain and diverse geohazard events such as rockfalls, landslides, debris flows, and flooding. Traditional observational methods, including ground-based rainfall stations, streamflow gauges, and in-situ soil moisture sensors, are often constrained by cost, logistical feasibility, and accessibility, leading to sparse spatial coverage, infrequent sampling, and incomplete temporal records. Even the record of major events is sparse with only relatively recent efforts attempting to consolidate an inventory (*7*). Consequently, infrastructure decision makers and their trusted advisors are frequently forced to make critical risk management decisions based on partial or completely absent local data. In such circumstances, engineers and decision-makers increasingly rely on expert opinion or highly extrapolated or reanalyzed data. As Parker (*8*) underscores, reanalysis datasets differ fundamentally from direct observations, as they blend real measurements with numerical model outputs, introducing uncertainties tied to model assumptions and observational biases (*9*).

Given the acknowledged uncertainties associated with our data sources and the original purposes for which inferred data were developed, the availability of high-resolution remote sensing datasets from Planet Labs, such as vegetation cover, soil moisture and land surface temperature with rapid revisit frequencies, becomes particularly significant. These combined data streams enable detailed, spatially continuous representations of geohazard dynamics, which are especially valuable in remote or rugged regions. For example, during a rockslide event in the Wind River Canyon (Wyoming) (Figure 6), satellite-based soil moisture observations provided critical insights despite the absence of comprehensive ground-based monitoring.

The availability of 7-10 years of observational data at varying resolutions is now beginning to provide sufficiently large datasets to correlate hazard occurrences with environmental conditions on a global scale. Given the complexity and scale of these data, empirical methods (especially data-driven and machine-learning techniques) are becoming essential tools to establish reliable correlations between observational datasets and geohazard events.

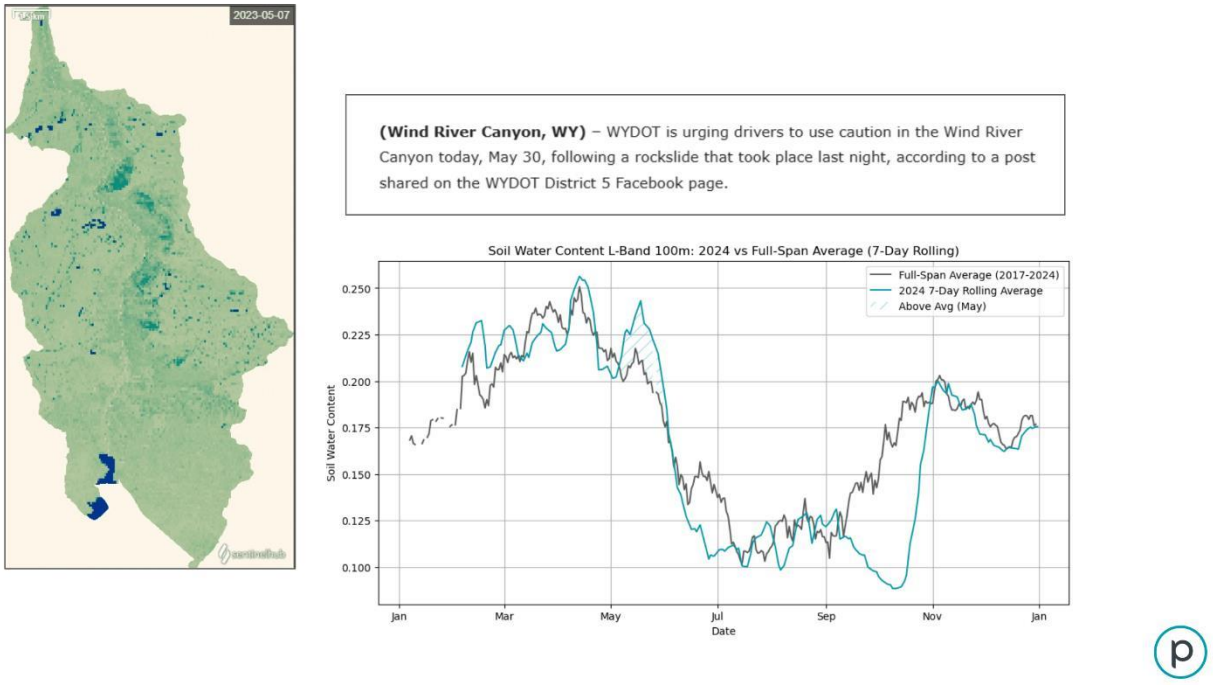


Figure 6 - Soil moisture data for Wind River Canyon, comparing annual averages against a specific landslide-inducing event in May 2023. Note that this representation is incomplete, as soil moisture alone, despite rapidly increasing during the event, does not capture the total water volume generated or fully describe the conditions triggering the landslide (image and analysis provided by Planet Labs)

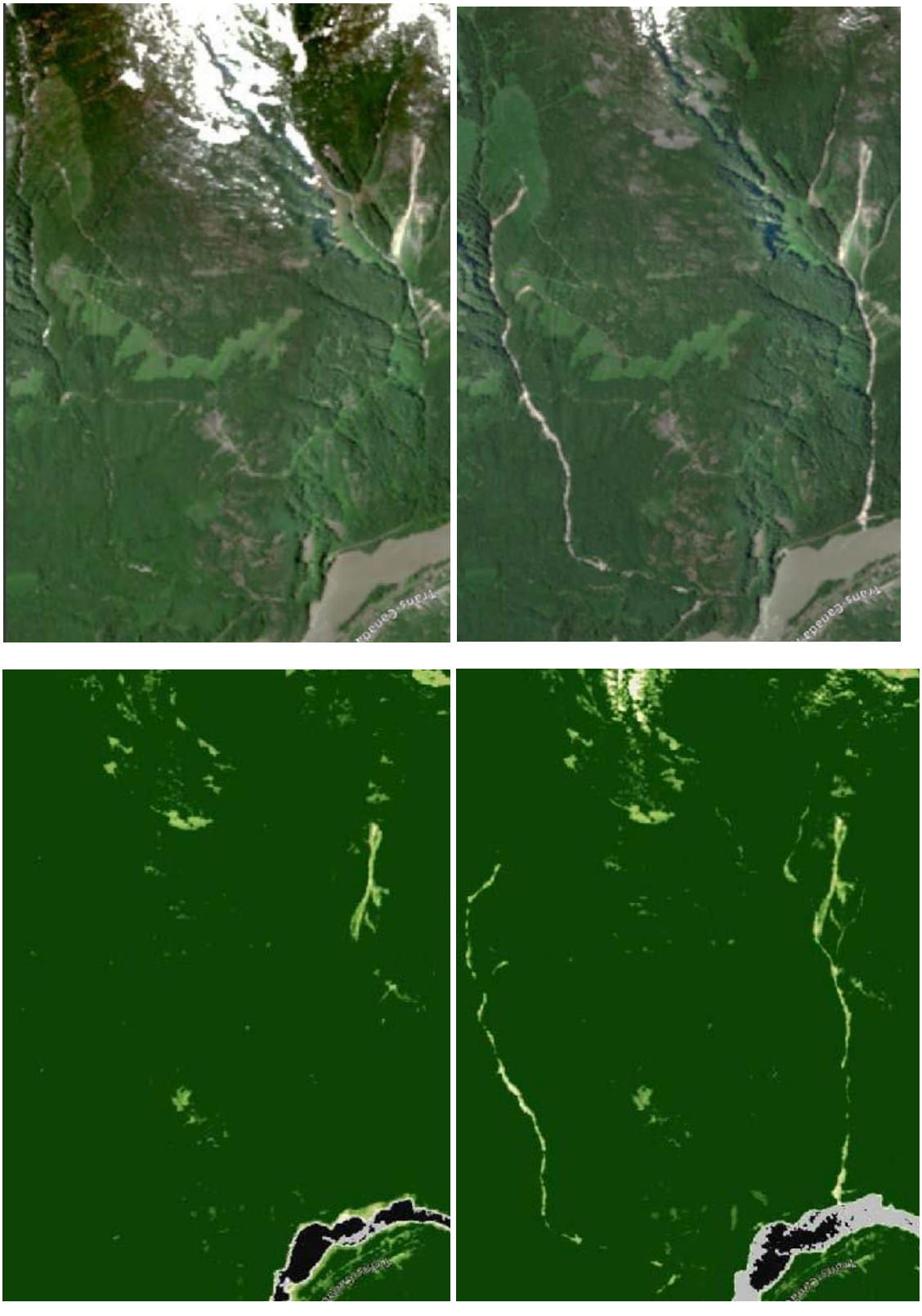


Figure 7 - Land Sat Images (top) and NVDI images (bottom) for landslides in the BC Pacific Coast mountains before (left) and after (right) the November 2021 Atmospheric River Event.

GETTING COMFORTABLE WITH SOME UNCERTAINTY

Incorporating data from advanced observational, modeling, and machine learning methodologies into a comprehensive decision support system (DSS) transforms complex geohazard-climate interactions into actionable insights. These insights come with inherent uncertainties, which is expected given the unpredictable nature of geohazard triggering. Understanding, quantifying, and reducing these uncertainties over time should be a goal of any geohazard DSS. However, it is crucial for users to recognize that no geohazard tool will ever be perfect. The benefits of having a comprehensive DSS and being able to evaluate different climate and financial investment scenarios greatly outweigh its limitations.

Many owners may feel uncertain about where to start when evaluating geohazard risk, but the key is to begin and become comfortable with some level of uncertainty. Embracing this approach enables more informed decision-making and proactive risk management, even in the face of imperfect data.

CONCLUSION

The success of our decision support system (DSS) will not be measured solely by the acceptance of tools and datasets, but by the extent to which clients and owners understand data gaps, improve data collection, recognize uncertainties in their decision-making, and utilize the DSS to prioritize monitoring and mitigation of geohazard threats affecting their assets.
Our approach has demonstrated that integrating advanced weather modeling, machine learning, and continuous hazard quantification frameworks can significantly enhance the precision and utility of geohazard risk assessments. By leveraging these technologies, we can provide location-specific risk profiles with daily resolution, enabling both real-time operations and long-range planning.

The practical applications of our methodology, as exemplified by our collaboration NZTA, highlight the potential for broader implementation in geohazard risk management. The near real-time rockfall risk management system developed for them has proven effective in operational risk management, pre-positioning resources, and conducting road closures in advance of potential landslide activities.

Furthermore, our work on Colorado SH 133 demonstrates the value of a risk-based geohazard management approach in prioritizing mitigation projects and reducing risk exposure. The successful implementation of mitigation projects has resulted in a significant reduction in risk exposure compared to construction costs.

In conclusion, our DSS and risk-based assessment methodologies offer a scalable, adaptable, and data-driven approach to managing geohazard risks. By continuously refining risk assessments with new data and integrating machine learning insights, we can elevate risk analysis from static tables to living, learning systems that evolve alongside the landscape and climate. This approach not only enhances immediate response capabilities but also contributes to long-term resilience and proactive risk management.

REFERENCES

1. Roccati, A. et al., GIS-Based Landslide Susceptibility Mapping for Land Use Planning and Risk Assessment, Land, 10(2), 2021, p. 162. Available at: https://doi.org/10.3390/land10020162

2. Kreft, J., M. Easton, and R. Topham, Automating New Zealand's Rockfall Risk Management: A Shaky Start to a Seismic Shift?, New Zealand, 2021.

3. Post, R., R. Pihl, N. Oester-Mapes, and B. Group. Geohazard Management on Colorado SH 133 From Planning to Mitigation. Tacoma WA, 2023.

4. Beven, K.. Towards an Alternative Blueprint for a Physically Based Digitally Simulated Hydrologic Response Modelling System, *Hydrological Processes* 16, no. 2, 2002, pp. 189–206. https://doi.org/10.1002/hyp.343

5. Beven, K., How to make advances in hydrological modelling, Hydrology Research, 50(6), 2019 pp. 1481–1494. Available at: https://doi.org/10.2166/nh.2019.134.

6. TseKiChun, Random forest explain [image], 2021. Retrieved from https://commons.wikimedia.org/wiki/File:Random_forest_explain.png

7. Brideau, M.A., C.A. Hancock, D. Brayshaw, P. Lipovsky, D. Cronmiller, P. Friele, and G. Wells, *Preliminary Canadian Landslide Database (9.0) [Data set]*, Zenodo, 2024. https://doi.org/10.5281/zenodo.13924556

8. Parker, W. S., Reanalyses and Observations: What's the Difference?, Bulletin of the American Meteorological Society, 97(9), 2016, pp. 1565-1572. https://doi.org/10.1175/bams-d-14-00226.1

9. Bosilovich, M. G., J. Kennedy, D. Dee, R. Allan, and A. O'Neill, On the reprocessing and reanalysis of observations for climate, In: A. Ghassem and J.W. Hurrell (eds.), Climate Science for Serving Society: Research, Modeling and Prediction Priorities, 2013, pp. 51–71, https://doi.org/10.1007/978-94-007-6692-1_3

OpenRoads, OpenBridge, Open…Frog?
Imagining the 3D World of Geological Design with Bentley's Latest Subsurface Modeling Tool

David Crotsley, PG, CPG
Senior Geologist
HDR Engineering, Inc.
1670 Broadway, Suite 3400
Denver, CO 80202
(303) 764-1520
david.crotsley@hdrinc.com

Will Brandenberger, PG, PE
Geotechnical Engineer
HDR Engineering, Inc.
1670 Broadway, Suite 3400
Denver, CO 80202
(303) 764-1520
will.brandenberger@hdrinc.com

Prepared for the 74th Highway Geology Symposium, August, 2025

Disclaimer

Statements and views presented in this paper are strictly those of the authors, and do not necessarily reflect positions held by their affiliations, the Highway Geology Symposium (HGS), or others acknowledged above. The mention of trade names for commercial products does not imply the approval or endorsement of HGS.

Copyright Notice

Copyright © 2025 Highway Geology Symposium (HGS)

All Rights Reserved. Printed in the United States of America. No part of the publication may be reproduced or copied in any form or by any means – graphic, electronic, or mechanical, including photocopying, taping, or information storage, and retrieval system – without prior written permission of the HGS. This excludes the original author(s).

ABSTRACT

The integration of advanced 3D geological modeling tools with civil infrastructure design platforms marks a transformative shift in how geotechnical data informs engineering decisions. This paper explores the synergistic use of *Leapfrog Works*, a powerful subsurface modeling software developed by Seequent, with Bentley *OpenRoads* and *OpenBridge* platforms. Traditionally, geological and civil design workflows have operated in silos, often leading to inefficiencies, miscommunication, and costly design revisions. By bridging these domains, the integration enables a unified, data-rich environment where geological complexity is visualized and incorporated directly into infrastructure design.

Leapfrog's ability to rapidly generate and refine 3D geological models from borehole logs, geophysical surveys, and other subsurface datasets allows for a more accurate and dynamic understanding of site conditions. When combined with OpenRoads and OpenBridge, this capability enhances the precision of roadway alignments, bridge foundations, and slope stability analyses. The result is a more resilient, cost-effective, and constructible design that proactively addresses geotechnical risks.

This paper presents two case studies that illustrate the practical application and benefits of this integrated approach: the I-70 Floyd Hill project in Colorado, which involved complex rockfall mitigation and slope design, and the Corridor H Roaring Run Bridge project in West Virginia, which required detailed foundation modeling in variable bedrock conditions. These examples demonstrate how the integration supports early hazard identification, optimized design geometry, and improved collaboration among geologists, engineers, and project stakeholders.

In addition to highlighting the technical advantages, the paper discusses implementation challenges such as data standardization, model performance, and the need for interdisciplinary training. A comparative analysis of traditional versus integrated workflows is provided, along with key lessons learned from the field. The paper concludes with a forward-looking perspective on how such integrations will shape the future of infrastructure design in increasingly complex geological settings.

INTRODUCTION

Infrastructure projects are increasingly challenged by complex geotechnical conditions, environmental constraints, and the need for sustainable design. Traditional workflows often separate geological modeling from civil design, leading to inefficiencies, miscommunication, and costly design and construction errors. Blending the surface design world with the subsurface has provided a more comprehensive understanding of the project to avoid these problems. The specific tool known as LeapFrog, a Seequent product which is owned by Bentley Systems, has advanced as a leader in integration with such common design programs like OpenRoads and OpenBridge. This integration enables seamless data exchange between the civil and geotechnical teams to make informed decisions based on accurate geological context.

TECHNOLOGY OVERVIEW

Seequent LeapFrog Works

Seequent Leapfrog Works (Leapfrog) is a 3D geological modeling software designed for civil engineering and environmental projects. It allows users to build dynamic geological models from borehole data, geophysical surveys, and other subsurface datasets. Key features include implicit modeling for rapid model updates, integration with geological databases like OpenGround, visualization of complex geological structures, and support for groundwater and contaminant modeling. Long used in the tunneling, dams, and the mining sector, LeapFrog is rapidly becoming more utilized in road, bridge, and rail projects where understanding the subsurface is critical to design.

Bentley OpenRoads and OpenBridge

Bentley's OpenRoads and OpenBridge Designer programs are part of Bentley's civil design suite. OpenRoads provides corridor modeling and roadway alignment development, allows the designer to apply roadway templates across larger areas, and provides cut and fill balances throughout. OpenBridge then provides a means to develop the bridge geometry, evaluate the structural design, drainage and utility integration, and constructability. Both programs are part of Bentley's iTwin technology, enabling real time collaboration and model synchronization.

BENEFITS TO INTEGRATION

Enhanced Design Accuracy

By incorporating accurate geological models into the design process, design teams can optimize road and bridge alignments for cut/fill balances, design foundations based on real subsurface conditions, and avoid conflicts with identified geological hazards. All of this leads to a more resilient and cost-effective infrastructure design.

Risk Mitigation

According to the CRUX Insight 2024 report, developed by HKA, geotechnical risks are a leading cause of project delays and cost overruns, with average claims exceeding hundreds of millions of dollars. The integration helps mitigate risk by identifying problematic conditions

early in the design process, enabling proactive design adjustments, and reducing reliance on assumptions and outdated data.

Improved Collaboration

Collaboration is the key item when using Leapfrog on larger design projects. Integrating work from geologists, engineers, project managers and stakeholders allows for an open and transparent model environment. Data can be shared or updated in real time through cloud based sharing, which allows for quicker and smoother data integration, and reduces the likelihood of errors.

Challenges and Considerations

Despite its benefits, the integration of the various moving parts presents natural challenges that the design team needs to be cognizant of throughout the process. As with most current programs, consistent and standardized data is required across platforms. Additionally, dealing with large datasets and complicated processing, the design team needs to balance the level of detail with the performance and usability of the model. Then lastly, and most importantly from a geologic standpoint, is the training required to understand how to model subsurface conditions at a project site. Blending the core geology courses of structural geology, sedimentation and stratigraphy, geomorphology, and then considering the needs from the civil engineering side is critical to consider during the project.

CASE STUDIES

I-70 Floyd Hill – Clear Creek County, Colorado

Introduction

The project site is located along Interstate 70 (I-70), from Floyd Hill to the Veteran's Memorial Tunnels, near Clear Creek County, Colorado. This phase of the project was the design and evaluation for the western section of the project, which included two (2) bridge replacements along with a larger, >250-foot high rock cut and rockfall mitigation. Refer to Figure 1 below for a project location map.

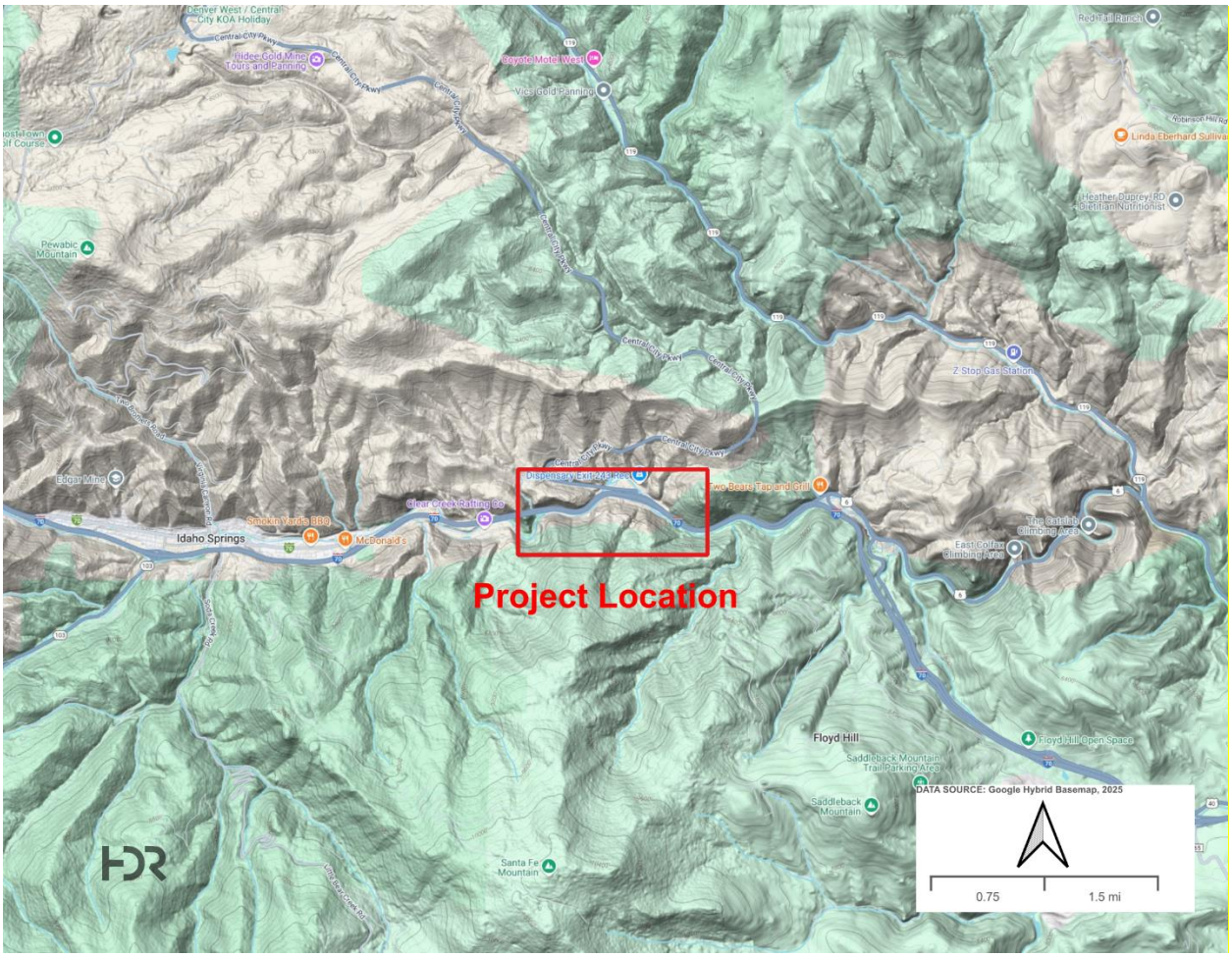


Figure 1 – Floyd Hill Project Location Map

Geologic Setting

The project is located in the Southern Rocky Mountains physiographic province, and consists of a variety of alluvium, colluvium, and bedrock outcrops. Bedrock consists of various Precambrian era Gneiss with interlayered areas of Amphibolite. The Floyd Hill fault was mapped by Sheridan and Marsh in 1976 (*1*), and generally parallels the existing roadway alignment between the US-6 interchange and the eastern limit of the proposed corridor.

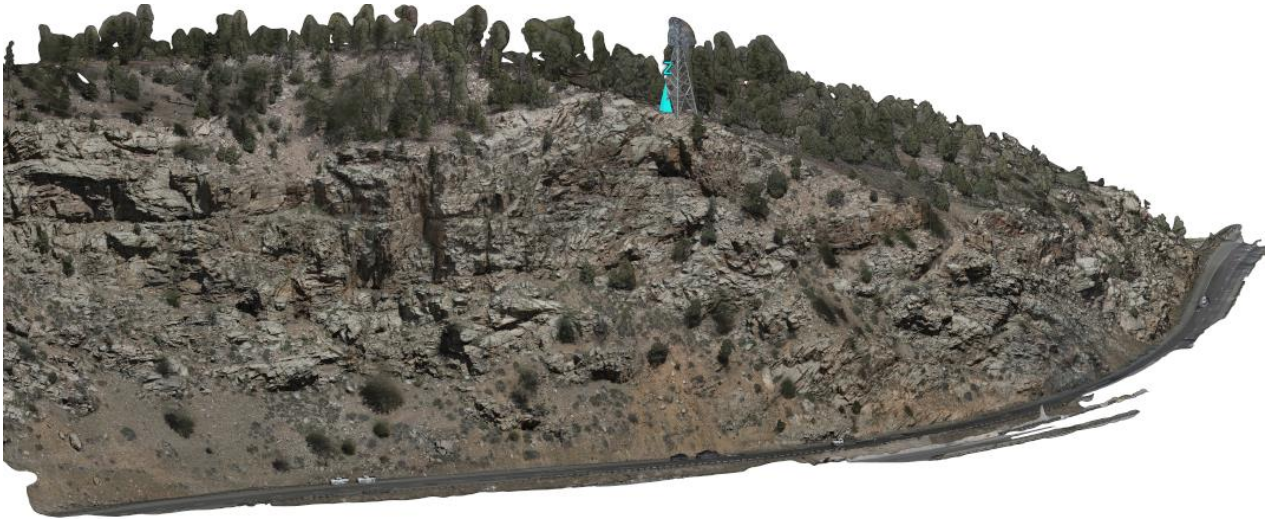


Figure 2 – View of West Cut UAV Data

The subject slope in particular is adjacent to the previously constructed Veteran's Memorial Tunnels. Reaching more than 300 feet above the roadway, the existing slope has a history of rockfall reaching the roadway and beyond. The proposed realignment of I-70 would require significant blasting and rock removal, with a blasting timeline of approximately one year. HDR was the geotechnical lead for the west section, as well as the lead designer for the rockfall mitigation. A separate subconsultant was responsible for the cut design.

Data Collection

Detailed photogrammetric imagery was collected by Chinook Landscape Architecture, LLC, as a subcontractor to HDR. Point cloud data was processed and provided to HDR, to support the design analyses and recommendations. The results of the photogrammetric survey were utilized in evaluating rockfall concerns throughout the corridor, as well as developing parameters for the analyses.

In addition to the photogrammetric survey, HDR personnel performed a site visit on March 23, 2023. The site visit was performed in order to evaluate existing site conditions, verify areas of concern and parameters used for the rockfall analyses, and to verify the anticipated extents of the rockfall treatments. The site was snow covered during the time of the site visit; however, the general slope geometries, vegetation conditions, and existing rockfall shape and size were in general accordance with historical imagery and past experience in the area.

Geotechnical borings were performed by others for the project, as well as four (4) lines of seismic refraction. Two (2) borings were performed at the top of the cut, then tied into the seismic data to evaluate the top of rock line.

Geologic Model

Bedrock in the project area was considered massive with little identifiable structure. Therefore, the design hinged primarily on the dominant foliation planes and the general strength of the rock itself. For the rockfall design portion, we collaborated with the roadway designers to incorporate the OpenRoads model to evaluate the rock cut benches and potential catchment

areas. The image below incorporated the UAV mesh showing the natural ground surface where there would be no cut (red), hard rock area with 1H:6V cut (orange), slope rounding (yellow), and difficult blasting areas (blue)

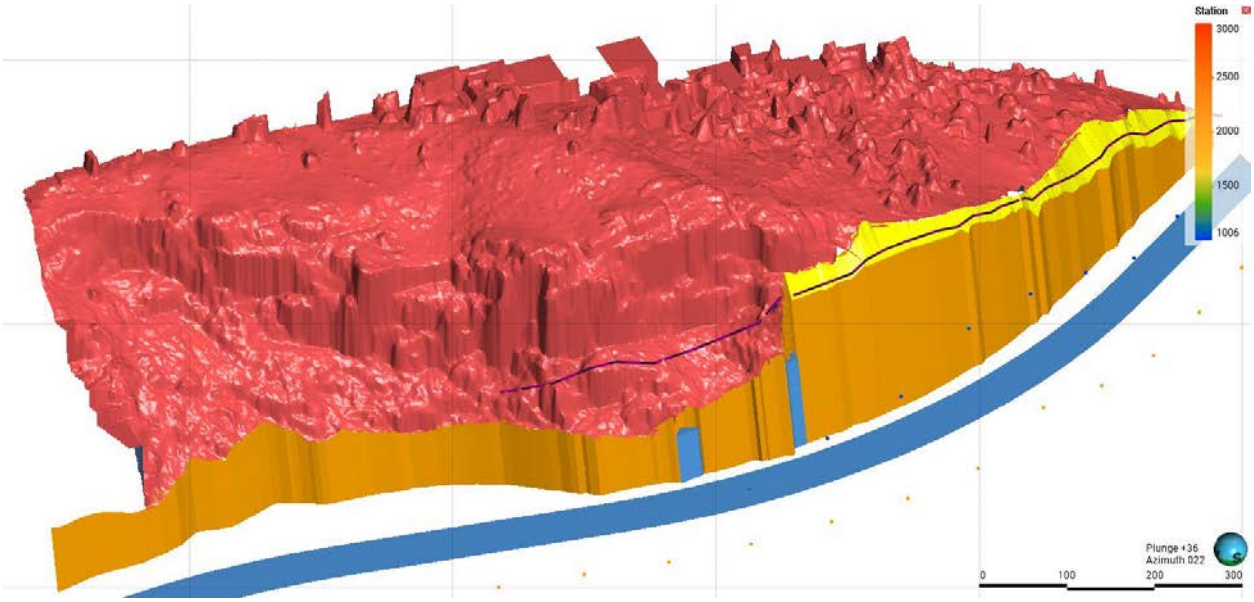


Figure 3 – Floyd Hill LeapFrog Model

Analysis and Interpretation

Rockfall analyses were performed utilizing RocScience's RocFall2 design program. The geometry was provided by the roadway team, and incorporated into the design runs. Rockfall analyses were performed along the cut location to identify areas of concern based on existing and proposed slope geometry, shoulder/ditch width, and existing vegetation on the slopes. The controlling cross sections were utilized to analyze the slope.

In general, due to the complexity of the slope and the limited catchment location, the design recommendation for the area was to use a draped mesh from the top of the slope to the cut line or adjacent bench location, which would then filter any rockfall into a hybrid barrier system funneling rock to the existing ditch. Therefore, rockfall is intended to be minimized throughout.

The design of the rockfall attenuator fence and mesh were developed utilizing the energies estimated from past experience with draped systems, and applying them to the various components of the attenuator fence. The perpendicular anchors were analyzed based on impact, shear, and pullout forces, and the wire ropes were analyzed based on the weight of the supported mesh to ensure suitable capacity. The draped mesh anchors were analyzed using the mass of the mesh itself, and assuming a nominal mass suspended behind the mesh.

Project Benefit

During development of the cut slope, HDR was concerned about the blasting efforts and the phasing that was being proposed. Noticing a gap in information from the 25-foot cross sections, HDR developed the geologic model with the proposed cut angles, showing that there would be two locations that would require extensive additional work to get equipment onto the

blast bench. As a result, the team collaborated with the blasting leads to rework the slope angles in the area to provide a suitable working bench, saving the team additional issues during construction.

Corridor H Roaring Run Bridge – Tucker County, West Virginia

Introduction

The Roaring Run Bridge project was developed to provide recommendations for the design of foundations associated with the bridge structure carrying US 48 over United States Route 219 (US-219) Seneca Trail, and Roaring Run. The project is located in Tucker County, West Virginia, near the city of Parsons. The project location is shown below in Figure 4.

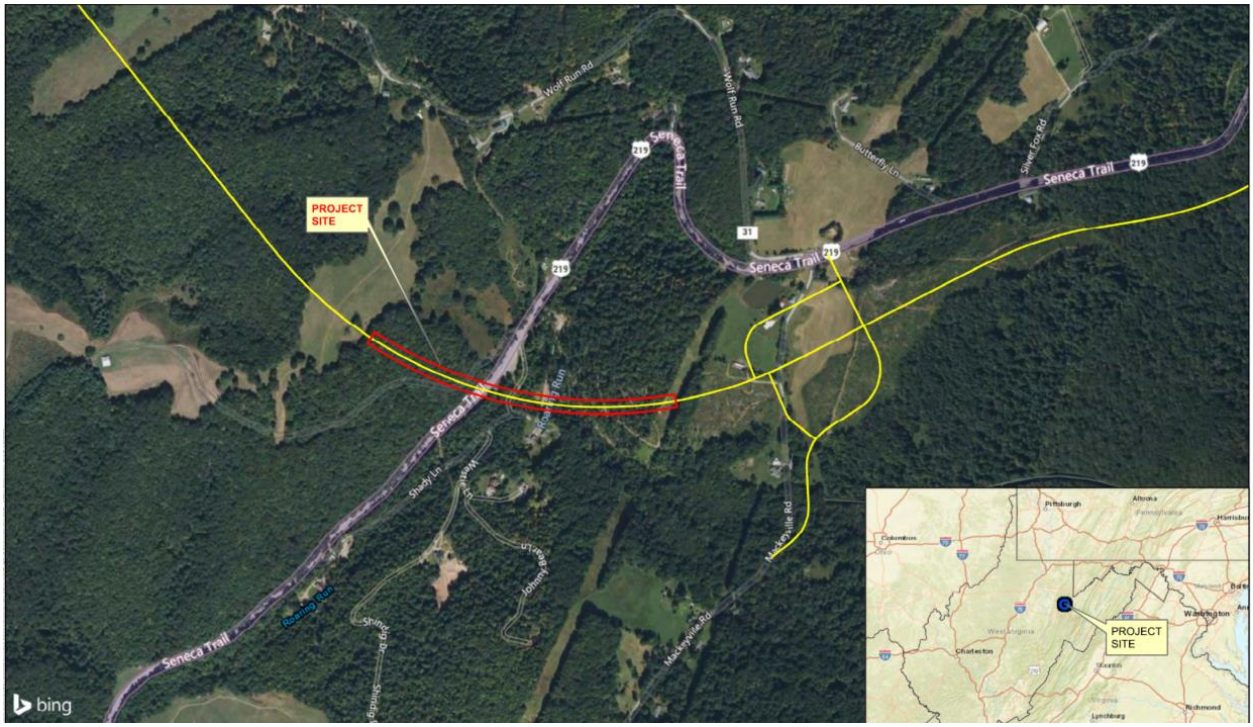


Figure 4 – Roaring Run Project Location Map

Geologic Setting

The bridge structure is located within the Hampshire formation (Dhs), generally consisting of interbedded mudstones, shales, siltstones, and micaceous sandstone. Sandstones can be fine to medium grained, occasionally bioturbated or with shale clasts. Thin to medium planar beds and cross-beds are common, with occasional massive beds may be observed. Contact with the overlying Price formation is marked by the unconformable transition from the red and green shales and sandstones of the Hampshire Formation to the gray shales and brown, coarse-grained to conglomeratic sandstones of the overlying Price Formation (Pocono Group).

The underlying Upper Devonian-aged Greenland Gap Group consists of siltstone and sandstone interbedded with shale and conglomerates. The formation is mostly marine and may be fossiliferous.

The Deer Park anticline is located approximately 4.5 miles west and the North Potomac syncline is located approximately 5.0 miles east of the bridge structure. Both the anticline and syncline trend northeast. The bedrock within the project area gently dips west.

Data Collection

Initially, twelve (12) borings were performed for the approximate bridge location by Michael Baker in 2016, then HDR performed a supplemental boring program consisting of 29 borings. Soil samples of the overburden soils were obtained using split-spoon sampling procedures through hollow-stem augers. Standard Penetration Test (SPT) samples are taken at 5-foot intervals in accordance with WVDOH Standard Core Boring Contract Documents and ASTM D 1586, and all samples were visually classified in accordance with USCS and AASHTO classification systems. SPT N-values were recorded to estimate the in-situ relative density of granular soils. Where pocket penetrometer readings could not be taken, SPT N-values were used to estimate the consistency of the soil. An automatic hammer was used to drive the split-spoon sampler. SPT N-values were corrected for hammer efficiency of the automatic hammer. The recovered SPT samples were placed in glass jars for retention. Where needed, auger soil cuttings were collected in bulk bag samples for subsequent laboratory testing. Upon completion of each boring, each borehole was backfilled with soil cuttings to existing grade. Finally, ground water readings were taken in each boring, unless a boring was backfilled immediately upon completion for safety reasons.

Upon achieving SPT refusal on bedrock, rock coring was performed to prescribed depths using a NQ2-size double-tube wire-line core barrel with a diamond bit. A split inner core barrel was used for all rock coring.

Laboratory testing for the project consisted of soil classifications, direct shear, unconfined compressive strength of rock, slake durability, and corrosion series.

Geologic Model

The geologic model was developed to better understand the conditions present at the foundation locations, estimate cut/fill volumes, and identify areas of concern for any deep foundation elements.

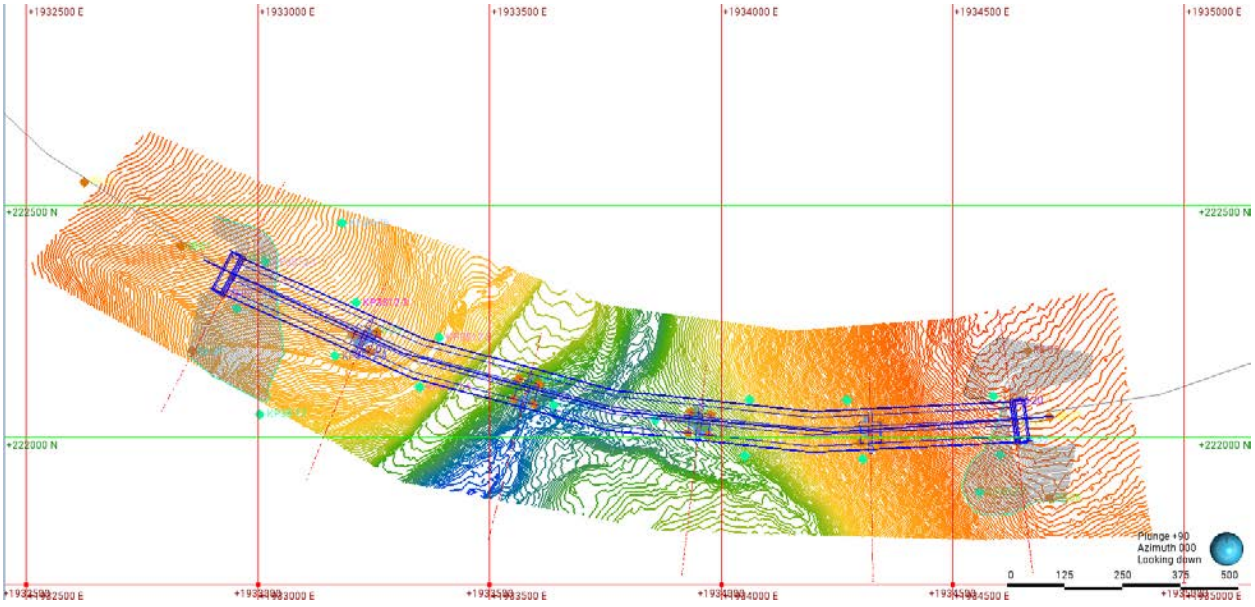


Figure 5 – Roaring Run Preliminary LeapFrog Model

Analysis and Interpretation

The basis of design of the proposed foundations relies on engineering parameters of soil and rock, the geometry of the proposed substructures relative to site topography and other constraints, and geotechnical resistances and deformations of available bearing materials. Early foundation discussions considered both deep and shallow foundation types. Boring analysis revealed several rock types and conditions encountered at the proposed substructures. Overall, the rock dip appeared favorable to shallow foundations, however weathering and hardness of the rock formations varied with location. Sandstone at the abutments was observed to be weathered to depths which would be unsuitable to shallow foundations. For this reason, and because of the fill height required to reach proposed roadway superelevation, the abutments will be founded on predrilled HP 14x102 piles driven to refusal on sound bedrock. Because of the downdrag forces induced from continued embankment placement following driving, and because they are to be predrilled, the piles will be installed plumb, without a batter. The use of hardened steel pile shoes is recommended. Full height (bottom of footing to bottom of approach slab) EPS foam and reinforced backfill (woven geotextile with Class 1 aggregate) will be utilized behind both abutments to the lengths specified.

Loading demands at the piers were compared with surficial rock bearing resistances. Through analysis, it was determined that the footing size requirements would be cost prohibitive, requiring considerable excavation on the steep slopes where the pier are proposed. For this reason, CIP reinforced concrete single-column piers with a footing, founded on drilled shafts with rock sockets are proposed at each of the piers. Careful analysis of the bedrock at each corner of the proposed piers was performed in order to determine minimum caisson lengths at each substructure. The proposed diameters of the caissons are 6 feet, with 5.5 foot rock sockets

supported by skin friction within bedrock, and limited consideration for end bearing. For further discussion, refer to the geotechnical report. Variability in rock types resulted in rock socket lengths ranging from 25 feet to 40 feet in length, with the greatest lengths at Pier 4 where an extended layer of soft to medium hard siltstone was encountered.

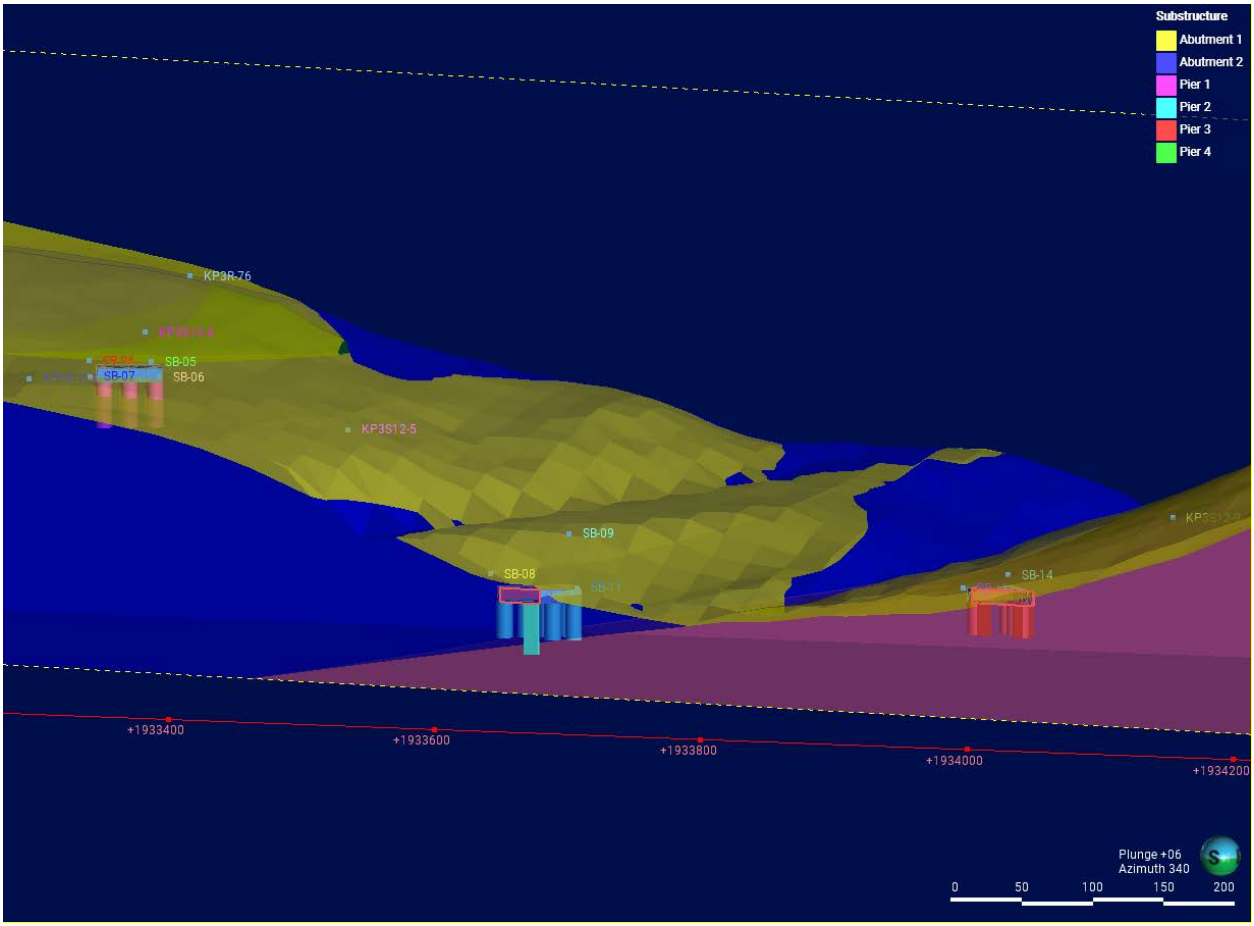


Figure 6 – Roaring Run LeapFrog Model

Project Benefit

Incorporating the LeapFrog model into the project design allowed the design team to develop an efficient model of where the deep foundations would bear and the quantity of overburden that was anticipated to be excavated. HDR was able to refine the foundation locations to limit excessive earthwork while maintaining suitable pile resistances. The collaboration between structural, roadway, and geotechnical engineers, and the ability to visualize the above and below ground design together was critical in a completing a successful project.

CONCLUSIONS AND FUTURE OUTLOOK

The integration of Seequent's Leapfrog Works with Bentley's OpenRoads and OpenBridge platforms represents a significant advancement in infrastructure design. By bridging the gap between surface and subsurface modeling, this integration improves design accuracy, reduces risk, and fosters collaboration. As infrastructure projects grow in complexity, such integrated workflows will be essential for delivering resilient, efficient, and sustainable outcomes.

REFERENCES

1. Marsh, Sherman P. and D. M. Sheridan, *Rutile in Precambrian sillimanite-quarts gneiss and related rocks, east-central Frong Range, Colorado*, USGS 1976.

a. Bentley Systems, Inc., LeapFrog v.2025.1.1, 2025

b. HDR, *Final Geotechnical Engineering Report*, 2023.

c. HDR, *West Section Rockfall Mitigation Design Memorandum*, 2023.

*References a-c are not cited in body of text.

HIGHWAY GEOLOGY AND PALEONTOLOGY AND THEIR IMPORTANCE TO UNDERSTANDING EARTH'S HISTORY

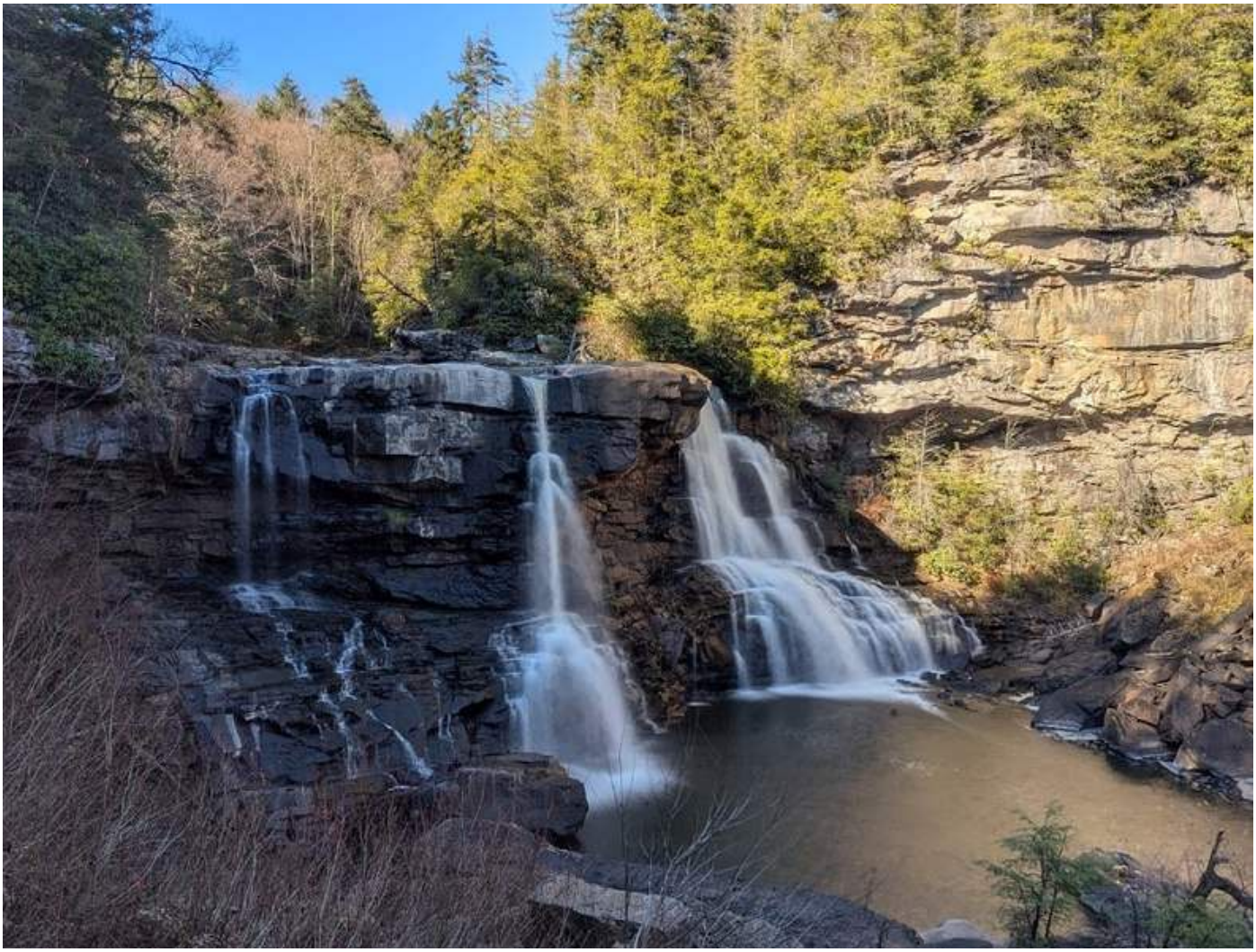
E. Ray Garton
West Virginia Geological and Economic Survey Museum
1 Mont Chateau Rd, Morgantown, WV 26508
eraygarton@gmail.com

ABSTRACT

Highway construction has almost always involved exposing bedrock, creating the opportunity for interesting, even incredible, discoveries to be made. Highway cuts have uncovered breathtaking geologic exposures and vistas. More importantly, many highway cuts have uncovered unknown fossils and prehistoric life treasures providing a wealth of information about the history of life on this planet spanning at least 500 million years. Thousands of sites have uncovered significant find and paleontologists and museums have benefited greatly from the discoveries made possible by the geologists and engineers designing and building our transportation systems. This presentation will explore just a few of those discoveries.

Thank you for attending the 74th Highway Geology Symposium!

See you next year in Reno, Nevada.



Blackwater Falls State Park, WV



SUNSET OVER BACKBONE MOUNTAIN, TUCKER CO., WV